EFFECTS OF STARCH BLENDS AND PROCESSING TECHNIQUE ON SOME PROPERTIES OF BIODEGRADABLE POLYMER DRILLING MUDS

BY

CHIKE-ONYEGBULA, CATHERINE OLUCHI
(B. ENG., M. Sc.)
REG. NO: 20094704078

A THESIS SUBMITTED TO

THE POSTGRADUATE SCHOOL
FEDERAL UNIVERSITY OF TECHNOLOGY, OWERRI

IN PARTIAL FULFILMENT OF THE REQUIREMENTS FOR THE AWARD OF DOCTOR OF PHILOSOPHY (Ph.D) DEGREE IN POLYMER SCIENCE

JULY, 2016

CERTIFICATION

This is to certify that the work entitled **"Effects of Starch blends and Processing Technique on Some Properties of Biodegradable Polymer Drilling Muds"** was carried out by **CHIKE-ONYEGBULA, CATHERINE OLUCHI (REG.NO: 20094704078)** in accordance with the regulations governing the award of Doctor of Philosophy, Ph.D (Polymer Science) in the Postgraduate School at Federal University of Technology, Owerri, Imo State, Nigeria.

Prof. O. Ogbobe
Supervisor
.....
Signature and Date

Engr. Prof. I. C. Madufor
CO-Supervisor/Head of Department
Polymer and Textile Engineering Department
.....
Signature and Date

Engr. Dr. M. U. Obidiegwu
CO-Supervisor
19/09/16
.....
Signature and Date

Engr. Prof. G. I. NWANDIKOM
Dean, SEET
19/09/16
.....
Signature and Date

Prof. (Mrs.) N. N. Oti
Dean, Postgraduate School
.....
Signature and Date

Prof. F. E. Okieimen
External Examiner
20/7/16
.....
Signature and Date

DEDICATION

This thesis is dedicated to the Almighty God.

I also dedicate this thesis to my late father, Mr G. E. Ukachukwu, who passed on when this work was in progress.

ACKNOWLEDGEMENTS

I express my profound gratitude to Prof. O. Ogbobe, whose academic advice and other immense contributions helped me in the accomplishment of this work. I am also grateful to my other lecturers, Prof. A. E. Iheonye, Prof. C. B. C. Ohanuzue, Prof. I. Igwe, Engr. Prof. I. C. Madufor, Dr. G. N. Onyeagoro, Engr. Dr. M. U. Obidiegwu, and other colleagues in the Department of Polymer and Textile Engineering, FUTO, for their assistance during the course of this work.

My gratitude goes to Engr. A. A. Imoh of TOTAL FINA ELF Oil Company, Engr. C. E. Bode and Mr C. Onyeukwu of SIFANE Group of Companies and Mrs Anunobi of Biology Department, FUTO, for their technical advice and assistance.

I am also thankful for the wonderful encouragement and assistance given to me by some of my friends and well wishers like Engr. U. Ezeamaku, Engr Dr. H. C. Obasi, Mr U. Onyeje, Mr K. I. Aniagbaoso, Engr F. Onuoha, Dr. (Mrs.) J. E. Nnanna, Mrs. L. N. Amaefula, Engr. Dr. (Mrs) C. C. Anyanwu.

I am very grateful to my husband, Chief B. Chike Onyegbula, my mother, Mrs. J. N. Ukachukwu, my brothers, Rev. P. C. Ukachukwu, Mr C. C. Ukachukwu, Chief A. N. Ukachukwu, Pastor T. C. Ukachukwu, Mr E. O. Ukachukwu, my sisters, Mrs A. N. Ukwuoma, Mrs U. V. Nduka, and my aunt, Mrs J. O. Uwakwe for their financial support and other encouragement to the success of this work.

My great appreciation goes to my lovely children, Chiamaka and Chizitere for their time, patience and understanding shown to me during the period of this work.

CHIKE-ONYEGBULA, CATHERINE OLUCHI

TABLE OF CONTENTS

CHAPTER FIVE: CONCLUSION AND RECOMMENDATIONS

LIST OF TABLES

LIST OF FIGURES

ABSTRACT

This research was carried out on "Effects of Starch blends and Processing Technique on some Properties of Biodegradable Polymer Drilling Muds". Several biodegradable polymer drilling muds were prepared using starches from local corns and millet pregelatinized and blended by extrusion technique in the absence of any solvents or chemicals. The filtration and rheological properties of the new muds and three already existing muds were studied at 25^{o}C-450^{o}C temperature range and at 0.01-0.05g/ml concentration of each starch using filter loss method and viscometric method respectively. The biodegradation properties of the muds were studied with their respective starches using soil burial test method and plant growth method. The experimental results were also modelled using MATLAB software method of modelling. Experimental results showed that the new polymer drilling muds have excellent filtration control behaviours and thermal stability at all the temperatures. The three already existing muds showed thermal degradation at 250^{o}C, 350^{o}C and 450^{o}C temperatures. The values of flow index were found to be less than 1.0 showing pseudoplastic flow behaviour of the muds. Consistency index, Shear stress and yield stress increased with increase in concentration. Viscosity decreased with increasing shear rate showing shear thinning behaviour of the muds. The highest percent weight loss of 65.70% and lowest percent weight loss of 10.34% were obtained with one of the new starch blends and one of the already existing starches respectively for biodegradability. The polymer drilling muds obeyed Henri Darcy and API models for filtration as well as power law and Herschel Bulkely models for fluid rheology. The results from Matlab model showed that the values of coefficient of regression, (R^2) and the Sum of Squared Errors, (SSE) were respectively close to "1" and "0"signifying good fit for all the new muds. The behaviours of the muds showed that there is proximity between the Matlab's modelled results and the experimental results based on the already existing models.Therefore, the polymer muds containing the new starch blends are purer, more suitable and more environmentally friendly than the already existing muds. The new muds are therefore recommended to be used for drilling operations in all areas including high temperature and environmentally-sensitive areas.

Keywords: starch-blends, biodegradable-polymer, drilling-mud, extrusion, filtration, rheology.

CHAPTER ONE

INTRODUCTION

1.1 Background of Study

Starch is a polymer that is widely used in all types of drilling muds including water-based muds (Cyracus, 2012; Robert & Bell, 2011; Andrew & Robert, 2007; Timmerman & Dakota, 2000). With the development of specialty drilling and completion technologies, starch is also chosen as one of the components of drill-in-fluids. Non-damaging drilling and completion fluids have gained considerable interest during the last decades because high angle well, multilateral and slim-hole technologies require fluids with special properties (Bernu, 2011; Zereek & Bruce, 2010; Long & Jolly, 2004; Bhattacharya et al., 2002). Deviated drilling operations need shear-thinning fluids with a good carrying capacity (Anthony & Robert, 2010). Efficient clean-up ability of drilling fluids is important in reservoirs for maximizing the well productivity. The changes in drilling fluid rheology have shifted the requirements for the drilling fluid components. One of these components is starch. Starch is a biodegradable polymer, which is susceptible to biological or micro-organisms attack (Adrian & Gareth, 2009). There are four biodegradation environments for polymeric products namely soil, aquatic, landfill, and compost with each environment having its special conditions for degradation and containing different micro-organisms (Obasi, 2012). The biodegradation rates in biopolymers depend on a number of factors which include the nature of biopolymer, the biodegradability of each component and the quality of the interface (Scott et al., 2007). In the soil, fungi are mostly responsible for degradation of organic matter including polymer.

Over the past decades, starch has been used in producing drilling muds so as to control the fluid loss properties of the muds. In this present time, numerous modified starch derivatives have been produced for oil field applications and some of them have been commercialized. Some modified starches which have been in use for preparing muds include hydroxyl propyl starch, carboxyl methyl starch, and others (Amanullah & Long, 2004). These modified starches are produced by gelatinization in the presence of a solvent and chemicals (Bryan et al., 2010; Ben & Joe, 2006; Dickson & Philipp, 2006; Bill & Mark, 2007; Weir & Bailey, 2004; Amanullah & Long, 2004). The modification is carried out to produce a range of starches with higher tolerance to thermal, mixing and pH effects, and to generate easy swelling characteristics in the presence of water. In the drilling operation, a well bore is drilled to dislocate the rocks to the surface from different depth, in order to obtain some useful substances which are extractable from the interior part of the earth crust (Amanullah et al., 1997). The process of extraction through well bores involves drilling for: Exploitation of petroleum (crude oil) and gas, Geological prospecting and exploration for new reserves of useful substances, Execution of mines and ventilation, Water from water-beds for agriculture, industries and household use, Ground and soil investigation before building construction.

The fluid circulated round the well bore during drilling operation is a major component in the drilling of an oil well (Bernu, 2011). It performs a variety of functions that influence the drilling rate and the cost, efficiency and safety of the operation. As a result of technological advancement in the drilling industries since 1963, drilling fluid technology has expanded enormously in scope and sophistication (Gray & Darley, 1990). An example is the great increase in the use of polymers to

obtain more favourable mud properties. Indeed, a well can now be drilled with a mud consistency of nothing but polymer and water or oil as its base fluid. Drilling, therefore, uses a range of specialized fluids, which are multi – component dispersions and polymeric solutions (Amanullah & Long, 2004). Virtually all rock particles and other solids are removed at the surface by improved mechanical separators. Also the most important aim in this age of oil shortage is that well productivity can be increased by the use of special completion and work over fluids that do not damage the formation (Jones & Mark, 2006). These advanced technologies were not readily available as far back as 1963. The formulation of an ideal drilling mud for any particular job is a complex task because of the required functions. But the knowledge of the geological conditions and the model of the relevant drilling operation can be used to specify the particular combination of mud properties required (Zhang et al., 2006). Rheology of drilling muds and the associated annular hydraulics are related directly to how effectively a well bore is drilled and the hole-stability. An understanding of the rheology of drilling muds is very essential so that the well site engineers and mud engineers will most effectively accomplish the objective of drilling the well bore (Fordham et al., 2001). In fact, borehole stability remains the main concern during drilling and the selection of drilling fluid type and composition was at the origin of successful drilling (Pokar & Holt, 2002). In drilling fluid technologies, two main tendencies are currently developed in parallel: (i) search for new additives increasing the performances of water-based muds (WBM) and (ii) the development and introduction of new compounds into oil-based muds (OBM) (American Petroleum Institute, 1993). The drilling fluid must have certain physical characteristics. The most important of these are the viscosity, the thermal stability, and the water holding or retaining characteristics of the fluid (Cliff & Gerald, 2010;

Casmir et al., 2007; Vincent et al., 2001). It is well known that conventional or chemically- modified starches tend to break down or burn up at elevated temperatures for extended periods of time longer than four hours (Bernu, 2011; Brown, 2009; Dickson & Philipp, 2006). Higher temperatures for extended periods of time are often encountered in deeper wells during the drilling process. The breakdown of the chemically-modified starches causes an increase in the consumption of the starch needed in the mud. Chemically-modified starches are only suitable for drilling oil wells with low bottom-hole temperatures and not those with deep bottom-hole or elevated temperatures (Bernu, 2011; Brown, 2009; Dickson & Philipp, 2006). Therefore, there is still the need in the well-drilling industries for a starch which can operate for extended periods of time at elevated temperatures. The requirement for drill-in starches are quite different from those of the traditional starch based fluid loss reducing agents. The latter were designed to control filtration without contributing to the drilling fluid viscosity. Developments in the composition of fluids for drill-in and completion purposes led to an increased interest in starches that combined filtration-controlling properties with shear thinning properties and contribution to the low-end shear viscosity (Zereek and Bruce, 2010). Temperature restrictions of the current systems created demands for drilling muds with shear thinning effects and improved resistance to heat. In drilling fluids the polymer interacts with solid particles to enhance the seal of the filter cake on the well-bore, and to provide the required rheology (Brown, 2009; Dahlgreen & Helbig, 2008). During drilling operations the fluid rheology has to be controlled over a large temperature interval. Like many polymers, starches tend to degrade at high temperature. The degradation leads to increased fluid loss and changes of the fluid viscosity, which can result in fluid failure and lead to formation damage.

1.2 Statement of Problem

The use of non-degradable and non-environmentally-friendly drilling muds is a problem in the society because they have some components which are potentially non-degradable and hazardous to the environment (Bertts & Jerry, 2012; Iheaturu, 2006; Enie & Giles, 2001; Neff, 2000). These components include oil from oil- based muds and those based on mineral oil of the Isomerized Olefins (IO), Linear Alpha Olefins (LAO), N-paraffin or Polyalpha Olefins (PAO), salts such as Sodium and calcium chloride, soluble trace elements like zinc, lead, copper cadmium, nickel, mercury, arsenic, barium and chromium (Horner et al., 2001; Enie & Giles, 2001; Minton, 1991). The incomplete solubility of raw starch in water unless pregelatinized is also a problem hence producers incorporate harzadous chemicals or solvent to obtain complete starch solubility in aqueous solutions. Some past researchers had incorporated chemically modified starch-polymers in the preparation of drilling muds in which the biodegradability and environmental compatibility of the starch are completely reduced (Amani, 2012; Wylly & Chenevert, 2012; Bill & Mark, 2007; Casmir et al., 2007; Amanullah & Long, 2004; Bataille et al., 2000). Again, the wet method of production is low efficient, lacks purity and produces a large amount of industrial waste-water as a by-product (Amanullah & Long, 2004). It is also hard to graft two groups using this process, especially when one is hydrophilic and another is hydrophobic, in one reaction because they need different solvents. Furthermore, there is still the need to provide drilling muds that have high thermal stability for drilling wells with deep bottom-hole or high temperatures. Some researchers had prepared drilling muds that contained chemically-modified blend of starches or single starch or non chemically-modified single starch (Bertts & Jerry, 2012; Ukachukwu et al., 2010; Casmir et al., 2007). These drilling muds served some purposes but lacked such

desirable properties as either complete natural purity or thermal stability at elevated temperatures during the actual drilling operation. It is well known that one of the factors affecting the thermostability of a drilling fluid is the composition of the drilling fluid. Another factor is the nature and the chemical modification of the starch. The chemical modification including cross-linking, carboxymethylation and hydroxypropylation of the starches have not yet improved the properties of drilling muds at elevated temperatures (Bernu, 2011; Brown, 2009; Dickson & Philipp, 2006). Furthermore, the economic importance of the drilling muds is of great concern in the society. The high costs of producing widely used or already existing muds have been parts of the prolems of these drilling muds. These high costs have been confirmed to have arisen from the use of expensive raw materials in preparing the muds and costly processing techniques involving expensive equipments.

1.3 Objectives of Study

1.3.1 Main Objective

The main objective of this research work is to study the Effects of Starch Blends and Processing Technique on Some Properties of Biodegradable Polymer Drilling Muds.

1.3.2 Specific Objectives

The specific objectives of this study are:

(i) to provide drilling mud additives made up of starches extracted from local sources such as Guinea corn, Waxy corn, Popcorn of varying origins and millet.

(ii) to produce thermally-stable starch blends using extrusion technique without the addition of any solvents or chemicals.

(iii) to prepare water-based biodegradable polymer drilling muds, which have improved flow properties, low fluid loss, and high thermal stability, with the new starch blends.

(iv) to characterize the filtration properties, the rheological properties, and the thermal stability properties of the new polymer muds at 25^0C-450^0C temperature range and compare to those of three already existing drilling muds containing repectively a blend of chemically-modified carboxymethyl and hydroxypropyl starches, non-chemically-modified single starch, and chemically-modified single carboxymethyl starch.

(v) to determine the biodegradability of the muds using the starches, and the effects of the biodegradation products on plants' growths.

(vi) to model the experimental results obtained from the filtration and rheological tests on the muds using Matlab software.

1.4 Justification of Study

Starch was pre-gelatinized by extrusion technique in the absence of any solvent or chemical and complete solubility of the starch in water was obtained. Drilling operation involves the use of drilling mud that contains additives which are made up of polymers including starch which must be pre-gelatinized for complete solubility in water so as to display its special capacity of building solution's viscosity (Cliff and Gerald, 2010). The present study produced water-based drilling muds that are environmentally friendly and non-toxic. Many widely-used or standard drilling muds are formulated with synthetic polymers, which are non biodegradable and their waste cause a lot of hazard to the environment (Caleb & Dan, 2004). In recent years, some other muds have been formulated with biodegradable polymers like starch, cellulose, xanthan gum, etc but these muds lack purity and efficiency due to method of production (Kelvin, 2011; Amanullah & Long, 2004). The use of pure starch helps to keep intact the biodegradability and other environmental compatible properties of the mud. The production method or processing technique used in this work was of great

purity and high efficiency. Extrusion is a technology developed to carry out a production or processing reaction using an extruder (Ebewele, 2000; Fried, 2000). The technology has been developed in the last two decades and has been widely used to modify conventional polymers. The advantages of the technology are purity, flexibility, efficiency, non-use of solvent, and ability to carry out multi-reactions at one step. Therefore, the new starch blends used in preparing the drilling muds in this present research are totally pure and completely environmentally friendly. Also, there was no production of any industrial waste water to contaminate our environment and it was easy to graft two polymers at a step by this method. Also, the raw materials and processing equipments used in this study are locally available and cheap in cost. The reasons for choosing starch are its versatility, and compared to many biopolymers, its relative low cost. Millet and corns (Guinea corn, Popcorn and Waxy corn) which were the main sources for the starches were locally obtained and cheap in cost. Also, extrusion technique which involves the use of an extruder in this study is locally available and has low production cost. Again, the new polymer drilling muds containing the new starch blends possess high performance efficiency. The main functions of starch are fluid loss reduction and rheology control. The new muds have great potential to control fluid flow and reduce fluid loss. Also, the polymer drilling muds containing the new starch blends have high thermal stability. Therefore, the newly produced muds containing the new starch blends are very suitable for drilling deep bottom-hole or high temperature wells. It may be mentioned that several tons of chemically pre-gelatinized or modified starches are used by an oil-drilling rig annually. They are considered suitable for drilling oil wells that have low bottom-hole temperature, but unsuitable for deep bottom-hole temperature wells. In this work there

was provision of starches for the well-drilling industries which can operate for extended periods of time at elevated temperatures.

1.5 Scope of Study

The following were the limits for the study:

(i) Extraction of Starch; Starches were extracted from three different corn grains including Guinea Corn (Sorghum Bicolor), Waxy Corn (Zea Mays), and Popcorn (Zea Mays Averta) and Millet (Panicum Miliaceum) which were obtained locally.

(ii) Blending and Pre-gelatinization of the starches; The extracted starches were blended with one another to obtain six blends of starches and pre-gelatinized using extrusion technique without the use of any solvent or chemical in a machine called Extruder**.** Three already existing or widely used starches were also provided.

(iii) Provision of Biodegradable Polymer Drilling Muds; In one of the concepts of this study, several novel biodegradable polymer drilling muds containing each of the novel blends of starches were formulated and prepared.

(iv) Provision of three already existing or widely used Drilling Muds; In another concept, there was provision of three already existing or widely used drilling muds containing respectively the three already-existing starches for comparisons.

(v) Characterization of the Filtration properties of the various polymer muds were carried out and compared at the starch concentration of 0.01- 0.05g/ml and temperature range 25 ^{o}C-450^{o}C using a slurry filtration apparatus called standard filter press unit. The filtration properties included fluid loss (filter loss) behaviour, rate of filtration, fluid sorptivity and fluid diffusivity.

(vi) Determination of the Thermal Stability of the various drilling muds containing the various blends of starches was done by using the system of hot rolling treatment in an oven at elevated temperatures of 150 ^{o}C, 250 ^{o}C, 350 ^{o}C and 450 ^{o}C.

(vii) Characterization of the rheological properties of the various polymer muds were carried out and compared at the starch concentration of 0.01-0.05g/ml using Brookfield viscometer. The rheological properties determined included shear stress, viscosity, flow index, consistency index and yield stress.

(viii) The Biodegradability properties of the muds were determined and there was soil culturing to know the specific micro-organisms responsible for the biodegradation.

(ix) The effects of the biodegradation products from the new blends

of starches on the growth of plants were determined and compared to those of the already existing starches. The plants used were okra, wheat, soyabean and cucumber.

(x) The experimental results obtained from filtration and rheological tests on the new muds were modelled using Matlab softwar

CHAPTER TWO

LITERATURE REVIEW

2.1 Definition and Composition of Drilling Muds

Drilling mud is a suspension of solids in water or oil, or droplets of one of these liquids dispersed in the other (Bernu, 2012; Jack, 2008; Chris & James, 2005; Chilingarian & Varabutre, 2000; Andy et al., 2000). In actual drilling operations, various requirements are met through the quality and composition of drilling muds. The geological conditions of the well sites are also considered while formulating a particular mud (Jann et al, 2007). The continuous phase of any drilling mud may be gas, water or oil. But each of these phases give further divisions based on the composition or chemistry of the mud and the dispersed materials.

Most drilling muds in use today have water as their base and are referred to as water-based muds. These muds are composed of three phase systems (Chilingarian and Varabutre, 2000) viz: (i) water- the liquid phase (ii) active solids – substance that readily swell in water giving viscosity to the mud and designated as hydrophilic e.g. clay like Bentonite, polymers (iii) Inert solids- solids that do not hydrate or do not swell in water and are designated as hydrophobic e.g. Barium sulphate ($BaSO_4$) used for increasing density, sand, shales and so on. The mud Engineers' major concern is on the properties and qualities of the colloidal portion (active solids) of the muds. This is the portion that can be altered by the addition of clays and other chemicals for the desired composition and quality of the muds (Don & Benze, 2002; Mecktor et al., 2008). Bentonite clay and some other organic polymer have been in use for this colloidal portion of the muds. Bentonite is a high colloidal plastic clay which swells to several times its original volume when placed in water and forms thixotropic gels at smaller concentration and composed of montmorillonite clay minerals (Austin &

Christopher, 2008; Vincent & Iyklema, 2005; Velde, 1999; Grim, 1998). It is a viscosity – builder in drilling muds, used by various establishments all over the world. Clay deposits with an estimated reserve of over one billion metric tons have been discovered in Nigeria (Jimo, 2001) with different clay minerals. On the other hand, some organic polymers have strong affinity for water and develop high swollen gels in low concentrations. Thus, they serve a number of useful purposes in drilling muds. The most important of these purposes are to improve viscosity and control filtration of the muds. Some are strongly absorbed by clay particles and offer protection from contaminants by flocculation (Jimo, 2001). One of the most critical roles of this mud is as a lubricant. Drilling generates tremendous friction, which can damage the drill or the formation being drilled. Drilling mud cuts down on the friction, lowering the heat of drilling and reducing the risk of friction-related complications (Chilingarian & Varabutre, 2000). The mud also acts as a carrier for the materials being drilled, with material becoming suspended in the mud and then being carried up the drill to the surface. Using this substance protects the stability of a borehole by controlling variables such as friction and pressure. Different muds are needed for different circumstances, and the selection and formulation of mud is managed by a mud engineer. This engineer determines the correct viscosity level for the mud, and adjusts factors such as its density as well. Water, oil, and gas-based muds can all be used, with products ranging from true mud made with materials like biodegradable polymers to synthetic drilling muds. Drilling mud is recirculated throughout the drilling process. As it rises to the surface, it passes through screens that trap the materials from the borehole, before being cycled back into the system that delivers mud to the head of the drill bit (Fordham et al., 2001). This recirculation process is designed to cut down on waste by reusing as much mud as possible. Depending on the

materials being drilled, several screens may be needed to trap the materials, and sometimes the materials themselves are also coated in mud, which means that they will need to be cleaned even after filtration.

Petroleum drilling is the primordial step in the success of oilfield exploration. This success is based, on the one hand, on the important details derived from geological drilled formations mid, on the other hand, on the good drill-in reservoir conditions. Thus, the paramount drilling objective are to reach the target safely in the shortest possible time and at the lowest possible cost, with required additional sampling and evaluation constraints dictated by the particular application (Friedheim et al., 1999). Drilling the wellbore is the first and the most expensive step in the oil and gas industry.

Expenditures for drilling represent 25% of the total oilfield exploitation cost and are concentrated mostly in exploration and development of well drilling. In the 90s, drilling operations represented about $10S billions compared with $452 billions the total cost of US petroleum industry exploration and production (American Petroleum Institute, 1991). Drilling fluids, which represent till one fifth (15 to 18%) of the total cost of well petroleum drilling, must generally comply with three important requirements: they should be (i) easy to use, (ii) not too expensive,
(iii) environmentally-friendly (American Petroleum Institute API, 1991). The complex drilling fluids play several functions simultaneously. They are intended to clean the well, hold the cuttings in suspension, prevent caving, ensure the tightness of the well wall, flood diesel oil or water and form an impermeable cake near the wellbore area (Sorheim et al., 2000). Moreover, they also have to cool and lubricate the tool, transfer the hydraulic power and carry information about the nature of the

drilled formation by raising the cuttings from the bottom to the surface. Drilling fluids went through major technological evolution, since the first operations performed in the US, using a simple mixture of water and clays, to complex mixtures of various specific organic and inorganic products used nowadays to improve fluid rheological properties and filtration capability, and penetrate into the heterogeneous geological formations under the best conditions.

2.2 Classification of Drilling Muds

Drilling muds are classified according to the nature of the continuous phase. The continuous phase may be water or oil, but each broad classification has sub-divisions based on composition or chemistry of the mud or other dispersed phases (Chris & James, 2005; Bourgoyne,1996). The complexity of the problems met in petroleum drilling has led to emerging techniques for the formulation of appropriate fluids. Generally, drilling muds may be classified in the following three families: (i) Oil-Based Mud, (ii) Water-Based Mud, (iii) Gas-Aerated Mud (Chris & James, 2005; Amanullah& Long, 2004; Young & Maas, 2001; Chilingarian & Varabutre, 2000; Bland et al., 2003).

2.2.1 Oil- Based Muds (OBM)

Oil-Based Muds (OBM) are muds that have oil as the continuous phase (Bland, 2005; Chris and James, 2005; Salisbury & Deem, 1990). Example of such muds include synthetic oil-based muds containing ester base oil, synthetic oil-based muds or pseudo oil-based muds containing linear alpha olefins (LAO), isomerized olefins (IO), n-paraffin or polyalpha olefins (PAO) base oils and so on (Chris and James, 2005; Ghazi et al., 2008; Gieve, 1998; Saiers & Hornberger, 1999). The components of oil-based muds are:

- Oil which is the continuous phase that may be refined or crude
- Organophilic materials (surfactants) which induce viscosity and give body to the mud.
- Inert products which generally do not dissolve in oil, e.g. barite, sand.

Oil –Based Muds (OBM) are useful in drilling high temperature wells where water-based mud systems may be unstable or where problems may arise from water-sensitive shale formations or where corrosive gases such as hydrogen sulphide and carbon (IV) oxide may be encountered (Cambel et al., 2007; Serada & Solovyor , 2003; Skalli et al., 2006). Although oil-based muds have this great use, cost and environmental restriction limit their use.

The Oil-Based Mud (OBM) family is less used (5-10%). These drilling fluids have been developed for situations where Water-Based Mud was found inadequate (Young and Maas, 2001; Abrams, 2000). The OBM are oil- (usually, gas oil-) based muds. Generally, they are invert emulsions of brine into an oil major, continuous phase stabilized by surfactants (Caleb & Dan, 2004; Hans et al., 2003). Also, other additives are often added to the organic phase, such as organophilic modifiers of the clay surface. However, although OBM often give better performances, they have major drawbacks such as more expensive and less ecologically friendly than WBM. Although OBM give greater shale stability than WBM (Bland, 2002), these latter systems have also been developed by many researchers in order to respond to environmental regulations (Simpson et al., 1994; Friedheim et al., 1999; Young and Maas, 2001; Patel et al., 2001; Schlemmer et al., 2002).

2.2.2 Water–Based Muds (WBM)

Water-based muds are typically suspensions of bentonite clay (largely sodium or calcium montmorillonite), polymers, and surfactants to which further minerals usually barites are added to optimize the rheology and other properties for a particular application (Gautier & Lecourtier, 2001; Rogers, 1991; Gray & Darley, 1990).

Water-based muds are also muds whose continuous phase is water (Amani, 2012; Argillier et al., 2001; Chenevert & Pernot, 1998; Cliffe et al., 2005). The WBM family, in which fresh-, salt-, or sea-water is the continuous phase, is the most used 90-95% (Khodja et al., 2010; Qartar & Giacelo, 2010). The WBM are mainly composed of aqueous solutions of polymers and clays in water or brines, with different types of additives incorporated to the aqueous solution.

2.2.2.1 Components of Water-Based Muds

Water-based muds basically consist of four distinct components viz: Water – water is the base and major component by volume, which may contain emulsified oil (i.e., emulsion of oil in water), Active colloids – clays and polymers constitute the colloidal system that gives viscosity and body to the muds. The clays are either deliberately added or from formation e.g. natural clays of organic colloids and soluble products in excess, Inert solid – these are weighting materials or drilled out solid contaminants e.g. Barite /Barium sulphate [$BaSO_4$], Haematite [$Fe2SO_3$], ilmenite, sand, dolomites, etc.**,** Additives / chemicals – e.g. surfactants (Gautier and Lecourtier, 2001; Alderman et al, 2008). The proportions of the various components and interactions among them lead to the diversed and varied properties of the muds (Chris & James, 2005).

2.2.2.1.1 Water

Water is the continuous phase for water-based muds. The water may be fresh, hard or salty. Water provides the initial viscosity which depends on the temperature and the dissolved salt's concentration. This viscosity of water can be modified to obtain any desirable rheological properties (Chris & James, 2005). As the temperature of water increases, the volume also increases, resulting in lower molecular friction and consequently, a higher flow rate (Chris & James, 2005; Gautier & Lecourtier, 2001; Reid et al., 1993).

Water cools the bit and reduces the friction on the surfaces of the drilling shaft better than other liquids. At a sufficiently high flow rate, it can very effectively remove the drilled-out rock cuttings from the bottom hole of the well-bore (Chris & James, 2005; Downs et al., 1993). Water is satisfactorily cleared from fragments of the drilled-out cuttings even in comparatively simple water settling system since it is devoid of thixotropic properties.

Water exerts less pressure on the bottom hole face. It penetrates freely the micro-fractures in the rocks, prevents closure of the later and then facilitates breaking up the face with the bit. Therefore, with water-based muds, the breakdown speed, while flushing out the rock cuttings is higher than those of other muds (oil- based muds) under review (Chris & James, 2005; Gautier & Lecourtier, 2001; Carl, 1990). Moderate viscosity of water helps it to gain access into the minutest pores of the unstable rocks, which accelerates their deformation and caving. Water also acts as a medium for transferring the surface hydraulic horsepower to the bit on the bottom of the well (Chris & James, 2005; Fordham et al., 2001; Stamatakis et al., 1995).

2.2.2.1.2 Active Colloids

In water –based muds, active colloids are added to increase viscosity, gel strength, yield point, and density (Chimere, 2011; Fordham et al, 2001). The colloids also decrease fluid loss of the muds. The main substances that serve as colloids for muds are clays and polymers. These materials are soluble in water and form gel so as to build up the viscosity of the muds. According to Katchy, a polymer is a large or giant molecule or macro- molecule formed by an almost endless repetition of smaller units called monomers (Katchy, 2000). If only one specie of monomer is used to build up the macromolecule, the product is a homopolymer, but if two species are used, a copolymer is produced (Katchy, 2000; Lamberti, 1999).

Polymers posses more viscous and gel-strength properties than any other drilling mud constituent. Besides clays, polymers are used in the formulation of muds to reduce the fluid loss and to control the flow of fluids. Another advantage of using polymers is that these organic substances can impart maximum viscosity at a minimum solid content (Enie & Giles, 2001). The emergence of degradable, high performance polymers was a major reason behind the success of water –based muds over oil-based muds (Eyler & Pastecck, 2005; Enie & Giles, 2001; Alderman et al., 2008). One of the past developments that appeared to offer significant advantage was the use of cationic polymer species. Present day water – based mud technology is based on anionic polymer ranging from carboxy methyl starch, hydroxyl propyl starch, carboxy methyl cellulose to poly-acrylamide (Jones, 2006).

Clays are chemically active electrolyte-solid systems (Rashid, 1999; Van, 1997; Sibel & Tuncan, 1991). Their macrofabric and physicochemical forces determine much of their physical and chemical properties, and subsequent mechanical behaviour. Clay

minerals belong to a class of crystalline material that is uniquely layered in plate-like structures (Partheniades, 2000; Sibel & Tuncan, 1991; Behker et al., 2000; Faniran & Areola, 2000). Clays are classified as Hydrous Aluminium Silicates (phyllosilicates), and the particles are usually less than two micrometer (>2 μm) in size (Van-Oort et al., 1996; Roy & Dzombak, 1996; Van-Oort et al., 1999; Hans, 1990; Jones et al., 1996.). The very common clay minerals which are used in drilling muds are kaolinites, Bentonites (smectites) and illites. Details of clay mineralogy and classification have been given by Grim and Mitchel (Audibert & Dalmazzone, 2006; Baghdikian et al., 2000; Muniz et al., 2004; Grim, 1998). Bentonite is the most commonly used clay mineral because of its superior ability to swell uniformly in fresh water upon shear application, resulting in a more homogeneous clay- water mixture.

Clays used in water- based muds have two different sources, (Parkson et al, 2000; Partheniades, 2000; Saddok et al.,, 1997; Bailey et al., 1994): viz

-Commercial clays: these are clays added purposely to impart rheological properties and to control fluid loss.

-Natural clays: these are clays encountered while drilling through various argillaceous formations. The clays are incorporated into the muds as drilling continues. Selected characteristics of the common clay particles are also taken into consideration. The size, shape, specific gravity, specific surface and cation Exchange capacity (CEC) are important properties of the clay minerals that are needed in clay microstructure and flow interaction behavior (Bergaya et al., 2006; Parkson et al., 2000; Partheniades, 2000). For intance, flocculation and setting velocity are affected by the shape, size, specific gravity, CEC and specific surface of the interacting particles (Parkson et al, 2000; Partheniades, 2000; Sibel and Tuncan, 1991).

2.2.2.1.3 Inert Solids

Inert solids are materials or substances that add weight to the muds (Nair, 2004; Hans, 1990). At times, drilled-out solid contaminants can serve as inert solids. The final weight and the type of mud desired determine the particular inert solids to be used. The inert solids or weighting materials must be of high specific gravity, ground to an optimum particle size distribution, and not be reactive with the continuous phase of the muds (Piltinitakis et al., 2002; Rosana et al., 2000; Ogden et al., 1991). Barium sulphate (Barite, $BaSO_4$) meets all these requirements and it is used for increasing the density of muds throughout the world (Daniel, 1990) because of its high specific gravity. It is fairly soft and non abrasive, inert in both water and oil. It is generally available in adequate quantities of satisfactory purity and economical in use.

Alternative inert materials with higher specific gravities exist. These include ilmenite, Galena, Haematite (Fe_2SO_4), which can be used to prepare extremely heavy muds that are sometimes needed to control abnormally high formation pressures(Durant et al., 2005).

2.2.2.1.4 Chemical Additives

The component often added to influence the properties of drilling muds are called chemical additives (Mayes, 2003; Dons & Billy, 2001; Debussy, 1992). They include thinners and conditioners typically low molecular weight anionic polyelectrolyte, they are designed to reduce the sensitivity of muds' properties to factors such as pH and temperatures. Other minor additives, both organic and inorganic will invariably be present to influence, amongst other things, the continuous phase, viscosity, and the interactions of the muds and the rocks (Mecktor et al., 2008; Roberts et al., 2005; Robert, 2002).

2.2.2.2 The Mixture of Clay and Water

The mixture formed by clay and water has attracted much attention from scientists of clay research because of its agricultural, economic and industrial importance (Labby, 2001; Mecktor, 2008; Fritz & Marine, 1993; Locher, 1992). The physical and chemical properties of clay and associated process are intimately related to the interaction between the clay particles and water molecules (Ruehrwein & Ward, 2002; Dollimore & Horridge, 1993). Moreover, clay minerals on account of their electro-chemical and structural properties offer a high degree of complexity, and have been studied previously (Jilani et al., 2002; Velde, 1999; Van-Oort, 1994). For instance, absorption of water molecules by colloidal clay particle surfaces is known to be a function of the nature of the mineral surface and the associated exchangeable cations (Ruehrwein & Ward, 2002; Paulsen, 2001).

Also, when increasing amount of water is added to dry clay powder, a typical sequence of rheological conditions or consistency is normally traversed (Grolimund et al., 2001). Three principal changes can be distinguished according to Houwink and Dedecker (Balser et al., 1996; Houwink & Dedecker, 1991). In the first stage, clay particles aggregate to form crumbs or a mass that crumbles when it is deformed. The mass behaves more or less like brittle solids. In the second stage, the mass will sustain large deformation without rupturing. After removal on the stress, the mass retains its deformed shape, that is, it behaves like a plastic solid. In the third stage, the mass is so easily deformed that it cannot retain its shape against the forces of gravity or gentle shaking. At this point, it behaves like a liquid.

Finally, viscosity of colloidal clay suspensions gives valuable information about the influence of the clay particles upon the structure of the absorbed water (Quintero,

2002; Valentine, 1997; Raymond & Benco, 1992). The viscosity of a liquid refers to the internal friction between the molecules of the liquid (Civan, 2001; Theng, 1999; Schamp & Huylebroeck, 1993; Clark & Saddok, 1991). In a colloidal suspension, friction takes place between the particles and the molecules of the dispersing medium, which is water in hydrated colloidal system.

2.2.3 Gas Aerated Mud

The third family of drilling fluids comprises gas, aerated muds (classical muds with nitrogen) or aqueous foams (Coussot et al., 2004). These drilling fluids are used when their pressure is lower than that exerted by the petroleum located in the pores of the rock formation.These fluids are called underbalanced fluids. This underbalanced drilling technology is generally adopted for poorly consolidated and/or fractured formations (Indigo, 2009; Khodja et al., 2005; Lomba et al., 2000; Bennion & Thomas, 1994). Controlled drilling rate tests in various rocks have confirmed that air or gas is a faster drilling fluid than water or oil. Water should be the fastest drilling fluid's base, however, in this case, drilling tests show that the most commonly used additives have detrimental effects on the drilling rate (Modv & Tale, 1993). Choosing a mud system begins with the selection of a mud family, according to the nature of the rock formation, and should take into account environmental and economic constraints. The choice of the mud formulation will be the second step, where one has to decide on the range of desired properties, leading to use minimum amounts of additives.

2.3 Polymers used in Drilling Muds

A number of polymers are used in preparing drilling muds. Some polymers are used for oil-based muds while others are suitable for water-based muds (Chimere, 2011; Ukachukwu et al., 2010; Cisco & Whistler, 2008). The choice of a particular polymer

for a particular type of mud depends on the desired properties and qualities of the muds. Another factor to be considered in the choice of a polymer for a mud, is the ability of the polymer to interact well with the continuous phase or base of the mud (Robert & Bell, 2011; Longey, 2006; DeNooy et al, 2002). For instance, polymers for water-base muds should be soluble in water before they will be able to build up the viscosity of the mud and to control fluid loss. Cationic and non-degradable polymers have been in use for especially oil-based mud since the past years (Zhang et al., 2004; Ward et al., 1997). Present day water –based muds are prepared with anionic and degradable polymers like hydroxyl propyl starch, carboxy methyl starch, carboxy methyl cellulose, partially hydrolysed polyacrylamide, and others (Obong, 2004).

The diversity in composition and properties of polymers used in muds preparation requires an examination of the factors involved in the selection of the product for a specific application. Among the factors, that affect the performances of substances used in formulating drilling muds, are shear conditions, temperature, dissolved salts, pH conditions, and so on (Robert and Bell, 2011; Wilcox & Hool, 2010; Wikky, 2008; Van-Oort, 2003).

2.3.1 Natural and Biodegradable Polymers used for Muds

The development of natural or green polymers from plants or crop has presently been a success (Clever et al., 2012; Gronski & Hellmann, 2003). Some naturally occurring polymers are now made available through the use of biotechnology on some crops like corn (Sevens, 2002). Examples of naturally- occurring polymers that are developed from corn and other plants include starch, poly (lactic acid) (PLA), Polyhydroxy alkanoates (PHA), xanthan Gum, Guar Gum, etc (Clever et al., 2012; Gronski & Hellmann, 2003; Sevens, 2002).

Biodegradable polymers are used in the preparation of drilling muds (Clever et al., 2012; Ukachukwu et al., 2010; Eyler & Pastecck, 2005; Scott et al., 2007; Gronski & Hellmann, 2003; Sevens, 2002). However, most polymers are not biodegradable. Polymers, like polyamides, polycarbonates, polyfluoro carbons, polyethylene, polypropylene, are highly resistant to microbial attack (Jeffrey, 2007; Marck & Hercules, 2004; Giavasis et al., 2002). Some synthetic polymers like polyurethanes (especially polyether-polyurethanes) are susceptible to biological degradation (Joel et al., 2006). Generally, many naturally-occurring polymers (Green polymers) are more biodegradable than synthetic polymers (Gronski & Hellmann, 2003; Fried, 2000). More specifically, polymers containing ester linkages particularly aliphatic polyesters are potentially biodegradable. It is believed that biodegradation of these polymers proceeds by attack of the ester groups by nonspecific esterases produced by ground microflora combined with hydrolytic attack. Products of the degradation can be quickly metabolized by micro-organisms (Scott et al., 2007; Gronski & Hellmann, 2003; Fried, 2000).

One commercially important group of biodegradable polymers is the naturally-occurring polyesters, the poly (β-hydroxy alkanoates) (Cambel et al., 2007; Lenz, 1993). These polyhydroxy alkanoates have commercial potential as biomaterials due to their biodegradability. Originally identified in 1925, poly (β-hydroxy-butyrate, PHB) is synthesized by the bacterium *alcaligenes eutrophus* (Fried, 2000; Lenz, 1993), which uses globules of PHB as energy – storage medium analogous to fat in animals or starch in plants. The polymer is accumulated in discrete membrane bound granules in the cytoplasm of the bacterium. The thermal decomposition temperature of this polymer is 200^{o}C (Fried, 2000). Poly (β-hydroxy-valerate, PHV) can be

produced by *A-eutrophus* as well as another bacterium *P. Oleovorans* depending upon the type of carbon substrates available during the fermentation process (Fried, 2000). Another important biodegradable polyester is poly (lactic acid) (PLA), which is polymerized through the self- condensation of lactic acid (Mario & Mark, 2003). The lactic acid is obtained by the fermentation of potato waste (Bada, 2005).

The relatively high cost of these biodegradable polymers may be reduced by larger scale production and advances in biotechnology (Sevens, 2002; Feiffer & Vierty, 2002; Enie & Giles, 2001; Gautier & Lecourtier, 2001). For example, the gene that synthesizes PHB has been recently identified and it should therefore be possible to produce these polyesters in higher- productivity bacteria such as *E. coli* or even crops such as potatoes or tunnips (Bada, 2005; Mario & Mark, 2003; Lenz, 1993).

2.3.1.1 Starch

Starch is a polymer of anhydroglucose units with alpha- 1, 4 (α- 1, 4) linkages (Adrian & Gareth, 2009; Casmir et al., 2007; Herman et al., 2002; Fischer,2002; Glinel et al., 2000; Swanson et al., 1993). Starch is the second most abundant biomass found in nature, next to cellulose (Cyracus, 2012, Bernu, 2011; Rolly, 2012; Ukachukwu et al, 2010; Amanullah & Long, 2004; Heinze, 2005; Heinze & Liebert, 2001). Specifically, crop grains like corns, millet, wheat, are the major sources of starch used industrially. The grains are processed into granules ranging from 2 to 50 microns in diameter (Cyracus, 2012; Gronski & Hellmann, 2003; Swanson, 1993). Starch consists of two major components. Chemically, it contains amylose linear polymer with a molecular weight in the range of 100,000 – 500,000kg/mol and amylopectin highly branched polymer with a molecular weight in the range of 1-2 million g/mol. Physically, it has both amorphous and crystalline regions (Cyracus, 2012, Bernu, 2011; Amanullah & Long, 2004). The short branch chains in the amylopectin are the main crystalline

component in granular starch. The relative ratios of amylose and amylopectin vary depending on the origin and nature of the starch. Variation in the amount of amylose and amylopectin in a starch changes the behaviour of the starch. The amylose component of starch controls the gelling behaviour since gelling is the result of re-association of the linear chain molecules. Amylopectin is usually larger in size. The large size and the branched nature of amylopectin reduce the mobility of the polymer and their orientation in an aqueous environment (Whistler et al., 2007; Amanullah & Long, 2004). The abundance of hydroxyl groups in the starch molecules impart hydrophilic properties to the polymer and thus its potential to disperse in water.

Starch in its raw form is not soluble in aqueous solution (Cliff & Gerald, 2010; Amani, 2010). It simply floats around as granular particles. This granular starch is not suitable as mud's constituent. Therefore, to prepare an effective starch-polymer mud, it is very necessary to rupture the protective shell of amylopectin in order to release the inner amylase. This is done by rupturing the cells of the starch granules through a process known as pregelatinzation (Jones, 2006; Swanson, 1993). The starch then becomes hydrophilic. That is to make starch soluble in water, the outside amylopectin shell is ruptured by heat, liberating the amylose inside which absorbs water and swells to form gel. The gelling capacity of starch enables it to form sponge-like bags called filter cake in drilling mud which helps to reduce fluid loss by a plugging action. Therefore, for mud and most applications, starch must be made soluble or dispersible in solution by cooking it in water until the granules swell and rupture (Ebewele, 2000). This is known as pre-gelatinization. Such aqueous dispersion of starch is extremely viscous. In order to reduce the viscosity of such dispersion, starch must be modified through processes that involve partial depolymerization or re-arrangement of molecules (Fried, 2000). To effect this conversion, starch must be subjected to

hydrolytic, oxidative, or thermal processes (Ebewele, 2000). All these processes involve the use of solvents and other chemicals. Conversion processes cause weakening and solubilization of starch granules, resulting in products that are more readily dispersible in solution. For instance, thin boiling starches (acid converted starches) are produced by reactions of granular starch with warm mineral acids such as HCl or H_2SO_4 (Amani, 2010; Ebewele, 2000; Fried, 2000). Oxidized starches are made by the reaction of starch with sodium hypochlorite. These reactions introduce carbonyl and carboxyl groups and cleave the glycosidic linkages. Dextrins are degradation products of starch produced by heating starch in the presence of hydrolytic agents (Ebewele, 2000). This conversion process for dextrins is complex, but is thought to involve hydrolytic breakdown of starch molecules into smaller fragments followed by their re-arrangement/ repolymerization into a branched polymer structure.

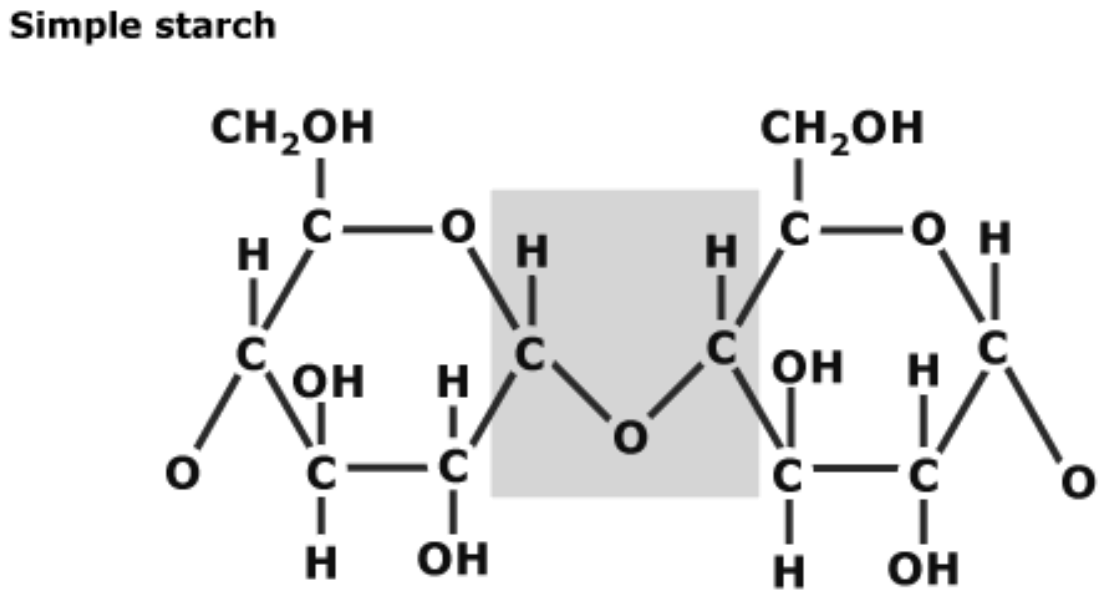

Figure 2.1 (a): Simsple Starch Structure (Cyracus, 2012; Jones, 2006; Kenie & Stan, 2010)

Starch is nonionic and when pre-gelatinized becomes soluble in both saturated salty water and fresh water (Austin & Christopher, 2008; Bill & Mark, 2007; Ebewele, 2000). It is not expensive and is readily available. Starch is totally biodegradable and serves as a viscosity builder and used to reduce fluid loss in drilling muds (Bernu, 2011; Ukachukwu et al., 2010; Jill & Poka, 2003). Corn-starch retains about 6% to 20% moisture but is thermally stable up to 250^{o}C temperature or above with some modifications (Bernu, 2011). The structures of starch components are given below:

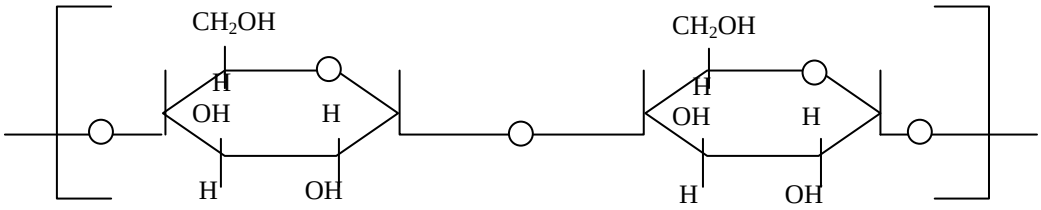

Figure 2.1 (b): Linear amylose

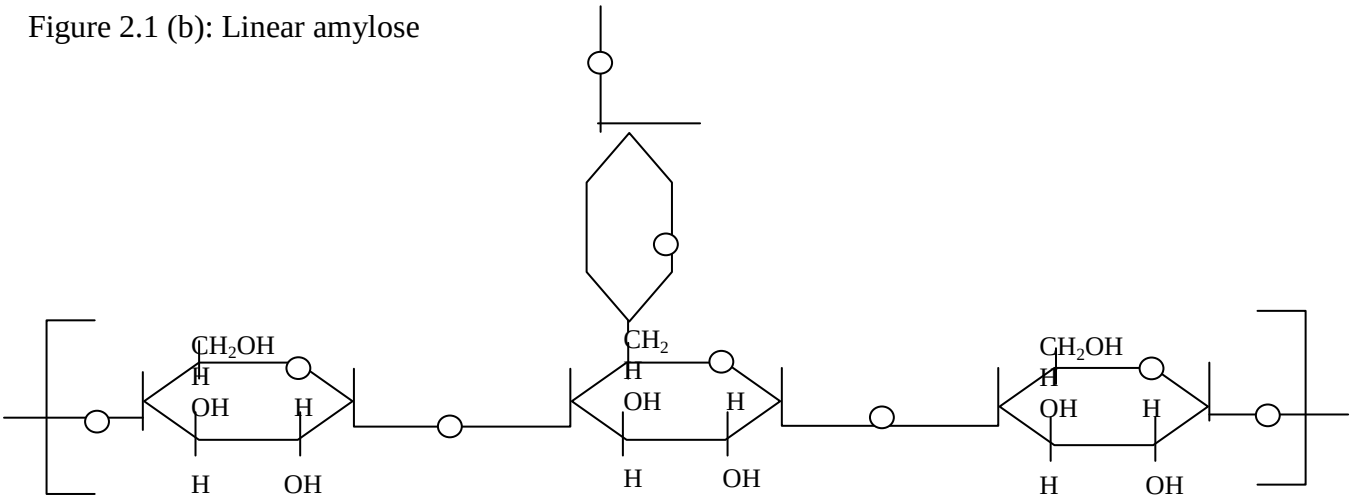

Figure 2.1 (c): Branched amylopectin

(Bernu, 2011; Kenie & Stan, 2010; Dahlgreen & Helbig, 2008; Linus, 2002; Amanullah & Long, 2004; Timmerman & Dakota, 2000).

The range of industrial applications for starch is enormous (Whistler et al., 2007). The uses of these water-soluble polysaccharide polymers are dependent on their wide range of functional properties. One of the main importances in the characteristics of starch is its ability to modify the properties of the polar solvents that it is dissolved into by thickening, stabilizing, swelling, forming suspension or to form gels (Albert & Mark, 2001). These properties have led to applications for starch ranging from thickeners in foods, explosives, polishes, blends with synthetic polymers to obtain fluid loss reduction in drilling muds (Albert & Mark, 2001). Starches are natural polymers from renewable resources and their physical and chemical properties such as biocompatibility, biodegradability, and nontoxicity have led to their increasing exploitation as commercial materials (Bernu, 2011; Jax, 2010; Andrew & Robert, 2007; Ben & Joe, 2006; Glinel et al., 2000; Carriere, 2009).

Starches are subject to bacterial attack unless protected by high salinity or bactericide. Drilling-grade natural starch has API/ISO specifications for quality (API, 2003; American Petroleum Institute, 1993). Starches are carbohydrates of a general formula $(C_6H_{10}O_5)_n$ and are derived from corn, wheat, oats, rice, potatoes, yucca millet and similar plants and vegetables (Clement & Bona, 2009; Van-Oort et al, 2001). The two starch components namely linear polymer (amylose) and branched polymer (amylopectin) are intertwined within starch granules. Granules are insoluble in cold water, but soaking in hot water or under steam pressure or by the use of chemicals ruptures their covering and the polymers hydrate into a colloidal suspension (Cliff & Gerald, 2010; Clement & Bona, 2009). This product is a pregelatinized starch and has been used in muds for many years. Amylose and amylopectin are nonionic polymers that do not interact with electrolytes. Amylose section of starch is responsible for the gelling function, while amylopectin reduces polymers movements and profusion in

hydroxyl assemblies within the starch molecules and expresses hydrophilic property of the polymers and therefore makes it possible to dissolve in water. Starch is typically applied in drilling fluids technology by customized forms because of its solubility in water. They are principally applied to diminish the filtration of virtually all types of water based drilling fluids, owing to their swelling ability. This swelling assortment diminishes muds permeability, decreases the mud filtering ability and hence causing fluid loss on borehole areas (Clement & Bona, 2009). There is an opportunity of filtration management by appropriate consumption of starch ingredients and their combination with polymers and bentonite. Among the most commonly used filtration control agents reported are biopolymers, synthetic polymers and sodium bentonite. A fluid loss phenomenum occurs when a superior hydrostatic force applies to mud formation (Van-Ort et al., 2001). The leakage of fluid may present multiple drilling tribulations such as structure destruction and stuck pipe. Therefore, by applying a fluid loss control agent (also known as filtrate reducing additives), tendency of drilling mud fluid loss will be diminished. A study by Chin revealed that incorporating particles into the mud system has a significant role in preventing fluid loss.

Derivatized starches, such as hydroxypropyl and carboxymethyl starches are used in drill-in fluids, completion fluids and various brine systems as well as in drilling-mud systems. The use of starch typically causes an increase in viscosity while effectively controlling fluid loss. Some of newly developed local starch products (with high amylose content and high water absorption capacity) have similar or better filtration control properties than the filtration control properties of a widely used imported starch (Clement & Bona, 2009).

2.3.1.2 Guar Gum

Guar gum is a non-ionic, branched-chain polysaccharide (a Galactomanan) (Christopher & Perlin, 2010; Candy & Justus, 2006; Mario, 2003; Dakky & Gronski, 2000). Guar gum is also a naturally occurring polymer obtained from *cyamopsis tetragonologus* (Michael, 2009; Gronski & Hellmann, 2003; Sevens, 2002), whose straight chain has a galactose branch. It produces viscous solutions in either fresh or salty water at a concentration of 3 – 6kg/m^3, and is very effective as drag-reducing agent (Jeffrey, 2007; Eyler & Pasteck, 2005). The gum is used in formulating low solid muds. It helps in reducing fluid loss and improving hole stability (Sevens, 2002). The gum degrades rapidly when the temperature is above 150^{o}C, and this limits its application to shallow well bores (Feiffer & Vierty, 2002; Gautier & Lecourtier, 2001). Its effect on viscosity decreases with rise in temperature. The structures of Guar Gum are shown below:

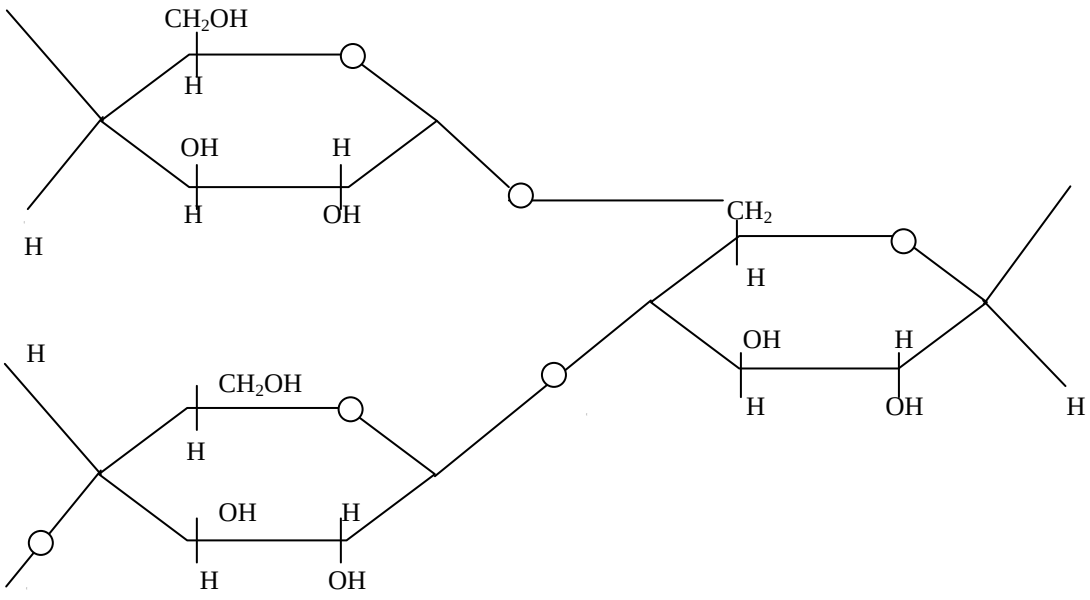

Figure 2.2 (a) Schematic Structure of Guar Gum (Candy & Justus, 2006)

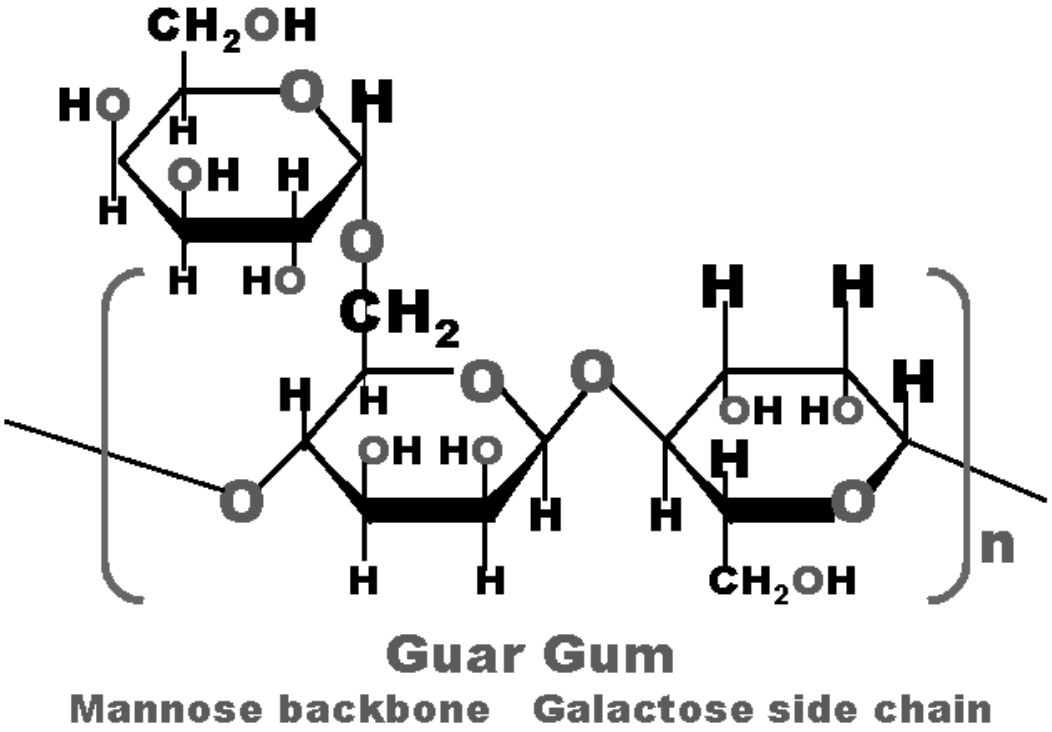

Figure 2.2 (b): Simple Structure of Gur Gum (Michael, 2009; Feiffer & Vierty, 2002; Dakky & Gronski, 2000)

2.3.1.3 Carboxymethyl Starch [CMS]

Carboxymethyl starch is a starch derivative (Bertts & Jerry, 2012; Bill & Mark, 2007; Casmir et al., 2007; Zac et al., 2002; Bataille et al., 2000; Jones & Mark, 2006). Starch can be modified in a such away that it can posses some special properties which make it more suitable for drilling muds (Jason & Henry, 2004; Bataille et al., 2000). It is therefore necessary to impact into starch such properties as high temperature stability, good preservative capacity (if the drilling mud should be stored for a period of time).This modification is obtained by incorporating certain chemicals which will induce these desired properties without affecting the biodegradability of starch (Clement & Bona, 2009; Dickson & Philipp, 2006; Timmerman & Dakota, 2000). Carboxymethyl starch [CMS] is one of the derivatives of starch (Kelvin, 2011;

Cisco & Whistler, 2008; Linus, 2002).The carboxymethyl starch undergoes carboxylated substitution reaction at either the hydroxymethyl group or at either of the two hydroxyl groups on the ring structure. The substitution occurs most readily at the hydroxymethyl group like it happens in carboxymethyl cellulose. Carbonxymethyl starch controls fluid loss and gives high viscosity in most water-based drilling fluids (Kelvin, 2011; Jay & Bruce, 2005; Heinze & Liebert, 2001). It has a temperature stability similar to carboxymethyl cellulose which is up to 300^{o}F (149^{o}C) and it does not require a bactericide (Bertts & Jerry, 2012; Bill & Mark, 2007; Clement & Bona, 2009; Casmir et al, 2007; Dickson & Philipp, 2006; Zac et al., 2002; Bataille et al., 2000). It is compatible with all water-based systems and performs at any pH level. The structure of carboxymethyl starch is given below.

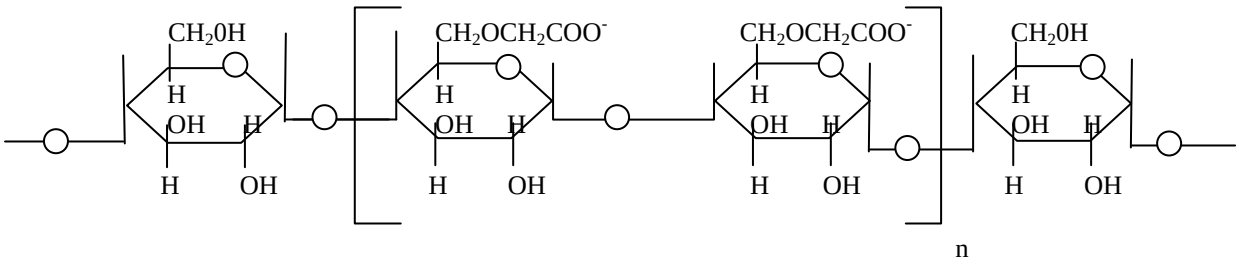

Figure 2.3: Structure of Carboxymethyl Starch

(Bertts & Jerry, 2012; Kelvin, 2011; Casmir et al., 2007; Zac et al., 2002; Bataille et al., 2000)

2.3.1.4 Hydroxypropyl Starch [HPS]

Hydroxypropyl starch is another modified starch derivative. It is produced by reacting starch with propylene oxide and the resulting modified starch is nonionic and is water-soluble (Rolly, 2012; Kelvin, 2011; Bernu, 2011; Rob et al., 2006; Wikky, 2008). Like in CMS, the substitution occurs at either the hydroxymethyl group or any of the two available hydroxyl groups on the ring structure (Rolly, 2012; Rob et.al,

2006). However, the hydroxymethyl group is the most reactive site where the substitution readily occurs. The result is a substitution of propoxylated groups. The degree of polymerization (DP) of the propoxylated groups is known as the Molar substitution [M.S] (Kelvin, 2011; Rob et.al, 2006; Fried 2000) which is the average number of propylene oxide molecules that have reacted with each starch unit. Many types of hydroxypropyl starch are available but their properties vary with the degree of polymerization. Hydroxy propyl starches are used primarily for fluid loss control (James, 2012). They are very compatible with calcium carbonate and are unlike poly acrylamide muds. The HP starch works in conjunction with calcium carbonate to remove acid-soluble filter cake. It has a unique viscosifying characteristic that makes it suitable for drilling muds. It is thermally stable to about 200^{o}C and does not need a bactericide (Wikky, 2008; Rob et.al, 2006). It is very compatible with most brines including sea water, NaCl, KCl, $CaCl_2$, NaBr and formate brines.

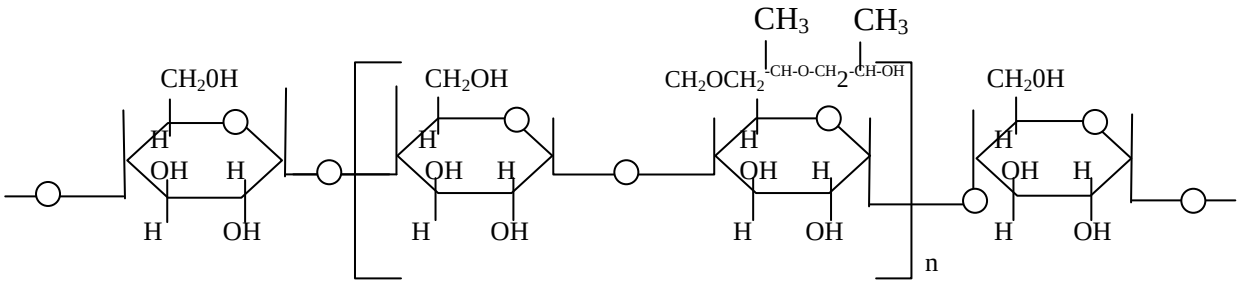

Figures 2.4: Structure of Hydroxy Propyl Starch

(Kelvin, 2011; Wikky, 2008; Rob et al, 2006)

2.3.1.5 Xanthan Gum

Xanthan Gum is a natural polymer produced by bacterial action (Marries, 2001). The bacterial Xanthamonas campestris produces the gum during its normal life cycle via a complex enzymatic process (Mario, 2003; Marries, 2001). It is water soluble, slightly anionic and highly branched. It has a molecular weight in the 2 to 3 million range

which is relatively high and good for drilling fluids (Marries, 2001). Xanthan gum is a five-ring respective structure consisting of a two-ring backbone which is made up of glucose residues identical in structure to cellulose and a three-ring side chains of additional sugar residue on which is attached various functional groups (carboxyl, carbonyl, hydroxyl and others) which give this xanthan gum its unique high viscosity properties (Christopher & Perlin, 2010). Under static conditions, xanthan polymer displays thixotropic characteristics providing gels. The concentration of xanthan molecules necessary to develop thixotropic properties depend on the make-up water. Only 0.5lb/bbl may be sufficient for a highly weighed fresh water system while it may take 2 to 3lb/bbl in a kCl or NaCl salinity system (Weir & Bailey, 2004; Marries, 2001; Sobie, 1994). In high salinity brines, xanthan polymer does not hydrate easily rather it remains coiled. In fresh water, the polymer expands and the branches form hydrogen bonding which results in the development of higher thixotropy (Weir and Bailey, 2004; Marries, 2001). Xanthan gum is a very good substitute for clay in the formulation of drilling muds (Marries, 2001). It is a great viscosity builder and a good suspending agent (Edmund & Hellmann, 2000). It easily develops gel strength and easily suspends acid-soluble material like $CaCO_3$, thereby giving maximum hole-cleaning (Edmund & Hellmann, 2000; Weir & Bailey, 2004). More specifically, it is totally biodegradable like starch.

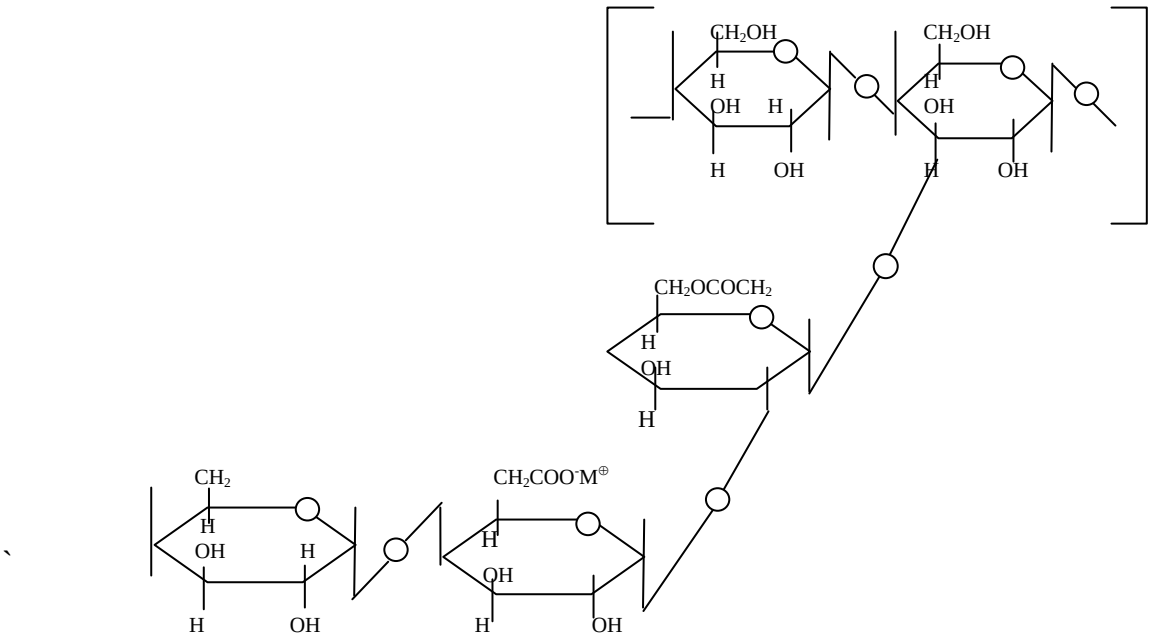

Figure 2.5 (a): Schematic Structure of Xanthan Gum

(Edmund & Hellmann, 2000; Weir & Bailey, 2004; Marries, 2001)

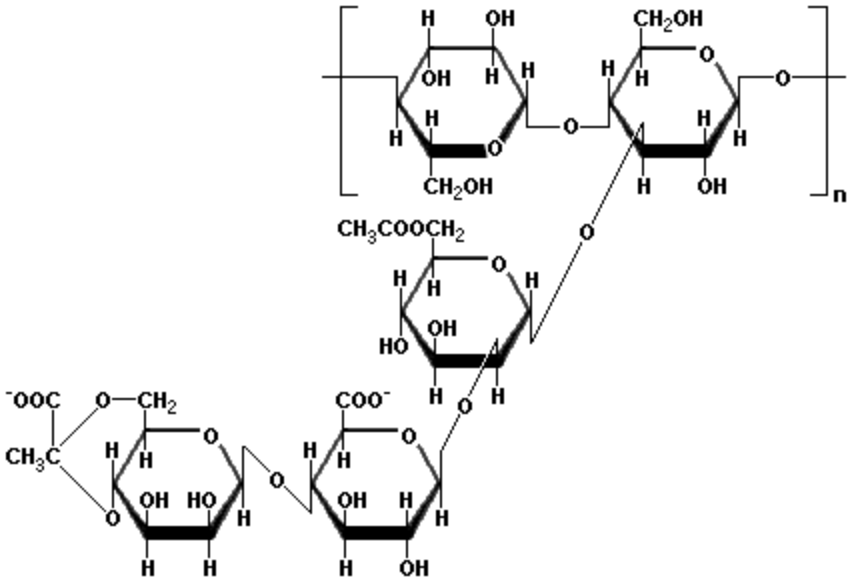

Figure 2.5 (b): Simple Structure of Xanthan Gum

(Edmund & Hellmann; Weir & Bailey, 2004)

Xanthan gum is an anionic polysaccharide polymer with high molecular weight generated after fermentation of xanthomonas campestris.

It has also emerged as a highly preferable drilling mud additive that helps in minimizing associated work problems. Basically, it is a polysaccharide and an immensely essential biological polymer that is made from carbohydrates (Edmund & Hellmann). Some of the most distinct properties of Xanthan Gum that makes it an ideal additive for drilling fluids include:

(i) It can be used as a stabilizer, a thickener, an emulsifier and a suspending agent for drilling fluids.

(ii) It can effectively enhance the viscosity of drilling mud or fluids as well as enhance shear force. Therefore, it is widely used in drilling fluids for the non solid phases, for workover fluids as well as completion fluids in order to restrict formation damage.

(iii) It is highly pH stable and heat stable too.

(iv) It possesses unique rheological properties. The viscosity of the drilling fluid decreases fast though shear action once the shearing ceases. Subsequently, the viscosity levels are restored within no time.

(v) It also possesses fairly strong anti oxidant as well as anti enzyme properties.

2.3.1.6 Cellulose

Cellulose is the most abundant, renewable polymer resource available worldwide. Haven been estimated that by photosynthesis, 1011-1012 tons are synthesized annually in a rather pure form, e.g. in the seed hairs of the cotton plant, but mostly are combined with lignin and other polysaccharides (so- called hemicelluloses) in the cell wall of wood plants (Caskey et al., 2004; Cisco & Whistler, 2008). Cellulose is a versatile starting material for chemical conversions, aiming at the production of artificial, cellulose derivative used in many areas of industry and domestic life. As

demand for oil and gas increases, so does the need for extremely economic techniques to recover these resources. The process of drilling must however be safe, cost effective and environmental friendly. One of the major challenges of the indigenous petroleum companies is the importation of mud additives or the drilling mud itself and this has not allowed them to compete favorably with foreign counterparts (Cole, 2004).

2.3.1.6.1 Occurrence and natural sources

The main source of cellulose is that of polysaccharides in different types of plants, often combined with other. The primary occurrence of cellulose is lignocellulosic materials found in woods which are the most important and common sources (Derek & Perlin, 2003). Other cellulosic materials include agricultural residue, water plant, grasses and other plant substances. Besides cellulose, they contain hemicelluloses, lignin and a comparably small amount of extracts. Commercial cellulose production concentrates on harvested sources such as wood or on naturally pure source such as cotton.

2.3.1.6.2 Structure and analysis

Cellulose is a polydisperse linear homopolymers consisting of regio-and enantioselectively β-1, 4- glycosidic linked D-glucopyranose units (so-called) anhydroglucose unit (Fannon et al., 2004). It has been shown by spectroscopy that the β-D-glucopyranose adopts the 4C chain information, the lowest free energy conformation of the molecule. As a consequence, the hydroxyl groups are positioned in the ring plane while the hydrogen atoms are in the vertical position (axial). The polymer contains free hydroxyl groups at the C-2, C-3, and C-6 atoms. Based on the OH groups and the oxygen atoms of both the pyranose ring and the glycosidic bond,

ordered hydrogen bond systems form various types of supramolecular semi-crystalline structures (Fischer et al., 2000).

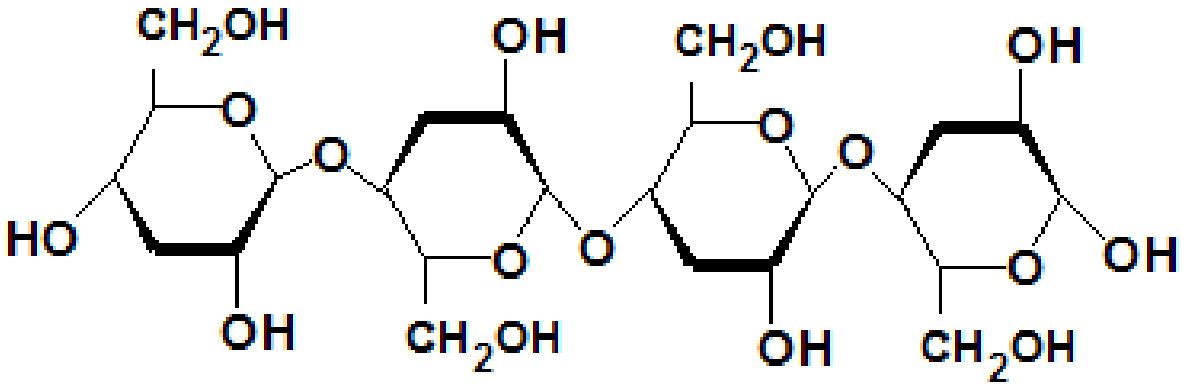

Figure 2.6 (a): Simple Structure of Cellulose

(Derek & Perlin, 2003; Fischer et al., 2000)

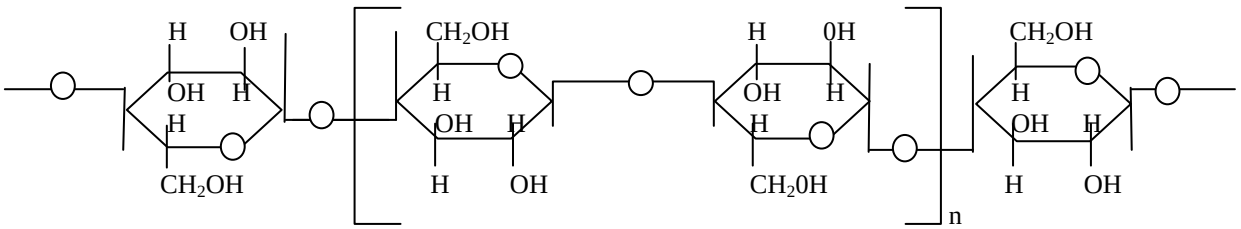

Figure 2.6 (b): Schematic Structure of cellulose

(Cisco & Whistler, 2008)

2.3.1.6.3 Polyanionic cellulose

Polyanionic cellulose (PAC) is a kind of anionic cellulose ether of high purity and high degree of substitution, prepared with natural cellulose through chemical modification (Lann, 2005; Derek & Perlin, 2003). Its sodium salt is often utilized. PAC is available in two types (high or low viscosity grade), both of which impart the same degree of fluid loss control but different degrees of viscosity (Lann, 2005). The temperature stability of PAC is 149 °C and is not subjected to bacterial degradation.

At present, polyanioniccellulose (PAC), a cellulose based fluid loss agent is one of the commonly used fluid loss control agents in drilling mud industry (Swartz & Gschwend, 1999). In view of the fact that the importation of PAC is costly, there is a necessity for less expensive polymers, preferably local resources like corn, potato starch as an alternative to the PAC. PAC has showed a better function in water based mud when it‘s combined with a sulfonatic polymer and aged in the temperature of 300°F. Polyanionic cellulose additives for the oilfield are high quality and purity and meet industry standards. We supply both PAC high viscosity and low viscosity grades. High viscosity polyanionic cellulose for the oilfield gives high rheology, shale inhibition and fluid loss control. Low viscosity polyanionic cellulose provides shale inhibition and fluid loss control without excessive viscosity buildup (Wylly & Chenevert, 2012). The unique properties of PAC result from the high degree of carboxy methyl substitutions on the cellulose backbone. This chemical modification gives cellulose its ability to viscosify water at low concentrations as well as providing high temperature stability while resisting contaminants such as alkaline metal salts and high chloride content brines. At temperatures above 300^0F, an oxygen scavenger can be added to protect the properties of polyanionic cellulose.

Drilling mud treated with Polyanionic Cellulose can form a thin filter cake with low permeability, and thus can reduce the mud loss and collapse of well bore phenomena resulting from water loss of mud. The mud with the addition of Polyanionic Cellulose is seldom affected by bacteria so no need to maintain high pH value or use preservatives (Wylly & Chenevert, 2012; Benna et al., 1999). PAC will remain stable with corresponding decrease of the usage amount of other chemical agents, or even within a certain range of temperature variation during the drilling process. PAC-HV additions to the mud with require small usage amounts that will increase viscosity and

reduce fluid loss. A small amount of Polyanionic Cellulose HV can replace a significant amount of clay and thus reduce the difficulties resulting from encountering calcium sulfate or other contaminants during drilling process (Wylly & Chenevert, 2012; Benna et al., 2001). PAC-LV can reduce the fluid loss but have little effect on the viscosity.

2.3.1.6.4 Carboxymethyl Cellulose [CMC]

Carboxymethyl cellulose (CMC) is a derivative of cellulose (Bertts & Jerry, 2012; Wyllly & Chenevert, 2012; Fannon et al., 2004; Fischer, 2002). Cellulose is a natural polymer obtained from wood pulp and cotton (Fischer et.al, 2000). Cellulose can be modified to carboxymethyl cellulose to become soluble in water (Wyllly & Chenevert, 2012; Jones, 2006; Fannon et al., 2004). The solubility of this CMC in water occurs because CMC has affinity for water through the anionic group (Bertts & Jerry, 2012). Both cellulose and cellulose derivatives are very biodegradable. A typical CMC is sodium carboxymethyl cellulose which is formed by the reaction between sodium salt of monochloroacetic acid ($ClCH_2COONa$) and cellulose (Bertts & Jerry, 2012; Wyllly & Chenevert, 2012; Jones, 2006; Fannon et al., 2004; Fischer, 2002). A substitution occur most often at the [$-CH_2OH$] group of the cellulose to form a soluble poly electrolyte. High degree of polymerization (DP) of sodium carboxymethyl cellulose causes high molecular weight and viscosity (Wyllly & Chenevert, 2012; Derek & Perlin, 2003). Sodium Carboxymethyl cellulose is very useful in water-based mud. It controls fluid loss in fresh water, seawater, and salt water. It develops viscosity to a degree that is dependent on the solids concentration, salinity and make-up water chemistry (Bada, 2005). It is thermally stable to 140^oC.

Sodium Carboxymethyl cellulose is a chemically modified cellulose, and possesses the natural properties of cellulose that have been modified by the addition of chemicals (Clever et al., 2012). It is biodegradable because of the presence of natural cellulose. It is compatible with all common mud-treating additives. It encapsulates shale particles to inhibit swelling and dispersion (Fannon et al., 2004). The structure of sodium carboxymethyl cellulose is given below.

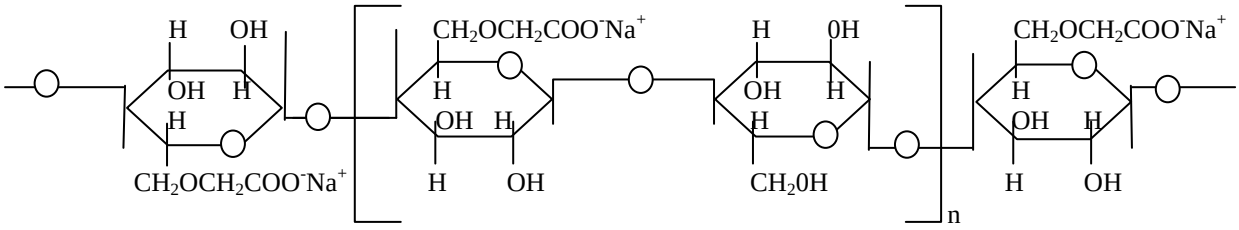

Figure 2.7: Structure of sodium carboxymethyl cellulose

(Bertts & Jerry, 2012; Wyllly & Chenevert, 2012; Fannon et al., 2004)

Carboxymethyl cellulose (CMC) is a semi-flexible anionic cellulose ether polymer that is produced by reacting alkali cellulose with sodium monochloroacetate under rigidly controlled conditions. It is a chemical derivative of cellulose where some of the hydroxyl groups (-OH) are substituted with carboxymethyl groups (-CH_2COOH) (Kobert, 2009). It is an ionic polymer produced by treating cellulose with caustic soda and monochloro acetate, molecular weight ranges between 50,000 and 400,000 (Wylly & Chenevert, 2012). CMC is another popular additive being increasingly considered for easing the challenges associated with borehole drilling mechanisms. CMC is basically a technical grade, low viscosity, and dispersible additive (Kennedy et al., 2002). Chemically, it is a Carboxymethyl Cellulose compound. It reduces the

API filtration rate through minimum enhancement in viscosity with respect to aqueous drilling fluids (Clerk & Clem, 2003).

2.3.1.7 Gum Arabic

Gum arabic is a complex mixture of polysaccharides and glycoproteins that is used for various purposes including viscosity control and can be used in drilling fluid formulation (Christopher & Perlin, 2010; Kenie & Stan, 2010). Gum Arabic in its crude form is solid with golden coloration which readily dissolves in water to form a sweet smelling gel-like fluid. Gum Arabic is the trade name for a natural forest product from the genus Acacia (Christopher & Perlin, 2010). It is manly obtained from Acacia Senegal var. Senegal locally known as Hashab. Gum Arabic tree is about 5 to 20ft height and has a life span of 25 to 30 years. It grows in poor sandy, reddish soils and the colors of flowers are white or of cream. It has a deep–dark yellow to light brown on gray branches and the length of the leaf is 1 to 6 cm. The name Acacia is derived from the Greek word (akis) meaning (sharp point) and relates to the thorny sharps and trees of tropical Africa and Western Asia that were the only known acacia at the time where the name was published. Synonym names include gum Arabic (Acacia Senegal), Gum Hashab, Kordofanian Gum, Gum Arabic, Acacia Gum, Arabic Gum (Christopher & Perlin, 2010). Acacia Senegal is found in the Sudan throughout the states of Darfur, Kordafan Blue Nile part of White Nile, Upper Kassala and Gedaref. The main area of its occurrence is the part of Sudan where the species is uniform and is found in pure stands, giving Sudan the advantage of being the major producer and exporter of the best quantity Gum Arabic supplying about 80% of the annual world requirements (Christopher & Perlin, 2010).

2.3.1.7.1 Properties and Characteristics

Gum Arabic readily dissolves in water to produce solutions of low viscosity and hence finds little application as a thickening agent. The Gum Arabic solutions viscosity decreases in the presence of electrolyte and at high and low pH levels (Jeffery, 2007). The viscosity of Gum Arabic solutions shows an irreversible decrease after heating due to denaturation at pH and precipitation of the high molecular, mass protein and rich components. It is used as an emulsifier in the encapsulation of oils for long prior to bottling. Gum Arabic also has the ability to form thick visco-elastic films at the oil– water interface. Size exclusion chromatography studies have shown that Gum Arabic from Acacia Senegal consists of two main components, proteins deficient major component and acetous which for on 30% of the total thus emphasizing the total dispersion of gum and confirming that gum Arabic is an arabinose galacton protein complex The gum has been fractionated using hydrophobic interaction chromatography to three fractions. A protein deficient arabinose galacton fraction froms 89.4% of the total and has a molecular mass of 2.79×103 g/mol and was low in protein 0.44% (Weight/Weight (w/w)), which is designated as an arabinogalacton fraction. The second major fraction forms 10.4% of the total (w/w) has a higher molecular mass of 1.45×106 g/mol and a greater proportion of protein 9.18% (w/w). The third fraction as the glycol protein, it is major fraction of about 1% of the total (w/w) and a molecular mass of 0.25%. Gum Arabic is used to maintain the required properties of water-based drilling fluid (Christopher & Perlin, 2010).

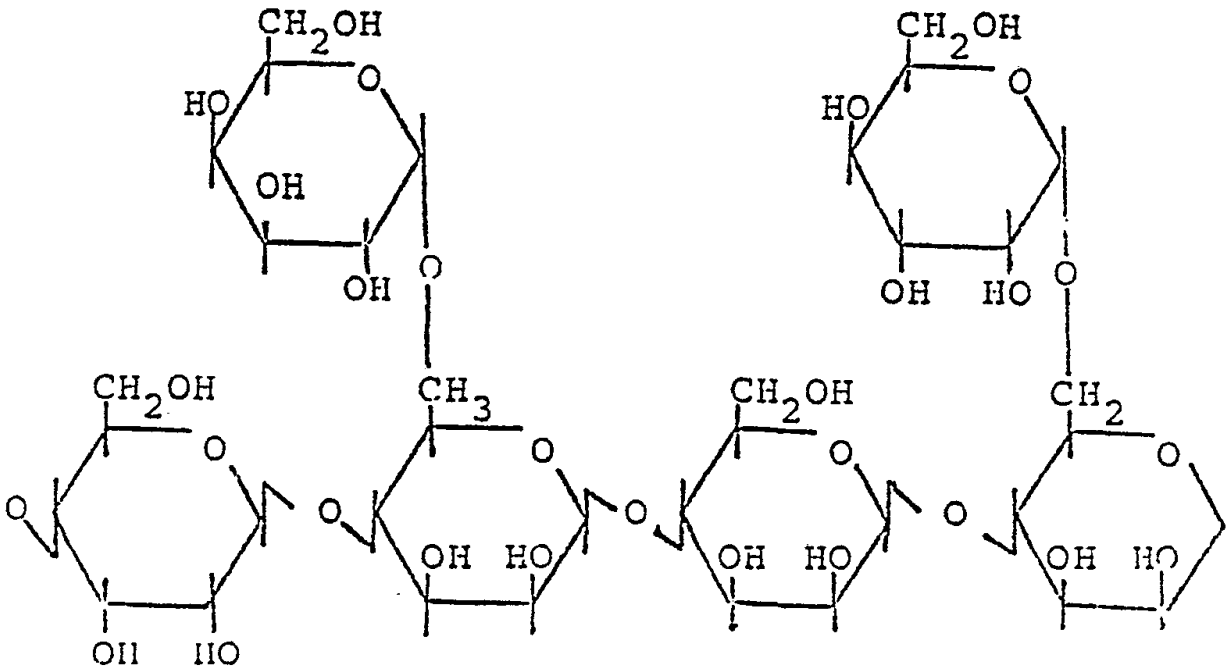

Figure 2.8: Structure of Gum Arabic (Jeffery, 2007)

2.3.1.8 Polyhydroxy Alkanoates [PHA]

Polyhydroxy alkanoates are naturally-occurring polyesters which are totally biodegradable (Cambel et al., 2007; Calistus & Mathew, 2004; Lenz, 1993). Typical examples of poly hydroxyl alkanoates are poly (β – hydroxy butyrate, PHB), n = 1 synthesized by the bacterium Akaligenes eutrophus, and poly (β -hydroxy valerate, PHV), n = 1 synthesized by A. eutrophus and P. eleovorans (Cambel et al., 2007; Calistus & Mathew, 2004).

Polyhydroxy alkanoates (PHA) like poly-lactic acid (PLA) are obtained from corn (Cambel et al., 2007; Sevens, 2002). But PLA requires chemical steps (hydrolysis and fermentation) to synthesize it, while PHA naturally accumulates with the microbes as granules that can constitute up to 90% of a single cell's mass. These micro-organisms (bacteria eutropha) convert sugar directly into the polymer: polyhydroxy alkanoate (Cambel et al., 2007).

Recently, researchers have developed a new method of producing polyhydroxy alkanoates directly from agricultural plant (corn plant) instead of from the corn grains. This was initiated in the mid 1980s when the genes that enable the bacteria to make the polymer were isolated, and inserted into a plant from which acety co-enzyme A (a Compound that forms naturally as the plant converts sunlight into energy) was converted into a polymer (Sevens, 2002). In 1992, a group of researchers introduced the genes into the plant Arabidopsis thaliana to produce PHA. Two years later Mosanto used the same genes to produce PHA on corn plant. The parts of the plant that are mainly used for the production of this polymer are the stem and the leaves generally called the STOVER (Catia, 2005; Sevens, 2002; Carraha-Chrales & Sperling, 1996). Polyhydroxy alkanoates are suitable for making drilling muds because they are highly crystalline (65% to 85%) which results in high viscosity of the mud. PHA is thermally stable up to temperatures above 200^{o}C, which is good for work over or well completion fluid (Cambel et al., 2007; Calistus & Mathew, 2004; Peddy, 2002). PHA in its natural state is soluble in water and totally biodegradable.

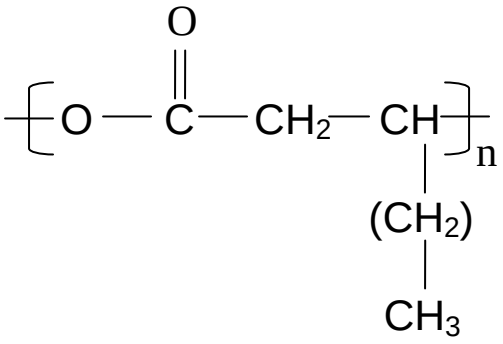

Figure 2.9: General structure for poly hydroxy alkanoate (PHA)

(Catia, 2005; Sevens, 2002)

2.3.2 Synthetic Polymers Used for Muds

Some synthetic polymers also can be biodegraded often with the help of specific micro-organisms adaptation or the addition of agents to promote chemical degradation (Qartar & Giacelo, 2010; Middleton, 2000; Sobie, 1994). Therefore drilling muds made from these polymers are biodegradable. Synthetic polymers are chemically or synthetically produced usually from petroleum-derived products, unlike natural polymers and their derivatives (Neff, 2000; Sobie, 1994). Synthetic polymers are built up from relatively smaller molecules, and they afford an almost unlimited flexibility in their design. They can be tailor-made to fit almost any application. The sizes and chemical composition can be made to produce properties for almost any function.

Synthetic polymers are most often prepared from substituted ethylene or substituted vinyl group (Ebewele, 2000). The polymerization process occurs through an addition reaction where the substituted groups are added to the end of the polymer chain. In the figure below, the substituted group "A" can be any functional group.

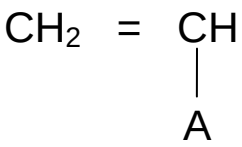

Figure 2.10: Substituted Vinyl Group (Ebewele, 2000).

Note, the carbon–carbon backbone and the unlimited substitution possibilities. The carbon -carbon back bone is a more stable linkage than the carbon-oxygen linkage encountered earlier with starch and cellulose – base polymers. The carbon – carbon linkage is resistant to bacteria attack and has temperature stability in excess of 700^{o}F (Ebewele, 2000). Biodegradation is introduced into the polymer chain by the

substituted groups, which most likely will degrade before the carbon – carbon linkage. Examples of these biodegradable synthetic polymers are polyacrylate and partially hydrolysed polyacrylamide (Qartar & Giacelo, 2010; Stewart, 2009).

2.3.2.1 Polyacrylate

The specific polyacrylate is sodium polyacrylate (Qartar & Giacelo, 2010). The polymerization of acrylic acid and the subsequent neutralization give sodium polyacrylate (SPA) (Katchy, 2000). This sodium polyacrylate is a highly anionic polymer that functions either as a deflocculant at low molecular weight (less than 1000) or a fluid loss control additive (depending on the molecular weight of the polymer) (Wilcox & Hool, 2010; Katchy, 2000). It functions at much lower concentrations than lignosulfonates. Typical concentrations 0.25 to 1.0 ib/bbl are sufficient to control rheological properties. SPA functions well at any pH level and is stable to temperatures up to 500^{o}F (260^{o}C) (Anthony & Robert, 2010; Beneth & Godfrey, 2006). SPA performs best in water-based mud because it is a surface-active material but sensitive to high concentration of solids (Qartar & Giacelo, 2010).

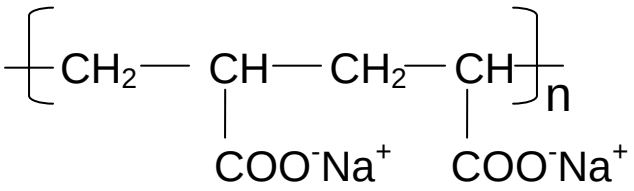

Figure 2.11: Sodium Polyacrylate

(Qartar & Giacelo, 2010; Katchy, 2000)

2.3.2.2 Partially Hydrolysed Polyacrylamide

Partially Hydrolysed Polyacrylamide (PHPA) is often used to identify the hydrolysis of polyacrylamide (Stewart, 2009). Polymethacrylamide is an example of partially hydrolysed polyacrylamide. Partially hydrolysed polyacrylamide is used in preparing drilling muds by the oil industry as a flow and fluid loss reduction agent (Anthony & Robert, 2010; Zereek & Bruce, 2010; Caskey et al., 2004; Ogden, 1991). It has good thermal stability but degradation occurs upon prolonged heating at elevated temperatures like above 200^{o}C (Parkson et al., 2000; Lancen et al., 1994). The polymer is infinitely soluble in water giving clear solution (Enie & Giles, 2001). The viscosity of PHPA and water solution depends on concentrations, molecular weight, temperature, shear rate, and past history (Ogden, 1991). The properties of PHPA are affected by the molecular weight and the ratio of the carboxyl group to the amide group (Stewart, 2009). The PHPA is anionic polymer and water-soluble. PHPA has exceptional thermal stability and biodegradability. Its anionic properties are affected by hardness and cationic surfaces. It produces high gel strength and increases the viscosity of the muds (Stewart, 2009). The efficiency of PHPA is reduced by salt saturation (high salinity). The polymer remains coiled at high salinity without hydration which results in less viscosifying capacity. Another characteristic of PHPA is that it is sensitive to soluble calcium. The anionic sites react with the calcium to yield undesirable effects. It is therefore recommended to add chemicals to the mud system that can precipitate the calcium (Stewart, 2009).

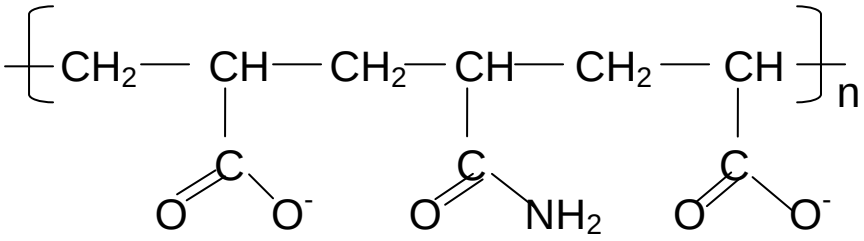

Figure 2.12: Partially Hydrolysed Poly acrylamide (PHPA)

(Stewart, 2009)

2.3.3 General Methods for Producing Biodegradable Polymers

Two basic methods are employed in the production of biodegradable polymers. These include: Direct extraction from natural plants and Conversion of biomass to bionomers and further conversion to biopolymers (Scott et al., 2007; Gronski & Hellmann, 2003).

2.3.3.1 Direct Extraction from Natural Plants

Natural polymers such as cellulose, starch, proteins, fibres and vegetable oils are extracted directly from plants or agricultural crops (Gronski & Hellmann, 2003; Mario & Mark, 2003). Then these natural polymers are the main raw materials for developing biodegradable polymers. The figure below illustrates this:

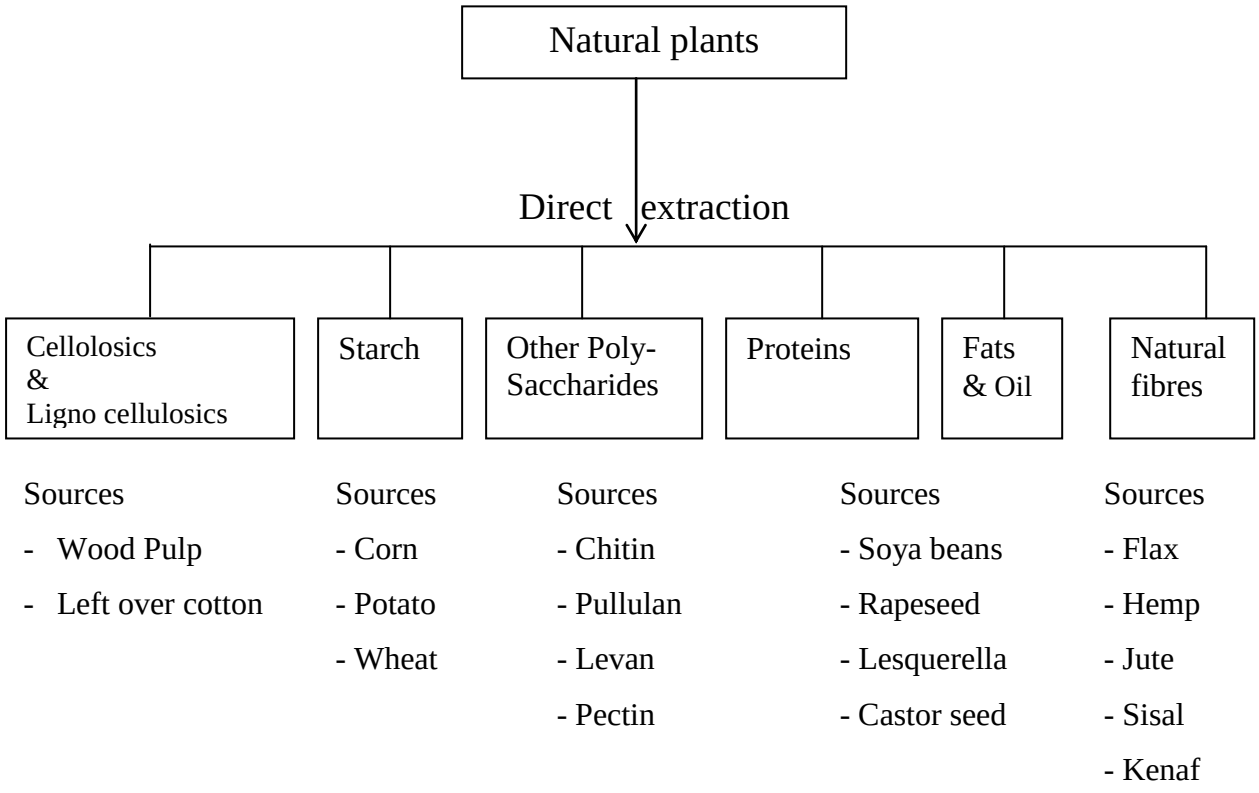

Figure 2.13: Direct Extraction to produce Biopolymers

(Gronski & Hellmann, 2003; Mario & Mark, 2003)

2.3.3.2 Conversion of Biomass to Biomonomers and further Conversion to Biopolymers

Bio based products/Biomass (one of the product of biodegradation) can be converted to biomonomers by hydrolysis or fermentation. These biomonomers then undergo either chemical process or Bioprocess to yield the specific biodegradable polymers (Scott et al., 2007; Mario, 2003). In the chemical process, the monomers are converted to biodegradable polymers (e.g. Polylactic acid) by chemical synthesis. In the bio process, the biomonomers are converted to biodegradable polymers (e.g. Polyhydroxy alkanoates) by microbial synthesis. This is illustrated in the figure below.

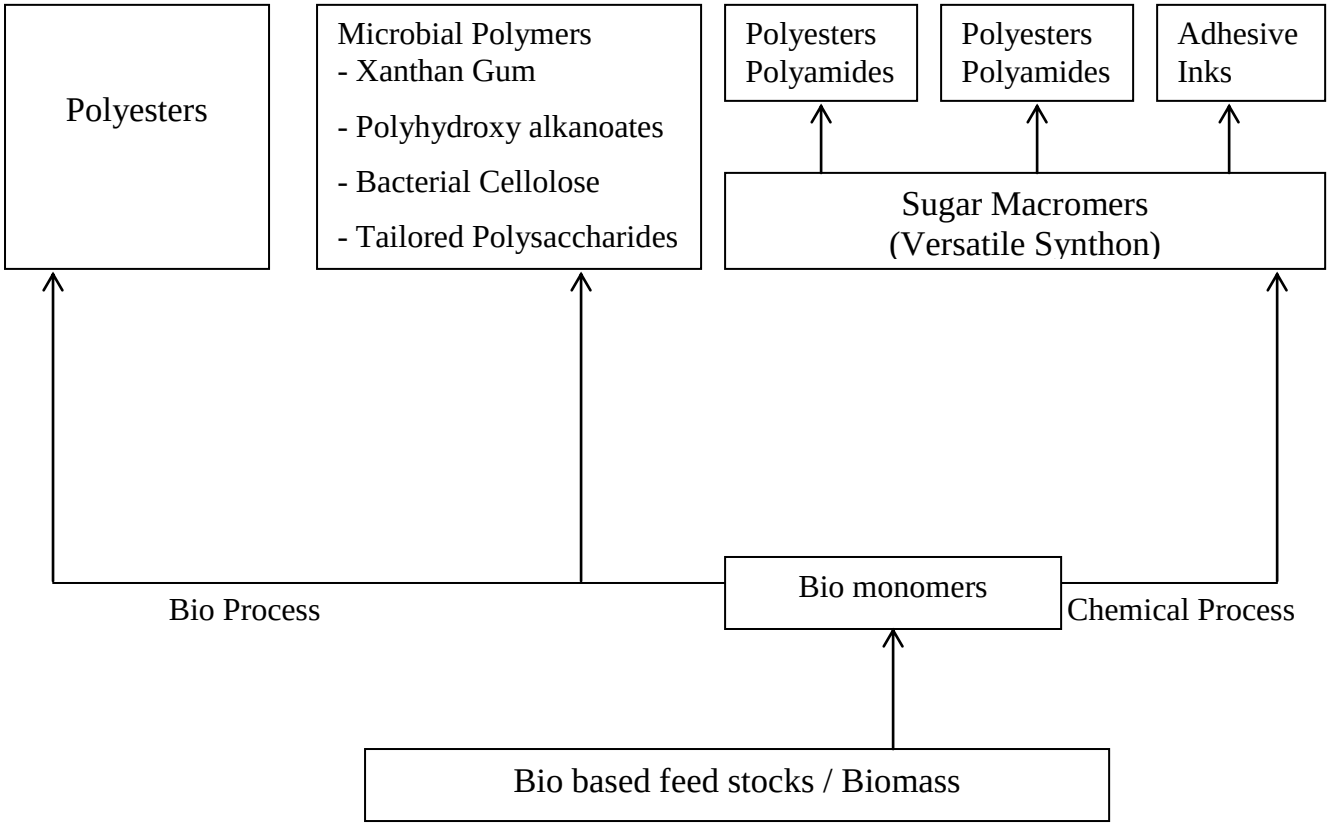

Figure 2:14: Conversion of Biofeed stocks /Biomass to Biopolymers

(Scott et al, 2007; Gronski & Hellmann, 2003; Mario & Mark, 2003)

2.3.4 Biodegradable Polymers

A Biodegradable polymer is a type of polymer that is attacked by microorganisms after its intended purpose (Mario & Mark, 2003; Ukachukwu et al., 2010). Biopolymers break down to result in natural byproducts such as gases (CO_2, N_2), water, biomass, and inorganic salts. These polymers are found both naturally and synthetically made, and largely consist of ester, amide, and ether functional groups. Their properties and breakdown mechanism are determined by their exact structure. These polymers are often synthesized by condensation reactions, ring opening polymerization, and metal catalysts. There are vast examples and applications of biodegradable polymers. Natural polymers are

available in large quantities from renewable sources, while synthetic polymers are produced from non-renewable petroleum resources. Biodegradation of polymeric biomaterials involves cleavage of hydrolytically or enzymatically sensitive bonds in the polymer leading to polymer erosion. A vast number of biodegradable polymers have been synthesized recently and some microorganisms and enzymes capable of degrading them have been identified.

Biodegradable polymers have a long history and since many are natural products, the precise timeline of their discovery and use cannot be accurately traced. One of the first medicinal uses of a biodegradable polymer was the catgut suture, which dates back to at least 100 AD. The first catgut sutures were made from the intestines of sheep, but modern catgut sutures are made from purified collagen extracted from the small intestines of cattle, sheep, or goats. The concept of synthetic biodegradable plastics and polymers was first introduced in the 1980s. In 1992, an international meeting was called where leaders in biodegradable polymers met to discuss a definition, standard, and testing protocol for biodegradable polymers (Mario & Mark, 2003). Also, oversight organizations such as American Society for Testing of Materials (ASTM) and the International Standards Organization (ISO) were created.

2.3.4.1 Classification of Biodegradable Polymers

Biodegradable polymers represent a growing field. A vast number of biodegradable polymers (e.g. cellulose, chitin, starch, polyhydroxyalkanoates, polylactide, polycaprolactone, collagen and other polypeptides) have been synthesized or are formed in natural environment during the growth cycles of organisms. Some microorganisms and enzymes are capable of degrading such polymers. Biodegradable polymers can be classified according to their chemical composition, origin and

synthesis method, processing method, economic importance, application, etc (Clever et al., 2012; Chimere, 2011; Carraha-Charles & Sperling, 1996).

Based on structure, Biodegradable polymers can be classified into two main categories:

- The agro-polymers (category i)
- The biodegradable polyesters or biopolyesters (categories ii–iv).

2.3.4.1.1 Agro-polymers

The agro-polymers are those derived from biomass. They include polysaccharides, like starches found in corns, tubers (potatoes, cassava, etc) or wood, and proteins, such as animal based whey or plant derived gluten. Polysacharides consist of glycosidic bonds which take a hemiacetal of a saccharide and bind it to an alcohol via loss of water (Cisco & Whistler, 2008). Proteins are made from amino acids, which contain various functional groups. These amino acids come together again through condensation reactions to form peptide bonds, which consist of amide functional groups.

2.3.4.1.2 Biodegradable polyesters

This group consists of biopolyesters, which are those derived from microorganisms or synthetically made from either natural or synthetic monomers.

Examples of biopolyesters includes polyhydroxybutyrate and polylactic acid.

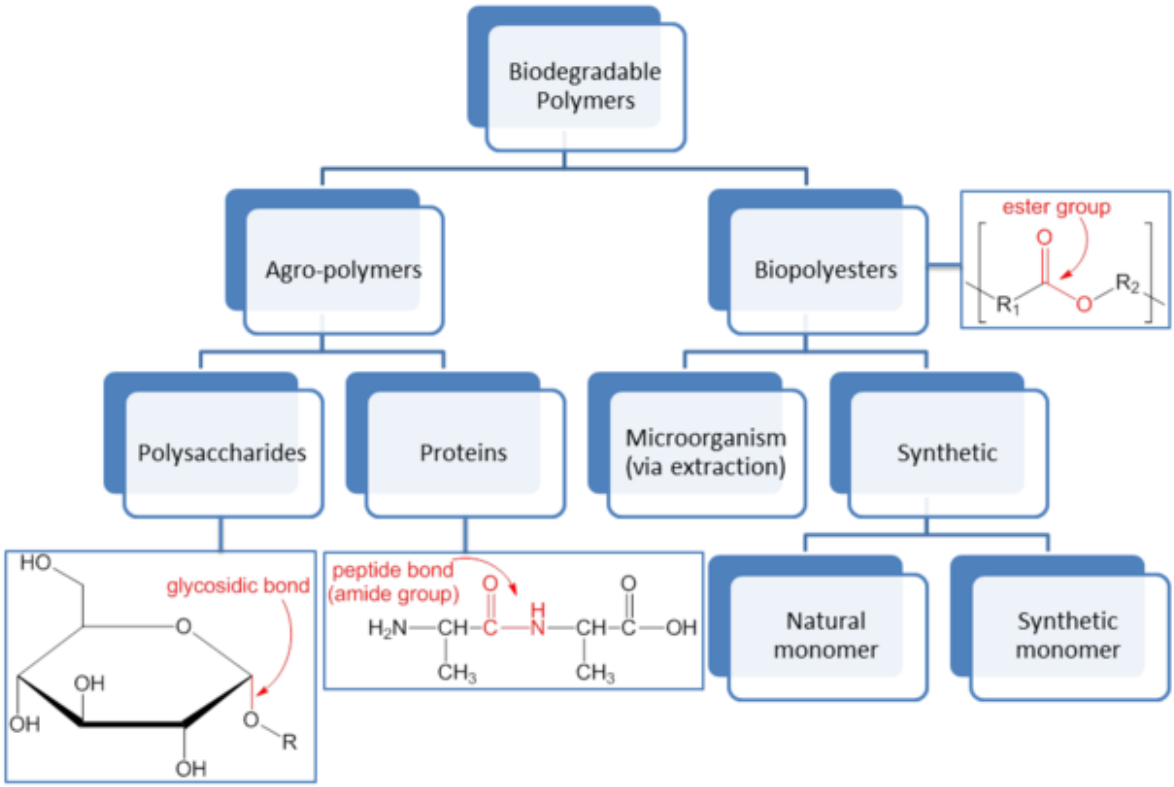

Figure 2.15 Biodegradable Polymers organization based on Structure and Occurrence (Marck & Hercules, 2004; Mangelsdorf, 2004)

2.3.4.2 Properties of Biodegradable Polymers

- All biodegradable polymers should be stable and durable enough for use in their particular application, but upon disposal they should easily breakdown.
- A high surface area is common as it allows easy access for the chemical, light, or organism.
- Crystallinity is often low as it also inhibits access to end groups.
- A low degree of polymerization to allow more accessible end groups for reaction with the degradation initiator.
- They are Hydrophobic

- They are non-toxic
- They are capable of maintaining good mechanical integrity until degraded.
- Capable of controlled rates of degradation.

2.3.4.3 Factors Affecting Biodegradation

2.3.4.3.1 Effect of polymer structure

Natural macromolecules, e.g. protein, cellulose, and starch are generally degraded in biological systems by hydrolysis followed by oxidation (Marck & Hercules, 2004). It is not surprising, then, that most of the reported synthetic biodegradable polymers contain hydrolyzable linkages along the polymer chain; for example, amide enamine, ester, urea, and urethane linkages are susceptible to biodegradation by microorganisms and hydrolytic enzymes. Since most enzyme-catalyzed reactions occur in aqueous media, the hydrophilic–hydrophobic character of synthetic polymers greatly affects their biodegradabilities. A polymer containing both hydrophobic and hydrophilic segments seems to have a higher biodegradability than those polymers containing either hydrophobic or hydrophilic structures only.

2.3.4.3.2 Effect of polymer morphology

One of the principal differences between proteins and synthetic polymers is that proteins do not have equivalent repeating units along the polypeptide chains (Mario & Mark, 2003). This irregularity results in protein chains being less likely to crystallize. It is quite probable that this property contributes to the ready biodegradability of proteins. Synthetic polymers, on the other hand, generally have short repeating units, and this regularity enhances crystallization, making the hydrolyzable groups inaccessible to enzymes. Microorganisms produce extracellular enzymes responsible for the selective degradation. This selectivity can be attributed to the less-ordered

packing of amorphous regions, which permits easier access for the enzyme to the polymer chains. The size, shape and number of the crystallites all have a pronounced effect on the chain mobility of the amorphous regions and thus affect the rate of the degradation. Biodegradation proceeds differently from chemical degradation. Studies on the degradation by solutions of 40% aqueous methylamine have shown a difference in morphology and molecular weight changes and in the ability of the degrading agents to diffuse into the substrate.

2.3.4.3.3 Effect of radiation and chemical treatments

Photolysis with UV light and the g-ray irradiation of polymers generate radicals and/or ions that often lead to cleavage and crosslinking. Oxidation also occurs, complicating the situation, since exposure to light is seldom in the absence of oxygen. Generally this changes the material's susceptibility to biodegradation. Initially, one expects the observed rate of degradation to increase until most of the fragmented polymer is consumed and a slower rate of degradation should follow for the crosslinked portion of the polymer. A study of the effects of UV irradiation on hydrolyzable polymers confirmed this. Similarly, photooxidation of polyalkenes promotes (slightly in most cases) the biodegradation (Gronski & Hellmann, 2003). The formation of carbonyl and ester groups is responsible for this change. For polyglycolide and poly (glycolide-*co*-lactide), the pH of the degradation solution decreased as the process proceeded.

2.3.4.3.4 Effect of molecular weight

There have been many studies on the effects of molecular weight on biodegradation processes. Most of the observed differences can be attributed to the limit of detecting the changes during degradation, or, even more often, the differences in morphology

and hydrophilicity– hydrophobicity of polymer samples of varying molecular weight (Ching et al., 1993). Microorganisms produce both exoenzymes [degrading polymers from terminal groups (inwards)] and endoenzymes (degrading polymers randomly along the chain). One might expect a large molecular effect on the rate of degradation in the ease of exoenzymes and a relatively small molecular weight effect in the case of endoenzymes. Plastics remain relatively immune to microbial attack as long as their molecular weight remains high (Ching et al., 1993). Many plastics, such as PE, PP and PS do not support microbial growth. Low molecular weight hydrocarbons, however, can be degraded by microbes. However, these processes do not function well (if at all) in an extracellular environment, and the plastic molecules are too large to enter the cell. This problem does not arise with natural molecules, such as starch and cellulose, because conversions to low molecular weight components by enzyme reactions occur outside the microbial cell. However, photodegradation or chemical degradation may decrease molecular weight to the point that microbial attack can proceed (Ching et al., 1993).

2.3.4.4 Applications and Uses of Biodegradable Polymers

Biodegradable polymers are of significant interest to a variety of fields including medicine, agriculture, and packaging. One of the most active areas of research in biodegradable polymer is in controlled drug delivery and release.

2.3.4.4.1 Medicine

Biodegradable polymers are of great interest in the field of drug delivery and nanomedicine (Zhanpeng et al., 2002). The great benefit of a biodegradable drug delivery system is the ability of the drug carrier to target the release of its payload to a specific site in the body and then degrade into nontoxic

materials that are then eliminated from the body via natural metabolic pathways. The polymer slowly degrades into smaller fragments, releasing a natural product, and there is controlled ability to release a drug. The drug slowly releases as polymer degrades. For example, polylactic acid, poly (lactic-co-glycolic) acid, and poly (caprolactone), all of which are biodegradable, have been used to carry anti-cancer drugs (Zhanpeng et al., 2002). Encapsulating the therapeutic in a polymer and adding targeting agents decreases the toxicity of the drug to healthy cells.

Biodegradable polymers and biomaterials are also of significant interest for tissue engineering and regeneration. Tissue engineering is the ability to regenerate tissue with the help of artificial materials. The perfection of such systems can be used to grow tissues and cells *in vitro* or use a biodegradable scaffold to construct new structures and organs *in vitro*. For these uses, a biodegradable scaffold is obviously preferred as it reduces the risk of immunological reaction and rejection of the foreign object.

2.3.4.4.2 Agricultural applications

Since the introduction of plastic films in the 1930s and 1940s for greenhouse coverings, fumigation and mulching, agricultural applications of polymers have grown at an enormous rate (Feiffer & Vierty, 2002). All principal classes of polymers, i.e. plastics, coatings, elastomers, fibres and watersoluble polymers are presently utilized in applications which include the controlled release of pesticides and nutrients, soil conditioning, seed coatings, gel plantings and plant protection.

However, degradable plastics are also of interest as agricultural mulches and agricultural planting containers. Ultimate biodegradability, as in composting, is also

of some interest as it would permit degradable plastics to be combined with other biodegradable materials and converted into useful soil-improving materials.

2.3.4.4.3 Packaging

Biodegradable polymers are often used to reduce the volume of waste in packaging materials. There is also significant effort to replace materials derived from petrochemicals with those that can be made from biodegradable components. One of the most commonly used polymers for packaging purposes is polylactic acid, PLA (Feiffer & Vierty, 2002; Ching et al., 1993). The production of PLA has several advantages, the most important of which is the ability to tailor the physical properties of the polymer through processing methods. PLA is used for a variety of films, wrappings, and containers (including bottles and cups). In 2002, FDA ruled that PLA was safe to use in all food packaging. BASF markets a product called Ecovio (Feiffer & Vierty, 2002) which is a blend of the company's biodegradable plastic Ecoflex and PLA. An application for this biodegradable material is for thin plastic films such as shopping bags or trash bags.

2.3.4.4.5 Drilling Fluids

Drilling fluids are fluids used to drill boreholes into the earth, and are used while drilling oil and natural gas wells and on exploration drilling rigs. Drilling fluid is often called drilling mud. The three main categories of drilling fluids are water-based muds (which can be dispersed and non-dispersed), non-aqueous muds, usually called oil-based mud or invert, and gaseous drilling fluid, in which a wide range of gases can be used (Feiffer & Vierty, 2002). The main functions of drilling fluids include providing hydrostatic pressure to prevent formation fluids from entering into the well bore, keeping the drill bit cool and clean during drilling, carrying out drill cuttings,

and suspending the drill cuttings while drilling is paused and when the drilling assembly is brought in and out of the hole. The drilling fluid used for a particular job is selected to avoid formation damage and to limit corrosion

Nowadays, various polymers, which can be in the form of natural (e.g. starch), synthetic, and/or modified (e.g. carboxymethyl cellulose or CMC) polymers, are used in order to control the fluid loss and viscosity of drilling fluids (Fischer, 2002). In oil-drilling, these polymers reduce filtrate, modify rheological properties, stabilize shale and reduce drag, and can be used in advanced oil recovery (AOR) processes.

2.3.4.5 Mechanism of breakdown during Biodegradation Process

In general, biodegradable polymers break down to form gases, salts, and biomass (Chimere, 2011; Catia, 2005; Micky & Duke, 2005; Klirk, 2002). Complete biodegradation is said to occur when there are no oligomers or monomers left.The breakdown of these polymers depend on a variety of factors including the polymer and also, the environment the polymer is in (Klirk, 2002). Polymer properties that influence degradation are bond type, solubility, and copolymers among others. The surrounding environment of the polymer is just as important as the polymer structure itself. These factors included items such as the pH, temperature, microorganisms present, and water as just a few examples. There are two primary mechanisms through which biodegradation can occur. One is through physical decomposition through reactions such as hydrolysis and photodegradation, which can lead to partial or complete degradation. The second mechanistic route is through biological processes which can be further broken down into aerobic and anaerobic processes. The first involves aerobic biodegradation, where oxygen is present and important. In this case

the general equation seen below where $C_{residue}$ represents smaller fragments of the initial polymer such as oligomers (Micky & Duke, 2005).

$$C_{polymer} + O_2 \longrightarrow C_{residue} + C_{biomass} + CO_2 + H_2O$$

General equation for aerobic biodegradation

The second mechanism of biodegradation is by anaerobic processes, where oxygen is not present (Micky & Duke, 2005).

$$C_{polymer} \longrightarrow C_{residue} + C_{biomass} + CO_2 + CH_4 + H_2O$$

General equation for anaerobic biodegradation

2.4 Interaction Between Polymer and Solid Surfaces

The information on the mechanisms of interaction of simple organic compounds with solids is used to understand the interaction between polymer and solid surfaces (Vincent & Iyklema, 2005; Labby, 2001; Theng, 1999; Shamp & Huylebroeck, 1993). The positively charged organic micro molecules are adsorbed by an exchange reaction between the charge-balancing inorganic cations at the solid surfaces and the uncharged polar compounds (Jimo, 2001). The interaction principally occurs between the functional group and the exchangeable cations. A number of excellent general reviews on the adsorption of polymers from solution onto solid adsorbent have been written (Jimo, 2001; Labby, 2001). These principles would apply to the adsorption organic macromolecules whose interactions with solids differ in some respects from those of simple non-polymeric species. The differences arise from the fact that besides being long, a polymer chain is flexible and often polyfunctional

2.4.1 Polymer and Clay Interaction

According to Lagaly, adsorption of polymer molecules by clay minerals is more strongly governed by structural aspects (Jimo, 2001). Clay minerals bind polymer compounds by adsorption, ion exchange and intercalation (Jimo, 2001; Labby, 2001; Velde, 1999), which may take place on the external and internal surfaces. The ideal situation is coating the clay particles with a polymer producing a stable suspension of clay and polymer kaolinite and other clay minerals can be used in polymer- clay interactions studies. These kaolinites are very useful because they are very inert chemically and very stable in different pH level and Oxidation potential environment (Lancen et al., 1994).

Experimentally, the action of flocculating agents (e.g. polymer) on clay dispersion is governed by a number of principles (Jimo, 2001; Roberts et al., 2005). One of these principles is the solubility of the polymer in the medium and the ability to compete effectively with solvent for surface sites, and the concentration for effective flocculation is much less than that needed for surface saturation. The effect may be assessed in a variety of ways based on the changes in a given property of either the total system (e.g. its Rheology) or the aggregate formed (e.g. its filtration property) (Roberts et al., 2005).

In the past, a concept was developed that polyelectrolytes can flocculate clay suspension by forming interparticle bond (Regan & Hardy, 2002; Raymond & Benco 1992). From this concept, single polymeric chain was capable of attaching itself to more than one particle surface. Progress in explaining this mode of interaction had been made in the recent theories on the structure of flexible polymers confined to a solid –liquid interface (Vincent & Iyklema, 2005). The bridge is formed when part of the polymer attaches to a solid particle surface whereas other sections of the chain

may extend out into the solution and become attached to a free site on a second particle. Rashid, (Rashid, 1999), described this mechanism as it applies to the sedimentation of floccules of clay and organic complexes in the marine environment and stressed the role of saline water in promoting flocculation.

The ability of polymers to sensitise and protect mineral suspension at low and high amounts absorbed respectively had been demonstrated by Van Olphen in 1977 using MC [Carboxy Methyl Cellulose] and sodium (Na^+) montorillonite (Jimo, 2001; Theng, 1999; Valentine, 1997). He noted that there was a narrow range of polyanion concentration ($1x10^{-4}$ – $10x10^{-4}$ g /100ml) over which the flocculation value (i.e. the amount of NaCl required to cause flocculation) was less than that shown in the absence of CMC.

Indeed unchanged polyacrylamide has been used extensively both as flocculant of mineral suspensions and soil aggregate stabilizer (Theng, 1999). It has advantage over polyvinyl alcohol in that both negatively and positively charged functional groups and the polymer are strongly and virtually adsorbed (Schamp & Huylebroeck, 1993).

2.5 Functions of Drilling Muds

The functions of drilling muds include:

- Removal of cuttings from the hole of well bore,
- Controlling the Sub-surface pressures,
- Cooling and lubricating the bit and drill pipe,
- Preventing the walls from caving,
- Releasing the cutting and sand at the well's surface,
- Supplying of down-hole information.

2.5.1 Removal of Cuttings

There are many factors that determine the effective removal of cuttings (drilled out particles or drilled out rock debris) from a well bore (McDonald & Portier, 2003; Greaves, et al., 2001). Some of these factors include; Rheology (viscosity), Density, and Annular velocity. Density and Rheology (viscosity) depend only on the mud, but Annular Velocity depends also on the hole and drill pipe (Greaves et al., 2001; Carl, 1990). Annular Velocity is the velocity at which the mud travels up the hole or annulus of the well (Perricou et al., 2010; Mayes, 2003; Greaves et al., 2001; Carl, 1990). As the mud moves up the annulus carrying the cuttings to the surface, the cuttings tend to slip back down the hole depending on their sizes, shapes and densities. If the pump capacity is able to provide adequate annular velocity, then these cuttings will be effectively deposited on the well surface. The viscosity of the mud is another factor in carrying and lifting of the cuttings. Increase in the mud viscosity results in better lifting and removing of the cuttings (Mayes, 2003).

2.5.2 Controlling the Sub-Surface pressures

The weight of the mud should be greater than that exerted from the formation pressures that have been penetrated whether these encountered pressures are due to water, oil or gas (Mayes, 2003). The hydrostatic pressure of the mud exerted against the formation is of great importance, although there are factors to consider, such as keeping the hole full on trips, and maintaining low gel strength to prevent swabbing (Mayes, 2003) when removing the drill pipe from the hole.

2.5.3. Cooling and Lubricating the Bit and String of the Drill Pipe

There is great heat generated by the drill string, and also by the bottom of the hole. The drilling mud maintains a trouble free hole by lubricating the bit and by forming a

slick surface to the drill string (Fordham et al., 2001). While circulating, the mud flowing to the surface is at a lower temperature than the formation, and this enable the mud to reduce the temperature of the drill string and bit when re-injected. Thus, the generated heat is transferred to the water (the aqueous phase of the drilling fluid) and carried to the surface where it is dissipated (Fordham et al., 2001).

2.5.4 Preventing the Walls from Caving

The drilling mud acts as a suspending agent by forming filter cake against the permeable formations (Perricou et al., 2010; Fordham et al., 2001). The filter cake formation depends on the colloidal fraction of the drilling mud. The filter cake reduces fluid loss to the formations by forming a plugging action against the formation (Mayes, 2003). The cake tends to wall the unconsolidated formations and retards their invasions over the fluid. In troublesome shale areas, the caving of these shales results in fluid invasion which leads to loss of fluid circulation (Chilingarian & Varabutre, 2000). Therefore the mud must not only carry cuttings while circulating but must be able to hold them in suspension when circulation is interrupted.

2.5.5 Supplying of Down–Hole Information

The mud supplies information about the changes in lithology and formation fluids encountered during drilling operation (Perricou et al., 2010; Don & Benze, 2002). This information can be interpreted thus:

- Drill cuttings brought to the surface with mud indicates formations drilled. The mud should alter them as little as possible with its changes in physical and / or chemical properties.
- A change in mud weight indicates a slight kick, not yet discernable by volume increase in surface pit.
- A change in chloride content indicates the presence of evaporates.

2.6 Properties of Drilling Muds

The physical and chemical properties of drilling muds play important roles in the success of a drilling operation. The properties of drilling muds are perhaps the only variables of the entire drilling process that can be easily altered to improve drilling efficiency (Qartar & Giacelo, 2010). These mud properties include:

(a) Density
(b) Filtration properties
(c) Rheological properties
(d) pH value (Acidity and Alkalinity)

2.6.1 Density

Density is very a important property of drilling muds. It is the weight per unit volume of the mud, and has a buoyancy effect upon the particles (Chilingarian & Varabutre, 2000). It should be sufficiently high so that the hydrostatic pressure of the mud acting on the formation should prevent formation's sloughing and influx of fluids (kick), to the well bore (Fordham et al., 2001). It should not exceed a value for which the hydrostatic pressure of the muds exceeds the critical pressure of the rocks at any point in the open hole. The hydrostatic pressure varies with the depth of well and with the mud weight (measured with the mud balance).

The density is related to hydrostatic pressure by this equation (Fordham et al., 2001):

$$d = \frac{10\ p}{h} \qquad 2.1$$

d = Density, p = Hydrostatic pressure, h = Depth

It is necessary to note that;

(a) An increase in density while drilling indicates;

- An increase in the solid content from the formation

- The inflow of a fluid of high density than the density of the mud.

(b) A decrease in density while drilling indicates;

- Inflow of fluids of lower density than that of mud
- Aeration of mud.

2.6.2 Filtration Properties of Drilling Muds

Filtration is the process of separating a heterogenous mixture of fluid and particle of solid (Scarlet & Brene, 2010; API, 2003; Clifford & Cain, 1999; API, 1997; Gray & Darley., 1990; Rogers, 1991). It is a widely used solid – liquid separation process accomplished by means of a filter medium such as screen, filter paper, cloth or porous bed, which permits the flow of the filtrate but retains the solid particles (Anthony & Robert, 2010; Calistus & Mathew, 2004). In the drilling operation, the substance flows vertically onto the filter surface (filter cake) being formed in the process (Jax, 2010; Chilingarian & Varabutre, 2000; Rogers, 1991; Sbittle, 2000). If the driving force (pressure gradient) is constant, the filtration rate decreases with time, that is filtration is inherently a batch operation if particles are allowed to accumulate and are different from filter suspensions of colloidal or even micro sized particles (Troy et al., 2008; Al-Riyainy & Sharma, 2004). Filtration media which retain these particles are often very susceptible to plugging.

Fine particle filtration is often preceded by a pretreatment step such as flocculation or coagulation to increase the particle size of the solids that must be retained (Benna et al., 2001; Clifford & Cain, 1999; Coulson et al., 1999). Through these processes the filtration efficiency is promoted by the introduction of polyelectrolytes to the stream. These polymers provide a variety of effects, including floc formation, molecular bridging and charge reversal (Andrew & Robert, 2007).

These polymers tend to form floc (cake) that covers the filter media in a relatively short time. In a typical operation, the cake gradually builds up on the medium and the resistance of flow progressively increases (Hall & Hoff, 2012; Scarlet & Brene, 2010; Hans, 1990). During the initial period of filtration the flow particles are deposited in the surface layer of the medium forming the true filtering medium. Hence, the factors (Anthony & Robert, 2010; Scarlet & Brene, 2010; Clifford & Cain, 1999; Troy et al., 2008) that determine the rate of filtration include;

(a) Pressure

(b) Time

(c) Area of the filtering surface

(d) Viscosity of the filtrate

(e) Resistance of the filter cake

(f) Temperature

The flow of fluid through porous formations had been described by Henri Darcy (Hall & Hoff, 2012; Scarlet & Brene, 2010; Ukachukwu et al., 2010; Andrew & Robert, 2007; Brandy, 1997). The relations which describes the flow through a filter cake at any particular instance, is the basic filtration equation given as

$$U = \frac{1}{A}\frac{dv}{dt} = \frac{k(-\Delta P)}{\mu L} \qquad 2.2$$

where u = Velocity, based on total area A, v = Volume of filtrate (cm^3), t = Time in minutes, k = Permeabilities in Darcies, p = Differential pressure across the filter cake (atm), μ = Viscosity of filtrate in centipoises, L = Thickness of the filter cake in centimeter.

When the pressure is constant, the filtration rate progressively decreases, and when the pressure increases, the filtration rate becomes constant (Scarlet & Brene, 2010; Calistus & Mathew, 2004). In filtration operation, solid particles are deposited over a period of time, thereby increase the resistance to flow and causing a decrease in filtration rate (Sbittle, 2000). Therefore, it is necessary to determine the rate at which filtrate (the continuous liquid phase of mud) is forced out from the sample under a specified pressure given the filtrate volume (Troy et al., 2008; Longey, 2006; Enie & Giles, 2001).

The filtration properties of drilling muds are indicative of the ability of the solid components or colloidal portions of mud to form a filter cake, and magnitude of cake permeability (Longey, 2006; Enie & Giles, 2001; Chilingarian & Varabutre, 2000). The lower permeability causes thicker filter cake and lower volume of filtrate from the muds of comparable solids concentration. Filtration property is dependent upon the amount and physical state of colloidal materials in the mud (Edmund & Hellmann, 2000; Rogers, 1991). Two types of filtration are involved in drilling an oil well (Hall & Hoff, 2012; Scarlet & Brene, 2010; Chilingarian & Varabutre, 2000):

* Static filtration
* Dynamic filtration

Static filtration occurs when the mud is not in circulation (no circulation) and the formation of filter cake is not disturbed. Dynamic filtration is obtained when the mud is in circulation and the formation of filter cake is not limited by the erosive action of the mud stream (Scarlet & Brene, 2010). Dynamic filtration rates are much higher than static filtration rates and most of the filtrate invading sub-surface formations does so under dynamic conditions (Scarlet & Brene, 2010). When the surface of the rock is first exposed, the rate of filtration is very high and the cake grows rapidly.

However, the growth rate decreases as time goes on until eventually, it is equal to the erosion rate.

The filtration properties of drilling muds are usually evaluated and controlled by the AP1 (American Petroleum Institute) filter loss tests, which is a test under static condition only (Hall & Hoff, 2012; American Petroleum Institute API, 2003; Andy et al., 2000). Therefore it is not a reliable guide to downhole filtration unless both the static and dynamic filtrations are evaluated (Scarlet & Brene, 2010; Horner et al., 2001). However, the AP1 tests are more directly relevant under static condition (during any stopped circulation) while drilling (Andy et al., 2000). Experimentally, it has been found that for static filtration with negligible medium resistance as in the AP1 tests the total fluid loss V per unit area has a square root dependence on time (Hall & Hoff, 2012; Bernu, 2011; Andy et al., 2000; Scarlet & Brene, 2010; Ukachukwu et al., 2010; American Petroleum Institute (API), 2003).

$$V = S\sqrt{t} \quad = St^{½} \qquad 2.3$$

Where S is a constant

This expression shows that the filter cake is continually building up (until no more free suspension remains) and consequently the fluid loss rate ($^{dv}/_{dt}$), decreases with time.

2.6.2.1 Theory of Static Filtration

Assuming unit volume of a stable suspension of substances is filtered against a permeable substrate and x volumes of filtrate are expressed, the 1 – x volume of cake will be deposited on the substrate (Andy et al., 2000; Scarlet & Brene, 2010; Ukachukwu et al., 2010).

Therefore, if Q_c be the volume of cake and Q_f is the volume of filtrate, then

$$\frac{Q_c}{Q_f} = \frac{1-x}{x} \qquad 2.4$$

And the cake thickness (L) per unit area of cake in unit time will be

$$L = \frac{1-x}{X} Q_f \qquad 2.5$$

According to Darcy,

$$\frac{dv}{dt} = \frac{kp}{\mu l} \qquad 2.6$$

Therefore,

$$\frac{dv}{dt} = \frac{kp}{\mu Q_f} \left(\frac{x}{1-x} \right)$$

$$Q_f^2 = \frac{2kp}{\mu} \left(\frac{x}{1-x} \right) t \qquad 2.7$$

From equations (2.4) and (2.6),

$$Q_f^2 = \frac{2kp}{\mu} \left(\frac{Q_f t}{Q_c} \right) \qquad 2.8$$

If A is the area of the filter cake, then

$$Q_f^2 = \frac{2kpA^2}{\mu} \left(\frac{Q_f t}{Q_c} \right) \qquad 2.9$$

It has been found that if a mud is filtered through filter paper at constant temperature and pressure, Q_f is proportional to $t^{1/2}$, apart from a negligible zero error. It follows that for a given mud, $^{Qf}/_{Qc}$ and k in equation 9 are constant with respect to time. This forms the basis for the mechanics of static filtration (Hall & Hoff, 2012; Andy et al., 2000; Scarlet & Brene, 2010; Ukachukwu et al., 2010).Thus, the filtration properties of diverse muds can be evaluated by measuring the filtrate volume accumulating in a given time and standard conditions.

2.6.3 Rheological Properties of Drilling Muds

Rheology is the science of the de-formation and flow of matter (Bryan et al., 2010; Candy & Justus, 2006; Qartar & Giacelo, 2010; Dahlgreen & Helbig, 2008; Beihoffer et al., 2008; Jay & Bruce, 2005; Akran, 1992; Alderman et al., 2008; Utrack, 2001). It has its greatest impart on the flow behaviour of suspension in pipes and other conduits (Bryan et al., 2010; Alderman et al., 2008; Benna et al., 1999). The important rheological characteristic required of drilling mud for good operational performance is that it should be capable of sustaining a sufficiently large stress to maintain cuttings in suspension, particularly when fluid circulation is stopped (Qartar & Giacelo, 2010; Dahlgreen & Helbig, 2008). The viscosity of the mud should also be moderate for efficient pumping (Stewart, 2009; Candy & Justus, 2006). The rheological properties of suspensions containing polymerically stabilized particles have been studied (Brown, 2009; Eyler & Pastecck, 2005; Hale & Mody, 1996). The effect of polyacrylate and fatty alcohol (different thickness) on the rheological properties of finely dispersed oil/water emulsion studied showed a simple non Newtonian flow behaviour with a yield points (Hofmann et al., 1995). An understanding of the rheology of drilling muds is very essential so that the mud engineers will effectively carry out their functions at the rig-site.

2.6.3.1 Viscosity

Viscosity is the resistance to the flow of a fluid when the fluid is subjected to shear stress (Lee, 2012; Qartar & Giacelo, 2010; Rob et al, 2006; Carriere, 1999; Alderman, et al., 2008). It is very important in drilling muds because it affects the efficiency of their lifting capacity. The rheologists are primarily interested in the relationship between flow pressure and flow rate as well as the influence of the flow characteristics of the fluid (Bryan et al, 2010; Troy et al, 2008; Mandy, 2001; Bingham, 2000; Uttrack, 2001; Akran, 1992; Barnes, et al., 1999). There are basically two flow regimes (Bryan et al., 2010):

(a) The laminar flow regime:- this prevails at low viscosities. In this relationship, flow is orderly and the pressure-velocity relationship is a function of the viscous properties of the fluid.

(b) The turbulent flow regime: this prevails at high viscosities. Flow is disorderly and is governed by the inertia properties of the fluid in motion.

The laminar flow equations relating flow behaviour to the flow characteristics of the fluid are based on certain flow models namely; the Newtonian, the Bingham plastic (Bingham bodies), the Pseudoplastic, and the Dilatant (Staben et al., 2004; Bingham, 2000; Akran, 1992). Only the first three are of importance in drilling mud technology (Bryan et al., 2010; Staben et al., 2004; Alderman et al., 2008; Gray & Darley, 1990; Rogers, 1991). Most drilling muds do not conform exactly to any of these models but their behaviours can be predicted with accuracy sufficient for practical purposes by one or more of the models (Staben et al., 2004). Flow models are usually visualized by means of consistency curves, which are plots either of flow pressure versus flow rate or shear stress versus shear rates (Obong, 2004; Staben et al., 2004; Alderman et al., 2008). The concept involving

shear stress and shear rate and their measurement enables the mathematical description of the flow of drilling muds (Staben et al., 2004). The amount of force applied to a fluid determines the shear rate, which in oil field is determined by the flow rate of the mud through a particular geometrical configuration. Resistance of the fluid to the applied rate of shear or force is called the shear stress (Obong, 2004; Staben et al., 2004). Thus,

$\gamma = dv/dr$ 2.10

Where γ = rate of shear, v = velocity, r = distance from a pipe wall.

The shear stress τ is given as:

$\tau = F/A$ 2.11

Where F = applied force, A = surface area to the force. Shear rate and shear stress are two basic measurements that are widely utilized in the petroleum or oil industries and their relationship defines the type of flow of their relationship mud. Measurement of the relationship between the shear stress and shear rate in drilling muds employs the use of viscometers (Obong, 2004; Staben et al., 2004; Alderman et al., 2008)The most common viscometer include cup and bob type, field viscometers, capillary viscometers and rotational viscometer, etc. (Staben et al., 2004).

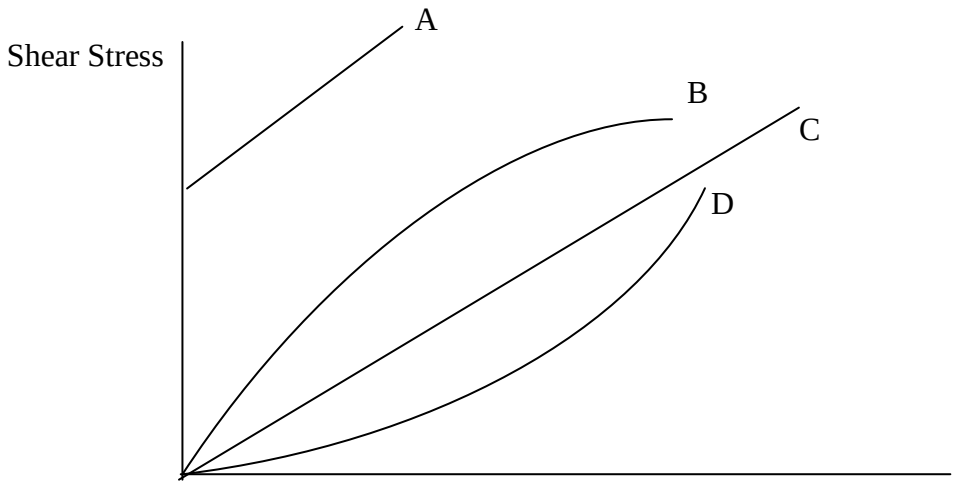

Figure 2.16: Relationship between shear stress and shear rate for various fluids. A = Bingham Plastic, B = Pseudoplastic, C = Newtonian, D = Dilatant. (Michael, 2009; Alderman et al., 2008; Obong, 2004; Staben et al., 2004; Mandy, 2001)

2.6.3.1.1 Newtonian Flow Model

Flow curves or viscosity curves are used to describe the flow behaviours of fluids (Alderman et al., 2008; Stewart, 2009; Obong, 2004; Staben et al., 2004). In flow curves, the shear rate of a sample is plotted against the shear stress which produces shearing. If the flow curve passes through the origin of the co-ordinate system and if there is a linear relationship between shear stress and shear rate, the fluid is said to be Newtonian (Stewart, 2009; Alderman et al., 2008; Obong, 2004; Staben et al., 2004). In Newtonian fluid, the constant of proportionality between shear stress and shear rate is the viscosity (Stewart, 2009).

$$\text{Viscosity} = \frac{\text{Shear stress}}{\text{Shear rate}} \qquad 2.12$$

2.6.3.1.2 Bingham Plastic Flow Model

Bingham plastic fluids are non-Newtonian fluids which have no linear relationship between shear stress and shear rate at the origin (Stewart, 2009; Michael, 2009; Alderman et al., 2008; Bingham, 2000). Non-Newtonian fluids are broadly classified as time independent fluids (Stewart, 2009). This means that the relationship between shear stress and shear rate in a non-Newtonian fluid does not depend on the time for which the fluid has been previously sheared, that is its previous history. In time independent fluids, the rate of shear at any point in the fluid is some function of the shear stress at that point. Examples of these fluids are fluids which have the characteristics of both viscous liquids and elastic solids and exhibit partial elastic recovery after deformation, the so called viscoelastic fluids (Carriere, 2009; Houwink & Dedecker, 1991). Another particular species of non- Newtonian fluids are those which have a yield value. The yield value is the minimum shear stress needed to produce viscous flow and the viscosity of these fluids is dependent on the shear rate, and is known as apparent viscosity (Michael, 2009; Vincent et al., 2001; Mandy, 2001).

Plastic fluids were first recognized by Bingham and are referred to as Bingham plastics or Bingham bodies (Carriere, 2009; Mandy, 2001; Houwink & Dedecker, 1991). They are distinguished from Newtonian fluids with the fact that they require a finite stress to initiate flow and are successfully used to describe drilling muds. Bingham plastic consistency curve tends to be linear at rotor speed /very high shear stress above that required to keep all the fluid in the annulus in laminar flow (Carriere, 2009; Houwink & Dedecker, 1991). But drilling muds deviate from linearity at low shear rates. This deviation becomes apparent when behaviours are examined in a multispeed viscometer. The degree of deviation from linearity in the consistency

curves of drilling muds using rotary viscometer differ from mud to mud, depending on the concentration, size and shape of the particles (Carriere, 2009; Rogers, 1991).

The viscosity, of Newtonian fluids such as water and mineral oil is a function of temperature and pressure but independent of shear rate, while the viscosity of non-Newtonian fluids depends on temperature, pressure, shear rate and molecular weight (Rogers, 1991).

2.6.3.1.3 Pseudoplastic Flow Model

Pseudoplastic fluids are fluids whose consistency curves pass through the origin and are non linear, but approach linearity at high shear rates (Bryan et al., 2010; Michael, 2009; Obong, 2004; Staben et al., 2004; Mandy, 2001). They have no yield point except when the stress reading are taken at high shear rate extrapolated back to axis. Suspensions of long chain polymers are typical pseudoplastic (Bryan et al., 2010; Staben et al., 2004; Mandy, 2001).

The equation relating shear stress and shear rates under these experimental conditions is called Power Law equation (Bryan et al., 2010; Ukachukwu et al., 2010; Qartar & Giacelo, 2010; Michael, 2009; Obong, 2004; Staben et al., 2004; Mandy, 2001), given as:

$$\tau = k \gamma^{n} \qquad 2.13$$

Where τ = shear stress, k = consistency index, γ = shear rate, n = power law index which characterize the type of fluids flow. The value of n describes three flow models:

(a) Newtonian, n = 1, viscosity does not change with shear rate.

(b) Pseudoplastic, n < 1, viscosity decreases with shear rate.

(c) Dilatant, n > 1, viscosity increases with shear rate.

Herschel – Bulkely equation, $\tau = \tau_o + k \gamma^n$, is also in use, where τ_o = yield stress and k = consistency index (Bryan et al., 2010; Qartar & Giacelo, 2010; Obong, 2004; Staben et al., 2004).

2.6.3.1.4 Thixotropic Flow Model

This flow model is time dependent. Thixotropy is a phenomenon by which the viscosity of a fluid decreases with time (Jax, 2010; Gray & Darley, 1990). Most fluids are thixotropic (viscosity decreases with time under constant shear stress or shear rate) while some are rheopectic or antithixotropic (viscosity increases with time under constant shear stress or shear rate) (Jax, 2010; Eyler & Pasteck, 2005). The term thixotropy was first used to describe an isothermal reversible decrease of viscosity due to mechanical agitation. The phenomena, observable in multiphase systems, are related to molecular or macroscopic changes in association (Eyler & Pasteck, 2005; Utrack, 2001). The effect of thixotropy on the evaluation of the rheological parameters of drilling muds was first investigated by Jones and Babson (Gray & Darley, 1990). They observed the changes in torque with the passage of time, when thixotropic muds were sheared at constant rate in a MacMicheal viscometer.

Thixotropic fluids form gels under dynamic conditions (Rob et al., 2006). Most water-based muds exhibit this property because of the electrically charged particles that tend to link together at low shear rates (Rob et al., 2006; Vincent et al., 2001; Leung & Steig, 1992). The strength of the gel structure formed is a function of the amount and type of solids or colloidal particles, time, temperature and chemical constituents of the mud.

2.6.3.1.5 Factors that affect viscosity

Viscosity has the following dependence:

(a) shear rate dependence

(b) molecular weight dependence

(c) temperature dependence

(d) pressure dependence

(e) time dependence

2.6.3.1.5.1 Shear- Rate Dependence

Most non Newtonian solutions are defined with power law equation (see equation 2.13).

Newton's law of viscosity for Newtonian fluid is defined as:

$$\tau = \mu \gamma \qquad 2.14$$

The above equation 2.14 is called the Generalized Newtonian Fluid (GNF) model (Stewart, 2009; Bingham, 2000; Alderman et al., 2008; Barnes et a l., 1999). The actual analytical relationship between shear stress (τ) and shear rate (γ) and therefore, the dependence of viscosity (μ) on shear rate are given by the constitutive equation of the material.

Polymers prepared in concentrated solutions display three characteristic regions as illustrated in fig.2.17. At low shear rates, μ is nearly independent of γ (i.e., Newtonian behaviour) and approaches a limiting zero shear rate value of μ_o. At higher γ, μ decreases with increasing γ. Fluids that display this behaviour are termed shear thinning (Qartar & Giacelo, 2010; Alderman et al., 2008; Staben et al., 2004; Rogers, 1991). Finally, μ once again approaches a limiting Newtonian plateau, $\mu\infty$, at very high γ.

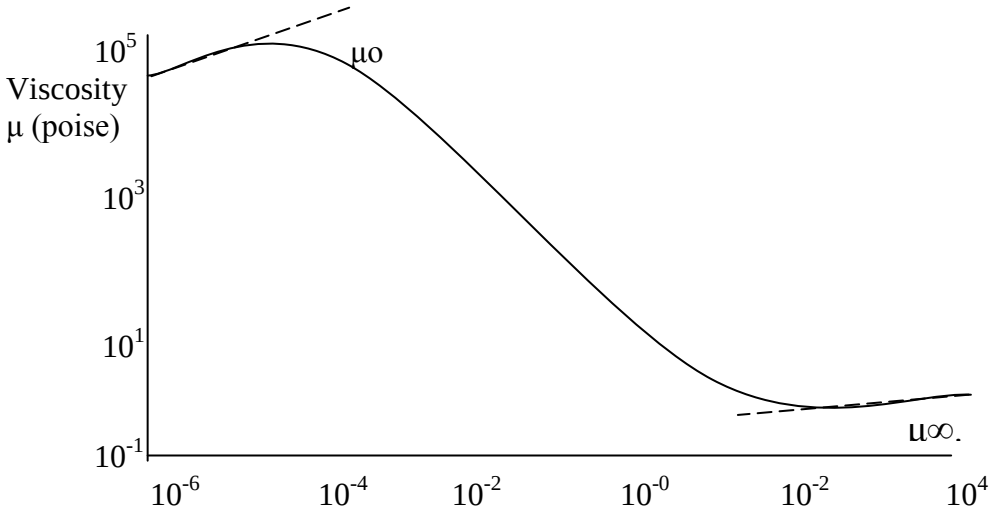

Figure 2.17: Typical shear rate dependence of viscosity.

(Qartar & Giacelo, 2010; Staben et al., 2004; Rogers, 1991)

The molecular basis for shear thinning behaviour is the effect of shear on entanglements. At low shear rates, the entanglements impede shear flow and, therefore, viscosity is high. As the shear rate in creases, chains begin to orient in the flow direction and disentangle from one another, the viscosity begin to decrease. Finally, the molecules become fully oriented in the flow direction at very high shear rates. At this point, stable entanglements are no longer possible and the viscosity reaches a low level that is again independent of shear rate (Qartar & Giacelo, 2010; Staben et al., 2004; Rogers, 1991Alderman, 2008).

2.6.3.1.5.2 Molecular Weight Dependence

The significance of entanglement to shear thinning flow suggests that molecular weight should significantly influence the rheological properties of polymers (Candy & Justus, 2006; Staben et al, 2004). The zero – shear viscosity μo is directly related to the weight – average molecular weight, Mw (Candy & Justus, 2006). In addition, the onset of shear thinning behaviours occurs at progressively lower shear rate as

molecular weight increases (Dahlgreen & Helbig, 2008). The viscosity of polymer mud increases with increase in molecular weight. Therefore high molecular weight polymers build high viscosity of the drilling muds (Candy & Justus, 2006). The presence of some very high molecular weight polymer in drilling muds provides drag reduction along the walls of their hole, and so increases output rate or general flow rate (Candy & Justus, 2006; Fordham et al., 2001). These polymers enhance the lubricating properties of muds due to the chemical nature of the oil-wetting surfactants and the inherent lubricity of the oil itself.

2.6.3.1.5.3 Pressure Dependence

Viscosity of polymer muds can be significantly affected by pressure. This pressure dependence may be an important consideration in the choice of materials for the formulation of drilling muds and design of drilling operations. At constant temperature, the effect of pressure on viscosity can be approximated by the relation (Fordham et al., 2001; Fried, 2000).

$$\text{In}\left[\frac{\mu}{\mu_r}\right] = \beta[P - P_r] \qquad 2.15$$

Where μ_r = reference viscosity, P_r = reference pressure, β = pressure coefficient in the range 0.87 to 4.93 x 10^{-8} pa^{-1}.

Also, the effect of pressure on the viscosity of muds in the annulus in the case of laminar flow can be determined by this Bingham equation (Stewart, 2009; Fordham et al., 2001):

$$\Delta p = \frac{LY_p}{225d} + \frac{LP_v}{1500d} \times V_f \qquad 2.16$$

Where Δp = pressure drop, L= length or depth,

Y_p = yield point, p_v = plastic viscosity,

V_f = velocity of the drilling mud.

d = hole diameter minus pipe diameter

2.6.3.1.5.4 Temperature Dependence

Temperature equally affects the viscosity of the drilling muds. With increase in temperature, there is decrease in molecular cohesion and this decreases viscosity (Fried, 2000).

2.6.3.1.5.5 Time Dependence

In some cases, the viscosity of some fluid decrease with time. The subsequent flow behaviour of a previously sheared fluid may depend upon the prior shear history and the time allowed for recovery. A fluid whose viscosity is reduced by prior deformation or decrease with time under conditions of constant stress or shear rate is called thixotropic (Fried, 2000). Eventually, the viscosity will recover (increase) once the stress is removed. Similarly, a fluid whose viscosity has increased as a result of prior deformation history increase with time under application of constant stress or strain is called antithixotropic (Fried, 2000).

2.6.3.2 Gel Strengths

Gel strength indicates the thixotropic properties of a drilling mud and the measurements of attractive forces under static conditions in relation to time (Rob et al., 2006; Carl, 1990). It occurs in drilling muds due to the pressure of electrically charged particles when fluid circulation is stopped. It depends upon solid concentration, chemical treatment, time and temperature (Vincent et al., 2001).

There is no well established mathematical means of predicting gel strengths in any mud system (Rob et al, 2006). Generally, gel strength increases with time and amount of solids and temperature. If the mud system is not successfully treated for temperature stability, the gel strength developed after a bit trip becomes a major factor in the pressure required to break the circulation. Gel strength of drilling muds used for drilling wells with low bottom hole temperature is measured with instruments that

have coaxial cylinders such as the “Fann direct indicating viscometer” (Vincent et al., 2001). High gel strength is necessary for restoring lost circulation.

In addition, initial gel strength in a weighted mud system must be sufficient to prevent setting of weight materials (Vincent et al., 2001). Therefore the drilling mud engineer must be concerned with sufficient initial gel strength of the mud. Gel strength is a major rheological property of drilling mud, which is observed when a coagulative structure is formed and helps to suspend the drilled particles of the rock during any stopped circulation (Vincent et al., 2001). The strength of this structure is accessed by the magnitude of stress required to make the fluid flow. It is conventionally common in drilling mud by two operations to characterize the strength, namely (Vincent et al., 2001; Rogers 1991).

Initiate Θ_1- which is measured 1 minute after stirring

Initiate Θ_{10}- which is measured 10 minutes after stirring

Two types of Gel strength occur in drilling muds- progressive gel strength and fragile gel strength (Rob et al., 2006).

A progressive gel strength increases substantially with time. This type of gel strength requires increased pressure to break circulation after shutdown. A fragile gel-strength increases only slightly with time, but may be higher initially than a progressive gel-strength. If gel strength measurements are taken after 30 minutes, the strength of the gel formed by the mud can easily be determined (Rob et al., 2006). Progressive and fragile gel strengths are illustrated below:

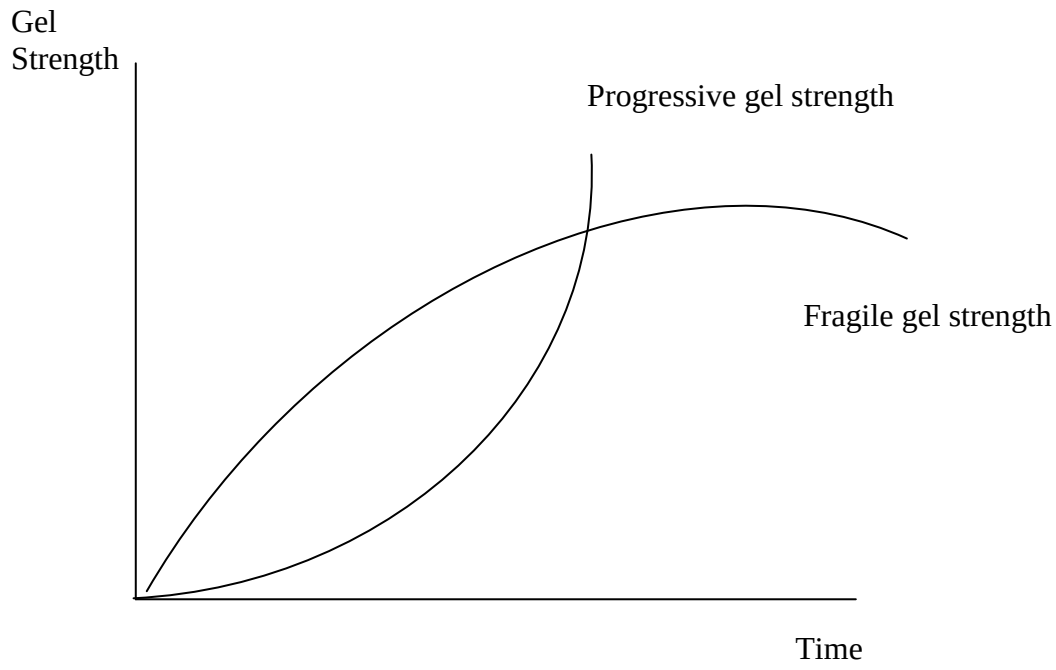

Figure 2.18: illustration of progressive and fragile gel strength. (Rob et al., 2006)

2.6.3.3 Shear Thinning

The viscosity of an ideal drilling mud decreases with increasing shear rate, and this is called shear thinning (Bryan et al., 2010; Qartar & Giacelo, 2010; Ukachukwu et al., 2010; Rob et.al, 2006; Rogers, 1991; Alderman et al., 2008). Water-based muds generally exhibit shear thinning but oil based muds may not be shear- thinned because in most cases their viscosities increase with increasing shear rate (Qartar & Giacelo, 2010). The drilling rate is affected by viscosity which affects the bottom hole cleaning, cuttings removal and hydraulics (Rob et al., 2006). The teeth of the bit impart large shear to the drilling mud, thin it, and displace it before rock is contacted. The energy required for this purpose is viscosity dependent. For instance, very high viscosity of drilling muds provide an effective viscous cushion, which softens and reduces the impact of the bit teeth resulting in slower penetration rate (Bryan et al.,

2010; Rob et al., 2006). In the case of a polymer mud, which is a shear thinning mud, decreasing the upward velocity in the large portion of bore hole is automatically compensated for by an increase in viscosity (Bryan et al., 2010; Rob et al., 2006). Conversely in the case of other types of muds, the pumping rate must be increased or more viscosities must be added to increase the pressure drop in the annulus Therefore, a better hole-cleaning is achieved with shear thinning muds because of a flatter velocity profile in the annulus (Bryan et al., 2010; Rob et al., 2006).

2.6.3.4 Yield Point And Plastic Viscosity

Yield point and plastic viscosity are dynamic proepties and should not be confused with static properties (Bryan et al., 2010; Rob et al., 2006). However, yield point and gel strength are slightly related because yield point decreases as gel strength decreases (Bryan et al., 2010; Rob et al., 2006; Vincent et al., 2001). Sliding of layers (typical feature of the laminar flow of the Newtonain Liquid) in a flowing plastic fluid is observed at the peripheral part of the stream (Bryan et al., 2010). The central part of the plastic fluids stream is a plastic body and it moves like a plug. The velocities of the plugs layers are the same. On the boundaries of the plug, the tangential stresses are equal to the yield value τ_o (Bryan et al., 2010). To destroy part of the plug, it is necesaary that the tangential stresses between the adjacent layers in this part should exceed the yeild value. The flow of a plastic body is described by this Bingham equation (Bryan et al., 2010; Rob et al., 2006).

$$\tau = \mu \frac{dv}{dr} + \tau_o \qquad 2.17$$

where μ = plastic viscosity in Pa.s, τ_o = yield value in Pascal.

The velocity profiles of laminar flow of a plastic fluid (e.g polymer mud) differ in the central part of the stream from the velocity profiles of the corresponding laminar flow of a Newtionian fluid (Bryan et al., 2010; Rob et al., 2006) . Therefore, the laminar mode of flow in a plastic fluid is commonly referred to as plastic flow (the velocities profiles in the central part of the stream do not change). The profiles of flow velocities for plastic fluid and Newtonian fluid are shown below.

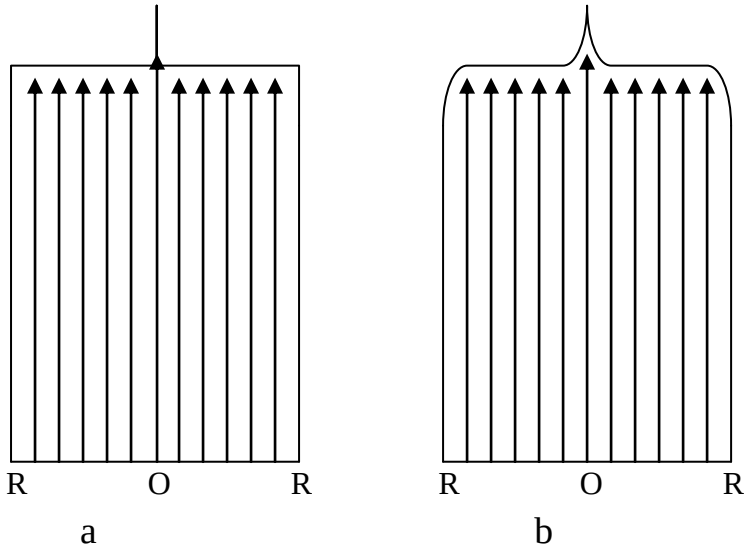

Figure 2.19: (a) Plastic flow velocities of a plastic fluid

(b) Laminar flow velocities of a Newtonian fluid

(Bryan et al., 2010; Rob et al., 2006)

Yield point and plastic viscosity are important rheologocal parameters that are used as parts of maintenance guide at the well site to evaluate drilling mud performance (Rob et al., 2006; Vincent et al., 2001). The plastic viscosity is sensitive to concentration of cuttings, hence needs dilution treatment. Also, the yield point is sensitive to electro-chemical environment,hence needs chemical treatment. Both the yield point, yp and plastic visocosity Pv are determined with the aid of Fann V.G. viscometer (a rotational viscometer) (Bryan et al., 2010; Rob et al., 2006; Vincent et al., 2001).

2.6.4 Biodegradable properties of Drilling Muds

Biodegradable properties of polymers are those properties that make polymers susceptible to biological or micro- organisms' attack (Scott et al., 2007; Mickey & Duke, 2005; ; Mario, 2003; Lenz, 1993). Biodegradation of polymers is the degradation process by which micro-organisms decompose or break-down polymers into their smaller units or micro molecules such as carbon dioxide , methane, water, or biomass (Mickey & Duke, 2005; Mario, 2003). It is not all polymers that are biodegradable; naturally-occurring polymers are more biodegradable than synthetic polymers (Mickey & Duke, 2005; Mario, 2003; Gautier & Lecourtier, 2002). More specifically, polymers containing ester functionality, particularly aliphatic polyesters, are potentially biodegradable. It is believed that biodegradation of these polymers proceeds by attack of the ester groups by nonspecific esterases produced by ground microflora combined with hydrolytic attack (Mickey & Duke, 2005; Gautier & Lecourtier, 2001). Products of the degradation can be quickly metabolized by micro-organisms. Most naturally occurring polymers are completely biodegradable. Therefore, drilling muds produced from biodegradable polymers are biodegradable ((Scott et.al, 2007; Jones & Mark, 2006; Mickey & Duke, 2005).

Generally, degradation of polymers has been known since the earliest times and there are several examples, such as the deterioration of cellulose in wood etc (Jones & Mark, 2006). The types of degradation process vary depending on the environmental conditions in which the polymer is used, the manufacturing history and the structure of the polymer (Feiffer & Vierty, 2002).

Traces of impurities and various structural irregularities are often taken to be responsible for either causing or accelerating degradation of polymers. For many

polymers, hydroperoxides, carbonyl groups (unsaturated carbonyl), radicals (Benzoyl peroxide) are among the major initiating factors of degradation in the polymers (Fried, 2000).

However, biodegradation is specific to only polymers which contain functional groups that are attacked by micro-organisms (Scott et.al, 2007; Mickey & Duke, 2005). Polymer muds prepared from these polymers also possess the property of biodegradability. ASTM standard D-5488-94 defines biodegradable as "capable of undergoing decomposition into carbon dioxide, methane, water, inorganic compounds, or biomass in which the predominant mechanism is the enzymatic action of micro organism, that can be measured by standard tests, in a specified period of time, reflecting available disposal conditions" (Mickey & Duke, 2005; Mario, 2003; ASTM, 2000).

Most polymers obtained from natural resources are completely biodegradable. Standards have been developed by some organization like International Standard Organization and the American Society for Testing and Materials (ASTM) (Mario, 2003; ASTM, 2000), specifying the Conditions at which a polymer biodegrades, what constitutes a biodegradable polymer and the number of additives used in the polymer. Biodegradability is also dependent on particular environmental conditions. Among these conditions are two necessary factors, which include high temperature and water, and in the absence of either of these factors, biodegradation will be inhibited (Mickey & Duke, 2005; Mario, 2003). Again, some polymers are biodegraded in a specific period of time.

2.7 Biodegradability of Drilling Fluids

The biodegradability of petroleum products is dependent on the chemical structure of their various components (Chimere, 2011). Compound resistance to biodegradation increases with increasing molecular weight. The oils used in OBM can be classified according to their aromatic hydrocarbon concentration, which contributes to fluid toxicity (Zac et al., 2012). However, the relations between hydrocarbon physico-chemical properties and biodegradability have been little studied. Several works (Zhanpeng et al., 2002), dealing with - laboratory techniques of biodegradability determination and the influence- of experimental conditions, showed the variation of the results according to the used method and considered conditions. In general, the more soluble, lighter petroleum hydrocarbons are more biodegradable than the less soluble, heavier members of the group. Viscosity is also known to have an important impact on biodegradability. Highly viscous hydrocarbons are less biodegraded because of the inherent physical difficulty in establishing contact among contamination and microorganisms, nutrients, and electron acceptors compounds (Cole, 2004). The viscous diesel oil at high amount (>10%) shows low biodegradation rate (4%), but, in the presence of mixed culture *(Enterobracter sp., Citrohactcr freundii, Erogenous Pseudomonas, Staphylococcus auricularis, Bacillus thuringiensis, micrococcus varians,…..)* it presents good biodegradation properties (Khodja, 2008). Moreover; the biodegradation behaviour of diesel oil does not obey that of individual compounds. With high amount of aromatics in diesel oil (33%), the difficulty was considerable to relate diesel oil biodegradability to its composition. Numerous works showed good correlation between biodegradability and some physical and chemical parameters (Haus et al., 2003) demonstrated that biodegradability decreased with increasing amounts of aromatic and/or polar

compounds. He showed that kinematic viscosity is the significant factor in biodegradability variation with chemical composition and oil physical and chemical properties. (Hongwei et al., 2004; Zhanpeng et al., 2002) based their method to calculate biodegradability on three parameters: F30D5/COD (biological oxygen demand after 5 days/ chemical oxygen demand) ratio, CO_2 production and microorganism activity by ATP (adenosine triphosphate). On the chemical structure scale, some works (Hongwei et al., 2004) showed that biodegradability was a function of total energy and molecular diameter.

2.8 Drilling Fluid Technology

Drilling fluid technology is in constant evolution due to: (i) rapid expanding needs due to more severe conditions, such as high temperature and pressure, tight gas and shale-gas reservoirs, (ii) increasing technical demands, such as increased lubricity requirements in air drilling and (iii) growing restrictions on oil-based systems, such as environmental remediation (Paulsen et al., 2002; Song et al., 1990). To comply with the new government regulations restricting the use of some technologies or practices, drilling fluid manufacturers have responded by developing acceptable alternatives (Caleb & Dan, 2004, April 16; Bland, 1998; Ward & Williamson, 1996). However, these solutions usually have substantial added costs and limitations that are sometimes prohibitive. In summary, drilling fluid's development needs to encompass the design of new environmentally acceptable WBM and oil-like systems that will provide alternatives to OBM. Such new drilling fluids should provide superior filtration control to minimize fluid invasion damaging permeable zones. The properties of the resultant mud cakes should prevent sticking of the drill pipe against the borehole wall due to differential-pressure (Himel & Lee, 1991). Particularly, in horizontal or high-angle wells, these new fluids should also provide adequate hole- cleaning capabilities.

The study of cuttings transport flow, air foam behavior and fluid viscoelastic behavior will help understanding and improving this process (Growcock et al., 2002; Getliff et al., 2000).

In order to attain greater efficiencies and cost savings, the main point in a Research and Development (R & D) program is the consideration of all the consequential aspects of drilling technology or drilling and Excavation technologies (Hudson, 1999, April 15). Such additional R & D should focus on the 'Development of environmentally-friendly drilling fluids', designing non-toxic drilling fluids and foams as alternatives to toxic OBM which are moreover difficult to remove from the drill hole (Perricou et al., 2010; Caleb & Dan, 2004, April 16; Retz et al., 1991).

2.8.1 Optimization of drilling fluid performances

Drilling optimization in oilfields is usually formulated by using mathematical models. In these models, some parameters appear to be fundamental. These include:

- **Fluid density**

Density is the first parameter to consider. For desired densities greater or lower than 1, WBM or OBM can be used, respectively (Prutt & Iudson, 1998). The latter are recommended especially for clay formations where this density should be sufficient for drilling. Generally, for both WBM and OBM, mud weight (density) can be increased by adding various solids or soluble materials. Other undesirable solids issued from geological drilled formations are not easily removed but will be reduced to finer particles, which could have some adverse effects on mud properties (Rahman et al., 1995; Renard & Dupuy, 1991). The way to avoid such undesirable phenomena is to use high-speed shale shakers. In additional stages, to remove finer solids down to the 1 jam range, these devices are equipped with 50- to 100-mesh screens, using

desanders, desilters, mud cleaners, and centrifuges (Shenglai et al., 2008; Tare & Mody, 2000; et al., 1997; WardZamori et al., 1990). Undesirable solids that are less than 1 jam can only be removed chemically using medium- to high-molecular-weight flocculants. In addition, some recommendations specify the effects of size on rheology and fluid performances. Solids less than 1 jam have 12 times more effect on drilling rate than larger particles (Likos et al., 2004; Pernot, 1999). For these solids less than 1 jam, the shearing stress required to start the fluid motion will be greater than for larger particles.

- **Viscosity**

The second parameter to consider is viscosity. It is a general term used to define the internal friction generated by a fluid when a force is applied to cause it to flow. This internal friction is a result of the attraction between the molecules of a liquid and is related to a shear stress. The greater is the resistance to the shear stress, the greater is the viscosity. In fact, standard viscosity measurements do not define flow behavior within shear rate ranges imposed at the annulus, and pits. The viscosity at the bit affects penetration rate, which will be better when viscosity is lower. The viscosity in the annulus affects hole cleaning efficiency and the viscosity in the pits influences the effectiveness of solids separation techniques (Cambel et al., 2007; Civan, 2000; Cook et al., 1993).

Numerous additives are added to the formulation in order to reach optimized specific purposes which are sometimes contradictory. For example, mud has to be viscous enough in order to be able to lift the cuttings to the surface, but at the same time, viscosity must not be too high in order to minimize friction pressure loss (Clark et al., 2006; Edmund & Hellman, 2000; Horsud et al., 1998).

- **Fluid loss**

The loss of drilling fluids is the last considered parameter. It is generally defined as the volume of the drilling mud that passes into the formation through the filter cake formed during drilling (Shahri, 2012). It is often minimized or prevented by blending the mud with additives (Dalmazzone et al., 2006; Chang & Civan, 1997). A number of factors affect the fluid-loss properties of a drilling fluid, including time, temperature, cake compressibility; but also the nature, amount and size of solids present in the drilling fluid (Darly, 1999).

In high-pressure and high-temperature environments, optimization of the above mentioned three parameters is essential to lighten instability problems when drilling through shale sections (Lee, 2012; Shadravan, 2012; Thaemlitz, 2009; Van-Oort et al., 2001). Under these conditions, selection of suitable mud parameters can benefit from analyses that consider significant thermal and chemo-mechanical processes involved in shale-drilling fluid interactions (Van-Oort et al., 1996).

Nevertheless, some other factors are not taken into consideration in these mathematical models For instance, it has been widely experienced that random factors related to soil layers, drill bits, and surface equipment, greatly affect drilling performance (Shadravan, 2009). Optimization involves the post-appraisal of offset well records to determine the cost effectiveness of related variables, which include mud and bit types, weight on bit, and rotary speed (Anderson et al., 1991). Stochastic models are introduced to describe such random effects. This more practical model provided a better characterization for real oilfield situations as compared with other deterministic models, and has been demonstrated to be more efficient in solving real design problems. For drilling fluid additive evaluation, five important parameters

have been proposed: Main function and chemical nature, Compatibility/salt tolerance with other additives and temperature limitations, Recommended treatment range and cost, History/success of using, Interferences, damage and risk such as geological interpretation effects, formation damage, health safety and environment (HSE) and waste treatment.

2.8.2 Drilling costs

Remediation costs attributable to drilling are not easily estimated. The difficulty of access, the type of pollutant present, and the nature and time of derived treatment will influence the total cost. In oilfield operations, drilling costs typically account for 50 to 80% of exploration finding costs, and about 30 to 80% of subsequent field development costs (Anderson et al., 1991). Typical costs for shallow hydrocarbon wells (up to 1250ft depth) drilled in the United States are about $27/ft (Anderson et al., 1991). The boreholes required for environmental remediation will be shallow, so it might be expected that their cost will range between $20 to $30/ft. similar to shallow petroleum wells. However, special circumstances may increase these costs substantially. If the drilled solids contain toxic or radioactive substances, the drilling cost may increase dramatically because of the need to collect, document, and dispose the cuttings and to decontaminate drilling equipment (Hudson, 1999, April, 15; Iudson & Nicholson, 1999).

2.8.3 Shale problems during drilling

The stability of a drilling fluid is generally guaranteed by its homogeneity after a long aging period (Bol et al., 2002; Amaefule et al., 1998). For OBM systems, a phase separation and a viscosity decrease are direct indications of drilling fluid degradation. In WBM, phase separation is also an indicator of mud instability.

Mud viscosity affects the dispersion and the swelling of shales and decreases the diffusion velocity on porous medium. Muds with high viscosity and a minimum filtrate volume are preferred for inhibition efficiency, according to classical filtration equations (Uachukwu et al., 2010; Hale & Mody, 1992). In terms of its composition and properties, the mud column (i.e., the vertical column of drilling mud in the borehole) is a dynamic system whose characteristics are frequently changing dramatically both in time and space (Bradley, 1999; Ding et al., 1996). Mud composition changes as shales migrate into the column and are dispersed into the mud, or by chemical interaction between the mud and the formation.

2.8.4 Shale instability

Wellbore instability is the largest source of trouble, waste of time and over costs during drilling. This serious problem mainly occurs in shales (principally clays), which represent 75% of all formations drilled by the oil and gas industry (Bol et al., 2002). The remaining 25% are composed of other minerals such as sand, salt, etc. The physical properties and behavior of shale exposed to a drilling fluid depend on the type and amount of clay in the shale.

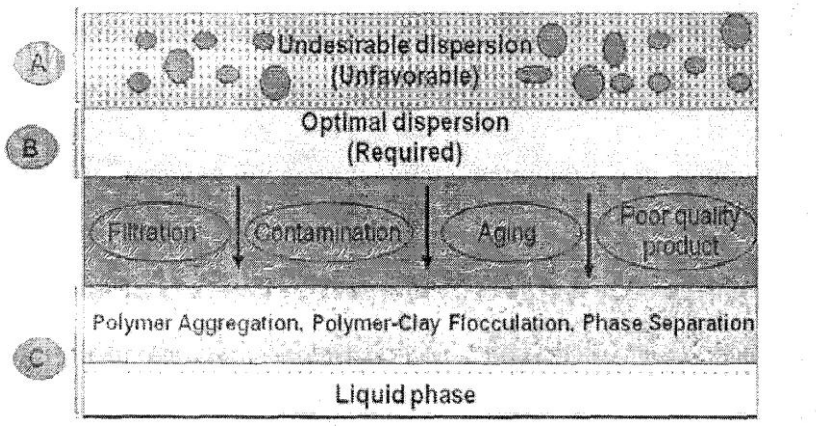

Figure 2.20: Representation of drilling fluid destabilization (Phase separation: low viscosity and high filtrate) (Khodja et. al, 2010; Bol et al., 2002)

A: Undesirable dispersion with an inhornogeneous additive repartition. Solid-liquid, polymer-solution, dispersed phase-continuous phase are inhomogeneous and unstable.

B: Optimal dispersion with a uniform repartition of additives. The mud system is stable and exhibits good rheological and filtration characteristics.

C: The mud system is unstable for one of the following reasons: dramatic filtration conditions (pressure and temperature), use of incompatible additive (contaminant) or of poor quality products, or considerable aging. Solids, polymers, and salt in WBM, dispersed phase, emulsifiers or others additives in OBM are separated from continuous phase. The system presents a phase separation, involving a degradation of rheological parameters and a high lilirate volume.

Wellbore stability issues were not seriously addressed until the end of the 70s, when a famous published paper initiated great interest for this topic in the industry. Since that time, wells became more complex and drilling operations were routinely carried out in more difficult environments. In addition to a technical challenge, the occurrence of any weilbore instability-related problems will significantly add to the already high well costs. It is estimated that at least 10% of the well budget is used to perform unplanned operations resulting from welibore instability. This cost may approach $1 billion/yr. worldwide (Bol et al., 2002). Various aspects of weilbore instability have been presented recently. Shale-fluid interactions can be manipulated to enhance cuttings and weilbore stabilization as well as improving hole-making ability in shale formations (van-Oort, 2003). A membrane transport model was developed for calculating the diffusion potential and the reflection coefficient in shales under different conditions (Rosana et al., 2000). The ionic composition of the fluid saturating the shale appeared to control the magnitude of the membrane potential. This suggests that at least at early time, the type of cations in the drilling fluid is much

less important than their concentration since this parameter controls the water activity. Thus, the stability of clay-rich shales is profoundly affected by their complex physical and chemical interactions with drilling fluid.

Most borehole stability and drilling fluid-related problems can be handled with present technology in well-defined environments if stringent quality control actions are maintained. Nevertheless, severe complex drilling situations still present serious challenges to economically viable drilling. Efforts and progress by several Companies have led to new patented technologies usually available for license, applied in the field but rarely used in laboratories and scarcely published in the accessible literature. When wellbore walls become unstable, the spilling of cuttings causes a disastrous change in the rheological properties of the mud (Beihoffer et al., 2008). Several studies on shale-fluid interactions confirm that various causes are at the origin of borehole instability: water adsorption, osmotic swelling and cation exchange. Different approaches to Water-Based Mud design have been suggested depending on given shale formation. Other recent studies focused on shale-fluid interactions (Lomba et al., 2000; Schiemmer et al., 2002; Van-Oort, 2003). Consideration is given to maintain borehole stabilization in reactive shales by reducing hydration (swelling) and/or dispersion. The process is generally\ referred to as ‘inhibition’. Clay wettability and inhibition properties were studied by analyzing’ the behaviour of water-clay-polymer-electrolyte systems. These properties are connected to the rheological and filtration characteristics for both mud and filtrate. Considering the replacement of OBM by WBM, (Van-Oort, 2003) showed that additives, such as polymer and KC1, tend to reduce shale instability. Cuttings characterization is a key parameter to explain how salt, added to WBM, affects shale stabilization. Although, as in most engineering disciplines, a wide gap appears between R&D studies and field

applications, some important research areas could yield significant advances and benefits. In addition to new development, efforts should be made to transfer some of the old existing technologies that could immediately solve problems encountered in borehole stability or formation characterization and validation. The main critical parameters that should be determined are the constitution and strength of the formation, its discontinuities as well as abrasively, permeability, pore pressure and stress state. Several studies were conducted in order to understand some contradictory data and propose adequate mechanisms and solutions for drilling. Aldol (2004) intended to visualize that a good field modeling, based on the understanding of the underlying physics is the key for development of wellbore technologies and practices.

2.8.5 Clay swelling

Clay swelling is at the origin of well instability during drilling. In 1958, Low and Anderson presented osmotic pressure equations for determination of the swelling properties, considering clays like semi-permeable membranes. In 1969, Chenevert stated that the main reason of instability during drilling by WBM systems is the swelling of clays, adjusted the water activity of OBM systems, to prevent water adsorption on clays (Bol et al., 2002). Steiger (1993) studied clay hydration in a triaxial apparatus by measuring the swelling pressure of clays exposed to different drilling fluids with different water activities. He showed that the addition of potassium salts can reduce the water activity of clay and consequently the swelling pressure. In experiments conducted on site, he observed that the presence of KC1 in the drilling fluid improves the stability of clay formations. Modv and Tale (1993) developed a model of stability supporting the interaction between drilling fluids and clay formation. This model identified the optimum drilling fluid parameters, such as density and salinity, for the elimination of instability problems during the use of

WBM and OBM. They reported that the chemical potential difference between water in the clays and in the drilling fluid is the most important parameter. Simpson et al., (1994), using an experimental approach, showed that OBM containing an emulsified water phase can prevent moisture and thus the weakening of the clay. According to these authors, the use of a hydrophilic organic compound, namely cyclic with multiple hydroxyl groups (methyiglucoside) can also afford other characteristics similar to those of OBM, such as lubrication.

2.8.6 Laboratory methods for stability evaluation

Hale and Mody (1996) conducted experimental tests to study the direct impact of moisture on the mechanical properties of clay and tried to understand the mechanisms behind the instability of the wells, Van-Oort et al. (1996) used the pressure transmission test (PT) (based on the work of Fritz and Marine, 1983) to measure the effectiveness of the clay membranes. They observed that, after increasing the upstream pressure, the outlet pressure increases due to a higher pressure in pore caused by the hydraulic flow. Horsud et al. (1998) have also studied the phenomenon of swelling pressure in clays and concluded that osmosis does not play a role, but that pressure (or suction) is the main parameter that controls the development of the swelling. Pernot (1999) quantified the effect of the swelling pressure of a variety of fluids in contact with several types of clays and concluded that the methyiglucoside type 'Gumbo' stops clay swelling. The created barrier blocked the flow of ions and water in clays. Concentrated salt solutions show a low membrane reflection coefficient. Muniz et al. (2004) described the equipment used for the evaluation of clay-fluid interactions. The idea is to combine water and ionic gradients to estimate both the efficiency of the membrane reflectivity and the permeability coefficient and to integrate them into a program for stability evaluation. Zhang et al. (2006)

developed the gravimetric swelling test (GST) and showed that water motion is not controlled only by osmosis (water activity) but is also influenced by capillary suction and ionic diffusion. The contact of fluid with clays changes their physico-chemical and mechanical properties. Drilling fluid additives able to inhibit the swelling and dispersion of clays will be considered.

2.8.7 Shale characterization and Inhibition

2.8.7.1 Inhibition diagnosis and shale characterization

The mechanism of inhibition is dependent on the choice of the polymer-salt system. It can be identified by the following features (Bol et al., 2002):

- Increase of filtrate viscosity,
- Reduction of clay permeability,
- Balancing of the flow of mud filtrate in the clays with pore water by the effect of osmotic pressure ($a_{df} < a_{wsh}$)

Wellbore instability is due to the dispersion of the clay into ultra-fine colloidal particles and this has a direct impact on the drilling fluid properties. Clay characterization is the main parameter allowing understanding borehole stability. Solid particles are divided into three groups according to size. Colloids from about 0.005 to 1 µm impart the viscous and filtration properties, silt and barite (sometimes called “inert solids”) from 1 to 50 pm provide density, but are otherwise deleterious and sand from 50 to 420 pm, apart from bridging large opening in very porous formations, is objectionable because of its abrasive property. Clay minerals are considered as particularly active colloids (Bergaya et al., 2006), partly because of their anisotropy due to shape (tiny platelets) and partly because of their molecular structure which presents high negative charges mainly on their basal surfaces, and possible positive charges on their edges. Interaction between these opposite charges

strongly influences the viscosity of clay at low velocities, and is responsible for the formation of a reversible gel structure when the mud is at rest.

The main methods developed for shale characterization and fluid inhibition performances deal with composition, reactivity, mechanical and physico-chemical properties of shales (composed in majority of clay). A succinct list of usual methods is presented here.

- **XRD,** X-Ray Diffraction analysis to determine qualitative mineral content,
- **CEC,** Cation Exchange Capacity to evaluate reactivity of drilled cuttings. The methylene blue test (MBT) method was recommended by API (2003),
- **GST,** Gravimetric Swelling Test, used to measure water and ion motion during shale/mud interaction (Zhang et al., 2004),
- **CST**, Capillary Suction Time for the determination of filtration properties and salt up U I Hi za Lion (Wilcox & Hool, 2010),
- **ROP**, Rate of Penetration measured with a penetrometer to estimate the degree and depth of softening (Reid et al., 1993) or with a Bulk Hardness Test designed to give an assessment of the hardness of shale following exposure to a test fluid (Patel et al., 2001),
- **DCM,** Dielectric Constant Measurement to quantify swelling clay content and to determine specific area (Leung & Steig, 1992),
- Triaxial test for pore pressure measurements, carried out in down-hole simulation cell (DSC) for compressive stress/strain behavior (Salisbury & Deem, 1990),
- **Oedorneter** test for pore pressure modification and chemical potential influence (Bol et al., 2002),

- **SDT**, Slake Durability Test, a standard method originally used in geotechnical studies when measuring the weathering and stability of rock slope, reapproved 1992 (Likos et al., 2004; ASTM, 2000),
- **DSCA,** Differential Strain Curve Analysis for in situ measuring stress orientation and intensity (Fischer, 2002),
- **Hot-Rolling Dispersion Test** (shale disintegration resistance or cuttings dispersion test), the most widely used technique in optimizing drilling fluid. Appreciated for its simplicity, low cost and duration, it has been recommended by several laboratories and adopted by American Petroleum Institute (API, 2003).
- **Shale Pellet Inhibition** (pellet dispersion test): pellets and fluid are introduced into a steel bomb and processed as above (hot-rolling dispersion test). For comparison and reference, an OBM system is generally used (Modv & Tale, 1993).
- **Pressure Transmission Test**, used for confined or unconfined shale (Van-Oort, 1994). Muniz et al. (2004) described an apparatus designed to evaluate shale-drilling fluid interaction and estimate shale permeability, coefficient of reflectivity (membrane efficiency) as well as ionic diffusion coefficient,
- **Microbit Drilling Equipment,** requiring core sample availability and costly investment (Lamberti, 1999).

The comparison between all these techniques shows an important contribution of each of them. However, these methods are often criticized regarding feasibility, cost, precision and conditions used.

2.8.8 A new approach for inhibition evaluation

Swelling measurement is a key test when selecting and developing inhibitive WBM. However new methods are proposed, combining dispersion and pellet tests. The aim is to protect the initial quality of cuttings, to minimize grinding and to avoid moistening, while opting for a preliminary wash to eliminate the contamination of cuttings by the different additives like polymers, surfactants, etc (Adibhatla et al., 2006).

A new approach using a wet-cell X-ray diffraction method is proposed by some researchers (Khodja, 2008). The advantage of this method is to evaluate clay swelling after fluid contact and to estimate differences in the rate of solution adsorption between various WBM systems. The principle is to combine in-situ X-ray diffraction in wet-cell with the evaluation of liquid adsorption. This latter method combines filtrate data (volume and rate) with rheological and inhibitive properties. The API fluid loss test (30 mins, P= 100 psi through N°50 Whatman filter paper, ambient temperature) is the standard static filtration test used in the industry; however, because it uses very fine mesh paper as filter medium, all of the bridging particles are stopped at the surface of the paper and the spurt-loss phase is not simulated properly. A better static filtration test is the permeability plugging test (PPT), which uses a 1/4-inch-thick ceramic disk of known permeability (API, 2003). But in this test, mineralogy variation is not taken into account. In the new test, experiments were carried out by replacing Whatman 50 filter paper by the pellet in the API filtration cell (Khodja et. al., 2008; Khodja et.al, 2010). The slurry was exposed to a 100 psi pressure for 30 mins to obtain filtrate. The compaction force, linked to the deposit mode of the sediments, has a significant influence on the permeability. When using different inhibitive polymers, almost no difference in recovered weight is noticed

between cuttings samples from different geological formations and with different mineralogical compositions. It is recommended to use, in dispersion tests, preferably small size cuttings, which are in close contact with all additives used in drilling fluid systems. Moreover, when using small size cuttings, clays are fully exposed to the fluid and aggregation effect is eliminated (Khodja, 2008). Polymers are added as viscosifiers. The inhibition mechanism also depends on the type of polymer used, controlled by plugging of clay pores, thus reducing the dispersion (PAG), or by surface coating (film formation with PHPA or silicate). Practically, drilling engineers need to optimize formulatinns in opposite ways depending on whether they deal with upper geological layers or reservoir formation (Bishop, 2001). In the former case, minimum filtrate, optimal viscosity and high damage are required in fluid formulation selection. In the latter one, low damage is the principal selection parameter. In response to environmental constraints, new families of compounds are proposed such as sugars and their derivatives (saccharides). Sugars increase the viscosity of the filtrate and reduce the flow of water in clays (van-Oort, 1994). In addition, they provide a low water activity and generate an osmotic pressure favorable to clay dehydrenun. The problem with sugars is their susceptibility to biological attack, making them difficult to maintain unspoiled when stored on site. However, methylglucoside (MEG) and generally methylated saccharides are less susceptible to biological attack (Simpson et al., 1994). MEG is a derivative of glucose, supplied as liquid containing 70% solids. Made from corn starch, it is classified as "biodegradable". Saccharides are generally recommended for the stabilization of clays. Added salts to saccharide systems allowed effective dehydration of clays, reduction of "bit-balling' and increasing ROP. These MEG systems have a good filtrate and produce environmentally acceptable cuttings (Chenevert & Pernot, 1998).

Soluble in water, MEG has many hydroxyl groups in a ring structure capable of reducing the water activity of the drilling fluid and may be a good additive to WBM.

2.9 Corn

Corn is an agricultural crop grown in many parts of the world. It is also known as maize. It is also grown locally in many parts of Nigeria including Imo state and examples are waxy corn (white and yellow colours), Guinea corn, etc (Ukachukwu et al, 2010). It is made up of grains arranged and harvested on cobs at maturity. Corn is processed to obtain corn starch. Corn is one of the most diverse grain crops found in nature. The most common types of corn include flint corn, flour corn, dent corn, pop corn, sweet corn and waxy corn (Mangelsdorf, 2004; Schopmeyer, 2003). The physical appearance of each corn kernel or corn grain type is determined by its pattern of endosperm composition as well as quantity and quality of endosperm (Amanullah, 2004). Grains of flint corn have mostly hard, glassy endosperms with smooth, hard seed coats (pericarps). Flour corn endosperms are made of soft starch with thin pericarps. Dent corns with flinty sides and soft cores of starch cause the end of the grains to collapse or dent during drying. Popcorns are basically small grain type of corns. The wrinkled, glassy appearance of sweet corn kernels or grains is the result of a sugary gene that retards the normal conversion of sugar to starch during endosperm development (Mangelsdorf, 2004; Schopmeyer, 2003). Waxy corn carries a gene that produces 100% amylopectin, a complex form of starch (Amanullah, 2004). The domestic and industrial uses of corn starch are versed. Some of its applications include food, adhesives, drilling fluid or drilling mud preparation, etc. The various groups include sweet corns, field corns, etc.

2.9.1 Sweet Corn

Sweet corn (zea mays saccharata or zea rugosa) also called sugar corn or pole corn is a variety of maize with high sugar content. Sweet corn is the result of naturally occurring recessive mutation in the genes which control conversion of sugar to starch inside the endosperm of the corn kernel (Mangelsdorf, 2004). Unlike field corn varieties, which are harvested when the kernels are dry and mature (dent stage), sweet corn can be pitched when immature (milk stage) and prepared and eaten as a vegetable rather than a grain. Since the process of maturation involves converting sugar to starch, sweet corn stores poorly and must be eaten fresh, canned, or frozen, before the kernels become tough and starchy.

Figure 2.21: Sweet Corn

(Mangelsdorf, 2004; Schopmeyer, 2003)

2.9.2 Field Corns

Field corns are corns grown specifically for industrial purposes. They have high starch content. Field corn is the variety of maize that is not grown primarily for consumption as human food in the form of fresh kernels in the United States.

The varieties of field corn are: Dent corn, Flint corn, Flour corn, including blue (*Zea mays amylacea*) and Waxy corn (Mangelsdorf, 2004).

2.9.2.1 Dent Corn

Dent corn (Zea mays var. Indentata), with varieties as Reid's yellow dent corn, white dent corn, is a type of maize or corn with a high soft starch content. It received its name because of the small indentation at the crown of each kernel on a ripe ear of corn. It is a variety developed by northern Illinois farmer James L, Reid. Reid and his father, Robert Reid, moved from Brown country Ohio to Tazewell country, Illinois in 1846 bringing with them a red corn variety known as Gordon Hickories and crossed it with varieties of flint corn and floury corn. Dent corn (Zea mays var, indentata) a fast growing and similar to many other varieties of zea mays (Mangelsdorf, 2004). More commonly grown to height of 2-3 meters (6.9 feet), Zea mays typically grows with a single, hollow main stem often called a stulk (culm) which exhibits internodes that are cylindrical in the upper part, and alternately grooved on the lower part with a bud in the groove, and with one or occasionally two lateral branches in the leaf axils in the upper part of the plant. He leaves of zea mays alternate with broad sword-shaped leaf blades, parallel veins with a prominent mid-rib, and small ligules. The kernels vary from variety to variety, and what distinguishes zea mays var. Indentata from other varieties of zea mays is the small indentation ("dent") that develops at the crown of each kernel.

Figure 2.22: Dent corn Cobs and Grains

(Mangelsdorf, 2004)

2.9.2.2 Waxy corn

Waxy corns tarch is relatively easy to gelatinize, produces a clear viscous paste with a sticky or tacky surface (Mangelsdorf, 2004; Schopmeyer, 2003). The paste rheology resembles pastes of root or tuber starches, such as potato starch or tapioca starch (made from cassava) (Schopmeyer, 2003). Amylopectin starch has also a lower tendency to retrogradate and is thus more viscosity stable. The clarity and viscous stability of amylopectin starch make it especially suitable for thickening purposes. Waxy maize starch is also the preferred starting material for the production of maltodextrins because of improved water solubility after drying and greater solution stability and clarity. Waxy corn on the cob is popular in China and Southeast Asia, and may be found in frozen or precooked forms in Chinatowns. Waxy corn is the most popular corn in China for fresh consumption. Starch from waxy maize differs from regular maize starch in both molecular structure and pasting characteristics. Pastes made from waxy starch are long and cohesive; whereas, pastes made from

regular maize starch are short and heavy bodied. Waxy maize starch is a major starch component in adhesives used for making bottle labels. This waxy starch based adhesive imparts re-solubilizing resistance to the labels which prevents their soaking off the bottle if immersed in water or being subjected to very high humidity conditions. Moreover, waxy maize starches are commonly used in the USA for the manufacture of gummed tapes and envelope adhesives (Mangelsdorf, 2004).

Figure 2.23 (a): Yellow Waxy Corn on Cobs

(Mangelsdorf, 2004; Schopmeyer, 2003)

Figure 2.23 (b): Yellow Waxy Corn Grains

(Schopmeyer, 2003)

Figure 2.23 (c): White Waxy Corn on Cobs

(Mangelsdorf, 2004; Schopmeyer, 2003)

Figure 2.23 (d): Purple Waxy Corn on Cobs

(Mangelsdorf, 2004; Schopmeyer, 2003)

CHAPTER THREE

MATERIALS AND METHODS

3.1 Materials

The following materials were used for the work:

Waxy corn (a field corn) (Zea mays)

Millet (Panicum Miliaceum)

Pop corn (Zea mays Averta or Zea mays Var. Everta)

Guinea corn (Sorghum Bicolor)

Double distilled water

Sodium Hydroxide (NaOH)

Bentonite Clay

Carboxymethyl starch (CMS, standard/wdely-used)

A Blend of Caboxymethyl starch and Hydroxypropyl starch (CMS:HPS, standard/widely-used)

Non-chemically- modified single starch (W, already existing single starch)

Soybean seeds

Okro seeds

Wheat grains

Cucumber seeds

Top soil (Alluvial)

Nutrient Agar (NA)

Sabourauid Dextrose Agar (SDA)

Mineral Salt Agar (MSA)

MacConkey Agar

3.1.1 Sources of Materials

Waxy corn, a field corn was obtained from a local farm in Imo State. Millet and Guinea corn were obtained from a local farm at Jos, Plateau State in Nigeria. Pop corn was bought from Owerri main market, Imo State. The double distilled water was obtained from the Quality control Department of NichBen Group of Companies Limited in Awo-Omama, Imo State. The Sodium Hydroxide was purchased from MacDonald Scientific Laboratory at Port-Harcourt in Rivers State. The Bentonite Clay, Carboxymethyl starch (CMS, standard/wdely-used), and a Blend of Caboxymethyl starch and Hydroxypropyl starch (CMS:HPS, standard/widely-used) were obtained from Trans-Ocean Oil Company Limited based in Port-Harcourt, Rivers State, Nigeria. Soybean seeds, Okro seeds, Wheat grains, Cucumber seeds and Top soil (Alluvial) were obtained from Imo State. Nutrient Agar (NA), Sabourauid Dextrose Agar (SDA), Mineral Salt Agar (MSA), and MacConkey Agar (MA), were obtained from Federal University of Technology, Owerri (FUTO), Imo State.

Images of Corns and Millet used for the study

Figure 3.1 (a): Waxy Corn Grains in cobs

(Mangelsdorf, 2004; Schopmeyer, 2003)

Figure 3.1 (b): Image of Waxy Corn Grains

(Schopmeyer, 2003)

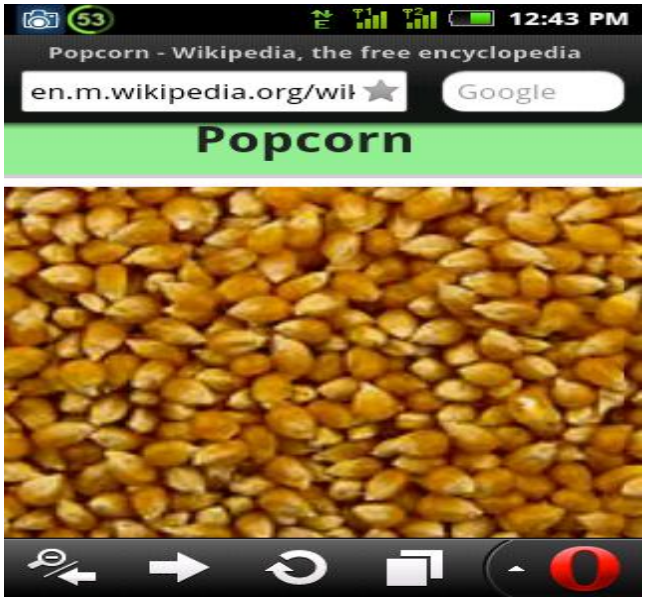

Figure 3.1 (c): Image of Popcorn Grains

(Mangelsdorf, 2004)

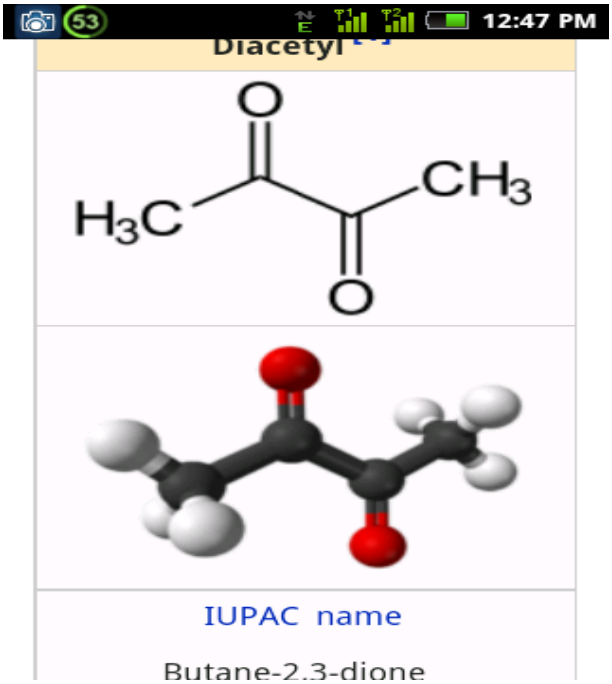

Figure 3.1 (d): Chemical Structure of Diacetyl (Butane-2,3-dione) from Popcorn (Fischer, 2002).

Figure 3.1 (e): Guinea Corn Grains (Mangelsdorf, 2004).

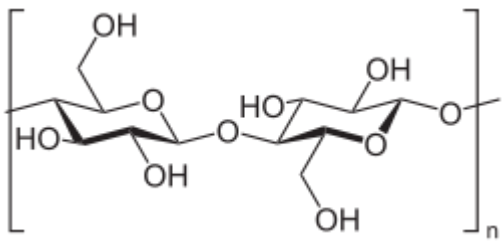

Figure 3.1 (f): Chemical Structure of extact from Guinea Corn (Mangelsdorf, 2004)

Figure 3.1 (g): Millet Grains (Ukachukwu et al, 2010).

3.1.2 Apparatus

The following instruments were used.

Extruder

Oven

Weighing balance

Cloth bag

Mechanical shaker

Endecotts laboratory test sieve (< 45 μm mesh size)

Grinder/Blender

Cups

Measuring cylinder

Beakers

Conical flasks

Constant temperature water bath

Filter papers

Thermometer

Funnels

Stop clock

Brookfield Viscometer (synchro-lectric model)

Standard Filter Press Unit

Polyethylene films

Small Plastic buckets

3.1.3 Description of Some of the Apparatus

3.1.3.1 Extruder

An extruder is a machine used to carry out extrusion process. Extrusion is a production or processing technique for coverting polymer materials in powdered or granular form into a continuous uniform melt, which is shaped into items of uniform cross-sectional area by forcing it through a die (Adrain & Gareth, 2009; Fried, 2000). The two principal components of an extrusion or an extrusion operation are the extruder and the die. The extruder consists of a hopper that holds the resin stock (usually in the form of small pellets or powder) and the extruder barrel which can be conceptually divided into three sections on the basis of function. These are called the feed, compression, and metering section (Fried, 2000). In the feed section, the solid feed is conveyed by the rotating screw from the hopper to the compression zone where the resin begins to melt due to the action of electrical heater attached to the barrel wall. By the time the resin reaches the metering zone, all the resin has melted, and the shearing action of the screw rotating against the inner wall of the extruder barrel forces the melt out of the extruder and through a die (Adrain & Gareth, 2009). The die shapes the extrudate to the desired form. After the extrudate leaves the die, it is cooled and chopped to the desired length. In commercial polymer production, powder from a polymerization reactor can be fed directly to an extruder that has an opening for venting volatiles (a process called devolatilization). Examples of volatile contaminants include residual monomer and solvent that may be used during

polymerization process (Adrain & Gareth, 2009). The extruded melt is then passed through a die, cooled and chopped to form small pellets. Single screw extruder and twin screw extruder are in use. Figure 3.2 (a) and (b) illustrate diagrams of a single screw extruder.

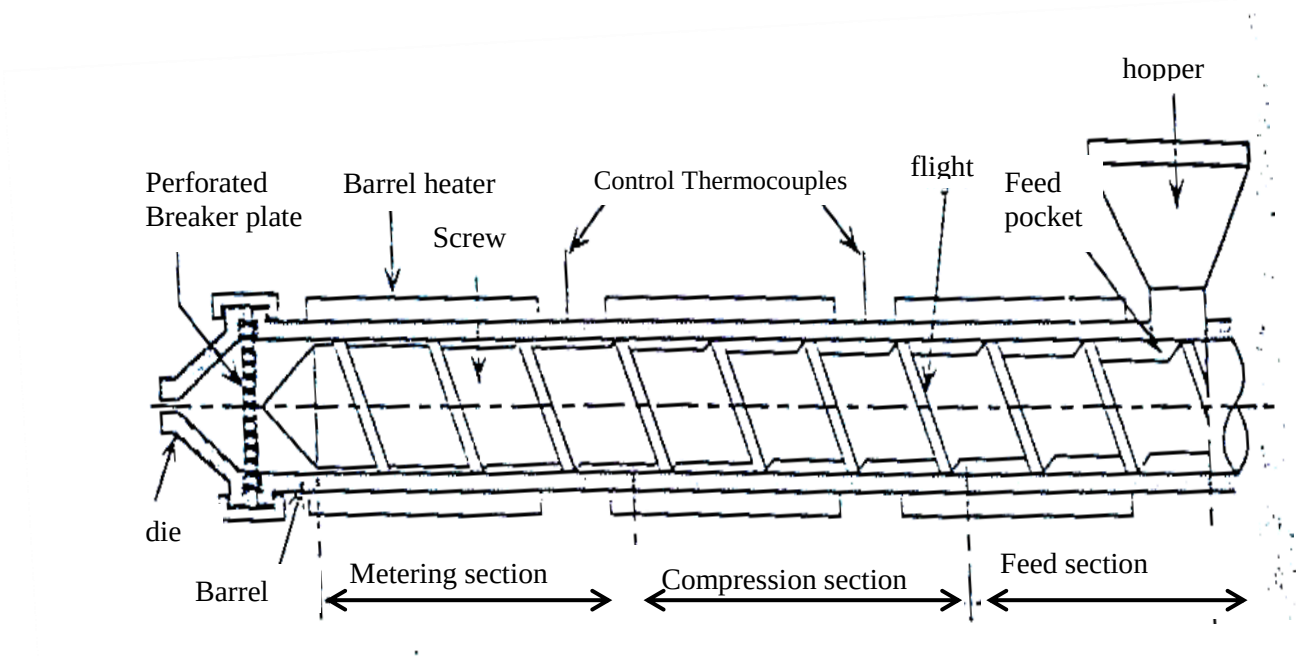

Figure 3.2 (a): Schematic diagram of an Extruder (culled from Ukachukwu et al., 2010)

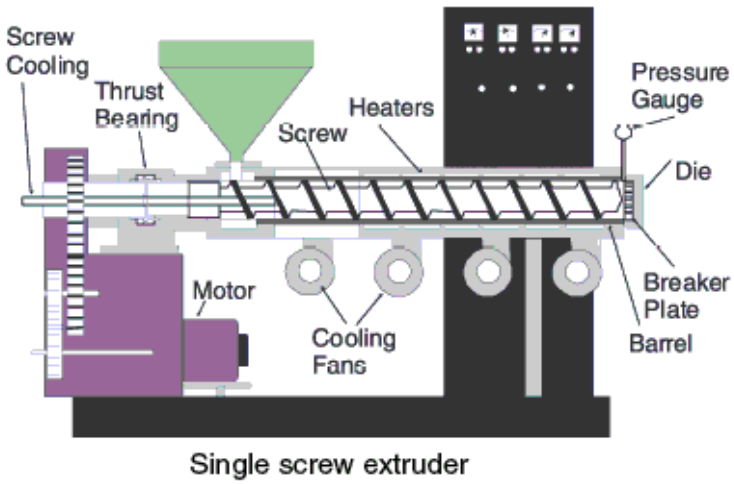

Figure 3.2 (b): Single Screw Extruding Machine

(culled from Adrain & Gareth, 2009)

3.1.3.2 Brookfiled Viscometer

The Brookfield viscometer is used for viscous fluid with moderate shear rates. The original and most common sensor is a disk rotating in an infinite sea of fluid. A factor finder applies to Brookfield viscometer with standard spindles (Bryan et al., 2010; Dahlgreen & Heibig, 2008). The viscometer features lie on the fact that its readings are easily transformed to values of viscosity using measurements taken at different speed in revolutions per minute (rpm), with four different spindles. Before the measurement, slide is usually inserted in sleeve so that appropriate viscometer model is visible in the window such that the first two letters of the models designation are shown, i.e. LV applies to LVF. To convert viscometer dial reading to MilliPascal seconds (MPa.S) or poises, slide is adjusted until viscometer model and spindle number being used appear in window (Dahlgreen & Heibig, 2008). The reading noted on viscometer is being used for measurement, such that viscosity= dial reading x factor (MPa.S). The speed at which viscosity is determined is preset with the aid of the square knob at the side. Figure 3.3 shows schematic diagram of a Brookfield viscometer (Obong, 2004).

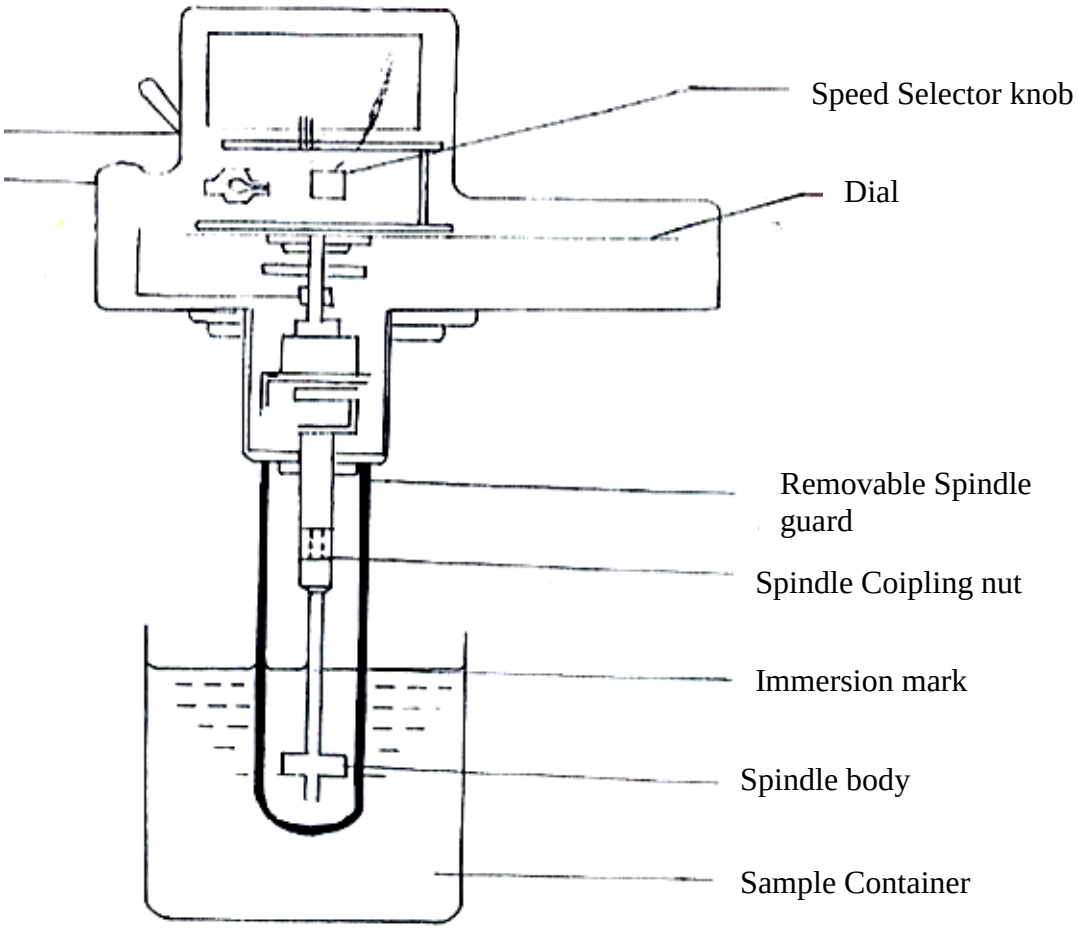

Figure 3.3: Schematic diagram of Brookfield Viscometer (culled from Dahlgreen & Heibig, 2008; Obong, 2004)

3.1.3.3 Standard Filter Press

The filtration properties were determined by means of the standard filter press. It consists of mud reservoir mounted on a frame, filter medium for filtering, collecting and discharging filtrate, measuring cylinder for measuring the filtrate volume; pressure source, etc (Al-Riyainy & Sharma, 2004; Obong, 2004). The filter press contains a filter medium made up of a sheet of specially designed hardened filter paper (9cm in diameter) which fits on the screen in the base cap. The function of the filter medium is generally to act as a support for the filter cake, while the initial layers of the cake provide the filter medium. A graduated glass cylinder is used to collect and measure the volume of the filtrate. Pressure source is a cylinder of compressed air (veller compressor). A pressure - gauge is used to ensure and maintain constant pressure throughout a particular experiment (Anthony & Robert, 2010**;** Al-Riyainy & Sharma, 2004). Figure 3.4 (a) and 3.4 (b) illustrate the diagrams of a standard filter press unit (Slurry filtration Apparatus).

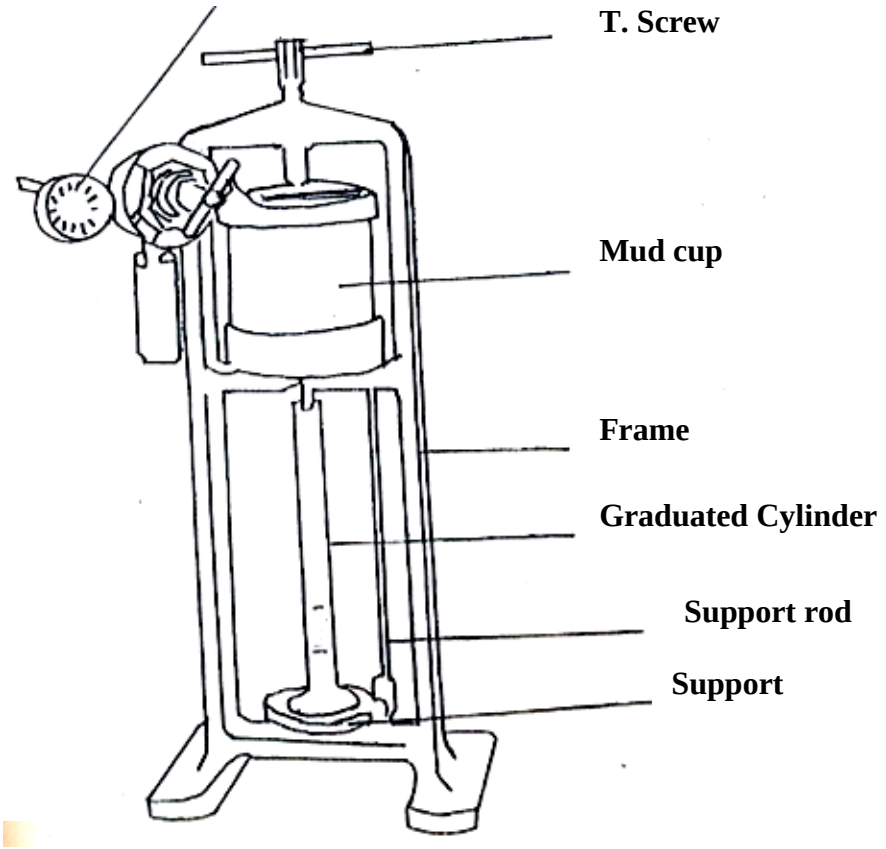

Figure 3.4 (a): Schematic diagram of standard filter press unit (culled from Ukachukwu et al., 2010; Al-Riyainy & Sharma, 2004)

Figure 3.4 (b): Standard Filter Press Unit (Slurry Filtration Apparatus)

(culled from Anthony & Robert, 2010)

3.2 Methods

3.2.1 Methods for Preparation of Samples

The samples were prepared in three stages namely; extraction of starches, extrusion of starches, and preparation of muds.

3.2.1.1 Extraction of Starches

Different starches were extracted from local Corns and millet. The corns that were used included Waxy corn (field corn), Guinea corn and Pop corn. The grains of each corn and the millet were separately softened by soaking them overnight in water. The softened grains were then removed from water and ground to a moderately fine consistency. The mash was sieved through a cloth bag into a sufficient volume of distilled water (Andrew & Robert, 2007; Amanullah & Long, 2004). The whole extract was allowed to stand for an hour, then, the water was pressed out to obtain the starch, which was dried at a low temperature for 24 hours.

3.2.1.2 Pre-gelatinization and Blendingof Starches by Extrusion Technique

The starches were extruded to obtain blends of novel starch products for preparing muds. The new blends of starch products are known in this work as G:W (a blend of Guinea corn starch and Waxy corn starch) , M:W (a blend of Millet starch and Waxy corn starch) , P:W (a blend of Pop corn starch and Waxy corn starch), G:M **(**a blend of Guinea corn starch and Millet starch), G:P (a blend of Guinea corn starch and Pop corn starch) , M:P (a blend of Millet starch and Pop corn starch), and they were prepared by gelatinization and blending using extrusion technique in the absence of a solvent. The process was carried out for each blend of starches by putting two different starches and water in the ratio of 85:85:45 into an extruder. The extrusion

was carried out at 80 x 10^5 Nm^{-2} pressure and 120^oC temperature (Amanullah & Long, 2004). The approximate resident time during the extrusion process was about three minutes. The moisture content of the extruded starches was in the range of 12-13%. After extrusion, the extruded starches were shredded to 2-3mm sizes. The shredded samples were dried at a temperature of 105^oC for 24 hours, and then ground to obtain less than 45 micron meter (< 45 μm) size fraction that was used for preparing muds.

In addition, each extrudate, that is, extruded starch blend was collected exactly as it comes out from the extruder, and dried (without shredding or grinding it) at a temperature of 105^oC for 24 hours to obtain strong sample material for characterizing each blend of starches for biodegradation properties (Obasi, 2012).

3.2.1.3 Production of widely- used Chemically-modified single starch (Carboxymethyl starch, Hydroxypropyl starch)

The chemically-modified single starch was produced by first crosslinking a single starch with epichlorohydrin, suitably in a basic starch suspension, or slurry, at a temperature and for a period of time such that the viscosity of the slurry exceeds the maximum viscosity which can be obtained in the starch suspension and then drops to about 50% or less of the maximum viscosity as determined experimentally (Rolly, 2012; Weir & Bailey, 2004). Typically the slurry contains at least 25% by weight starch granules. The maximum viscosity is eached at a very low crosslinking density and then drops with further crosslinking, as the crossliked system becomes increasingly dense. The viscosity varies by the amount of crosslinking and the test conditions, i.e, temperature, concentrations, etc (Fannon et al., 2004). Preferably, the crosslinking is continued until the viscosity decreases to a value in the range of from

about 35% to 5% of the maximum viscosity. When the desired viscosity is reached, the crosslinking reaction is terminated (Wikky, 2008; Rolly, 2012; Weir & Bailey, 2004). The next stage is to either carboxymethylate the crosslinked starch to obtain carboxymethyl starch or hydroxypropylate it to obtain hydroxypropyl starch.

In the case of carboxymethyl starch, carboxymethylation is accomplished by reacting the epichlorohydrin crosslinked starch with chloroacetic acid or its sodium salt (Zac et al., 2012; Rolly, 2012; Wikky, 2008). Such reactions are well known. The degree of substitu tion (ds) in the starch is at least 0.1, more desirably at least 0.3, and preferably at least 0.4 carboxymethyl groups per anhydroglucose unit in the starch polymer. Polymers with ds of about 0.4 or higher are especially preferred because they are stable against fermentation however, this degree of substitution is much higher than can conventionally be achieved in a slurry reactor. Therefore for this reaction the starch slurry is desirably transferred to a paste or autoclave reactor (Zac et al., 2012; Rolly, 2012; Wikky, 2008). The carboxymethyl starch was marked in this work as CMS.

In the case of hydroxypropyl starch, hydroxypropylation is achieved by reacting of the epichlorohydrin crosslinked starch with propylene oxide to form hydroxypropyl ether (Weir & Bailey, 2004). The reaction of propylene oxide and starch is based catalyzed. Aqueous slurry reactions are generally catalyzed by 0.5 to 1% sodium hydroxide based on the dry weight of starch. Sodium sulfate or sodium chloride may be added to keep the starch from swelling during reaction with propylene oxide. Reaction temperatures are generally in the range of about 38^0 to about 55^0C. Propylene oxide levels generally range from about 1% to about 10% based on the dry weight of starch. Propylene oxide-starch reactions take approximately 24 hours to

complete under the conditions decribed and are about 60% efficient with respect to the propylene oxide (Bill & Mark, 2007; Weir & Bailey, 2004). It is preferred that the epichlorohydrin crosslinked hydroxypropylated contain from about 0.5% to about 20% reacted propylene oxide based on the dry weight ("moisture free basis" or"MBS") of starch (James, 2012; Weir & Bailey, 2004; Linus, 2002).

3.2.1.4 Production of widely-used Chemically-modified Blend of starches (a blend of Carboxymethyl starch and Hydroxypropyl starch)

The carboxymethyl starch and hydroxypropyl starch were subjected to a higher water dilution or a solvent might be employed in a high speed mixer or slurry reactor for proper blending (Zac et al., 2012; Jones & Mark, 2006; Heinze, 2005; Weir & Bailey, 2004). Suitably the reacted starches are then drum-dried and milled to obtain a dry product (a blend of carboxymethyl starch and hydroxypropyl starch). The milled dry product can then be incorporated into the oil well drilling fluid at the drill site (Bertts & Jerry, 2012; Jones & Mark, 2006).

The blend of chemically-modified carboxymethyl starch and hydroxypropyl starch was marked in this work as CMS:HPS.

3.2.1.5 Prodution of an already existing non-Chemically-modified single starch

The non-chemically-modified single starch was produced by preheating single waxy corn starch under specific pressure and temperature without the incorporation of any solvent or chemical (Ukachukwu et al., 2010). After preheating, the starch was dried in an oven and then ground to obtain powdered product for drilling mud preparation. The non-chemically-modified single starch was marked in this work as W.

3.2.1.6 Preparation of Muds

Several biodegradable polymer muds that were water-based were prepared using first 8, 16, 24, 32, 40, grams of each of the new starch-blend products (extruded blends of starches) in 800ml of water giving rise to 0.01-0.05g/ml concentration of each starch blend and then each of 4, 8, 12, 16, 20, grams of the same new starch-blend products (G:W, M:W,P:W, G:M, G:P, M:P) in each 400ml of water giving rise to 0.01-0.05 g/ml concentration of each starch-blend.These new polymer muds were compared to the already existing or widely-used(standard) mud prepared respectively with a blend of chemically modified starches (a blend of Carboxymethyl Starch and Hydroxypropyl Starch; CMS:HPS), non-chemically modified single starch (W), chemically modified single starch (CMS) of the same concentration as above. The base component (water) of the muds was mixed with Bentonite for 20 minutes using a high speed mixer (Amani, 2012; Austin & Christopher, 2008). At the end of mixing the components, starch product was added slowly to the agitated mud to avoid any scope of lump formation within the mud system. pH of the mud was adjusted by adding and mixing suitable amount (25ml) of Sodium hydroxide (NaOH) to the mud (Austin & Christopher, 2008). Each mud system contained about 6% Bentonite by weight of starch (Austin & Christopher, 2008; American Petroleum Institute, 1993). All preparations were made using double distilled water. The various mud samples and their identification marks were as shown below:

Table 3.1: The various Mud samples and their Identification marks.

Mud samples	Identification marks
• Biodegradable Polymer Drilling Mud Prepared with extruded blend of Guinea corn starch and Waxy corn starch.	**G:W-mud**
• Biodegradable Polymer Drilling Mud Prepared with extruded blend of Millet starch and Waxy corn starch.	**M:W-mud**
• Biodegradable Polymer Drilling Mud Prepared with extruded blend of Pop corn starch and Waxy corn starch	**P:W-mud**
• Biodegradable Polymer Drilling Mud Prepared with extruded blend of Guinea corn starch and Millet starch.	**G:M-Mud**
• Biodegradable Polymer Drilling Mud prepared With extruded blend of Guinea corn starch and Pop corn starch.	**G:P-Mud**
• Biodegradable Polymer Drilling Mud prepared With extruded blend of Millet starch and Pop corn starch.	**M:P-Mud**
• Already existing and widely used Drilling Mud prepared with a blend of Chemically modified Carboxymethyl starch and Hydroxypropyl Starch.	**CMS:HPS-Mud**
• Already Existing Mud prepared with non-chemically-modified single Waxy corn starch.	**W-Mud**
• Already Existing and widely used Mud Prepared with chemically- modified Singe Carboxymethyl starch.	**CMS-Mud**

3.2.2 Methods of Experiment

Filter loss method and viscometric method were respectively used to determine the filtration properties and rheological properties of the various muds, while soil burial test method and plants's growth method were used to determine the biodegradable properties of the muds' additives (blended and unblended starches).

3.2.2.1 Filter Loss Method

Filter loss method were used to determine the filtration properties of the muds. Various filtration tests were run on the mud systems using filter loss method. The apparatus that was used for the tests was the standard filter press unit (a slurry filtration apparatus) under constant pressure of 100Psi (Hall & Hoff, 2012; Anthony & Robert, 2010**;** Al-Riyainy & Sharma, 2004; American Petroleum Institute, 2003). After assembling the accessories of the filter press, 800ml of each of the newly produced Biodegradable Polymer Drilling Muds (G:W-Mud, M:W-Mud, P:W-Mud, G:M-Mud, G:P-Mud, M:P-Mud) containing 0.01-0.05g/ml concentration of the extruded blend of starches were poured into the cup of the filter press. The tests were run on each mud for various time intervals at 25^{o}C. At the end of each time interval, the volume of the filtrate was collected as the fluid loss and measured using the graduated cylinder. The thermal stability of the muds was assessed by carrying out a standard Hot Rolling Dispersion test at 150^{O}C, 250^{o}C, 350^{o}C, and 450^{o}C. Each of the mud samples that were recovered from the hot test was remixed with a blender (Anthony & Robert, 2010**;** Al-Riyainy & Sharma, 2004). Then, filtration test was run on each of the mud samples. Three tests were run on each mud at all the temperatures and the result of the average of the three tests was taken for accuracy. The whole procedures were repeated for the already existing and widely used muds, (CMS:HPS-mud, W-mud, CMS-mud)**,** containing respectively 0.01-0.05g/ml concentration of

blend of chemically modified starches (CMS:HPS), non-chemically- modified single starch (W), chemically- modified single starch (CMS). All the results were recorded and tabulated.

The Sorptivity was computed using this equation 3.1 (Hall & Hoff, 2012; Bernu, 2011; Anthony & Robert, 2010; Scarlet & Brene, 2010; American Petroleum Institute, 2003; Andy et al., 2000).

$$V=St^{½} \qquad 3.1$$

Where V is the filtrate volume or fluid loss or filter loss, S is the sorptivity of fluid, and was obtained as the slope of the plot, t is the filtration time in minutes.

The diffusivity was computed using equation 3.2 (Hall & Hoff, 2012; Bernu, 2011; Anthony & Robert, 2010; Scarlet & Brene, 2010; American Petroleum Institute API, 2003; Andy et al., 2000).

$$\Phi(R) = \Phi_o \exp^{-Dt} \qquad 3.2$$

Where Φ_o and Φ are initial and final filtration rates respectively, D is the diffusivity of fluid, and was obtained as the slope of the plot, t is time in minutes.

3.2.2.2 Viscometric Method

Viscometric method was used to determine the rheological properties of the muds. The apparatus used was the Brookfield viscometer. 400ml of each of the new Biodegradable Polymer Drilling Muds (G:W-Mud, M:W-Mud, P:W-Mud, G:M-Mud, G:P-Mud, M:P-Mud) containing 0.01-0.05g/ml concentration range of the respective blended and unblended starches was used for the test. Each 400ml volume of each mud containing each of the starch concentration was agitated by re-mixing it for about

20 minutes, and then subjected to four different speeds of (60, 120, 300 and 600) rpm under the shear rate range of 0.1-1.0s^{-1} (Bryan et al., 2010; Ukachukwu et al., 2010; Qartar & Giacelo, 2010; Michael, 2009; Obong, 2004; Staben et al., 2004). The whole procedure were repeated for CMS:HPS-mud, W-mud and CMS-mud. Viscosities and shear stresses were obtained and all the results were recorded and tabulated and used to plot graphs.

The flow index was determined using the power law equation (see equation 3.3) (Bryan et al., 2010; Ukachukwu et al., 2010; Qartar & Giacelo, 2010; Michael, 2009; Obong, 2004; Staben et al., 2004).

$$\tau = k\gamma^{n} \qquad 3.3$$

Where τ is the shear stress, γ is the shear rate, n is the flow index which will be obtained as the slope of the logarithmic plot under the above equation. The intercept of the plot gave the consistency index K.

The yield stress was computed using the Herschel Bulkely equation (see equation 3.4) (Bryan et al., 2010; Qartar & Giacelo, 2010; Obong, 2004; Staben et al., 2004).

$$\tau = \tau_o + k\,\gamma^{n} \qquad 3.4$$

Where τ is the shear stress, τ_o is the yield stress, K is the consistency index, γ is the shear rate, and n is the flow index.

3.2.2.3 Soil Burial Test Method

A soil burial test method was used to determine the biodegradability of the various of starches (G:W, M:W, P:W, G:M, G:P, M:P)**.** In the first place, definite weight of 50g and length of 10cm for each starch blend was used for the soil burial test, which lasted

for 100 days. Wet alluvial soil (cultured for the specific micro-organisms responsible for the biodegradation) was placed into plastic containers (small plastic buckets) with tiny holes perforated at the bottom, and on the side of the containers so as to increase air and water circulation (Obasi, 2012; Mickey & Duke, 2005). The soil was kept moist with water and the plastic containers containing the soil and the samples were covered with polyethylene films to prevent water from evaporating from the soil surface, and stored outside the room for 100 days at temperatures of 34-38^{o}C and ambient humidity of 72-78% (Obasi, 2012; Mickey & Duke, 2005). Each new blend of starches (G:W, M:W, P:W, G:M, G:P, M:P) was buried in the soil at a depth of 15cm from the soil surface. Care was taken to ensure that each sample blend is covered completely with soil. Before burying each sample blend in the container of soil, the sample was weighed, and the weight (50g) obtained was recorded as initial weight of the sample. The already existing blended and unblended starches (CMS:HPS, W, CMS) were used as the negative reference materials or for comparison. The biodegradation of the samples was estimated by monitoring the changes in their weights as a function of burial time. After each soil burial test of 10, 20, 30, 40, 50, 60, 70, 80, 90 and 100 days duration, each buried sample was removed from the soil and the debris on the sample was removed by washing it with distilled water. The specimen was then oven dried at 80^{o}C for 24 hours (Mickey & Duke, 2005). Then, the specimen was weighed again and the value was recorded as the final weight of the sample. The percentage weight loss of each sample, as a function of number of days, was determined as in this equation (Mickey & Duke, 2005):

$$\%\text{Weight Loss} = \frac{\text{Initial Weight of sample} - \text{Final Weight of sample}}{\text{Initial Weight}} \times \frac{100}{1} \qquad 3.5$$

3.2.2.4 Soil Culturing Method for Isolaion of Micro-organisms

The following media and methods were used for the soil culturing and isolation of microorganisms:

(a) Media: Nutrient Agar (NA)

Preparation Method: 28g of the Nutrient Agar powder was dissolved in 1 litre of distilled water and soaked for 10 minutes and later sterilized by autoclaving at 121^0C for 15 minutes.

Table 3.2(a): Formulation for Nutrient Agar (NA) for Soil Culturing

Formulation	**Composition (g)**
Peptone	5.0
Beef extract	3.0
Sodium Chloride (NaCl)	5.0
Agar Powder	15.0
pH (7.4 approximate)	

(b) Media: Sabouroid Dextrose Agar (SDA)

Preparation Method: 62g of the granules of the Sabouroid Dextrose Agar was dissolved in 1 litre of sterile distilled water. The solution was allowed to stay for 10 minutes and swirled to mix properly. Then it was put in autoclave at 121^0C for 15 minutes.

Table 3.2(b): Formulation for Sabouroid Dextrose Agar (SDA) for Soil Culturing

Formulation	**Composition (g)**
Mycological Peptoneoxide	10.0
Dextrose	40.0
Agar	15.0
pH (7.4 approximate)	

(c) Media: Mineral Salt Agar (MSA)

Preparation Method: 80g of the granules of the Mineral Salt Agar was dissolved in 1 litre of sterile distilled water. The solution was allowed to soak for 10 minutes and swirled to mix properly. Then it was put in autoclave at 121^0C for 15 minutes.

Table 3.2 (c): Formulation for Mineral Salt Agar (MSA) for Soil Culturing

Formulation	**Composition (g)**
Sodium Chloride (NaCl)	10.00
$NaNO_3$	0.42
KCl	0.29
$MgSO_4.7H_2O$	0.4
Na_2HPO_4	1.25
KH_2PO_4	0.83
Agar-Agar Powder	15.00

(d) Media: MacConkey Agar (MA)

Preparation Method: 52g of the MacconkeyAgar powder was dissolved in 1 litre of distilled water. The solution was allowed to stay for 15 minutes and turned to mix properly. Then it was later sterilized by putting it in autoclave at 121^0C for 15 minutes.

Table 3.2 (d): Formulation for MacConkey Agar (MA) for Soil Culturing

Formulation	**Composition (g)**
Peptone	20.00
Lactose	10.00
Salt	5.00
Sodium Chloride	5.00
Neutral red	0.75
Agar	12.00

3.2.2.5 Plant's Growth Method

The growth of Okro, Wheat, Soyabean and Cucumber plants was checked from the germination stage in order to find out whether or not the biodegradation products from the new polymer samples (new starch blends) and the three already existing samples (blended and unblended starches) affected the growths of plants. The crops were planted respectively in each of the plastic containers of soil from where the buried samples had been removed. The plants were allowed to grow for 50 days. The height of the shoots and the lengths of the roots were measured respectively for each sample. All the datas obtained were recorded and tabulated.

3.2.2.6 MATLAB Modelling Method

MATLAB requires a little knowledge of programming language. The dependent and independent variables were defined and the 'polyfit' command used to produce the modelling equations.

3.2.2.6.1 Opening Curve Fitting Tool

The Curve Fitting Tool is a graphical user interface (GUI) that can be used: (i) Visually to explore one or more data sets and fits as scatter plots. (ii) Graphically to evaluate the goodness of fit using residuals and prediction bounds. (iii) To access additional interfaces for importing, viewing, and smoothing data. (iv) In fitting data, and comparing fits and data sets. (v) In marking data points to be excluded from a fit. (vi) In selecting which fits and data sets are displayed in the tool. (vii) In interpolating, extrapolating, differentiating, or integrating fits. Curve Fitting Tool was opened with the 'cftool' command.

3.2.2.6.2 Importing Data

The data variables must exist in the MATLAB workspace before data could be imported into Curve Fitting Tool and stored in the MATLAB file ('.mat'). Alternatively, data could be imported into Curve Fitting Tool with the Data GUI. The GUI was opened by clicking the Data button on Curve Fitting Tool. The Data GUI consists of two panes: Data sets and Smooth. The appropriate variable names from the X Data and Y Data lists were selected to load the data set. The data was then displayed in the Preview window. The data import process was completed by clicking the 'create data set button'

3.2.2.6.3 Interactive Curve Fitting Procedure

Data was fitted with the Fitting GUI. The GUI was opened by clicking the Fitting button on Curve Fitting Tool. The Fitting GUI consists of two parts: the Fit Editor and the Table of Fits. The Fit Editor gave the new fit button.

3.2.2.6.4 The Data Fitting Procedure

This was begun by fitting data with a second degree polynomial. Then the fitting was continued with the data using polynomial equations up to sixth degree, and a single-term exponential equation. The data fitting procedure follows these general steps: (i) The new Fit button was opened from the Fit Editor. (ii) The Apply button was clicked. The library model, fitted coefficients, and goodness of fit statistics were displayed in the Results area. (iii) The additional library equations were fitted. For fits like polynomials, Copy Fit was used instead of New Fit because copying a fit retains the current fit type state thereby requiring fewer steps than creating a new fit each time.

3.2.2.6.5 Determining the Best Fit

To determine the best fit, both the graphical and numerical fit results were examined.

Examining the Graphical Fit Results, the initial approach in determining the best fit was a graphical examination of the fits and residuals.

Examining the Numerical Fit Results, because fits can no longer be eliminated by examining them graphically, the numerical fit results were examined. The two types of numerical fit results displayed in the Fitting GUI were goodness of fit statistics and confidence intervals on the fitted coefficients. The goodness of fit statistics helped to determine how well the curve fits the data. The confidence intervals on the coefficients determine their accuracy. The sum of squares due to error (SSE) and the adjusted *R*-square statistics were used to help determine the best fit. The SSE statistic gave the least-squares error of the fit, with a value closer to zero indicating a better fit. The adjusted *R*-square statistic was generally the best indicator of the fit quality when additional coefficients were added to the model.

3.2.2.6.6 Analyzing the Fit

The fit was evaluated over a specified data range with the analysis Graphic User Interface (GUI). The GUI was opened by clicking the Analysis button on Curve Fitting Tool. The appropriate MATLAB vector was entered in the Analyze at Xi field. The Evaluate fit was done at the Xi check box. The Plot results and Plot data set were selected. Then, the Apply button was clicked. This process was done for all the samples.

CHAPTER FOUR

RESULTS AND DISCUSSION

4.1 Results

The results and data obtained from the experiments done for Filtration properties, Rheological properties and Biodegradation properties and Soil Culturing for the isolation of specific Micro-organisms responsible for the biodegradation of the starches were respectively given in Table 4.1 to Table 4.45), Table 4.56 to Table 4.64 and Table 4.75 to Table 4.95. The data which were collected and studied under the filter loss method and tests for filtration properties of the samples included the fluid loss, the rates of filtration, Sorptivity and Diffusivity. The values of Soprtivity (S) were obtained as the slopes of fluid loss (V) versus square root of time ($t^{½}$) charts for the various Mud samples, through the use of equation 3.1 which is $V=St^{½}$ for filter loss test according to American Petroleum Institute (API). The values of diffusivity (D) were obtained as the slopes of filtration rate (dv/dt) versus time (t) charts for the various samples through the use of exponential equation 3.2, which is $\Phi (R) = \Phi_o$ exp-Dt) according to Henri Darcy. By definition, Sorptivity is a measure of the resistance on the flow of fluid passing through the built-up filter cake, while, Diffusivity is a measure of the flow rate of the fluid (Bernu, 2011; Andy et al., 2000; Scarlet & Brene, 2010).

The data, which were collected and studied under the viscometric method and tests for rheological propertie included viscosity (μ), Shear stress (τ), flow index (n), consistency index (K), and yield stress (τ_o) at four different shear rates (γ). The slopes of the logarithmic plots of shear stress versus shear rate gave the values of flow index using equation 3.3 which is ($\tau = k\gamma^n$) while the intercepts will give the consistency index (k) for the various samples (Bryan et al., 2010; Ukachukwu et al., 2010; Qartar

& Giacelo, 2010; Michael, 2009; Obong, 2004; Staben et al., 2004). The yield stress (τ_o) were computed from equation 3.4 which is

($\tau = \tau_o + k\ \gamma^n$) according to Herschel Bulkely (Bryan et al., 2010; Qartar & Giacelo 2010; Obong, 2004; Staben et al., 2004).

The data that were collected and studied under the experiments for biodegradation properties using soil burial test method and plant's growth method included Initial Weight, Final Weight, Weight Loss, Percentage Weight Loss, Height of plant's Shoot, and Length of plant's Root of all the samples (new blends of starches, already existing blended and unblended starches). The Percent Weight Loss (% Weight Loss) is obtained as in equation (3.5).

Table 4.1: Experimental Data and Results for the Filtration Properties of G:W–Mud sample at Room Temperature, 25^{o}C

Conc. (g/ml)	Time t (mins)	Square Root of Time (mins)	Fluid Loss Filtrate volume V (ml)	Rate of Filtration (fluid loss /Time)
0.01	50	7.07	32.00	0.64
	100	10.00	48.00	0.48
	150	12.25	63.00	0.42
	200	14.14	70.00	0.35
	250	15.81	76.00	0.30
	300	17.32	79.00	0.26
0.02	50	7.07	24.00	0.48
	100	10.00	34.00	0.34
	150	12.25	44.00	0.29
	200	14.14	49.00	0.25
	250	15.81	54.00	0.22
	300	17.32	57.00	0.19
0.03	50	7.07	18.00	0.36
	100	10.00	26.00	0.26
	150	12.25	37.00	0.25
	200	14.14	43.00	0.22
	250	15.81	47.00	0.19
	300	17.32	49.00	0.16
0.04	50	7.07	14.00	0.28
	100	10.00	22.00	0.22
	150	12.25	33.00	0.22
	200	14.14	40.00	0.20
	250	15.81	42.00	0.17
	300	17.32	44.00	0.15
0.05	50	7.07	12.00	0.24
	100	10.00	20.00	0.20
	150	12.25	30.00	0.20
	200	14.14	38.00	0.19
	250	15.81	41.00	0.16
	300	17.32	42.00	0.14

Table 4.2: Experimental Data and Results for the Filtration Properties of M:W–Mud sample at Room Temperature, 25^{o}C

Conc. (g/ml)	Time t (mins)	Square Root of Time (mins)	Fluid Loss Filtrate volume V (ml)	Rate of Filtration (fluid loss /Time)
0.01	50	7.07	54.00	1.08
	100	10.00	74.00	0.74
	150	12.25	93.00	0.62
	200	14.14	104.00	0.52
	250	15.81	110.00	0.44
	300	17.32	116.00	0.39
0.02	50	7.07	42.00	0.84
	100	10.00	57.00	0.57
	150	12.25	67.00	0.45
	200	14.14	77.00	0.39
	250	15.81	83.00	0.33
	300	17.32	90.00	0.30
0.03	50	7.07	30.00	0.60
	100	10.00	51.00	0.51
	150	12.25	63.00	0.42
	200	14.14	72.00	0.36
	250	15.81	80.00	0.32
	300	17.32	87.00	0.29
0.04	50	7.07	21.00	0.42
	100	10.00	40.00	0.40
	150	12.25	56.00	0.37
	200	14.14	66.00	0.33
	250	15.81	76.00	0.30
	300	17.32	80.00	0.27
0.05	50	7.07	20.00	0.40
	100	10.00	36.00	0.36
	150	12.25	51.00	0.34
	200	14.14	60.00	0.30
	250	15.81	67.00	0.27
	300	17.32	72.00	0.24

Table 4.3: Experimental Data and Results for the Filtration Properties of P:W–Mud sample at Room Temperature, 25^{o}C

Conc. (g/ml)	Time t (mins)	Square Root of Time (mins)	Fluid Loss Filtrate volume V (ml)	Rate of Filtration (fluid loss /Time)
0.01	50	7.07	67.00	1.34
	100	10.00	83.00	0.83
	150	12.25	96.00	0.64
	200	14.14	110.00	0.55
	250	15.81	115.00	0.46
	300	17.32	120.00	0.40
0.02	50	7.07	60.00	1.20
	100	10.00	75.00	0.75
	150	12.25	84.00	0.56
	200	14.14	93.00	0.47
	250	15.81	98.00	0.39
	300	17.32	105.00	0.35
0.03	50	7.07	52.00	1.04
	100	10.00	70.00	0.70
	150	12.25	79.00	0.53
	200	14.14	86.00	0.43
	250	15.81	92.00	0.37
	300	17.32	96.00	0.32
0.04	50	7.07	40.00	0.80
	100	10.00	59.00	0.59
	150	12.25	68.00	0.45
	200	14.14	75.00	0.38
	250	15.81	81.00	0.32
	300	17.32	84.00	0.28
0.05	50	7.07	29.00	0.58
	100	10.00	41.00	0.41
	150	12.25	54.00	0.36
	200	14.14	65.00	0.33
	250	15.81	73.00	0.29
	300	17.32	79.00	0.26

Table 4.4: Experimental Data and Results for the Filtration Properties of G:M–Mud sample at Room Temperature, 25^{o}C

Conc. (g/ml)	Time t (mins)	Square Root of Time (mins)	Fluid Loss Filtrate volume V (ml)	Rate of Filtration (fluid loss /Time)
0.01	50	7.07	82.00	1.64
	100	10.00	99.00	0.99
	150	12.25	110.00	0.73
	200	14.14	118.00	0.59
	250	15.81	126.00	0.50
	300	17.32	130.00	0.43
0.02	50	7.07	70.00	1.40
	100	10.00	87.00	0.87
	150	12.25	98.00	0.65
	200	14.14	108.00	0.54
	250	15.81	116.00	0.46
	300	17.32	120.00	0.40
0.03	50	7.07	61.00	1.22
	100	10.00	77.00	0.77
	150	12.25	88.00	0.59
	200	14.14	97.00	0.49
	250	15.81	104.00	0.42
	300	17.32	111.00	0.37
0.04	50	7.07	51.00	1.02
	100	10.00	68.00	0.68
	150	12.25	78.00	0.52
	200	14.14	87.00	0.44
	250	15.81	96.00	0.38
	300	17.32	101.00	0.34
0.05	50	7.07	42.00	0.84
	100	10.00	54.00	0.54
	150	12.25	67.00	0.45
	200	14.14	78.00	0.39
	250	15.81	89.00	0.36
	300	17.32	98.00	0.33

Table 4.5: Experimental Data and Results for the Filtration Properties of G:P–Mud sample at Room Temperature, 25^{o}C

Conc. (g/ml)	Time t (mins)	Square Root of Time (mins)	Fluid Loss Filtrate volume V (ml)	Rate of Filtration (fluid loss /Time)
0.01	50	7.07	98.00	1.96
	100	10.00	107.00	1.07
	150	12.25	120.00	0.80
	200	14.14	128.00	0.64
	250	15.81	135.00	0.54
	300	17.32	141.00	0.47
0.02	50	7.07	85.00	1.70
	100	10.00	102.00	1.02
	150	12.25	114.00	0.76
	200	14.14	123.00	0.62
	250	15.81	131.00	0.52
	300	17.32	134.00	0.45
0.03	50	7.07	75.00	1.50
	100	10.00	92.00	0.92
	150	12.25	104.00	0.69
	200	14.14	112.00	0.56
	250	15.81	119.00	0.48
	300	17.32	125.00	0.42
0.04	50	7.07	66.00	1.32
	100	10.00	83.00	0.83
	150	12.25	94.00	0.63
	200	14.14	103.00	0.52
	250	15.81	111.00	0.44
	300	17.32	117.00	0.39
0.05	50	7.07	58.00	1.16
	100	10.00	74.00	0.74
	150	12.25	84.00	0.56
	200	14.14	92.00	0.46
	250	15.81	99.00	0.39
	300	17.32	105.00	0.35

Table 4.6: Experimental Data and Results for the Filtration Properties of M:P–Mud sample at Room Temperature, 25^{o}C

Conc. (g/ml)	Time t (mins)	Square Root of Time (mins)	Fluid Loss Filtrate volume V (ml)	Rate of Filtration (fluid loss /Time)
0.01	50	7.07	116.00	2.32
	100	10.00	132.00	1.32
	150	12.25	142.00	0.95
	200	14.14	151.00	0.76
	250	15.81	160.00	0.64
	300	17.32	166.00	0.55
0.02	50	7.07	104.00	2.08
	100	10.00	118.00	1.18
	150	12.25	128.00	0.85
	200	14.14	139.00	0.70
	250	15.81	148.00	0.59
	300	17.32	153.00	0.51
0.03	50	7.07	93.00	1.86
	100	10.00	107.00	1.07
	150	12.25	117.00	0.78
	200	14.14	126.00	0.63
	250	15.81	134.00	0.54
	300	17.32	140.00	0.47
0.04	50	7.07	81.00	1.62
	100	10.00	96.00	0.96
	150	12.25	105.00	0.70
	200	14.14	114.00	0.57
	250	15.81	121.00	0.48
	300	17.32	127.00	0.42
0.05	50	7.07	69.00	1.38
	100	10.00	85.00	0.85
	150	12.25	96.00	0.64
	200	14.14	106.00	0.53
	250	15.81	114.00	0.46
	300	17.32	120.00	0.40

Table 4.7: Experimental Data and Results for the Filtration Properties of CMS:HPS–Mud sample at Room Temperature, 25^{o}C

Conc. (g/ml)	Time t (mins)	Square Root of Time (mins)	Fluid Loss Filtrate volume V (ml)	Rate of Filtration (fluid loss /Time)
0.01	50	7.07	157.00	3.14
	100	10.00	189.00	1.89
	150	12.25	212.00	1.41
	200	14.14	230.00	1.15
	250	15.81	240.00	0.96
	300	17.32	248.00	0.83
0.02	50	7.07	146.00	2.92
	100	10.00	176.00	1.76
	150	12.25	197.00	1.31
	200	14.14	213.00	1.07
	250	15.81	229.00	0.92
	300	17.32	239.00	0.80
0.03	50	7.07	140.00	2.80
	100	10.00	171.00	1.71
	150	12.25	191.00	1.27
	200	14.14	210.00	1.05
	250	15.81	223.00	0.89
	300	17.32	234.00	0.78
0.04	50	7.07	134.00	2.68
	100	10.00	164.00	1.64
	150	12.25	190.00	1.27
	200	14.14	204.00	1.02
	250	15.81	218.00	0.87
	300	17.32	230.00	0.77
0.05	50	7.07	130.00	2.60
	100	10.00	160.00	1.60
	150	12.25	183.00	1.22
	200	14.14	202.00	1.01
	250	15.81	214.00	0.86
	300	17.32	221.00	0.74

Table 4.8: Experimental Data and Results for the Filtration Properties of W–Mud sample at Room Temperature, 25^{o}C

Conc. (g/ml)	Time t (mins)	Square Root of Time (mins)	Fluid Loss Filtrate volume V (ml)	Rate of Filtration (fluid loss /Time)
0.01	50	7.07	207.00	4.14
	100	10.00	230.00	2.30
	150	12.25	258.00	1.72
	200	14.14	280.00	1.40
	250	15.81	300.00	1.20
	300	17.32	321.00	1.07
0.02	50	7.07	185.00	3.70
	100	10.00	220.00	2.20
	150	12.25	243.00	1.62
	200	14.14	263.00	1.32
	250	15.81	270.00	1.08
	300	17.32	289.00	0.96
0.03	50	7.07	170.00	3.40
	100	10.00	200.00	2.00
	150	12.25	216.00	1.44
	200	14.14	232.00	1.16
	250	15.81	249.00	0.99
	300	17.32	264.00	0.88
0.04	50	7.07	160.00	3.20
	100	10.00	183.00	1.83
	150	12.25	204.00	1.36
	200	14.14	225.00	1.13
	250	15.81	240.00	0.96
	300	17.32	256.00	0.85
0.05	50	7.07	148.00	2.96
	100	10.00	176.00	1.76
	150	12.25	201.00	1.34
	200	14.14	220.00	1.10
	250	15.81	230.00	0.92
	300	17.32	246.00	0.82

Table 4.9: Experimental Data and Results for the Filtration Properties of CMS–Mud sample at Room Temperature, 25^{o}C

Conc. (g/ml)	Time t (mins)	Square Root of Time (mins)	Fluid Loss Filtrate volume V (ml)	Rate of Filtration (fluid loss /Time)
0.01	50	7.07	220.00	4.40
	100	10.00	260.00	2.60
	150	12.25	289.00	1.93
	200	14.14	315.00	1.58
	250	15.81	336.00	1.34
	300	17.32	356.00	1.19
0.02	50	7.07	201.00	4.02
	100	10.00	242.00	2.42
	150	12.25	257.00	1.71
	200	14.14	277.00	1.39
	250	15.81	299.00	1.20
	300	17.32	319.00	1.06
0.03	50	7.07	192.00	3.84
	100	10.00	224.00	2.24
	150	12.25	254.00	1.69
	200	14.14	284.00	1.42
	250	15.81	307.00	1.23
	300	17.32	328.00	1.09
0.04	50	7.07	180.00	3.60
	100	10.00	205.00	2.05
	150	12.25	227.00	1.51
	200	14.14	249.00	1.25
	250	15.81	260.00	1.04
	300	17.32	281.00	0.94
0.05	50	7.07	165.00	3.30
	100	10.00	172.00	1.72
	150	12.25	188.00	1.25
	200	14.14	208.00	1.04
	250	15.81	234.00	0.94
	300	17.32	260.00	0.87

Table 4.10: Experimental Data and Results for the Filtration Properties of G:W–Mud sample at High Temperature, 150^{o}C

Conc. (g/ml)	Time t (mins)	Square Root of Time (mins)	Fluid Loss Filtrate volume V (ml)	Rate of Filtration (fluid loss /Time)
0.01	50	7.07	51.00	1.02
	100	10.00	69.00	0.69
	150	12.25	82.00	0.55
	200	14.14	91.00	0.46
	250	15.81	100.00	0.40
	300	17.32	108.00	0.36
0.02	50	7.07	48.00	0.96
	100	10.00	60.00	0.60
	150	12.25	75.00	0.50
	200	14.14	87.00	0.44
	250	15.81	94.00	0.38
	300	17.32	102.00	0.34
0.03	50	7.07	45.00	0.90
	100	10.00	57.00	0.57
	150	12.25	68.00	0.45
	200	14.14	79.00	0.39
	250	15.81	89.00	0.35
	300	17.32	97.00	0.32
0.04	50	7.07	40.00	0.80
	100	10.00	53.00	0.53
	150	12.25	60.00	0.40
	200	14.14	70.00	0.35
	250	15.81	80.00	0.32
	300	17.32	87.00	0.29
0.05	50	7.07	31.00	0.62
	100	10.00	47.00	0.47
	150	12.25	51.00	0.34
	200	14.14	63.00	0.31
	250	15.81	70.00	0.28
	300	17.32	76.00	0.25

Table 4.11: Experimental Data and Results for the Filtration Properties of M:W–Mud sample at High Temperature, 150^{o}C

Conc. (g/ml)	Time t (mins)	Square Root of Time (mins)	Fluid Loss Filtrate volume V (ml)	Rate of Filtration (fluid loss /Time)
0.01	50	7.07	80.00	1.60
	100	10.00	96.00	0.96
	150	12.25	110.00	0.73
	200	14.14	122.00	0.61
	250	15.81	132.00	0.53
	300	17.32	140.00	0.47
0.02	50	7.07	74.00	1.48
	100	10.00	88.00	0.88
	150	12.25	105.00	0.70
	200	14.14	114.00	0.57
	250	15.81	125.00	0.50
	300	17.32	135.00	0.45
0.03	50	7.07	68.00	1.36
	100	10.00	82.00	0.82
	150	12.25	95.00	0.63
	200	14.14	106.00	0.53
	250	15.81	115.00	0.46
	300	17.32	122.00	0.41
0.04	50	7.07	61.00	1.22
	100	10.00	77.00	0.77
	150	12.25	89.00	0.59
	200	14.14	103.00	0.52
	250	15.81	109.00	0.44
	300	17.32	118.00	0.39
0.05	50	7.07	56.00	1.12
	100	10.00	71.00	0.71
	150	12.25	84.00	0.56
	200	14.14	96.00	0.48
	250	15.81	108.00	0.43
	300	17.32	115.00	0.38

Table 4.12: Experimental Data and Results for the Filtration Properties of P:W–Mud sample at High Temperature, 150^{o}C

Conc. (g/ml)	Time t (mins)	Square Root of Time (mins)	Fluid Loss Filtrate volume V (ml)	Rate of Filtration (fluid loss /Time)
0.01	50	7.07	110.00	2.20
	100	10.00	127.00	1.27
	150	12.25	143.00	0.95
	200	14.14	157.00	0.79
	250	15.81	172.00	0.69
	300	17.32	185.00	0.62
0.02	50	7.07	102.00	2.04
	100	10.00	115.00	1.15
	150	12.25	130.00	0.87
	200	14.14	140.00	0.70
	250	15.81	150.00	0.60
	300	17.32	162.00	0.54
0.03	50	7.07	96.00	1.92
	100	10.00	109.00	1.09
	150	12.25	120.00	0.80
	200	14.14	131.00	0.66
	250	15.81	142.00	0.57
	300	17.32	151.00	0.50
0.04	50	7.07	88.00	1.76
	100	10.00	105.00	1.05
	150	12.25	118.00	0.79
	200	14.14	124.00	0.62
	250	15.81	134.00	0.54
	300	17.32	142.00	0.47
0.05	50	7.07	79.00	1.58
	100	10.00	90.00	0.90
	150	12.25	100.00	0.67
	200	14.14	110.00	0.55
	250	15.81	122.00	0.49
	300	17.32	128.00	0.43

Table 4.13: Experimental Data and Results for the Filtration Properties of G:M–Mud sample at HighTemperature, 150^{o}C

Conc. (g/ml)	Time t (mins)	Square Root of Time (mins)	Fluid Loss Filtrate volume V (ml)	Rate of Filtration (fluid loss /Time)
0.01	50	7.07	135.00	2.70
	100	10.00	150.00	1.50
	150	12.25	164.00	1.09
	200	14.14	178.00	0.89
	250	15.81	189.00	0.76
	300	17.32	199.00	0.66
0.02	50	7.07	128.00	2.56
	100	10.00	141.00	1.41
	150	12.25	156.00	1.04
	200	14.14	165.00	0.83
	250	15.81	175.00	0.70
	300	17.32	181.00	0.60
0.03	50	7.07	122.00	2.44
	100	10.00	134.00	1.34
	150	12.25	146.00	0.94
	200	14.14	156.00	0.78
	250	15.81	168.00	0.67
	300	17.32	173.00	0.58
0.04	50	7.07	113.00	2.26
	100	10.00	124.00	1.24
	150	12.25	138.00	0.92
	200	14.14	147.00	0.74
	250	15.81	154.00	0.62
	300	17.32	163.00	0.54
0.05	50	7.07	102.00	2.04
	100	10.00	115.00	1.15
	150	12.25	128.00	0.85
	200	14.14	139.00	0.70
	250	15.81	148.00	0.59
	300	17.32	154.00	0.51

Table 4.14: Experimental Data and Results for the Filtration Properties of G:P–Mud sample at High Temperature, 150^{o}C

Conc. (g/ml)	Time t (mins)	Square Root of Time (mins)	Fluid Loss Filtrate volume V (ml)	Rate of Filtration (fluid loss /Time)
0.01	50	7.07	162.00	3.24
	100	10.00	178.00	1.78
	150	12.25	192.00	1.28
	200	14.14	203.00	1.01
	250	15.81	215.00	0.86
	300	17.32	224.00	0.75
0.02	50	7.07	152.00	3.04
	100	10.00	165.00	1.65
	150	12.25	182.00	1.21
	200	14.14	195.00	0.98
	250	15.81	200.00	0.80
	300	17.32	210.00	0.70
0.03	50	7.07	145.00	2.90
	100	10.00	158.00	1.59
	150	12.25	170.00	1.13
	200	14.14	181.00	0.91
	250	15.81	190.00	0.76
	300	17.32	194.00	0.65
0.04	50	7.07	135.00	2.70
	100	10.00	148.00	1.49
	150	12.25	161.00	1.07
	200	14.14	174.00	0.87
	250	15.81	185.00	0.74
	300	17.32	190.00	0.63
0.05	50	7.07	126.00	2.52
	100	10.00	141.00	1.41
	150	12.25	152.00	1.01
	200	14.14	160.00	0.80
	250	15.81	169.00	0.68
	300	17.32	179.00	0.60

Table 4.15: Experimental Data and Results for the Filtration Properties of M:P–Mud sample at High Temperature, 150^{o}C

Conc. (g/ml)	Time t (mins)	Square Root of Time (mins)	Fluid Loss Filtrate volume V (ml)	Rate of Filtration (fluid loss /Time)
0.01	50	7.07	190.00	3.80
	100	10.00	206.00	2.06
	150	12.25	211,00	1.41
	200	14.14	225.00	1.13
	250	15.81	237.00	0.95
	300	17.32	246.00	0.82
0.02	50	7.07	182.00	3.64
	100	10.00	193.00	1.93
	150	12.25	207.00	1.38
	200	14.14	221.00	1.11
	250	15.81	229.00	0.92
	300	17.32	234.00	0.78
0.03	50	7.07	175.00	3.50
	100	10.00	188.00	1.88
	150	12.25	200.00	1.33
	200	14.14	210.00	1.05
	250	15.81	218.00	0.87
	300	17.32	224.00	0.75
0.04	50	7.07	165.00	3.30
	100	10.00	177.00	1.77
	150	12.25	189.00	1.26
	200	14.14	200.00	1.00
	250	15.81	208.00	0.83
	300	17.32	214.00	0.71
0.05	50	7.07	155.00	3.10
	100	10.00	167.00	1.67
	150	12.25	178.00	1.19
	200	14.14	188.00	0.94
	250	15.81	196.00	0.78
	300	17.32	208.00	0.69

Table 4.16: Experimental Data and Results for the Filtration Properties of CMS:HPS–Mud sample at High Temperature, 150^{o}C

Conc. (g/ml)	Time t (mins)	Square Root of Time (mins)	Fluid Loss Filtrate volume V (ml)	Rate of Filtration (fluid loss /Time)
0.01	50	7.07	230.00	4.60
	100	10.00	250.00	2.50
	150	12.25	265.00	1.77
	200	14.14	280.00	1.40
	250	15.81	292.00	1.17
	300	17.32	298.00	0.99
0.02	50	7.07	221.00	4.42
	100	10.00	240.00	2.40
	150	12.25	258.00	1.72
	200	14.14	272.00	1.36
	250	15.81	285.00	1.14
	300	17.32	292.00	0.97
0.03	50	7.07	215.00	4.30
	100	10.00	232.00	2.32
	150	12.25	247.00	1.65
	200	14.14	260.00	1.30
	250	15.81	272.00	1.09
	300	17.32	280.00	0.93
0.04	50	7.07	202.00	4.04
	100	10.00	220.00	2.20
	150	12.25	235.00	1.57
	200	14.14	246.00	1.23
	250	15.81	258.00	1.03
	300	17.32	268.00	0.89
0.05	50	7.07	175.00	3.50
	100	10.00	200.00	2.00
	150	12.25	214.00	1.43
	200	14.14	227.00	1.14
	250	15.81	239.00	0.96
	300	17.32	248.00	0.83

Table 4.17: Experimental Data and Results for the Filtration Properties of W–Mud sample at High Temperature, 150^{o}C

Conc. (g/ml)	Time t (mins)	Square Root of Time (mins)	Fluid Loss Filtrate volume V (ml)	Rate of Filtration (fluid loss /Time)
0.01	50	7.07	380.00	7.60
	100	10.00	430.00	4.30
	150	12.25	455.00	3.03
	200	14.14	480.00	2.40
	250	15.81	495.00	1.98
	300	17.32	511.00	1.70
0.02	50	7.07	360.00	7.20
	100	10.00	400.00	4.00
	150	12.25	435.00	2.90
	200	14.14	470.00	2.35
	250	15.81	485.00	1.94
	300	17.32	500.00	1.67
0.03	50	7.07	350.00	7.00
	100	10.00	370.00	3.70
	150	12.25	390.00	2.60
	200	14.14	420.00	2.10
	250	15.81	440.00	1.76
	300	17.32	475.00	1.58
0.04	50	7.07	310.00	6.20
	100	10.00	340.00	3.40
	150	12.25	375.00	2.50
	200	14.14	400.00	2.00
	250	15.81	436.00	1.74
	300	17.32	483.00	1.61
0.05	50	7.07	290.00	5.80
	100	10.00	320.00	3.20
	150	12.25	348.00	2.32
	200	14.14	373.00	1.87
	250	15.81	397.00	1.59
	300	17.32	423.00	1.41

Table 4.18: Experimental Data and Results for the Filtration Properties of CMS–Mud sample at High Temperature, 150^{o}C

Conc. (g/ml)	Time t (mins)	Square Root of Time (mins)	Fluid Loss Filtrate volume V (ml)	Rate of Filtration (fluid loss /Time)
0.01	50	7.07	485.00	9.70
	100	10.00	550.00	5.50
	150	12.25	600.00	4.00
	200	14.14	620.00	3.10
	250	15.81	645.00	2.58
	300	17.32	660.00	2.20
0.02	50	7.07	425.00	8.50
	100	10.00	465.00	4.65
	150	12.25	515.00	3.43
	200	14.14	560.00	2.80
	250	15.81	603.00	2.41
	300	17.32	631.00	2.10
0.03	50	7.07	405.00	8.10
	100	10.00	440.00	4.40
	150	12.25	475.00	3.17
	200	14.14	500.00	2.50
	250	15.81	527.00	2.11
	300	17.32	585.00	1.95
0.04	50	7.07	380.00	7.60
	100	10.00	424.00	4.24
	150	12.25	464.00	3.09
	200	14.14	480.00	2.40
	250	15.81	497.00	1.99
	300	17.32	540.00	1.80
0.05	50	7.07	365.00	7.30
	100	10.00	395.00	3.95
	150	12.25	447.00	2.98
	200	14.14	467.00	2.34
	250	15.81	483.00	1.93
	300	17.32	506.00	1.69

Table 4.19: Experimental Data and Results for the Filtration Properties of G:W–Mud sample at High Temperature, 250^{o}C

Conc. (g/ml)	Time t (mins)	Square Root of Time (mins)	Fluid Loss Filtrate volume V (ml)	Rate of Filtration (fluid loss /Time)
0.01	50	7.07	78.00	1.56
	100	10.00	95.00	0.95
	150	12.25	111.00	0.74
	200	14.14	126.00	0.63
	250	15.81	138.00	0.55
	300	17.32	148.00	0.49
0.02	50	7.07	72.00	1.44
	100	10.00	86.00	0.86
	150	12.25	98.00	0.65
	200	14.14	117.00	0.59
	250	15.81	128.00	0.51
	300	17.32	135.00	0.45
0.03	50	7.07	67.00	1.34
	100	10.00	80.00	0.80
	150	12.25	93.00	0.62
	200	14.14	104.00	0.52
	250	15.81	113.00	0.45
	300	17.32	121.00	0.40
0.04	50	7.07	60.00	1.20
	100	10.00	71.00	0.71
	150	12.25	85.00	0.57
	200	14.14	96.00	0.48
	250	15.81	106.00	0.42
	300	17.32	115.00	0.38
0.05	50	7.07	54.00	1.08
	100	10.00	65.00	0.65
	150	12.25	74.00	0.49
	200	14.14	81.00	0.41
	250	15.81	88.00	0.35
	300	17.32	94.00	0.31

Table 4.20: Experimental Data and Results for the Filtration Properties of M:W– Mud sample at High Temperature, 250^{o}C

Conc. (g/ml)	Time t (mins)	Square Root of Time (mins)	Fluid Loss Filtrate volume V (ml)	Rate of Filtration (fluid loss /Time)
0.01	50	7.07	106.00	2.12
	100	10.00	127.00	1.27
	150	12.25	145.00	0.97
	200	14.14	160.00	0.80
	250	15.81	171.00	0.68
	300	17.32	180.00	0.60
0.02	50	7.07	95.00	1.90
	100	10.00	116.00	1.16
	150	12.25	130.00	0.87
	200	14.14	143.00	0.72
	250	15.81	155.00	0.62
	300	17.32	167.00	0.56
0.03	50	7.07	87.00	1.74
	100	10.00	104.00	1.04
	150	12.25	117.00	0.78
	200	14.14	129.00	0.65
	250	15.81	138.00	0.55
	300	17.32	145.00	0.48
0.04	50	7.07	80.00	1.60
	100	10.00	92.00	0.92
	150	12.25	107.00	0.71
	200	14.14	119.00	0.60
	250	15.81	128.00	0.51
	300	17.32	137.00	0.46
0.05	50	7.07	72.00	1.44
	100	10.00	84.00	0.84
	150	12.25	95.00	0.63
	200	14.14	104.00	0.52
	250	15.81	112.00	0.45
	300	17.32	120.00	0.40

Table 4.21: Experimental Data and Results for the Filtration Properties of P:W–Mud sample at High Temperature, 250^{o}C

Conc. (g/ml)	Time t (mins)	Square Root of Time (mins)	Fluid Loss Filtrate volume V (ml)	Rate of Filtration (fluid loss /Time)
0.01	50	7.07	136.00	2.72
	100	10.00	158.00	1.58
	150	12.25	176.00	1.17
	200	14.14	198.00	0.99
	250	15.81	206.00	0.82
	300	17.32	216.00	0.72
0.02	50	7.07	125.00	2.50
	100	10.00	143.00	1.43
	150	12.25	157.00	1.05
	200	14.14	175.00	0.88
	250	15.81	191.00	0.76
	300	17.32	201.00	0.67
0.03	50	7.07	116.00	2.32
	100	10.00	131.00	1.31
	150	12.25	142.00	0.95
	200	14.14	152.00	0.76
	250	15.81	160.00	0.64
	300	17.32	167.00	0.56
0.04	50	7.07	109.00	2.18
	100	10.00	125.00	1.25
	150	12.25	137.00	0.91
	200	14.14	148.00	0.74
	250	15.81	155.00	0.62
	300	17.32	161.00	0.54
0.05	50	7.07	99.00	1.98
	100	10.00	113.00	1.13
	150	12.25	123.00	0.82
	200	14.14	132.00	0.66
	250	15.81	140.00	0.56
	300	17.32	150.00	0.50

Table 4.22: Experimental Data and Results for the Filtration Properties of G:M–Mud sample at High Temperature, 250^{o}C

Conc. (g/ml)	Time t (mins)	Square Root of Time (mins)	Fluid Loss Filtrate volume V (ml)	Rate of Filtration (fluid loss /Time)
0.01	50	7.07	167.00	3.34
	100	10.00	187.00	1.87
	150	12.25	204.00	1.36
	200	14.14	216.00	1.08
	250	15.81	226.00	0.90
	300	17.32	232.00	0.77
0.02	50	7.07	152.00	3.04
	100	10.00	168.00	1.68
	150	12.25	179.00	1.19
	200	14.14	193.00	0.97
	250	15.81	205.00	0.82
	300	17.32	216.00	0.72
0.03	50	7.07	140.00	2.80
	100	10.00	155.00	1.55
	150	12.25	167.00	1.11
	200	14.14	176.00	0.88
	250	15.81	184.00	0.74
	300	17.32	190.00	0.63
0.04	50	7.07	128.00	2.56
	100	10.00	142.00	1.42
	150	12.25	156.00	1.04
	200	14.14	167.00	0.84
	250	15.81	178.00	0.71
	300	17.32	185.00	0.62
0.05	50	7.07	112.00	2.24
	100	10.00	127.00	1.27
	150	12.25	138.00	0.92
	200	14.14	148.00	0.74
	250	15.81	158.00	0.63
	300	17.32	167.00	0.55

Table 4.23: Experimental Data and Results for the Filtration Properties of G:P–Mud sample at High Temperature, 250^{o}C

Conc. (g/ml)	Time t (mins)	Square Root of Time (mins)	Fluid Loss Filtrate volume V (ml)	Rate of Filtration (fluid loss /Time)
0.01	50	7.07	188.00	3.76
	100	10.00	207.00	2.07
	150	12.25	224.00	1.49
	200	14.14	237.00	1.19
	250	15.81	248.00	1.00
	300	17.32	260.00	0.87
0.02	50	7.07	174.00	3.48
	100	10.00	190.00	1.90
	150	12.25	204.00	1.36
	200	14.14	209.00	1.05
	250	15.81	226.00	0.90
	300	17.32	240.00	0.80
0.03	50	7.07	162.00	3.24
	100	10.00	176.00	1.76
	150	12.25	189.00	1.26
	200	14.14	201.00	1.01
	250	15.81	211.00	0.84
	300	17.32	220.00	0.73
0.04	50	7.07	145.00	2.90
	100	10.00	158.00	1.58
	150	12.25	172.00	1.15
	200	14.14	190.00	0.95
	250	15.81	200.00	0.80
	300	17.32	210.00	0.70
0.05	50	7.07	128.00	2.56
	100	10.00	144.00	1.44
	150	12.25	156.00	1.04
	200	14.14	166.00	0.83
	250	15.81	174.00	0.70
	300	17.32	181.00	0.60

Table 4.24: Experimental Data and Results for the Filtration Properties of M:P–Mud sample at High Temperature, 250^{o}C

Conc. (g/ml)	Time t (mins)	Square Root of Time (mins)	Fluid Loss Filtrate volume V (ml)	Rate of Filtration (fluid loss /Time)
0.01	50	7.07	209.00	4.18
	100	10.00	227.00	2.27
	150	12.25	243.00	1.62
	200	14.14	256.00	1.28
	250	15.81	268.00	1.07
	300	17.32	277.00	0.92
0.02	50	7.07	190.00	3.80
	100	10.00	210.00	2.10
	150	12.25	228.00	1.52
	200	14.14	240.00	1.20
	250	15.81	254.00	1.02
	300	17.32	265.00	0.88
0.03	50	7.07	182.00	3.64
	100	10.00	200.00	2.00
	150	12.25	216.00	1.44
	200	14.14	229.00	1.15
	250	15.81	240.00	0.96
	300	17.32	248.00	0.83
0.04	50	7.07	168.00	3.36
	100	10.00	185.00	1.85
	150	12.25	197.00	1.31
	200	14.14	215.00	1.08
	250	15.81	229.00	0.92
	300	17.32	236.00	0.79
0.05	50	7.07	150.00	3.00
	100	10.00	170.00	1.70
	150	12.25	188.00	1.25
	200	14.14	203.00	1.02
	250	15.81	216.00	0.86
	300	17.32	226.00	0.75

Table 4.25: Experimental Data and Results for the Filtration Properties of CMS:HPS–Mud sample at High Temperature, 250^{o}C

Conc. (g/ml)	Time t (mins)	Square Root of Time (mins)	Fluid Loss Filtrate volume V (ml)	Rate of Filtration (fluid loss /Time)
0.01	50	7.07	260.00	5.20
	100	10.00	290.00	2.90
	150	12.25	317.00	2.11
	200	14.14	337.00	1.69
	250	15.81	352.00	1.41
	300	17.32	364.00	1.21
0.02	50	7.07	251.00	5.02
	100	10.00	278.00	2.78
	150	12.25	306.00	2.04
	200	14.14	328.00	1.64
	250	15.81	346.00	1.38
	300	17.32	358.00	1.19
0.03	50	7.07	240.00	4.80
	100	10.00	267.00	2.67
	150	12.25	298.00	1.99
	200	14.14	318.00	1.59
	250	15.81	336.00	1.34
	300	17.32	348.00	1.16
0.04	50	7.07	230.00	4.60
	100	10.00	257.00	2.57
	150	12.25	275.00	1.83
	200	14.14	300.00	1.50
	250	15.81	320.00	1.28
	300	17.32	336.00	1.12
0.05	50	7.07	225.00	4.50
	100	10.00	245.00	2.45
	150	12.25	263.00	1.75
	200	14.14	289.00	1.45
	250	15.81	296.00	1.18
	300	17.32	304.00	1.01

Table 4.26: Experimental Data and Results for the Filtration Properties of W–Mud sample at High Temperature, 250^{o}C

Conc. (g/ml)	Time t (mins)	Square Root of Time (mins)	Fluid Loss Filtrate volume V (ml)	Rate of Filtration (fluid loss /Time)
0.01	50	7.07	572.00	11.44
	100	10.00	755.00	7.55
	150	12.25	755.00	5.03
	200	14.14	755.00	3.78
	250	15.81	755.00	3.02
	300	17.32	755.00	2.52
0.02	50	7.07	560.00	11.20
	100	10.00	754.00	7.54
	150	12.25	754.00	5.03
	200	14.14	754.00	3.77
	250	15.81	754.00	3.02
	300	17.32	754.00	2.51
0.03	50	7.07	559.00	11.18
	100	10.00	623.00	6.23
	150	12.25	754.00	5.03
	200	14.14	753.00	3.77
	250	15.81	753.00	3.01
	300	17.32	753.00	2.51
0.04	50	7.07	556.00	11.12
	100	10.00	623.00	6.23
	150	12.25	752.00	5.01
	200	14.14	750.00	3.75
	250	15.81	750.00	3.00
	300	17.32	750.00	2.50
0.05	50	7.07	550.00	11.00
	100	10.00	598.00	5.98
	150	12.25	625.00	4.17
	200	14.14	750.00	3.75
	250	15.81	750.00	3.00
	300	17.32	750.00	2.50

Table 4.27: Experimental Data and Results for the Filtration Properties of CMS–Mud sample at High Temperature, 250^{o}C

Conc. (g/ml)	Time t (mins)	Square Root of Time (mins)	Fluid Loss Filtrate volume V (ml)	Rate of Filtration (fluid loss /Time)
0.01	50	7.07	598.00	11.96
	100	10.00	764.00	7.64
	150	12.25	764.00	5.09
	200	14.14	764.00	3.82
	250	15.81	764.00	3.06
	300	17.32	764.00	2.55
0.02	50	7.07	590.00	11.80
	100	10.00	764.00	7.64
	150	12.25	764.00	5.09
	200	14.14	764.00	3.82
	250	15.81	764.00	3.06
	300	17.32	764.00	2.55
0.03	50	7.07	589.00	11.78
	100	10.00	764.00	7.64
	150	12.25	764.00	5.09
	200	14.14	764.00	3.82
	250	15.81	764.00	3.06
	300	17.32	764.00	2.55
0.04	50	7.07	585.00	11.70
	100	10.00	572.00	5.72
	150	12.25	764.00	5.09
	200	14.14	764.00	3.82
	250	15.81	764.00	3.06
	300	17.32	764.00	2.55
0.05	50	7.07	581.00	11.62
	100	10.00	566.00	5.66
	150	12.25	763.00	5.09
	200	14.14	763.00	3.82
	250	15.81	763.00	3.05
	300	17.32	763.00	2.54

Table 4.28: Experimental Data and Results for the Filtration Properties of G:W–Mud sample at High Temperature, 350^{o}C

Conc. (g/ml)	Time t (mins)	Square Root of Time (mins)	Fluid Loss Filtrate volume V (ml)	Rate of Filtration (fluid loss /Time)
0.01	50	7.07	104.00	2.08
	100	10.00	124.00	1.24
	150	12.25	144.00	0.96
	200	14.14	162.00	0.81
	250	15.81	177.00	0.71
	300	17.32	189.00	0.63
0.02	50	7.07	100.00	2.00
	100	10.00	115.00	1.15
	150	12.25	130.00	0.87
	200	14.14	146.00	0.73
	250	15.81	159.00	0.64
	300	17.32	170.00	0.57
0.03	50	7.07	93.00	1.86
	100	10.00	105.00	1.05
	150	12.25	116.00	0.77
	200	14.14	128.00	0.64
	250	15.81	140.00	0.56
	300	17.32	150.00	0.50
0.04	50	7.07	85.00	1.70
	100	10.00	97.00	0.97
	150	12.25	107.00	0.71
	200	14.14	120.00	0.60
	250	15.81	131.00	0.52
	300	17.32	148.00	0.49
0.05	50	7.07	79.00	1.58
	100	10.00	90.00	0.90
	150	12.25	101.00	0.67
	200	14.14	110.00	0.55
	250	15.81	118.00	0.47
	300	17.32	125.00	0.42

Table 4.29: Experimental Data and Results for the Filtration Properties of M:W–Mud sample at High Temperature, 350^{o}C

Conc. (g/ml)	Time t (mins)	Square Root of Time (mins)	Fluid Loss Filtrate volume V (ml)	Rate of Filtration (fluid loss /Time)
0.01	50	7.07	134.00	2.68
	100	10.00	159.00	1.59
	150	12.25	181.00	1.21
	200	14.14	198.00	0.99
	250	15.81	208.00	0.83
	300	17.32	217.00	0.72
0.02	50	7.07	130.00	2.60
	100	10.00	150.00	1.50
	150	12.25	171.00	1.14
	200	14.14	186.00	0.93
	250	15.81	199.00	0.80
	300	17.32	210.00	0.70
0.03	50	7.07	121.00	2.42
	100	10.00	139.00	1.39
	150	12.25	155.00	1.03
	200	14.14	170.00	0.85
	250	15.81	182.00	0.73
	300	17.32	193.00	0.64
0.04	50	7.07	118.00	2.36
	100	10.00	134.00	1.34
	150	12.25	148.00	0.99
	200	14.14	158.00	0.79
	250	15.81	167.00	0.67
	300	17.32	175.00	0.58
0.05	50	7.07	109.00	2.18
	100	10.00	126.00	1.26
	150	12.25	141.00	0.94
	200	14.14	151.00	0.76
	250	15.81	160.00	0.64
	300	17.32	168.00	0.56

Table 4.30: Experimental Data and Results for the Filtration Properties of P:W–Mud sample at High Temperature, 350^{o}C

Conc. (g/ml)	Time t (mins)	Square Root of Time (mins)	Fluid Loss Filtrate volume V (ml)	Rate of Filtration (fluid loss /Time)
0.01	50	7.07	162.00	3.24
	100	10.00	182.00	1.82
	150	12.25	201.00	1.34
	200	14.14	220.00	1.10
	250	15.81	235.00	0.94
	300	17.32	248.00	0.83
0.02	50	7.07	151.00	3.02
	100	10.00	172.00	1.72
	150	12.25	191.00	1.27
	200	14.14	205.00	1.03
	250	15.81	226.00	0.90
	300	17.32	239.00	0.80
0.03	50	7.07	140.00	2.80
	100	10.00	160.00	1.60
	150	12.25	176.00	1.17
	200	14.14	182.00	0.91
	250	15.81	196.00	0.78
	300	17.32	208.00	0.69
0.04	50	7.07	130.00	2.60
	100	10.00	147.00	1.47
	150	12.25	162.00	1.08
	200	14.14	178.00	0.89
	250	15.81	189.00	0.76
	300	17.32	201.00	0.67
0.05	50	7.07	119.00	2.38
	100	10.00	136.00	1.36
	150	12.25	152.00	1.01
	200	14.14	169.00	0.85
	250	15.81	181.00	0.72
	300	17.32	191.00	0.64

Table 4.31: Experimental Data and Results for the Filtration Properties of G:M–Mud sample at High Temperature, 350^{o}C

Conc. (g/ml)	Time t (mins)	Square Root of Time (mins)	Fluid Loss Filtrate volume V (ml)	Rate of Filtration (fluid loss /Time)
0.01	50	7.07	187.00	3.74
	100	10.00	208.00	2.08
	150	12.25	228.00	1.52
	200	14.14	243.00	1.23
	250	15.81	257.00	1.03
	300	17.32	271.00	0.90
0.02	50	7.07	177.00	3.54
	100	10.00	197.00	1.97
	150	12.25	215.00	1.43
	200	14.14	236.00	1.18
	250	15.81	244.00	0.98
	300	17.32	260.00	0.87
0.03	50	7.07	168.00	3.36
	100	10.00	186.00	1.86
	150	12.25	204.00	1.36
	200	14.14	226.00	1.13
	250	15.81	234.00	0.94
	300	17.32	246.00	0.82
0.04	50	7.07	156.00	3.12
	100	10.00	168.00	1.68
	150	12.25	181.00	1.21
	200	14.14	200.00	1.00
	250	15.81	216.00	0.86
	300	17.32	230.00	0.77
0.05	50	7.07	143.00	2.86
	100	10.00	158.00	1.58
	150	12.25	172.00	1.15
	200	14.14	184.00	0.92
	250	15.81	195.00	0.78
	300	17.32	204.00	0.68

Table 4.32: Experimental Data and Results for the Filtration Properties of G:P–Mud sample at High Temperature, 350^{o}C

Conc. (g/ml)	Time t (mins)	Square Root of Time (mins)	Fluid Loss Filtrate volume V (ml)	Rate of Filtration (fluid loss /Time)
0.01	50	7.07	213.00	4.26
	100	10.00	233.00	2.33
	150	12.25	253.00	1.69
	200	14.14	270.00	1.35
	250	15.81	286.00	1.14
	300	17.32	295.00	0.98
0.02	50	7.07	204.00	4.08
	100	10.00	222.00	2.22
	150	12.25	241.00	1.61
	200	14.14	258.00	1.29
	250	15.81	276.00	1.10
	300	17.32	282.00	0.94
0.03	50	7.07	195.00	3.90
	100	10.00	215.00	2.15
	150	12.25	232.00	1.55
	200	14.14	248.00	1.24
	250	15.81	261.00	1.04
	300	17.32	271.00	0.90
0.04	50	7.07	184.00	3.68
	100	10.00	208.00	2.08
	150	12.25	225.00	1.50
	200	14.14	238.00	1.19
	250	15.81	256.00	1.02
	300	17.32	266.00	0.88
0.05	50	7.07	170.00	3.40
	100	10.00	188.00	1.88
	150	12.25	203.00	1.35
	200	14.14	218.00	1.09
	250	15.81	236.00	0.94
	300	17.32	245.00	0.82

Table 4.33: Experimental Data and Results for the Filtration Properties of M:P–Mud sample at High Temperature, 350^{o}C

Conc. (g/ml)	Time t (mins)	Square Root of Time (mins)	Fluid Loss Filtrate volume V (ml)	Rate of Filtration (fluid loss /Time)
0.01	50	7.07	241.00	4.82
	100	10.00	265.00	2.65
	150	12.25	287.00	1.91
	200	14.14	299.00	1.50
	250	15.81	310.00	1.24
	300	17.32	320.00	1.07
0.02	50	7.07	235.00	4.70
	100	10.00	250.00	2.50
	150	12.25	267.00	1.78
	200	14.14	285.00	1.43
	250	15.81	297.00	1.19
	300	17.32	308.00	1.03
0.03	50	7.07	224.00	4.48
	100	10.00	239.00	2.39
	150	12.25	253.00	1.69
	200	14.14	265.00	1.33
	250	15.81	275.00	1.10
	300	17.32	285.00	0.95
0.04	50	7.07	215.00	4.30
	100	10.00	230.00	2.30
	150	12.25	246.00	1.64
	200	14.14	259.00	1.30
	250	15.81	269.00	1.08
	300	17.32	279.00	0.93
0.05	50	7.07	204.00	4.08
	100	10.00	215.00	2.15
	150	12.25	225.00	1.50
	200	14.14	237.00	1.19
	250	15.81	250.00	1.00
	300	17.32	265.00	0.88

Table 4.34: Experimental Data and Results for the Filtration Properties of CMS:HPS–Mud sample at High Temperature, 350^{o}C

Conc. (g/ml)	Time t (mins)	Square Root of Time (mins)	Fluid Loss Filtrate volume V (ml)	Rate of Filtration (fluid loss /Time)
0.01	50	7.07	400.00	8.00
	100	10.00	480.00	4.80
	150	12.25	560.00	3.71
	200	14.14	620.00	3.10
	250	15.81	680.00	2.72
	300	17.32	740.00	2.47
0.02	50	7.07	398.00	7.96
	100	10.00	477.00	4.77
	150	12.25	553.00	3.69
	200	14.14	619.00	3.10
	250	15.81	678.00	2.71
	300	17.32	739.00	2.46
0.03	50	7.07	397.00	7.94
	100	10.00	475.00	4.75
	150	12.25	550.00	3.67
	200	14.14	618.00	3.09
	250	15.81	677.00	2.71
	300	17.32	738.00	2.46
0.04	50	7.07	395.00	7.90
	100	10.00	473.00	4.73
	150	12.25	547.00	3.65
	200	14.14	616.00	3.08
	250	15.81	676.00	2.70
	300	17.32	736.00	2.45
0.05	50	7.07	393.00	7.86
	100	10.00	472.00	4.72
	150	12.25	545.00	3.63
	200	14.14	614.00	3.07
	250	15.81	675.00	2.70
	300	17.32	733.00	2.44

Table 4.35: Experimental Data and Results for the Filtration Properties of W–Mud sample at High Temperature, 350^{o}C

Conc. (g/ml)	Time t (mins)	Square Root of Time (mins)	Fluid Loss Filtrate volume V (ml)	Rate of Filtration (fluid loss /Time)
0.01	50	7.07	748.00	14.96
	100	10.00	766.00	7.66
	150	12.25	766.00	5.11
	200	14.14	766.00	3.83
	250	15.81	766.00	3.06
	300	17.32	766.00	2.55
0.02	50	7.07	765.00	15.30
	100	10.00	766.00	7.66
	150	12.25	766.00	5.11
	200	14.14	766.00	3.83
	250	15.81	766.00	3.06
	300	17.32	766.00	2.55
0.03	50	7.07	766.00	15.32
	100	10.00	766.00	7.66
	150	12.25	766.00	5.11
	200	14.14	766.00	3.83
	250	15.81	766.00	3.06
	300	17.32	766.00	2.55
0.04	50	7.07	764.00	15.28
	100	10.00	764.00	7.64
	150	12.25	766.00	5.11
	200	14.14	766.00	3.83
	250	15.81	766.00	3.06
	300	17.32	766.00	2.55
0.05	50	7.07	763.00	15.26
	100	10.00	764.00	7.64
	150	12.25	765.00	5.10
	200	14.14	766.00	3.83
	250	15.81	766.00	3.06
	300	17.32	766.00	2.55

Table 4.36: Experimental Data and Results for the Filtration Properties of CMS–Mud sample at High Temperature, 350^{o}C

Conc. (g/ml)	Time t (mins)	Square Root of Time (mins)	Fluid Loss Filtrate volume V (ml)	Rate of Filtration (fluid loss /Time)
0.01	50	7.07	765.00	15.30
	100	10.00	769.00	7.69
	150	12.25	771.00	5.14
	200	14.14	771.00	3.86
	250	15.81	771.00	3.08
	300	17.32	771.00	2.57
0.02	50	7.07	770.00	15.40
	100	10.00	770.00	7.70
	150	12.25	770.00	5.13
	200	14.14	770.00	3.85
	250	15.81	770.00	3.08
	300	17.32	700.00	2.57
0.03	50	7.07	769.00	15.38
	100	10.00	769.00	7.69
	150	12.25	769.00	5.13
	200	14.14	770.00	3.85
	250	15.81	770.00	3.08
	300	17.32	770.00	2.57
0.04	50	7.07	767.00	15.34
	100	10.00	768.00	7.68
	150	12.25	769.00	5.13
	200	14.14	769.00	3.85
	250	15.81	769.00	3.08
	300	17.32	769.00	2.56
0.05	50	7.07	768.00	15.36
	100	10.00	768.00	7.68
	150	12.25	768.00	5.12
	200	14.14	768.00	3.84
	250	15.81	768.00	3.07
	300	17.32	768.00	2.56

Table 4.37: Experimental Data and Results for the Filtration Properties of G:W–Mud sample at High Temperature, 450^{o}C

Conc. (g/ml)	Time t (mins)	Square Root of Time (mins)	Fluid Loss Filtrate volume V (ml)	Rate of Filtration (fluid loss /Time)
0.01	50	7.07	132.00	2.64
	100	10.00	153.00	1.53
	150	12.25	173.00	1.15
	200	14.14	195.00	0.98
	250	15.81	216.00	0.86
	300	17.32	248.00	0.83
0.02	50	7.07	119.00	2.38
	100	10.00	137.00	1.37
	150	12.25	156.00	1.04
	200	14.14	174.00	0.87
	250	15.81	192.00	0.77
	300	17.32	223.00	0.74
0.03	50	7.07	107.00	2.14
	100	10.00	126.00	1.26
	150	12.25	144.00	0.96
	200	14.14	165.00	0.83
	250	15.81	185.00	0.74
	300	17.32	203.00	0.68
0.04	50	7.07	98.00	1.96
	100	10.00	120.00	1.20
	150	12.25	135.00	0.90
	200	14.14	151.00	0.76
	250	15.81	169.00	0.68
	300	17.32	188.00	0.63
0.05	50	7.07	89.00	1.78
	100	10.00	109.00	1.09
	150	12.25	129.00	0.86
	200	14.14	140.00	0.70
	250	15.81	158.00	0.63
	300	17.32	174.00	0.58

Table 4.38: Experimental Data and Results for the Filtration Properties of M:W–Mud sample at High Temperature, 450^{o}C

Conc. (g/ml)	Time t (mins)	Square Root of Time (mins)	Fluid Loss Filtrate volume V (ml)	Rate of Filtration (fluid loss /Time)
0.01	50	7.07	176.00	3.52
	100	10.00	198.00	1.98
	150	12.25	222.00	1.48
	200	14.14	240.00	1.20
	250	15.81	267.00	1.07
	300	17.32	288.00	0.96
0.02	50	7.07	156.00	3.12
	100	10.00	170.00	1.70
	150	12.25	189.00	1.26
	200	14.14	212.00	1.06
	250	15.81	235.00	0.94
	300	17.32	259.00	0.86
0.03	50	7.07	143.00	2.86
	100	10.00	153.00	1.53
	150	12.25	177.00	1.18
	200	14.14	197.00	0.99
	250	15.81	216.00	0.86
	300	17.32	236.00	0.79
0.04	50	7.07	130.00	2.60
	100	10.00	148.00	1.48
	150	12.25	166.00	1.11
	200	14.14	180.00	0.90
	250	15.81	200.00	0.80
	300	17.32	220.00	0.73
0.05	50	7.07	116.00	2.32
	100	10.00	137.00	1.37
	150	12.25	151.00	1.01
	200	14.14	170.00	0.85
	250	15.81	190.00	0.76
	300	17.32	207.00	0.69

Table 4.39: Experimental Data and Results for the Filtration Properties of P:W–Mud sample at High Temperature, 450^{o}C

Conc. (g/ml)	Time t (mins)	Square Root of Time (mins)	Fluid Loss Filtrate volume V (ml)	Rate of Filtration (fluid loss /Time)
0.01	50	7.07	205.00	4.10
	100	10.00	226.00	2.26
	150	12.25	245.00	1.63
	200	14.14	264.00	1.32
	250	15.81	280.00	1.12
	300	17.32	295.00	0.98
0.02	50	7.07	191.00	3.82
	100	10.00	214.00	2.14
	150	12.25	233.00	1.55
	200	14.14	250.00	1.25
	250	15.81	269.00	1.08
	300	17.32	287.00	0.96
0.03	50	7.07	174.00	3.48
	100	10.00	196.00	1.96
	150	12.25	217.00	1.45
	200	14.14	235.00	1.18
	250	15.81	248.00	0.99
	300	17.32	264.00	0.88
0.04	50	7.07	160.00	3.20
	100	10.00	178.00	1.78
	150	12.25	194.00	1.29
	200	14.14	210.00	1.05
	250	15.81	227.00	0.91
	300	17.32	243.00	0.81
0.05	50	7.07	144.00	2.88
	100	10.00	157.00	1.57
	150	12.25	172.00	1.15
	200	14.14	186.00	0.93
	250	15.81	204.00	0.82
	300	17.32	225.00	0.75

Table 4.40: Experimental Data and Results for the Filtration Properties of G:M–Mud sample at High Temperature, 450^{o}C

Conc. (g/ml)	Time t (mins)	Square Root of Time (mins)	Fluid Loss Filtrate volume V (ml)	Rate of Filtration (fluid loss /Time)
0.01	50	7.07	234.00	4.68
	100	10.00	257.00	2.57
	150	12.25	277.00	1.85
	200	14.14	294.00	1.47
	250	15.81	310.00	1.24
	300	17.32	326.00	1.09
0.02	50	7.07	222.00	4.44
	100	10.00	246.00	2.46
	150	12.25	268.00	1.79
	200	14.14	289.00	1.45
	250	15.81	300.00	1.20
	300	17.32	318.00	1.06
0.03	50	7.07	202.00	4.04
	100	10.00	225.00	2.25
	150	12.25	244.00	1.63
	200	14.14	262.00	1.31
	250	15.81	286.00	1.14
	300	17.32	299.00	1.00
0.04	50	7.07	181.00	3.62
	100	10.00	205.00	2.05
	150	12.25	228.00	1.52
	200	14.14	251.00	1.26
	250	15.81	266.00	1.06
	300	17.32	281.00	0.94
0.05	50	7.07	160.00	3.20
	100	10.00	185.00	1.85
	150	12.25	208.00	1.39
	200	14.14	229.00	1.15
	250	15.81	250.00	1.00
	300	17.32	268.00	0.89

Table 4.41: Experimental Data and Results for the Filtration Properties of G:P–Mud sample at High Temperature, 450^{o}C

Conc. (g/ml)	Time t (mins)	Square Root of Time (mins)	Fluid Loss Filtrate volume V (ml)	Rate of Filtration (fluid loss /Time)
0.01	50	7.07	250.00	5.00
	100	10.00	272.00	2.72
	150	12.25	292.00	1.95
	200	14.14	309.00	1.55
	250	15.81	330.00	1.32
	300	17.32	347.00	1.16
0.02	50	7.07	235.00	4.70
	100	10.00	256.00	2.56
	150	12.25	275.00	1.83
	200	14.14	294.00	1.47
	250	15.81	311.00	1.24
	300	17.32	331.00	1.10
0.03	50	7.07	219.00	4.38
	100	10.00	238.00	2.38
	150	12.25	258.00	1.72
	200	14.14	282.00	1.41
	250	15.81	301.00	1.20
	300	17.32	320.00	1.07
0.04	50	7.07	199.00	3.98
	100	10.00	225.00	2.25
	150	12.25	247.00	1.65
	200	14.14	268.00	1.34
	250	15.81	287.00	1.15
	300	17.32	306.00	1.02
0.05	50	7.07	178.00	3.56
	100	10.00	202.00	2.02
	150	12.25	222.00	1.48
	200	14.14	243.00	1.22
	250	15.81	266.00	1.06
	300	17.32	289.00	0.96

Table 4.42: Experimental Data and Results for the Filtration Properties of M:P–Mud sample at High Temperature, 450^{o}C

Conc. (g/ml)	Time t (mins)	Square Root of Time (mins)	Fluid Loss Filtrate volume V (ml)	Rate of Filtration (fluid loss /Time)
0.01	50	7.07	299.00	5.98
	100	10.00	321.00	3.21
	150	12.25	343.00	2.29
	200	14.14	363.00	1.82
	250	15.81	381.00	1.52
	300	17.32	398.00	1.33
0.02	50	7.07	274.00	5.48
	100	10.00	293.00	2.93
	150	12.25	313.00	2.09
	200	14.14	334.00	1.67
	250	15.81	354.00	1.42
	300	17.32	375.00	1.25
0.03	50	7.07	251.00	5.02
	100	10.00	269.00	2.69
	150	12.25	289.00	1.93
	200	14.14	310.00	1.55
	250	15.81	332.00	1.33
	300	17.32	350.00	1.17
0.04	50	7.07	228.00	4.56
	100	10.00	253.00	2.53
	150	12.25	277.00	1.85
	200	14.14	298.00	1.49
	250	15.81	319.00	1.28
	300	17.32	336.00	1.12
0.05	50	7.07	203.00	4.06
	100	10.00	224.00	2.24
	150	12.25	246.00	1.64
	200	14.14	270.00	1.35
	250	15.81	292.00	1.17
	300	17.32	315.00	1.05

Table 4.43: Experimental Data and Results for the Filtration Properties of CMS:HPS–Mud sample at High Temperature, 450^{o}C

Conc. (g/ml)	Time t (mins)	Square Root of Time (mins)	Fluid Loss Filtrate volume V (ml)	Rate of Filtration (fluid loss /Time)
0.01	50	7.07	556.00	11.12
	100	10.00	788.00	7.88
	150	12.25	788.00	5.25
	200	14.14	788.00	3.94
	250	15.81	788.00	3.15
	300	17.32	788.00	2.63
0.02	50	7.07	550.00	11.00
	100	10.00	780.00	7.80
	150	12.25	780.00	5.20
	200	14.14	780.00	3.90
	250	15.81	780.00	3.12
	300	17.32	780.00	2.60
0.03	50	7.07	548.00	10.96
	100	10.00	780.00	7.80
	150	12.25	780.00	5.20
	200	14.14	780.00	3.90
	250	15.81	780.00	3.12
	300	17.32	780.00	2.60
0.04	50	7.07	540.00	10.80
	100	10.00	772.00	7.72
	150	12.25	772.00	5.15
	200	14.14	772.00	3.86
	250	15.81	772.00	3.09
	300	17.32	772.00	2.57
0.05	50	7.07	540.00	10.80
	100	10.00	770.00	7.70
	150	12.25	770.00	5.13
	200	14.14	770.00	3.85
	250	15.81	770.00	3.08
	300	17.32	770.00	2.57

Table 4.44: Experimental Data and Results for the Filtration Properties of W–Mud sample at High Temperature, 450^{o}C

Conc. (g/ml)	Time t (mins)	Square Root of Time (mins)	Fluid Loss Filtrate volume V (ml)	Rate of Filtration (fluid loss /Time)
0.01	50	7.07	790.00	15.80
	100	10.00	790.00	7.90
	150	12.25	791.00	5.27
	200	14.14	791.00	3.96
	250	15.81	791.00	3.16
	300	17.32	791.00	2.64
0.02	50	7.07	788.00	15.76
	100	10.00	790.00	7.90
	150	12.25	790.00	5.27
	200	14.14	790.00	3.95
	250	15.81	790.00	3.16
	300	17.32	790.00	2.63
0.03	50	7.07	788.00	15.76
	100	10.00	788.00	7.88
	150	12.25	790.00	5.27
	200	14.14	790.00	3.95
	250	15.81	790.00	3.16
	300	17.32	790.00	2.63
0.04	50	7.07	787.00	15.74
	100	10.00	788.00	7.88
	150	12.25	789.00	5.26
	200	14.14	789.00	3.95
	250	15.81	789.00	3.16
	300	17.32	789.00	2.63
0.05	50	7.07	785.00	15.70
	100	10.00	787.00	7.87
	150	12.25	789.00	5.26
	200	14.14	789.00	3.95
	250	15.81	789.00	3.16
	300	17.32	789.00	2.63

Table 4.45: Experimental Data and Results for the Filtration Properties of CMS–Mud sample at High Temperature, 450^{o}C

Conc. (g/ml)	Time t (mins)	Square Root of Time (mins)	Fluid Loss Filtrate volume V (ml)	Rate of Filtration (fluid loss /Time)
0.01	50	7.07	793.00	15.86
	100	10.00	794.00	7.94
	150	12.25	794.00	5.29
	200	14.14	794.00	3.97
	250	15.81	794.00	3.18
	300	17.32	794.00	2.65
0.02	50	7.07	793.00	15.86
	100	10.00	793.00	7.93
	150	12.25	793.00	5.29
	200	14.14	793.00	3.97
	250	15.81	793.00	3.17
	300	17.32	793.00	2.64
0.03	50	7.07	791.00	15.82
	100	10.00	791.00	7.91
	150	12.25	792.00	5.28
	200	14.14	792.00	3.96
	250	15.81	792.00	3.17
	300	17.32	792.00	2.64
0.04	50	7.07	790.00	15.80
	100	10.00	790.00	7.90
	150	12.25	791.00	5.27
	200	14.14	791.00	3.96
	250	15.81	791.00	3.16
	300	17.32	791.00	2.64
0.05	50	7.07	790.00	15.80
	100	10.00	790.00	7.90
	150	12.25	790.00	5.27
	200	14.14	790.00	3.95
	250	15.81	791.00	3.16
	300	17.32	791.00	2.64

4.2 Discussion

4.2.1 Filtration Properties

The filtration properties of the new Biodegradable Polymer Drilling Muds (G:W-Mud, M:W-Mud, P:W-Mud, G:M-Mud, G:P-Mud, M:P-Mud) prepared with blends of starches from Millet and corns pregelatinized in the absence of a solvent or any chemical, and three already existing muds (CMS:HPS-Mud, W-Mud, CMS-Mud) prepared with respective blend of chemically modified Carboxymethyl starch and Hydroxypropyl starch, non-chemically- modified single Waxy corn starch, and chemically- modified single Carboxymethyl starch, were determined at 25^{o}C, 150^{o}C, 250^{o}C, 350^{o}C, and 450^{o}C using filter loss method. Each of the muds contained 0.01-0.05g/ml concentration of starch. Table 4.1 to table 4.45 in Appendix 1 show the results and data obtained from the test run for the filtration properties of the various mud samples at 25^{o}C, 150^{o}C, 250^{o}C, 350^{o}C and 450^{o}C respectively. The charts and results obtained with the data were used to discuss the fluid loss behaviours, thermal stability, effects of varying starch concentrations on the fluid loss behaviours of the muds, filtration rates of the various muds and effects of varying starch concentrations on the filtration rates of the muds at the different temperatures.

4.2.1.1 Fluid Loss Behaviors of the Muds at Room Temperature, 25^{o}C

The experimental results and data for the fluid loss behaviors based on filtration properties of the muds at 25^{o}C are given Tables 4.1 to 4.9. The plots of fluid loss versus square root of time to show the fluid loss behaviours of the muds at room temperature are given in the figures below.

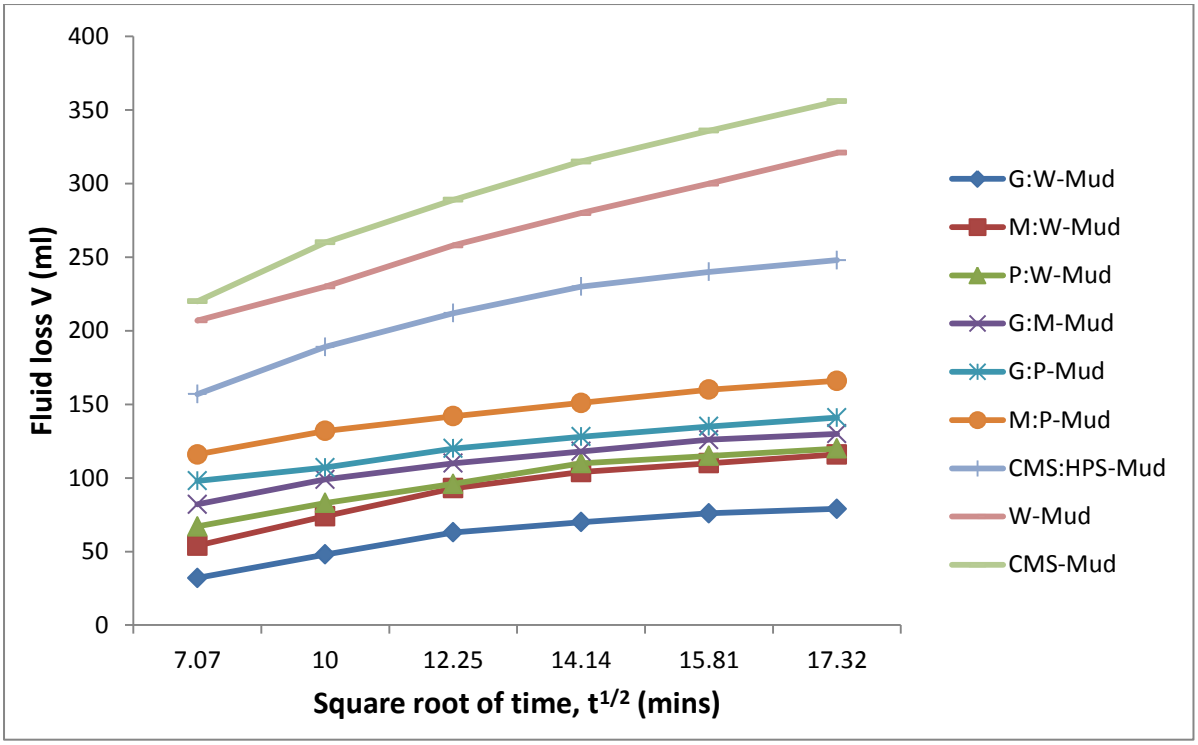

Figure 4.1: Plot of fluid loss versus square root of time for all the muds with 0.01g/ml starch concentration at room temperature, 25°C. (Data; Table 4.1-Table 4.9)

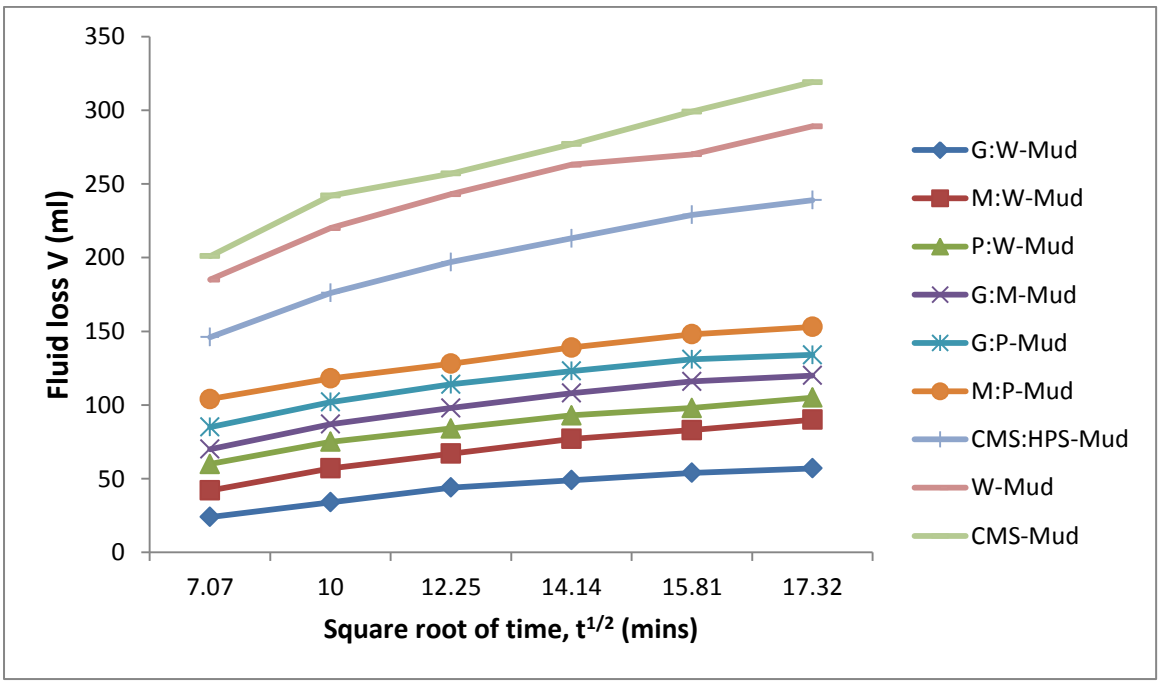

Figure 4.2: Plot of fluid loss versus square root of time for all the muds with 0.02g/ml starch concentration at room temperature, 25°C. (Data; Table 4.1-Table 4.9)

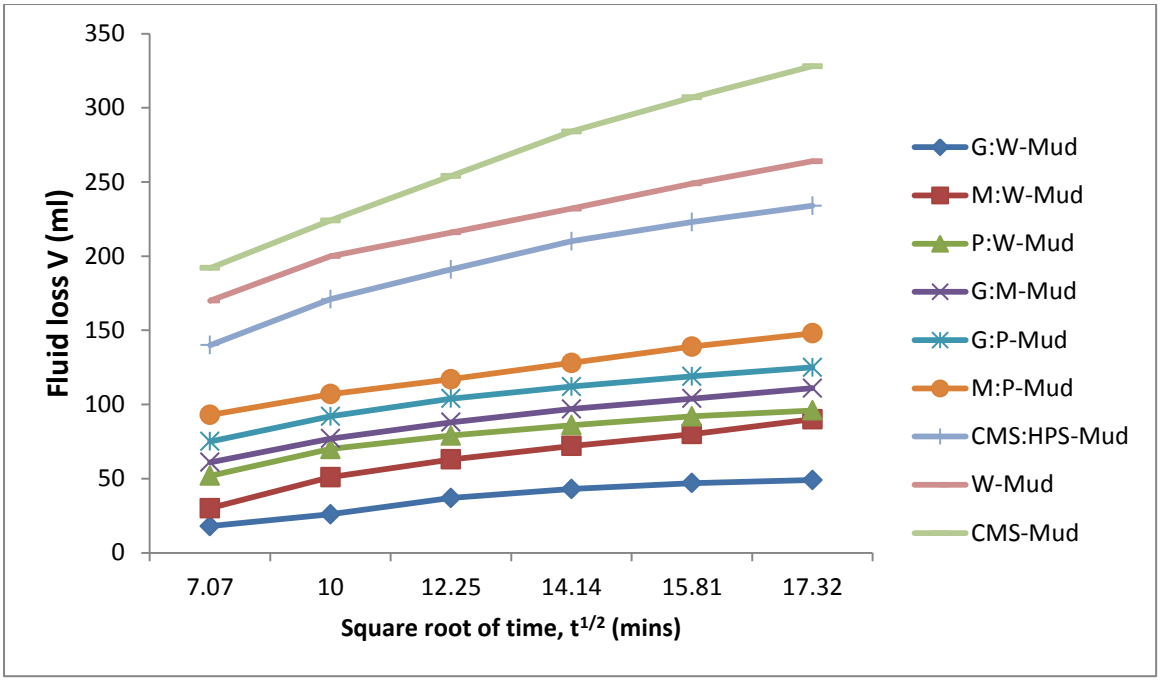

Figure 4.3: Plot of fluid loss versus square root of time for all the muds with 0.03g/ml starch concentration at room temperature, 25°C. (Data; Table 4.1-Table 4.9)

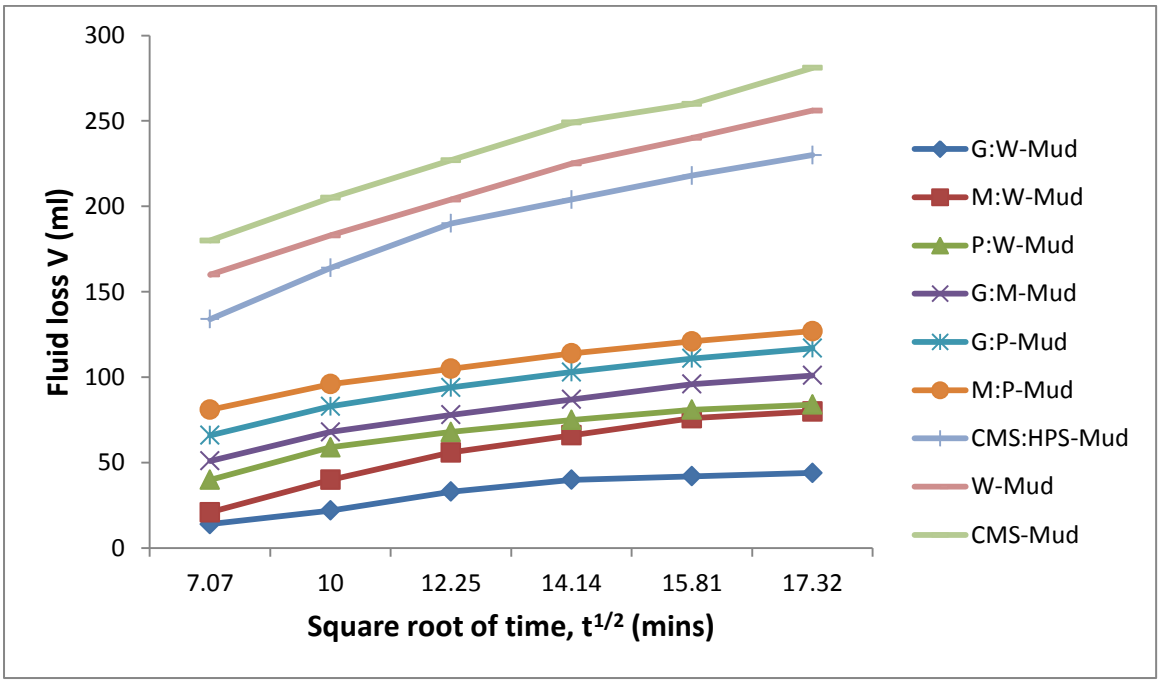

Figure 4.4: Plot of fluid loss versus square root of time for all the muds with 0.04g/ml starch concentration at room temperature, 25°C. (Data; Table 4.1-Table 4.9)

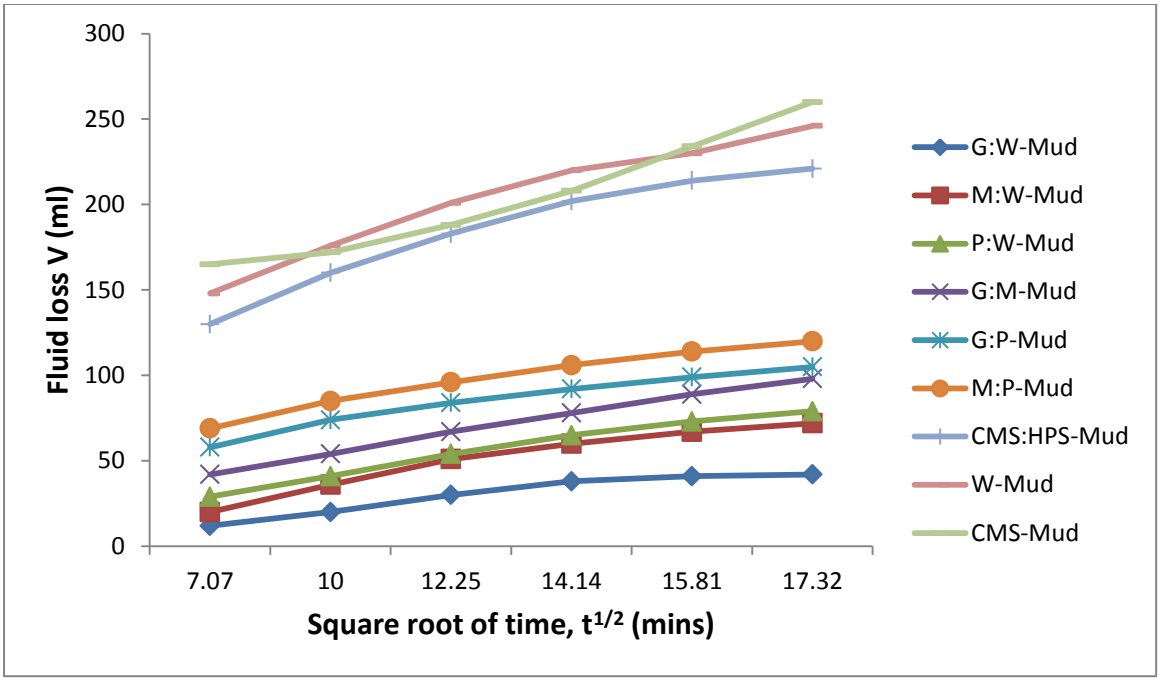

Figure 4.5: Plot of fluid loss versus square root of time for all the muds with 0.05g/ml starch concentration at room temperature, 25°C. (Data; Table 4.1-Table 4.9)

Figures 4.1, 4.2, 4.3, 4.4 and 4.5 show the plots of fluid loss versus square root of time for all the muds with 0.01-o.05g/ml starch concentrations at room temperature, 25°C. It was observed from the figures that the fluid loss of each mud varies almost linearly with square root of time. Further analysis of the figures shows that the fluid loss increases with increase in square root of time. The highest volume of fluid loss was obtained at the highest time of filtration. All the new polymer muds (G:W-Mud, M:W-Mud, P:W-Mud, G:M-Mud, G:P-Mud, M:P-Mud) containing starch blends showed less fluid loss values than the already existing muds (CMS:HPS-Mud, W-Mud, CMS-Mud) containing respectively blend of chemically modified starches, unblended non-chemically modified starch and unblended chemically modified starch. CMS-Mud containing unblended chemically modified Carboxymethyl starch gave the highest volume of fluid loss while the least volume of fluid loss was obtained with G:W-Mud at all the time intervals. The linear variation between fluid loss and

square root of time indicates that all the muds obeyed the American Petroleum Institute (API) model shown in equation 3.1, where the fluid loss volume is directly proportional to the square root of time (Hall & Hoff, 2012; Bernu, 2011; Anthony & Robert, 2010; Scarlet & Brene, 2010; American Petroleum Institute API, 2003; Andy et al., 2000). The less fluid loss capacity of the new polymer muds containing the new starch blends indicates that the new muds have better potentials and greater efficiency than the three already existing or widely-used muds, when used in actual drilling operation. This is because the ability of a mud to control fluid loss behavior is the ability to control circulation loss, wall caving and eventually formation damage during the actual drilling of a well.

In addition, each of the muds displayed different fluid loss behaviors with respect to time at room temperature of 25^{o}C. The difference, in the volumes of the filtrate or fluid loss by the muds, is a total indication of the extent of filtration control behavior of each of the muds during the actual drilling operation. More analysis of the figures at 25^{o}c temperature shows that there was reduction in all the fluid loss behaviors of all the new polymer muds (G:W-Mud, M:W-Mud, P:W-Mud, G:M-Mud, G:P-Mud and M:P-Mud). The fluid loss values of all the new polymer muds showed up to 50% decrease with respect to those of the already existing muds (CMS:HPS-Mud, W-Mud and CMS-Mud). The lower fluid loss values of the new muds indicate less scope of muds related formation damage during the actual drilling operation. However, fluid loss characteristics measured at room temperature may not be a better indicator of formation damage potential of a mud (Andrew and Robert, 2007; Amanullah 2004). The thermal degradation of the mud at elevated temperature may change the scenario. Therefore in comparison, the newly developed muds from the superior starch blend have better fluid loss control behaviours than the already existing muds. The better

fluid loss control behaviours of the new muds may be due to the combined strengths and efficiencies of the starch blends that are pure, pre-gelatinized and blended by a unique processing technique without the incorporation of any chemical or solvent.

4.2.1.2 Fluid loss Behaviours of the muds at High Temperature, 150^{0}C

The fluid loss behaviour of all the new polymer drilling muds and the three already existing muds containing 0.01-0.05g/ml range of starch concentrations at elevated temperature of 150^{0}c are shown in figure 4.6 to 4.10 below.

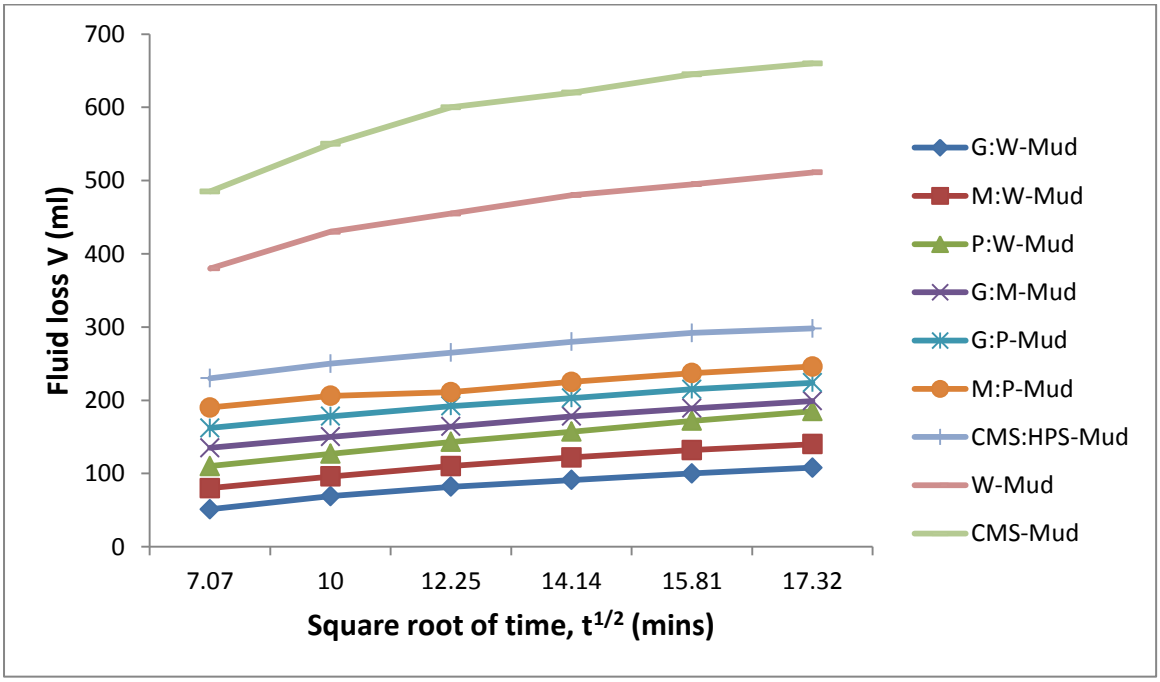

Figure 4.6: Plot of fluid loss versus square root of time for all the muds with 0.01g/ml starch concentration at high temperature, 150^{o}C. (Data; Table 4.10-Table 4.18)

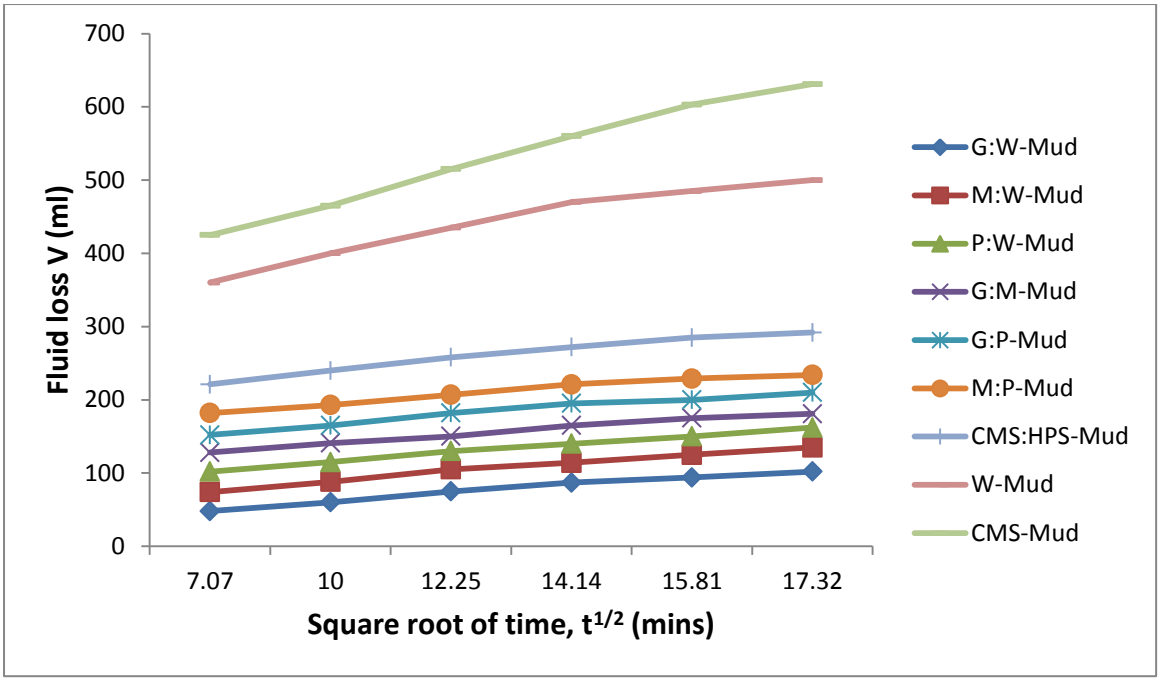

Figure 4.7: Plot of fluid loss versus square root of time for all the muds with 0.02g/ml starch concentration at high temperature, 150°C. (Data; Table 4.10-Table 4.18)

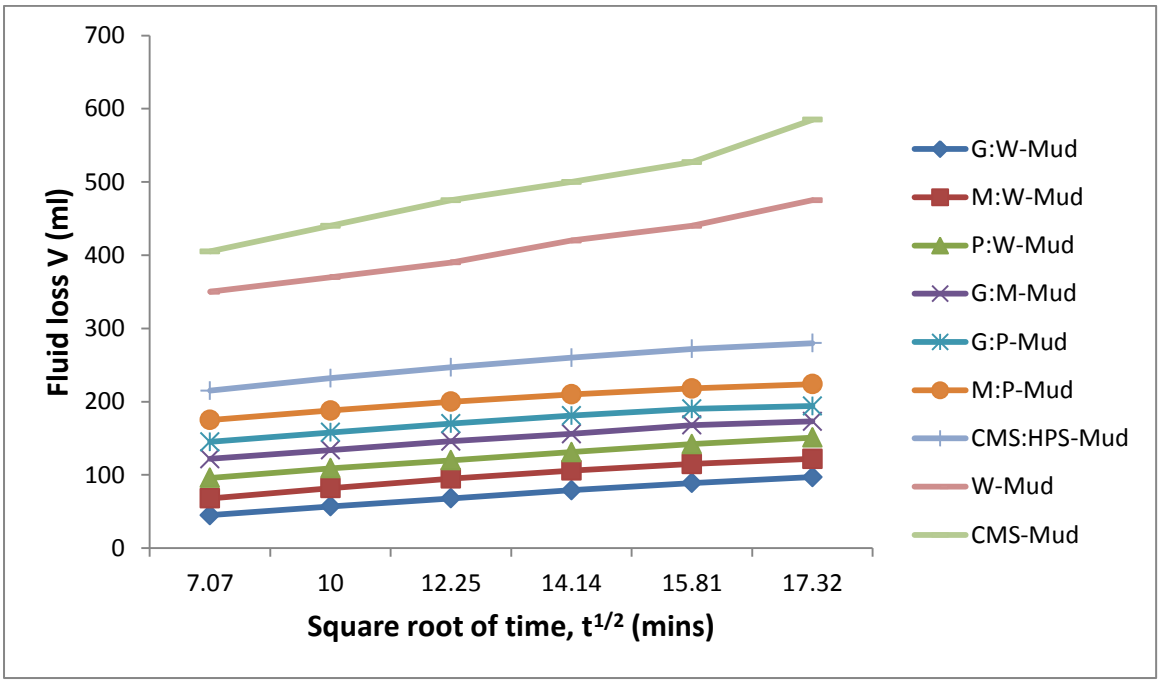

Figure 4.8: Plot of fluid loss versus square root of time for all the muds with 0.03g/ml starch concentration at high temperature, 150°C. (Data; Table 4.10-Table 4.18)

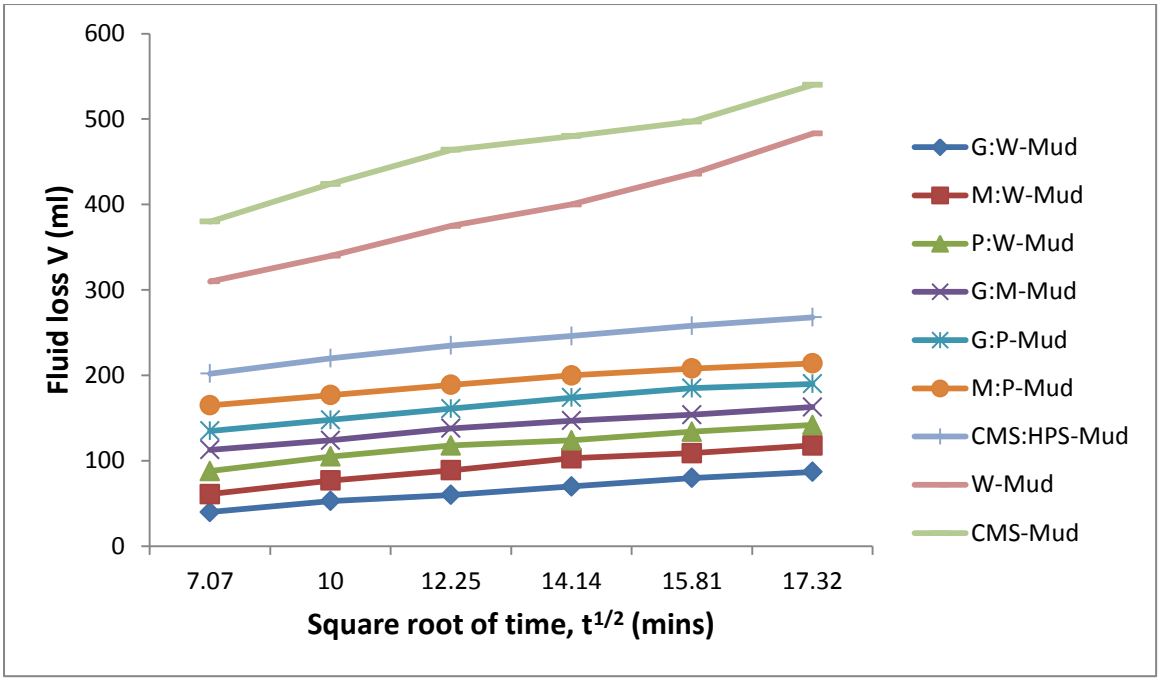

Figure 4.9: Plot of fluid loss versus square root of time for all the muds with 0.04g/ml starch concentration at high temperature, 150°C. (Data; Table 4.10-Table 4.18)

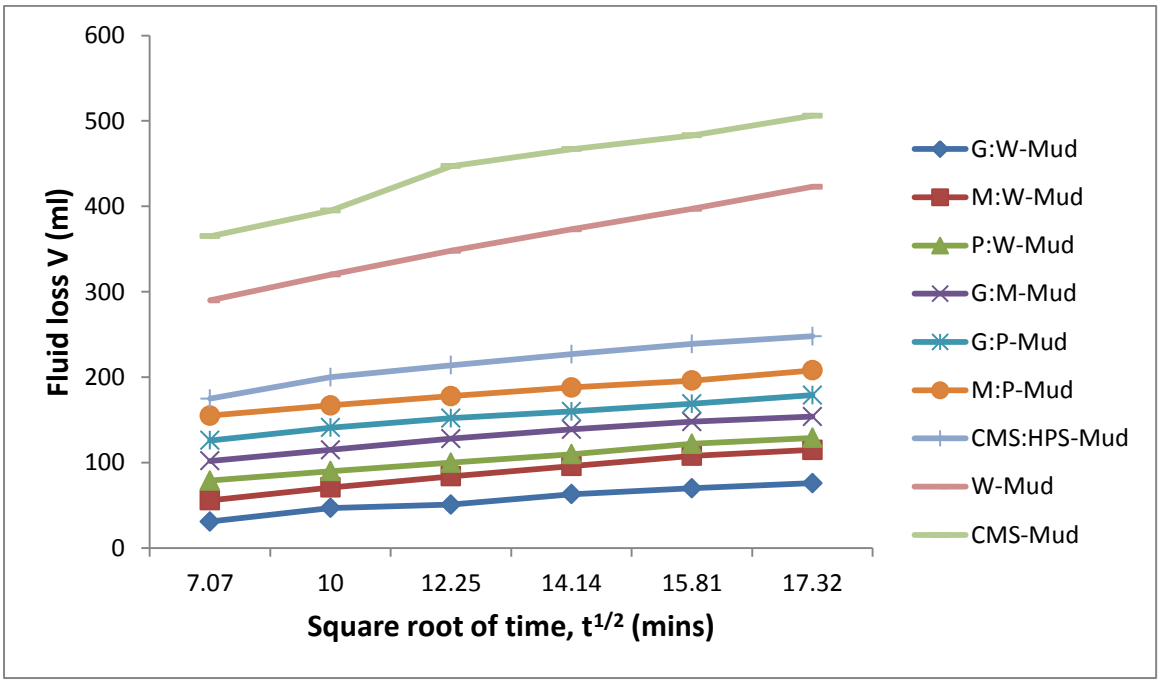

Figure 4.10: Plot of fluid loss versus square root of time for all the muds with 0.05g/ml starch concentration at high temperature, 150°C. (Data; Table 4.10-Table 4.18)

Figures 4.6, 4.7, 4.8, 4.9, and 4.10 show the plots of fluid loss versus square root of time for all the muds with 0.01-0.05g/ml starch concentration at elevated temperature of 150^0C put linear variation first. Analysis of the figures shows that all the muds posses good fluid loss behaviours and good thermal stability at the temperature of 150^0C. It is observed that after the thermal treatment of the muds, both the new polymer muds containing the novel blends of starches and the already existing muds were potentially thermally stable at 150^0C temperature. This is obvious in the area of filter loss or fluid loss behaviours of each of the muds, in which the difference in the volumes of filtrate or fluid loss, between a particular time interval and another, is minimal or small. It then implies that the quantity of fluid lost by each of the muds at 150^0C showed that the starches used in preparing the muds were still effective and efficient in building up filter cake that controlled the flow of fluid through it, even after the thermal treatment given at 150^oC. It should be recalled that the quantity or volume of filtrate or fluid loss, in any course of filtration, is also dependent on the ease or difficulty is fluid flow through the built-up filter cake (Herman et al., 2002). Generally, therefore, the good fluid loss behaviours of the new polymer muds (G:W-Mud, M:W-Mud, P:W-Mud, G:M-Mud, G:P-Mud, M:P-Mud) and the already existing muds (CMS:HPS-Mud, W-Mud, CMS-Mud), indicates that all the muds are efficient, thermally stable and suitable for drilling wells with bottom hole temperature of 150^0C.

The figures also show that the new polymer muds (G:W-Mud, M:W-Mud, G:W-Mud, G:P-Mud and M:P-Mud) have less fluid loss or filtrate values than the three already existing muds (CMS:HPS-Mud, W-Mud and CMS-Mud), although they are all thermally stable at 150^0C. This implies that each of the new muds possesses greater efficiency, thermal stability and more suitability than any of the three already existing

muds when used to drill wells with 150^{0}C hole temperatures. These better features of the new muds may be as a result of the nature of the new blends of starches used in preparing them.

4.2.1.3 Fluid Loss Behaviours of the muds at High Temperature, 250^{0}C

The fluid loss behaviours of all the new biodegradable polymer muds and the widely-used or already existing muds containing different starch concentrations at elevated or high temperature of 250^{0}C are displayed in the figures below.

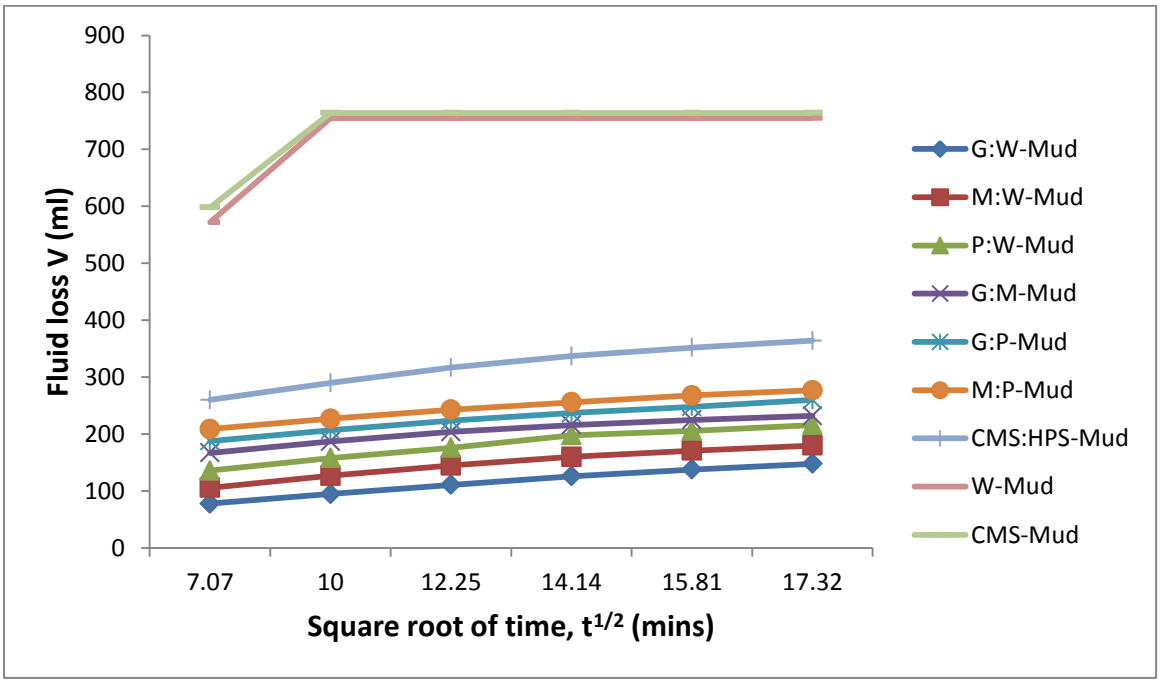

Figure 4.11: Plot of fluid loss versus square root of time for all the muds with 0.01g/ml starch concentration at high temperature, 250^{o}C. (Data; Table 4.19-Table 4.27)

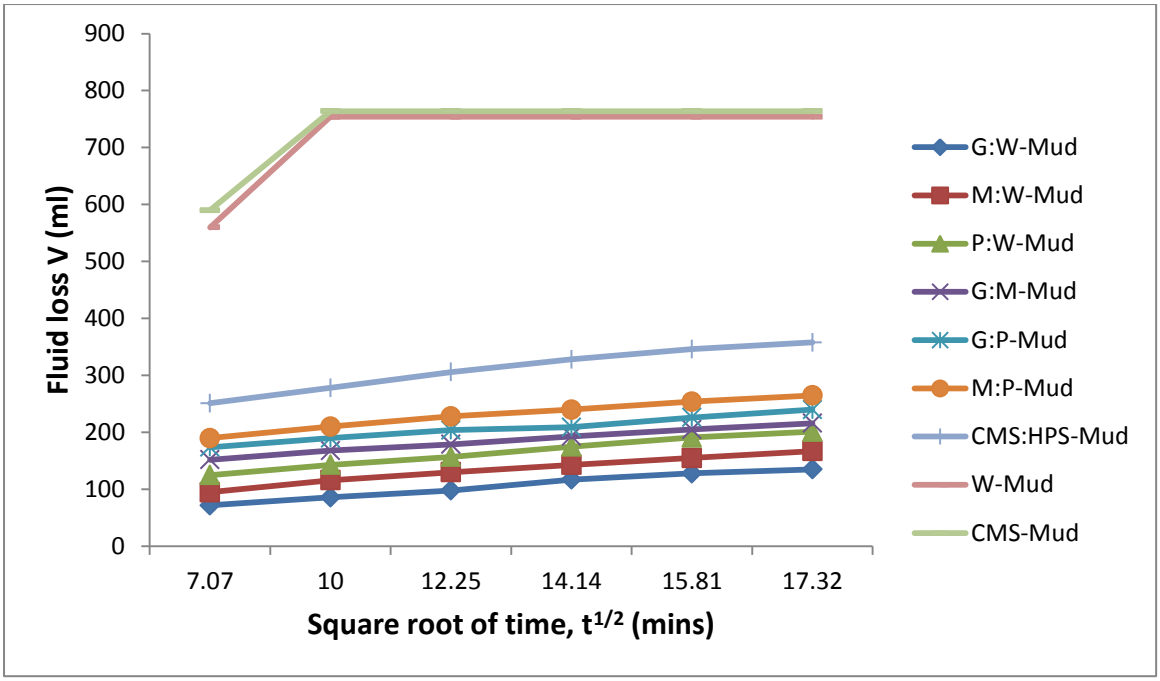

Figure 4.12: Plot of fluid loss versus square root of time for all the muds with 0.02g/ml starch concentration at high temperature, 250°C. (Data; Table 4.19-Table 4.27)

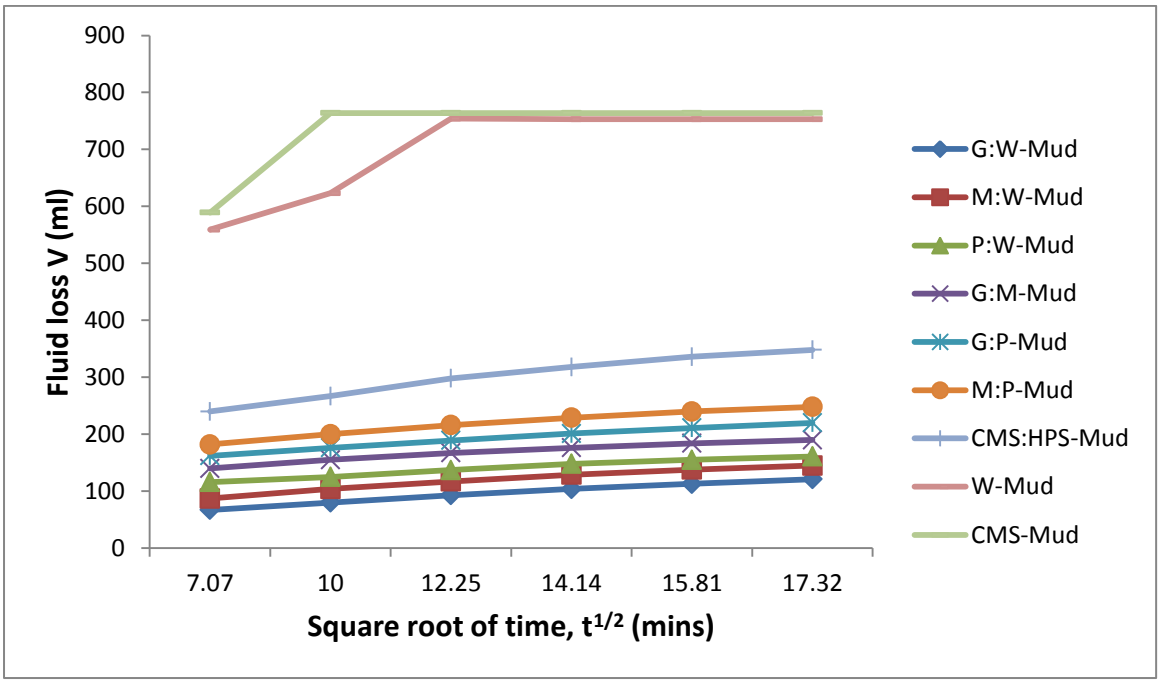

Figure 4.13: Plot of fluid loss versus square root of time for all the muds with 0.03g/ml starch concentration at high temperature, 250°C. (Data; Table 4.19-Table 4.27)

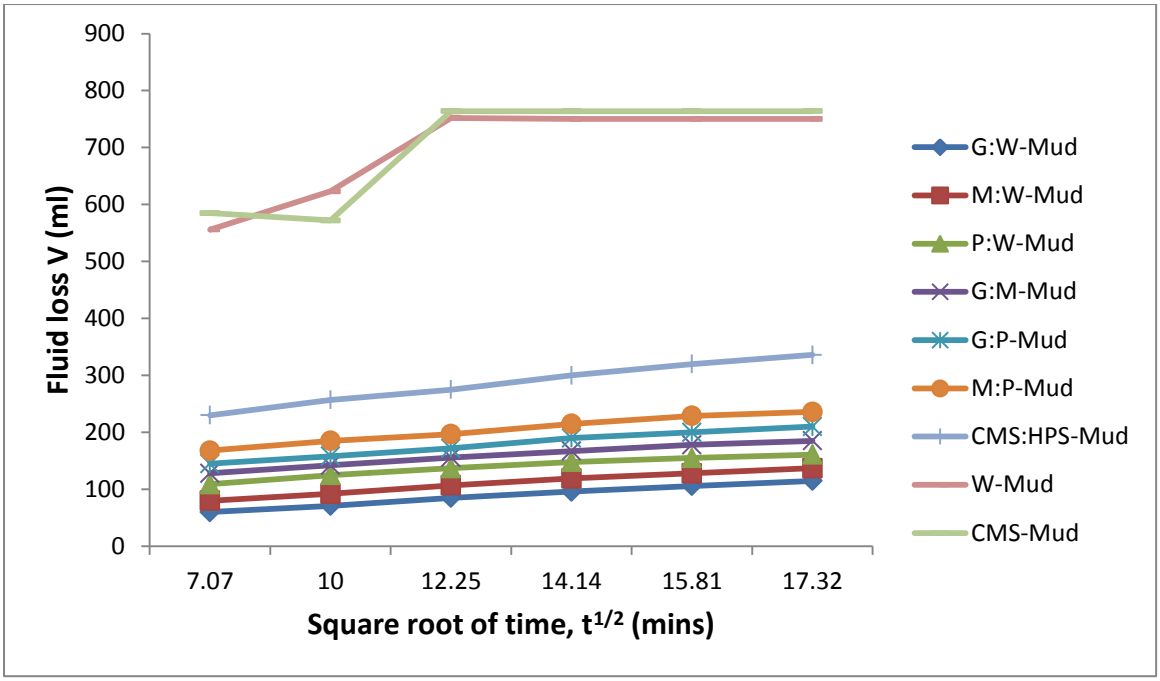

Figure 4.14: Plot of fluid loss versus square root of time for all the muds with 0.04g/ml starch concentration at high temperature, 250°C. (Data; Table 4.19-Table 4.27)

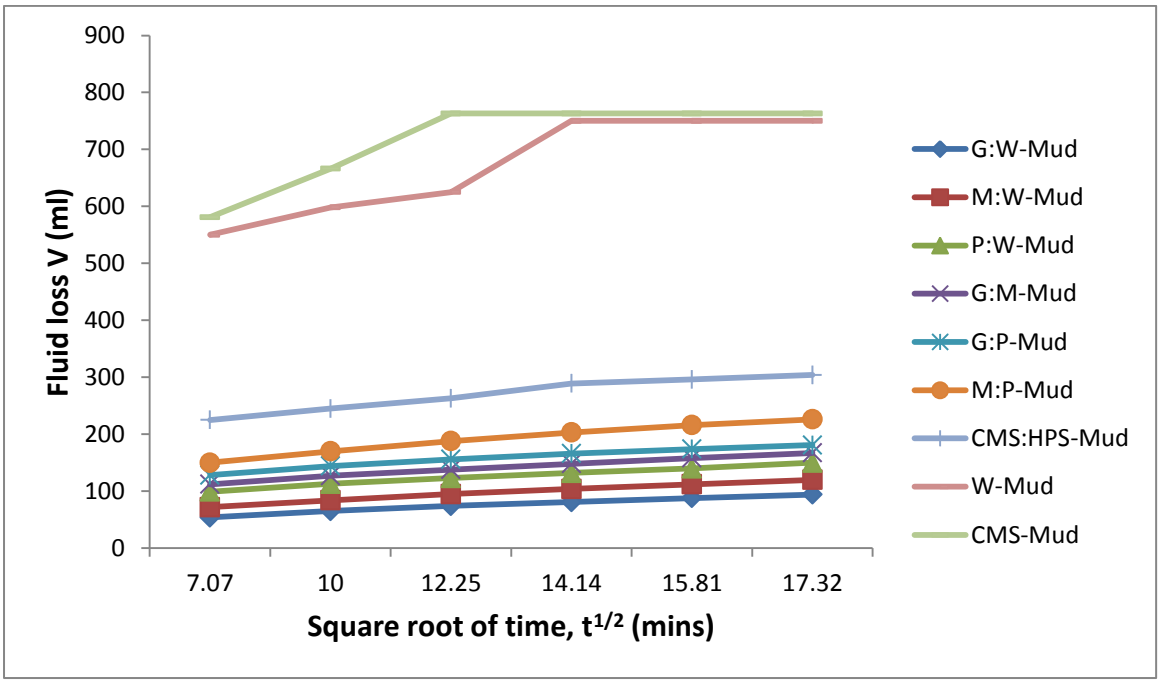

Figure 4.15: Plot of fluid loss versus square root of time for all the muds with 0.05g/ml starch concentration at high temperature, 250°C. (Data; Table 4.19-Table 4.27)

Figures 4.11, 4.12, 4.13, 4.14 and 4.15 show the plots of fluid loss versus squares root of time for all the muds with 0.01-0.05g/ml starch concentrations at 250^0C high temperature. The figures show that only the new polymer muds (G:W-Mud, M:W-Mud, P:W-Mud, G:M-Mud, G:P-Mud, M:P-Mud) and only one already existing mud (CMS:HPS-Mud) showed linear variations between the fluid loss and square root of time, while the other two already existing muds (W-Mud and CMS-Mud) did not. This implies that all the new muds and only one already existing mud (CMS:HPS-Mud) obeyed the American Petroleum Institute (API) model equation of Filtration, (equation 3.1), where the fluid loss volume is directly proportional to the square root of time (Hall & Hoff, 2012; Bernu, 2011; Anthony & Robert, 2010; Scarlet & Brene,2010; American Petroleum Institute API, 2003; Andy et al., 2000), while the other two muds (W-Mud, and CMS-Mud) did not. The failure by W-Mud and CMS-Mud to obey the API model is total indication of serious problems or catastrophy in the thermal stability and other features like filtration control of the muds. The shapes of the curves in the figures showed that the two already existing muds, W-mud and CMS-Mud, lost filtration control behaviour at 250^0C temperature, hence, their much greater fluid loss values than those of the new muds and CMS:HPS-Mud. The loss of filtration control by W-mud and CMS-Mud might have resulted from the fact that the starches contained by these muds were unblended and might have been easily made inactive by the high temperature of 250^0C. This means that the inactive starches could no longer swell to build up the viscosity of the muds, which on the other hand, could not build up effective amount of filter cakes to control the flow and passage of fluid through the cakes. The opposite was the case of the new polymer muds and CMS:HPS-Mud which contained blend of starches that were still excellent in controlling fluid loss and filtration activities at 250^0C.

Further analysis of figures 4.11-4.15 shows that all the new polymer muds containing pure blends of starches showed excellent thermal stability with low fluid loss values, one already existing mud CMS:HPS-Mud containing chemically modified blend of starches showed just good thermal stability with high fluid loss, while the other two already existing muds W-mud containing unblended pure starch and CMS-Mud containing unblended chemically modified starch, showed complete thermal degradation. The thermal degradation of W-mud and CMS-Mud is very clear when the curves in the figures at 250^0C are thoroughly viewed. It's obvious from the figures that the fluid loss values of W-mud and CMS-Mud appeared to vary linearly with square root of time at the initial stage, but changed later and became unusually high and constant as the square root of time increased. This really indicates complete thermal degradation of the two muds which might be due the presence of the unblended and chemically modified starches that might have been burnt up by the high temperature of 250^0C. The thermal stability of all the new muds and the widely used CMS:HPS-Mud may be as a result of the presence of the respective blends of starches in the muds, which were still effective and efficient in reducing fluid loss even at 250^0C. Therefore, the thermal stability of the new polymer muds and CMS:HPS-Mud proves that these muds can be used to drill wells with hole temperature of 250^0C and above. The thermal dergradation of W-Mud and CMS-Mud proves that the function of the unblended starches ceased at 250^0C and therefore, the muds are not suitable for drilling wells whose bottom hole temperatures are 250^0C and above.

4.2.1.4 Fluid Loss Behaviours of all the Muds at High Temperature of 350^{0}C

The fluid loss behaviours of the new muds and the already existing muds with 0.01-0.05g/ml starch concentration at high temperature of 350^{0}C are shown in the figures below.

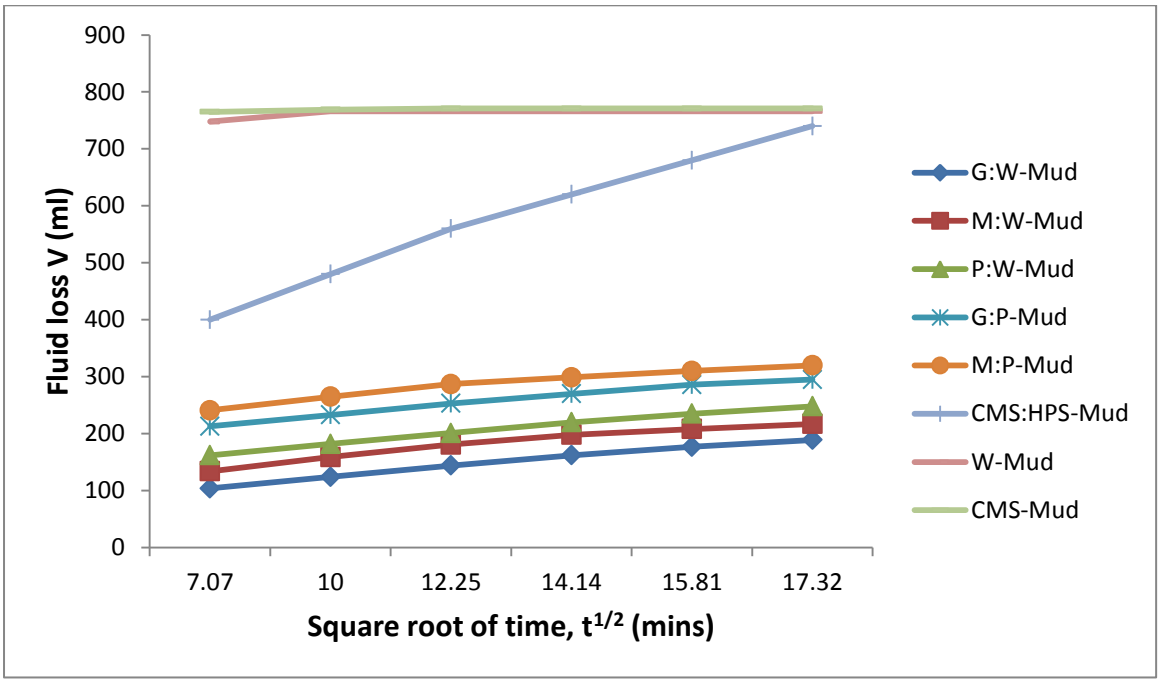

Figure 4.16: Plot of fluid loss versus square root of time for all the muds with 0.01g/ml starch concentration at high temperature, 350^{o}C. (Data; Table 4.28-Table 4.36)

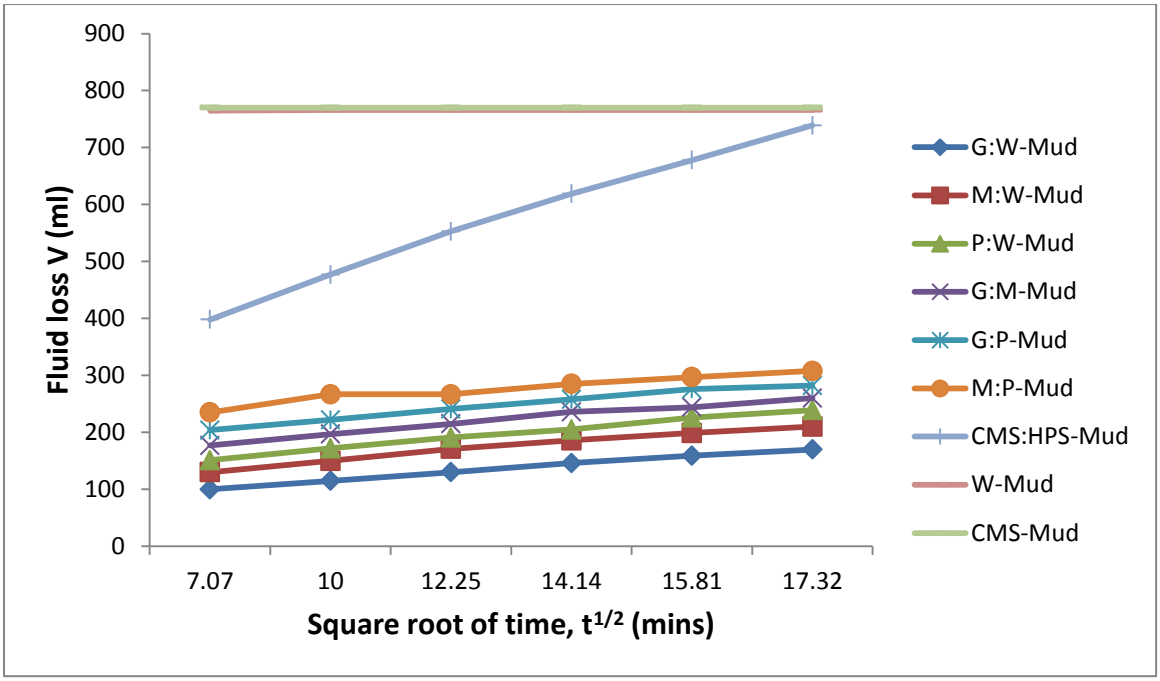

Figure 4.17: Plot of fluid loss versus square root of time for all the muds with 0.02g/ml starch concentration at high temperature, 350°C. (Data; Table 4.28-Table 4.36)

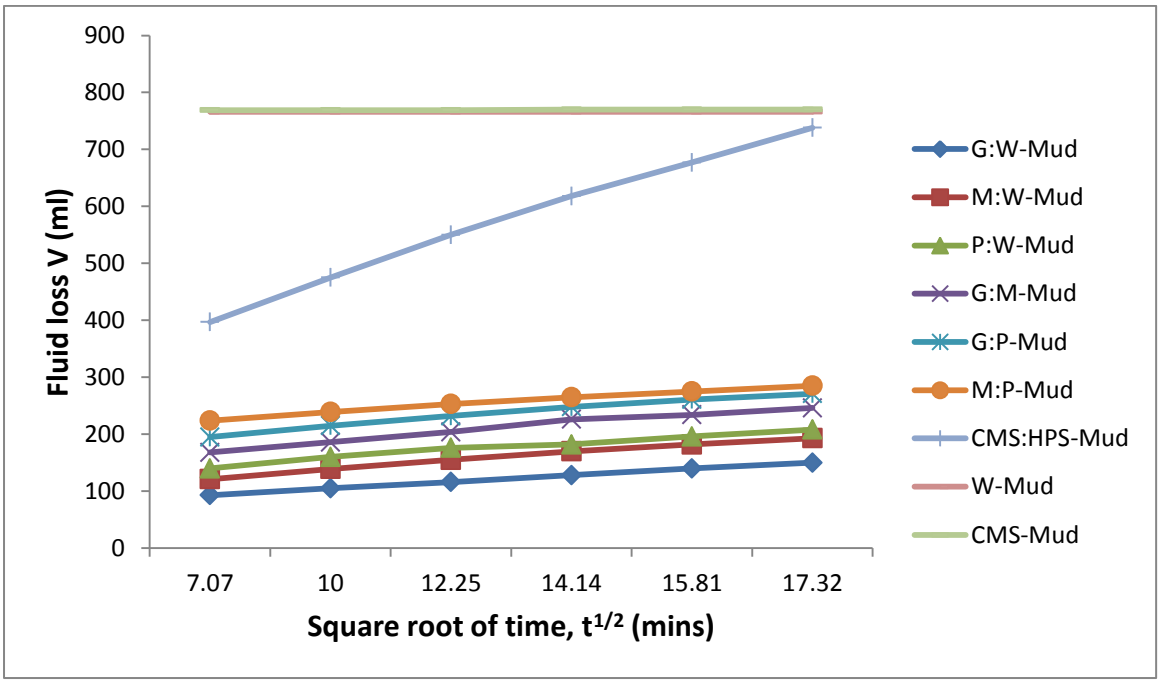

Figure 4.18: Plot of fluid loss versus square root of time for all the muds with 0.03g/ml starch concentration at high temperature, 350°C. (Data; Table 4.28-Table 4.36)

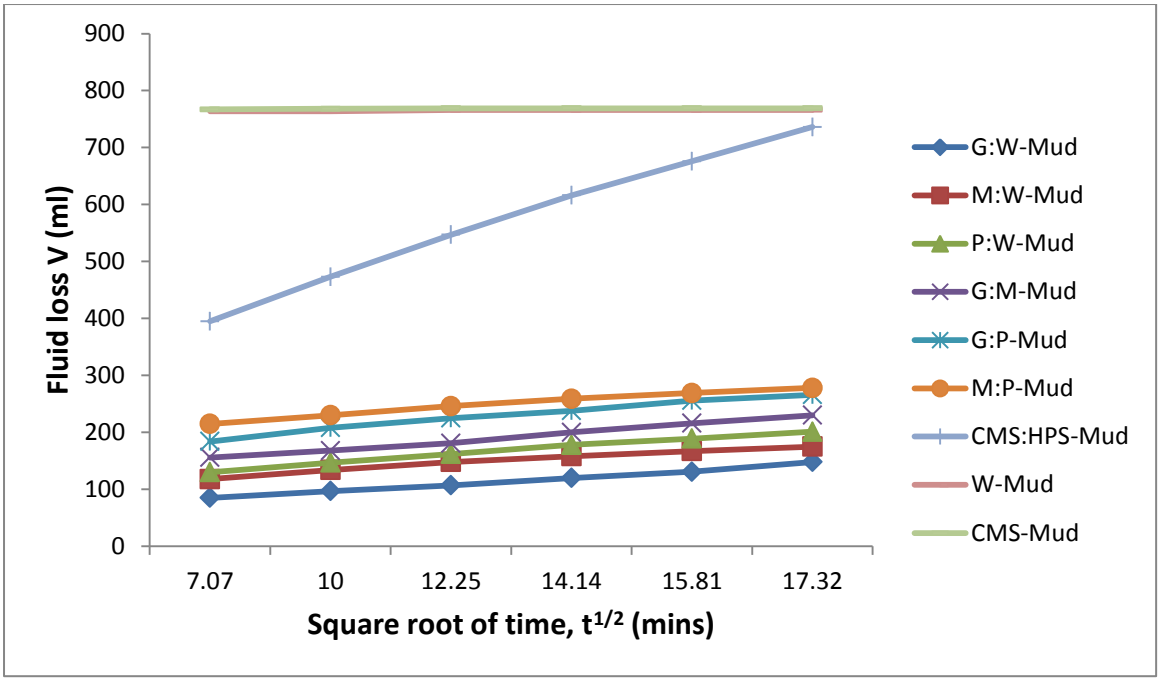

Figure 4.19: Plot of fluid loss versus square root of time for all the muds with 0.04g/ml starch concentration at high temperature, 350°C. (Data; Table 4.28-Table 4.36)

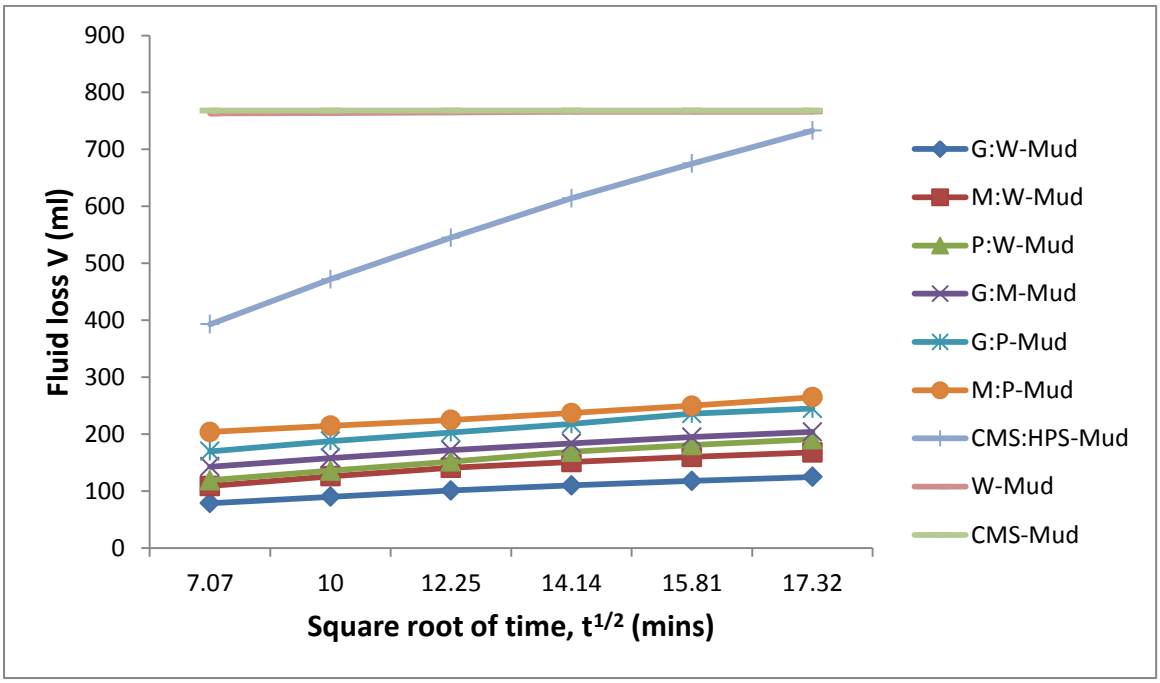

Figure 4.20: Plot of fluid loss versus square root of time for all the muds with 0.05g/ml starch concentration at high temperature, 350°C. (Data; Table 4.28-Table 4.36)

Figures 4.16, 4.17, 4.18, 4.19 and 4.20 show the plots of fluid loss versus square root of time for all the muds with 0.01-0.05g/ml starch concentrations at 450^0C high temperature. The figures show that the new muds and CMS:HPS-Mud containing starch blends showed linear variation between fluid loss and square root of time indicating compliance with the API filtration model, but W-mud and CMS-Mud did not comply with the model at all, indicating total in effectiveness and inactiveness of the muds. The failure in W-mud and CMS-Mud means that the unblended and chemically modified starches were not active at all to produce effective built-up filter cake to control fluid loss, at 350^0C. It then implies that W-mud and CMS-Mud are readily unstable to function at this high temperature, 350^0C.

Also, the figures 4.16- 4.20 show that the pattern of fluid loss by the new polymer muds differs from that of CMS:HPS-Mud although they all obeyed the API model. It was observed that all the new polymer muds containing the blends of non-chemically modified starches were very stable and showed no sign of thermal degradation while the already existing mud, CMS:HPS-Mud containing the chemically modified blend of starches showed some signs of thermal instability. All these could be seen in the volume of fluid loss. The shape of the curves, for the already existing chemically modified CHM:HPS-Mud, showed rapid increases at the various time intervals and different concentrations. The difference in volumes of fluid or filter loss between each set of similar time intervals at the varying concentrations were so little that it could be negligible. For the new polymer muds, opposite observations were the case, and this means that the starches used in preparing the muds were still active or effective in their functions which enabled the muds to still possess great efficiency in their fluid loss control behaviours even at this high temperature. For the already existing CMS:HPS-Mud, the efficiency of chemically modified starches might have been

reduced by the elevated temperature thereby reducing the fluid loss control behaviour of the mud. This might be due to the presence of the chemicals used in both pregelatinizing and blending the starches.

In the actual drilling operation, the effect is that each of the new polymer muds is still thermally stable and efficient to control its filtration behaviour so that the right quantity of fluid is circulated continuously round the walls of the well-bore throughout the drilling period. In the case of the already existing CMS:HPS-Mud containing the chemically modified starches, a unique experience occurs. At the initial time of drilling, the fluid is rapidly lost to give great volume of fluid loss at any time. After sometimes, the fluid remaining in the mud becomes very small and insufficient to control normal filtration behaviour and provide enough fluid for circulation round the walls of the well. This results in reduction of the mud's ability to aid continuation of actual drilling. This is an indication that total thermal degradation is about to set in (Brown, 2009).

4.2.1.5 Fluid Loss Behaviours of all the Muds at High Temperature, 450^0C

The fluid loss behaviours of all the muds including the new polymer drilling muds and the three already existing muds containing 0.01-0.05g/ml range of starch concentrations at 450^0C are presented in the figures below.

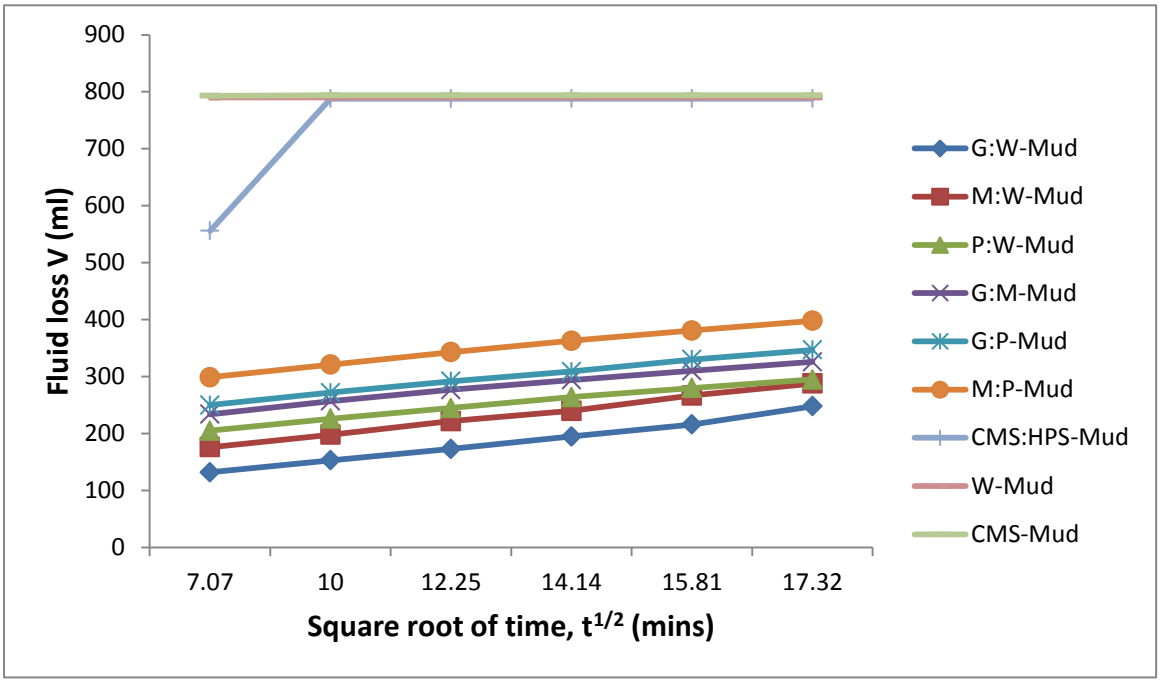

Figure 4.21: Plot of fluid loss versus square root of time for all the muds with 0.01g/ml starch concentration at high temperature, 450°C. (Data; Table 4.37-Table 4.45)

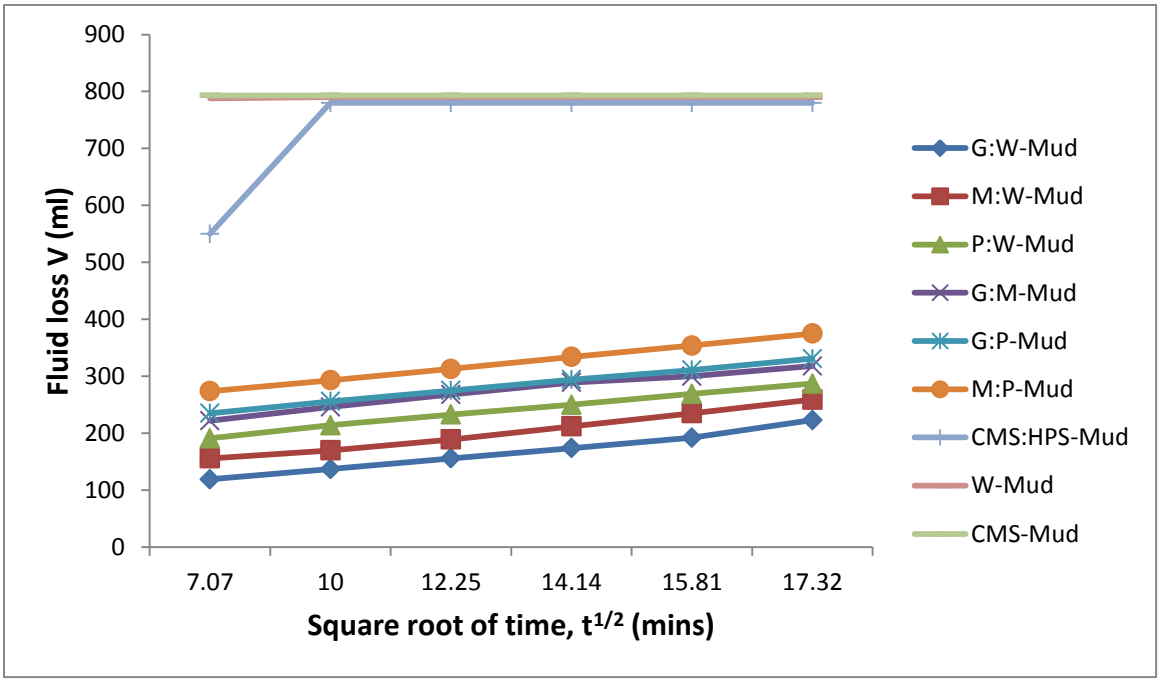

Figure 4.22: Plot of fluid loss versus square root of time for all the muds with 0.02g/ml starch concentration at high temperature, 450°C. (Data; Table 4.37-Table 4.45)

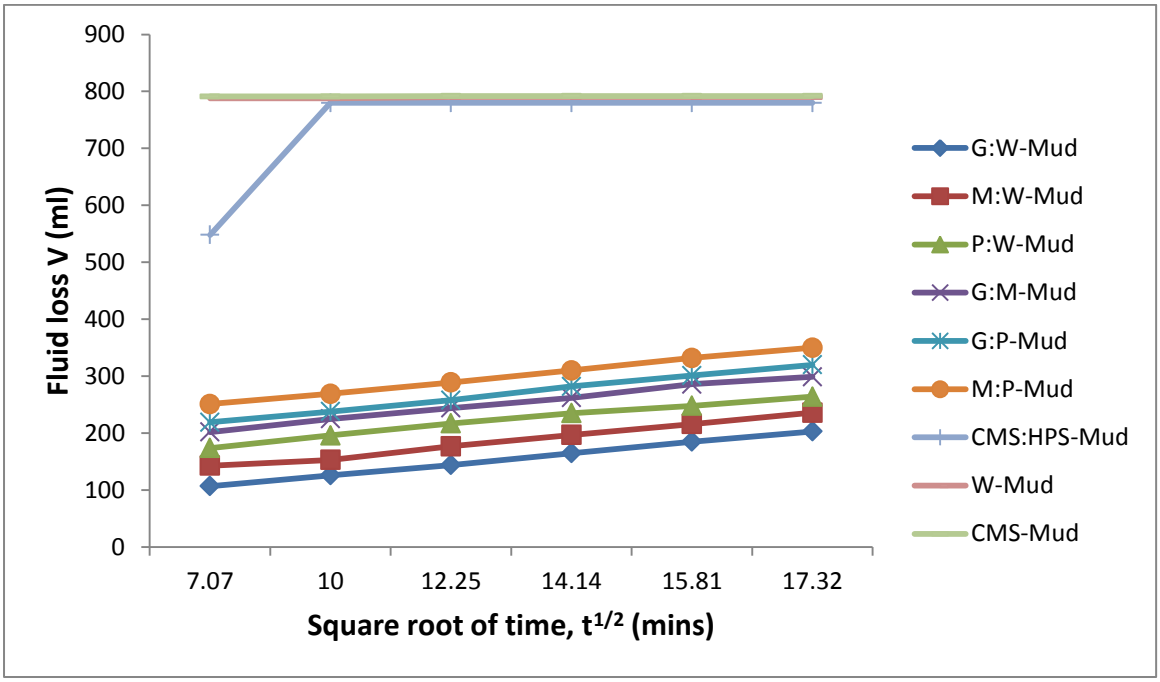

Figure 4.23: Plot of fluid loss versus square root of time for all the muds with 0.03g/ml starch concentration at high temperature, 450°C. (Data; Table 4.37-Table 4.45)

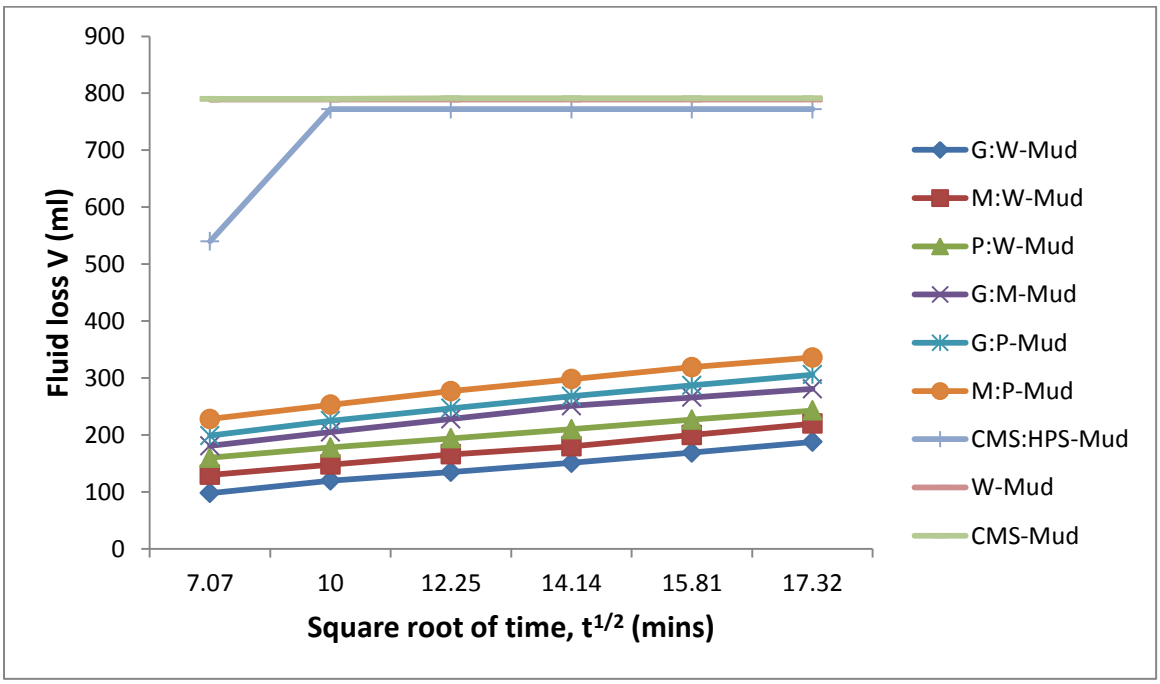

Figure 4.24: Plot of fluid loss versus square root of time for all the muds with 0.04g/ml starch concentration at high temperature, 450°C. (Data; Table 4.37-Table 4.45)

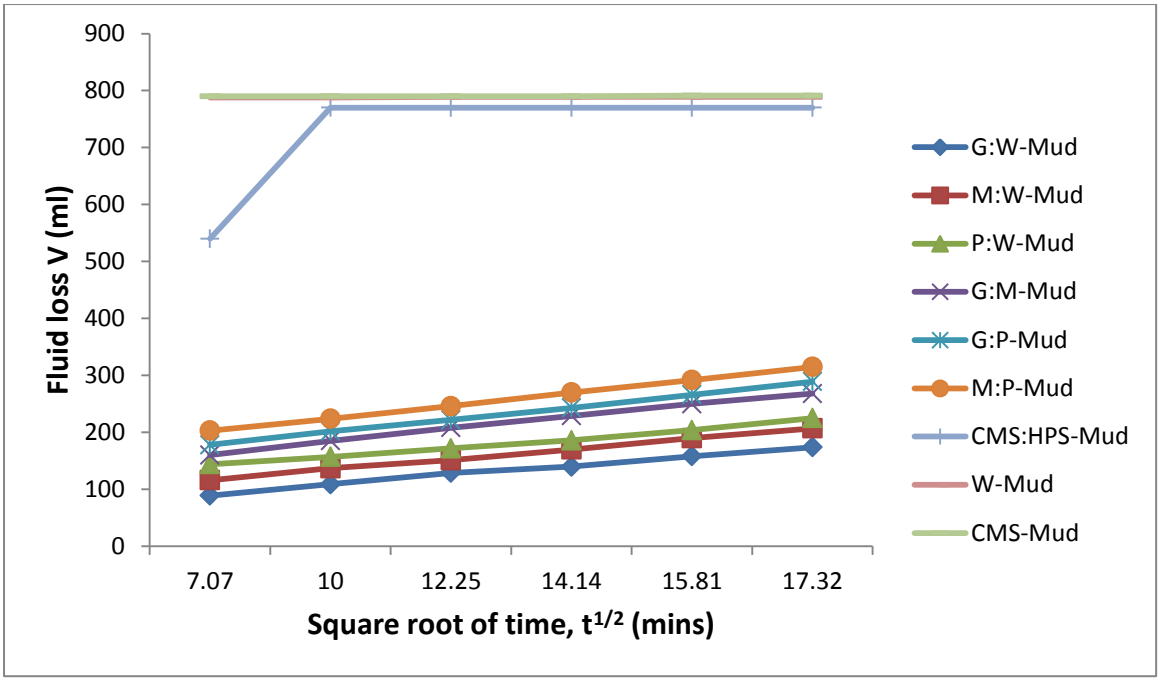

Figure 4.25: Plot of fluid loss versus square root of time for all the muds with 0.05g/ml starch concentration at high temperature, 450°C. (Data; Table 4.37-Table 4.45)

Figures 4.21, 4.22, 4.23, 4.24 and 4.25 show the plots of fluid loss versus square root of time for all the muds with 0.01-0.05g/ml starches concentration at high temperature of 450^0C. Analysis of the figures shows that the fluid loss of each of the new polymer muds (G:W-Mud, M:W-Mud, P:W-Mud, G:M-Mud, G:P-Mud and M:P-Mud) varied linearly with the square root of time, but the three already existing muds (CMS:HPS-Mud, W-Mud and CMS-Mud) did not show linear variation between fluid loss and square root of time. This means that at this high temperature, 450^0c, it was only the new muds that obeyed the API filtration model given in equation 3.1(Andy et al., 2010; Clifford & Cain, 2002). The lack of linear variation between fluid loss and square root of time by the already existing muds means that these muds have lost their strength and capability of controlling their filtration behaviours (Anthony & Robert, 2010). This might have resulted from the fact that the starches used in preparing the muds were no longer active or effective to produce or build up effective filter cake to

control their filtration characteristics. The starches of the already existing muds might have been burnt up at this high temperature, 450^0C. The presence of linear variation between fluid loss and square root of time in the new muds indicates that the new muds possess excellent filtration control ability, even at high temperature of 450^0C. This may be due to the high efficiency of the novel blends of starches used in preparing them.

More analysis of the figures shows that the new polymer muds containing the new blends of starches were thermally stable at 450^0C temperature. This is obvious in the fluid loss behaviours of the muds. The pattern or system of losing fluid by each new mud is usual and definite. For each of the new polymer muds, fluid loss increases with increase in square root of time in a usual manner. The pattern of the curves proved that the new polymer muds still possess fluid loss reducing behaviours even at high temperature of 450^0C. This implies that the new polymer muds are still thermally stable and efficient in their functions at this high temperature, 450^0C. This might base on the fact that the new blends of starches used in preparing these new muds have not been burnt up at 450^0C. Therefore, the new blends of starches were still efficient and active to build up effective filter cake that controlled and reduced the fluid loss. This means that the new muds are potentially thermally stable and efficient to be used in drilling wells with hole temperatures as high as 450^0C and above. This is because these new muds would be able to ensure continuous circulation of fluid round the walls of the well-bore without any catastrophe (Austin & Christopher, 2008). On the other hand, the figures show that the three already existing muds including CMS:HPS-Mud experienced total thermal degradation at 450^0C temperature. The fluid loss behaviors of the three already existing or widely-used muds showed unusual changes. The relationship between fluid loss and square root of time was not linear for

each of the three muds. From the figures, as square root of time was increasing, the fluid loss gave a great sharp increase after the initial time interval and then became almost profusely constant or steady. When a drilling mud starts to lose fluid more profusely than the usual manner at a particular temperature, and eventually no more fluid comes out as filtrate or filter loss, it said that the mud has lost thermal stability and filtration control at that temperature (Bernu, 2011; Anthony & Robert, 2010; Andrew & Robert, 2007). The pattern of steady or constant values of fluid loss with increasing square root of time, for each of the three widely used muds, is a total indication of thermal degradation of the muds at 450^0C high temperature. The thermal degradation of the muds might have resulted from the fact that the starches used in preparing the muds have been burnt up and lost their effectiveness or efficiency at this temperature. This may also be attributed to the use of unblended and chemically modified starches for preparing the three already existing muds. The implication, of this complete thermal degradation of the already existing muds, is that none of the muds can be used to drill well whose bottom hole temperature is as high as 450^0C or above.

The explanation to the above effect is that when there is no fluid to be lost from a drilling mud, there will be no fluid to be circulated round the walls of the well. Then, wall cracking and caving will set in, and eventually wall eruption, which falls back to the bottom hole of the well and causes “Formation Damage” (Bernu, 2011).

4.2.1.6 Effects of Varying Starch Concentrations on the Fluid Loss Behaviours of the Muds at all the Temperatures, 25^0C, 150^0C, 250^0C, 350^0C and 450^0C

The experimental results and data for the effects of varying starch concentrations on the muds' fluid loss behaviours are shown in Table 4.1 to table 4.45.

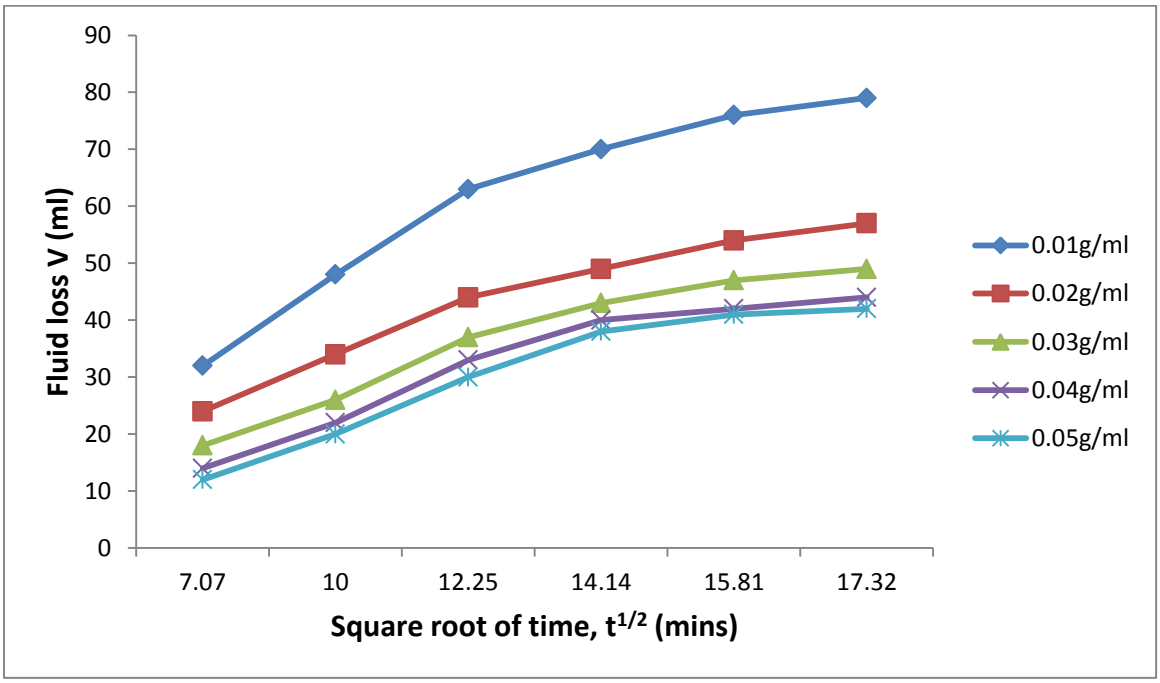

Figure 4.26: Plot of fluid loss versus square root of time for G:W-Mud sample with varying starch concentration at room temperature, 25^oC. (Data; Table 4.1)

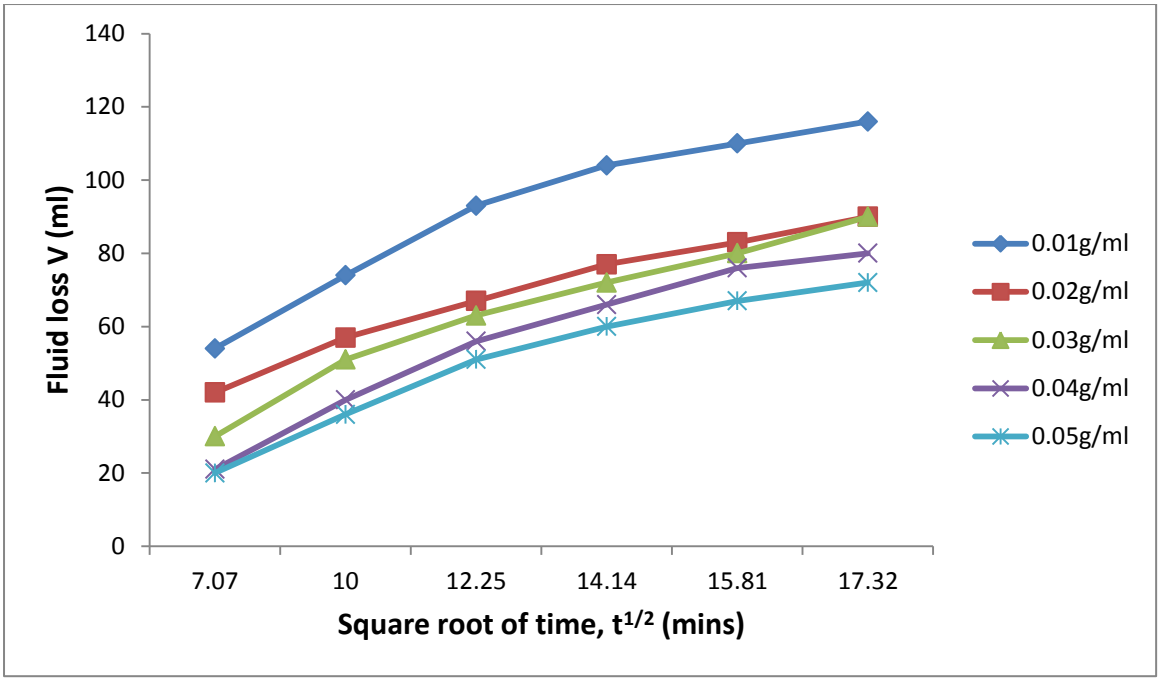

Figure 4.27: Plot of fluid loss versus square root of time for M:W-Mud sample with varying starch concentration at room temperature, 25°C. (Data; Table 4.2)

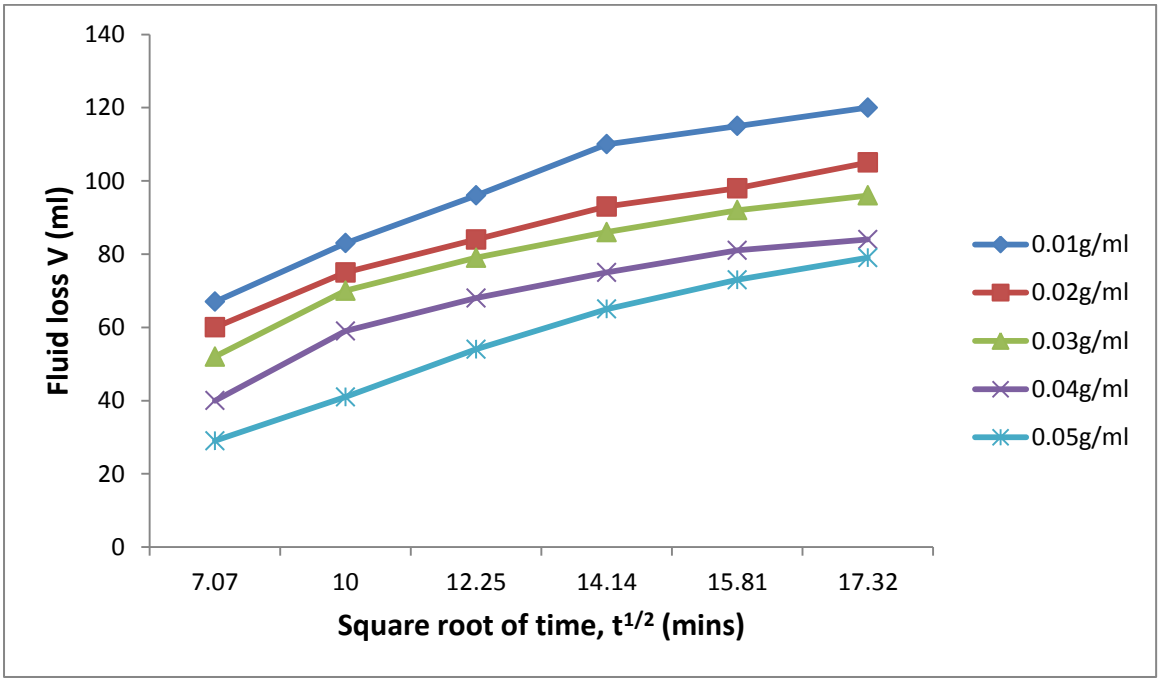

Figure 4.28: Plot of fluid loss versus square root of time for P:W-Mud sample with varying starch concentration at room temperature, 25°C. (Data; Table 4.3)

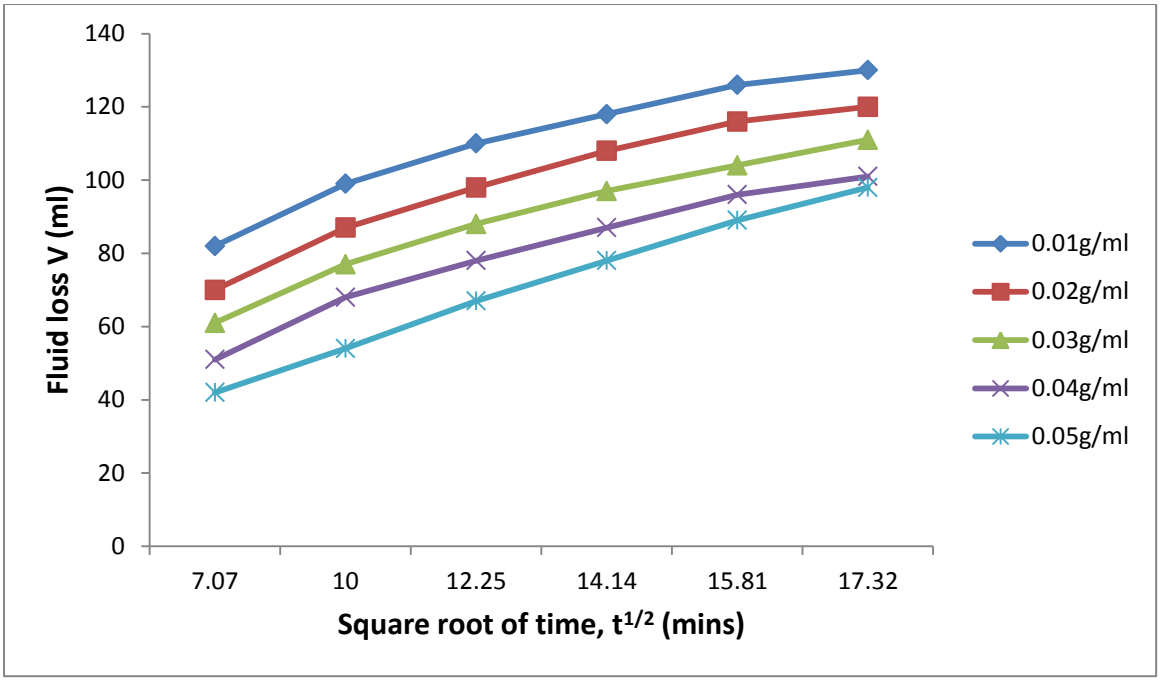

Figure 4.29: Plot of fluid loss versus square root of time for G:M-Mud sample with varying starch concentration at room temperature, 25°C. (Data; Table 4.4)

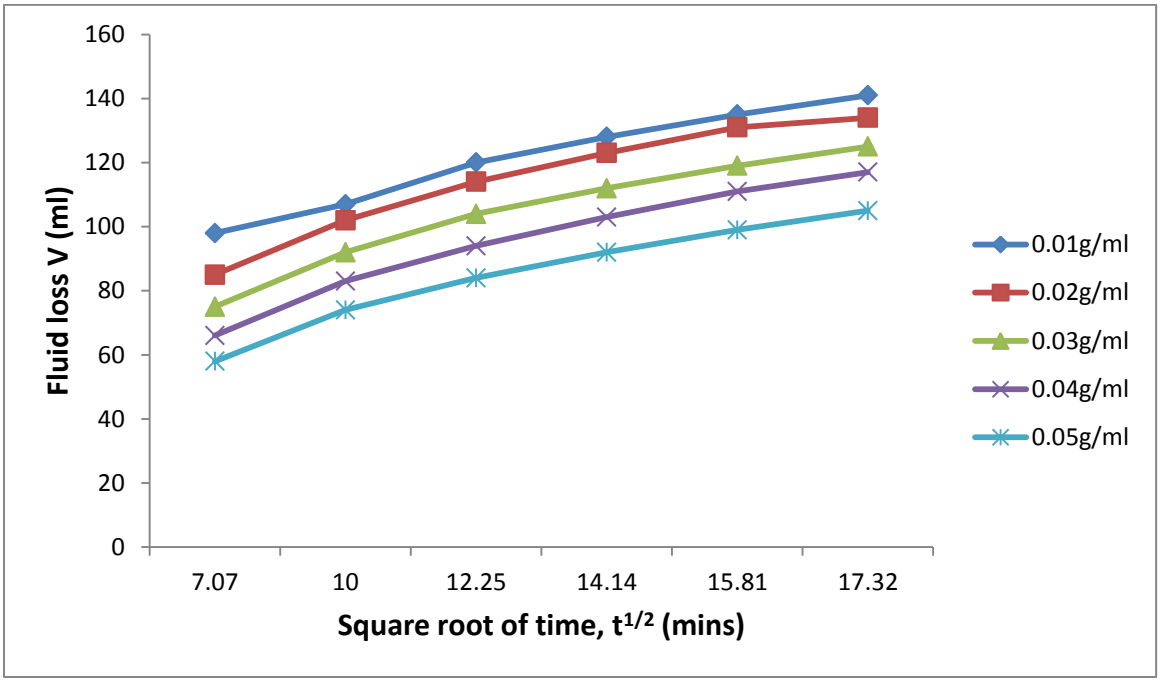

Figure 4.30: Plot of fluid loss versus square root of time for G:P-Mud sample with varying starch concentration at room temperature, 25°C. (Data; Table 4.5)

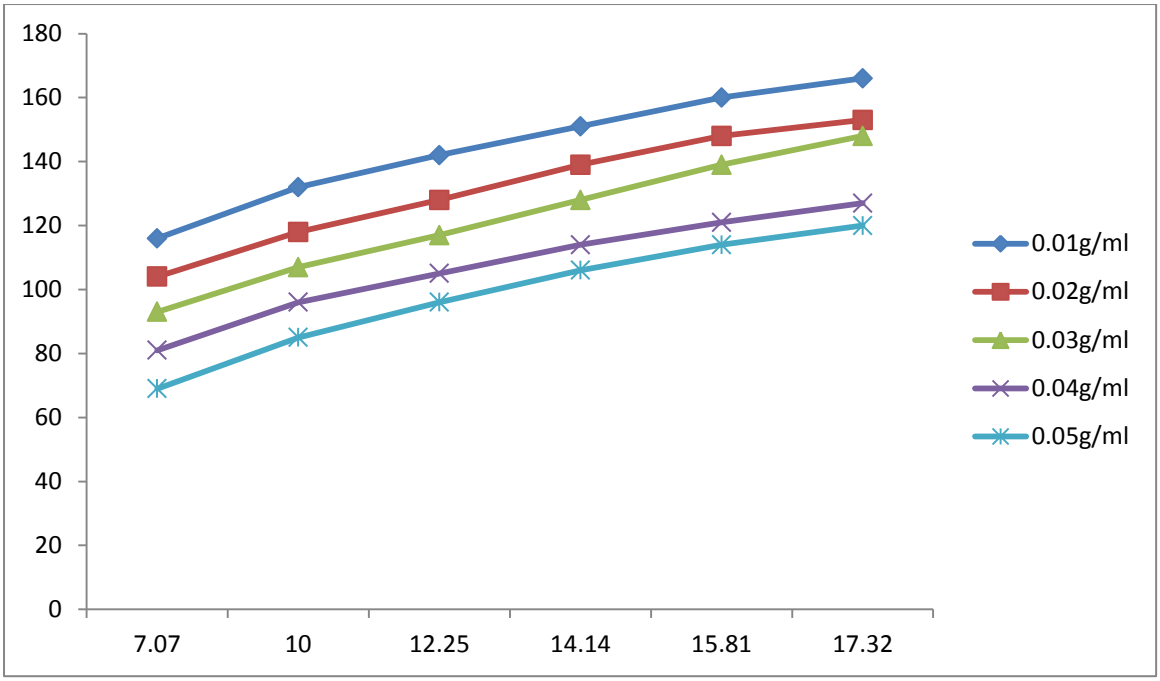

Figure 4.31: Plot of fluid loss versus square root of time for M:P-Mud sample with varying starch concentration at room temperature, 25°C. (Data; Table 4.6)

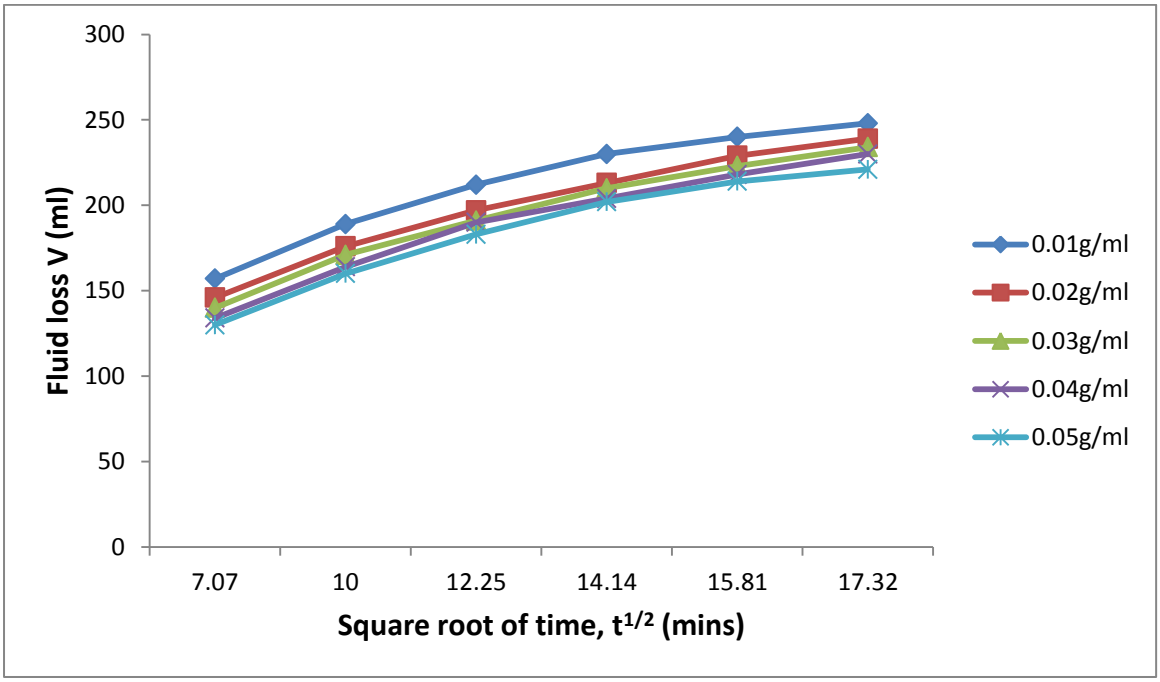

Figure 4.32: Plot of fluid loss versus square root of time for CMS:HPS-Mud sample with varying starch concentration at room temperature, 25°C. (Data; Table 4.7)

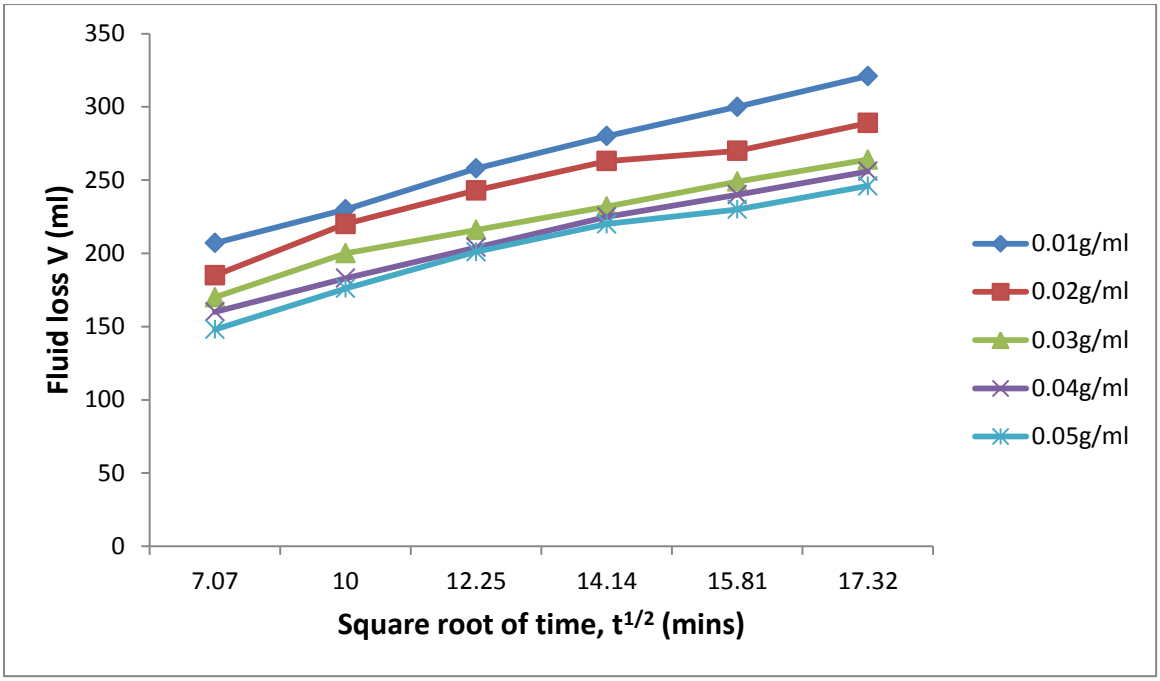

Figure 4.33: Plot of fluid loss versus square root of time for W-Mud sample with varying starch concentration at room temperature, 25°C. (Data; Table 4.8)

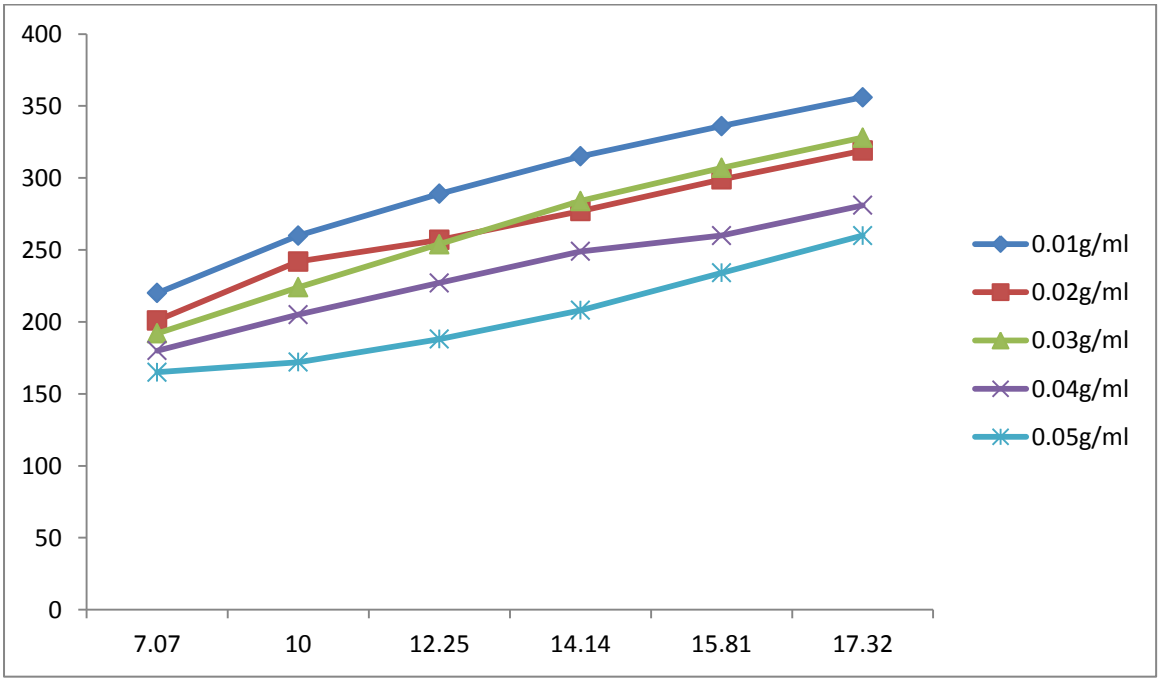

Figure 4.34: Plot of fluid loss versus square root of time for CMS-Mud sample with varying starch concentration at room temperature, 25°C. (Data; Table 4.9)

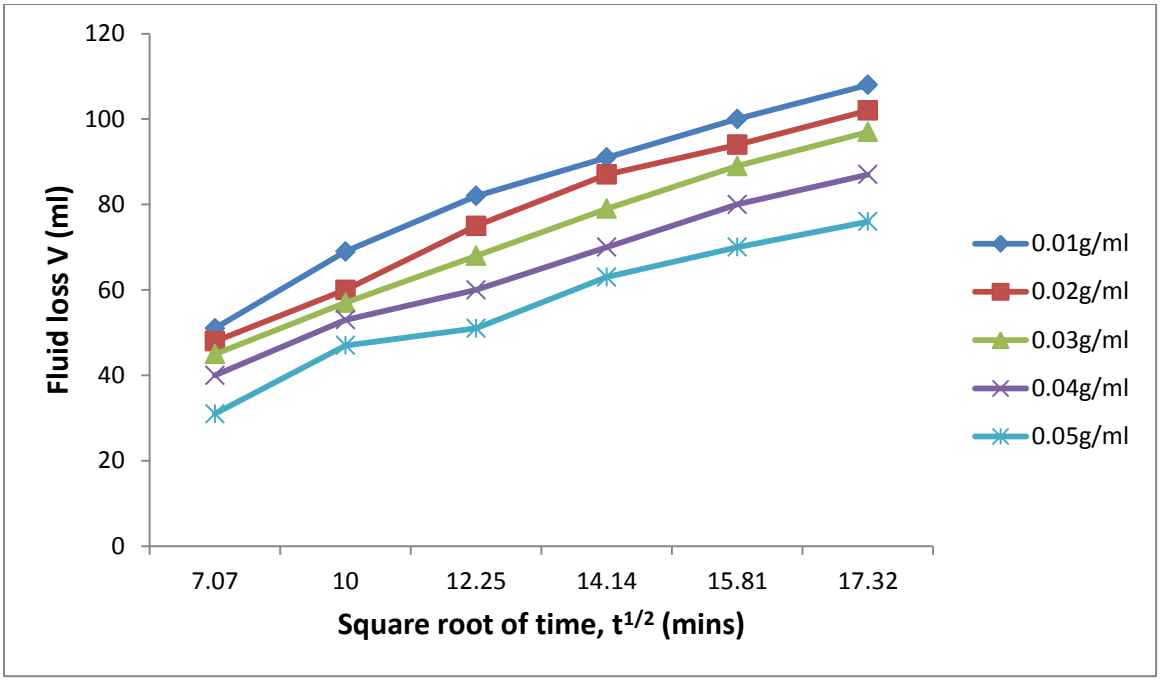

Figure 4.35: Plot of fluid loss versus square root of time for G:W-Mud sample with varying starch concentration at high temperature, 150°C. (Data; Table 4.10)

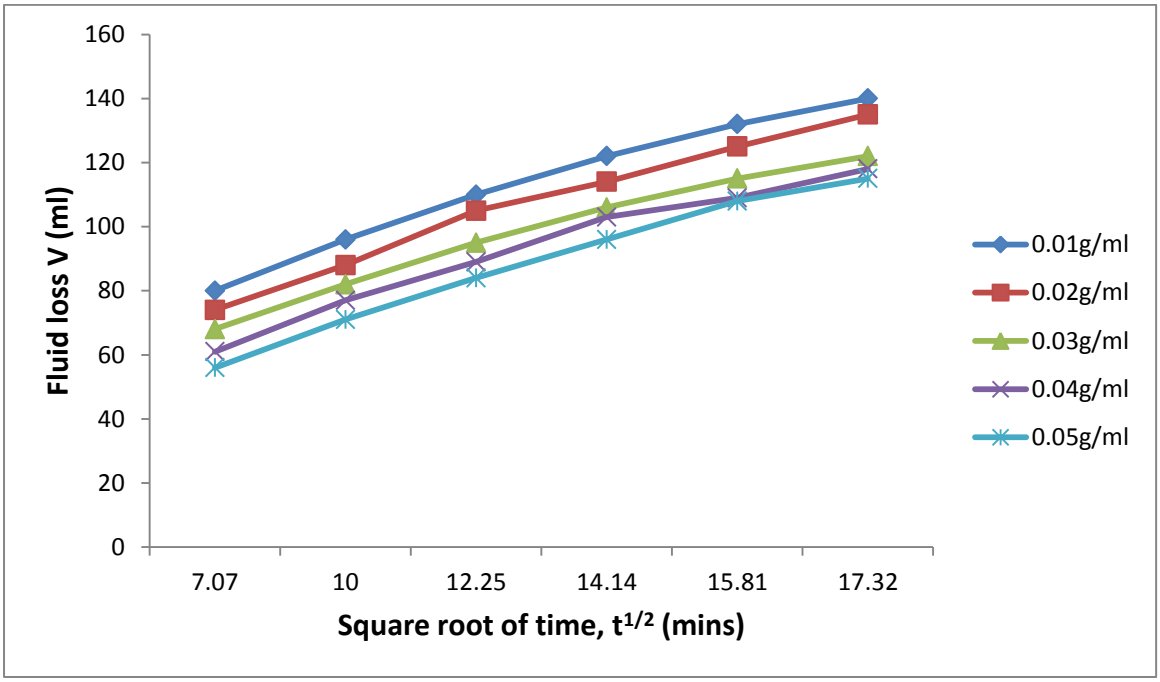

Figure 4.36: Plot of fluid loss versus square root of time for M:W-Mud sample with varying starch concentration at high temperature, 150°C. (Data; Table 4.11)

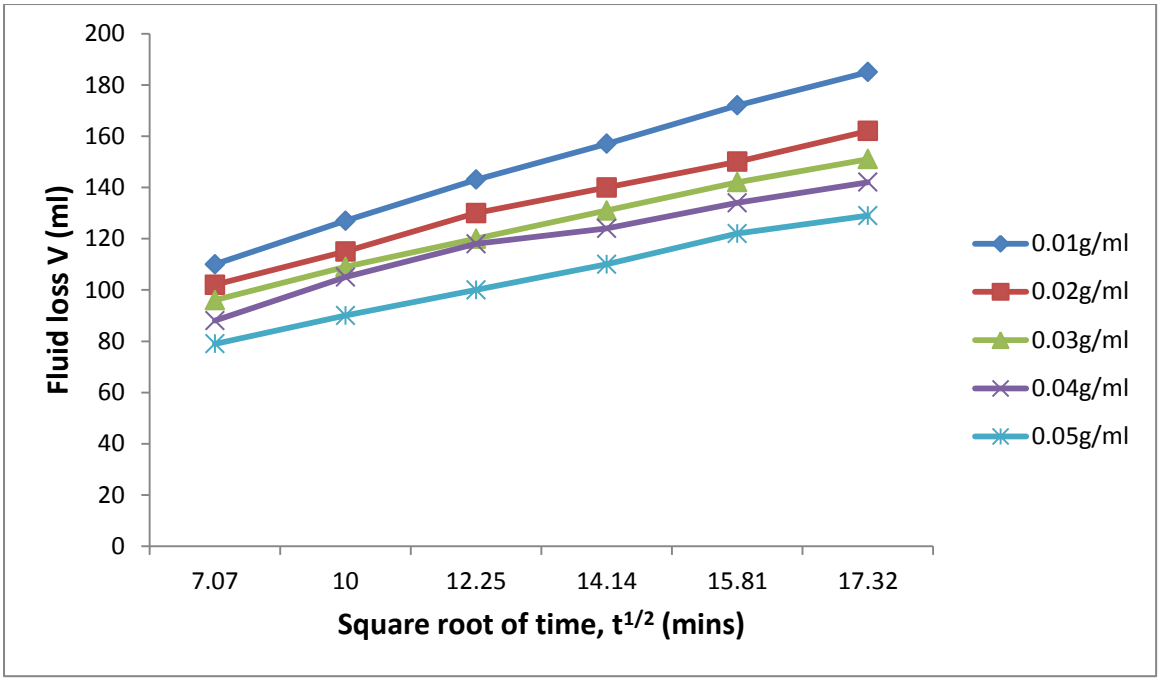

Figure 4.37: Plot of fluid loss versus square root of time for P:W-Mud sample with varying starch concentration at high temperature, 150°C. (Data; Table 4.12)

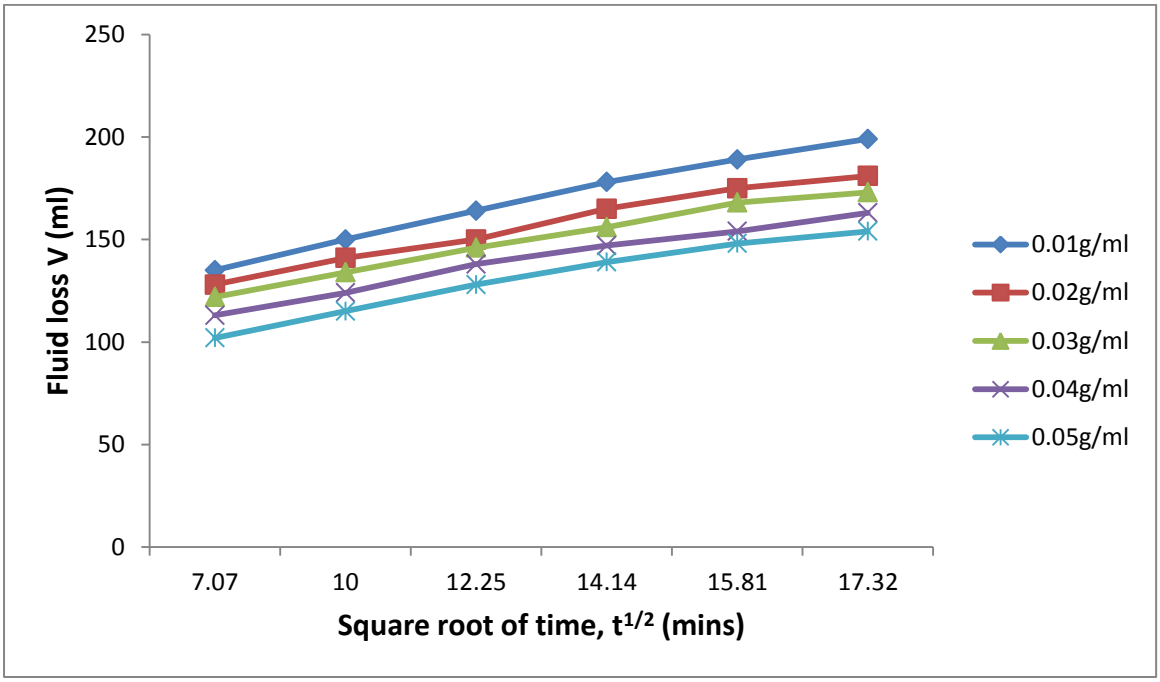

Figure 4.38: Plot of fluid loss versus square root of time for G:M-Mud sample with varying starch concentration at high temperature, 150°C. (Data; Table 4.13)

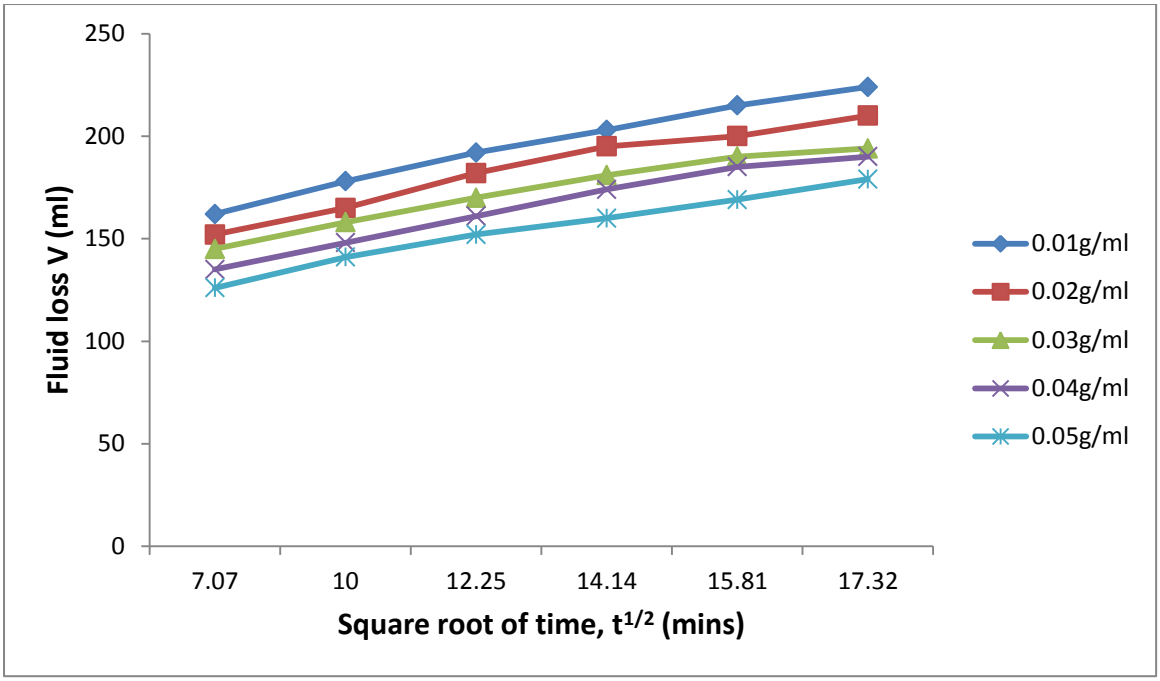

Figure 4.39: Plot of fluid loss versus square root of time for G:P-Mud sample with varying starch concentration at high temperature, 150°C. (Data; Table 4.14)

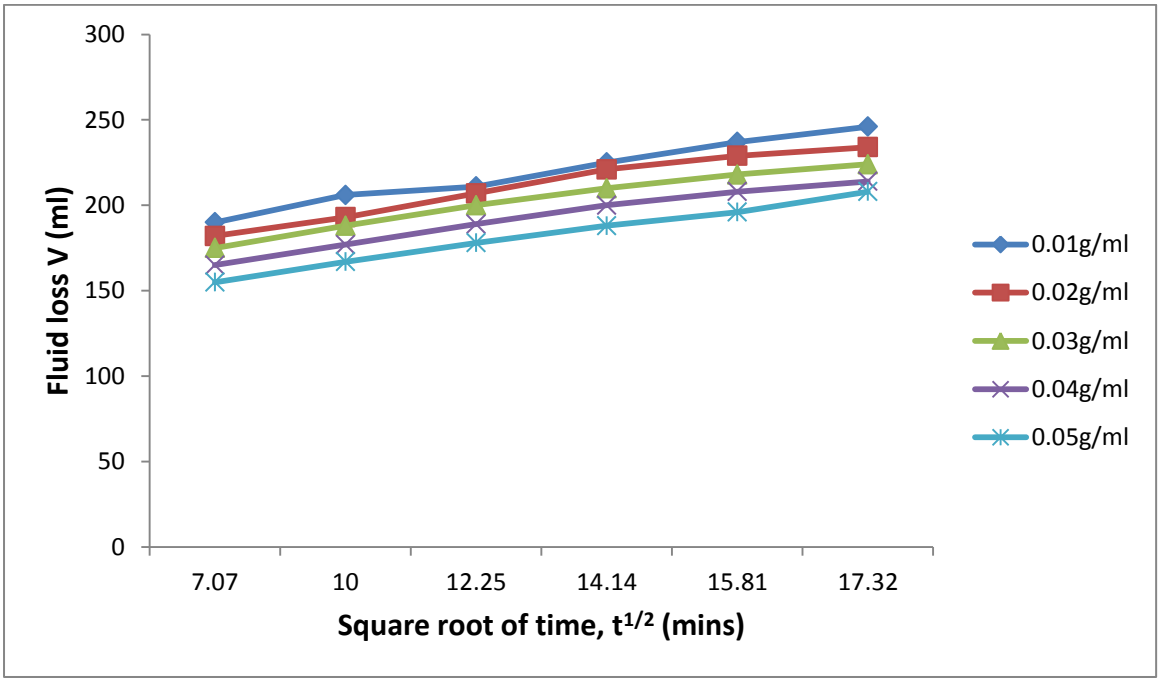

Figure 4.40: Plot of fluid loss versus square root of time for M:P-Mud sample with varying starch concentration at high temperature, 150°C. (Data; Table 4.15)

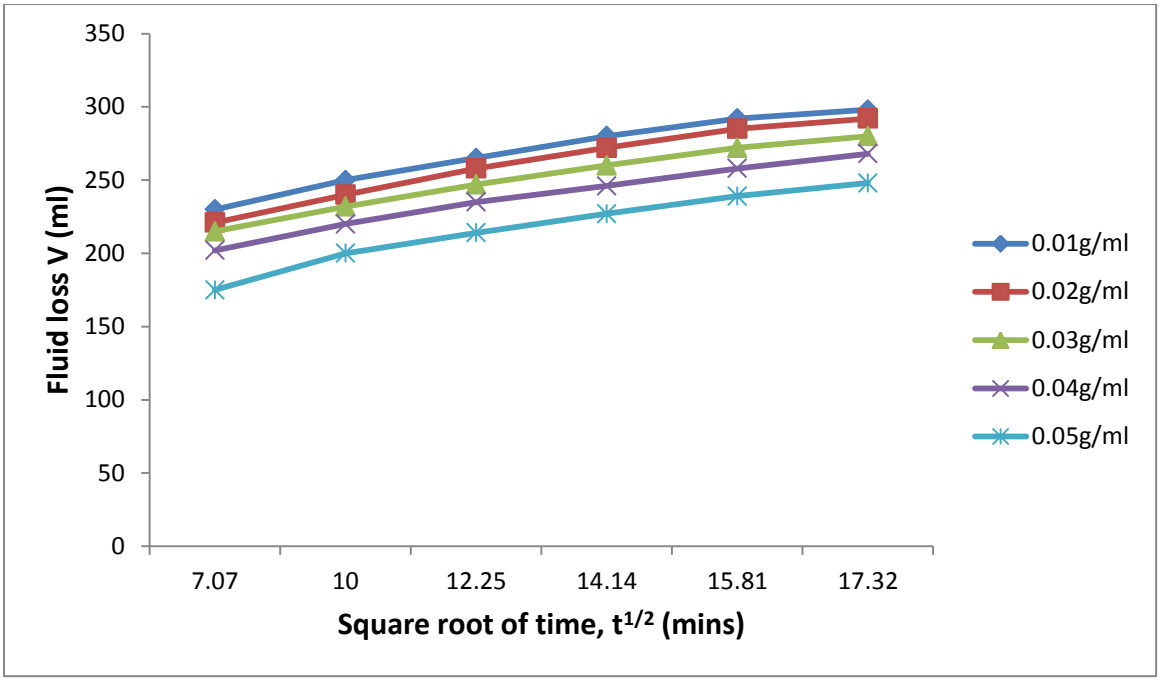

Figure 4.41: Plot of fluid loss versus square root of time for CMS:HPS-Mud sample with varying starch concentration at high temperature, 150°C. (Data; Table 4.16)

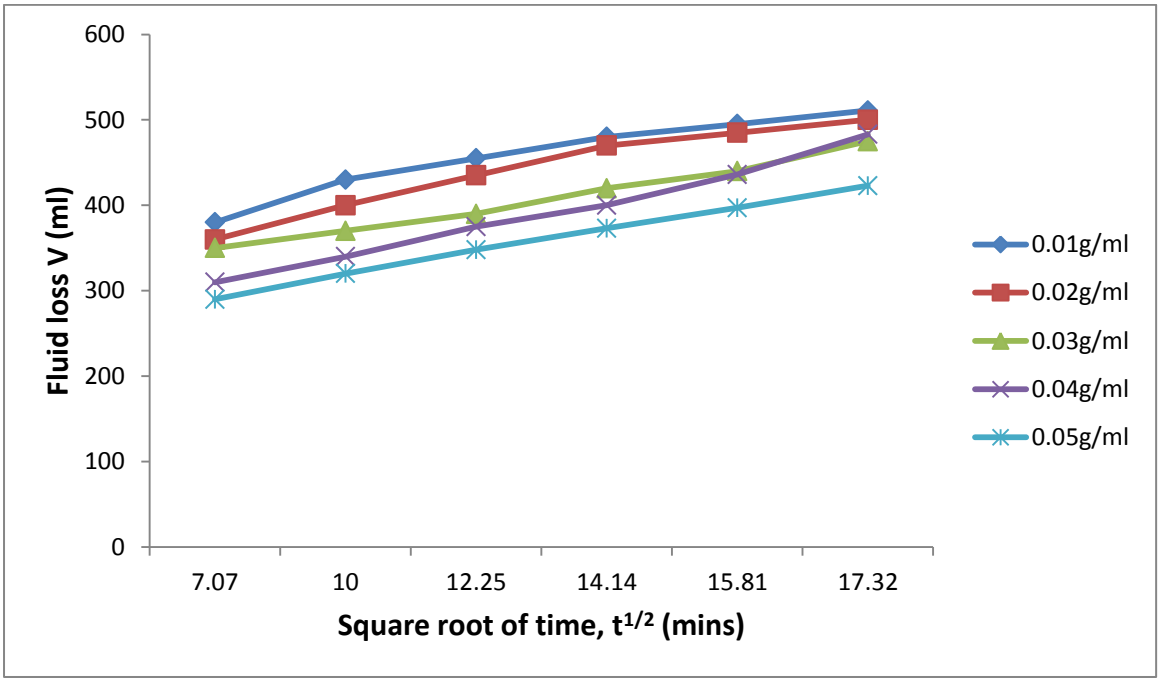

Figure 4.42: Plot of fluid loss versus square root of time for W-Mud sample with varying starch concentration at high temperature, 150°C. (Data; Table 4.17)

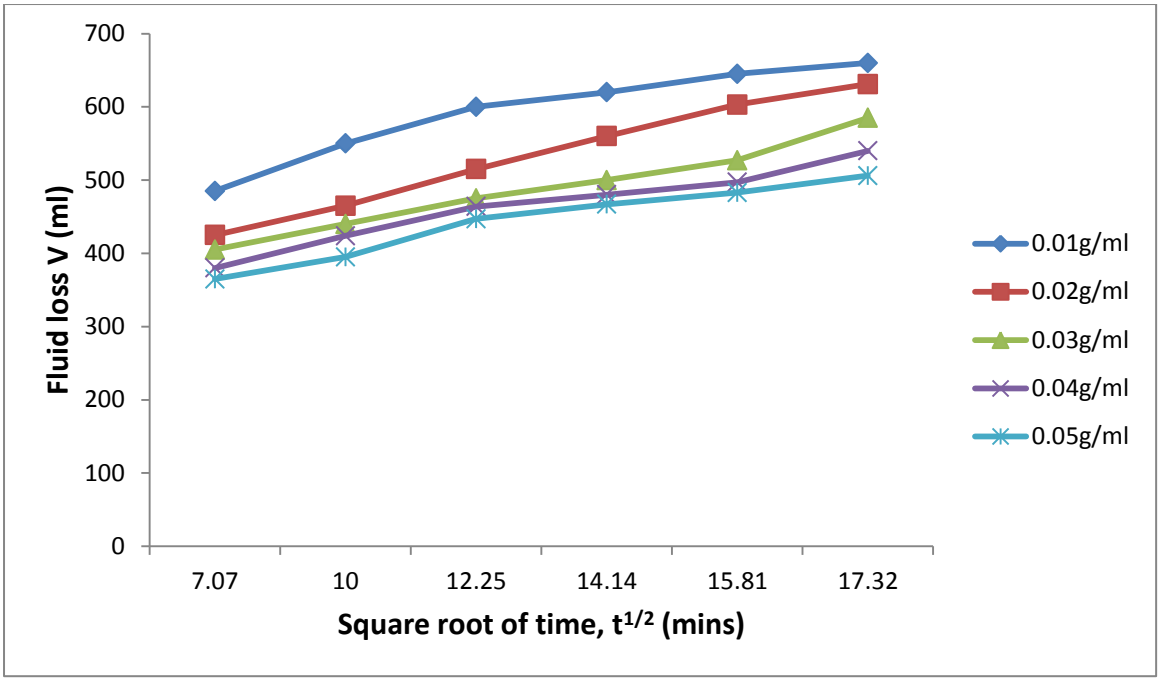

Figure 4.43: Plot of fluid loss versus square root of time for CMS-Mud sample with varying starch concentration at high temperature, 150°C. (Data; Table 4.18)

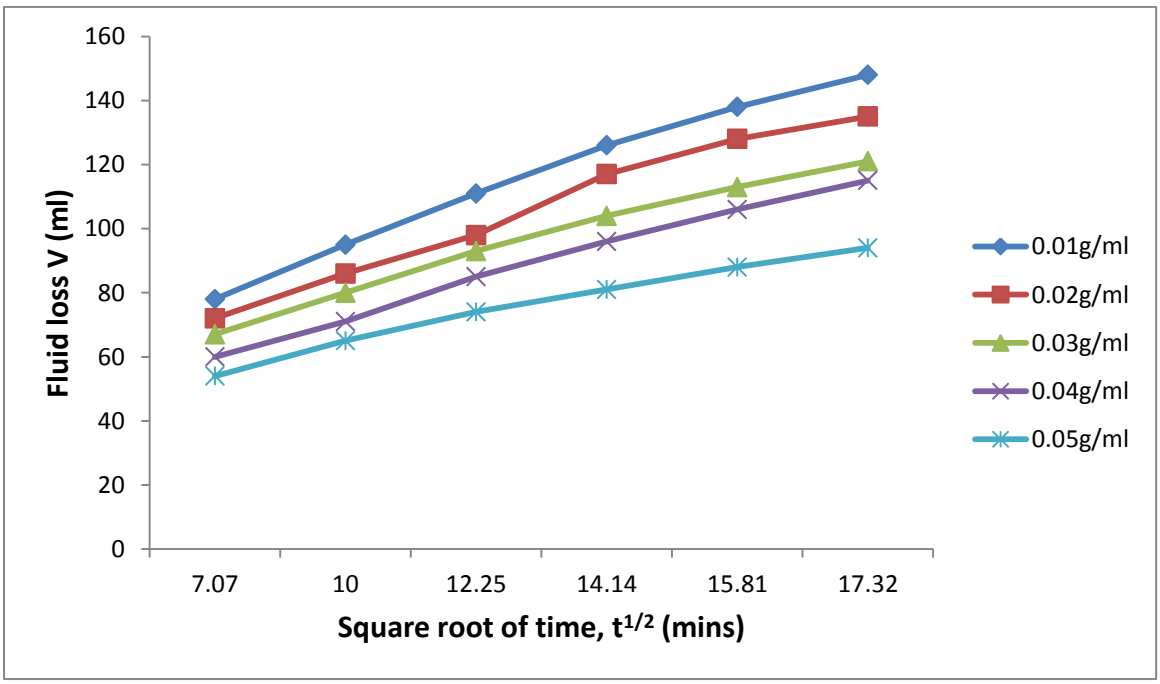

Figure 4.44: Plot of fluid loss versus square root of time for G:W-Mud sample with varying starch concentration at high temperature, 250°C. (Data; Table 4.19)

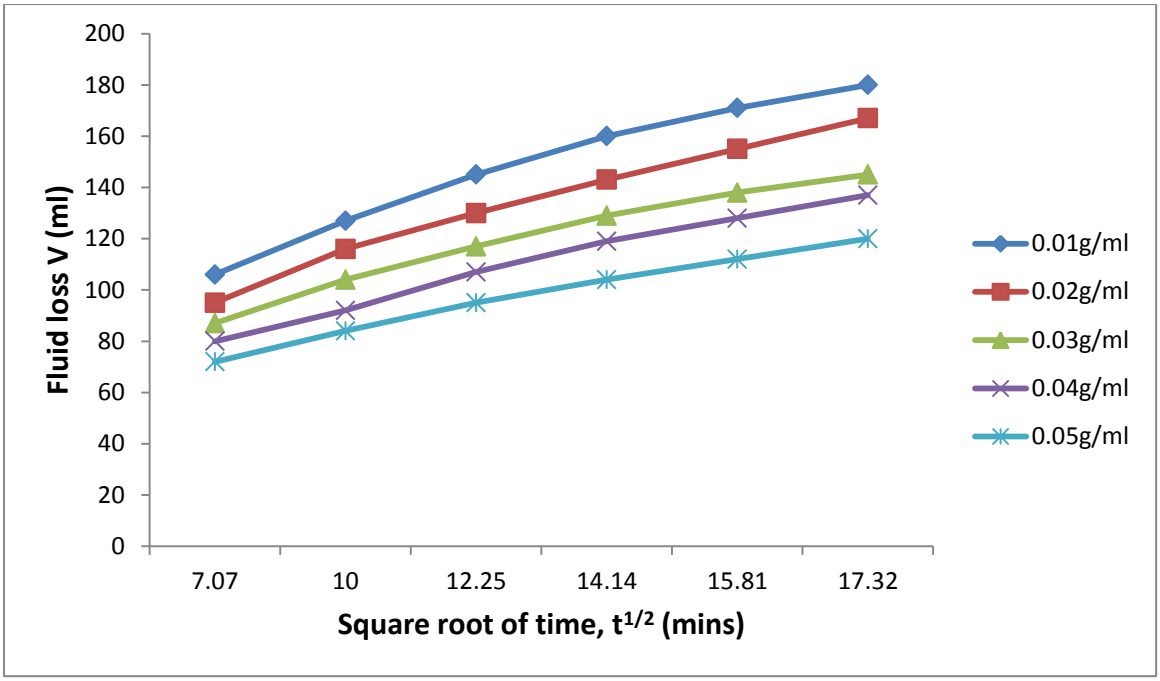

Figure 4.45: Plot of fluid loss versus square root of time for M:W-Mud sample with varying starch concentration at high temperature, 250°C. (Data; Table 4.20)

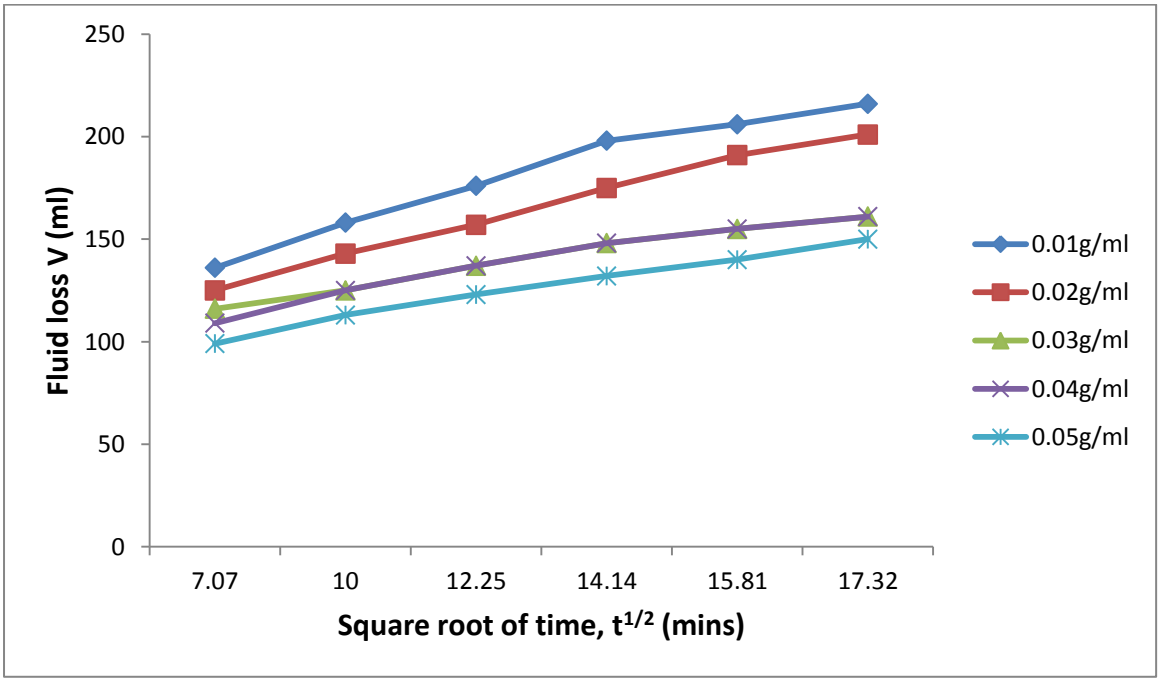

Figure 4.46: Plot of fluid loss versus square root of time for P:W-Mud sample with varying starch concentration at high temperature, 250°C. (Data; Table 4.21)

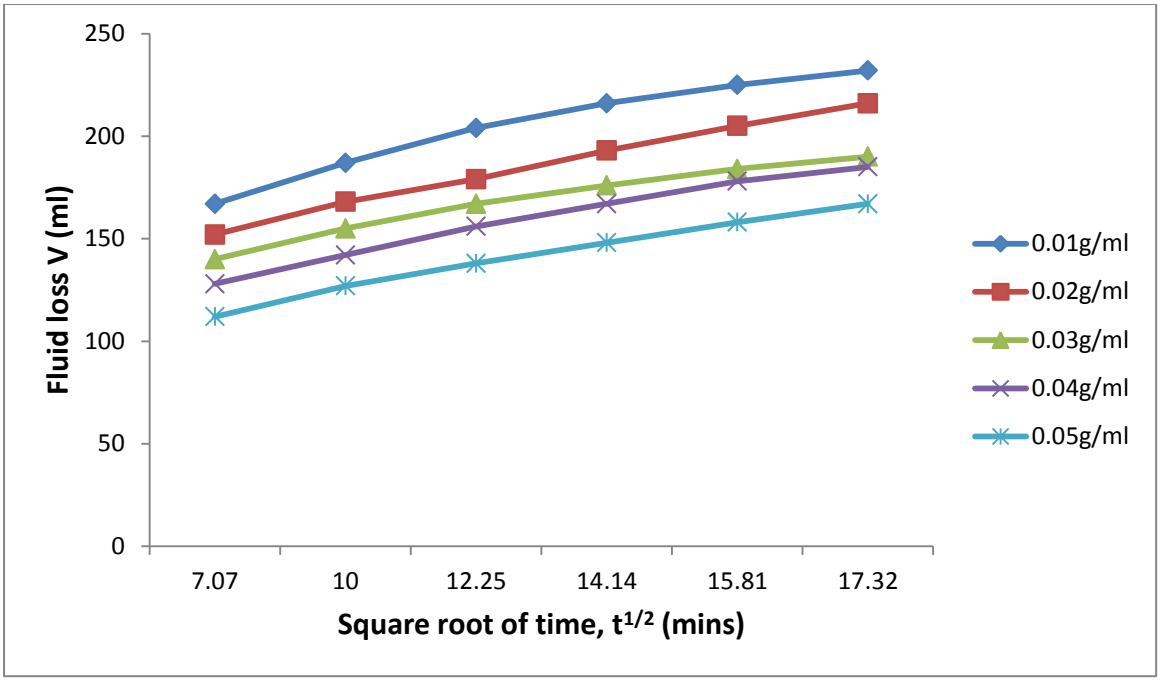

Figure 4.47: Plot of fluid loss versus square root of time for G:M-Mud sample with varying starch concentration at high temperature, 250°C. (Data; Table 4.22)

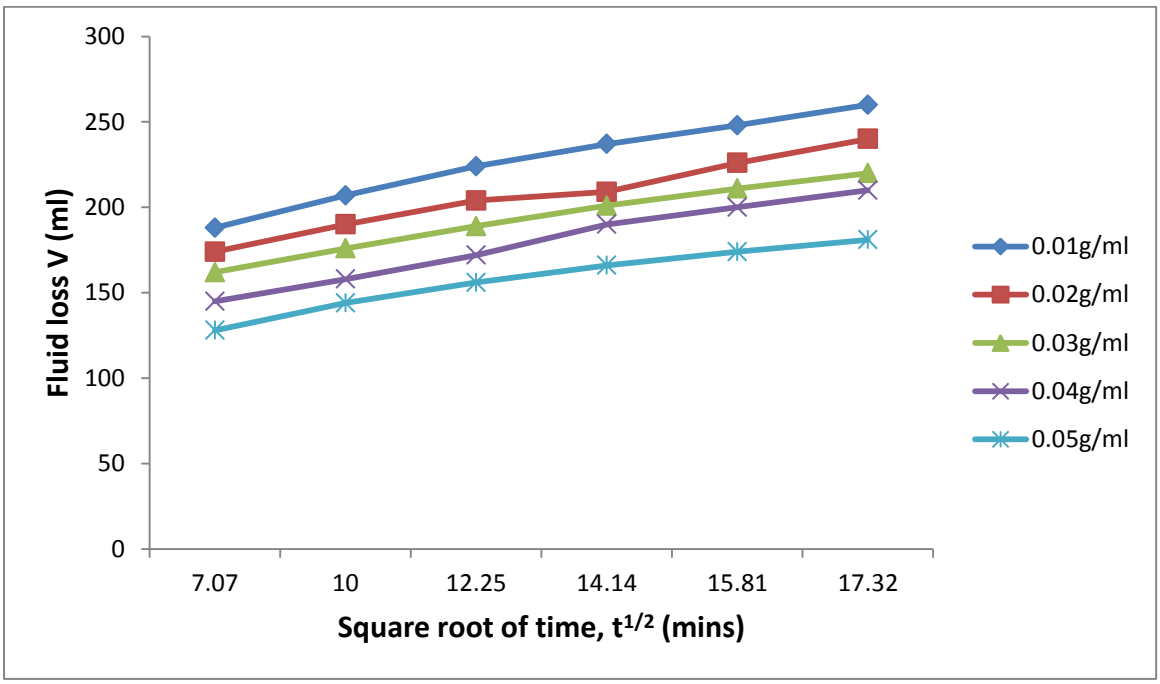

Figure 4.48: Plot of fluid loss versus square root of time for G:P-Mud sample with varying starch concentration at high temperature, 250°C. (Data; Table 4.23)

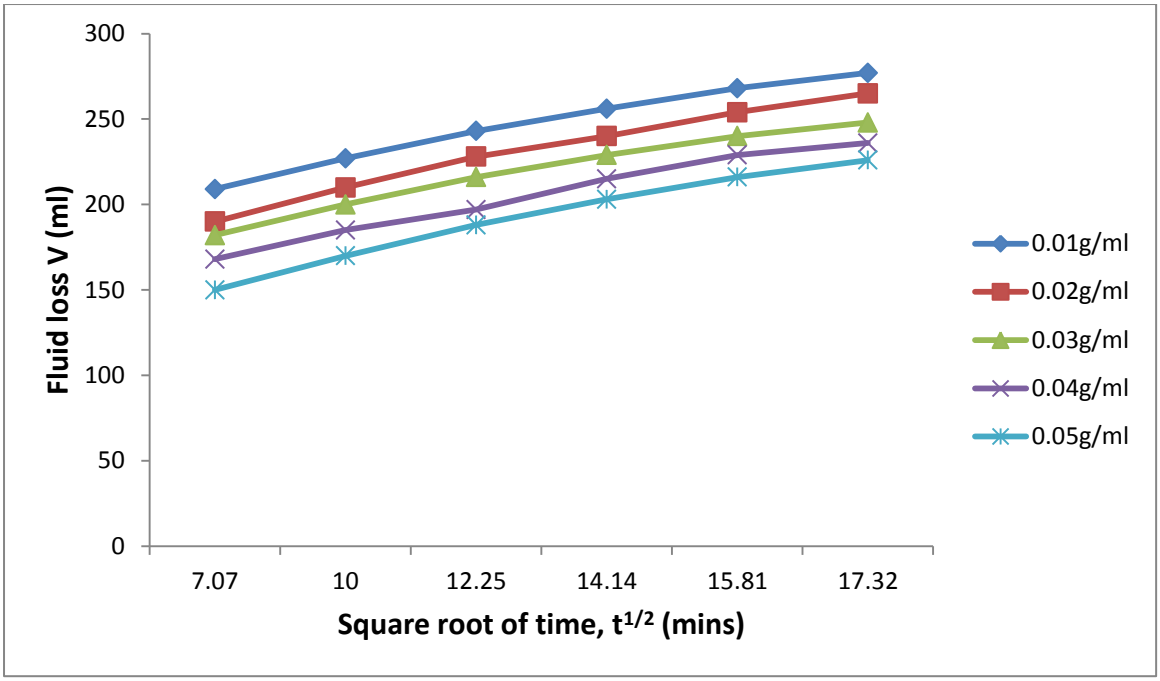

Figure 4.49: Plot of fluid loss versus square root of time for M:P-Mud sample with varying starch concentration at high temperature, 250°C. (Data; Table 4.24)

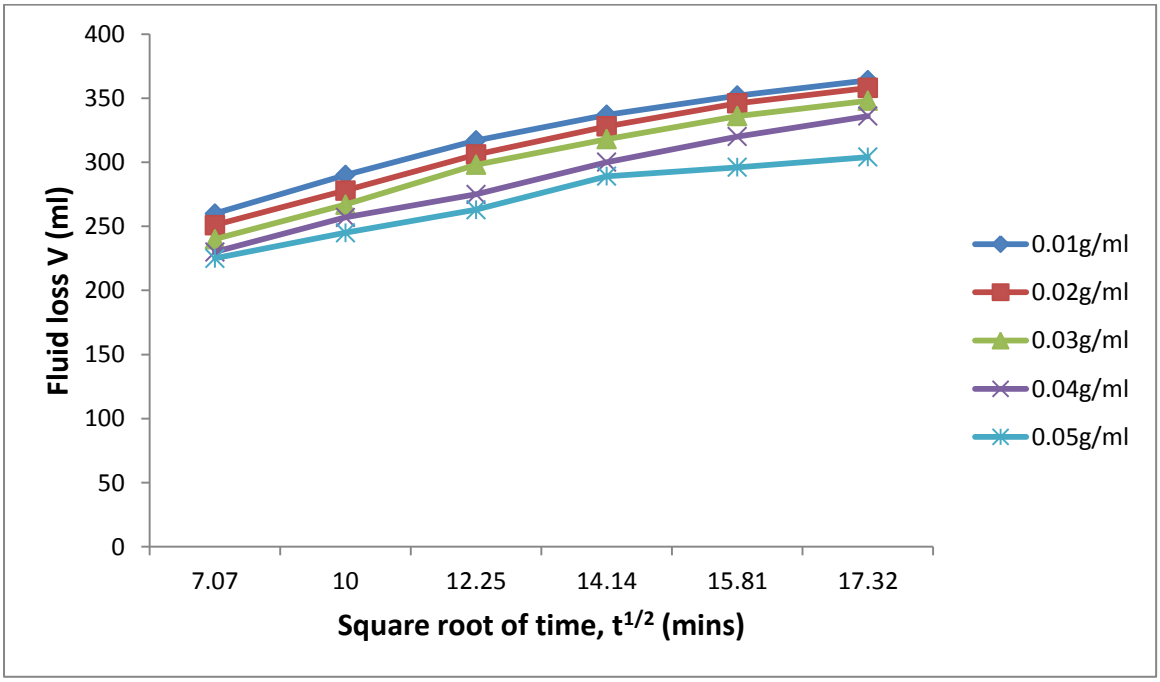

Figure 4.50: Plot of fluid loss versus square root of time for CMS:HPS-Mud sample with varying starch concentration at high temperature, 250°C. (Data;Table 4.25)

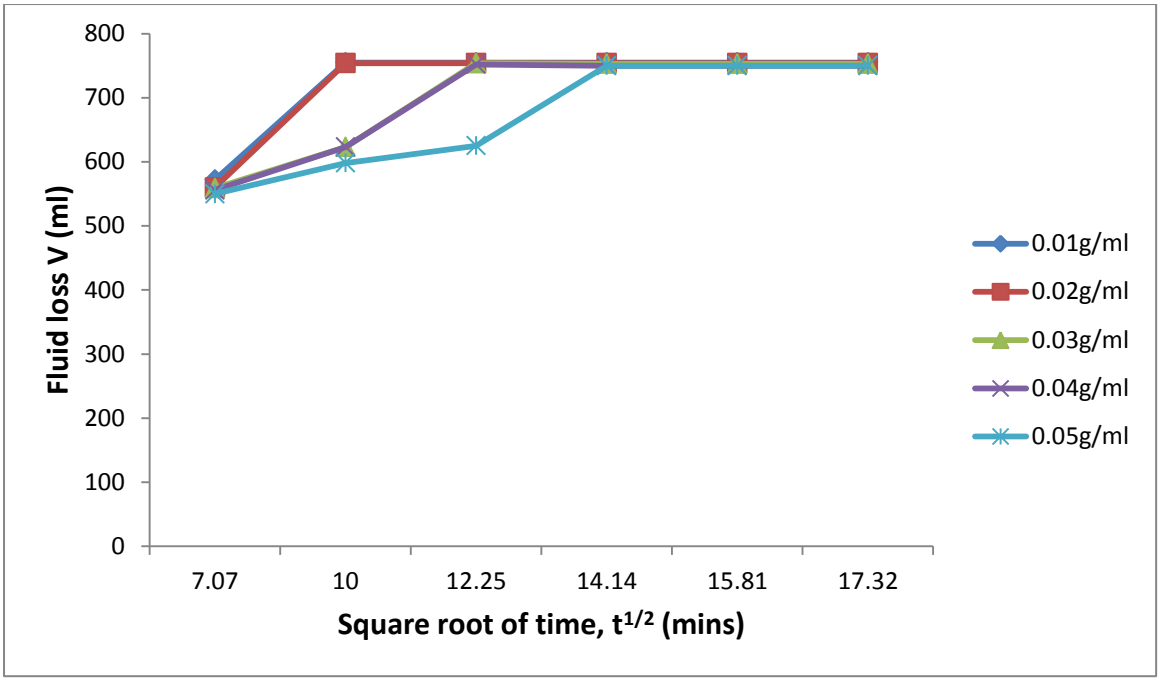

Figure 4.51: Plot of fluid loss versus square root of time for W-Mud sample with varying starch concentration at high temperature, 250°C. (Data; Table 4.26)

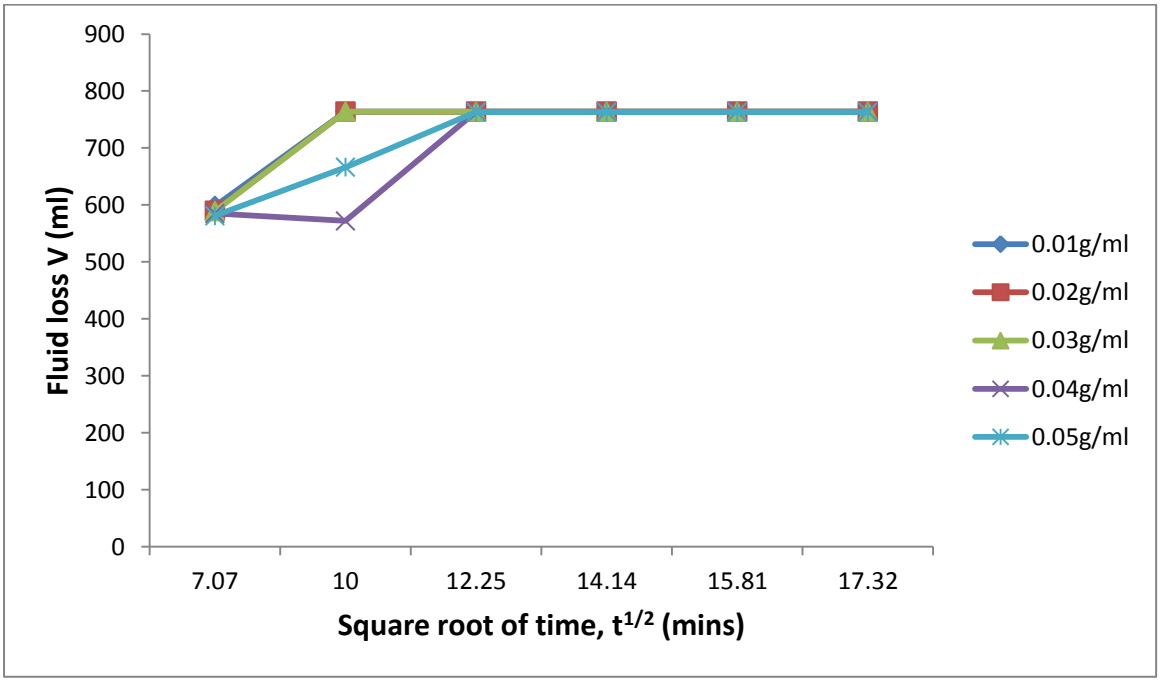

Figure 4.52: Plot of fluid loss versus square root of time for CMS-Mud sample with varying starch concentration at high temperature, 250°C. (Data; Table 4.27)

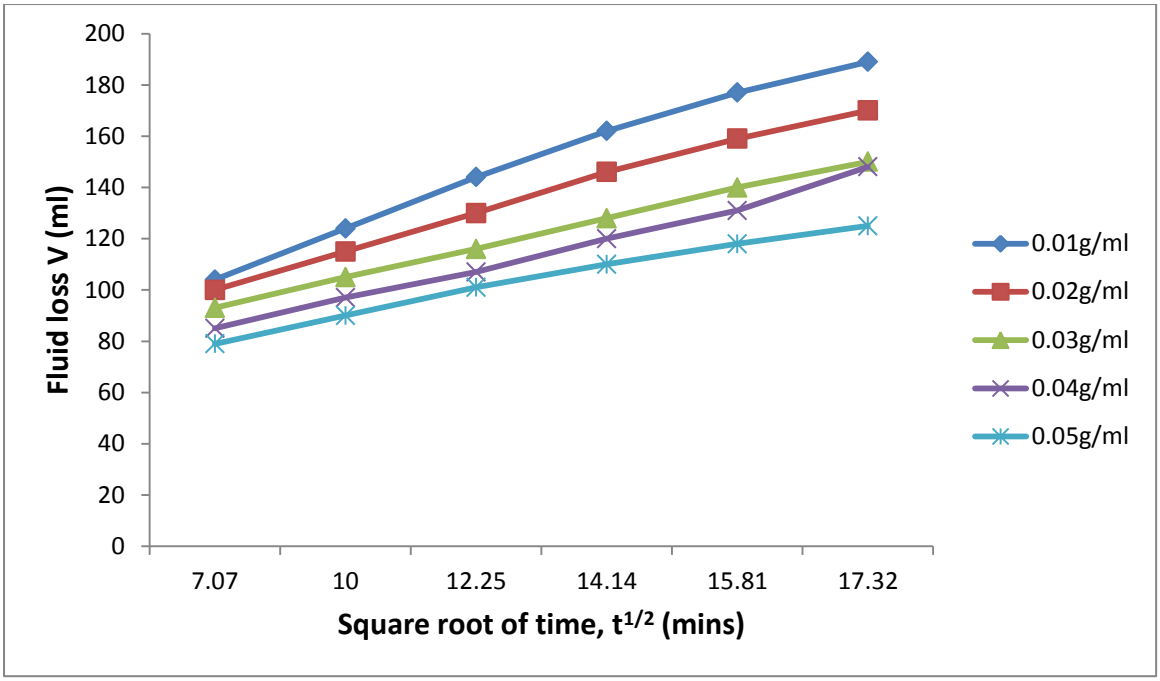

Figure 4.53: Plot of fluid loss versus square root of time for G:W-Mud sample with varying starch concentration at high temperature, 350°C. (Data; Table 4.28)

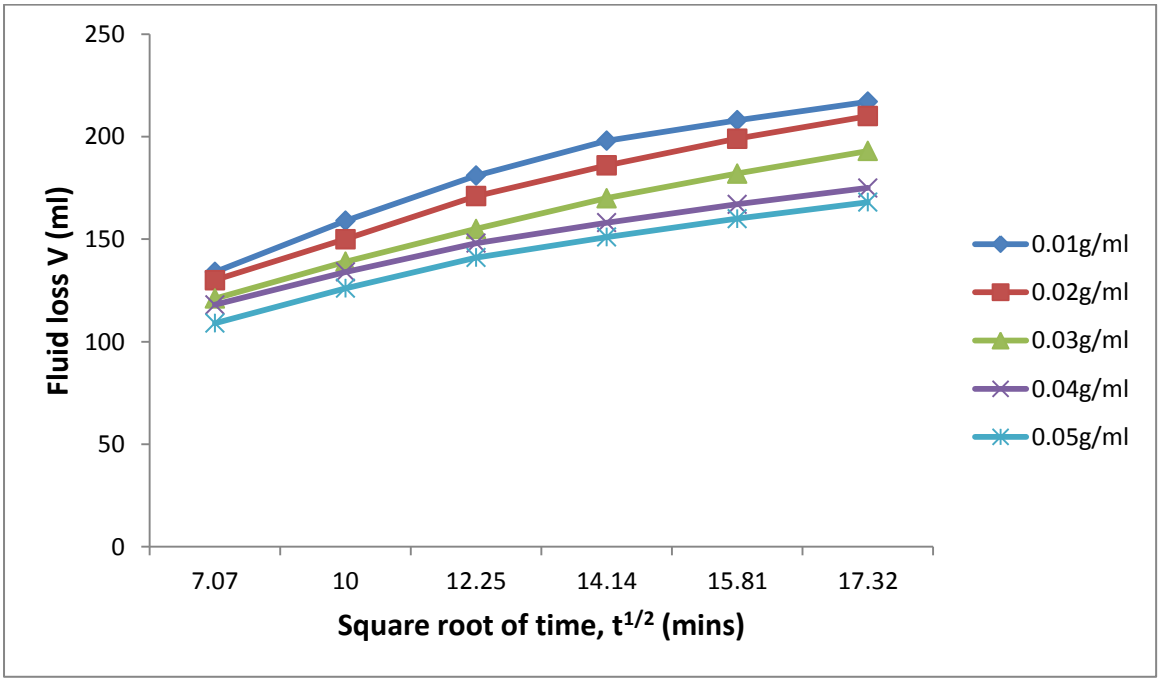

Figure 4.54: Plot of fluid loss versus square root of time for M:W-Mud sample with varying starch concentration at high temperature, 350°C. (Data; Table 4.29)

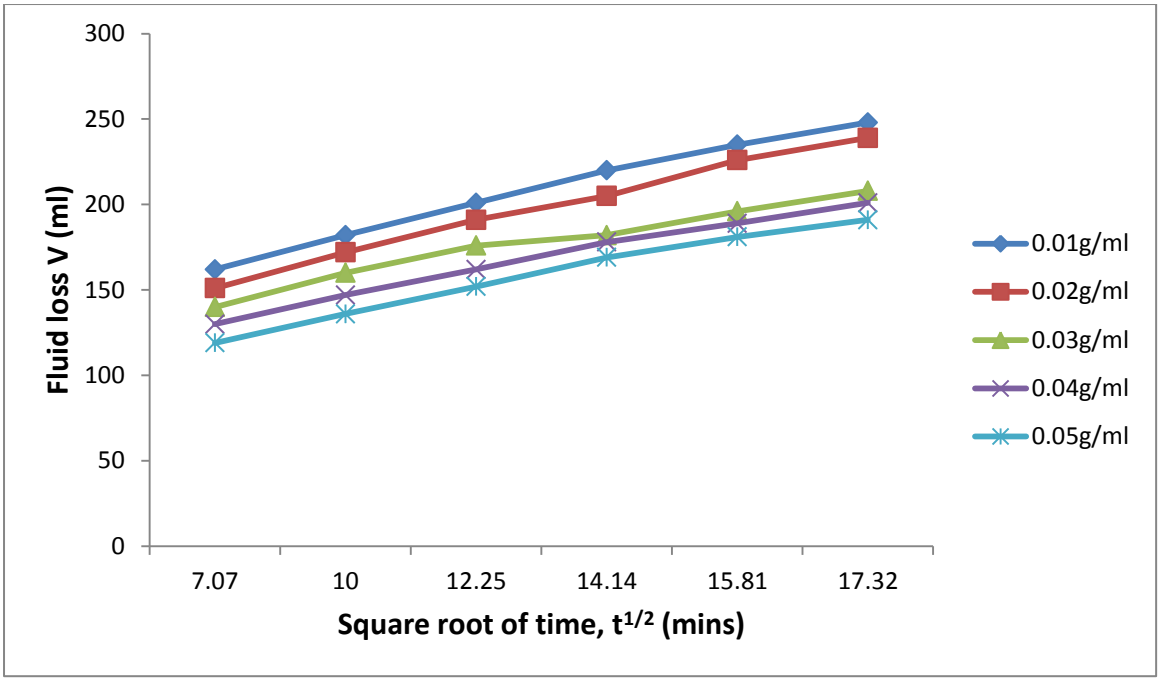

Figure 4.55: Plot of fluid loss versus square root of time for P:W-Mud sample with varying starch concentration at high temperature, 350°C. (Data; Table 4.30)

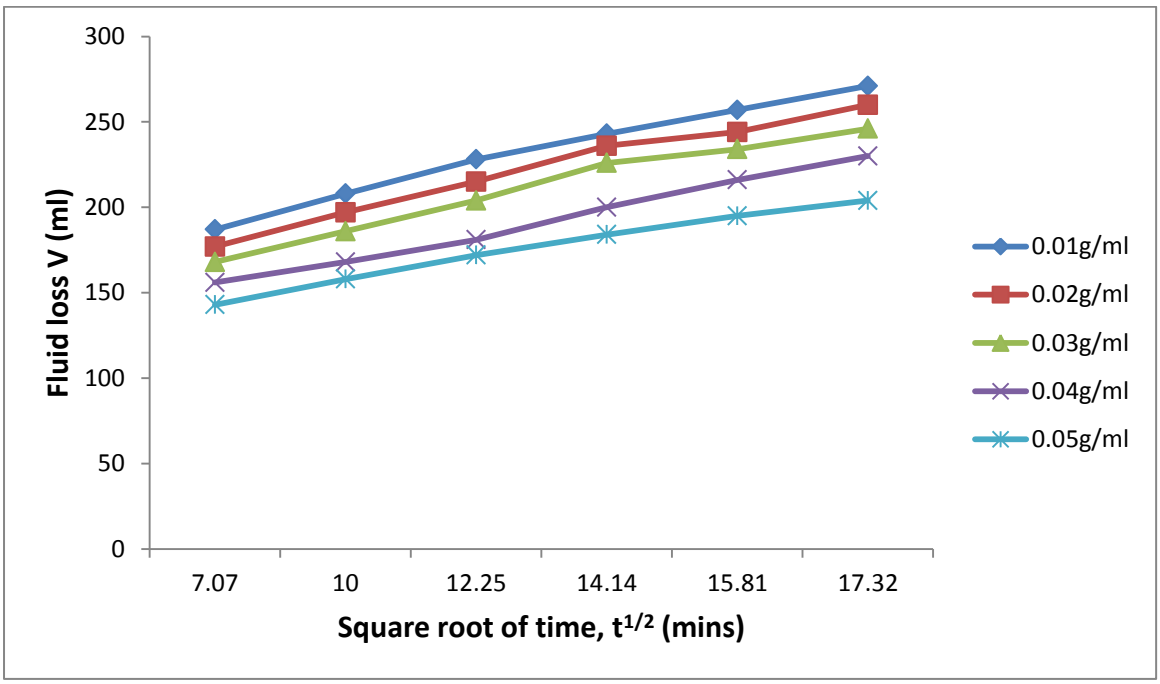

Figure 4.56: Plot of fluid loss versus square root of time for G:M-Mud sample with varying starch concentration at high temperature, 350°C. (Data; Table 4.31)

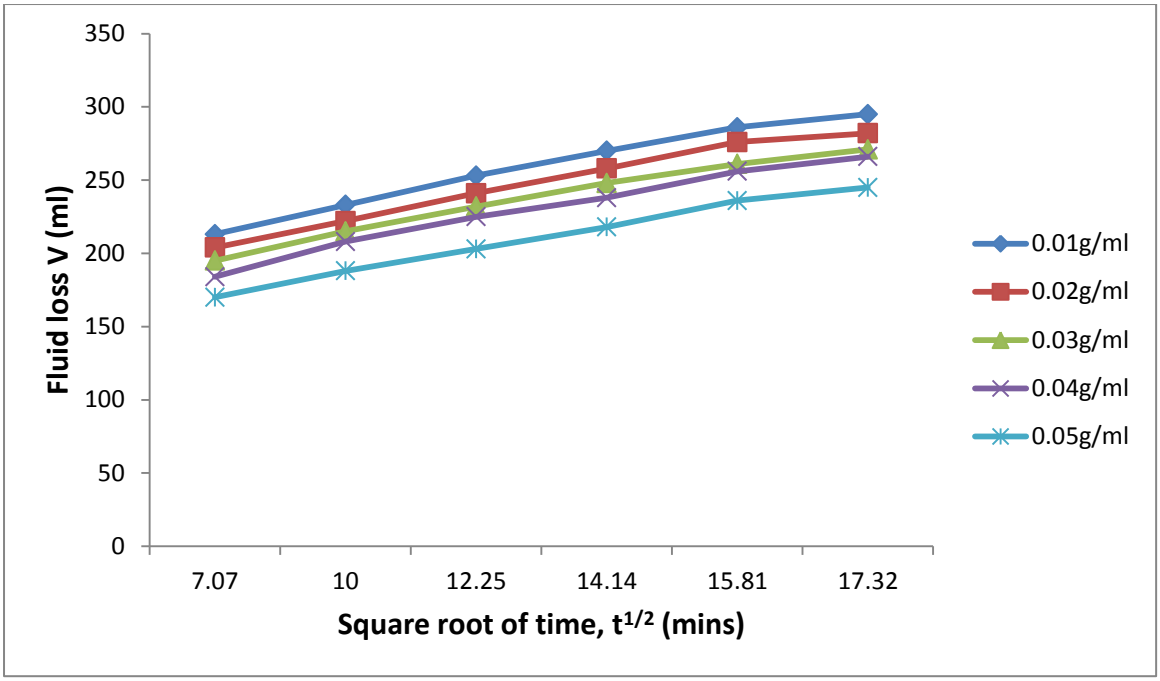

Figure 4.57: Plot of fluid loss versus square root of time for G:P-Mud sample with varying starch concentration at high temperature, 350°C. (Data; Table 4.32)

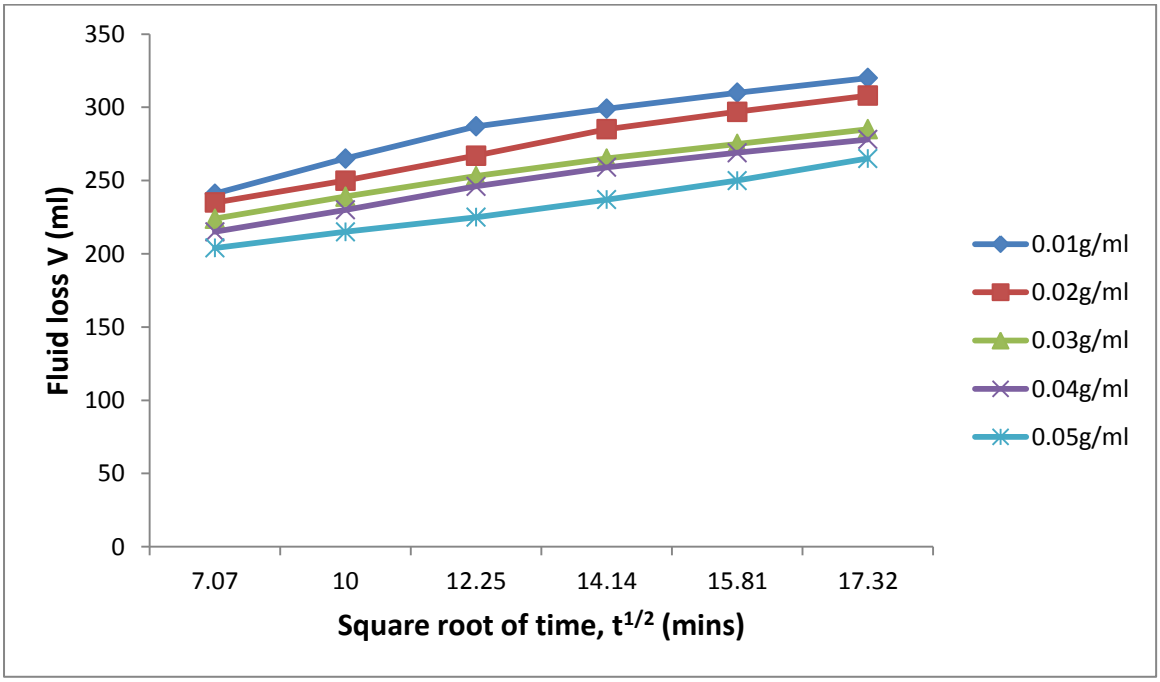

Figure 4.58: Plot of fluid loss versus square root of time for M:P-Mud sample with varying starch concentration at high temperature, 350°C. (Data; Table 4.33)

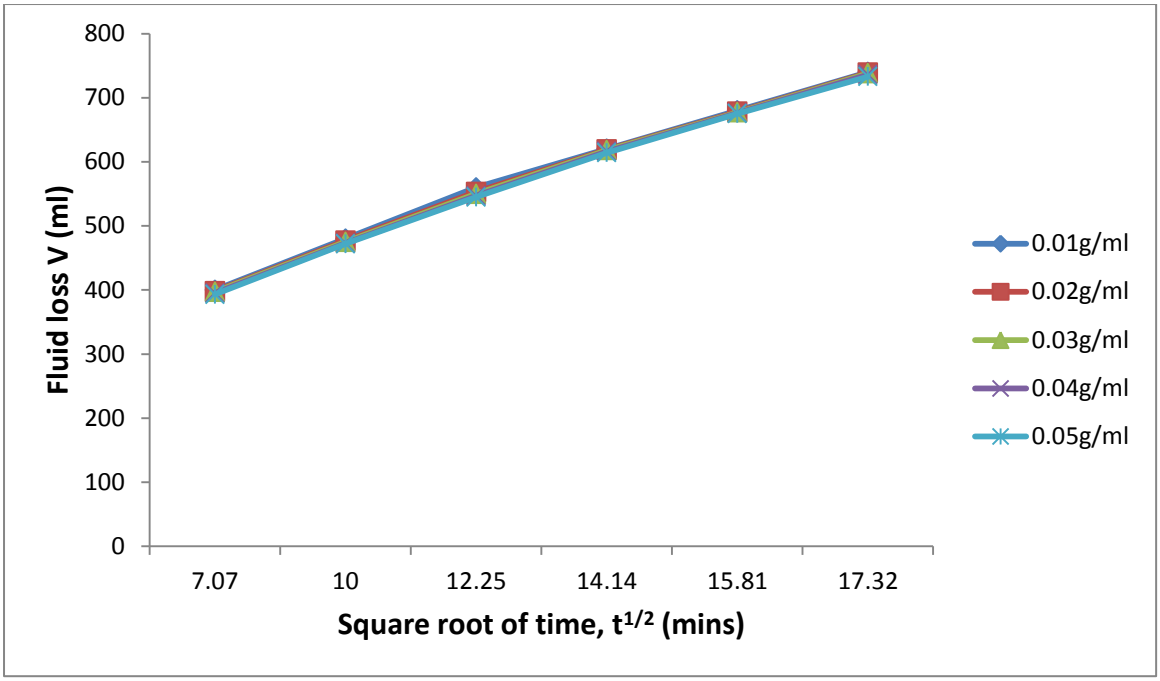

Figure 4.59: Plot of fluid loss versus square root of time for CMS:HPS-Mud sample with varying starch concentration at high temperature, 350°C. (Data;Table 4.34)

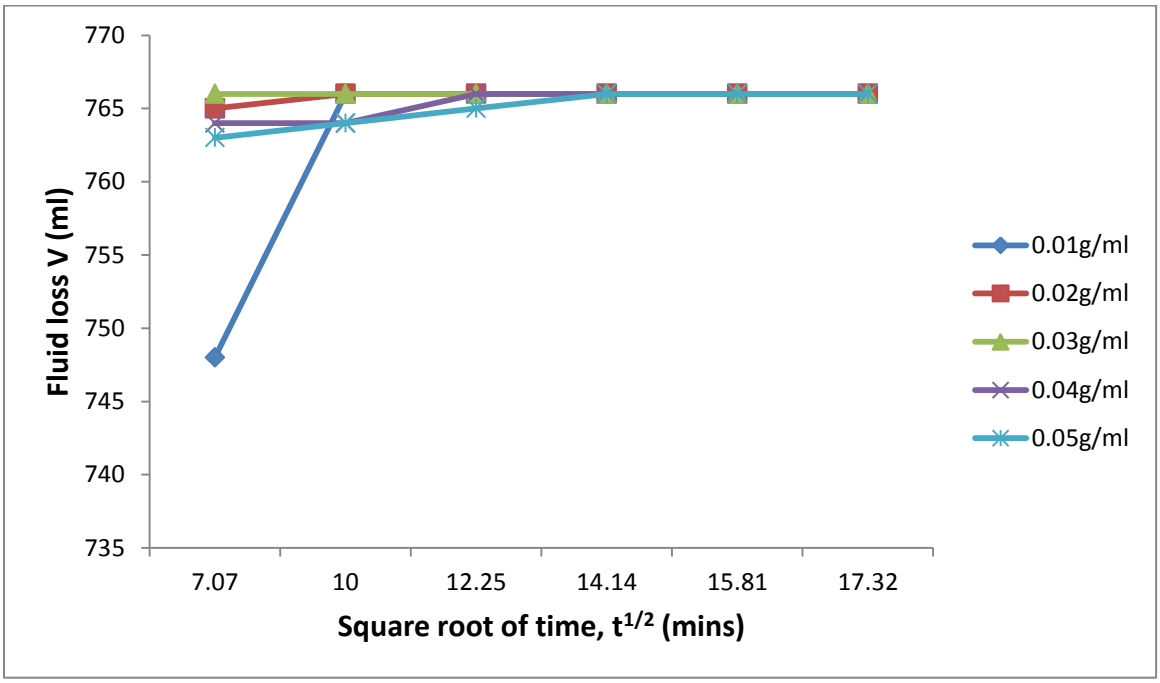

Figure 4.60: Plot of fluid loss versus square root of time for W-Mud sample with varying starch concentration at high temperature, 350°C. (Data; Table 4.35)

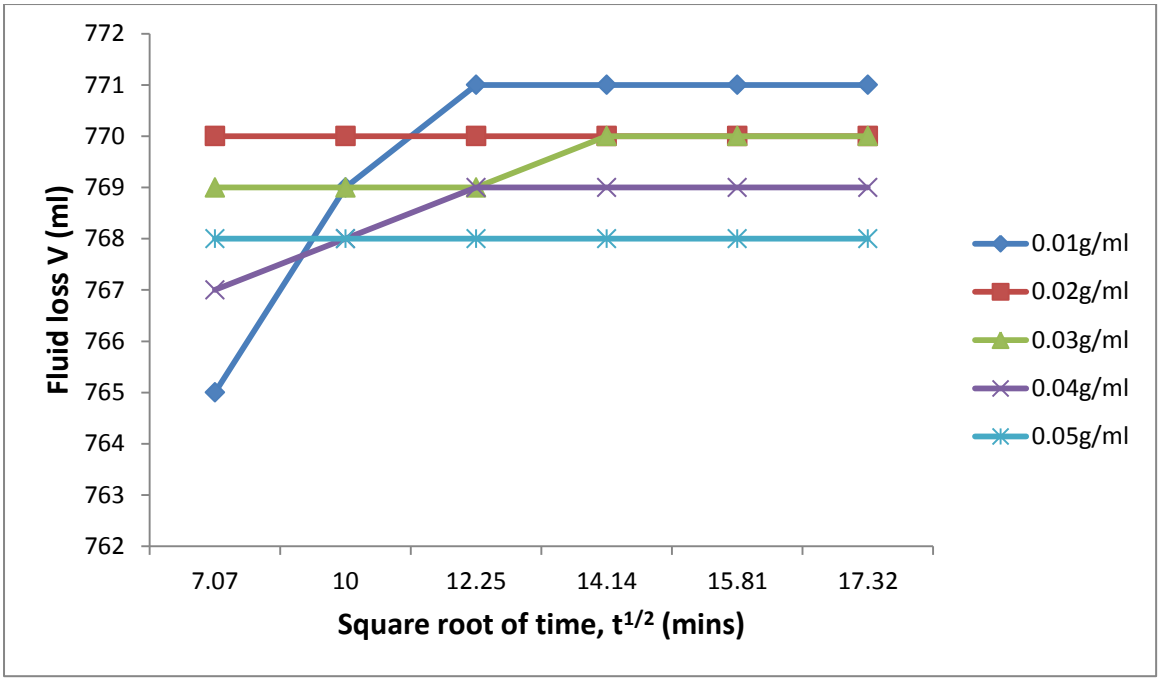

Figure 4.61: Plot of fluid loss versus square root of time for CMS-Mud sample with varying starch concentration at high temperature, 350°C. (Data; Table 4.36)

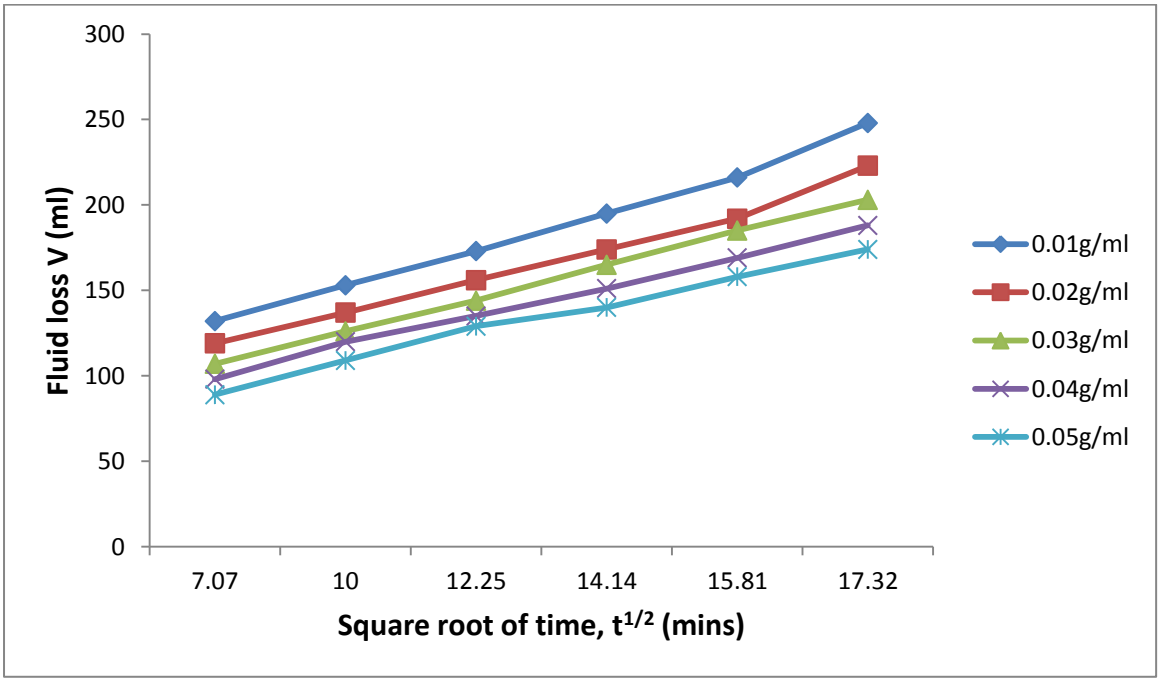

Figure 4.62: Plot of fluid loss versus square root of time for G:W-Mud sample with varying starch concentration at high temperature, 450°C. (Data; Table 4.37)

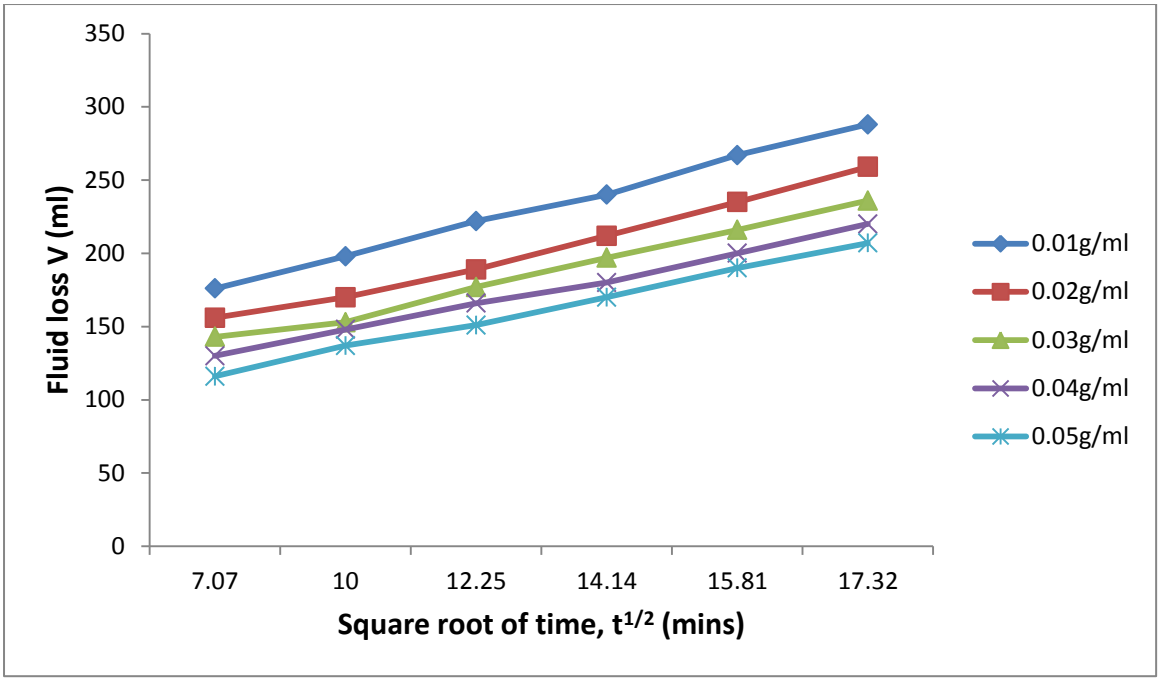

Figure 4.63: Plot of fluid loss versus square root of time for M:W-Mud sample with varying starch concentration at high temperature, 450°C. (Data; Table 4.38)

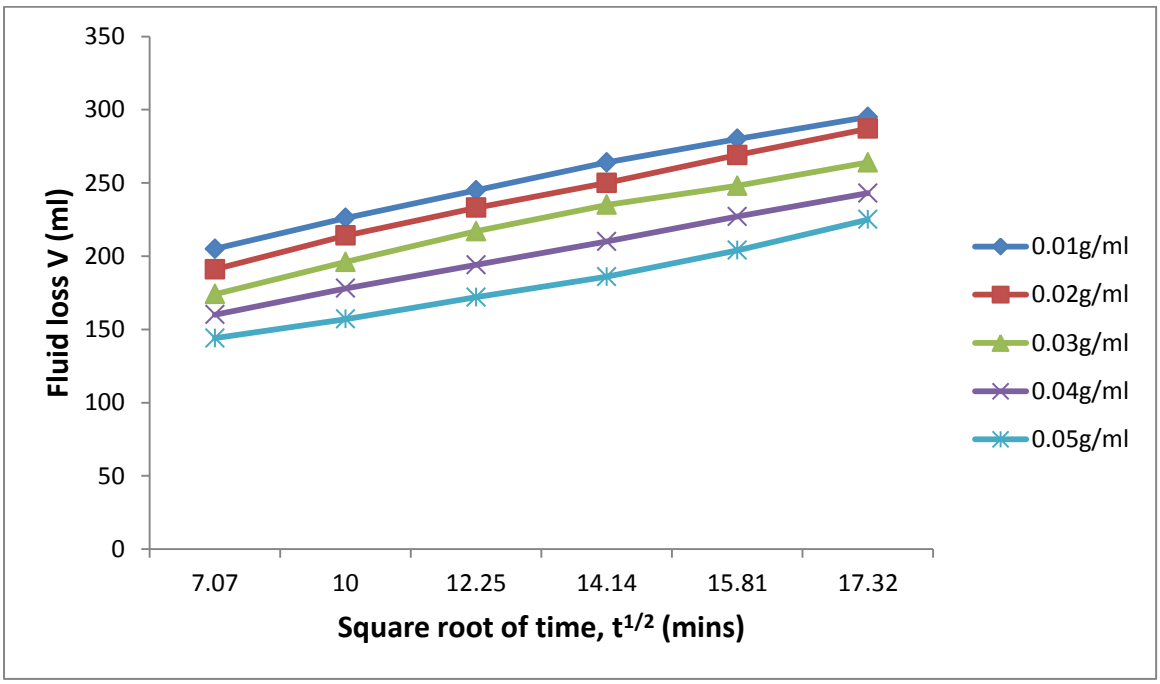

Figure 4.64: Plot of fluid loss versus square root of time for P:W-Mud sample with varying starch concentration at high temperature, 450°C. (Data; Table 4.39)

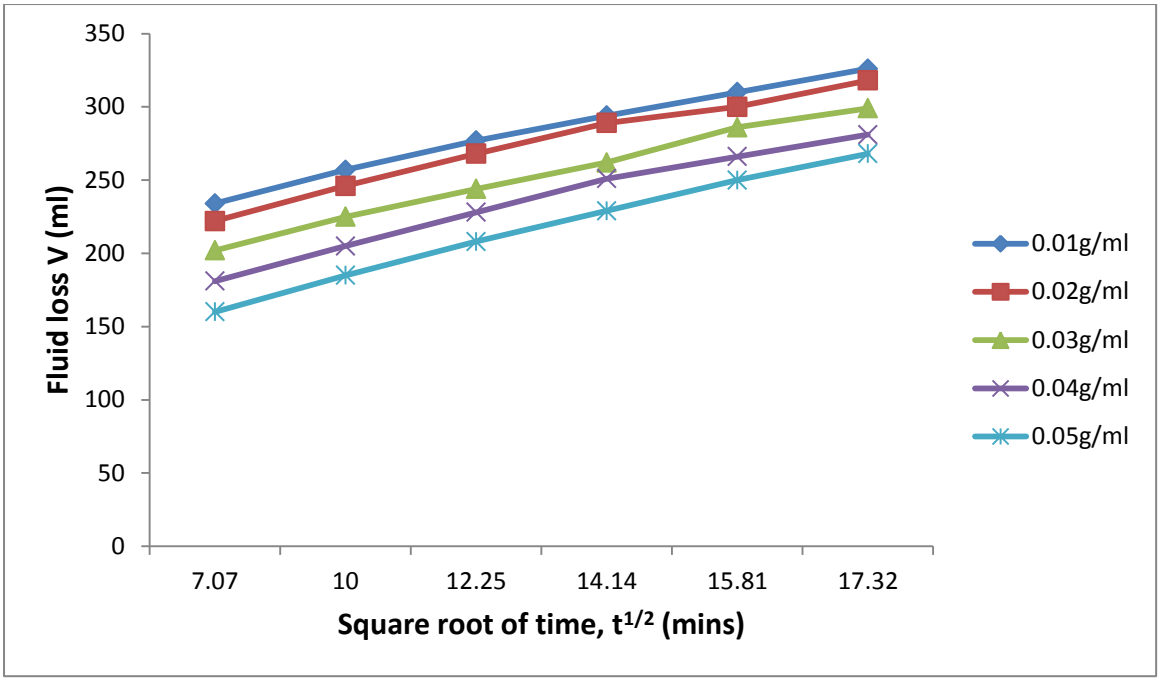

Figure 4.65: Plot of fluid loss versus square root of time for G:M-Mud sample with varying starch concentration at high temperature, 450°C. (Data; Table 4.40)

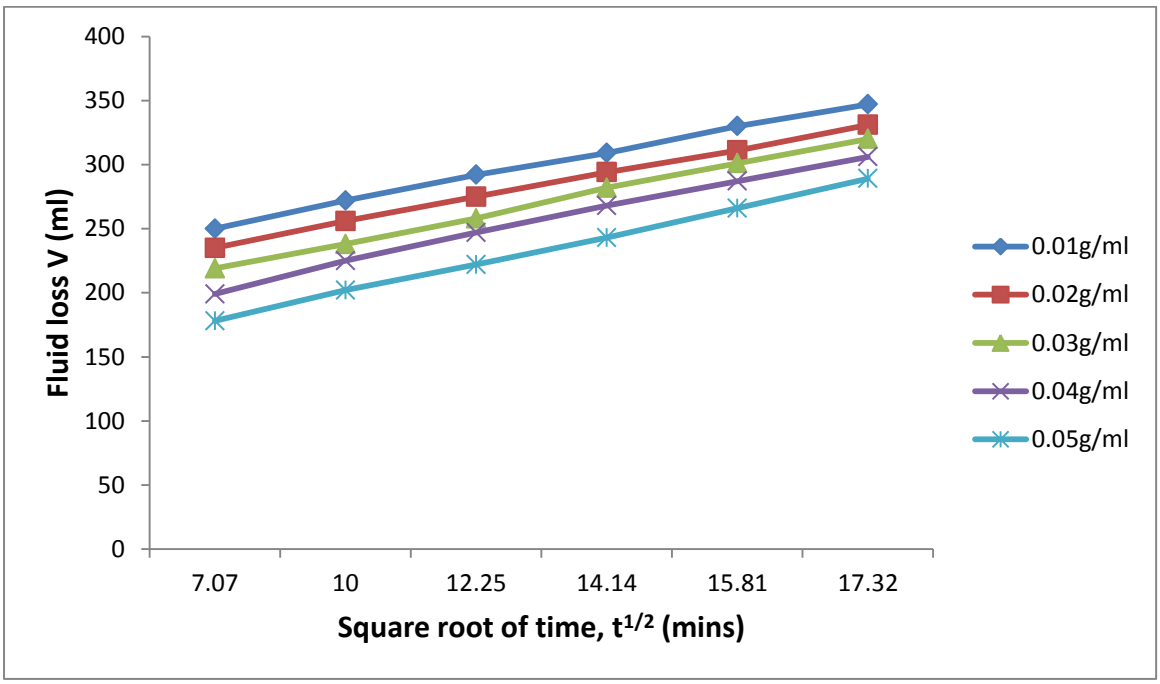

Figure 4.66: Plot of fluid loss versus square root of time for G:P-Mud sample with varying starch concentration at high temperature, 450°C. (Data; Table 4.41)

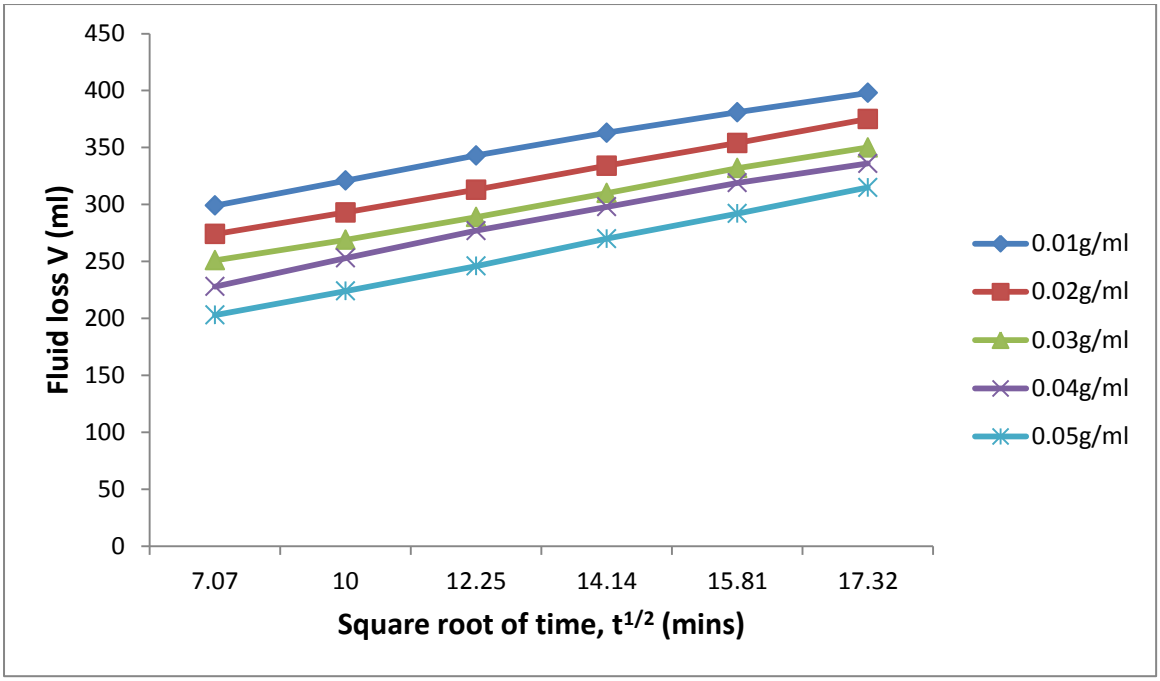

Figure 4.67: Plot of fluid loss versus square root of time for M:P-Mud sample with varying starch concentration at high temperature, 450°C. (Data; Table 4.42)

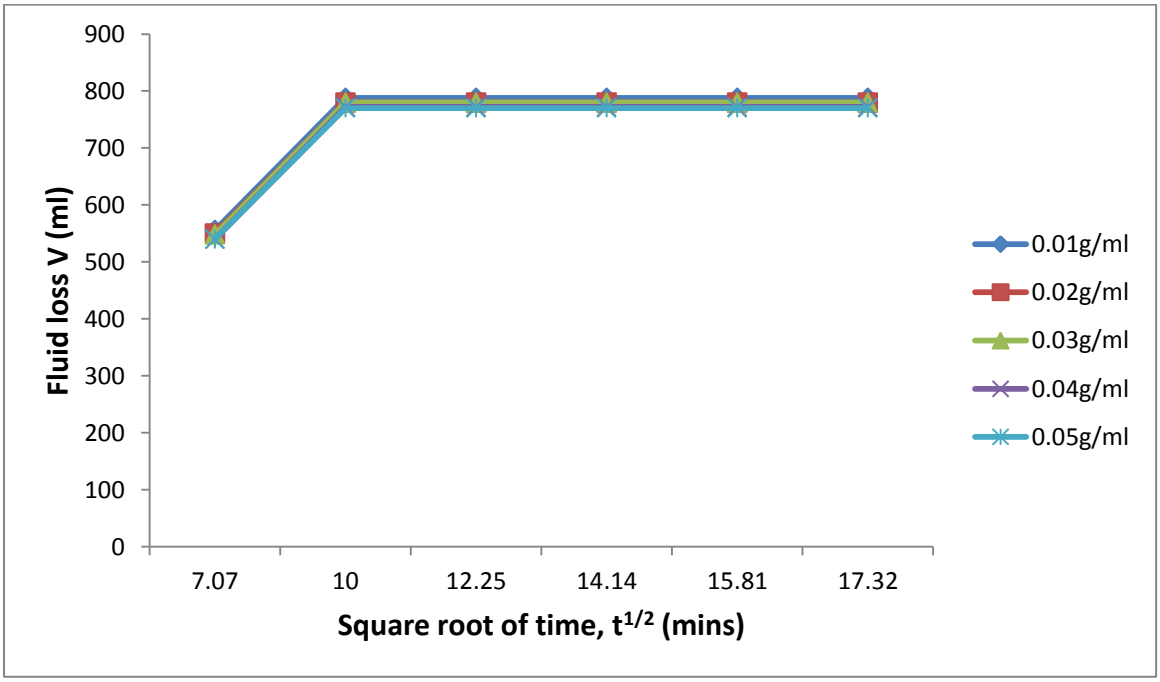

Figure 4.68: Plot of fluid loss versus square root of time for CMS:HPS-Mud sample with varying starch concentration at high temperature, 450°C. (Data;Table 4.43)

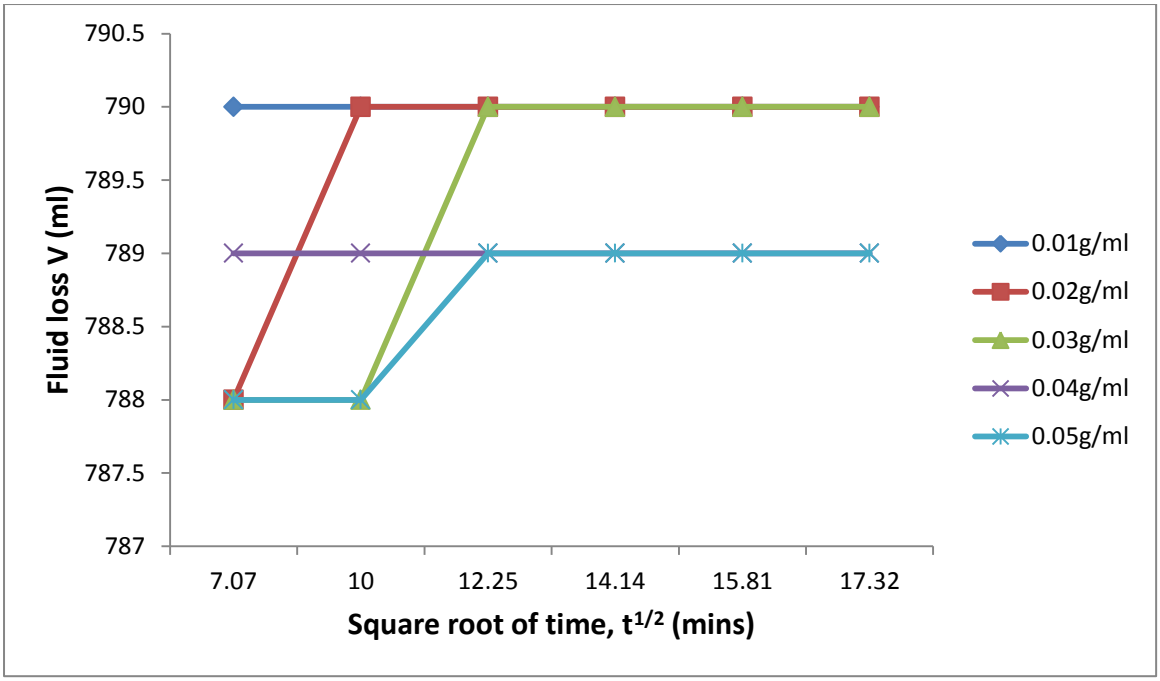

Figure 4.69: Plot of fluid loss versus square root of time for W-Mud sample with varying starch concentration at high temperature, 450°C. (Data; Table 4.44)

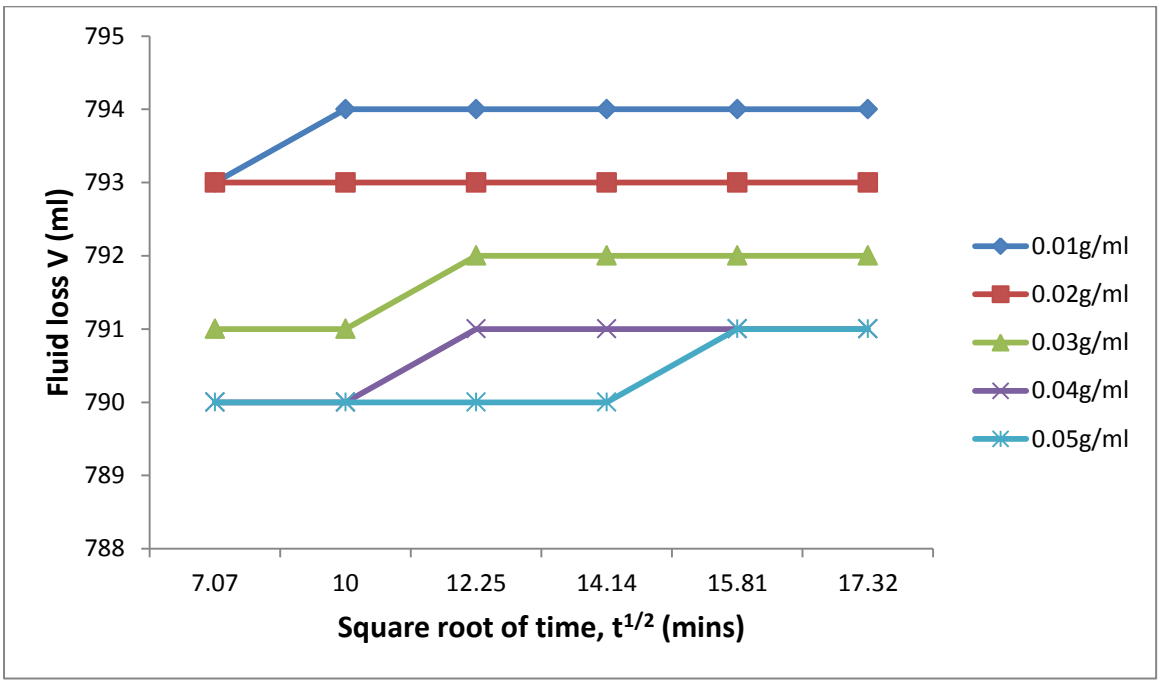

Figure 4.70: Plot of fluid loss versus square root of time for CMS-Mud sample with varying starch concentration at high temperature, 450°C. (Data; Table 4.45)

Figure 4.26 to 4.70 show the plots of fluid loss versus square root of time for each mud sample with varying starch concentration at room temperature 25^0C and elevated temperatures at 150^0C, 250^0C, 350^0C, 450^0C. Observations made from the figures shows that fluid loss also varies almost linearly with square root of time. Hence, fluid loss for each of the muds, with the starch concentration range of 0.01-0.05g/ml, increases with increase in square root of time. The figures also show that, for all the muds, the fluid loss values, with respect to time, reduce with increase in concentration of starch. An explanation to this is that since all the muds obey the API model for Filtration, an increase in starch concentration increased the amount of filter cake built-up by each mud during a particular filtration time and therefore caused an increase in the resistance to the flow of fluid through the filter cake. More evaluation of the figures shows that G:W-Mud gave the least volume of fluid loss with the varying starch concentration at all the temperatures. This means that G:W-Mud has the greatest ability to build up filter cake within any specific filtration time at all the temperatures. Furthermore, all the new biodegradable polymer muds (G:W-Mud, M:W-Mud, P:W-Mud, G:M-Mud, G:P-Mud and M:P-Mud) with the varying starch concentrations at all the temperatures gave less volumes of fluid loss than the three already existing muds (CMS:HPS-Mud, W-Mud and CMS-Mud). This indicates that the pure and superior blends of starches contained by the new muds at the varying concentrations are more capable of forming more viscous fluid and gelling strength, and therefore they are better fluid loss reducing agents than the already existing types of starches. Polymers are used in the formulation of muds to increase viscosity and reduce fluid loss (Jones & Mark, 2006). This is at total indication that the new muds with pure blend of starches have better filtration control behaviours than the already existing muds whose types of starches might have reduced their abilities at all the

temperatures. A fluid loss reducing agent helps drilling mud to retain fluid and maintain fluid circulation round the walls of the well for a long period of time even at high temperature (Bernu, 2011; Brown, 2009)

In addition, the figures show that although all the muds obeyed the API model of filtration (equation 3.1) at 25^0C and 150^0C, some changes occurred at 250^0C, 350^0C and450^0C temperatures. At 250^0C the fluid loss increased with increase in square root of time but reduced with increase in starch concentration for all the new polymer muds (G:W-Mud, M:W-Mud, P:W-Mud, G:M-Mud, G:P-Mud, M:P-Mud) and CMS:HPS-Mud, while for these already existing muds, W-Mud and CMS-Mud, fluid loss values showed negligible or no reducion as starch concentrations were increased. This indicates thermal degradation of the muds, W-Mud and CMS-Mud, at 250^0C temperature, which could neither be controlled nor stopped even with increase in starch concentration. This may be due to the nature of the unblended and chemically modified starches used in preparing the muds.

At 350^0C temperature, all the new polymer muds still showed usual decrease in fluid loss with increase in starch concentration. W-Mud and CMS-Mud showed no reduction rather the fluid loss values were very high and constant with increased and varying starch concentrations. CMS:HPS-Mud showed very little and almost negligible decrease in fluid loss as starch concentration increased. This is a sign that thermal instability is about to occur.When a mud begins to show slight strange fluid loss behaviour at a temperature, thermal instability is about to occur (Anthony & Robert, 2010).

At 450^0C temperature, all the new polymer muds still displayed reduced fluid loss with increase in starch concentrations. The three already existing muds (CMS:HPS-Mud, W-Mud and CMS-Mud) showed no decrease in fluid loss, rather, they displayed constantly high fluid loss values with increase and variation in starch concentrations. This is a complete indication of thermal degradation of these three muds at 450^0C.

Therefore, it means that all the new polymer biodegradable muds (G:W-Mud, M:W-Mud, P:W-Mud, G:M-Mud, G:P-Mud, M:P-Mud) are suitable for drilling wells whose hole temperatures are as high as 450^0C and above, while the functions of three already existing muds, W-Mud, CMS-Mud and CMS:HPS-Mud, would cease at 250^0C and450^0C respectively.

4.2.1.7 Fluid Flow Behaviours of the Drilling Muds at Different Temperatures, 25^0C, 150^0C, 250^0C, 350^0C, 450^0C

Inspection of figure 4.26-4.70 also shows that, at all the temperatures, the flow of fluid was higher at the initial time of filtration than towards the end of a particular time interval for all the muds. This is due to resistance on the flowing fluid by the built-up filter cake. There is negligible or no resistance on the flow of fluid at the initial time of filtration with filter paper, but the resistance become significant and reduce fluid flow later when the filter cake is built up. It is observed from the figures that above square root of time $t^{1/2}$ = 14.14, a straight line relationship exists between fluid loss and square root of time. This agrees with the theories of static filtration according to Henri Darcy and American Petroleum Institute (API), (Scarlet & Brene, 2010; API, 2003; Clifford & Cain, 2002). But below $t^{1/2}$ = 14.14, there is deviation from the root time law, and this shows filtration with insignificant resistance. This

means that there exists an initial spurt above which the resistance of the cake becomes very significant and obeys the root time law (see Equation 3.1).

In addition, figures 4.26-4.70 shows that the flow of fluid increases with increase in temperature. This implies that the higher the temperature, the more the molecules of the fluid are set into motion. As the temperature of fluid increases, the volume also increases, resulting in lower molecular friction and consequently, a higher flow rate (Chris & James, 2005; Gautier & Lecourtier, 2001; Andy et al., 2000). Also, the higher the temperature, the more the contents of the mud, including the starches, are burnt up, and the weaker or less effective the built-up filter cakes. All these result in increase in flow and freedom of passage of the fluid through the filter cakes. The new polymer muds, prepared with pure blends of starches, gave the least fluid flow at all the temperatures. The already existing mud, (CMS-Mud), prepared with chemically-modified single starch, showed the highest fluid flow at all the temperatures, and the highest flow of fluid was observed at 450^0C temperature. The level of fluid flow of the muds may depend on the nature of the starches. For the new polymer muds, the starches are pure and blended, so, that their excellent features, like viscosity-building agents and fluid flow or fluid loss reducing agents, are still order, and even increased. For the already existing or widely used muds, the non-blending and chemical modification of the starches have altered and reduced the purity and efficiencies of the starches.

The implication of all above is that the already existing muds (CMS:HPS-Mud, W-Mud and CMS-Mud) are more proned to thermal degradation than the new polymer muds (G:W-Mud, M:W-Mud, P:W-Mud, G:M-Mud, G:P-Mud and M:P-Mud). This is

because the higher the fluid flow, the more the fluid loss, then the greater the chance of thermal degradation, It is known, from literature, that polymers are used in the formulation of muds to control fluid flow and reduce fluid loss at a minimum solid content (Enie & Giles, 2001). However, some modifications may alter the natural state of polymers, and cause them to deviate from this fact. It should also be noted that the viscosity of a fluid can be modified to obtain any desirable flow properties (Chris & James, 2005). It, therefore, implies that the deviation by the already existing muds from the above facts may be due to the chemical modification and the unblended state of the starches used in preparing them.

4.2.1.8 Fluid Sorptivity (S) of the various Muds at different Temperatures

The values of fluid sorptivity for the muds at the different temperatures were obtained as the slopes of the curves of each plot of fluid loss versus square root of time, from the mathematical modeling the muds under the root time law equation (3.1) $V = St^{½}$ according to American Petroleum Institute (API). From the equation (3.1), S is the sorptivity defined as a measure of the resistance against the fluid flowing through the built-up filter cake (Anthony & Robert, 2010; Scarlet & Brene, 2010; Ukachukwu et al., 2010; American Petroleum Institute API, 2003). Sorptivity is also the tendency, or the measure of the ability, of a material to absorb and transmit water and other liquids by capillarity (Hall & Hoff, 2012). Also, sorptivity is the measure of the capacity of a filter medium to absorb and retain parts of fluid passing through it by capillarity (Bernu, 2011).

Table 4.46: Computed Values of Fluid Sorptivity (S) From The Modellng of the Muds Containing varying Concentrations of Starch at Room Temperature, 25 ^{o}C.

	Fluid Sorptivity (S) at 25^{o}C				
Muds/Samples	0.01g/ml	0.02g/ml	0.03g/ml	0.04g/ml	0.05g/ml
G:W-Mud	61.63	62.15	65.08	67.26	68.66
M:W-Mud	53.89	55.52	56.75	58.14	60.36
P:W-Mud	50.41	52.33	54.62	55.25	59.15
G:M-Mud	47.70	49.73	51.88	52.57	53.06
G:P-Mud	45.24	47.00	47.95	48.01	48.20
M:P-Mud	42.85	43.91	45.11	45.43	46.55
CMS:HPS-Mud	33.12	34.97	35.01	35.98	36.43
W-Mud	31.25	33.08	34.00	34.93	35.66
CMS-Mud	26.44	26.86	27.26	27.95	28.31

Table 4.47: Computed Values of Fluid Sorptivity (S) From The Modelling of the Muds Containing varying Concentrations of Starch at High Temperature, 150^{o}C.

	Fluid Sorptivity (S) at 150^{o}C				
Muds/Samples	0.01g/ml	0.02g/ml	0.03g/ml	0.04g/ml	0.05g/ml
G:W-Mud	57.38	58.90	62.83	64.18	65.25
M:W-Mud	48.75	49.18	51.96	53.22	54.73
P:W-Mud	45.14	48.82	49.26	51.45	52.97
G:M-Mud	40.36	42.68	44.35	45.75	47.64
G:P-Mud	37.83	40.92	43.24	45.15	46.33
M:P-Mud	35.65	36.46	38.66	41.23	42.62
CMS:HPS-Mud	25.32	27.11	28.35	29.83	32.15
W-Mud	22.74	23.36	25.13	26.41	28.27
CMS-Mud	18.05	19.22	20.40	21.62	21.93

Table 4.48: Computed Values of Fluid Sorptivity (S) From The Modelling of the Muds Containing varying Concentrations of Starch at High Temperature, 250^{o}C.

Fluid Sorptivity (S) at 250^{o}C

Muds/Samples	0.01g/ml	0.02g/ml	0.03g/ml	0.04g/ml	0.05g/ml
G:W-Mud	51.64	52.53	55.18	58.33	60.95
M:W-Mud	44.16	47.37	49.88	51.15	52.86
P:W-Mud	40.37	42.63	43.13	44.97	45.66
G:M-Mud	37.11	37.82	39.48	41.25	42.85
G:P-Mud	3.67	35.58	36.76	37.17	39.55
M:P-Mud	30.06	31.24	34.51	34.99	36.83
CMS:HPS-Mud	21.09	22.10	24.24	26.72	29.06
W-Mud	_	_	_	_	_
CMS-Mud	_	_	_	_	_

Table 4.49: Computed Values of Fluid Sorptivity (S) From The Modelling of the Muds Containing varying Concentrations of Starch at High Temperature, 350^{o}C.

Fluid Sorptivity (S) at 350^{o}C

Muds/Samples	0.01g/ml	0.02g/ml	0.03g/ml	0.04g/ml	0.05g/ml
G:W-Mud	44.21	45.73	48.10	50.38	52.15
M:W-Mud	38.66	39.89	41.25	42.44	45.90
P:W-Mud	34.23	36.15	37.80	38.03	40.38
G:M-Mud	31.54	33.25	35.39	36.84	37.12
G:P-Mud	29.16	30.46	32.57	34.26	35.41
M:P-Mud	26.73	28.61	30.15	31.62	32.56
CMS:HPS-Mud	16.95	17.10	17.52	17.93	18.11
W-Mud	_	_	_	_	_
CMS-Mud	_	_	_	_	_

Table 4.50: Computed Values of Fluid Sorptivity (S) From The Modelling of the Muds Containing varying Concentrations of Starch at High Temperature, 450°C.

	Fluid Sorptivity (S) at 450°C				
Muds/Samples	0.01g/ml	0.02g/ml	0.03g/ml	0.04g/ml	0.05g/ml
G:W-Mud	36.84	39.04	41.63	43.15	45.08
M:W-Mud	32.91	34.50	35.73	37.13	39.61
P:W-Mud	30.42	31.67	33.89	34.22	36.30
G:M-Mud	27.60	29.31	30.14	32.40	35.02
G:P-Mud	26.10	27.16	28.52	29.12	31.35
M:P-Mud	22.85	23.71	25.18	26.09	27.83
CMS:HPS-Mud	_	_	_	_	_
W-Mud	_	_	_	_	_
CMS-Mud	_	_	_	_	_

Tables 4.46, 4.47, 4.48, 4.49, and 4.50 show the values of sorptivity, S, for the various muds at the different temperatures of 25^{o}C, 150^{o}C, 250^{o}C, 350^{o}C and 450^{o}C. It is observed from the tables that values of Sorptivity decrease with increase in temperature. In addition, the values of sorptivity obtained with each of the new polymer muds (G:W-Mud, M:W-Mud, P:W-Mud, G:M-Mud, G:P-Mud and M:P-Mud) were higher than those of the already existing muds (CMS:HPS-Mud, W-Mud and CMS-Mud) at all the temperatures. The minimum sorptivity values of the new polymer muds were obtained at 450^{o}C, while the minimum sorptivity values of the already existing muds were obtained at 250^{o}C for W-mud and CMS-Mud, and at 350^{o}C for CMS:HPS-Mud. It, then, implies that each of the new muds has greater ability than any of the already existing muds in building up effective filter cake and absorbing flowing fluid. Ability to build up filter cake, to absorb fluid, to control fluid flow, and reduce fluid loss is dependent on viscosity (Obong, 2004; Clifford & Cain, 2002). Each of the new muds is therefore more viscous than any of the already existing muds. This may be due to the pure starch polymers used in preparing the new polymer muds. Highly viscous polymers have high coagulation strength and can easily clog the pores or interstitial openings between particles thereby building up filter cake to control the flow of fluid through the built-up cake (Obong, 2004; Clifford & Cain, 2002). Therefore, the higher the viscosity of a mud, the more the filter cake is built-up, and the higher the sorptivity.

Furthermore, the tables show that sorptivity increases with increase in concentration. An explanation to this is based on the fact that higher concentrations of the starches gave more viscous fluid. So, the higher the concentration, the higher the viscosity of each mud resulting in increased built-up filter cake, and higher sorptivity. It should also be noted that the above feature is obtainable with each mud if the built-up filter

cake is still effective in absorbing and retaining more of the fluid passing through it than the part that is lost. It then means that higher concentration results in higher viscosity and higher fluid loss reducing ability of a mud. This also means that the more the fluid loss reducing ability of a mud, the less the chance of losing fluid circulation round the walls of a well, and the less the occurrence of catastrophe with the mud in the actual drilling application (Wylly & Chenevert, 2012). The new polymer muds (G:W-Mud, M:W-Mud, P:W-Mud, G:M-Mud, G:P-Mud and M:P-Mud) gave higher values of sorptivity at all the concentrations than the already existing muds (CMS:HPS-Mud, W-Mud and CMS-Mud). The highest and lowest values of sorptivity was obtained with G:W-Mud and CMS-Mud at all the varying concentrations. This shows that the new polymer muds are better fluid loss reducing agents and better for drilling any type of well at any concentration than the already existing muds. The higher values of sorptivity and better behaviours of the new polymer muds at all the concentrations might have resulted from the purer and more effective starch blends used in preparing them.

Tables 4.46-4.50 further show that the fluid sorptivity decreases with increase in temperature. The decrease in the values of sorptivity with increased temperature is as a result of reduction in the fluid absorbing capacity of the built-up filter cake and the reduction in the viscosity of the muds. As the temperature of fluid increases, the volume also increases, resulting in lower molecular friction and consequently, a higher flow rate and lower sorptivity (Gautier & Lecourtier, 2001).This higher flow rate of mud gives rise to lower fluid loss reducing ability and lower sorptivity of the mud. When the temperature is high, the viscosity of the muds decreases due to lower molecular friction or lower compactness, the fluid flow increases with decrease in the ability of the mud's additives to clog the pores or interstitial openings between

particles. Also, effectiveness of the mud's additive (starch) reduces with high temperature, which results in reduction of the absorbing power of the particles of the built-up filter cake. All the above explanations result in decreased or lower sorptivity. The new polymer muds gave higher sorptivity values than the already existing muds at all temperatures under study. This shows that the new polymer muds have greater ability to absorb and retain parts of the flowing fluid, thereby, reduce fluid loss more than the already existing muds at the different temperatures. Two of the three already existing muds (W-Mud and CMS-Mud) showed infinite fluid sorptivity at 250^{o}C and 350^{o}C, which indicates thermal instability or thermal degradation of the muds at those temperatures. All the three already existing muds (CMS:HPS-Mud, W-Mud and CMS-Mud) gave infinite fluid sorptivity at 450^{o}C, and this is an indication of thermal degradation of the muds at 450^{o}C. The functions of a mud begin to cease when the mud is thermally degraded and deviation from the root time law is obtained (Andrew & Robert, 2007). It specifically means that the new muds (G:W-Mud, M:W-Mud, P:W-Mud, G;M-Mud, G:P-Mud and M:P-Mud) can be used to drill wells whose hole temperatures are as high as 450^{o}C and above, the functions of W-Mud and CMS-Mud would cease at about 250^{o}C, while the functions of CMS:HPS-Mud would cease at about 450^{o}C.

4.2.1.9 Rate of Filtration of the Muds at different Temperatures

The rates of filtration of the various muds are shown in figures 4.71-4.95. The figures comprise the curves of filtration rate against time for the muds at all the temperatures under study.

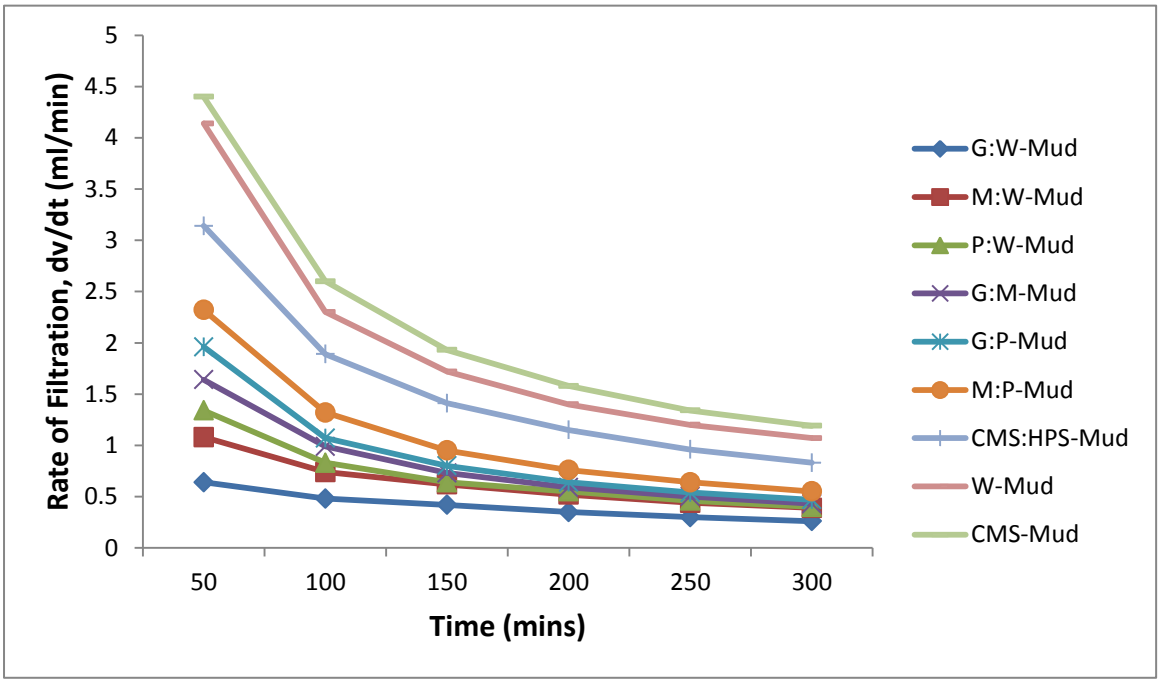

Figure 4.71: Plot of Rate of filtration versus time for all the muds with 0.01g/ml starch concentration at room temperature, 25°C. (Data; Table 4.1-Table 4.9)

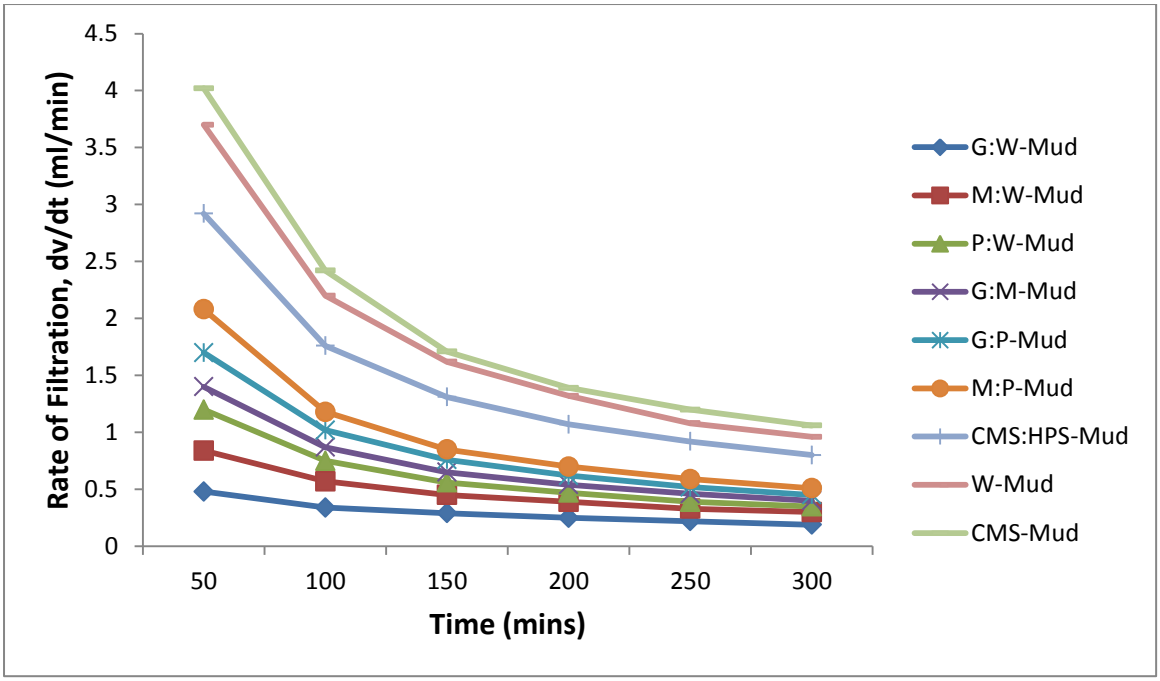

Figure 4.72: Plot of Rate of filtration versus time for all the muds with 0.02g/ml starch concentration at room temperature, 25°C. (Data; Table 4.1-Table 4.9)

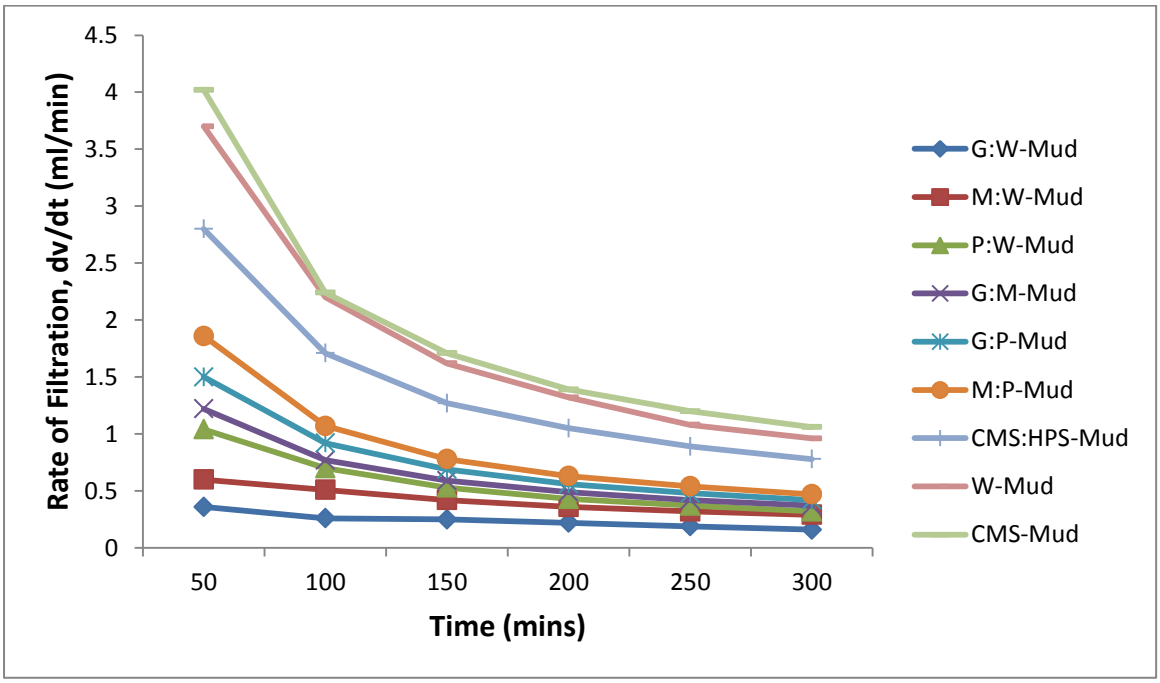

Figure 4.73: Plot of Rate of filtration versus time for all the muds with 0.03g/ml starch concentration at room temperature, 25°C. (Data; Table 4.1-Table 4.7)

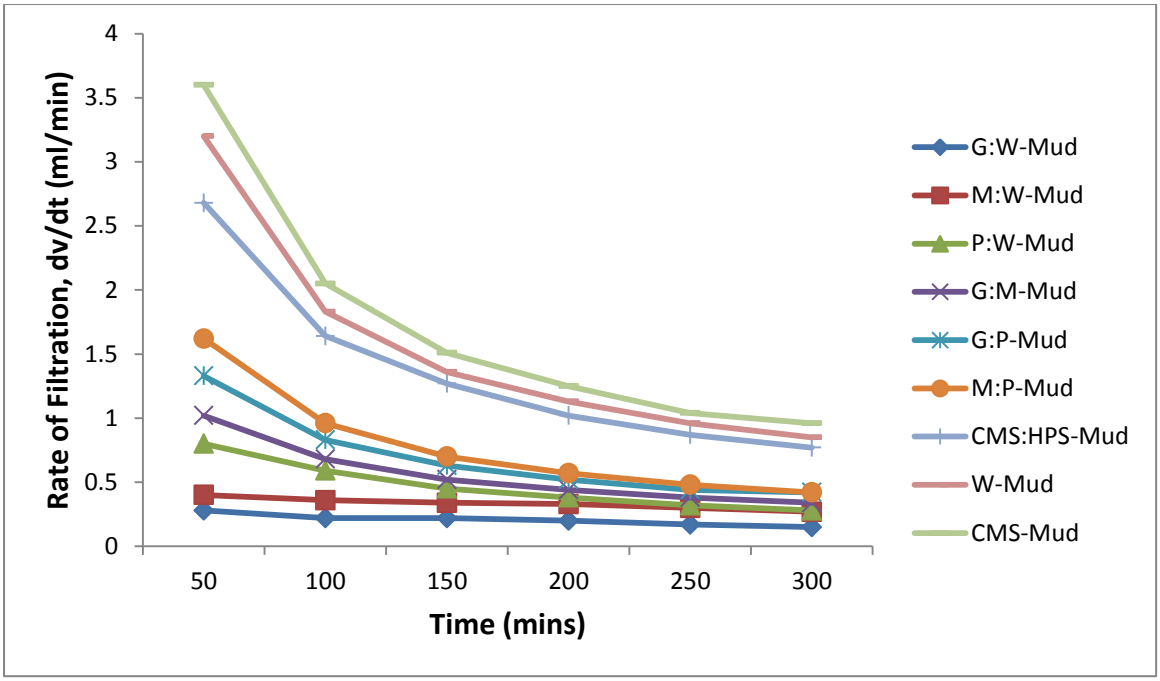

Figure 4.74: Plot of Rate of filtration versus time for all the muds with 0.04g/ml starch concentration at room temperature, 25°C. (Data; Table 4.1-Table 4.9)

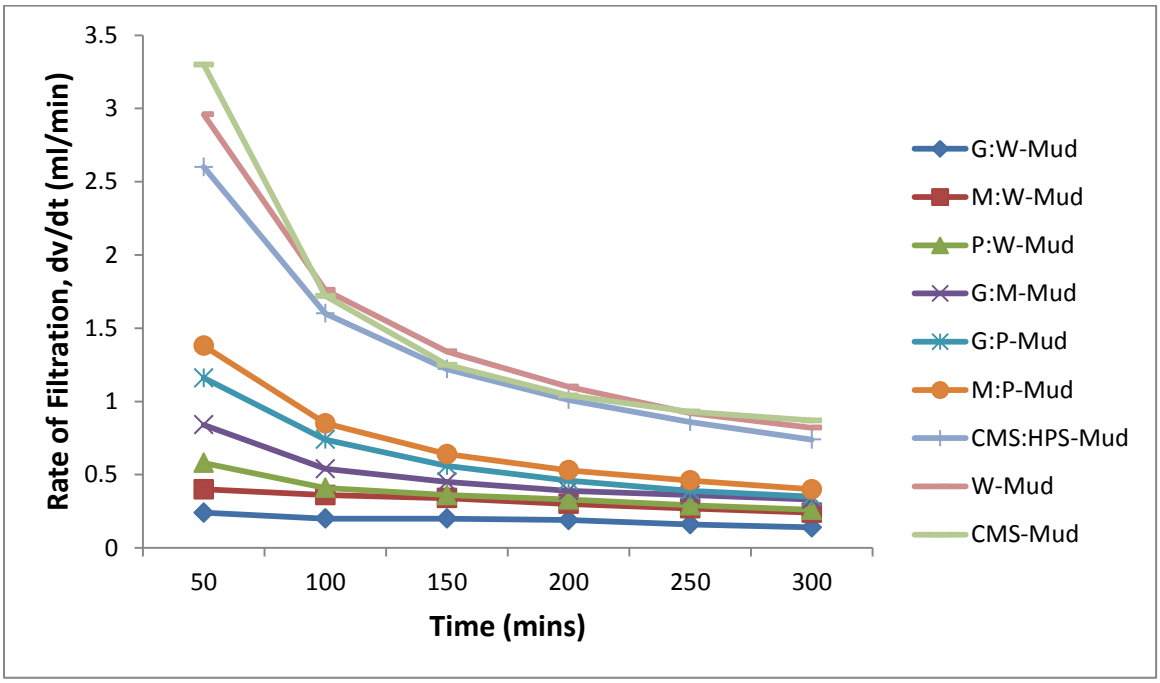

Figure 4.75: Plot of Rate of filtration versus time for all the muds with 0.05g/ml starch concentration at room temperature, 25°C. (Data; Table 4.1-Table 4.9)

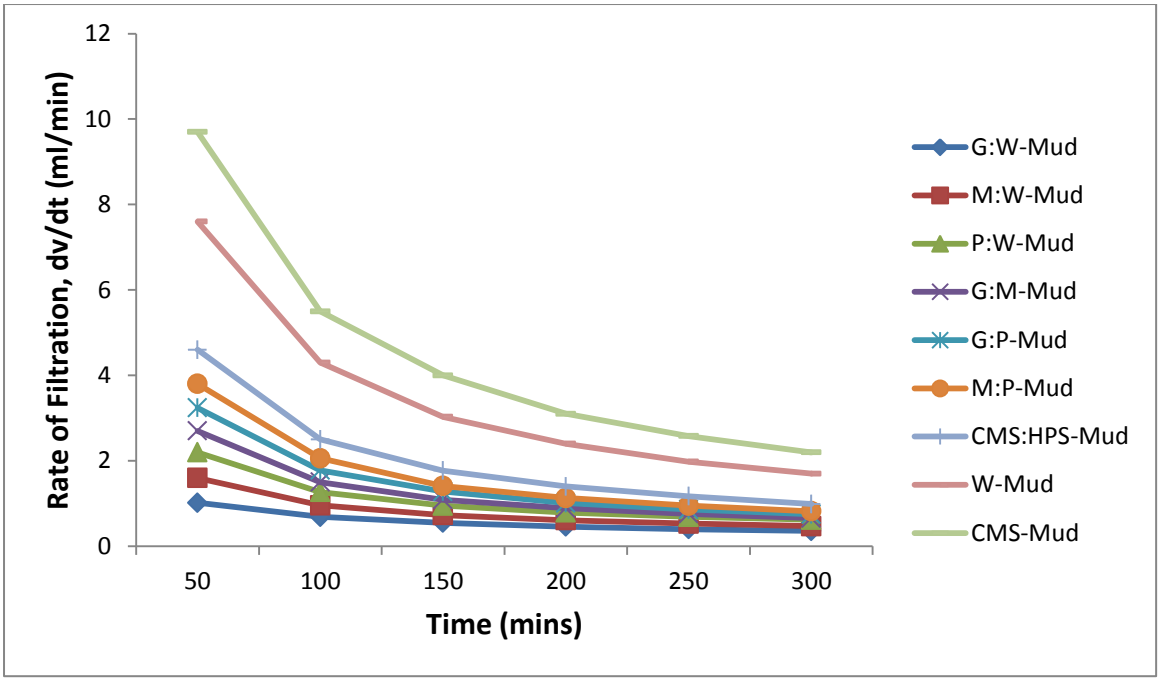

Figure 4.76: Plot of Rate of filtration versus time for all the muds with 0.01g/ml starch concentration at high temperature, 150°C. (Data; Table 4.10-Table 4.18)

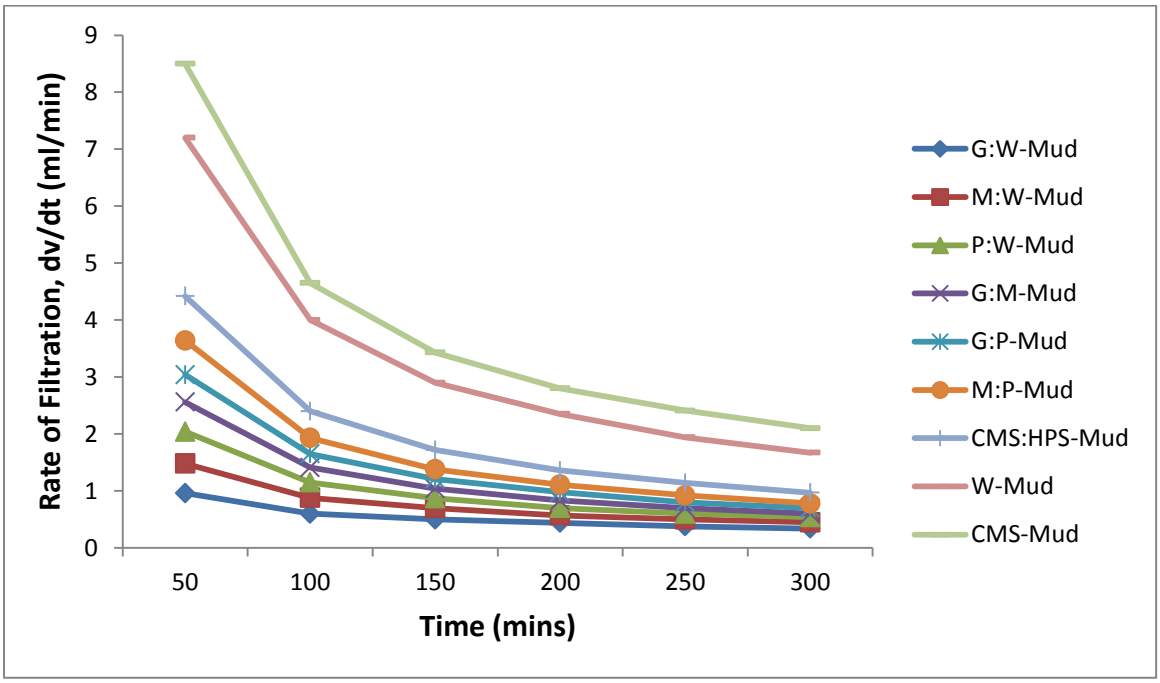

Figure 4.77: Plot of Rate of filtration versus time for all the muds with 0.02g/ml starch concentration at high temperature, 150°C. (Data; Table 4.10-Table 4.18)

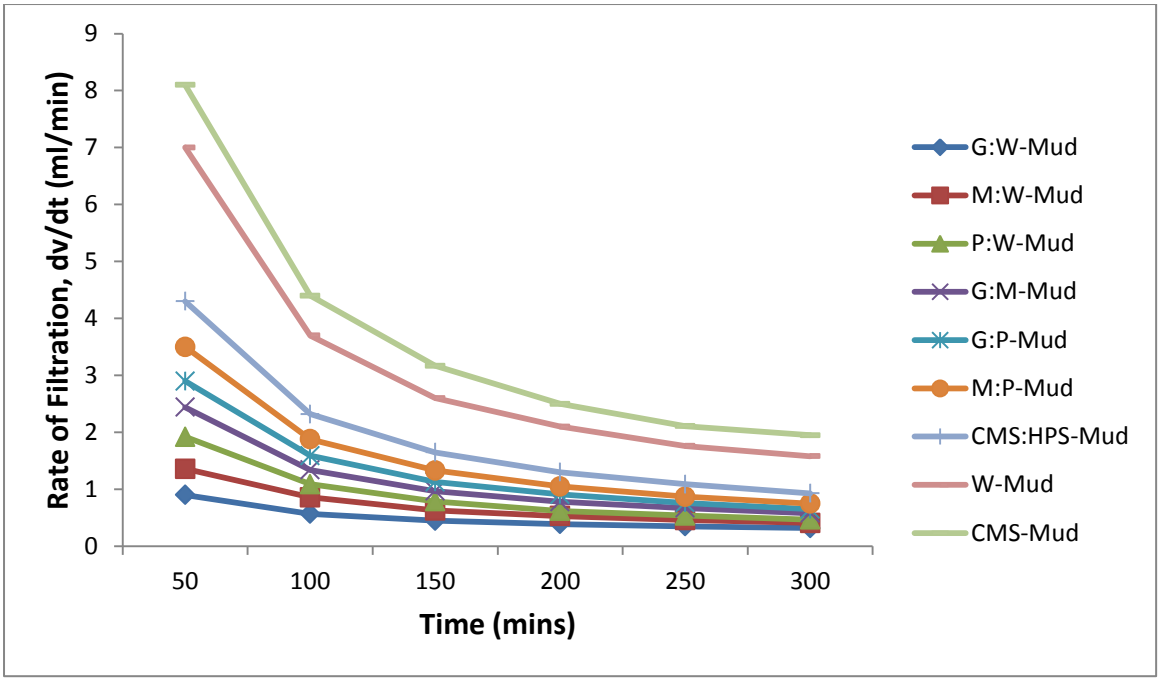

Figure 4.78: Plot of Rate of filtration versus time for all the muds with 0.03g/ml starch concentration at high temperature, 150°C. (Data; Table 4.10-Table 4.18)

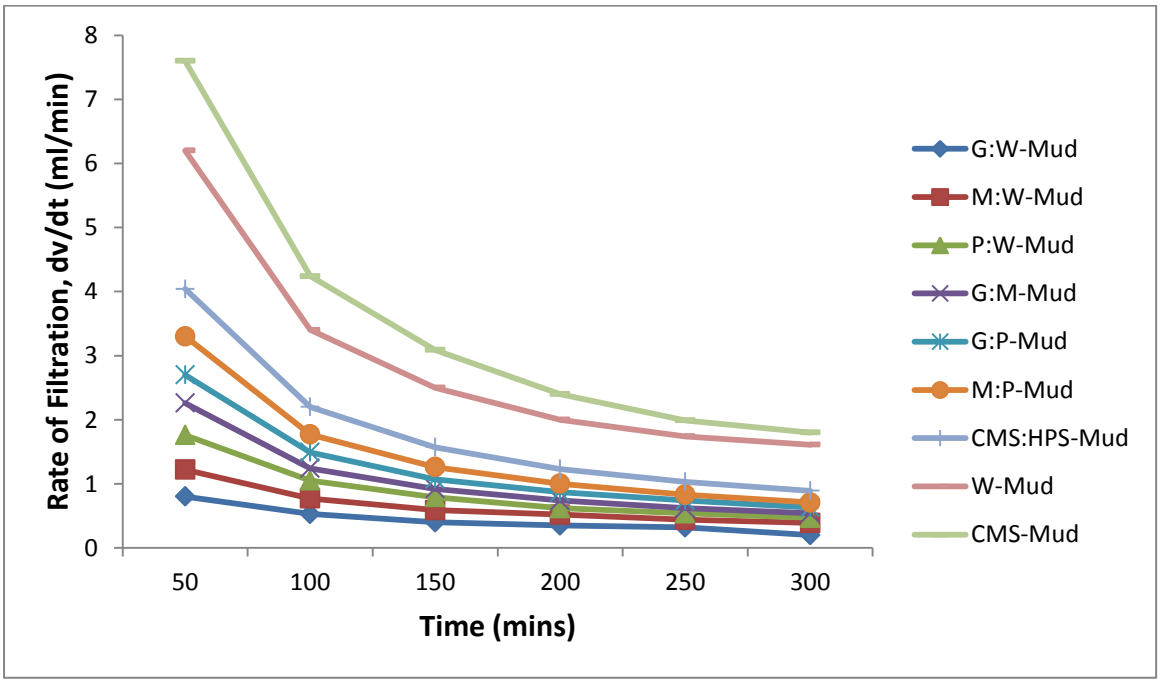

Figure 4.79: Plot of Rate of filtration versus time for all the muds with 0.04g/ml starch concentration at high temperature, 150°C. (Data; Table 4.10-Table 4.18)

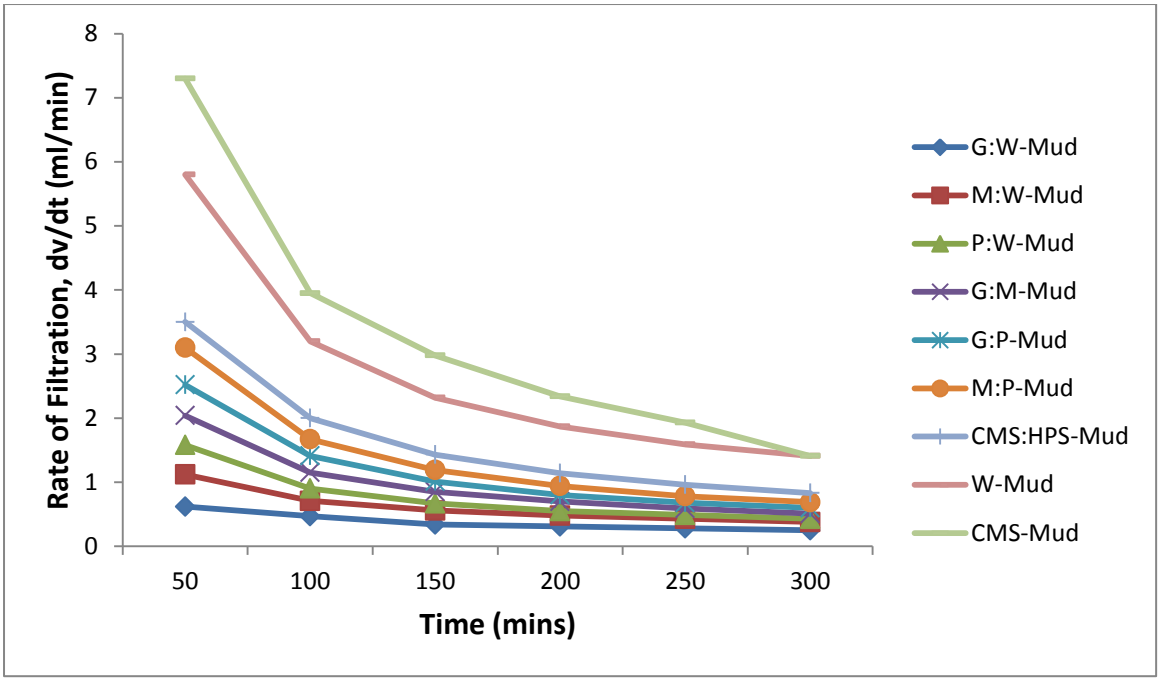

Figure 4.80: Plot of Rate of filtration versus time for all the muds with 0.05g/ml starch concentration at high temperature, 150°C. (Data; Table 4.10-Table 4.18)

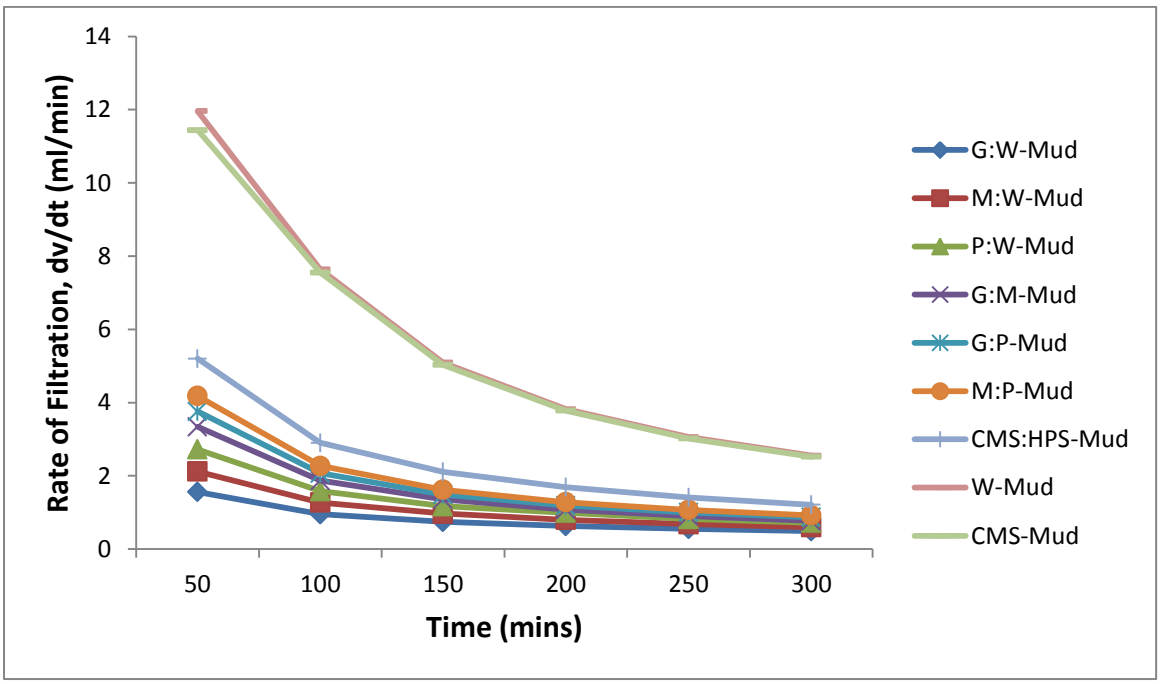

Figure 4.81: Plot of Rate of filtration versus time for all the muds with 0.01g/ml starch concentration at high temperature, 250°C. (Data; Table 4.19-Table 4.27)

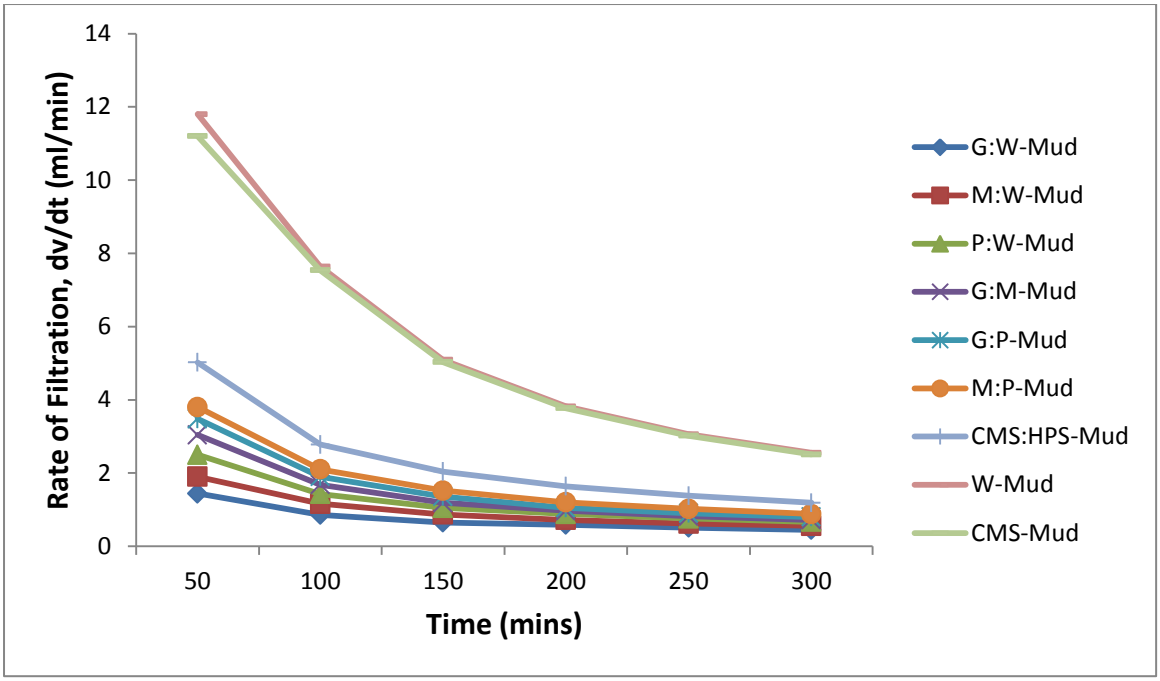

Figure 4.82: Plot of Rate of filtration versus time for all the muds with 0.02g/ml starch concentration at high temperature, 250°C. (Data; Table 4.19-Ttable 4.27)

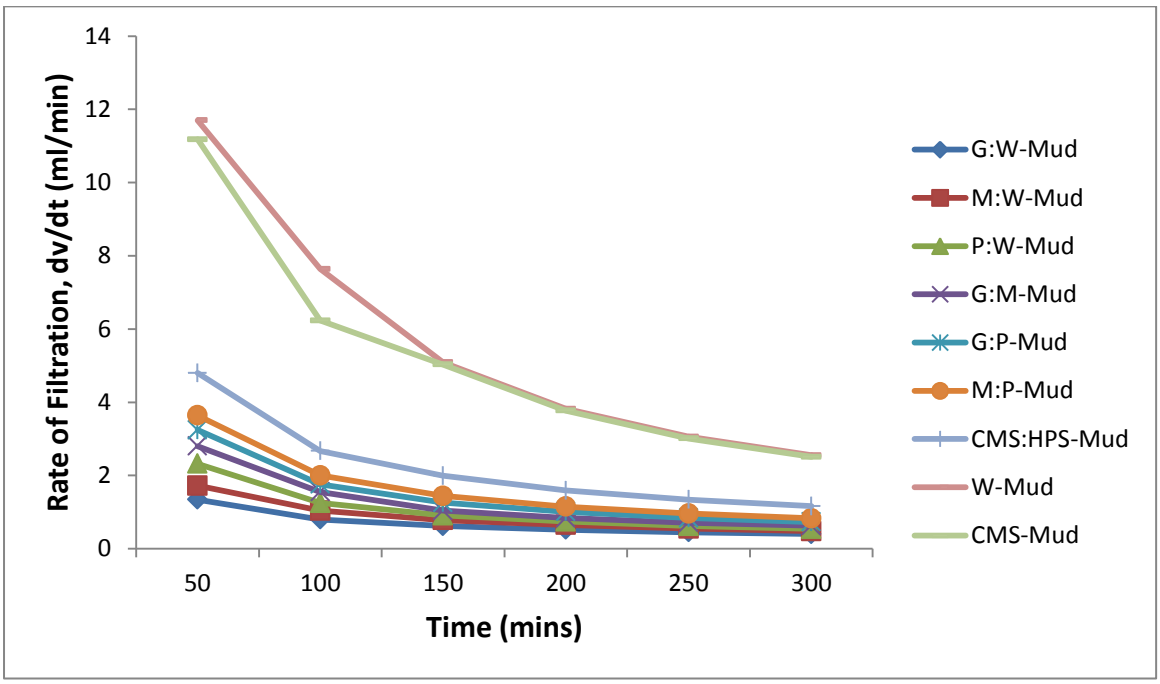

Figure 4.83: Plot of Rate of filtration versus time for all the muds with 0.03g/ml starch concentration at high temperature, 250°C. (Data; Table 4.19-Table 4.27)

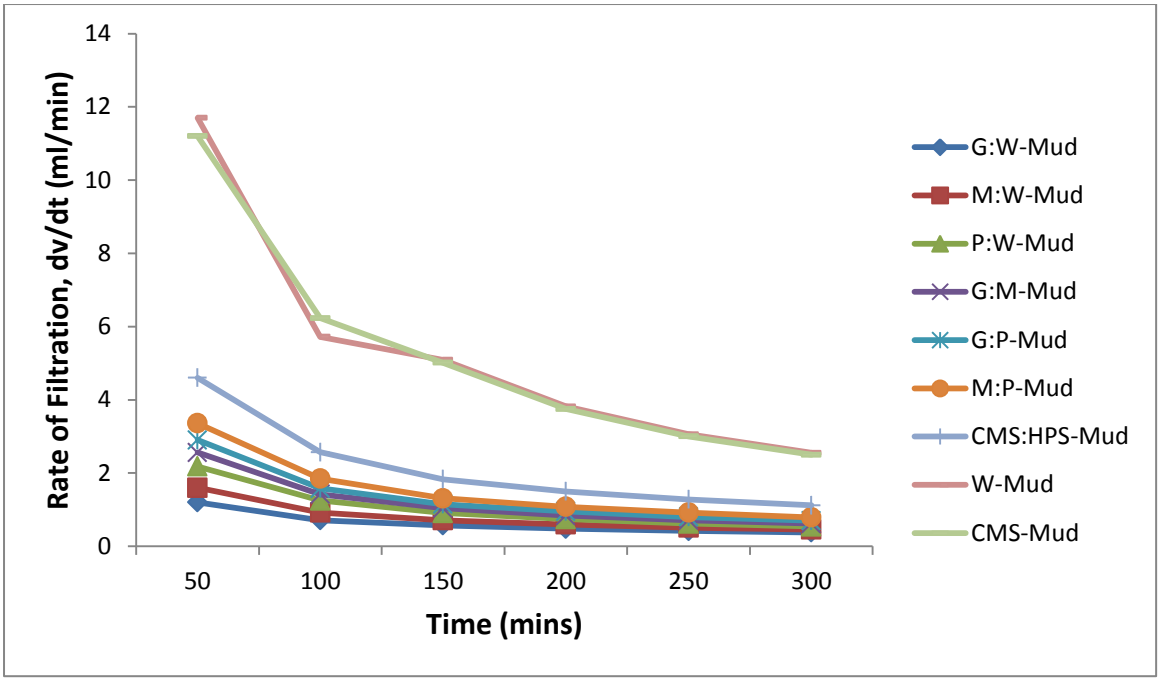

Figure 4.84: Plot of Rate of filtration versus time for all the muds with 0.04g/ml starch concentration at high temperature, 250°C. (Data; Table 4.19-Table 4.27)

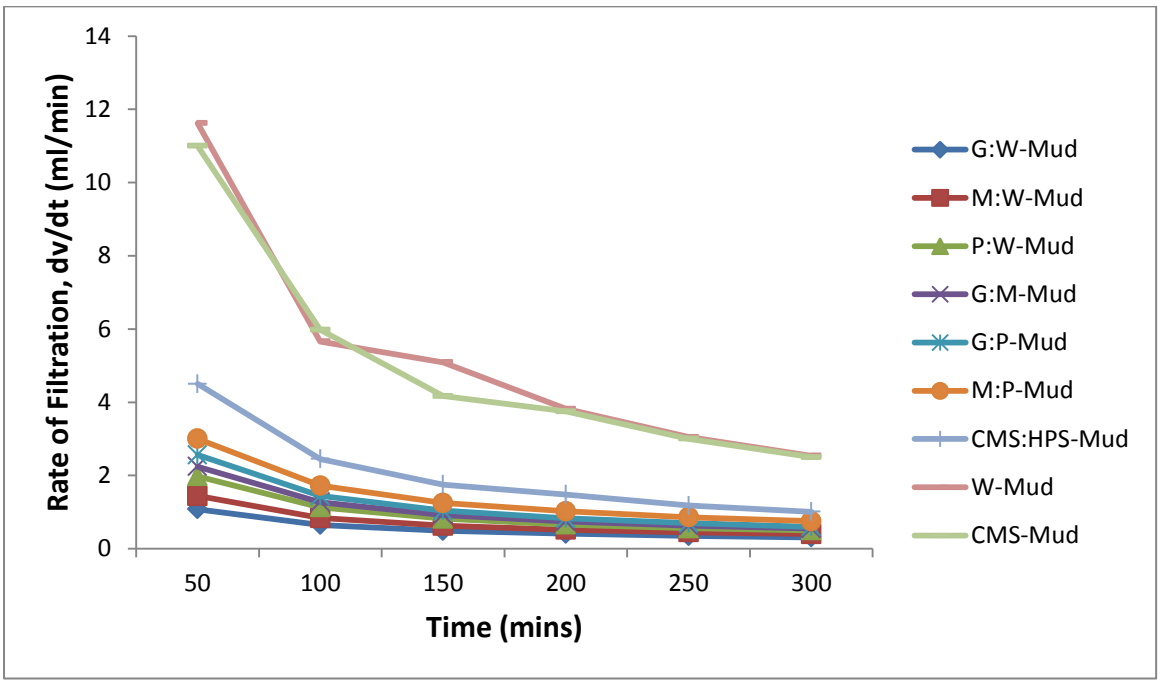

Figure 4.85: Plot of Rate of filtration versus time for all the muds with 0.05g/ml starch concentration at high temperature, 250°C. (Data; Table 4.19-Table 4.27)

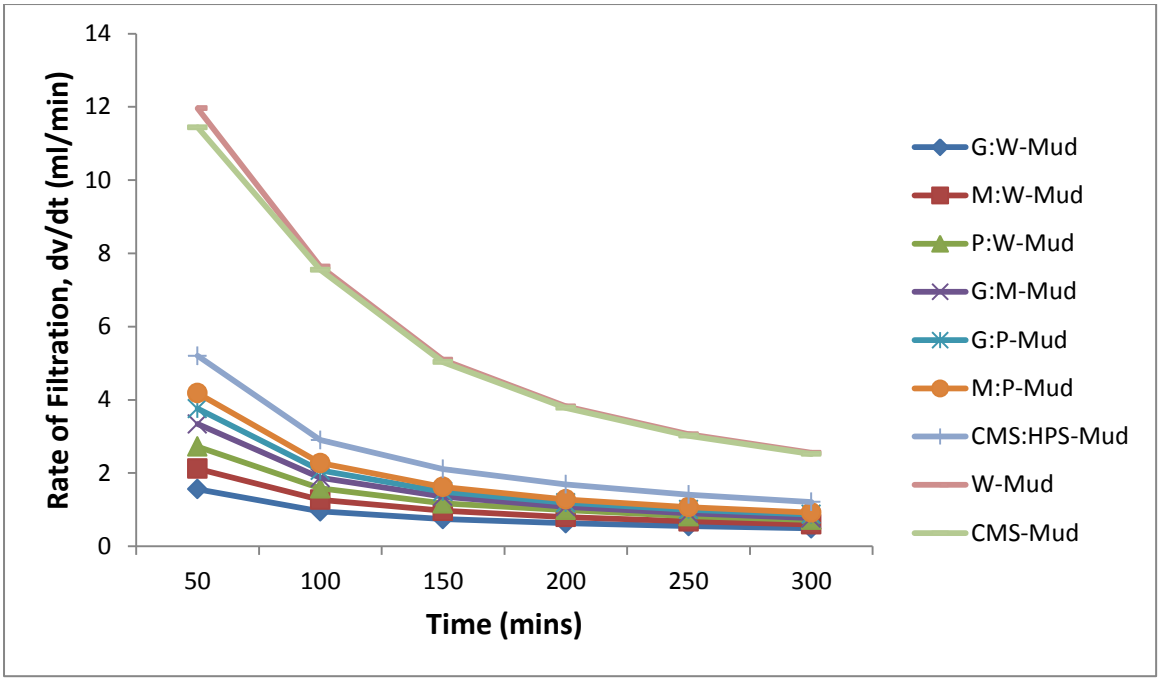

Figure 4.86: Plot of Rate of filtration versus time for all the muds with 0.01g/ml starch concentration at high temperature, 350°C. (Data; Table 4.28-Table 4.36)

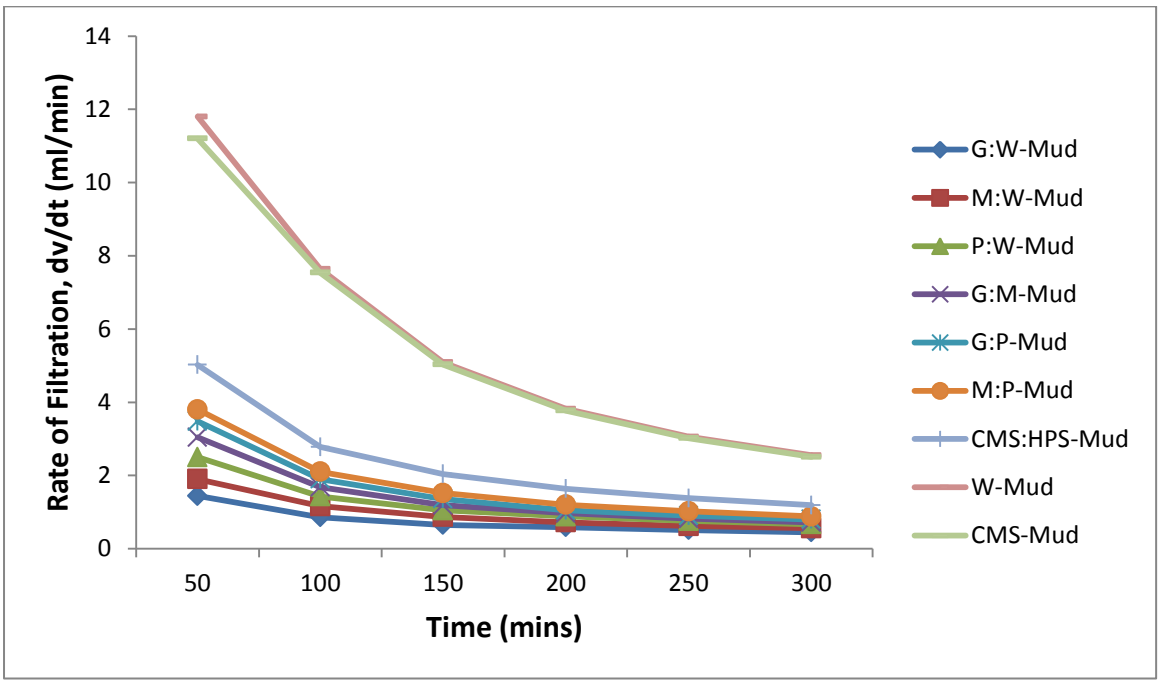

Figure 4.87: Plot of Rate of filtration versus time for all the muds with 0.02g/ml starch concentration at high temperature, 350°C. (Data; Table 4.28-Table 4.36)

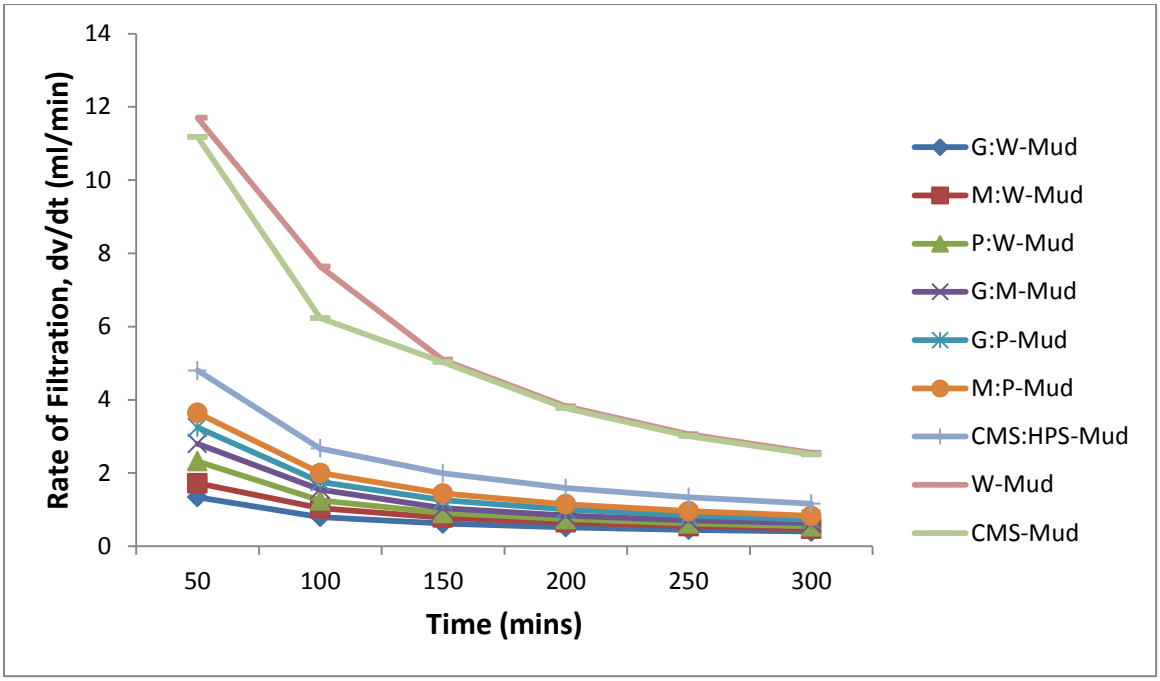

Figure 4.88: Plot of Rate of filtration versus time for all the muds with 0.03g/ml starch concentration at high temperature, 350°C. (Data; Table 4.28-Table 4.36)

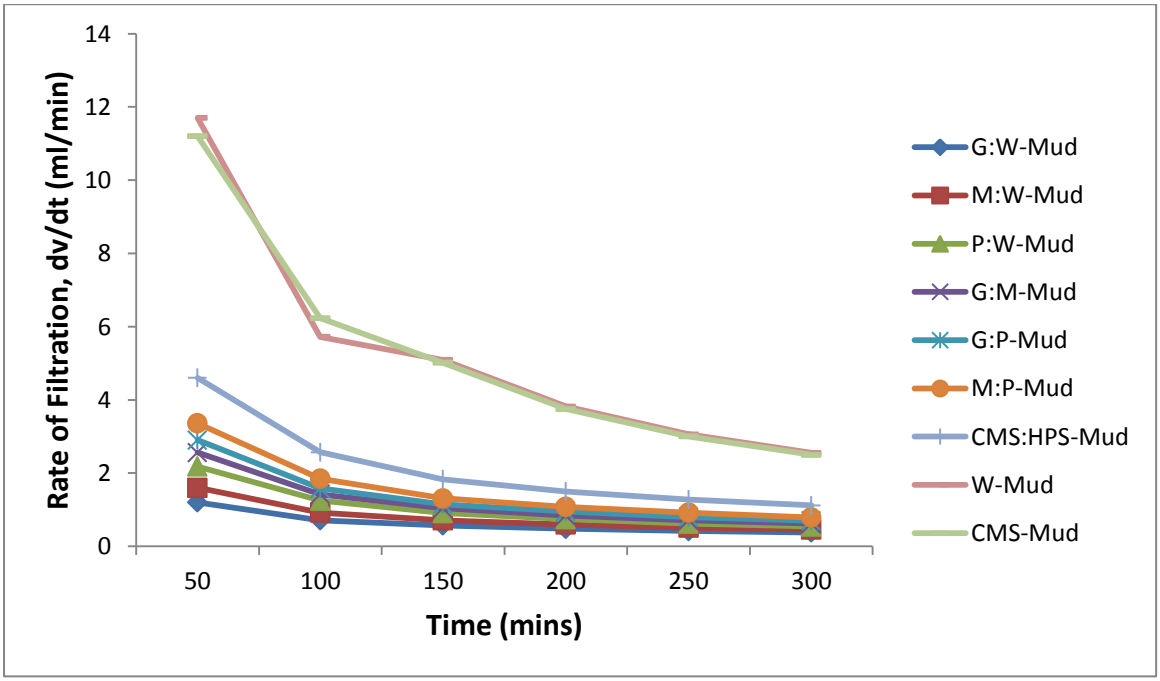

Figure 4.89: Plot of Rate of filtration versus time for all the muds with 0.04g/ml starch concentration at high temperature, 350°C. (Data; Table 4.28-Table 4.36)

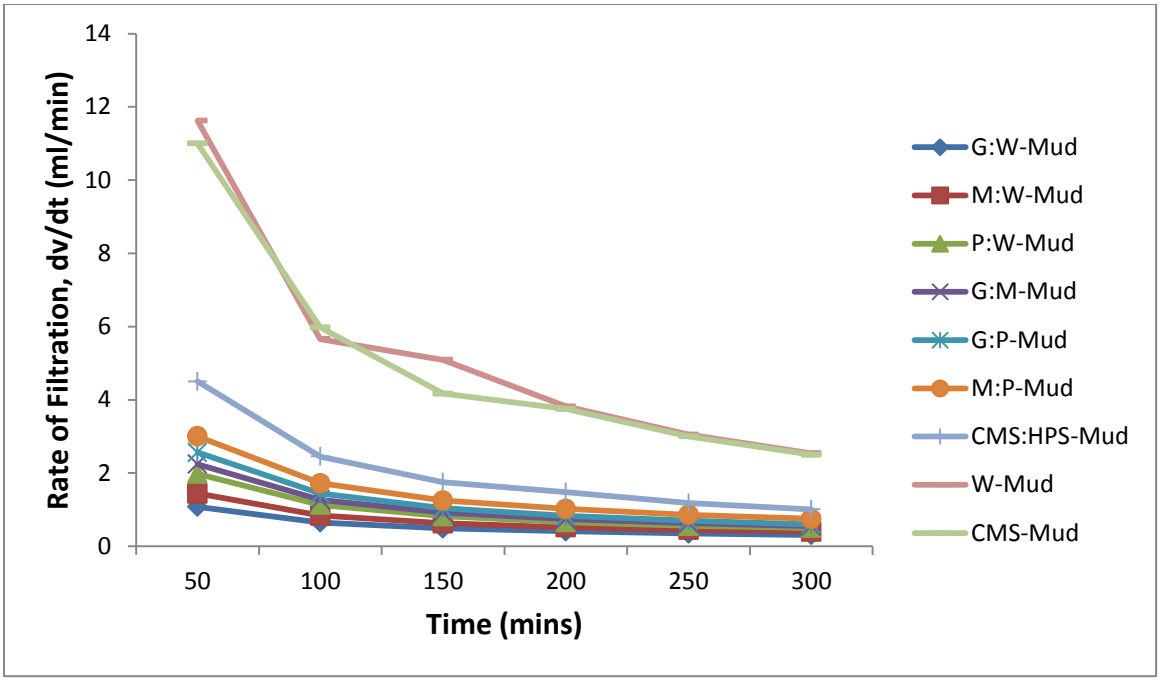

Figure 4.90: Plot of Rate of filtration versus time for all the muds with 0.05g/ml starch concentration at high temperature, 350°C. (Data; Table 4.28-Table 4.36)

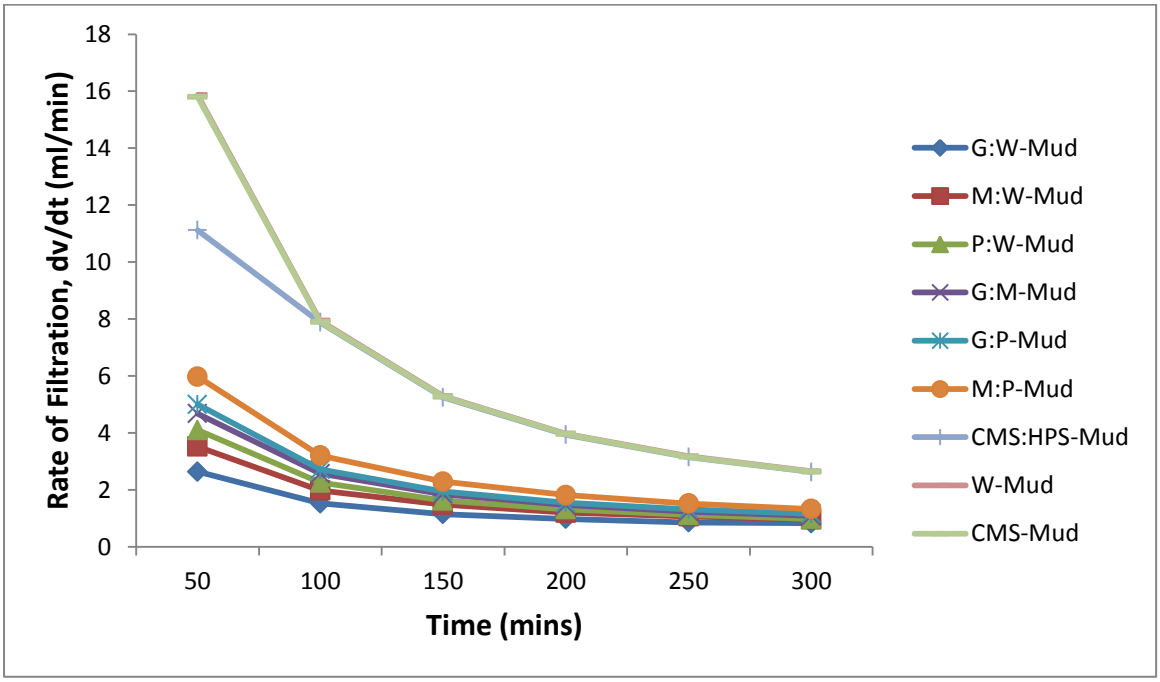

Figure 4.91: Plot of Rate of filtration versus time for all the muds with 0.01g/ml starch concentration at high temperature, 450°C. (Data; Table 4.37-Table 4.45)

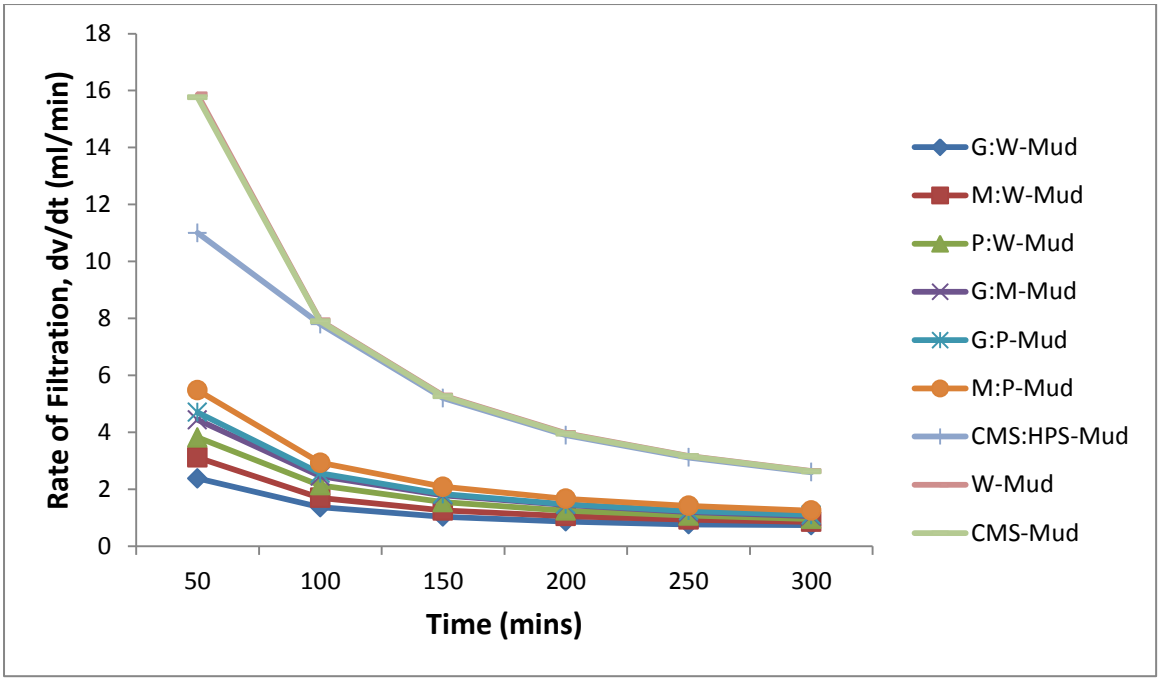

Figure 4.92: Plot of Rate of filtration versus time for all the muds with 0.02g/ml starch concentration at high temperature, 450°C. (Data; Table 4.37-Table 4.45)

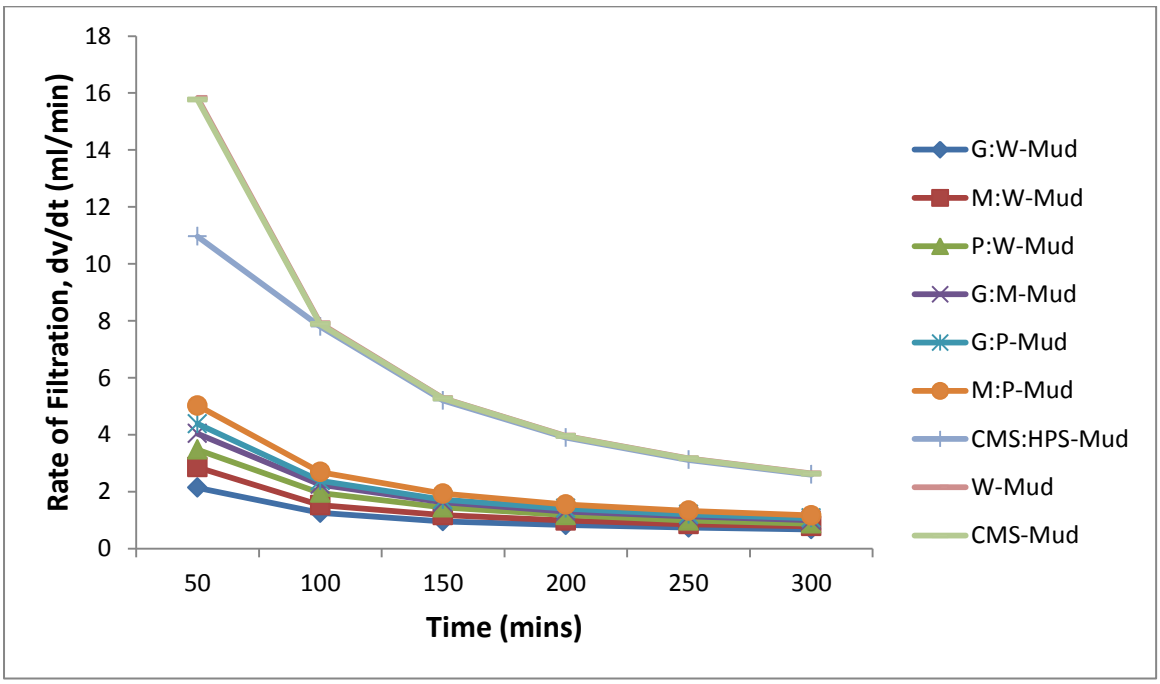

Figure 4.93: Plot of Rate of filtration versus time for all the muds with 0.03g/ml starch concentration at high temperature, 450°C. (Data; Table 4.37-Table 4.45)

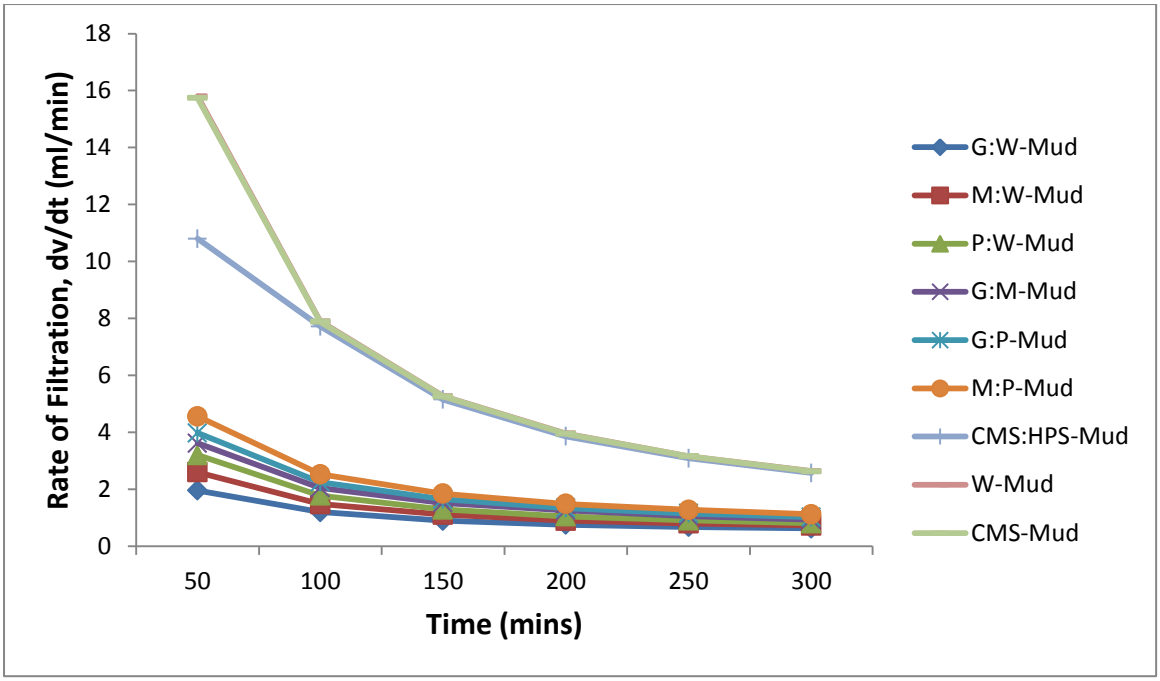

Figure 4.94: Plot of Rate of filtration versus time for all the muds with 0.04g/ml starch concentration at high temperature, 450°C. (Data; Table 4.37-Table 4.45)

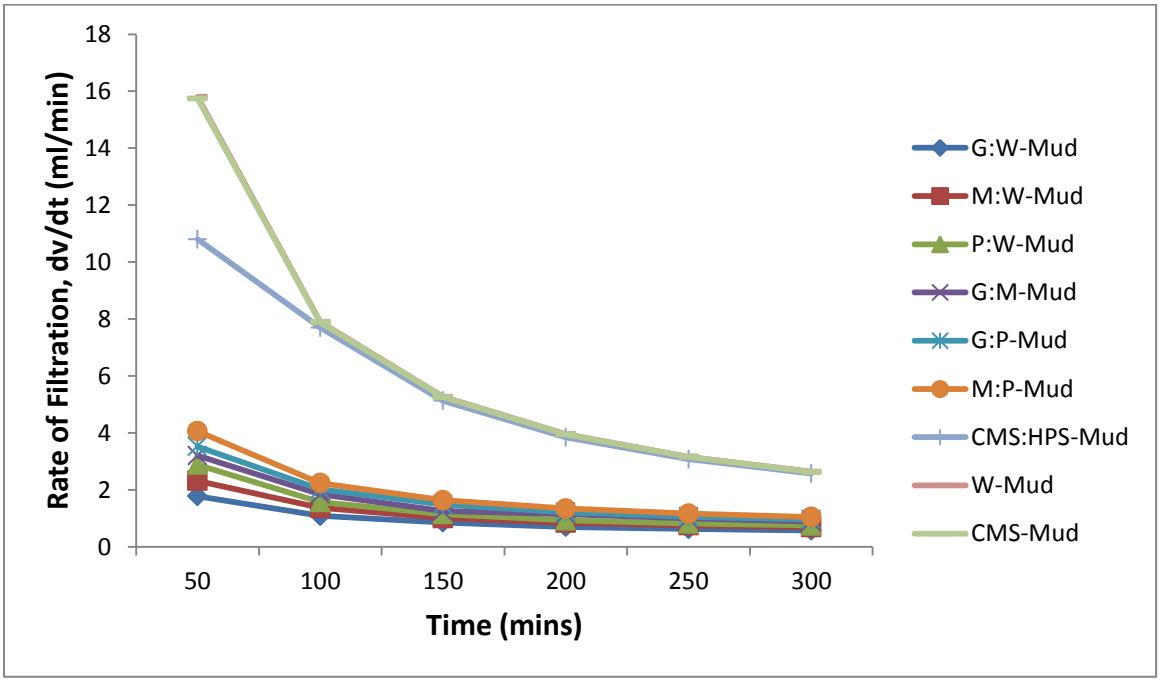

Figure 4.95: Plot of Rate of filtration versus time for all the muds with 0.05g/ml starch concentration at high temperature, 450°C. (Data; Table 4.37-Table 4.45)

Figures 4.71to 4.95 show the plots of Rate of Filtration versus Time for the muds at the different temperatures of 25^{o}C, 150^{o}C, 250^{o}C, 350^{o}C and 450^{o}C. Analysis of the figures shows that filtration rate decreases exponentially with increase in time. The figures also show that filtration rate increase with increase in temperature. Further analysis of the figures shows that the rate of filtration was maximum at the beginning of filtration for all the muds. At the beginning of filtration, the resistance to fluid flow is little but with increase in time, the filter cake builds up and begins to affect flow. Progressive building up of cake gradually slows down fluid flow which results in decrease in filtration rate. The filtration rate shows an exponential decrease for all the muds, as seen in Equation (3.2), ($\Phi R = \Phi_o \exp^{-Dt}$) (Hall & Hoff, 2012; Bernu, 2011; Anthony & Robert, 2010; Ukachukwu et al, 2010; American Petroleum Institute, 2003; Andy et al., 2001). This shows that all the muds obeyed the filtration rate equation.

In addition, the rate of filtration increases with increase in temperature. This is as a result of increase in the flow of fluid through the filter cake, which give rise to higher fluid loss. Higher temperature increases the flow of fluid with increase in the fluid volume due to reduction in the intermolecular friction (Chris & James, 2005). This increase in filtration rates with increase in Temperature denotes that the built-up filter cakes of the muds have been adversely affected and the effectiveness reduced by high temperature. Therefore, the flow of fluid increased and gave rise to higher filtration rate. The highest rate of filtration was obtained with CMS-Mud at all the temperatures.

4.2.1.10 Effects of Varying Starch Concentrations on the Filtration Rate of the Muds at different Temperatures

The effects of starch of varying concentration of starches on the rate of filtration of the muds at different temperatures are shown in these figures below. Figures 4.96 to 4.140 shows the plots of Filtration rate versus Time for each mud with varying starch concentrations range of 0.01-0.05g/ml at different temperatures of 25^{o}C, 150^{o}C, 250^{o}C, 350^{o}C and 450^{o}C. It is observed from the figures that filtration rate still decreases exponentially with increase in time at all the temperatures. This shows that the muds obeyed the exponential equation 3.2.

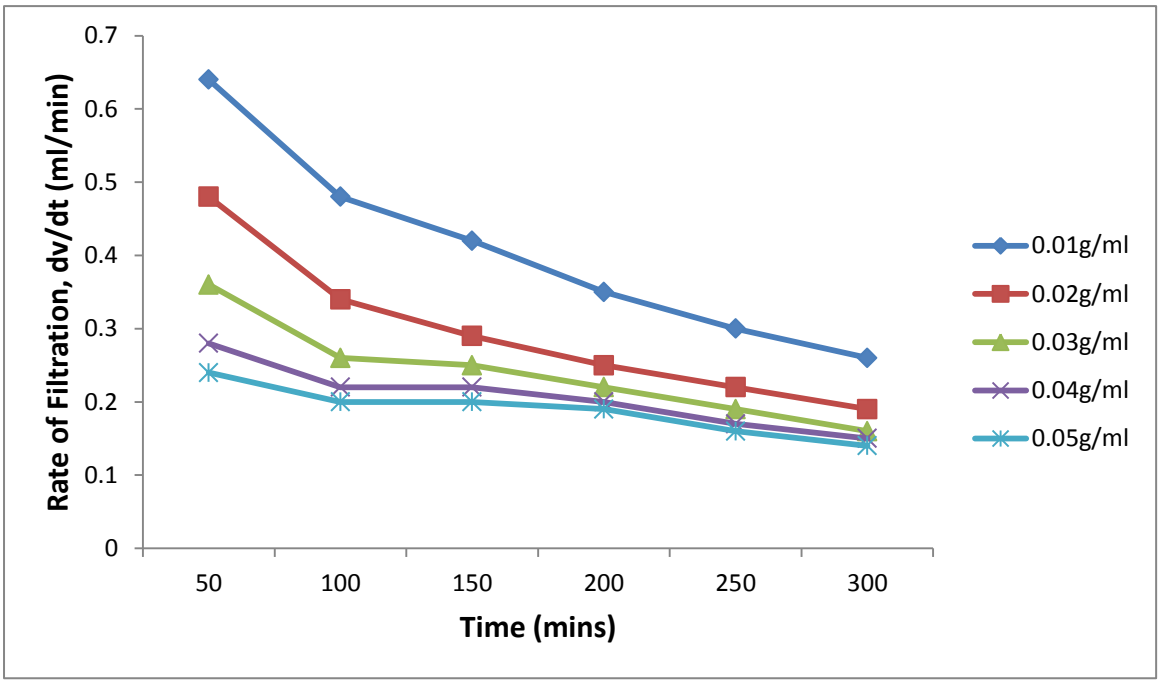

Figure 4.96: Plot of Rate of filtration versus time for G:W-Mud with varying starch concentration at room temperature, 25^{o}C. (Data; Table 4.1)

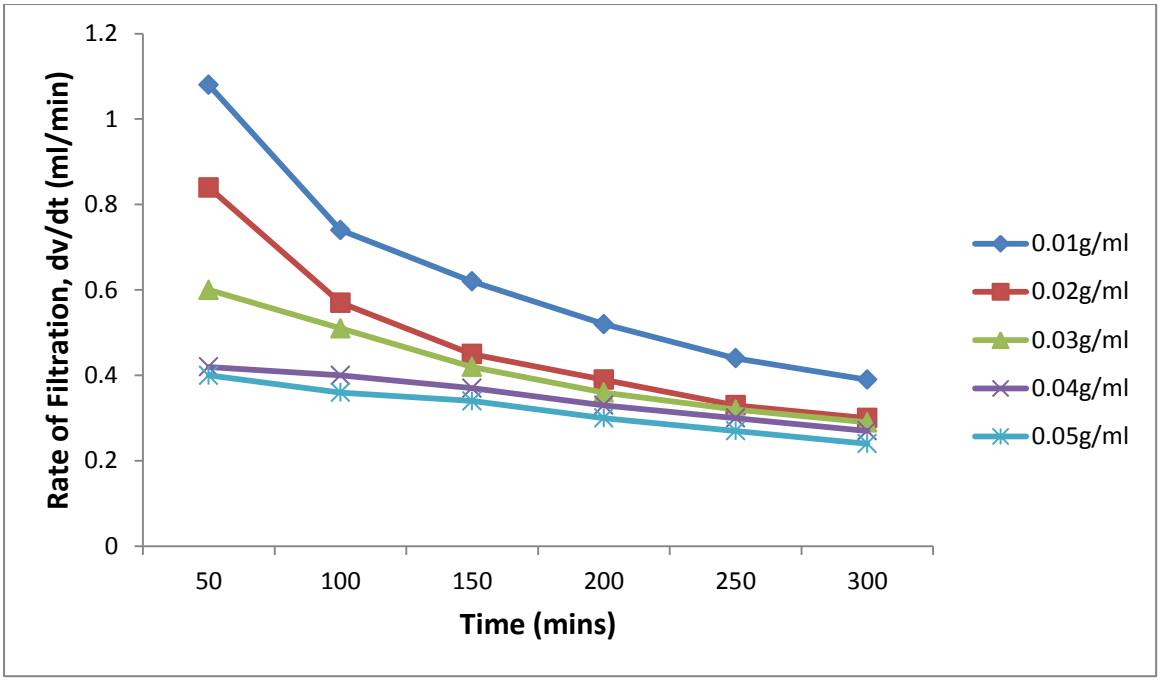

Figure 4.97: Plot of Rate of filtration versus time for M:W-Mud with varying starch concentration at room temperature, 25°C. (Data; Table 4.2)

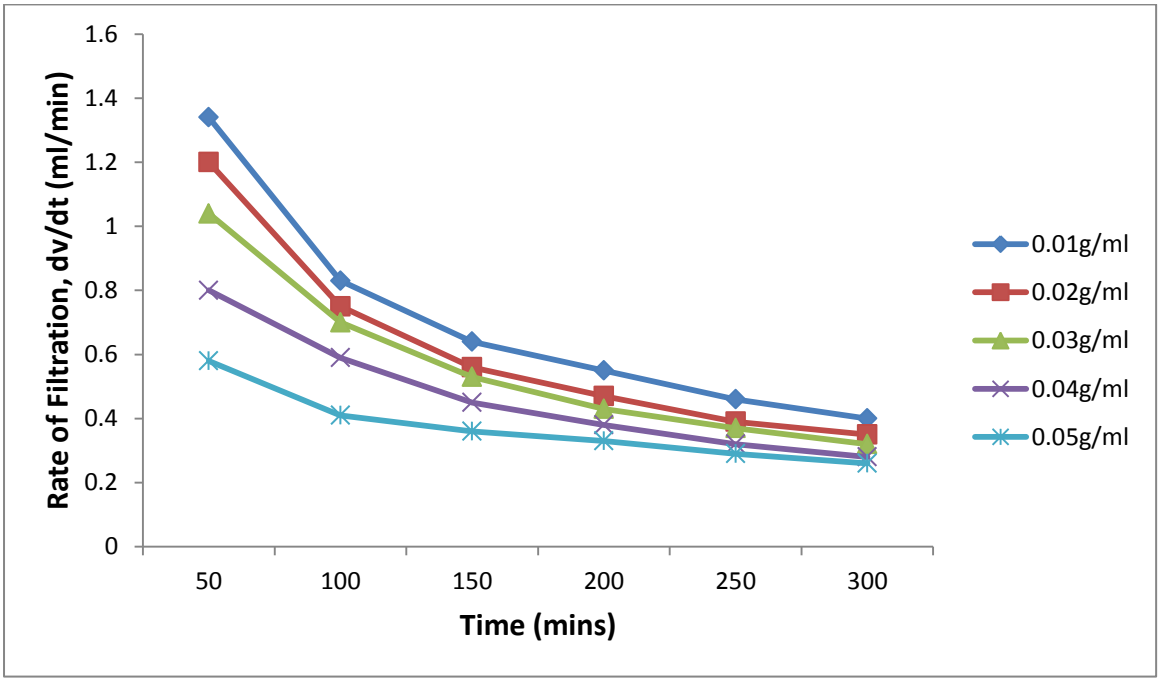

Figure 4.98: Plot of Rate of filtration versus time for P:W-Mud with varying starch concentration at room temperature, 25°C. (Data; Table 4.3)

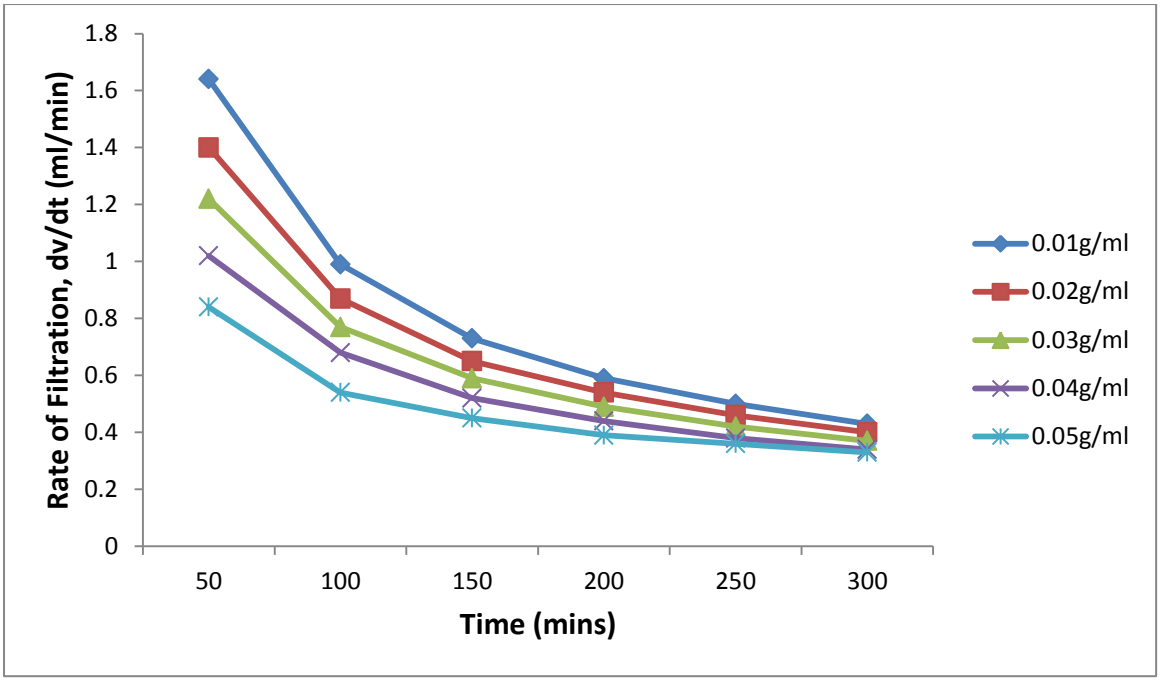

Figure 4.99: Plot of Rate of filtration versus time for G:M-Mud with varying starch concentration at room temperature, 25°C. (Data; Table 4.4)

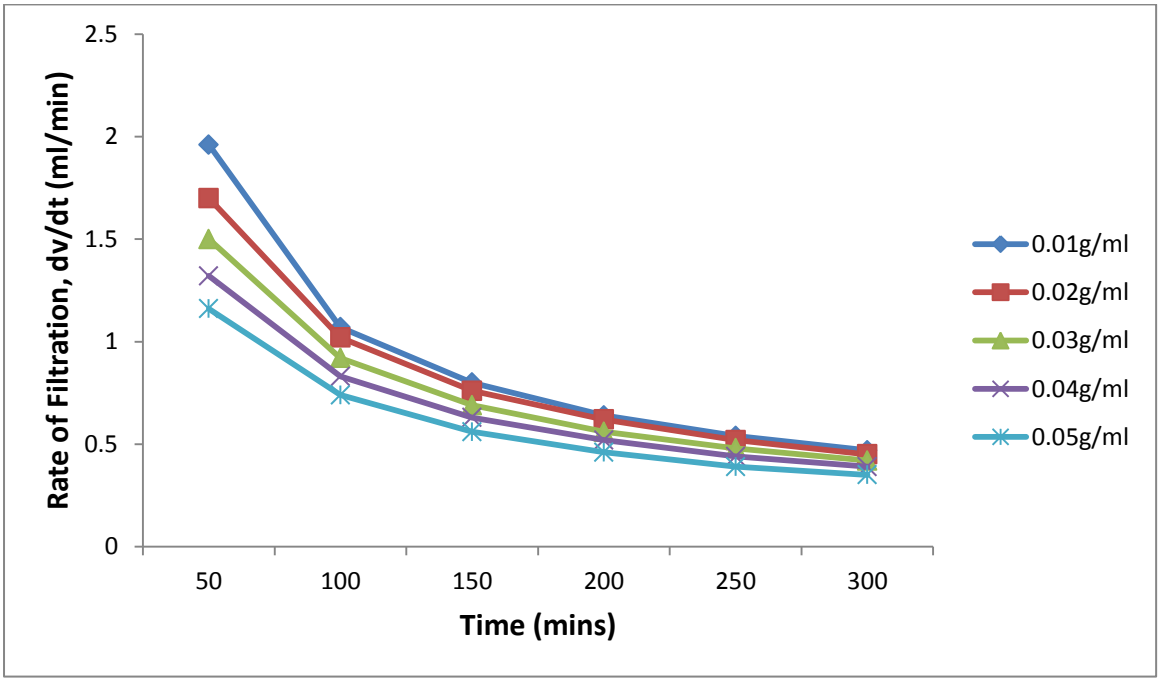

Figure 4.100: Plot of Rate of filtration versus time for G:P-Mud with varying starch concentration at room temperature, 25°C. (Data; Table 4.5)

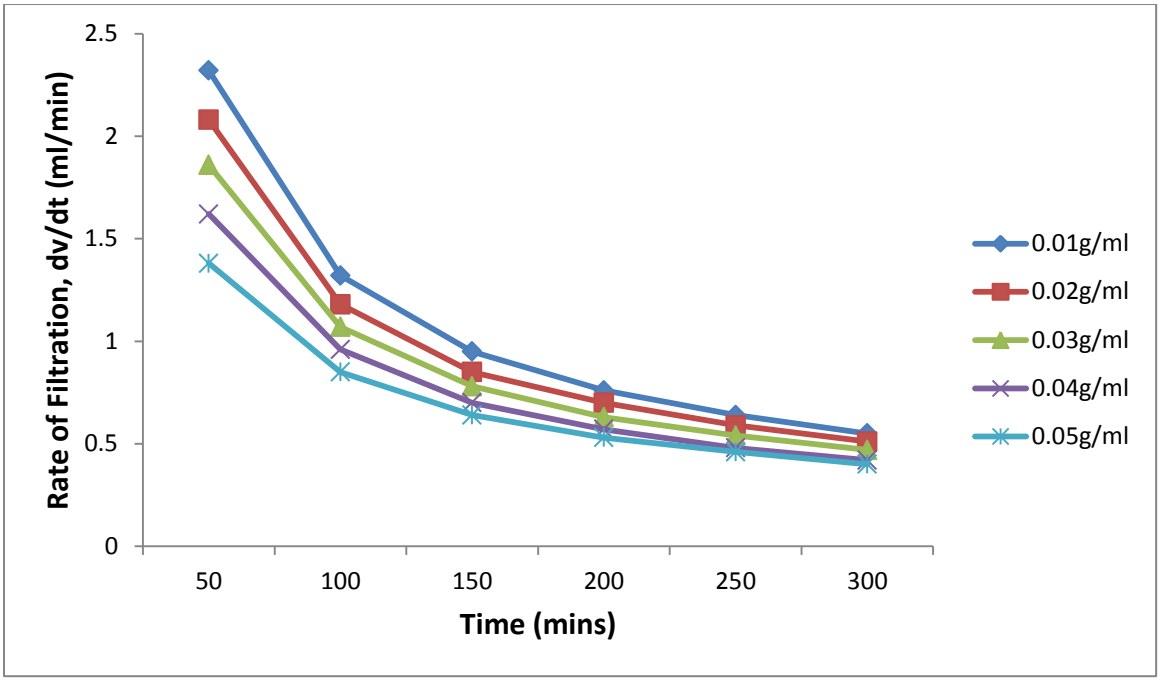

Figure 4.101: Plot of Rate of filtration versus time for M:P-Mud with varying starch concentration at room temperature, 25°C. (Data; Table 4.6)

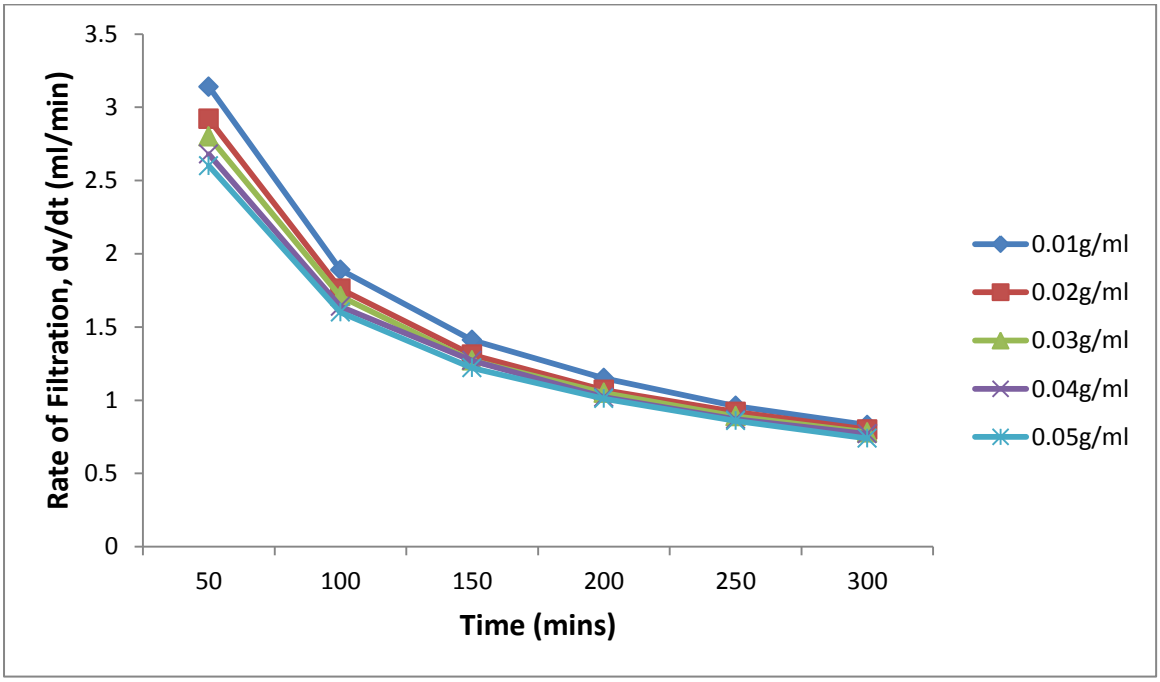

Figure 4.102: Plot of Rate of filtration versus time for CMS:HPS-Mud with varying starch concentration at room temperature, 25°C. (Data; Table 4.7)

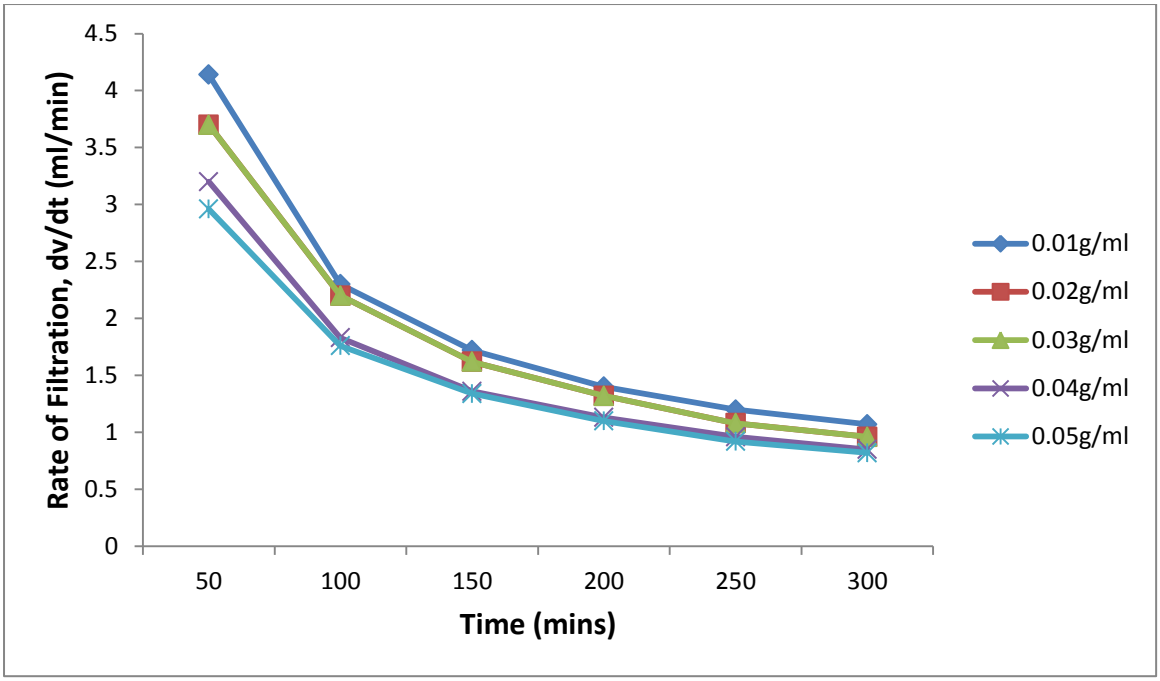

Figure 4.103: Plot of Rate of filtration versus time for W-Mud with varying starch concentration at room temperature, 25°C. (Data; Table 4.8)

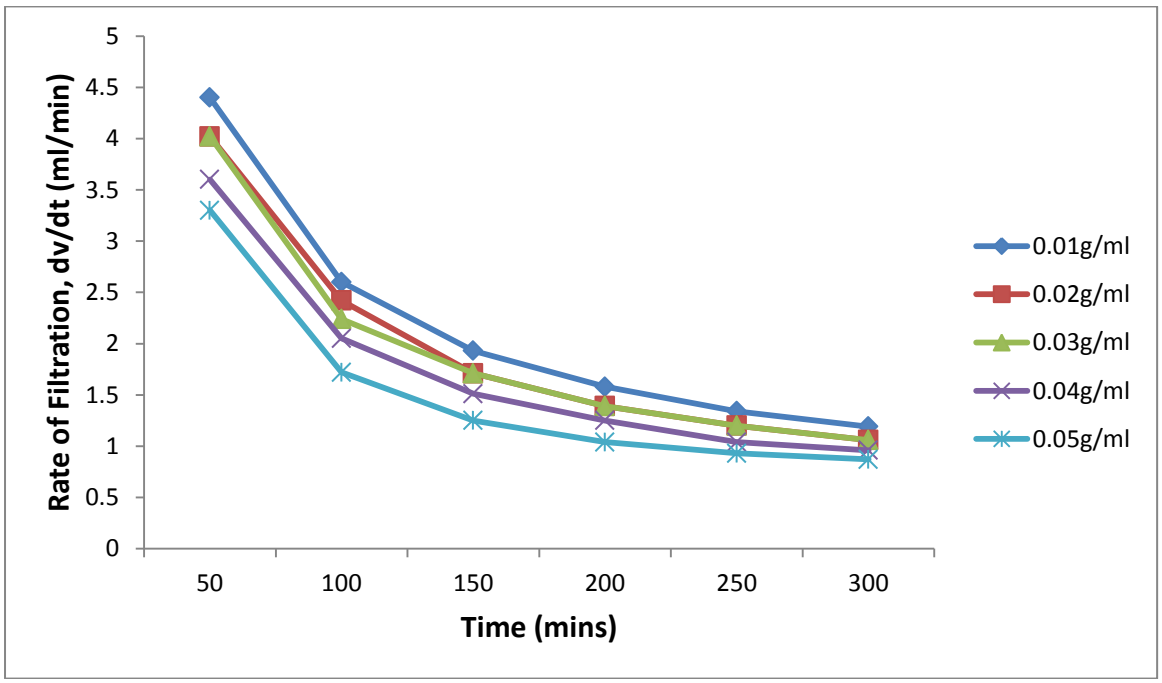

Figure 4.104: Plot of Rate of filtration versus time for CMS-Mud with varying starch concentration at room temperature, 25°C. (Data; Table 4.9)

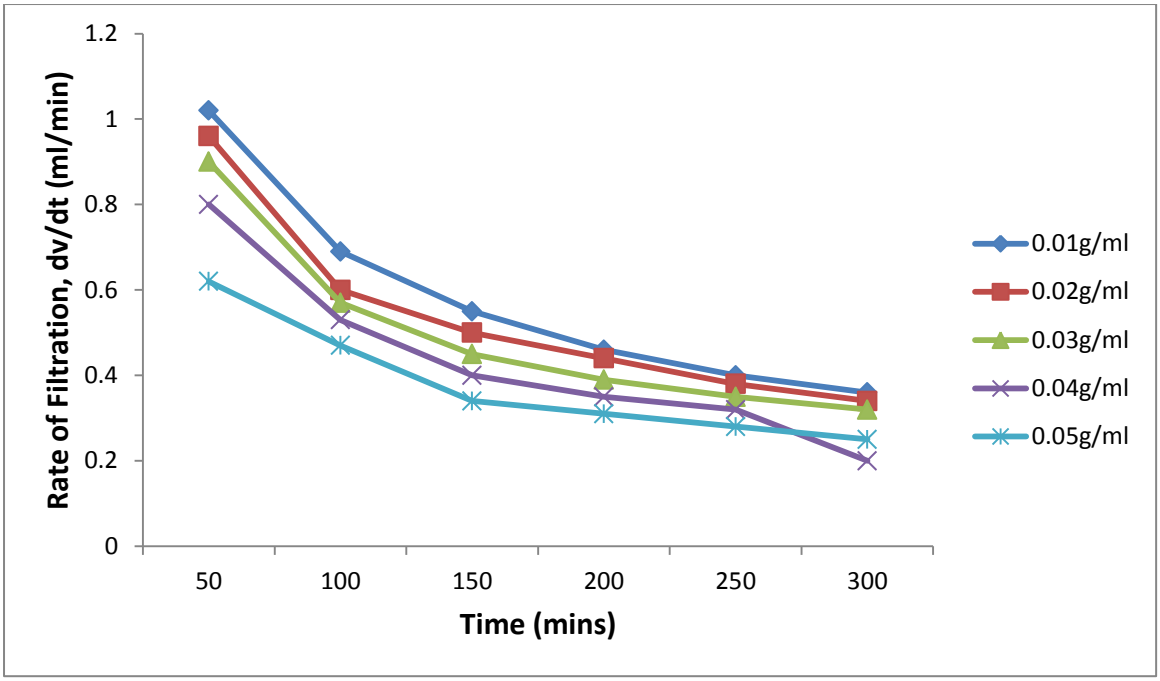

Figure 4.105: Plot of Rate of filtration versus time for G:W-Mud with varying starch concentration at high temperature, 150°C. (Data; Table 4.10)

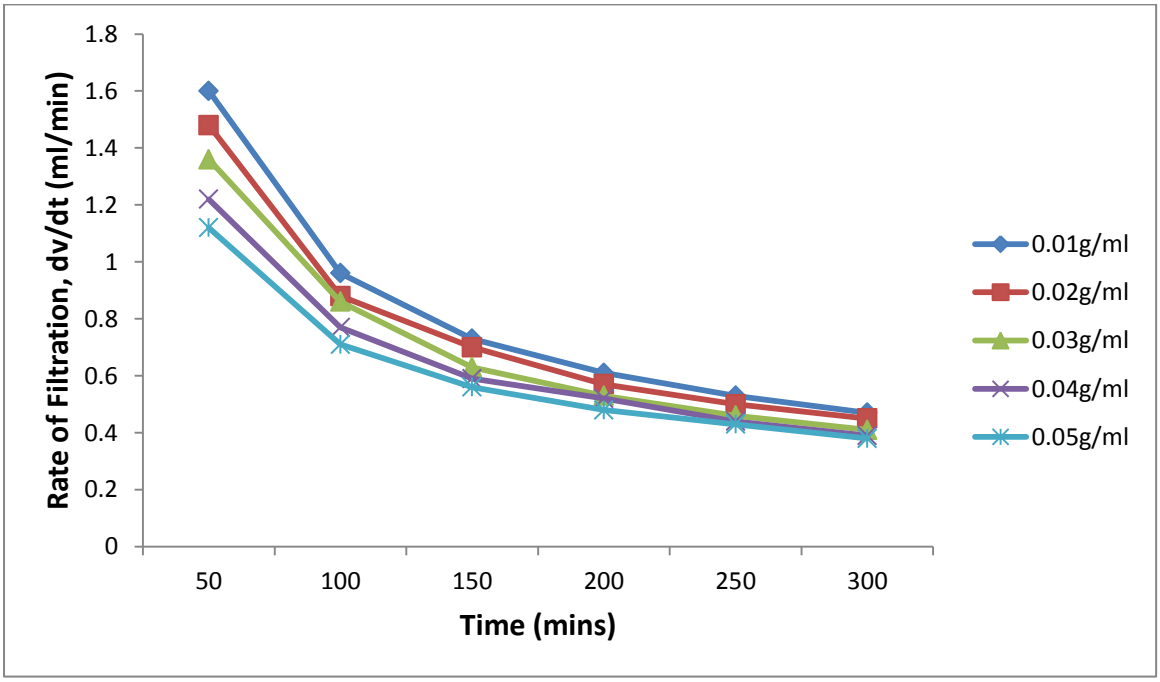

Figure 4.106: Plot of Rate of filtration versus time for M:W-Mud with varying starch concentration at high temperature, 150°C. (Data; Table 4.11)

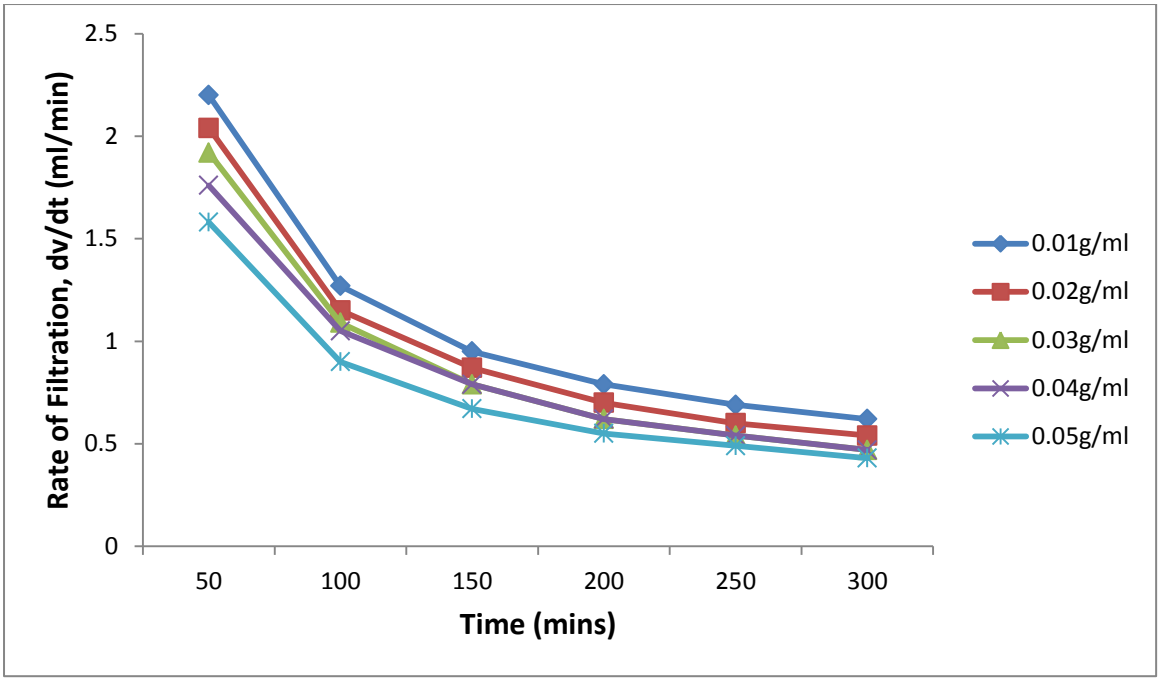

Figure 4.107: Plot of Rate of filtration versus time for P:W-Mud with varying starch concentration at high temperature, 150°C. (Data; Table 4.12)

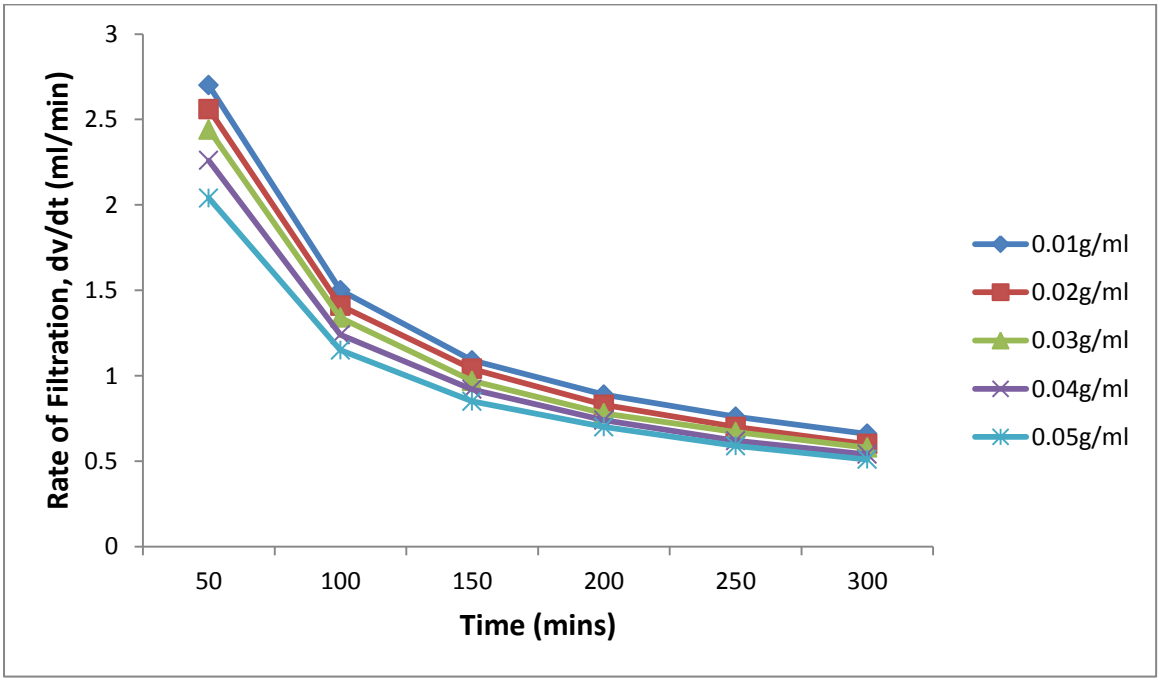

Figure 4.108: Plot of Rate of filtration versus time for G:M-Mud with varying starch concentration at high temperature, 150°C. (Data; Table 4.13)

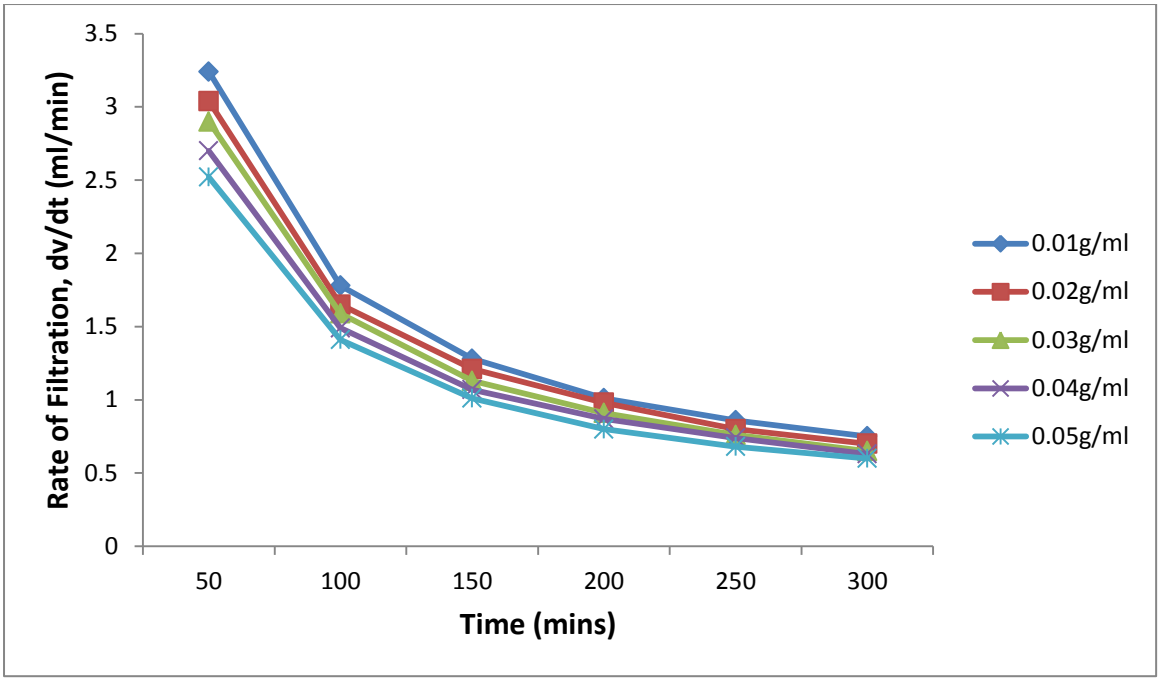

Figure 4.109: Plot of Rate of filtration versus time for G:P-Mud with varying starch concentration at high temperature, 150°C. (Data; Table 4.14)

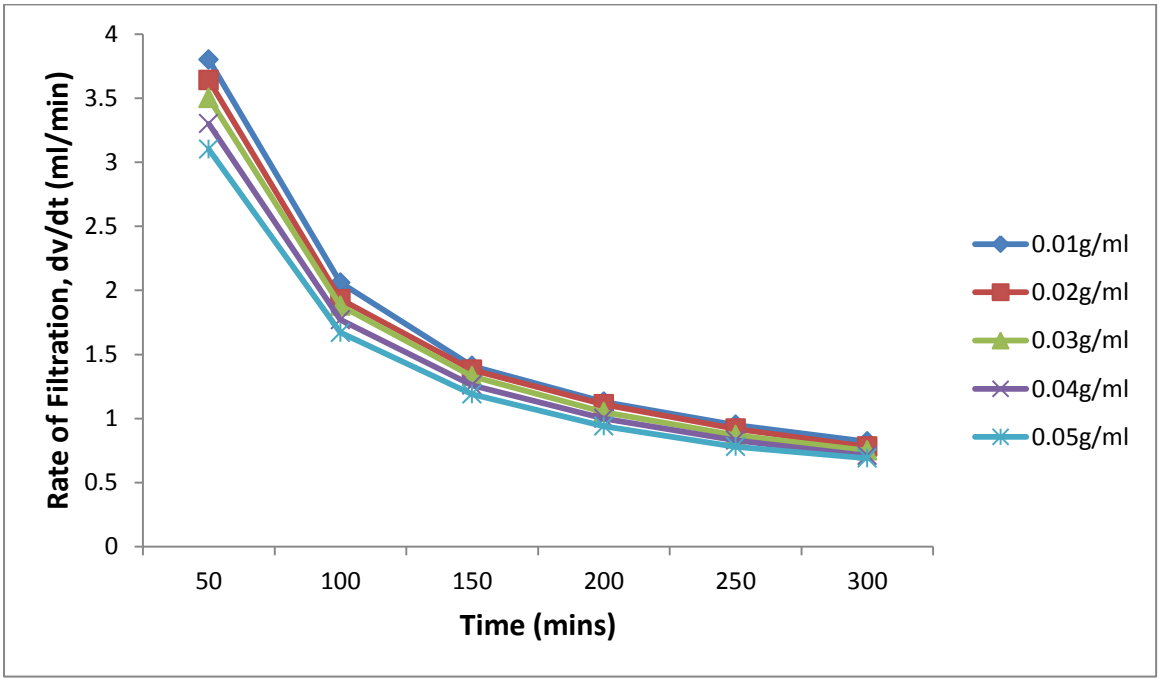

Figure 4.110: Plot of Rate of filtration versus time for M:P-Mud with varying starch concentration at high temperature, 150°C. (Data; Table 4.15)

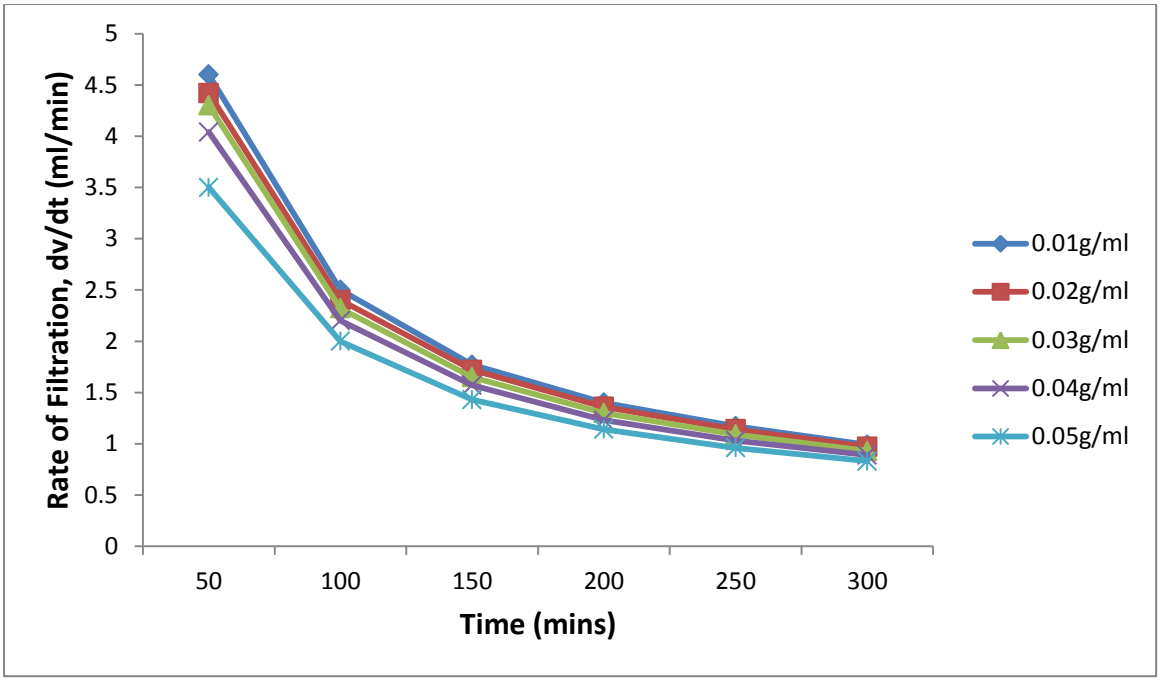

Figure 4.111: Plot of Rate of filtration versus time for CMS:HPS-Mud with varying starch concentration at high temperature, 150°C. (Data;Table 4.16)

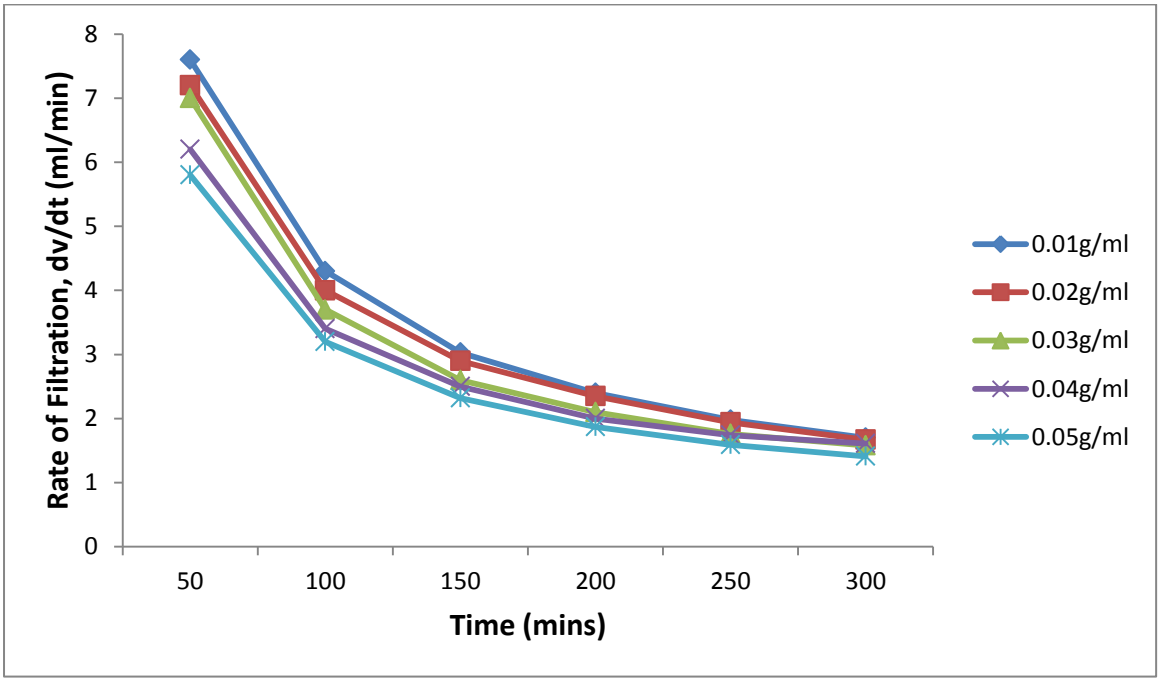

Figure 4.112: Plot of Rate of filtration versus time for W-Mud with varying starch concentration at high temperature, 150°C. (Data; Table 4.17)

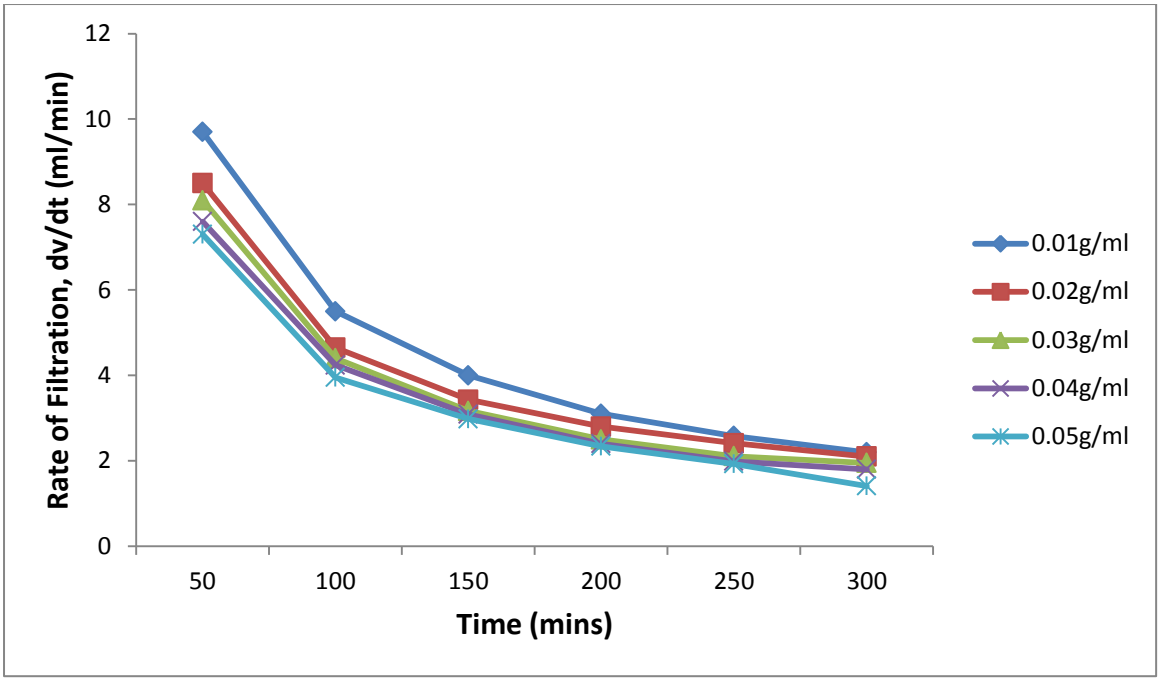

Figure 4.113: Plot of Rate of filtration versus time for CMS-Mud with varying starch concentration at high temperature, 150°C. (Data; Table 4.18)

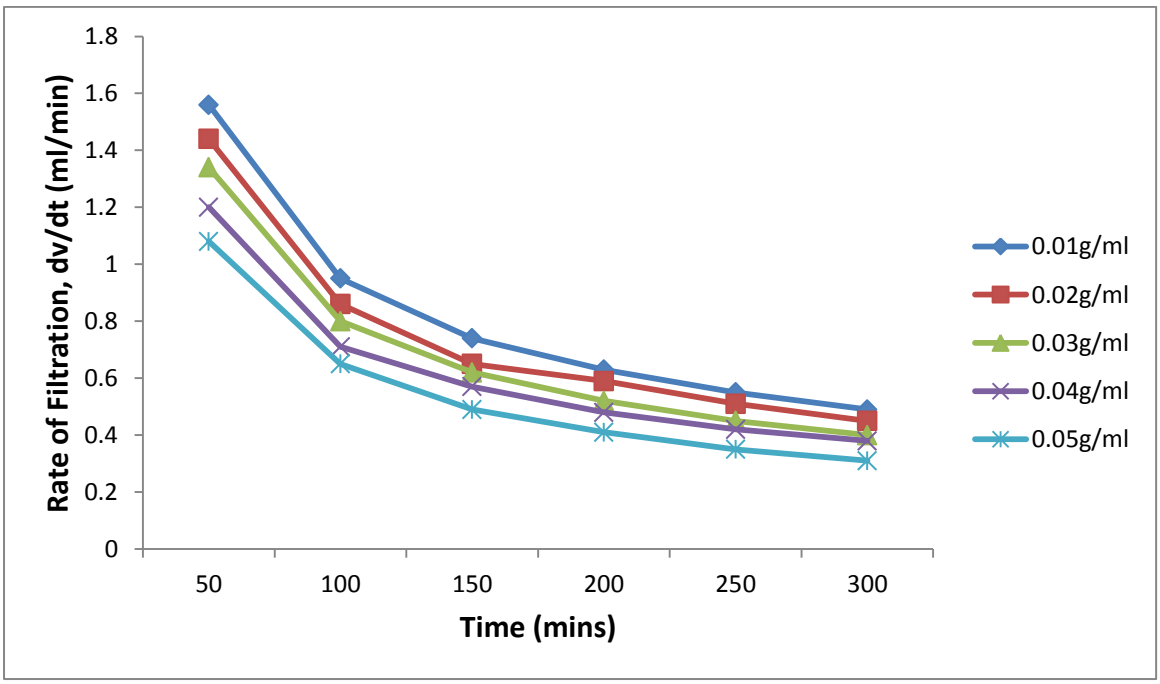

Figure 4.114: Plot of Rate of filtration versus time for G:W-ud with varying starch concentration at high temperature, 250°C. (Data; Table 4.19)

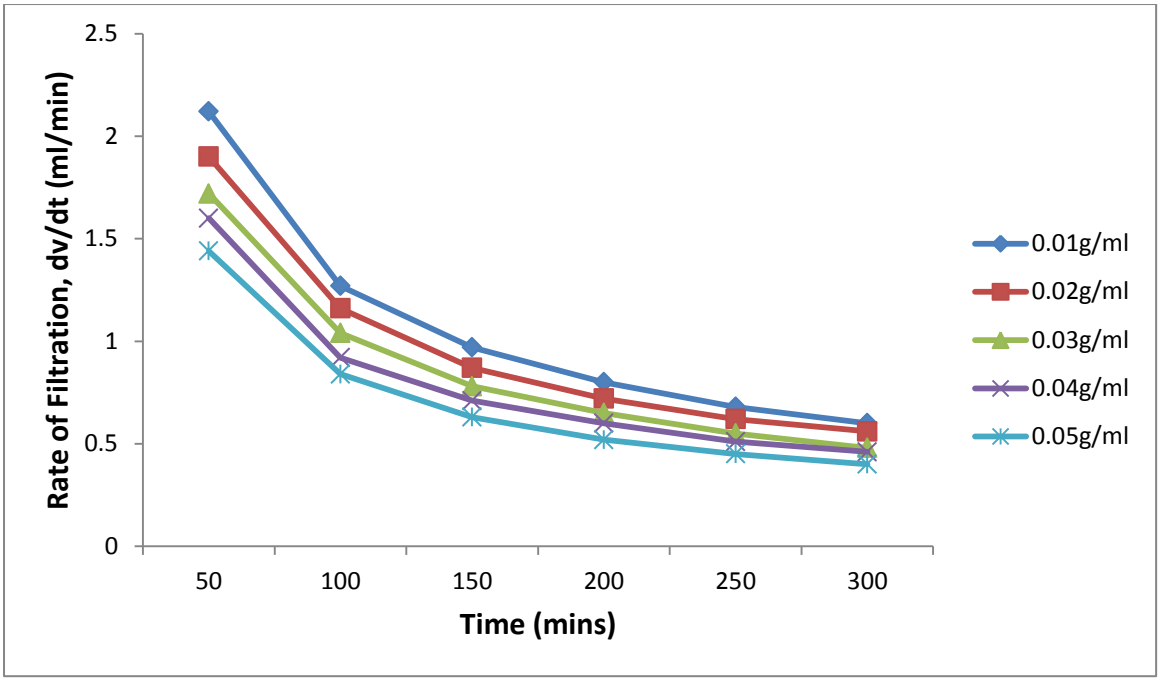

Figure 4.115: Plot of Rate of filtration versus time for M:W-Mud with varying starch concentration at high temperature, 250°C. (Data; Table 4.20)

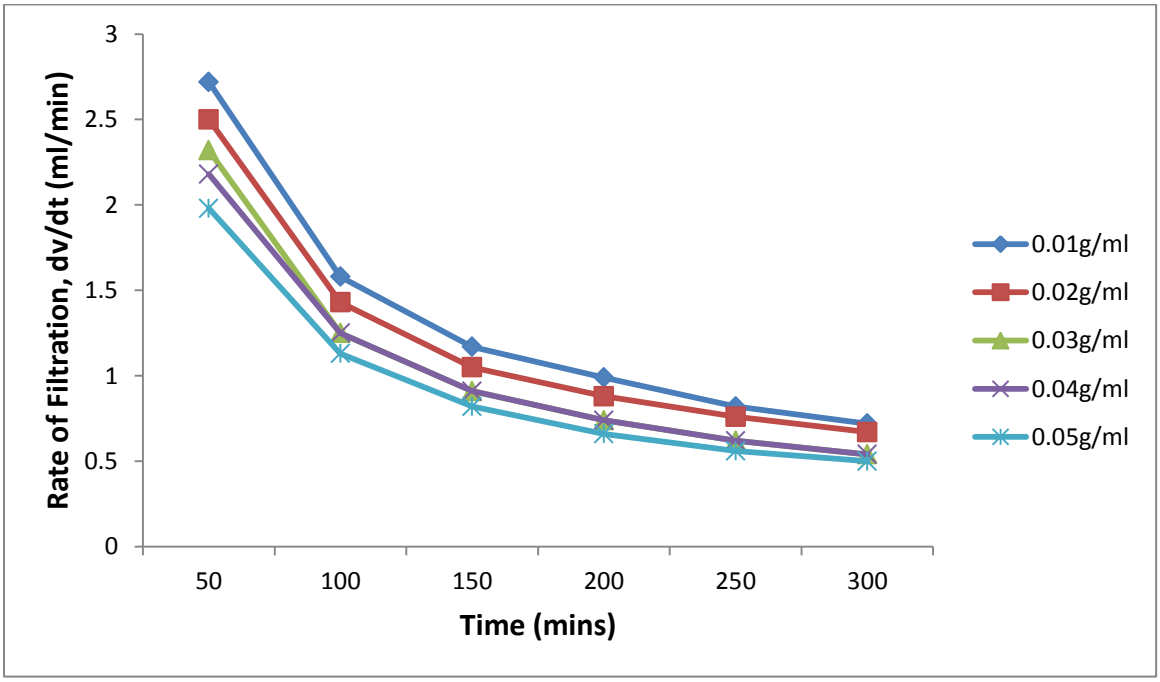

Figure 4.116: Plot of Rate of filtration versus time for P:W-Mud with varying starch concentration at high temperature, 250°C. (Data; Table 4.21)

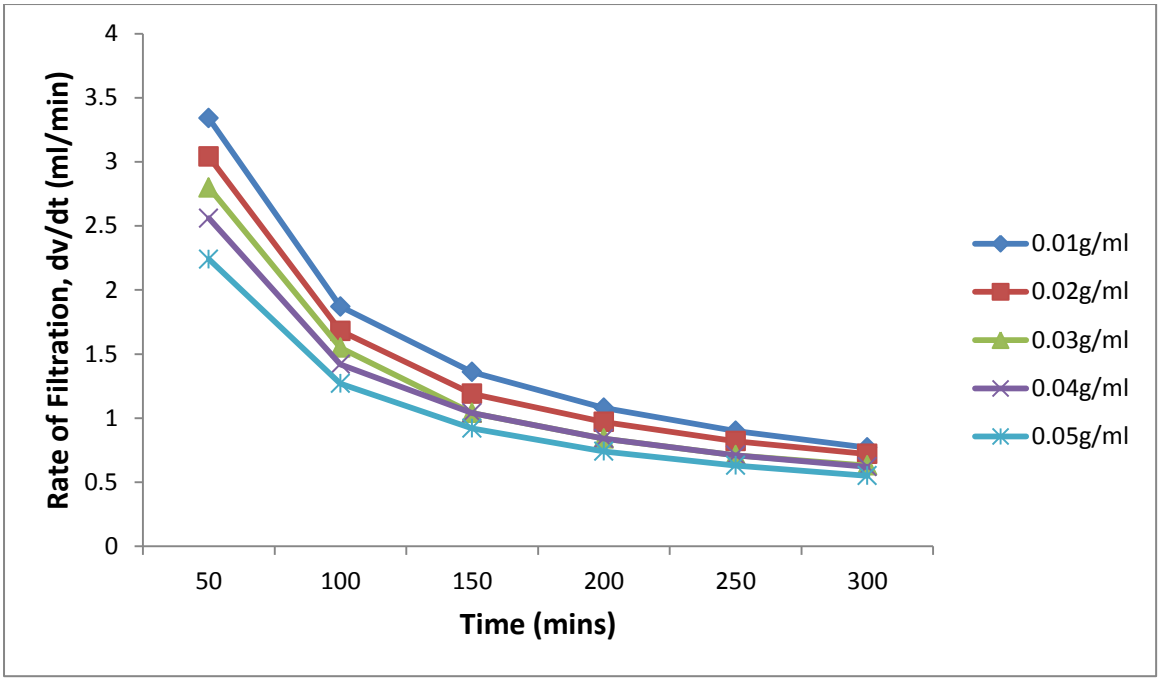

Figure 4.117: Plot of Rate of filtration versus time for G:M-Mud with varying starch concentration at high temperature, 250°C. (Data;Table 4.22)

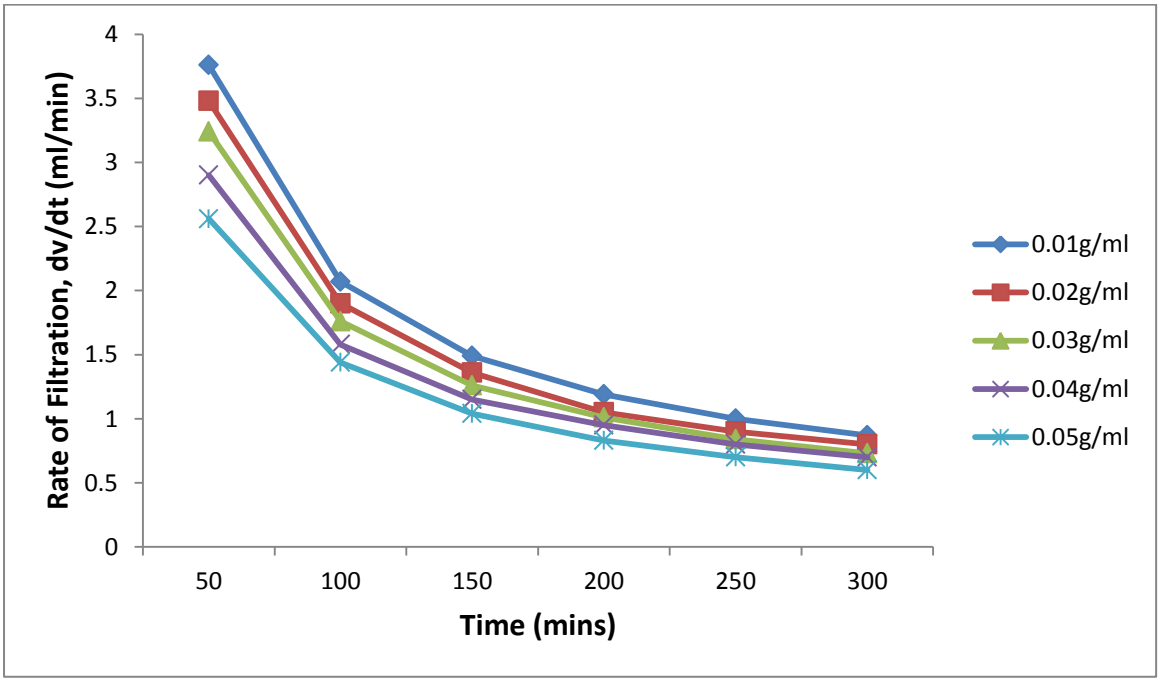

Figure 4.118: Plot of Rate of filtration versus time for G:P-Mud with varying starch concentration at high temperature, 250°C. (Data; Table 4.23)

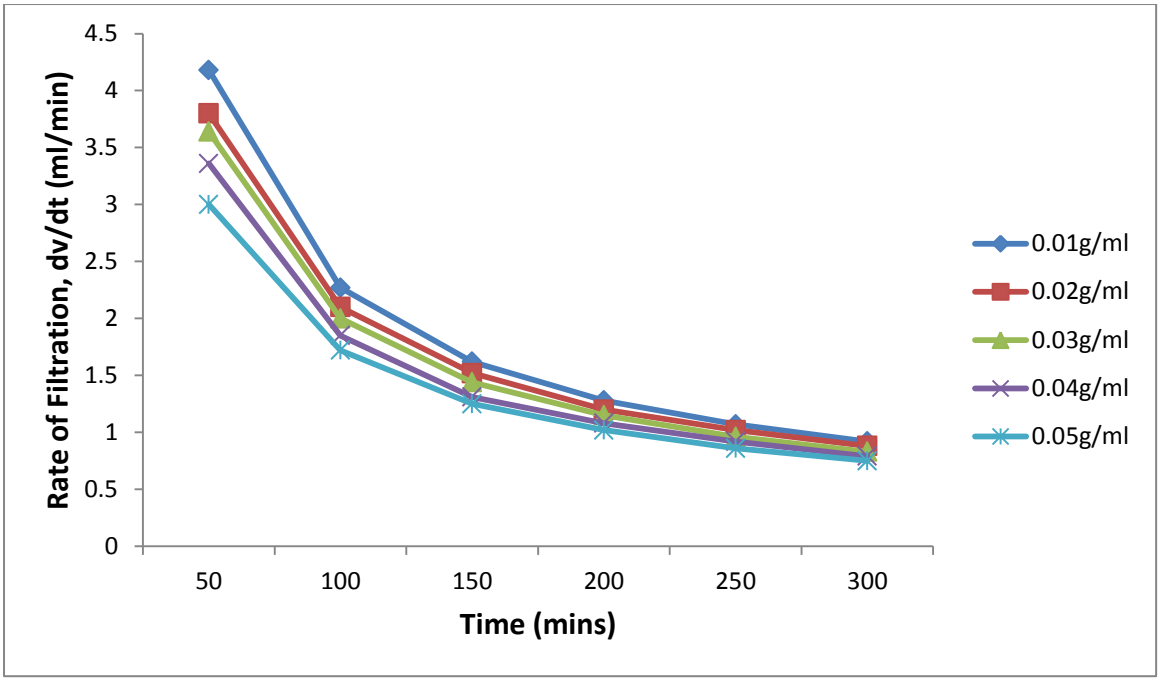

Figure 4.119: Plot of Rate of filtration versus time for M:P-Mud with varying starch concentration at high temperature, 250^{o}C. (Data; Table 4.24)

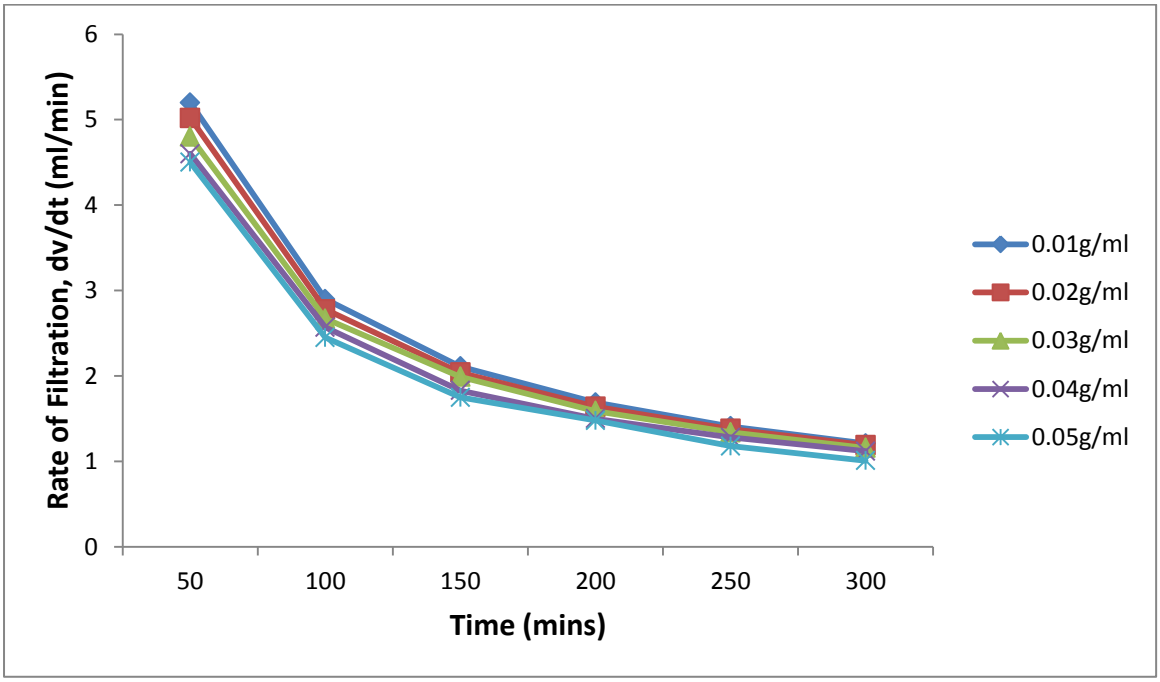

Figure 4.120: Plot of Rate of filtration versus time for CMS:HPS-Mud with varying starch concentration at high temperature, 250^{o}C. (Data; Table 4.25)

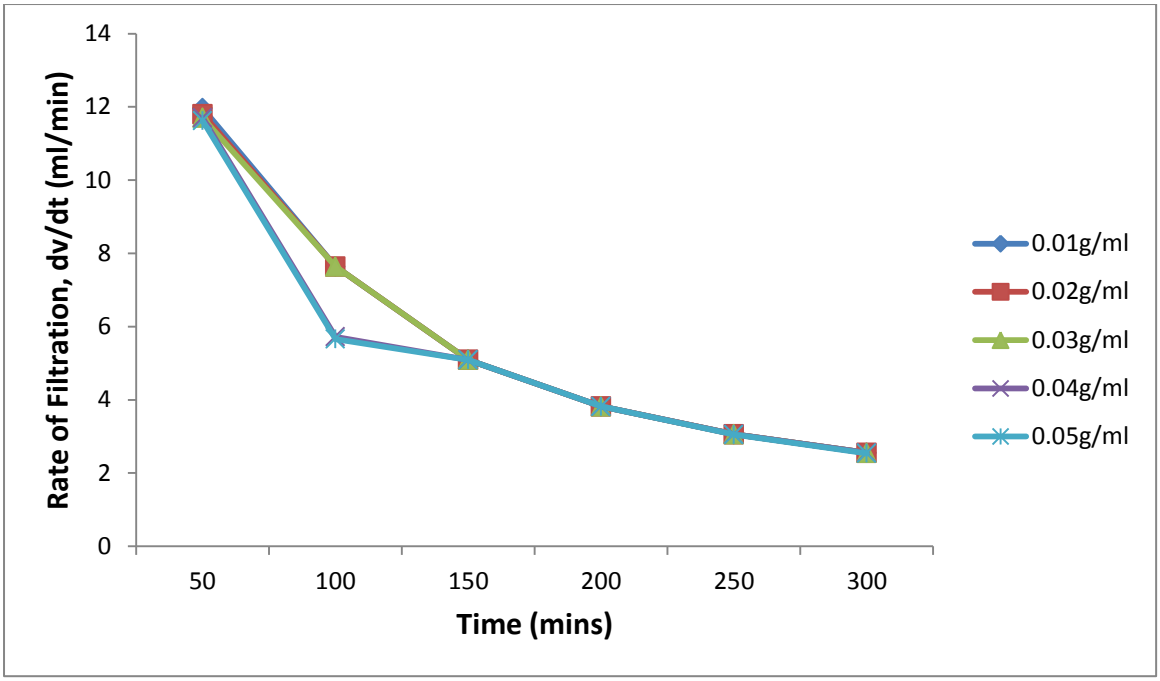

Figure 4.121: Plot of Rate of filtration versus time for W-Mud with varying starch concentration at high temperature, 250°C. (Data; Table 4.26)

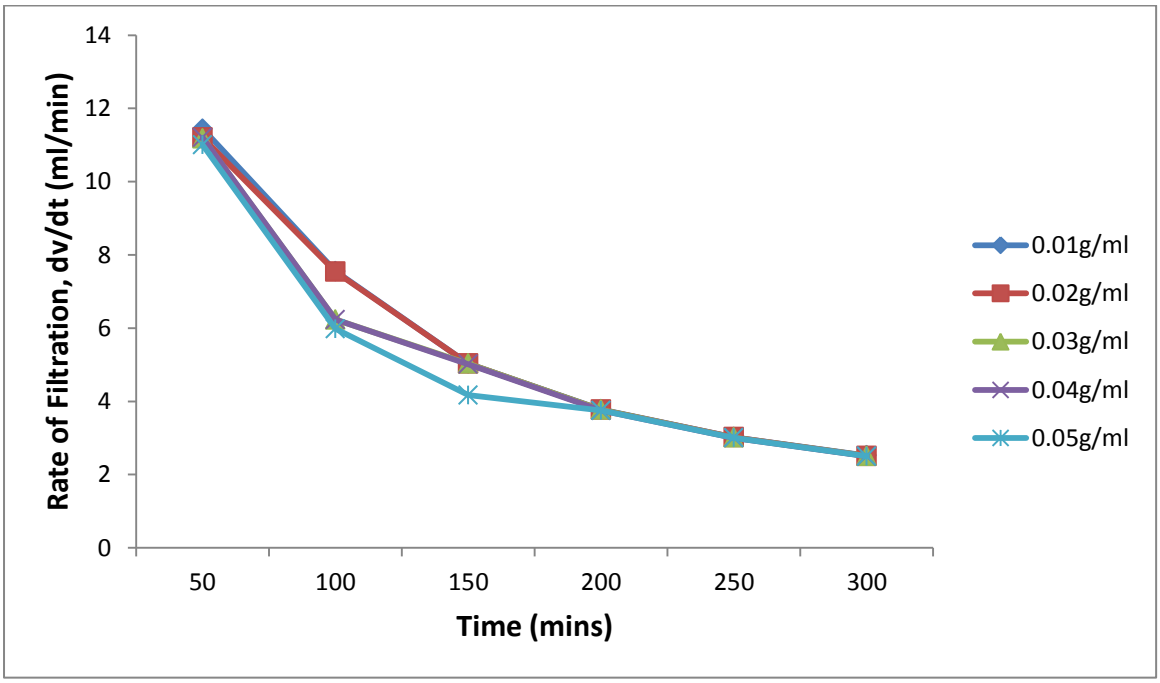

Figure 4.122: Plot of Rate of filtration versus time for CMS-Mud with varying starch concentration at high temperature, 250°C. (Data; Table 4.27)

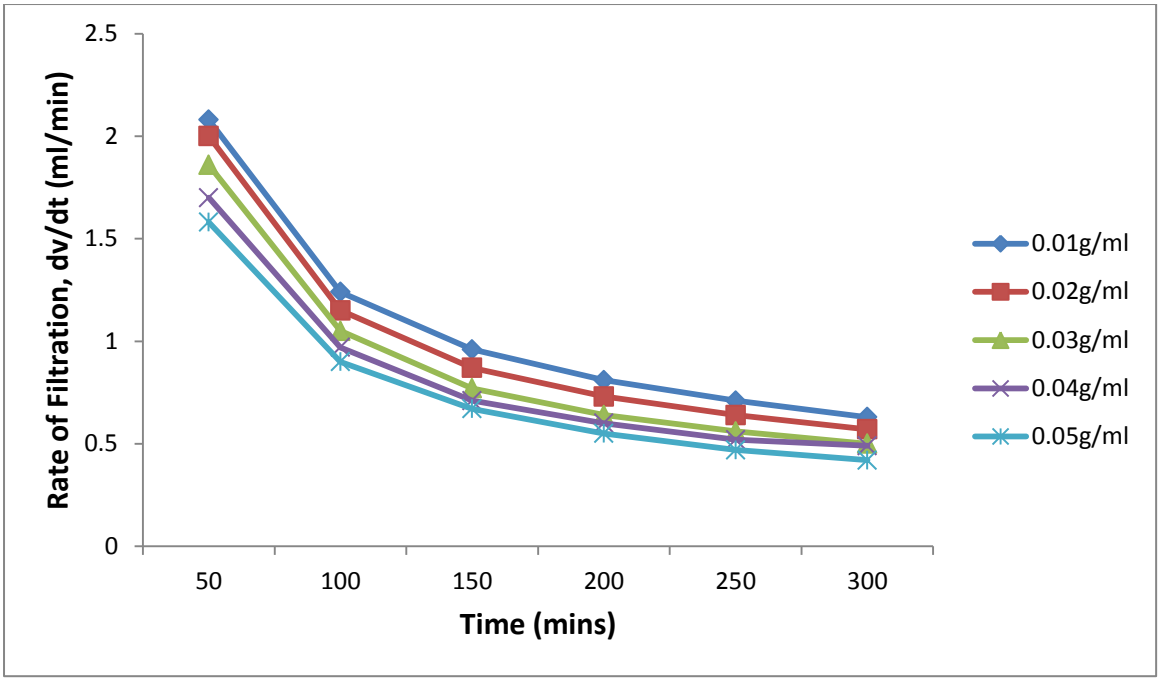

Figure 4.123: Plot of Rate of filtration versus time for G:W-Mud with varying starch concentration at high temperature, 350°C. (Data; Table 4.28)

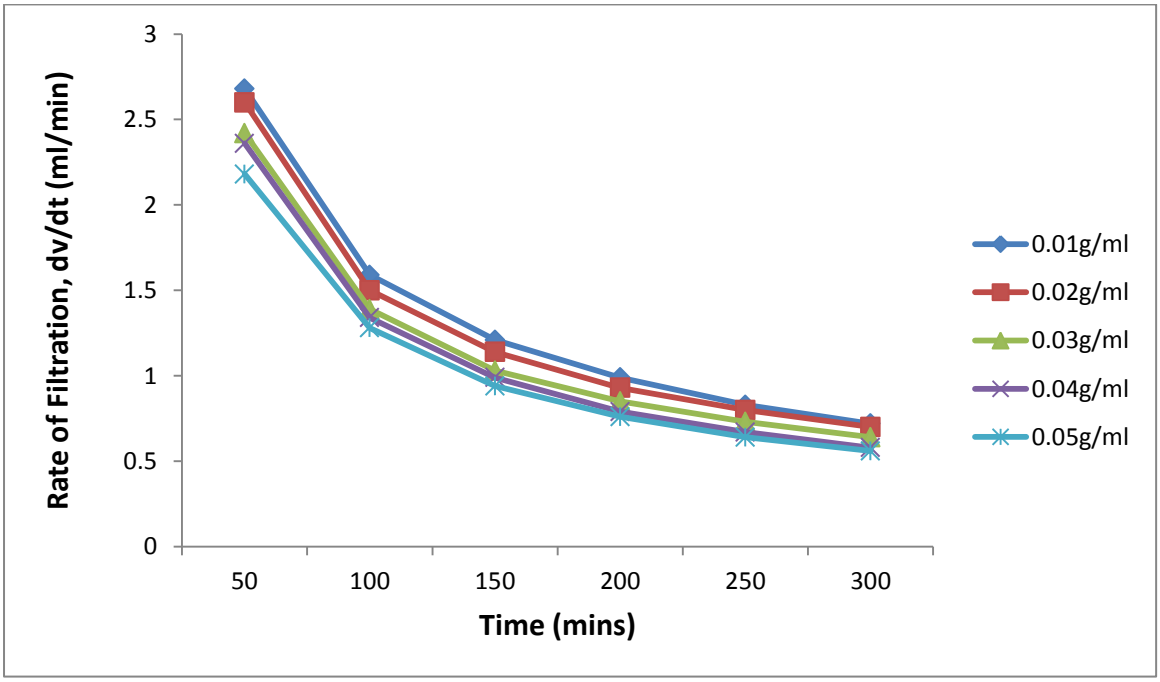

Figure 4.124: Plot of Rate of filtration versus time for M:W-Mud with varying starch concentration at high temperature, 350°C. (Data; Table 4.29)

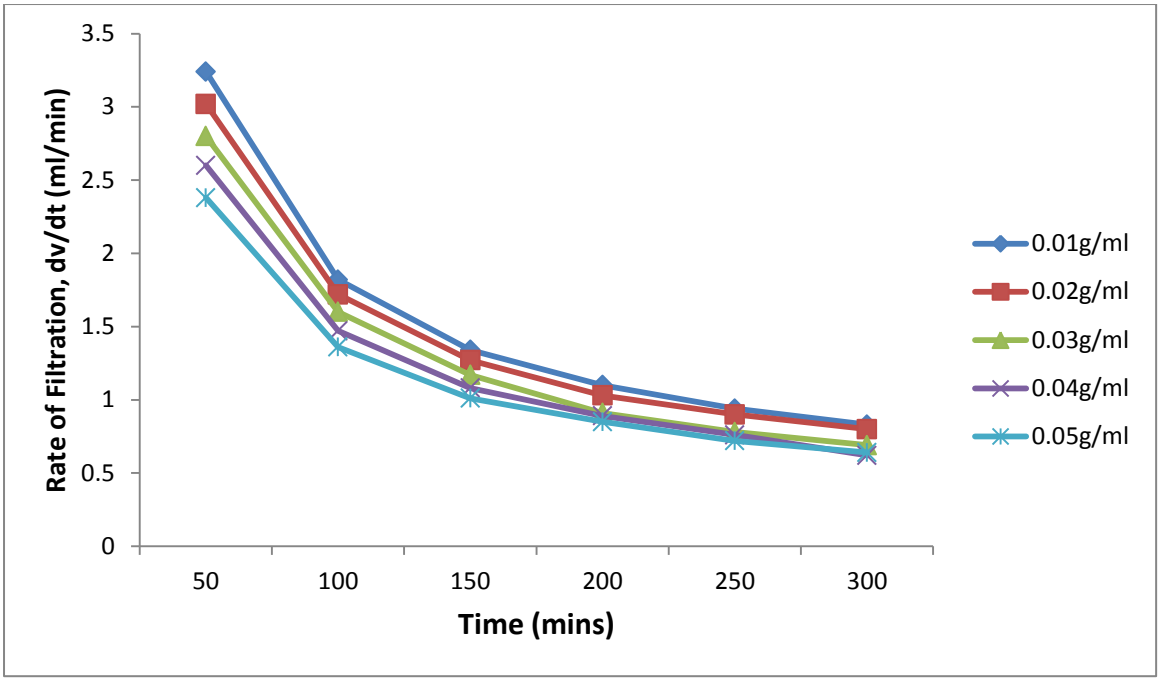

Figure 4.125: Plot of Rate of filtration versus time for P:W-Mud with varying starch concentration at high temperature, 350°C. (Data; Table 4.30)

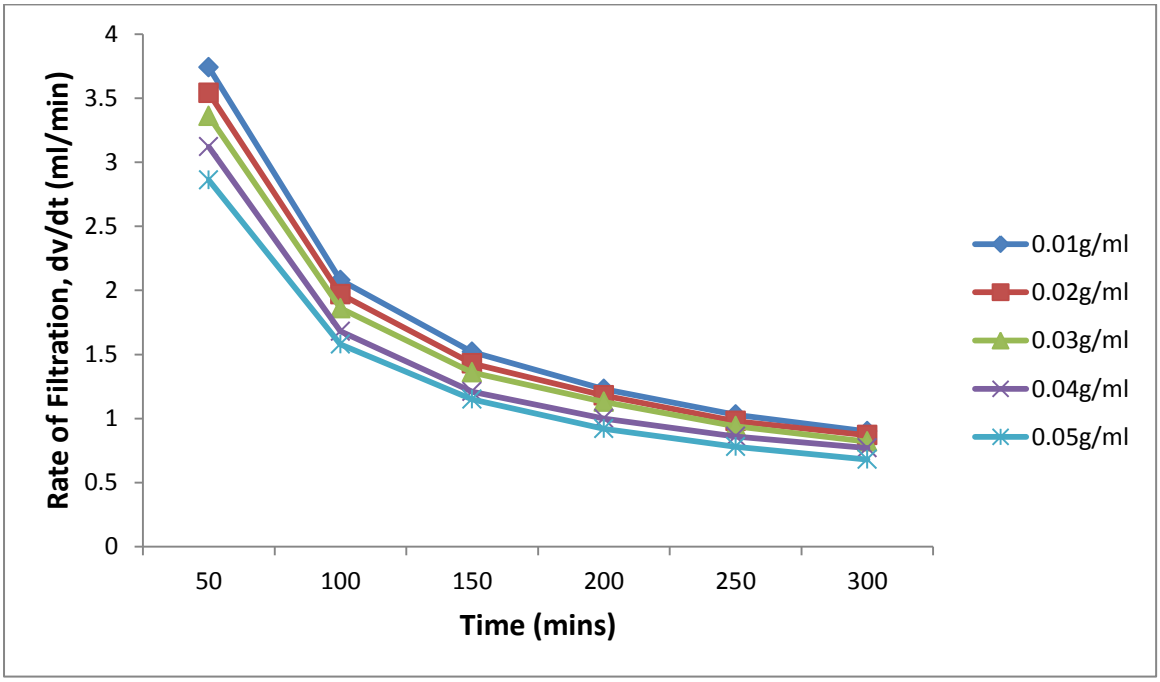

Figure 4.126: Plot of Rate of filtration versus time for G:M-Mud with varying starch concentration at high temperature, 350°C. (Data; Table 4.31)

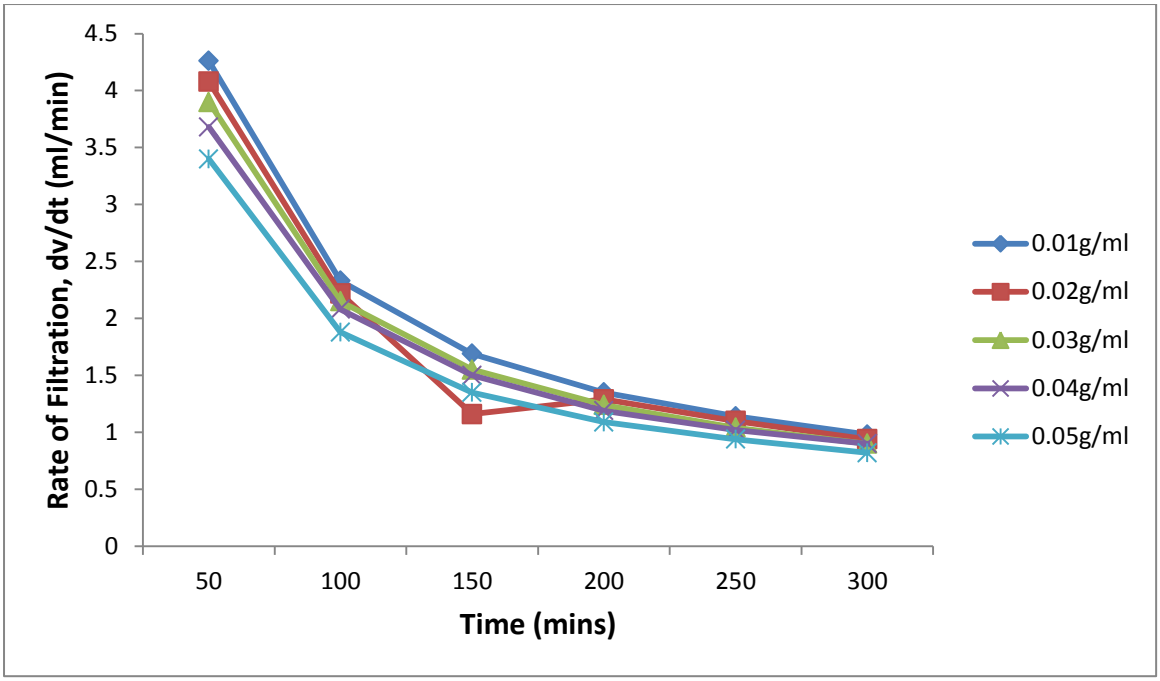

Figure 4.127: Plot of Rate of filtration versus time for G:P-Mud with varying starch concentration at high temperature, 350°C. (Data; Table 4.32)

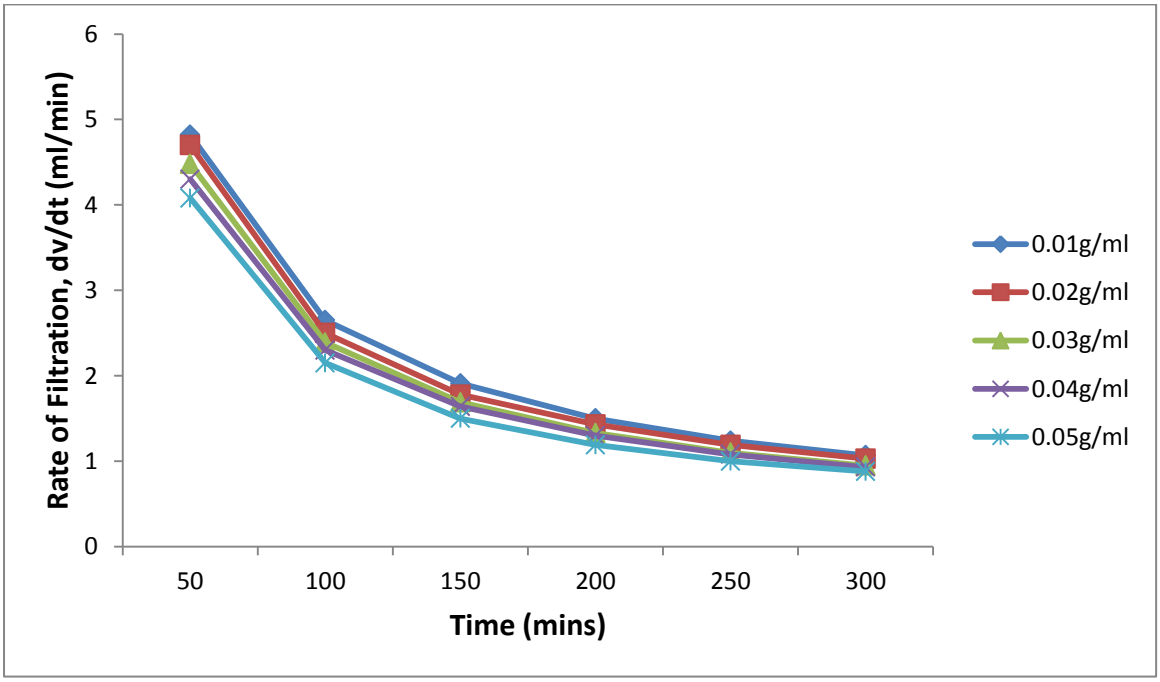

Figure 4.128: Plot of Rate of filtration versus time for M:P-Mud with varying starch concentration at high temperature, 350°C. (Data; Table 4.33)

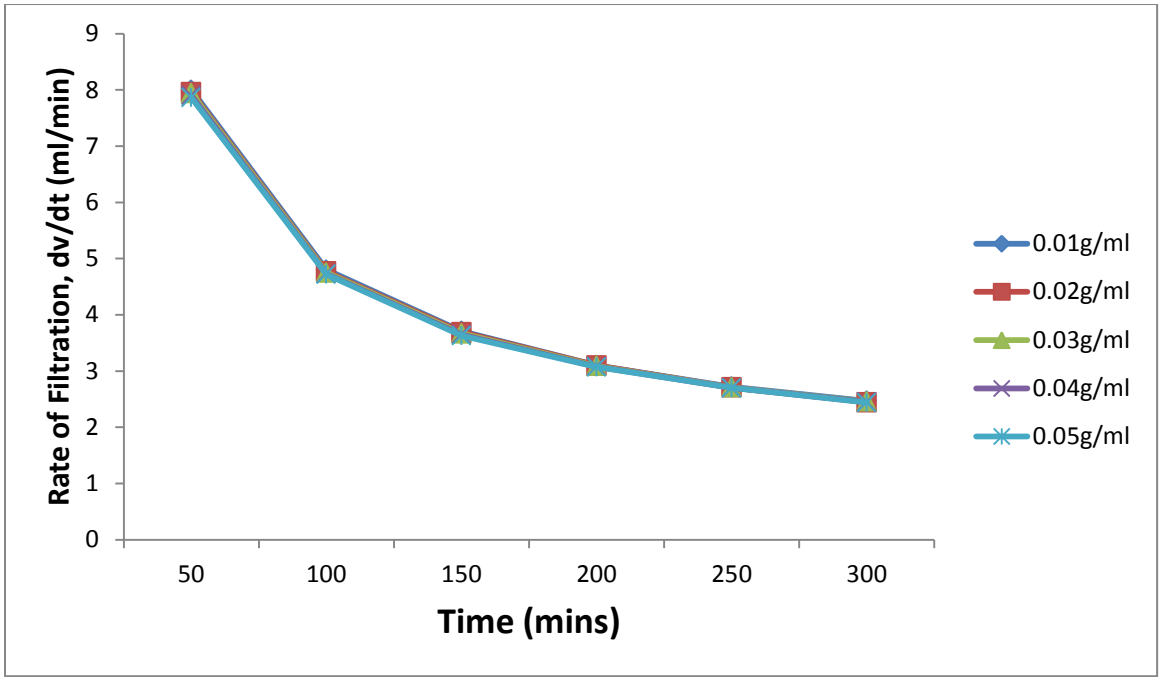

Figure 4.129: Plot of Rate of filtration versus time for CMS:HPS-Mud with varying starch concentration at high temperature, 350°C. (Data;Table 4.34)

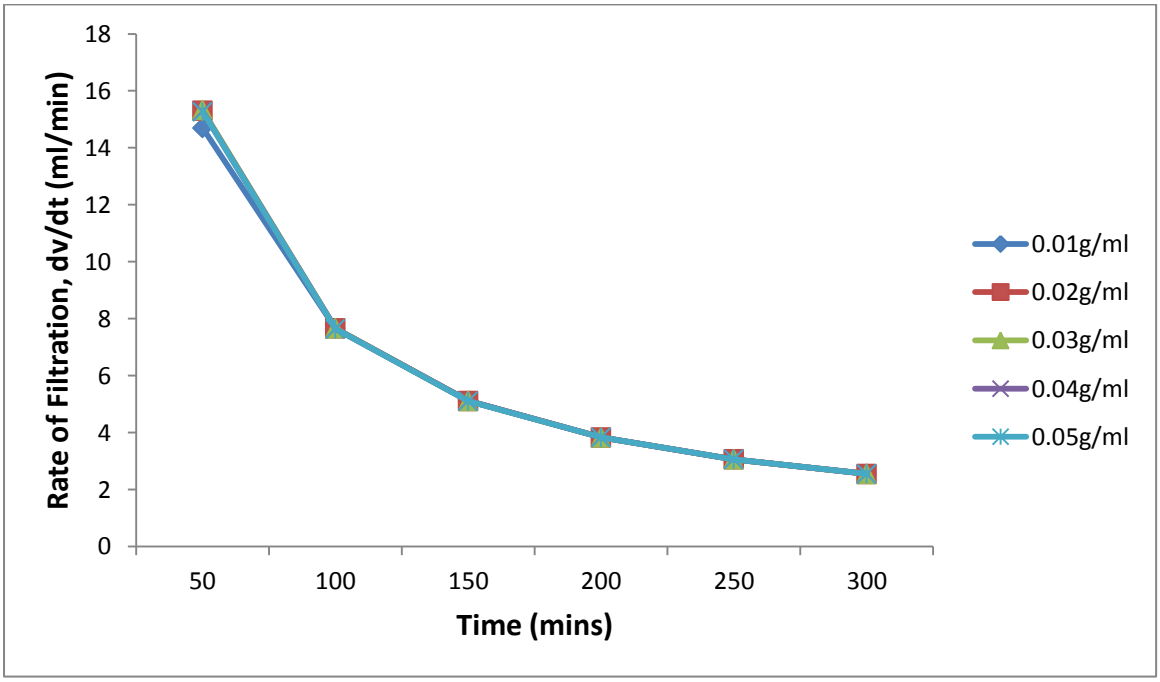

Figure 4.130: Plot of Rate of filtration versus time for W-Mud with varying starch concentration at high temperature, 350°C. (Data; Table 4.35)

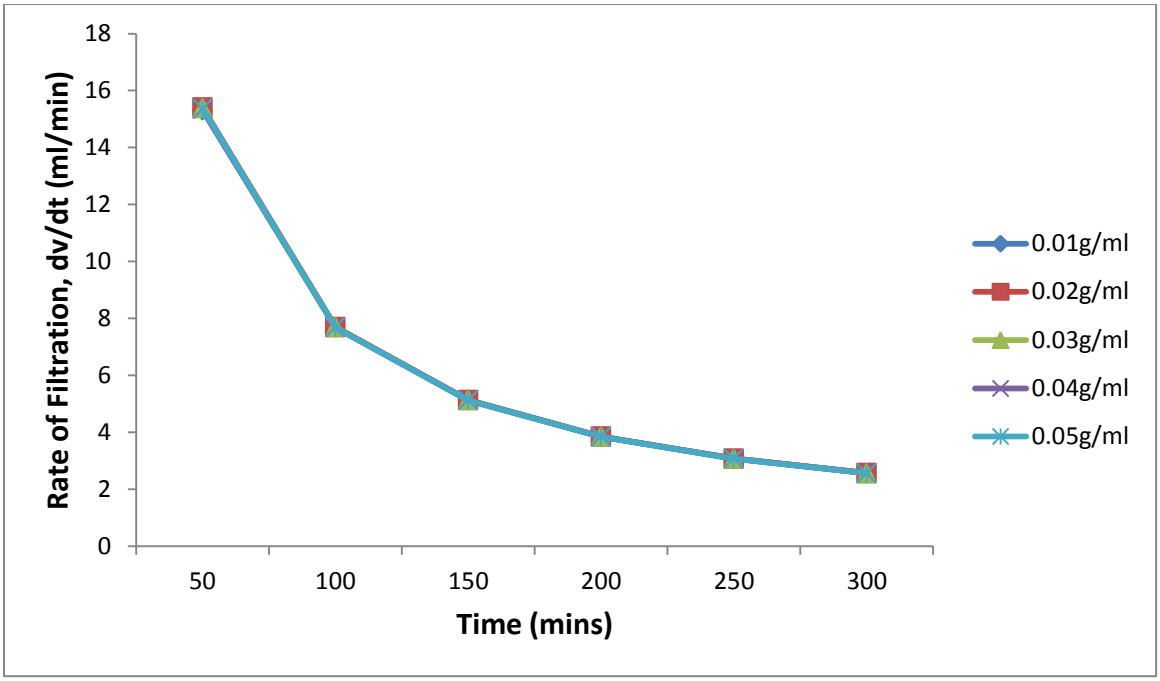

Figure 4.131: Plot of Rate of filtration versus time for CMS-Mud with varying starch concentration at high temperature, 350°C. (Data; Table 4.36)

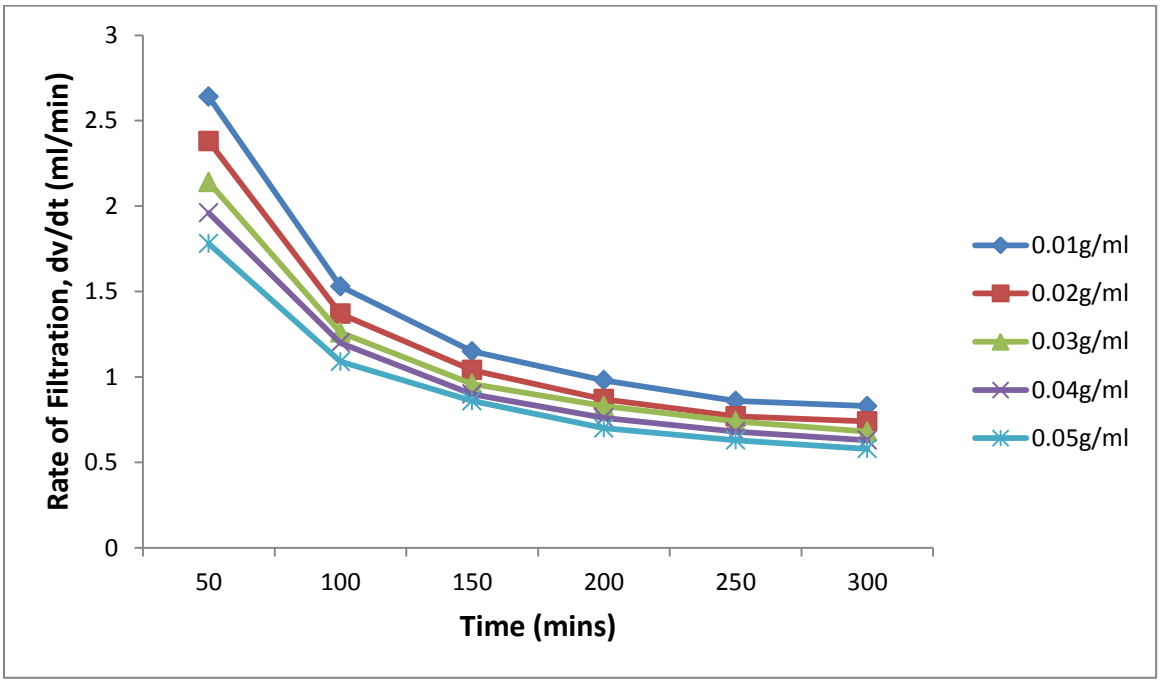

Figure 4.132: Plot of Rate of filtration versus time for G:W-Mud with varying starch concentration at high temperature, 450°C. (Data; Table 4.37)

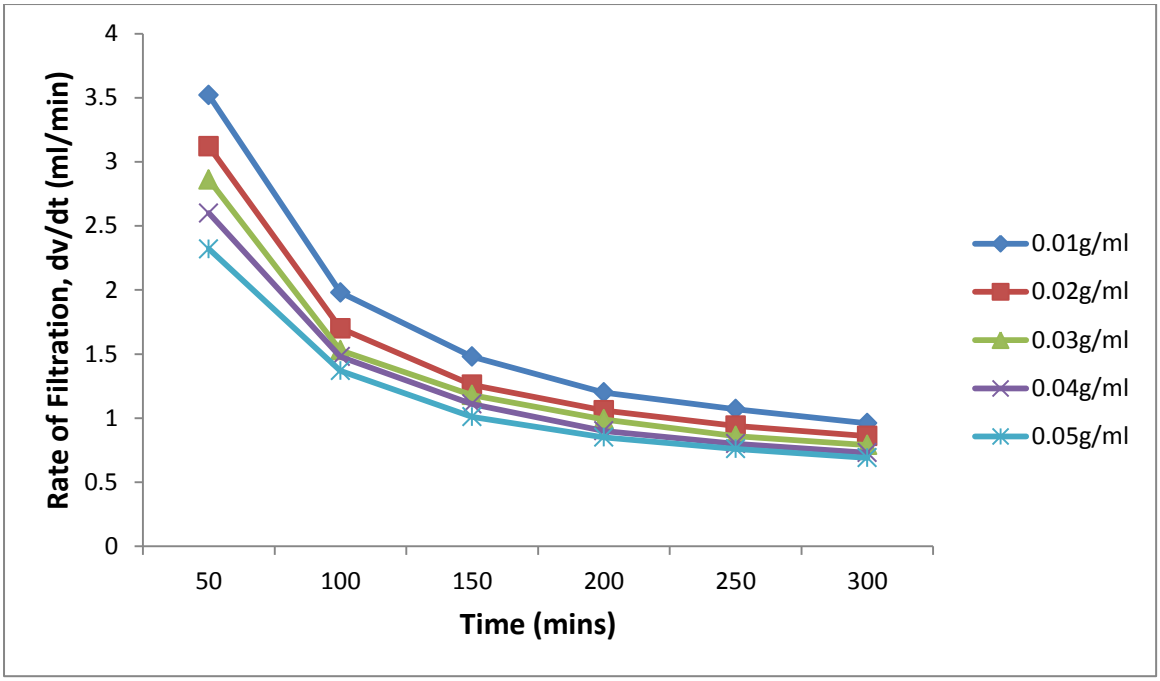

Figure 4.133: Plot of Rate of filtration versus time for M:W-Mud with varying starch concentration at high temperature, 450°C. (Data; Table 4.38)

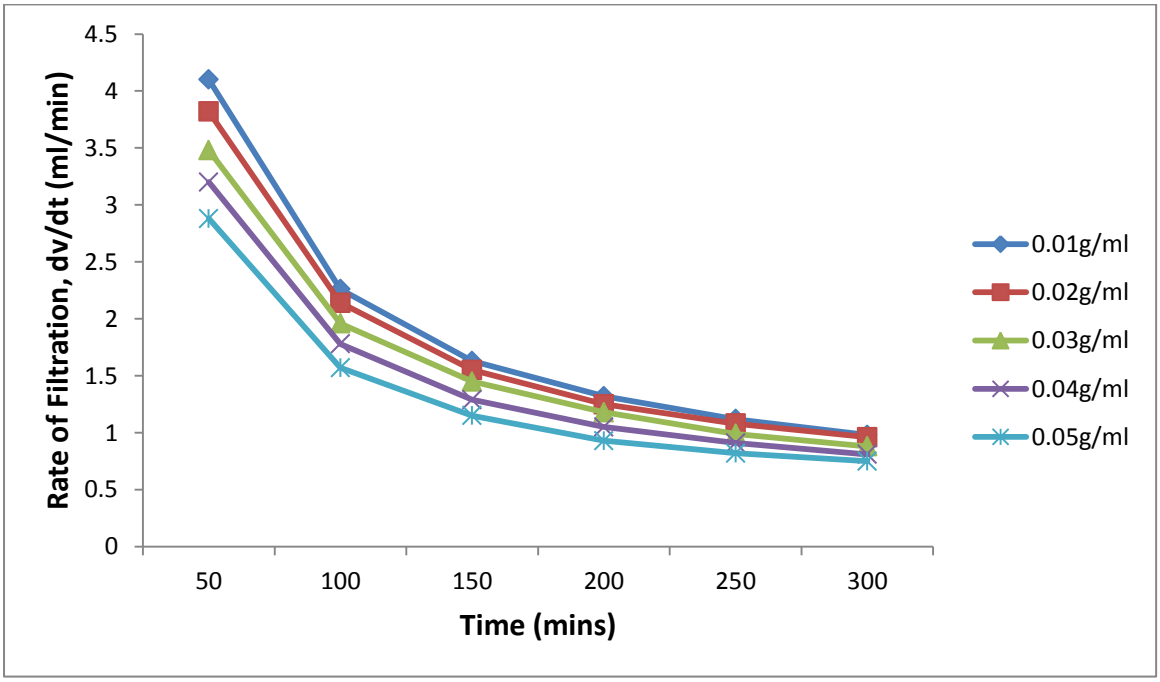

Figure 4.134: Plot of Rate of filtration versus time for P:W-Mud with varying starch concentration at high temperature, 450°C. (Data; Table 4.39)

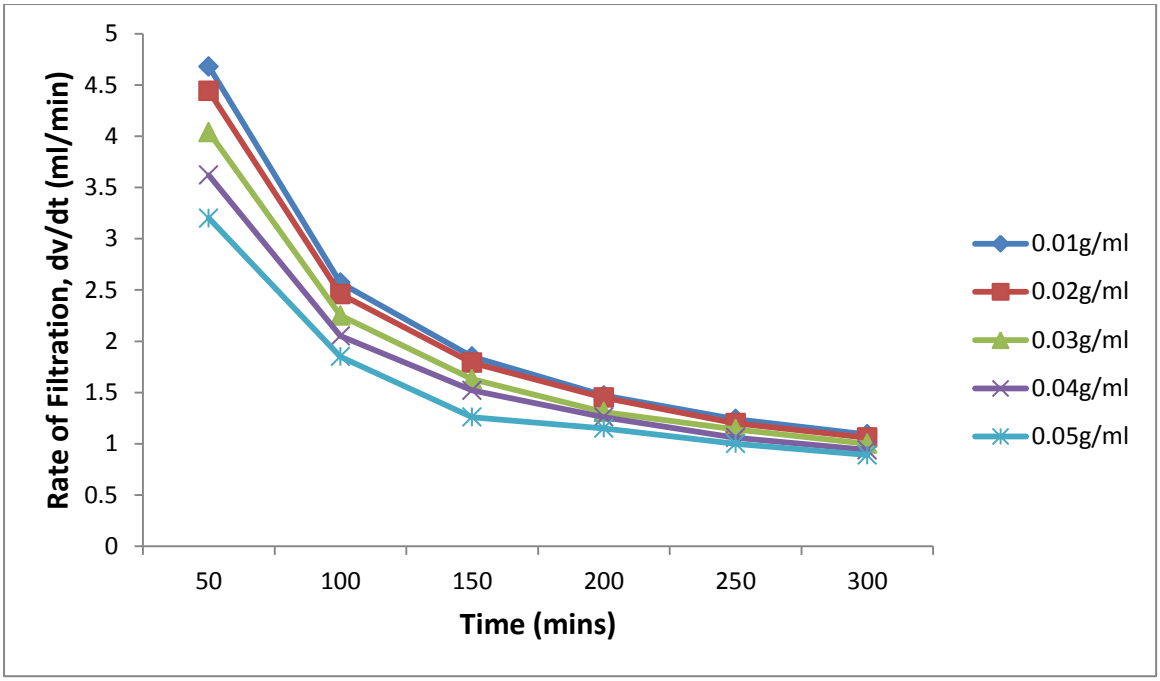

Figure 4.135: Plot of Rate of filtration versus time for G:M-Mud with varying starch concentration at high temperature, 450°C. (Data; Table 4.40)

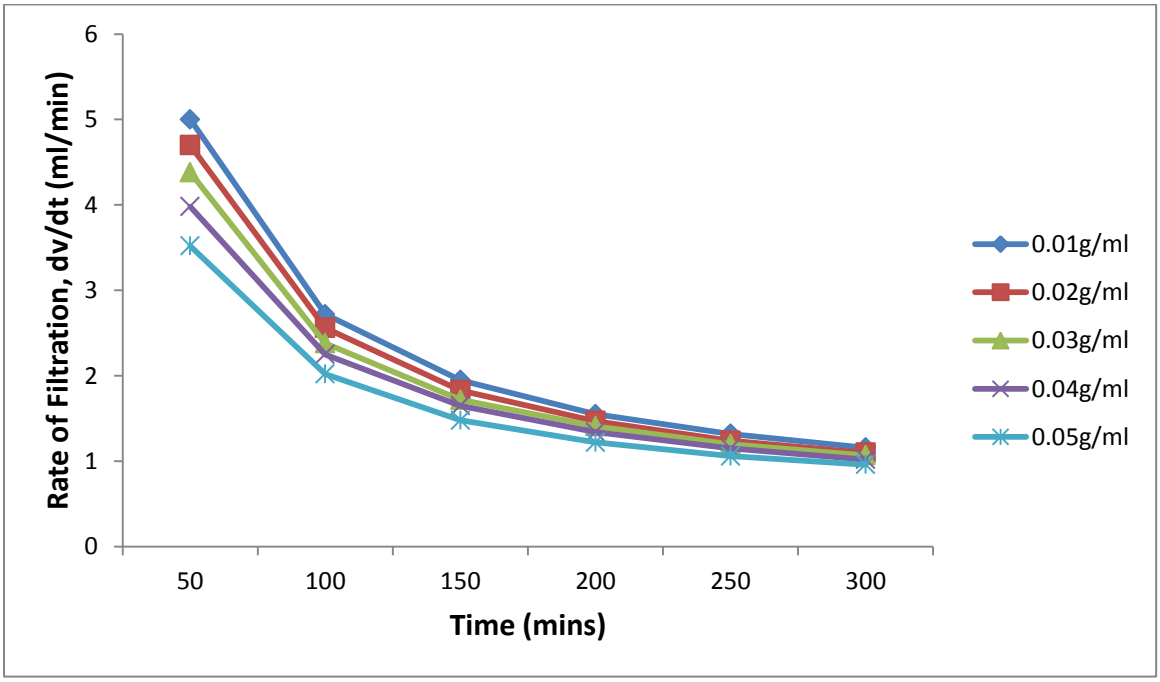

Figure 4.136: Plot of Rate of filtration versus time for G:P-Mud with varying starch concentration at high temperature, 450°C. (Data; Table 4.41)

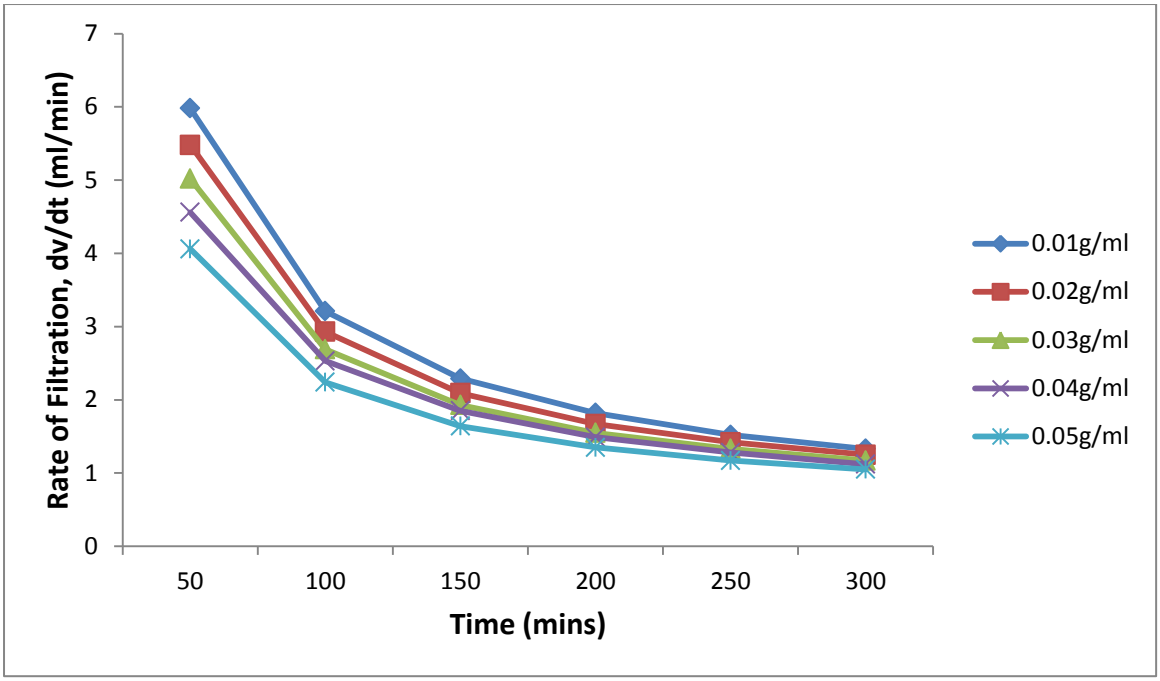

Figure 4.137: Plot of Rate of filtration versus time for M:P-Mud with varying starch concentration at high temperature, 450°C. (Data; Table 4.42)

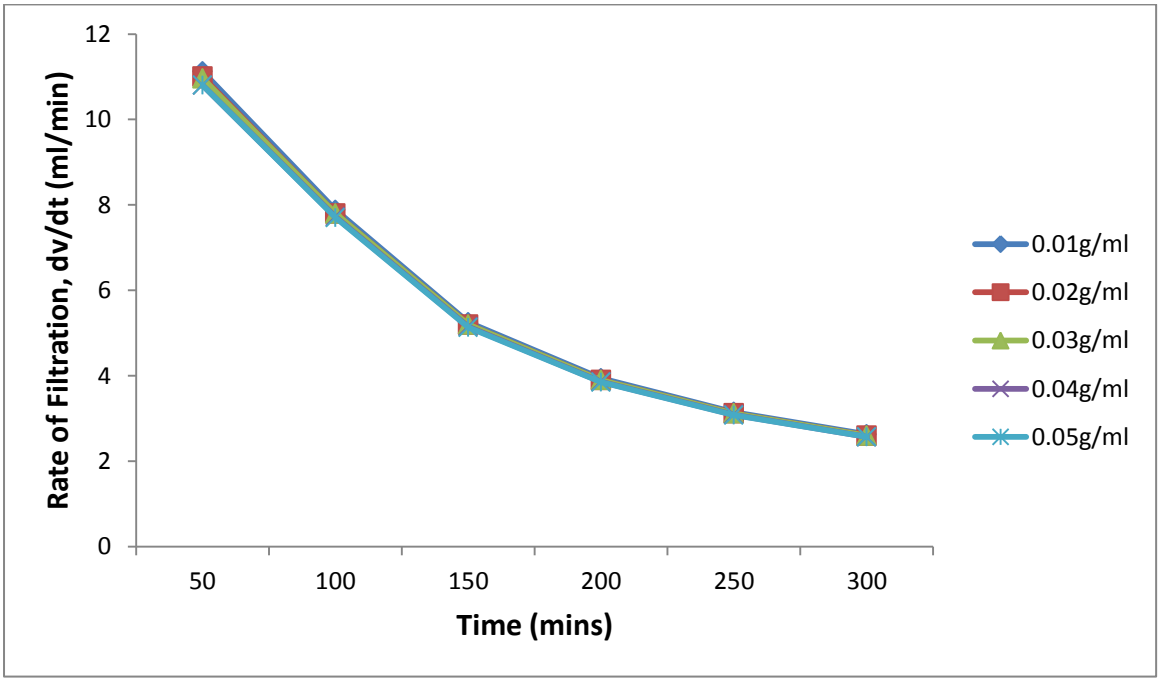

Figure 4.138: Plot of Rate of filtration versus time for CMS:HPS-Mud with varying starch concentration at high temperature, 450°C. (Data;Table 4.43)

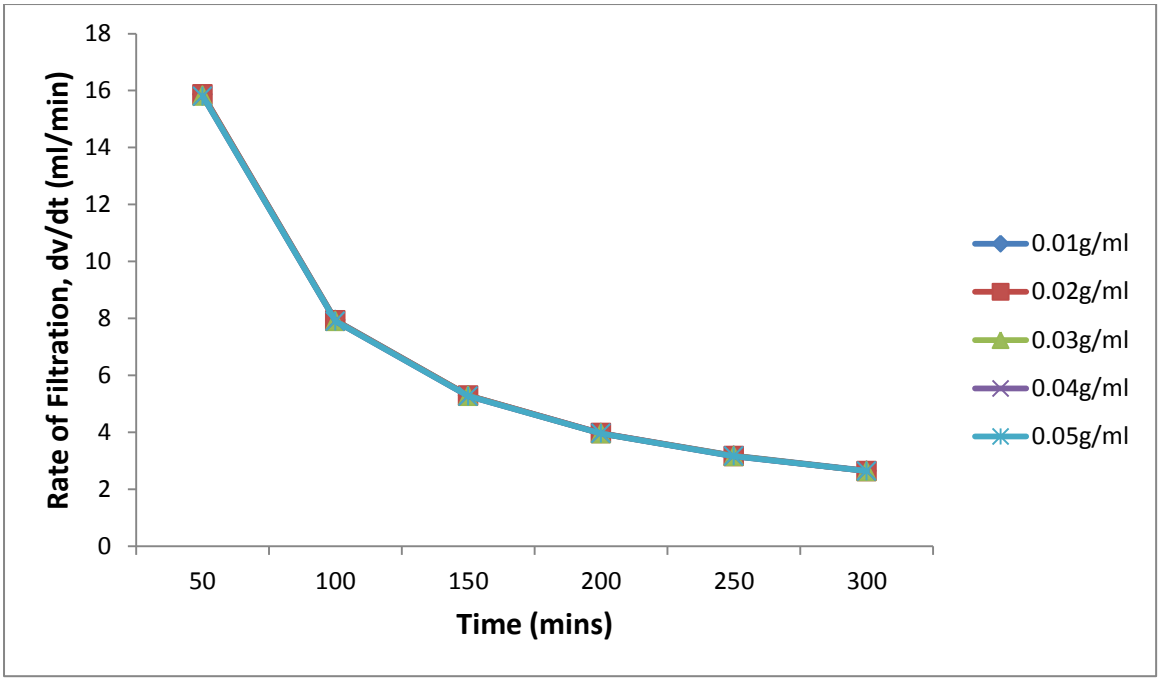

Figure 4.139: Plot of Rate of filtration versus time for W-Mud with varying starch concentration at high temperature, 450°C. (Data; Table 4.44)

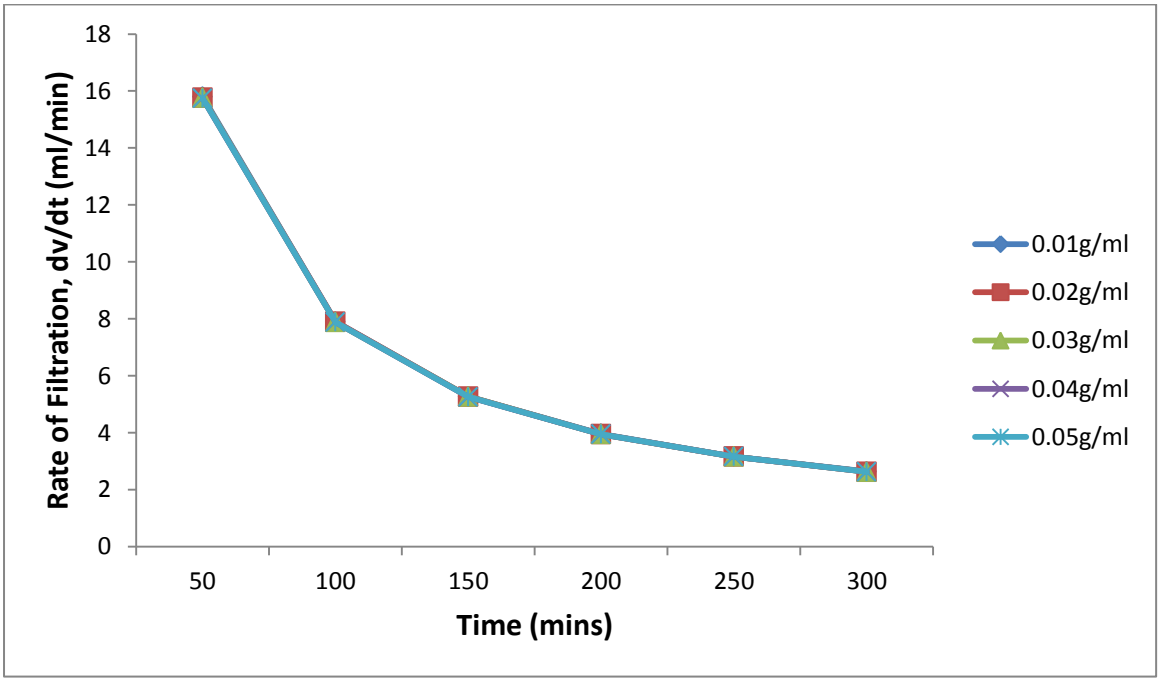

Figure 4.140: Plot of Rate of filtration versus time for CMS-Mud with varying starch concentration at high temperature, 450°C. (Data; Table 4.45)

More analysis of the figures shows that rate of filtration reduces with increase in starch concentrations. The least rate of filtration was obtained with each mud at 0.05g/ml starch concentration at all the temperatures. The reduction in filtration rate with increase in concentration shows that as concentration increases, the viscosity of fluid increases, resulting in more built-up filter cake and greater resistance to, and absorption of fluid passing through the cake, and consequently, a lower flow rate or filtration rate occurs.

All the muds showed normal behaviours with respect to filtration rate values until at 250^{o}C, 350^{o}C, and 450^{o}C temperatures, when increase in starch concentrations showed little or negligible reduction in filtration rates for W-Mud, CMS-Mud, and CMS:HPS-Mud. This an indication of thermal instability of the already existing muds at 250^{o}C, 350^{o}C and 450^{o}C.

4.2.1.11 Fluid Diffusivity of the Muds at different Temperatures

The diffusivity of all the muds was obtained as the slope of each plot of the rate of filtration versus time according to the mathematical modeling of the muds using equation (3.2), given as ($\Phi R = \Phi_o \exp^{-Dt}$). From the equation, D is the Diffusivity, which is defined as a measure of the rate of flow of fluid (Hall & Hoff, 2012; Bernu, 2011; Anthony & Robert, 2010; Scarlet & Brene, 2010; American Petroleum Institute API, 2003; Andy et al., 2001). The term Diffusivity is also defined as a measure of the ability of a substance to permit or undergo diffusion (Hall & Hoff, 2012; Jones & Mark, 2006). The values of diffusivity obtained with all the muds are given in the tables below.

Table 4.51: Computed Values of Fluid Diffusivity (D) From the Modelling of the Muds containing varying Concentrations of Starch at Room Temperature, 25°C.

	Fluid Diffusivity (D) at 25°C				
Muds/Samples	0.01g/ml	0.02g/ml	0.03g/ml	0.04g/ml	0.05g/ml
G:W-Mud	0.036	0.035	0.027	0.023	0.015
M:W-Mud	0.052	0.050	0.044	0.038	0.032
P:W-Mud	0.056	0.055	0.049	0.042	0.040
G:M-Mud	0.061	0.058	0.055	0.051	0.046
G:P-Mud	0.065	0.063	0.062	0.061	0.059
M:P-Mud	0.070	0.068	0.066	0.063	0.060
CMS:HPS-Mud	0.108	0.107	0.105	0.102	0.101
W-Mud	0.147	0.145	0.141	0.137	0.111
CMS-Mud	0.191	0.183	0.167	0.154	0.148

Table 4.52: Computed Values of Fluid Diffusivity (D) From the Modelling of the Muds containing varying Concentrations of Starch at High Temperature, 150°C.

	Fluid Diffusivity (D) at 150°C				
Muds/Samples	0.01g/ml	0.02g/ml	0.03g/ml	0.04g/ml	0.05g/ml
G:W-Mud	0.069	0.058	0.044	0.039	0.030
M:W-Mud	0.074	0.071	0.062	0.058	0.045
P:W-Mud	0.087	0.075	0.066	0.061	0.055
G:M-Mud	0.096	0.094	0.091	0.085	0.082
G:P-Mud	0.099	0.098	0.095	0.090	0.087
M:P-Mud	0.105	0.104	0.102	0,101	0.097
CMS:HPS-Mud	0.175	0.173	0.171	0.169	0.166
W-Mud	0.198	0.188	0.177	0.174	0.170
CMS-Mud	0.274	0.245	0.226	0.221	0.205

Table 4.53: Computed Values of Fluid Diffusivity (D) From the Modelling of the Muds containing varying Concentrations of Starch at High Temperature, 250°C.

	Fluid Diffusivity (D) at 250°C				
Muds/Samples	0.01g/ml	0.02g/ml	0.03g/ml	0.04g/ml	0.05g/ml
G:W-Mud	0.087	0.083	0.081	0.074	0.072
M:W-Mud	0.103	0.096	0.094	0.091	0.082
P:W-Mud	0.112	0.109	0.105	0.103	0.093
G:M-Mud	0.130	0.128	0.124	0.120	0.117
G:P-Mud	0.155	0.153	0.151	0.148	0.144
M:P-Mud	0.185	0.184	0.169	0.164	0.151
CMS:HPS-Mud	0.341	0.335	0.331	0.324	0.316
W-Mud	_	_	_	_	_
CMS-Mud	_	_	_	_	_

Table 4.54: Computed Values of Fluid Diffusivity (D) From the Modelling of the Muds containing varying Concentrations of Starch at High Temperature, 350°C.

	Fluid Diffusivity (D) at 350°C				
Muds/Samples	0.01g/ml	0.02g/ml	0.03g/ml	0.04g/ml	0.05g/ml
G:W-Mud	0.186	0.174	0.170	0,169	0.165
M:W-Mud	0,228	0,226	0.223	0.220	0,218
P:W-Mud	0.263	0.258	0.253	0.246	0.240
G:M-Mud	0.310	0.305	0.301	0.297	0.292
G:P-Mud	0.338	0.336	0.330	0,327	0.321
M:P-Mud	0.340	0,337	0.323	0.317	0.314
CMS:HPS-Mud	0.711	0.707	0.702	0.675	0.666
W-Mud	_	_	_	_	_
CMS-Mud	_	_	_	_	_

Table 4.55: Computed Values of Fluid Diffusivity (D) From the Modelling of the Muds containing varying Concentrations of Starch at High Temperature, 450^{o}C.

	Fluid Diffusivity (D) at 450^{o}C				
Muds/Samples	0.01g/ml	0.02g/ml	0.03g/ml	0.04g/ml	0.05g/ml
G:W-Mud	0.234	0.326	0.321	0.315	0.279
M:W-Mud	0.361	0.343	0.337	0.328	0.320
P:W-Mud	0.374	0.365	0.354	0.351	0.346
G:M-Mud	0.397	0.393	0.387	0.382	0,376
G:P-Mud	0.423	0.420	0,415	0.412	0,406
M:P-Mud	0.438	0.431	0.425	0.414	0.412
CMS:HPS-Mud	_	_	_	_	_
W-Mud	_	_	_	_	_
CMS-Mud	_	_	_	_	_

Tables 4.51 to 4.55 show the values of fluid diffusivity D the various muds containing varying starch concentrations of 0.01-0.05g/ml at 25^{o}C, 150^{o}C, 250^{o}C, 350^{o}C and 450^{o}C temperatures. It is observed from the tables that diffusivity D of the muds increases with increase in temperature. An explanation to this, on one aspect, is that as the temperature increases, the volume of fluid increases resulting in lower friction of the molecules, consequently, the flow rate increases resulting in higher diffusivity (Scarlet & Brene, 2010; Jones & Mark, 2006). Another aspect of the explanation is that as the temperature increases, the effectiveness of the muds' component, starch in particular, reduces resulting in less effective filter cakes with less resistance on fluid flow or less absorbing ability, consequently, the fluid flow rate increases resulting in higher fluid diffusivity (Anthony & Robert, 2010; Brown, 2009).

The tables also show that diffusivity of the muds reduces with increase in starch concentration, at all the temperatures. An increase in starch concentration causes an increase in the viscosity of the muds, which reduces the flow of fluid by fluid flow resistance and absorption, consequently, fluid flow rate reduces giving rise to lower diffusivity. Starch is a polymer and polymers are used to prepare drilling muds for controlling fluid flow and build the viscosity at a minimum content (Andrew & Robert, 2007).

The tables, further, show that the values of diffusivity D obtained with the new polymer muds (G:W-Mud, M:W-Mud, P:W-Mud, G:M-Mud, G:P-Mud and M:P-Mud) were lower than those of the already existing muds (CMS:HPS-Mud, W-Mud and CMS-Mud) at all the temperatures. G:W-Mud gave the lowest diffusivity values while CMS-Mud gave the highest diffusivity values at all the temperatures. The maximum diffusivity values of the muds were obtained at 450^{0}C temperature.

Diffusivity depends on molecular compaction characteristics and permeability (Clifford & Cain, 2002). The already existing muds, with higher diffusivity values than the new polymer muds, indicates that the already existing muds were less viscous due to less molecular compaction and higher permeability of the built-up filter cakes. Each of the new polymer muds has lower values of diffusivity because the mud has higher viscosity and the built-up filter cakes were less permeable. This may also be related to the fact that the new muds are made up of purer and more viscous blends of starch polymers, which clog the interstitial openings between particles resulting in lower fluid flow rate, and then lower diffusivity.

Furthermore, the tables show that the already existing muds, W-mud and CMS-Mud gave infinite diffusivity at 250^0C, 350^0C, 450^0C, while CMS:HPS-Mud gave infinite diffusivity at 450^0C temperature. All these values indicate thermal instability or thermal degradation of W-Mud, CMS-Mud and CMS:HPS-Mud at 250^0C, 350^0C and 450^0C high temperatures. When the diffusivity values of a mud at a particular temperarture are no longer specific or definite, it is said that the mud has deviated from the API and Henri Darcy models of filtration (Bertt & Jerry, 2012; Bernu, 2011; Bill & Mark, 2007; API, 2003). The deviation from the model is as a result of extraordinary flow rate of fluid, which usually occurs when the mud content (starch) has been burnt up by high temperature (Bernu, 2011).The thermal degradation of the muds at these temperatures might have resulted from the fact that W-Mud was prepared with single starch (unblended starch), CMS-Mud was prepared with chemically modified single starch, and CMS:HPS-mud was prepared with blend of chemically modified starches. The implication of this is that none of these already existing muds can be used in drilling any well whose hole temperature is as high as or above the temperature of its thermal degradation.

4.2.2 Rheological Properties

The rheological Properties of the new biodegradable polymer muds (G;W-Mud, M:W-Mud, P:W-Mud, G:M-Mud, G:P-Mud, M:P-Mud) and the already existing or widely used muds (CMS:HPS-Mud, W-Mud, CMS-Mud) were determined at 0.01-0.05g/ml concentration of each starch using viscometric method. The apparatus involved here was the Brookfield viscometer (see figure 3.2). Table 4.56 - Table 4.64, show the results and data obtained with the rheological tests run on the muds.The data were used to plot figures 4.141 – 4.167.

Table 4.56: Experimental Data and Results For Rheological Properties of G:W-Mud (Biodegradable Polymer Drilling Mud prepared with a blend of Guinea corn starch and Waxy corn starch)

Conc g/ml	Speed (rpm)	Viscosity μ(Poise)	Shear stress τ (mpa)	Shear rate $\gamma(s^{-1})$	Log τ	Log γ
0.01	60	3,730.00	373.00	0.1	2.57	-1.00
	120	3,450.00	690.00	0.2	2.84	-0.69
	300	2,820.00	1,410.00	0.5	3.15	-0.30
	600	2,310.00	2,310.00	1.0	3.36	0
0.02	60	4,800.00	480.00	0.1	2.68	-1.00
	120	3,920.00	784.00	0.2	2.89	-0.69
	300	3,260.00	1,630.00	0.5	3.21	-0.30
	600	2,789.00	2,789.00	1.0	3.45	0
0.03	60	5,850.00	585.00	0.1	2.77	-1.00
	120	4,550.00	910.00	0.2	2.96	-0.69
	300	3,500.00	1,750.00	0.5	3.24	-0.30
	600	3,030.00	3,030.00	1.0	3.48	0
0.04	60	6,980.00	698.00	0.1	2.84	-1.00
	120	5,350.00	1,070.00	0.2	3.03	-0.69
	300	3,840.00	1,920.00	0.5	3.28	-0.30
	600	3,440.00	3,440.00	1.0	3.54	0
0.05	60	7,940.00	794.00	0.1	2.90	-1.00
	120	6,770.00	1,354.00	0.2	3.13	-0.69
	300	4,308.00	2,154.00	0.5	3.33	-0.30
	600	3,940.00	3,940.00	1.0	3.60	0

Table 4.57: Experimental Data and Results For Rheological Properties of M:W-Mud (Biodegradable Polymer Drilling Mud prepared with a blend of Millet starch and Waxy corn starch)

Conc g/ml	Speed (rpm)	Viscosity μ(Poise)	Shear stress τ (mpa)	Shear rate $\gamma(s^{-1})$	Log τ	Log γ
0.01	60	3,350.00	335.00	0.1	2.53	-1.00
	120	3,080.00	616.00	0.2	2.79	-0.69
	300	2,640.00	1,320.00	0.5	3.12	-0.30
	600	2,120.00	2,120.00	1.0	3.33	0
0.02	60	4,400.00	440.00	0.1	2.64	-1.00
	120	3,520.00	704.00	0.2	2.85	-0.69
	300	2,872.00	1,436.00	0.5	3.16	-0.30
	600	2,416.00	2,416.00	1.0	3.38	0
0.03	60	5,380.00	538.00	0.1	2.73	-1.00
	120	4,120.00	824.00	0.2	2.92	-0.69
	300	3,240.00	1,620.00	0.5	3.21	-0.30
	600	2,760.00	2,760.00	1.0	3.44	0
0.04	60	6,490.00	649.00	0.1	2.81	-1.00
	120	4,880.00	976.00	0.2	2.99	-0.69
	300	3,536.00	1,768.00	0.5	3.25	-0.30
	600	3,220.00	3,220.00	1.0	3.51	0
0.05	60	7,410.00	741.00	0.1	2.87	-1.00
	120	6,260.00	1,252.00	0.2	3.10	-0.69
	300	4,176.00	2,088.00	0.5	3.31	-0.30
	600	3,690.00	3,690.00	1.0	3.57	0

Table 4.58: Experimental Data and Results For Rheological Properties of P:W-Mud (Biodegradable Polymer Drilling Mud prepared with a blend of Pop corn starch and Waxy corn starch)

Conc g/ml	Speed (rpm)	Viscosity μ(Poise)	Shear stress τ (mpa)	Shear rate $\gamma(s^{-1})$	Log τ	Log γ
0.01	60	3,050.00	305.00	0.1	2.48	-1.00
	120	2,800.00	560.00	0.2	2.75	-0.69
	300	2,592.00	1,296.00	0.5	3.11	-0.30
	600	1,810.00	1,810.00	1.0	3.26	0
0.02	60	3,990.00	399.00	0.1	2.60	-1.00
	120	3,100.00	620.00	0.2	2.79	-0.69
	300	2,796.00	1,398.00	0.5	3.15	-0.30
	600	2,140.00	2,140.00	1.0	3.33	0
0.03	60	4,890.00	489.00	0.1	2.69	-1.00
	120	3,680.00	736.00	0.2	2.87	-0.69
	300	3,176.00	1,588.00	0.5	3.20	-0.30
	600	2,573.00	2,573.00	1.0	3.41	0
0.04	60	6,060.00	606.00	0.1	2.78	-1.00
	120	4,390.00	878.00	0.2	2.94	-0.69
	300	3,400.00	1,700.00	0.5	3.23	-0.30
	600	2,880.00	2,880.00	1.0	3.46	0
0.05	60	6,870.00	687.00	0.1	2.84	-1.00
	120	5,730.00	1,146.00	0.2	3.06	-0.69
	300	4,130.00	2,065.00	0.5	3.31	-0.30
	600	3,370.00	3,370.00	1.0	3.53	0

Table 4.59: Experimental Data and Results For Rheological Properties of G:M-Mud (Biodegradable Polymer Drilling Mud prepared with a blend of Guinea corn starch and Millet starch)

Conc g/ml	Speed (rpm)	Viscosity μ(Poise)	Shear stress τ (mpa)	Shear rate $\gamma(s^{-1})$	Log τ	Log γ
0.01	60	2,720.00	272.00	0.1	2.43	-1.00
	120	2,510.00	502.00	0.2	2.70	-0.69
	300	2,256.00	1,128.00	0.5	3.05	-0.30
	600	1,670.00	1,670.00	1.0	3.22	0
0.02	60	3,560.00	356.00	0.1	2.55	-1.00
	120	2,700.00	540.00	0.2	2.73	-0.69
	300	2,530.00	1,265.00	0.5	3.10	-0.30
	600	1,990.00	1,990.00	1.0	3.30	0
0.03	60	4,380.00	438.00	0.1	2.64	-1.00
	120	3,230.00	646.00	0.2	2.81	-0.69
	300	2,598.00	1,479.00	0.5	3.16	-0.30
	600	2,380.00	2,380.00	1.0	3.38	0
0.04	60	5,530.00	563.00	0.1	2.75	-1.00
	120	3,850.00	770.00	0.2	3.89	-0.69
	300	3,180.00	1,590.00	0.5	3.20	-0.30
	600	2,690.00	2,690.00	1.0	3.43	0
0.05	60	6,330.00	633.00	0.1	2.80	-1.00
	120	5,200.00	1,040.00	0.2	3.02	-0.69
	300	3,760.00	1,880.00	0.5	3.27	-0.30
	600	3,186.00	3,186.00	1.0	3.50	0

Table 4.60: Experimental Data and Results For Rheological Properties of G:P-Mud (Biodegradable Polymer Drilling Mud prepared with a blend of Guinea corn starch and Pop corn starch)

Conc g/ml	Speed (rpm)	Viscosity μ(Poise)	Shear stress τ (mpa)	Shear rate $\gamma(s^{-1})$	Log τ	Log γ
0.01	60	2,480.00	248.00	0.1	2.39	-1.00
	120	2,200.00	440.00	0.2	2.64	-0.69
	300	2,020.00	1,010.00	0.5	3.00	-0.30
	600	1,480.00	1,480.00	1.0	3.17	0
0.02	60	3,110.00	311.00	0.1	2.49	-1.00
	120	2,560.00	512.00	0.2	2.71	-0.69
	300	2,320.00	1,160.00	0.5	3.06	-0.30
	600	1,880.00	1,880.00	1.0	3.27	0
0.03	60	3,890.00	389.00	0.1	2.58	-1.00
	120	2,770.00	554.00	0.2	2.74	-0.69
	300	2,420.00	1,210.00	0.5	3.13	-0.30
	600	2,250.00	2,250.00	1.0	3.35	0
0.04	60	5,200.00	520.00	0.1	2.72	-1.00
	120	3,310.00	662.00	0.2	2.82	-0.69
	300	2,920.00	1,460.00	0.5	3.16	-0.30
	600	2,560.00	2,560.00	1.0	3.41	0
0.05	60	5,800.00	580.00	0.1	2.76	-1.00
	120	4,670.00	934.00	0.2	2.97	-0.69
	300	3,240.00	1,620.00	0.5	3.21	-0.30
	600	2,980.00	2,980.00	1.0	3.47	0

Table 4.61: Experimental Data and Results For Rheological Properties of M:P-Mud (Biodegradable Polymer Drilling Mud prepared with a blend of Millet starch and Pop corn starch)

Conc g/ml	Speed (rpm)	Viscosity μ(Poise)	Shear stress τ (mpa)	Shear rate $\gamma(s^{-1})$	Log τ	Log γ
0.01	60	2,240.00	224.00	0.1	2.35	-1.00
	120	1,890.00	378.00	0.2	2.58	-0.69
	300	1,760.00	880.00	0.5	2.94	-0.30
	600	1,250.00	1,250.00	1.0	3.10	0
0.02	60	2,650.00	265.00	0.1	2.42	-1.00
	120	2,190.00	438.00	0.2	2.64	-0.69
	300	2,000.00	1,000.00	0.5	3.00	-0.30
	600	1,720.00	1,720.00	1.0	3.24	0
0.03	60	3,400.00	340.00	0.1	2.53	-1.00
	120	2,280.00	456.00	0.2	2.66	-0.69
	300	2,150.00	1,075.00	0.5	3.03	-0.30
	600	2,070.00	2,070.00	1.0	3.32	0
0.04	60	4,750.00	475.00	0.1	2.68	-1.00
	120	2,790.00	558.00	0.2	2.75	-0.69
	300	2,520.00	1,260.00	0.5	3.10	-0.30
	600	2,200.00	2,200.00	1.0	3.34	0
0.05	60	5,250.00	525.00	0.1	2.72	-1.00
	120	4,130.00	826.00	0.2	2.92	-0.69
	300	2,900.00	1,450.00	0.5	3.16	-0.30
	600	2,700.00	2,700.00	1.0	3.43	0

Table 4.62: Experimental Data and Results For Rheological Properties of CMS:HPS-Mud (Widely-used Drilling Mud prepared with a blend of chemically modified Carboxymethyl starch and Hydroxypropyl starch)

Conc g/ml	Speed (rpm)	Viscosity μ(Poise)	Shear stress τ (mpa)	Shear rate $\gamma(s^{-1})$	Log τ	Log γ
0.01	60	1,160.00	116.00	0.1	2.06	-1.00
	120	970.00	194.00	0.2	2.29	-0.69
	300	890.00	445.00	0.5	2.65	-0.30
	600	780.00	780.00	1.0	2.89	0
0.02	60	1,560.00	156.00	0.1	2.19	-1.00
	120	1,380.00	276.00	0.2	2.44	-0.69
	300	1,250.00	625.00	0.5	2.80	-0.30
	600	1,110.00	1,110.00	1.0	3.05	0
0.03	60	1,970.00	197.00	0.1	2.29	-1.00
	120	1,660.00	332.00	0.2	2.52	-0.69
	300	1,480.00	740.00	0.5	2.87	-0.30
	600	1,250.00	1,250.00	1.0	3.10	0
0.04	60	2,530.00	253.00	0.1	2.40	-1.00
	120	2,320.00	464.00	0.2	2.67	-0.69
	300	1,940.00	970.00	0.5	2.99	-0.30
	600	1,760.00	1,760.00	1.0	3.25	0
0.05	60	3,240.00	324.00	0.1	2.51	-1.00
	120	2,610.00	522.00	0.2	2.72	-0.69
	300	2,390.00	1,195.00	0.5	3.08	-0.30
	600	2,270.00	2,270.00	1.0	3.36	0

Table 4.63: Experimental Data and Results For Rheological Properties of W-Mud (Already Existing Drilling Mud prepared with non-chemically modified Waxy corn starch)

Conc g/ml	Speed (rpm)	Viscosity μ(Poise)	Shear stress τ (mpa)	Shear rate $\gamma(s^{-1})$	Log τ	Log γ
0.01	60	820.00	82.00	0.1	1.91	-1.00
	120	710.00	142.00	0.2	2.15	-0.69
	300	680.00	340.00	0.5	2.53	-0.30
	600	430.00	430.00	1.0	2.63	0
0.02	60	1,310.00	131.00	0.1	2.12	-1.00
	120	1,150.00	230.00	0.2	2.36	-0.69
	300	1,020.00	510.00	0.5	2.71	-0.30
	600	870.00	870.00	1.0	2.94	0
0.03	60	1,580.00	158.00	0.1	2.20	-1.00
	120	1,370.00	274.00	0.2	2.44	-0.69
	300	1,260.00	630.00	0.5	2.80	-0.30
	600	1,090.00	1,090.00	1.0	3.04	0
0.04	60	2,000.00	200.00	0.1	2.30	-1.00
	120	1,830.00	366.00	0.2	2.56	-0.69
	300	1,790.00	895.00	0.5	2.95	-0.30
	600	1,680.00	1,680.00	1.0	3.23	0
0.05	60	2,600.00	260.00	0.1	2.41	-1.00
	120	2,470.00	494.00	0.2	2.69	-0.69
	300	2,300.00	1,150.00	0.5	3.06	-0.30
	600	2,180.00	2,180.00	1.0	3.34	0

Table 4.64: Experimental Data and Results For Rheological Properties of CMS-Mud (Widely-used Drilling Mud prepared with Chemically modified Carboxymethyl starch)

Conc g/ml	Speed (rpm)	Viscosity μ(Poise)	Shear stress τ (mpa)	Shear rate $\gamma(s^{-1})$	Log τ	Log γ
0.01	60	580.00	58.00	0.1	1.76	-1.00
	120	490.00	98.00	0.2	1.99	-0.69
	300	390.00	195.00	0.5	2.29	-0.30
	600	270.00	270.00	1.0	2.43	0
0.02	60	1,090.00	109.00	0.1	2.04	-1.00
	120	960.00	192.00	0.2	2.28	-0.69
	300	730.00	365.00	0.5	2.56	-0.30
	600	560.00	560.00	1.0	2.75	0
0.03	60	1,330.00	133.00	0.1	2.12	-1.00
	120	1,100.00	220.00	0.2	2.34	-0.69
	300	880.00	440.00	0.5	2.64	-0.30
	600	670.00	670.00	1.0	2.83	0
0.04	60	1,640.00	164.00	0.1	2.21	-1.00
	120	1,410.00	282.00	0.2	2.45	-0.69
	300	1,080.00	540.00	0.5	2.73	-0.30
	600	920.00	920.00	1.0	2.96	0
0.05	60	2,230.00	223.00	0.1	2.35	-1.00
	120	1,720.00	344.00	0.2	2.54	-0.69
	300	1,380.00	690.00	0.5	2.84	-0.30
	600	1,270.00	1,270.00	1.0	3.10	0

4.2.2.1 Shear Stress and Shear Rate Relationship

The relationship between shear stress and shear rate helps to characterize the fluid types and flow models of fluids. Fluid types and flow models are usually visualized by means of consistency curves, which are plots of either flow pressure versus flow rate or shear stress versus shear rate (Alderman et al., 2008; Candy & Justus, 2006; Obong, 2004; Staben et al., 2004). The equation relating shear stress and shear rate under this experimental condition is equation (3.3) (Bryan et al., 2010; Ukachukwu et al., 2010; Obong, 2004; Staben et al., 2004). Drilling muds are based on certain flow models, which include the Newtonian, the Pseudoplastic, the Bingham plastic, and the Dilatant (Alderman et al., 2008; Obong, 2004; Staben et al., 2004). The figures below are plots of shear stress versus shear rate to show fluid types and flow models of the different muds.

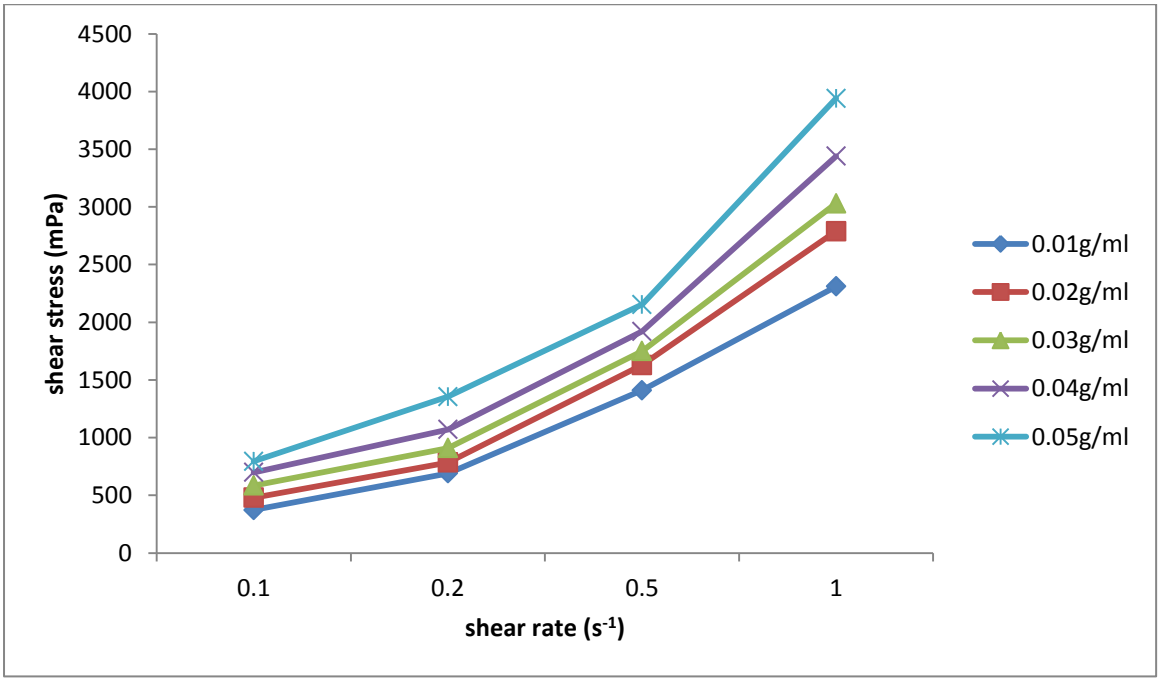

Figure 4.141: Plot of shear stress as a function of shear rate for G:W-Mud. (Data; Table 4.56)

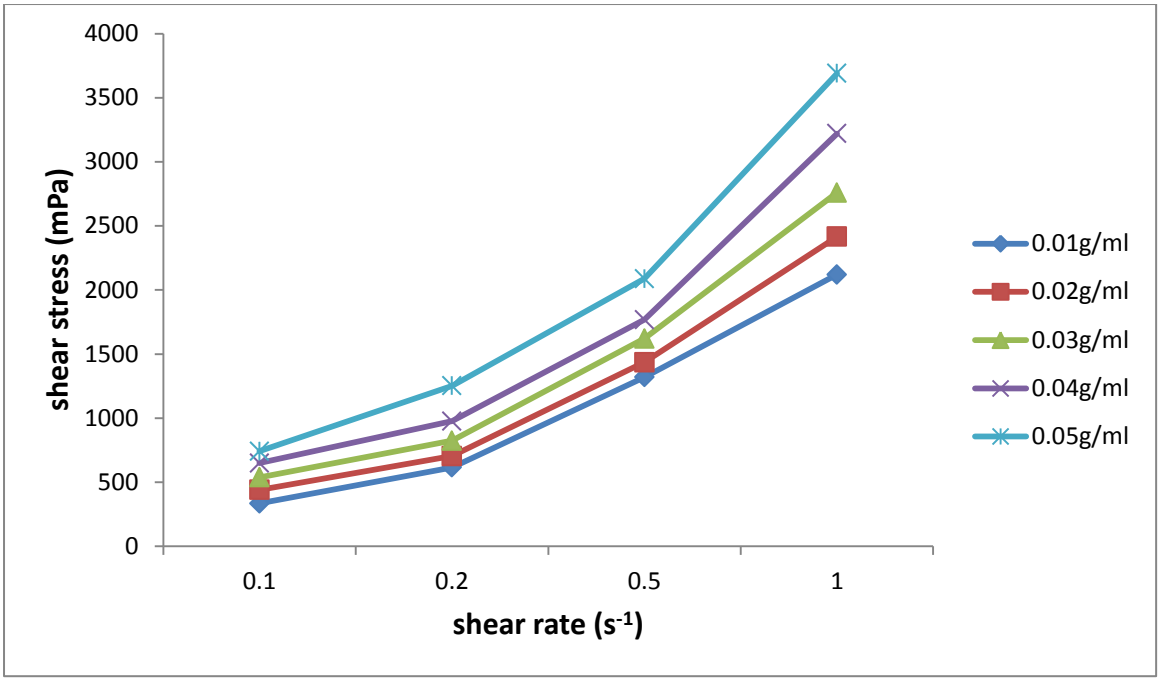

Figure 4.142: Plot of shear stress as a function of shear rate for M:W-Mud. (Data; Table 4.57)

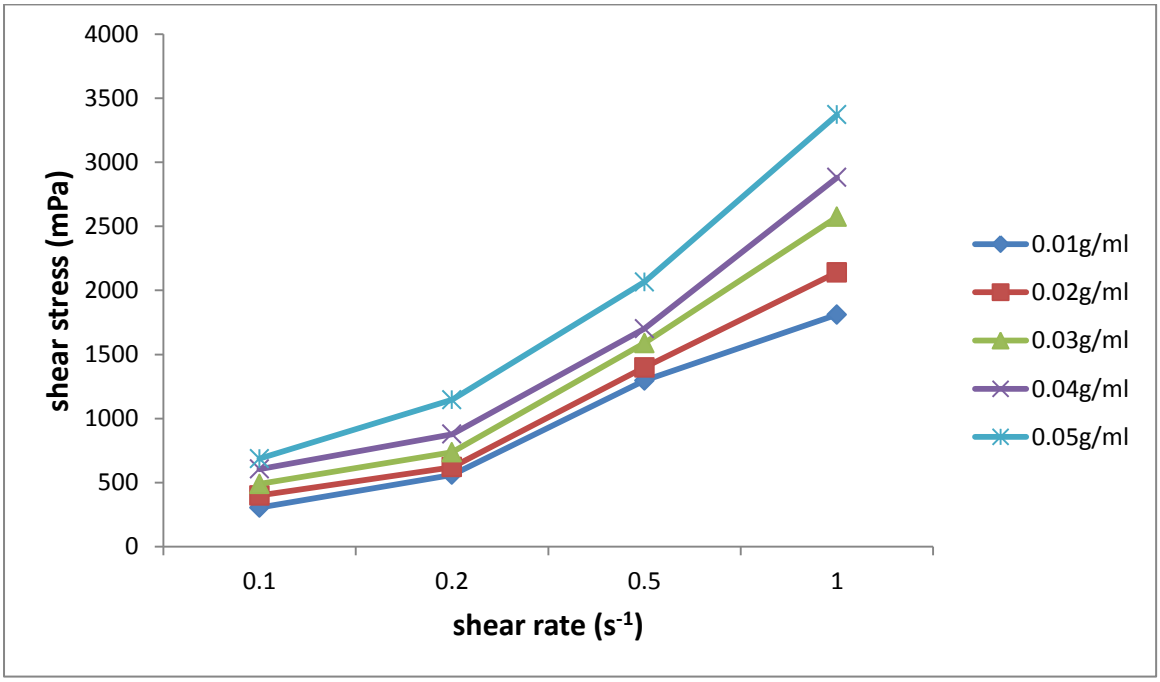

Figure 4.143: Plot of shear stress as a function of shear rate for P:W-Mud. (Data; Table 4.58)

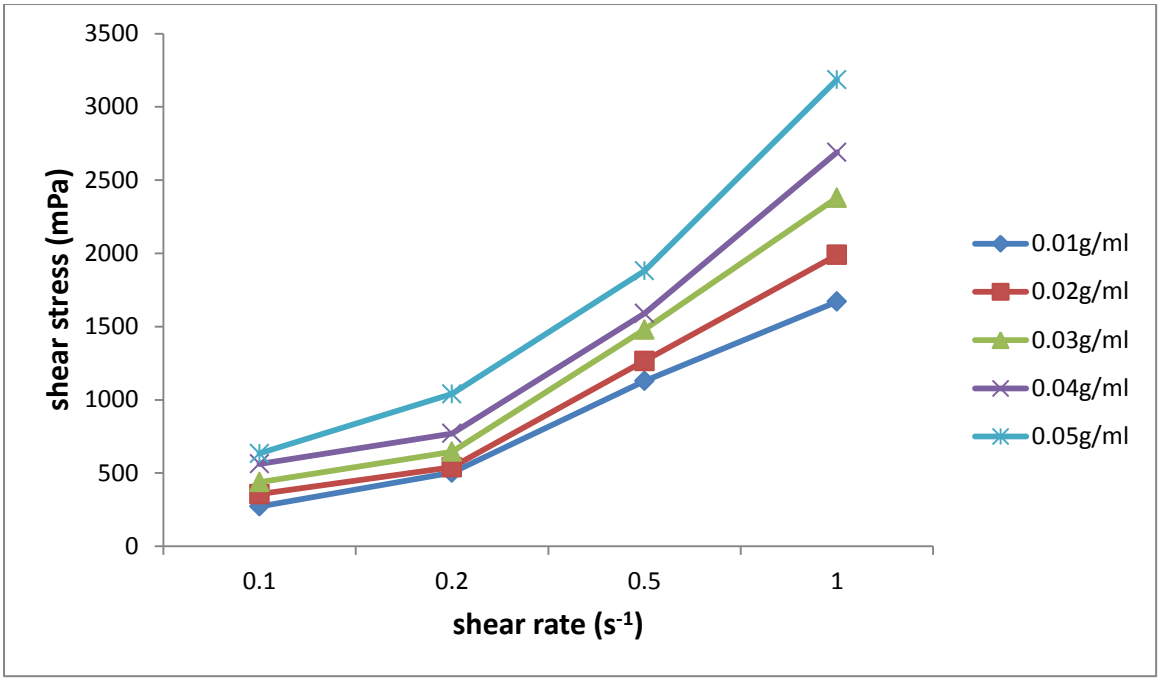

Figure 4.144: Plot of shear stress as a function of shear rate for G:M-Mud. (Data; Table 4.59)

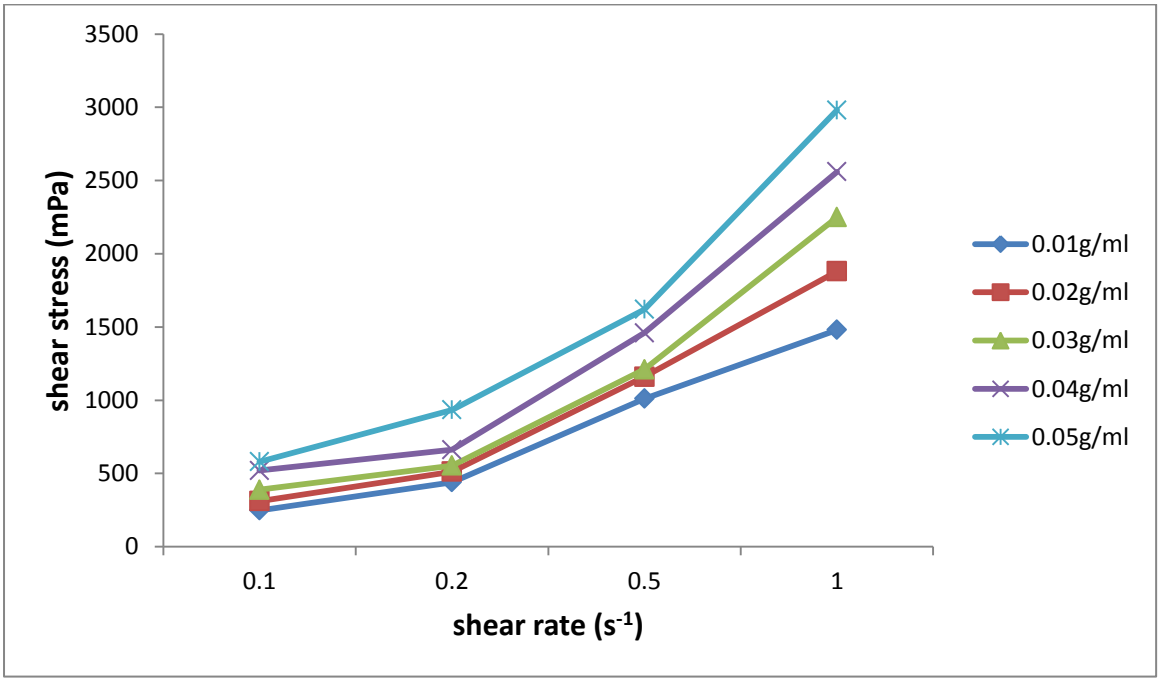

Figure 4.145: Plot of shear stress as a function of shear rate for G:P-Mud. (Data; Table 4.60)

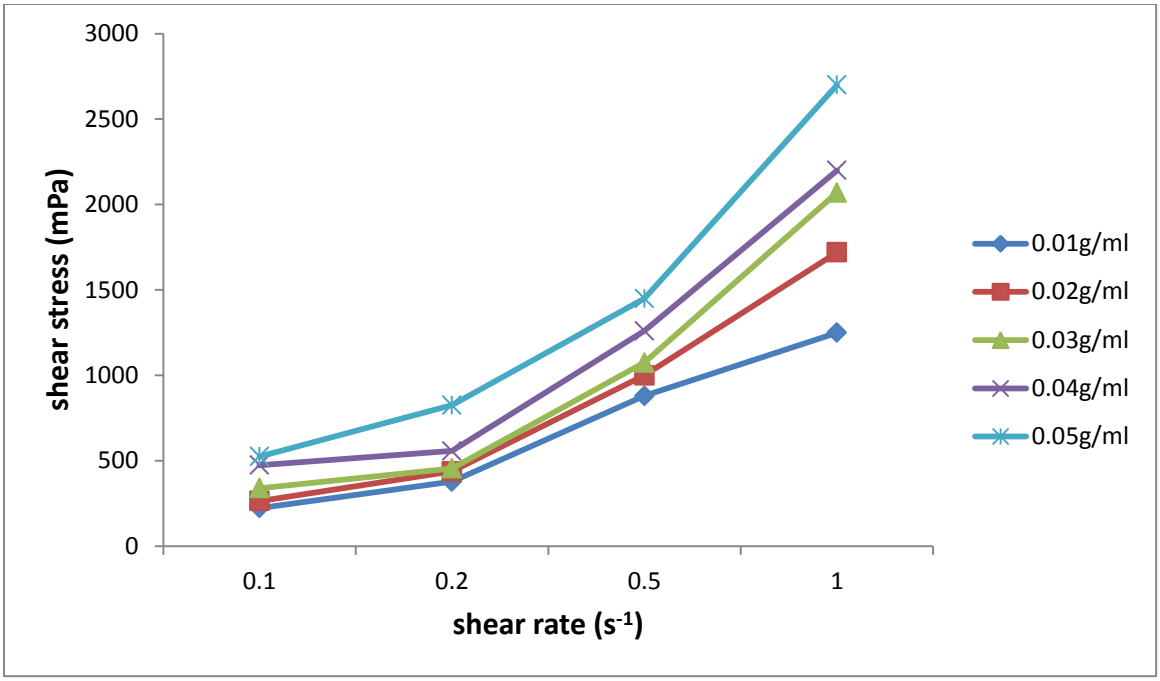

Figure 4.146: Plot of shear stress as a function of shear rate for M:P-Mud. (Data; Table 4.61)

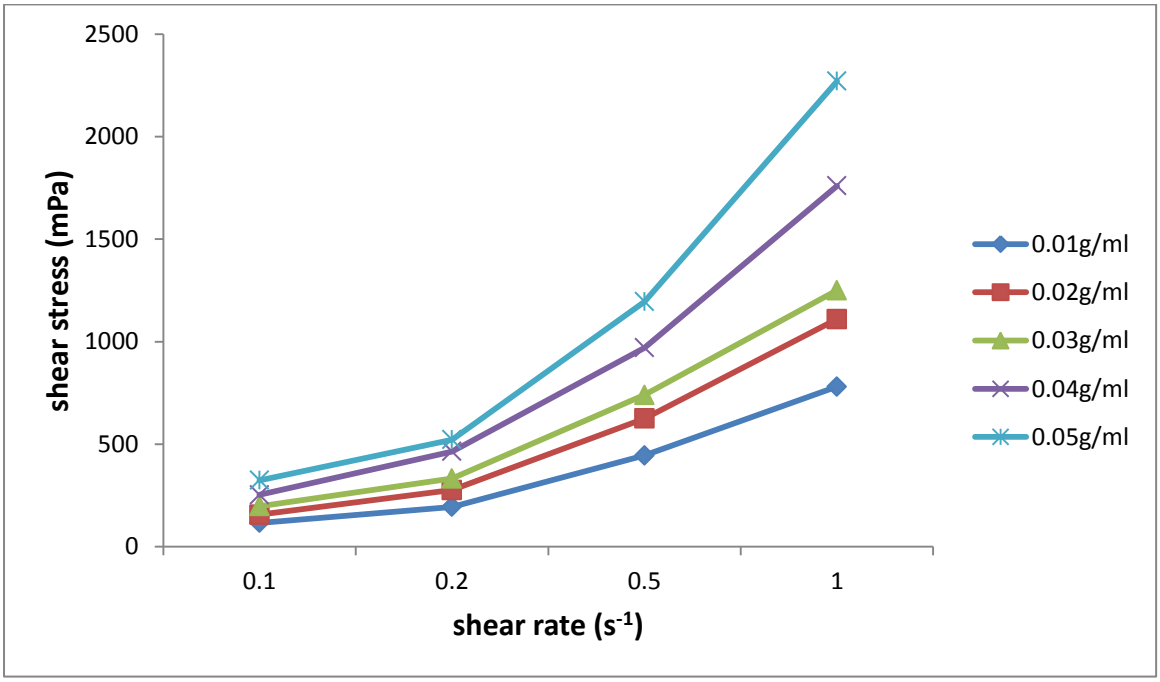

Figure 4.147: Plot of shear stress as a function of shear rate for CMS:HPS-Mud. (Data; Table 4.62)

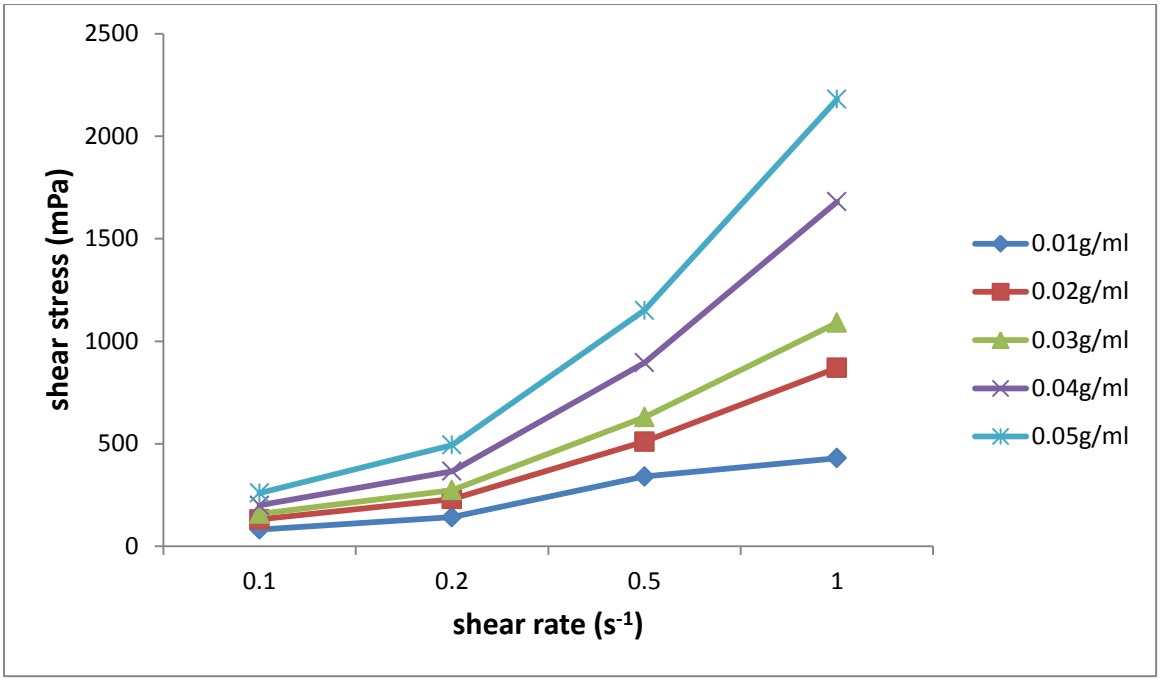

Figure 4.148: Plot of shear stress as a function of shear rate for W-Mud. (Data; Table 4.63)

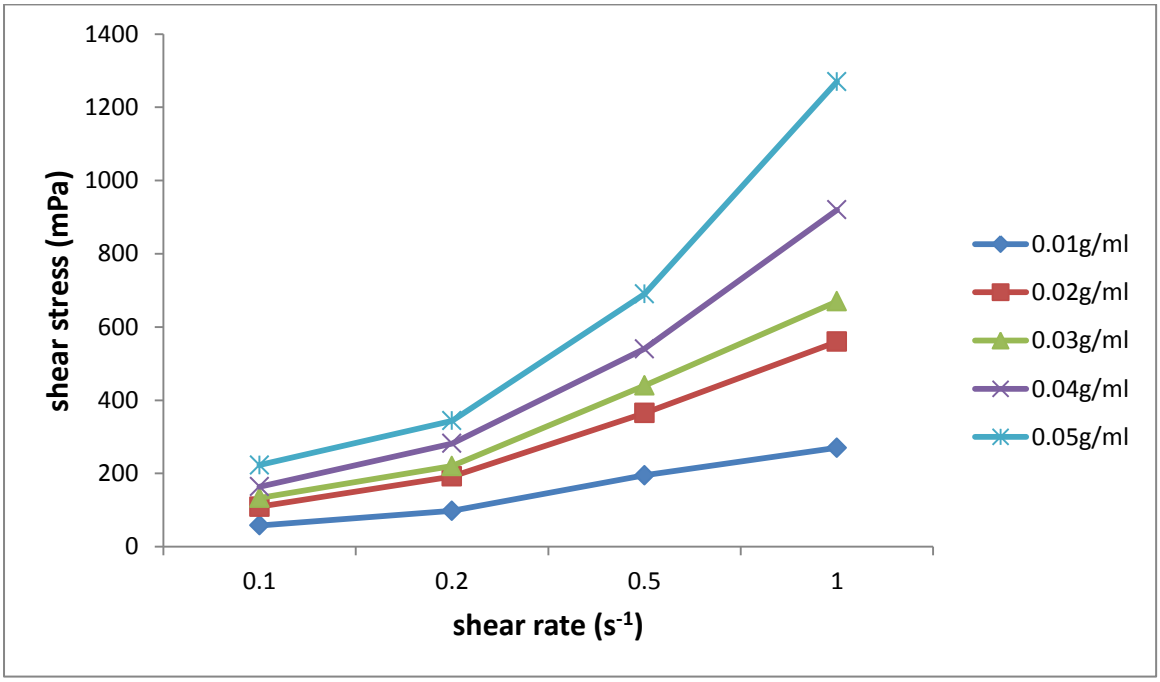

Figure 4.149: Plot of shear stress as a function of shear rate for CMS-Mud. (Data; Table 4.64)

Figures 4.141 to 4.149 show shear stress versus shear rate curves for G:W-Mud, M:W-Mud, P:W-Mud, G:M-Mud, G:P-Mud, M:P-Mud, CMS:HPS-Mud, W-Mud, and CMS-Mud. Inspection of the figures shows that the type of fluid displayed by the muds are Bingham plastic fluids or Pseudoplastic fluids according to the different concentrations within the shear rate range of 0.1-1.0 s^{-1}. Both Bingham plastic fluids and Pseudoplastic fluids are non-Newtonian fluids which have no linear relationship between shear stress and shear rate at the origin but can be linear at higher shear rate (Bryan et al., 2010; Qartar & Giacelo, 2010; Michael, 2009; Stewart, 2009; Alderman et al., 2008; Obong, 2004; Staben et al., 2004; Mandy, 2001). The patterns of the curves obtained under shear stress and shear rate relationship at the various concentrations show that the muds possess Pseudoplastic flow model. A mud is Pseudoplastic when the consistency curve obtained from shear stress and shear rate relationship, passes through the origin and is non linear, but approaches linearity at higher shear rate (Bryan et al., 2010; Qartar & Giacelo, 2010; Michael, 2009; Dahlgreen & Helbig, 2008; Obong, 2004; Staben et al., 2004; Gautier & Lecourtier, 2001). All the muds have non-linear consistency curves at the point of origin but the consistency curves could be linear at very high shear rate. The non-linear consistency curves and the level of non-linearity agree with the literature that drilling muds deviate from linearity at low shear rate, and the degree of deviation from linearity differ from mud to mud, depending on the concentration, size and shape of particles (Carriere, 2009; Rogers, 1991). Both Bingham plastic fluids and Pseudoplastic fluids are non-Newtonian. Non-Newtonian fluids are time independent, and this means that the relationship between shear stress and shear rate in a non-Newtonian fluid does not depend on the time for which the fluid has been previously sheared, that is its previous history (Stewart, 2009; Alderman et al., 2008). Also in time independent

fluids, the rate shear at any point in the fluid is some function of the shear stress at that point (Carriere, 2009). It is observed that the viscosity of each mud increase with increase in concentration of the starch-polymer. It is also observed that each of the new polymer muds (G:W-Mud, M:W-Mud, P:W-Mud, G:M-Mud, G:P-Mud, M:P-Mud) shows higher viscosity values than the already existing muds(CMS:HPS-Mud, W-Mud, CMS –Mud) at the various concentrations. Low concentration of the single and chemically modified starches shows little effect on the viscosity of the muds. This may be due to decrease in the particles' interaction on hydration caused by the unblending nature of the single starches and the chemicals used in the modification of the other two starches (Bryan et al., 2010; Amanullah, 2004). But, in the case of the new muds, relatively higher viscosity was obtained with low concentration of the pure and blended starches. Polymres are used in the formulation of muds to impart maximum viscosity at minimum solid content (Qartar & Giacelo, 2010; Stewart, 2009; Eyler & Pasteck, 2005; Enie & Giles, 2001). The maximum viscosity of each mud was obtained at the highest concentration, 0.05g/ml starch and the least shear rate, $0.1s^{-1}$. The values of viscosity and shear stress for the muds show that the new muds are more viscous and require to be sheared more than the already existing muds before they flow at all the concentrations. This may be due to the pure nature of the blends of starches used in preparing the muds. The viscosity of fluid can be modified to obtain any desirable rheological properties (Chris & James, 2005; Jay & Bruce, 2005).

4.2.2.2 Flow Models and Flow Patterns of the Muds

Flow behaviour or flow characteristics of fluids, including drilling mud, are based on certain flow models namely: the Newtonian, the Bingham plastic (Bingham bodies), the Pseudoplastic, and the Dilatant and only the first three are important to the drilling mud technology (Jax, 2010). Flow models can also be visualized by means of consistency curves, which are logarithmic plots of shear stress versus shear rate (Candy & Justus, 2006; Obong, 2004). This was obtained by putting equation (3.3) into logarithmic form. The flow model is Newtonian when the flow index n = 1, Pseudoplastic when n < 1, Dilatant when n > 1 (Byan et al., 2010; Ukachukwu et al., 2010; Obong, 2004; Staben et al., 2004). The flow models and the flow patterns of the new polymer muds and the already existing muds are shown in the figures below.

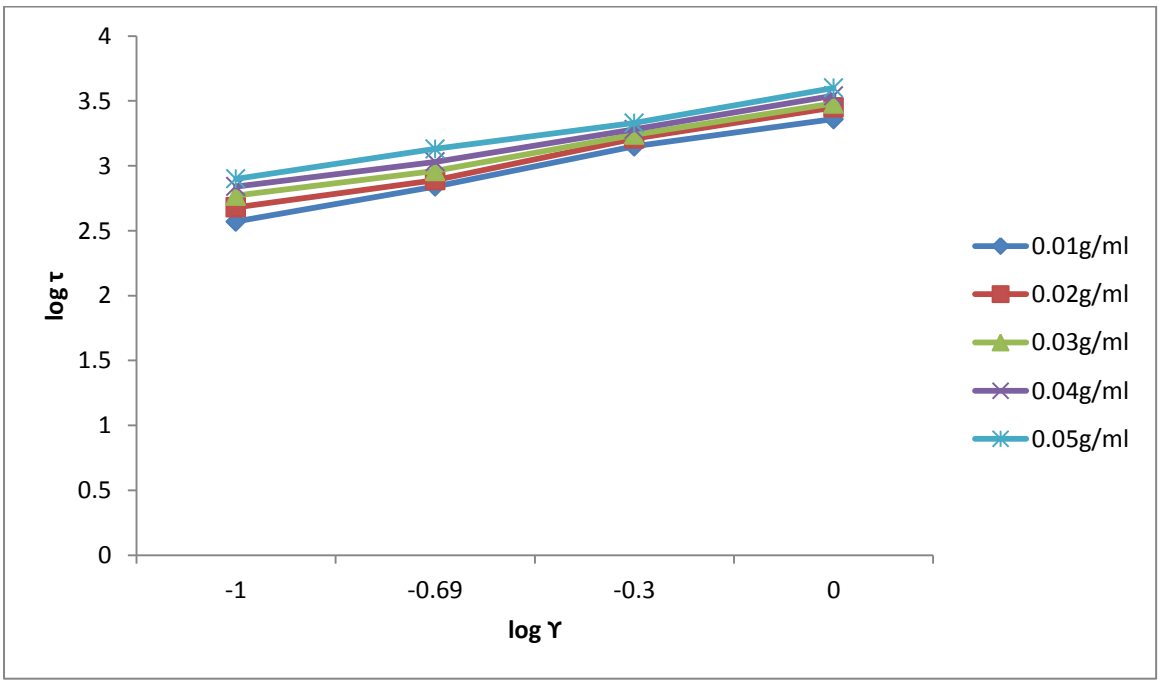

Figure 4.150: Plot of log shear stress (log τ) as a function of log shear rate (log Ϋ) for G:W-Mud. (Data; Table 4.56)

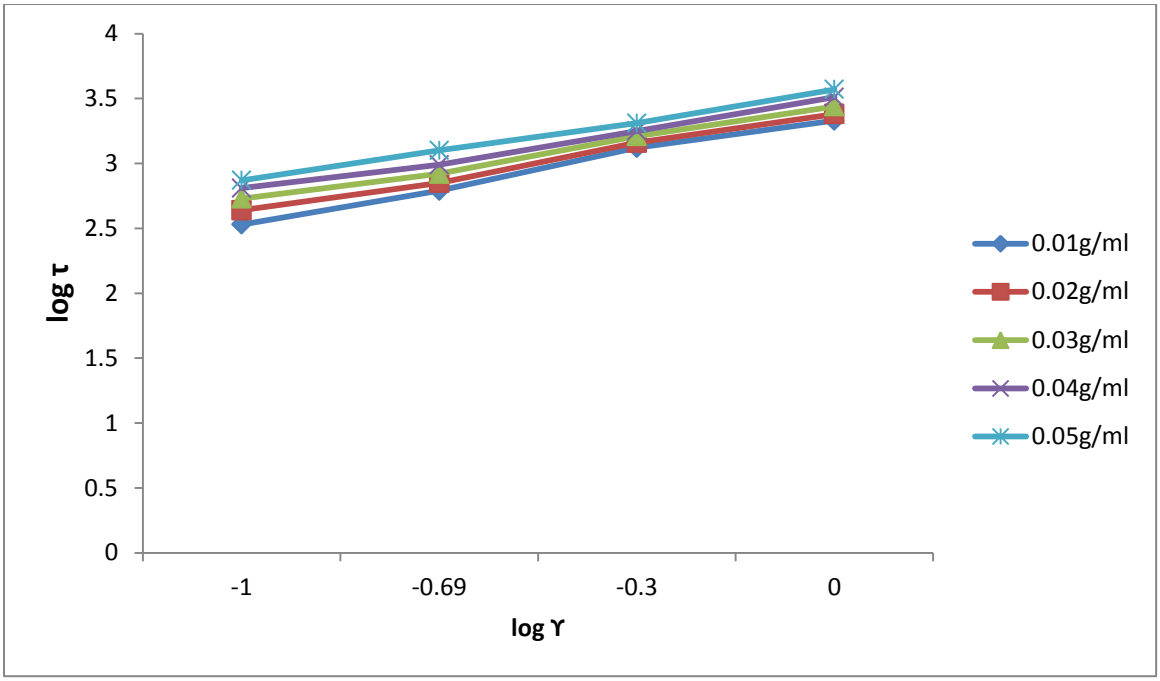

Figure 4.151: Plot of log shear stress (log τ) as a function of log shear rate (log Ϋ) for M:W-Mud. (Data; Table 4.57)

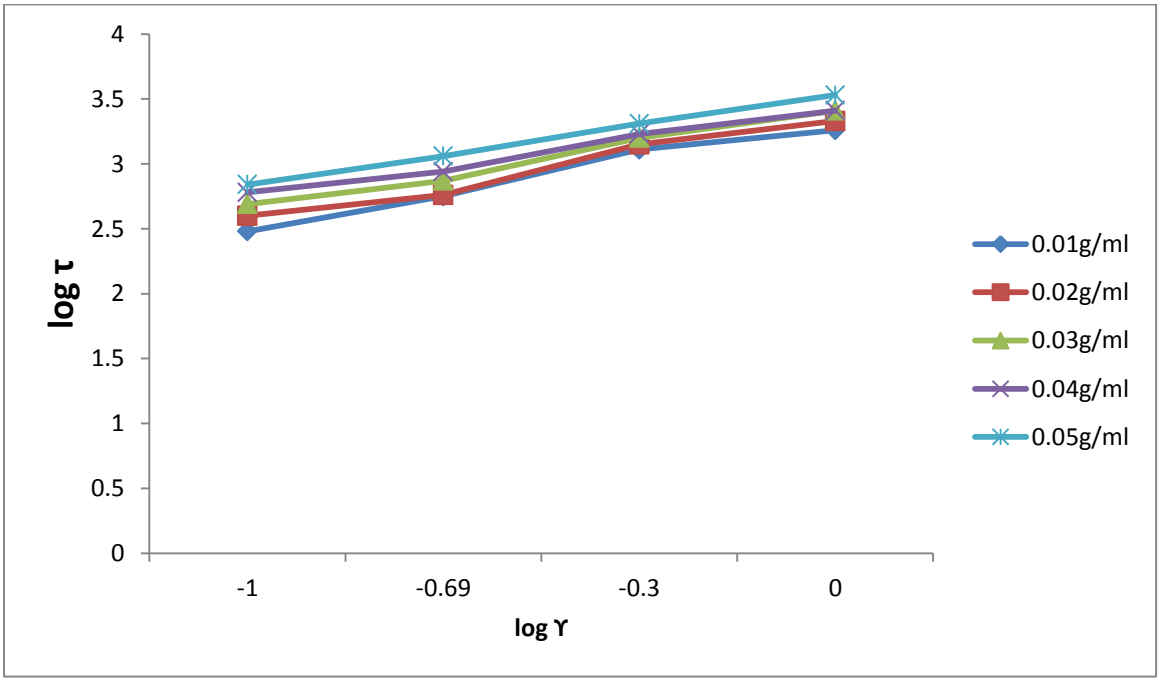

Figure 4.152: Plot of log shear stress (log τ) as a function of log shear rate (log Ϋ) for P:W-Mud. (Data; Table 4.58)

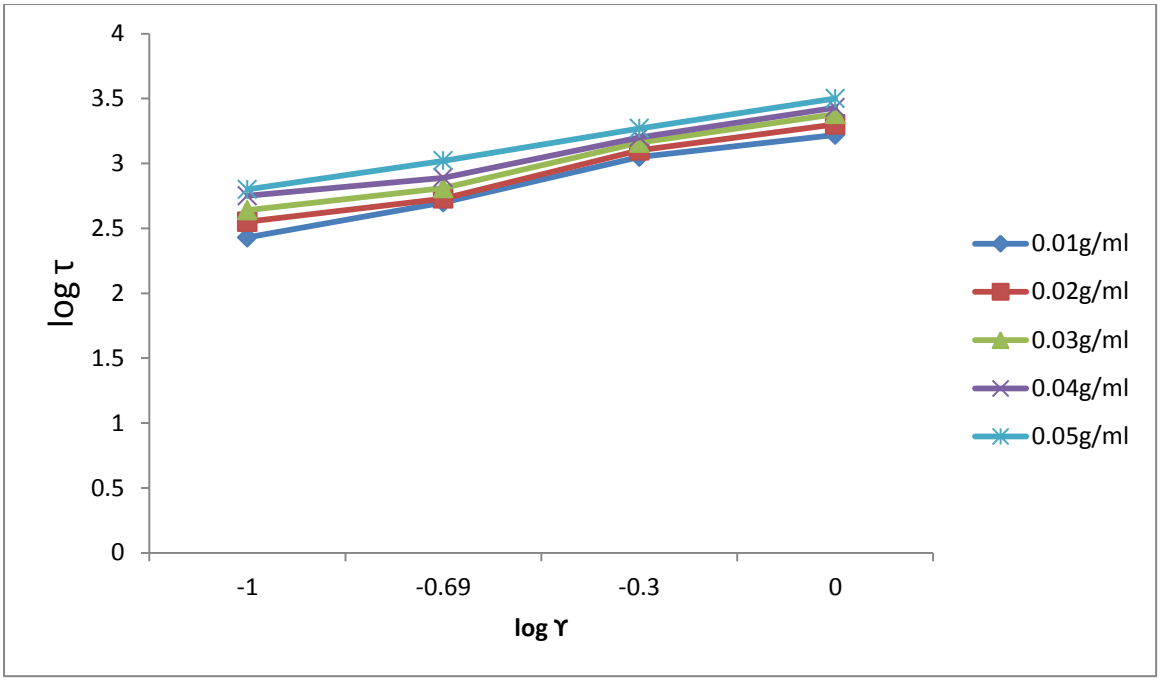

Figure 4.153: Plot of log shear stress (log τ) as a function of log shear rate (log Ɣ) for G:M-Mud. (Data; Table 4.59)

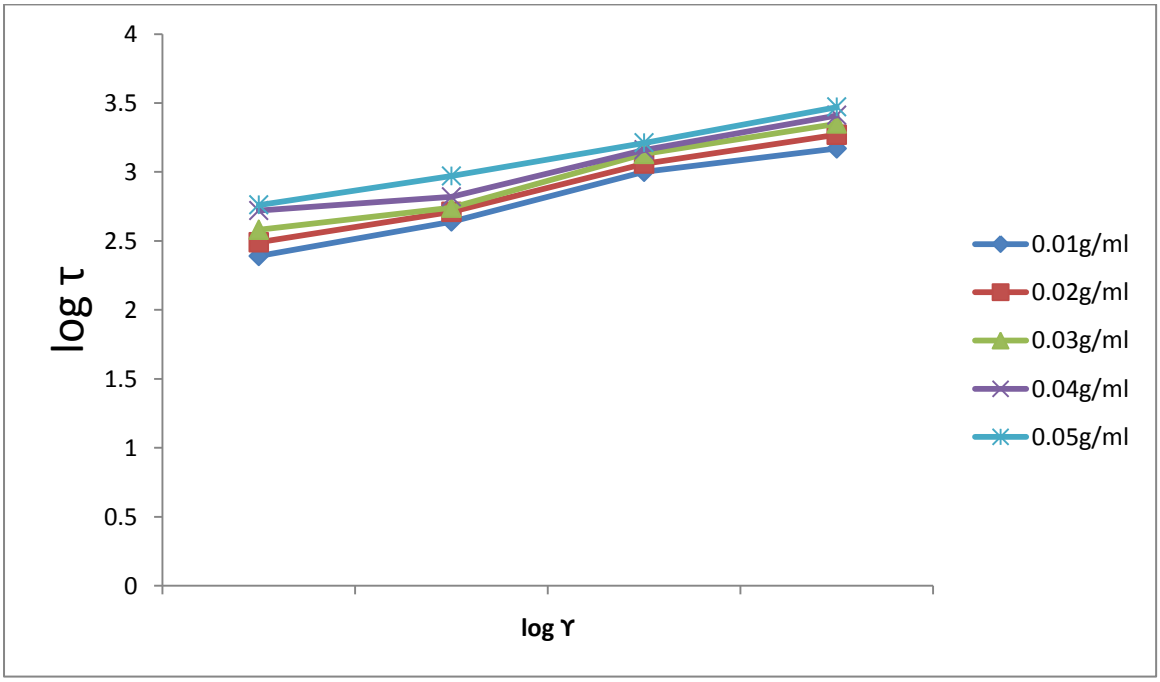

Figure 4.154: Plot of log shear stress (log τ) as a function of log shear rate (log Ɣ) for G:P-Mud. (Data; Table 4.60)

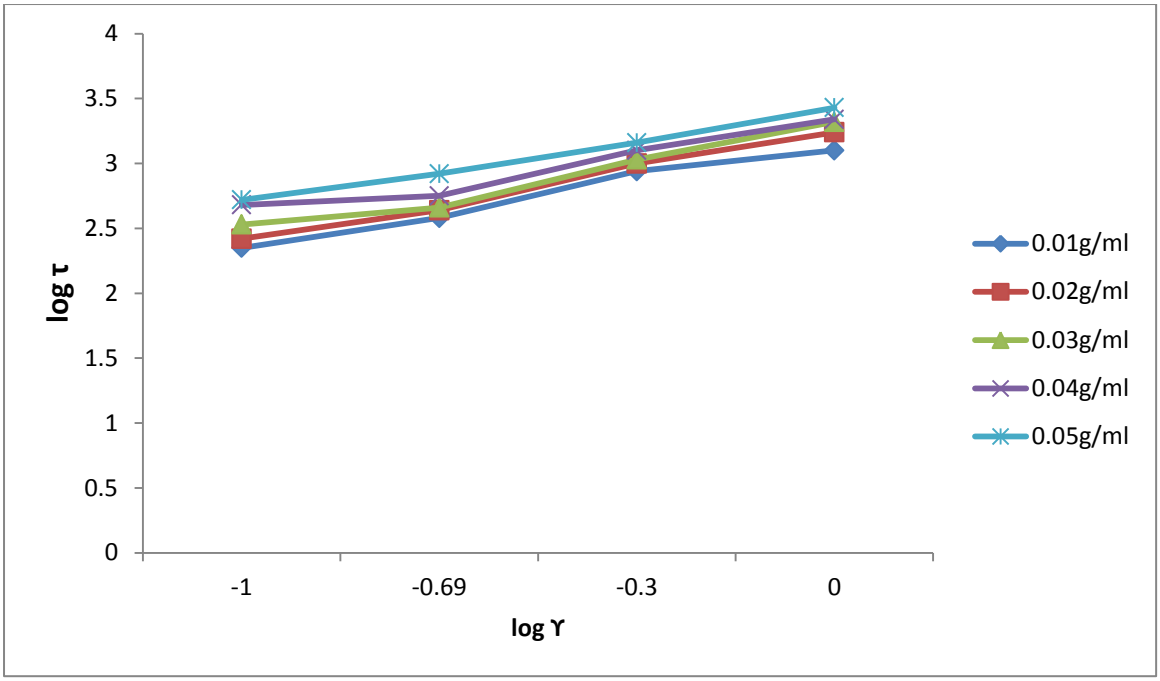

Figure 4.155: Plot of log shear stress (log τ) as a function of log shear rate (log Ɣ) for M:P-Mud. (Data; Table 4.61)

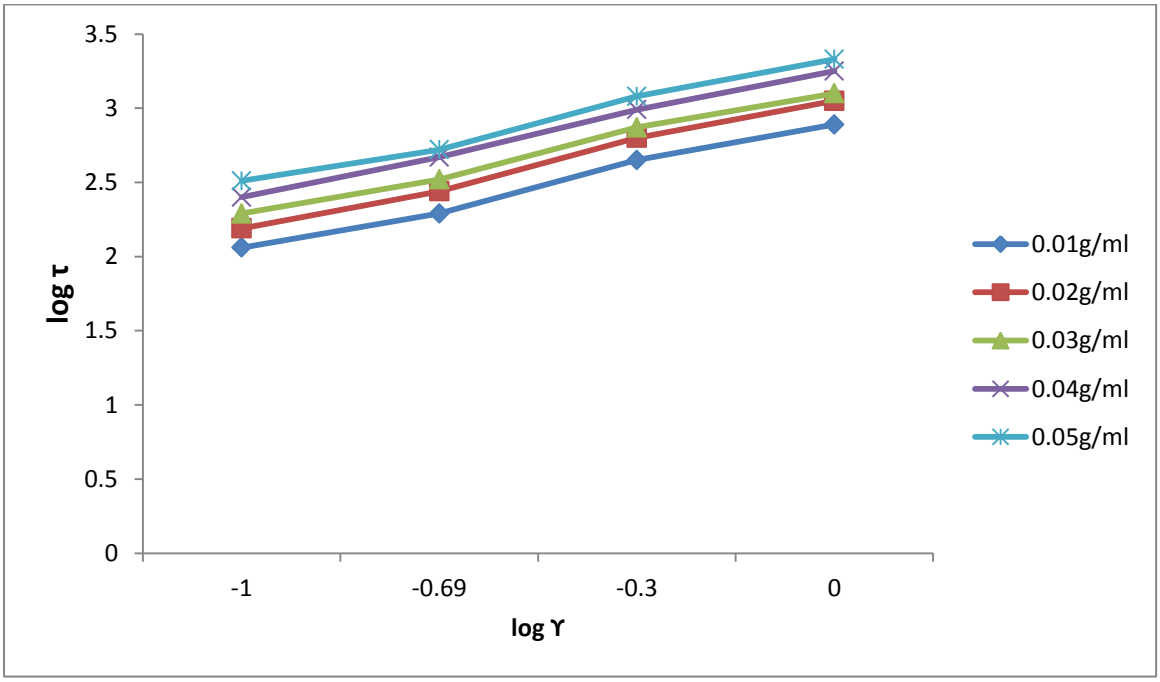

Figure 4.156: Plot of log shear stress (log τ) as a function of log shear rate (log Ɣ) for CMS:HPS-Mud. (Data; Table 4.62)

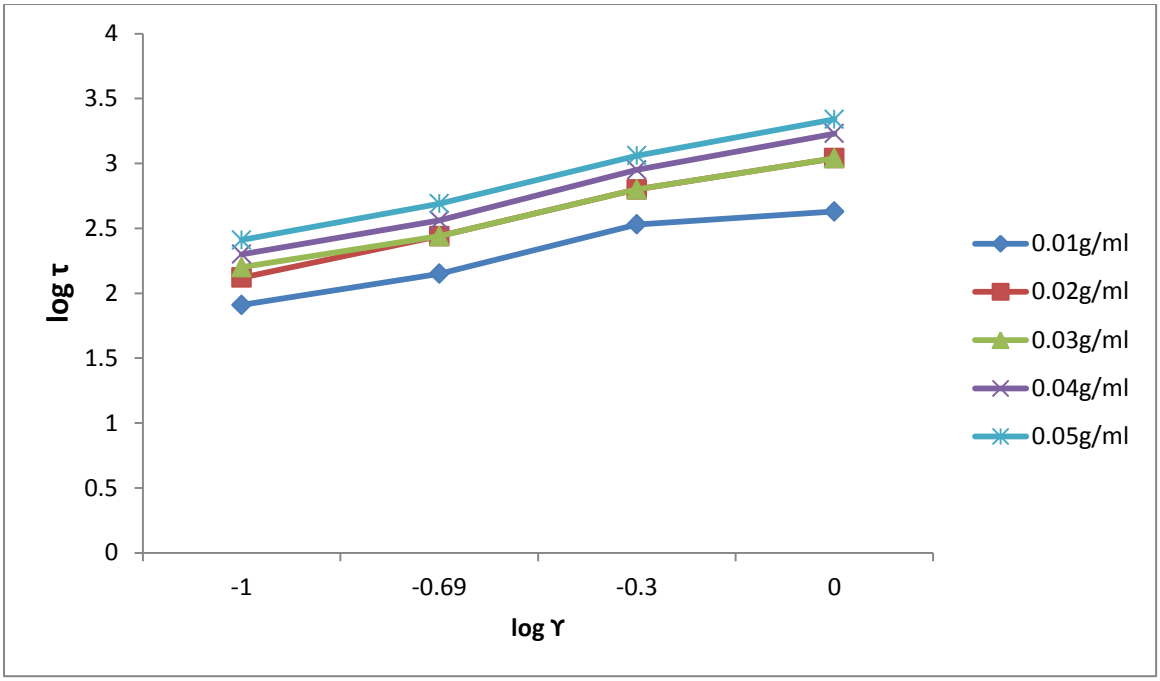

Figure 4.157: Plot of log shear stress (log τ) as a function of log shear rate (log Ɣ) for W-Mud. (Data; Table 4.63)

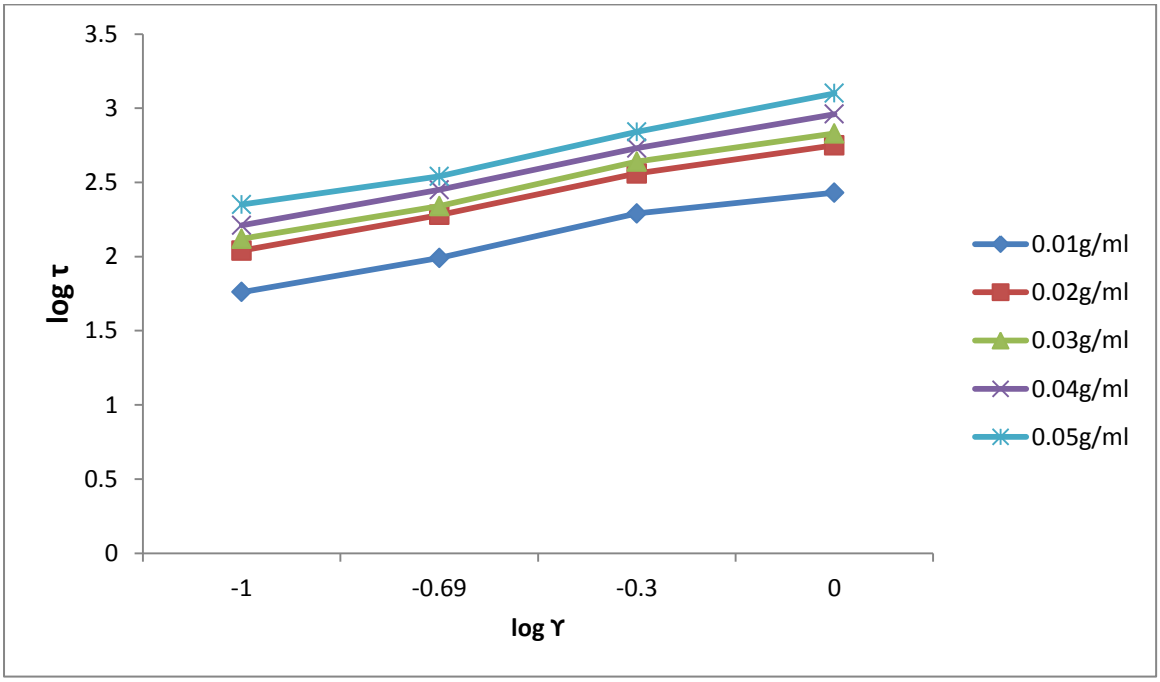

Figure 4.158: Plot of log shear stress (log τ) as a function of log shear rate (log Ɣ) for CMS-Mud. (Data; Table 4.64)

Figures 4.150 – 4.158 show logarithmic plots of shear stress (log τ) versus shear rate (log γ) for G:W-Mud, M:W-Mud, P:W-Mud, G:M-Mud, G:P-Mud, M:P-Mud, CMS:HPS-Mud, W-Mud and CMS-Mud. Analysis of the figures shows that there is linear variation between logarithm of shear stress and shear rate.

Tables 4.65 – 4.73 show the values of flow index n, and consistency index K, obtained using Power Law equation (see Equation 3.3). It is observed from the table that the flow index n is less than 1.0 for each mud at the various concentrations. This indicates that each of the muds shows Pseudoplastic flow model. The flow index n is a measure of the degree of flow behaviour of a fluid (Bryan et al., 2010; Staben et al., 2004). A fluid for which the value of n is less than 1 ($n < 1$) is said to have Pseudoplastic flow model (Bryan et al., 2010). The maximum and minimum flow index n values of 0.55 & 0.44, 0.59 & 0.50, 0.0.63 & 0.54, 0.68 & 0.55, 0.74 & 0.61, 0.77 & 0.65, 0.87 & 0.71, 0.91 & 0.75, and 0.96 & 0.80 were obtained for G:W-Mud, M:W-Mud, P:W-Mud, G:M-Mud, G:P-Mud, M:P-Mud, CMS:HPS-Mud, W-Mud and CMS-Mud respectively.

Further observation from the tables shows that the flow index n decreases, while the consistency index k increases with increase in concentration for each mud. The increase in the values of k with increase in concentration corresponds to the overall thickness of the mud. The consistency index k of a mud is a measure of the thickness of the mud and the extent to which it can carry cuttings (Ukachukwu et al., 2010; Obong, 2004; Staben et al., 2004). The maximum and minimum values of consistency index k obtained with G:W-Mud, M:W-Mud, P:W-Mud, G:M-Mud, G:P-Mud, M:P-Mud, CMS:HPS-Mud, W-Mud and CMS-Mud are 3.90 & 2.88, 3.86 & 2.79, 3.74 & 2.71, 3.69 & 2.67, 3.67 & 2.65, 3.56 & 2.61, 3.45 & 2.48, 3.26 & 2.31, and 3.19 & 2.26 respectively. The dependence of flow index and consistency index on concentration, and the values of n and k show that the muds obeyed power law model (Bryan et al., 2010; Qartar & Giacelo, 2010; Michael, 2009) shown in Equation 3.3.

Table 4.65 : Computed Values of Flow Index and Consistency Index for G:W-Mud sample with different Concentrations of Starch under Power Law Equation

Conc g/ml	Flow Index (n)	Consistency (κ)
0.01	0.55	2.88
0.02	0.53	2.99
0.03	0.47	3.68
0.04	0.45	3.76
0.05	0.44	3.90

Table 4.66 : Computed Values of Flow Index and Consistency Index for M:W-Mud sample with different Concentrations of Starch under Power Law Equation

Conc g/ml	Flow Index (n)	Consistency (κ)
0.01	0.59	2.79
0.02	0.58	2.89
0.03	0.54	3.61
0.04	0.51	3.69
0.05	0.50	3.86

Table 4.67: Computed Values of Flow Index and Consistency Index for P:W-Mud sample with different Concentrations of Starch under Power Law Equation

Conc g/ml	Flow Index (n)	Consistency (κ)
0.01	0.63	2.71
0.02	0.61	2.83
0.03	0.57	3.52
0.04	0.56	3.66
0.05	0.54	3.74

Table 4.68 : Computed Values of Flow Index and Consistency Index for G:M-Mud sample with different Concentrations of Starch under Power Law Equation

Conc g/ml	Flow Index (n)	Consistency (κ)
0.01	0.68	2.67
0.02	0.65	2.81
0.03	0.60	3.49
0.04	0.58	3.55
0.05	0.55	3.69

Table 4.69 : Computed Values of Flow Index and Consistency Index for G:P-Mud sample with different Concentrations of Starch under Power Law Equation

Conc g/ml	Flow Index (n)	Consistency (κ)
0.01	0.74	2.65
0.02	0.70	2.78
0.03	0.66	3.46
0.04	0.64	3.50
0.05	0.61	3.67

Table 4.70 : Computed Values of Flow Index and Consistency Index for M:P-Mud sample with different Concentrations of Starch under Power Law Equation

Conc g/ml	Flow Index (n)	Consistency (κ)
0.01	0.77	2.61
0.02	0.75	2.69
0.03	0.69	3.42
0.04	0.67	3.48
0.05	0.65	3.56

Table 4.71: Computed Values of Flow Index and Consistency Index for CMS:HPS-Mud sample with different Concentrations of Starch under Power Law Equation

Conc g/ml	Flow Index (n)	Consistency (κ)
0.01	0.87	2.48
0.02	0.83	2.54
0.03	0.76	3.38
0.04	0.74	3.43
0.05	0.71	3.45

Table 4.72: Computed Values of Flow Index and Consistency Index for W-Mud sample with different Concentrations of Starch under Power Law Equation

Conc g/ml	Flow Index (n)	Consistency (κ)
0.01	0.91	2.31
0.02	0.85	2.47
0.03	0.79	2.75
0.04	0.77	3.18
0.05	0.75	3.26

Table 4.73: Computed Values of Flow Index and Consistency Index for CMS-Mud sample with different Concentrations of Starch under Power Law Equation

Conc g/ml	Flow Index (n)	Consistency (κ)
0.01	0.96	2.26
0.02	0.93	2.38
0.03	0.84	2.64
0.04	0.81	2.99
0.05	0.80	3.19

4.2.2.3 Yield stress and Gel strength of the Muds

Table 4.74 shows the values of yield stress obtained using Herschel BuIkely equation (see Equation 3.4). It is observed from the table that yield stress increased with increase in concentration. Also, from the table, it is observed that the values of yield stress obtained with each starch concentration for each of the new muds (G:W-Mud, M:W-Mud, P:W-Mud, G:M-Mud, G:P-Mud, M:P-Mud), are higher than those of CMS:HPS-Mud, W-Mud and CMS-Mud. G:W-Mud gave the highest yield stress value as 2,069.00 mPa. Yield stress is the minimum shear stress needed to produce viscous flow and the viscosity of these fluids is dependent on the shear rate, and is known as "Apparent viscosity" (Bryan et al., 2010; Qartar & Giacelo, 2010; Obong, 2004; Vincent et al., 2001). Yield stress is related to gel strength of a mud, and the higher the yield stress, the higher the gel strength which results in higher viscosity (Michael, 2009; Chilingarian & Varabutre, 2000). This implies that a higher shear stress is required to break the gel structure of a more viscous polymer mud before flow starts. An explanation to this is, that at rest, the polymer chains are randomly

entangled, but they do not set up a structure because the electrostatic forces are predominantly repulsive. This leads to high viscosity, high gel strength and high yield stress. But when the mud is in motion, the chains tend to align themselves parallel to the direction of flow, and the alignment increases with increase in shear rate, and decrease in viscosity (shear thinning). Also, there is high inter-particles' interaction for highly viscous polymer mud which corresponds to a state of maximum flocculation (Michael, 2009; Jill & Poka, 2003). Each of the new polymer muds gave higher viscosity and showed better flocculation than the already existing, widely used muds. Moderate viscosity of fluid helps it to gain access into the minutest pores of the unstable rocks, which accelerates their deformation and caving (Chris & James, 2005). The estimated values of yield stress for all the muds are given below.

Table 4.74: Estimated values of yield stress from Herschel Bulkely model for the various muds with varying starch concentrations.

	Yield Stress Values (mPa)				
Muds/Samples	0.01g/ml	0.02g/ml	0.03g/ml	0.04g/ml	0.05g/ml
G:W-Mud	1,204.00	1,429.00	1,577.00	1,790.00	2,069.00
M:W-Mud	1,112.00	1,256.00	1,446.00	1,650.00	1,860.00
P:W-Mud	1,020.00	1,144.00	1,352.00	1,520.00	1,780.00
G:M-Mud	877.00	1,043.00	1,210.00	1,395.00	1,598.00
G:P-Mud	796.00	974.00	1,106.00	1,312.00	1,499.00
M:P-Mud	698.00	887.00	995.00	1,110.00	1,270.00
CMS:HPS-Mud	396.00	598.00	687.00	876.00	982.00
W-Mud	310.00	496.00	570.00	740.00	840.00
CMS-Mud	240.00	397.00	460.00	630.00	725.00

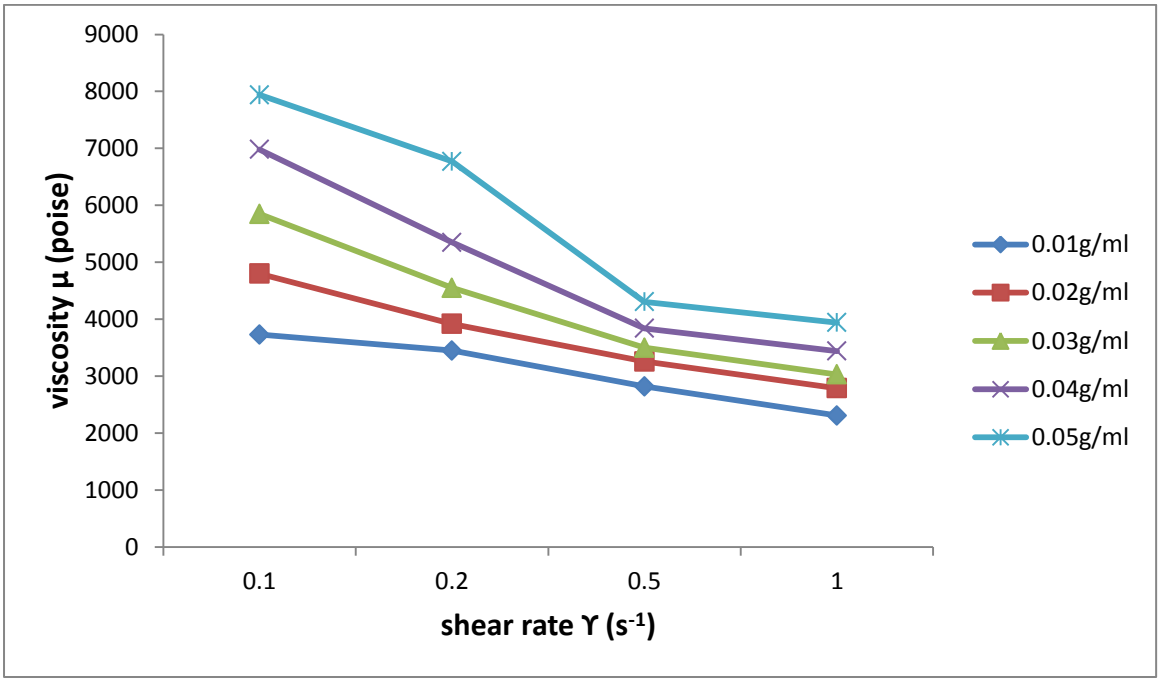

Figure 4.159: Plot of shear rate dependence of viscosity for G:W-Mud. (Data; Table 4.56)

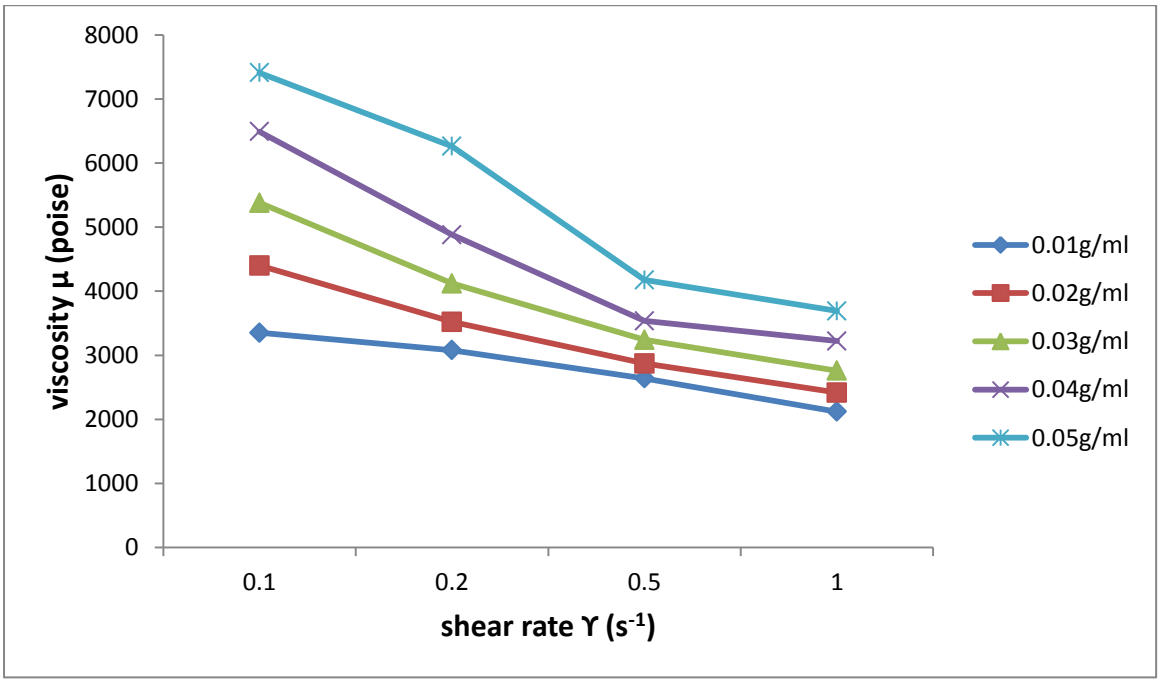

Figure 4.160: Plot of shear rate dependence of viscosity for M:W-Mud. (Data; Table 4.57)

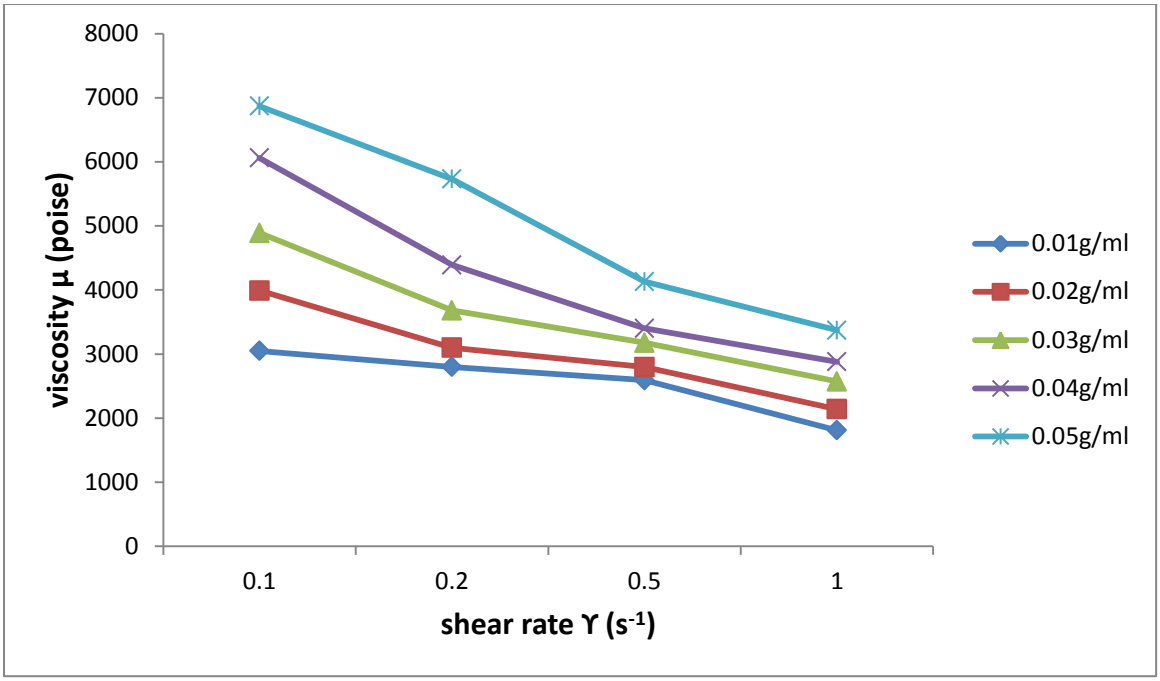

Figure 4.161: Plot of shear rate dependence of viscosity for P:W-Mud. (Data; Table 4.58)

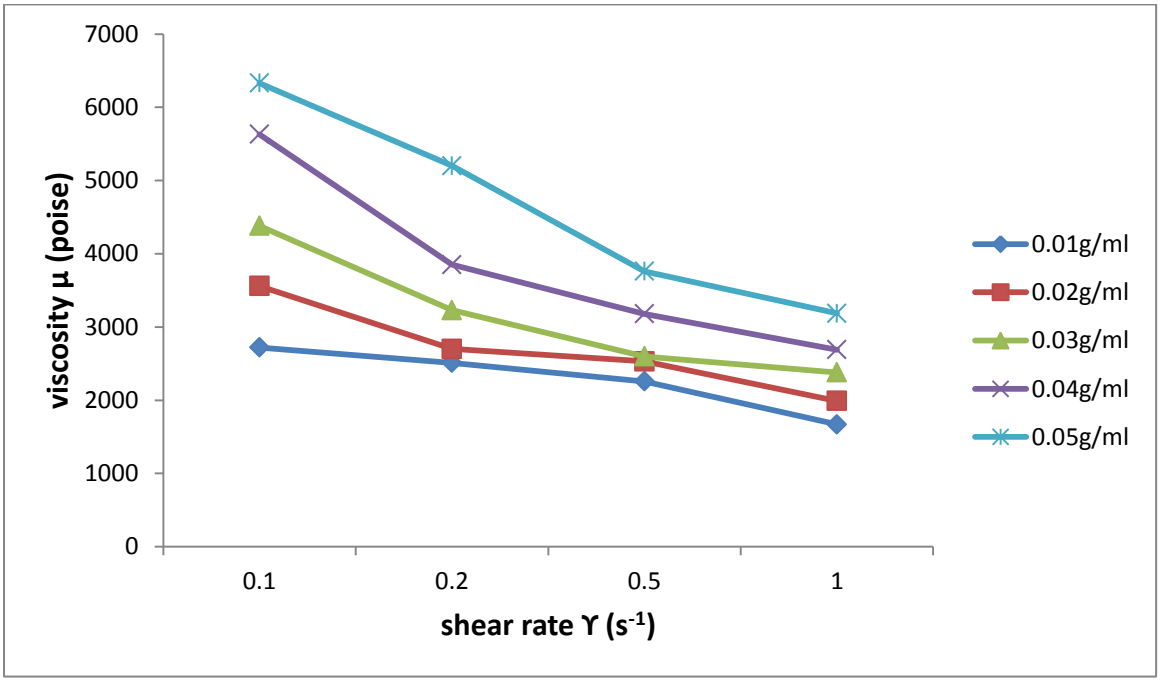

Figure 4.162: Plot of shear rate dependence of viscosity for G:M-Mud. (Data; Table 4.59)

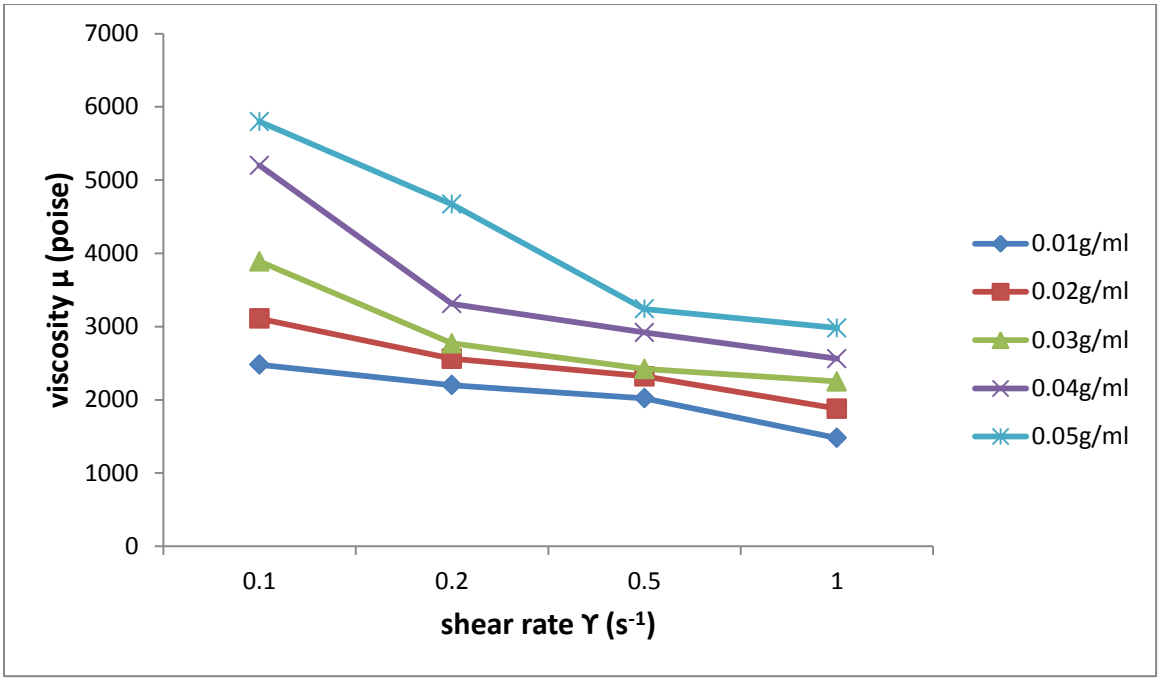

Figure 4.163: Plot of shear rate dependence of viscosity for G:P-Mud. (Data; Table 4.60)

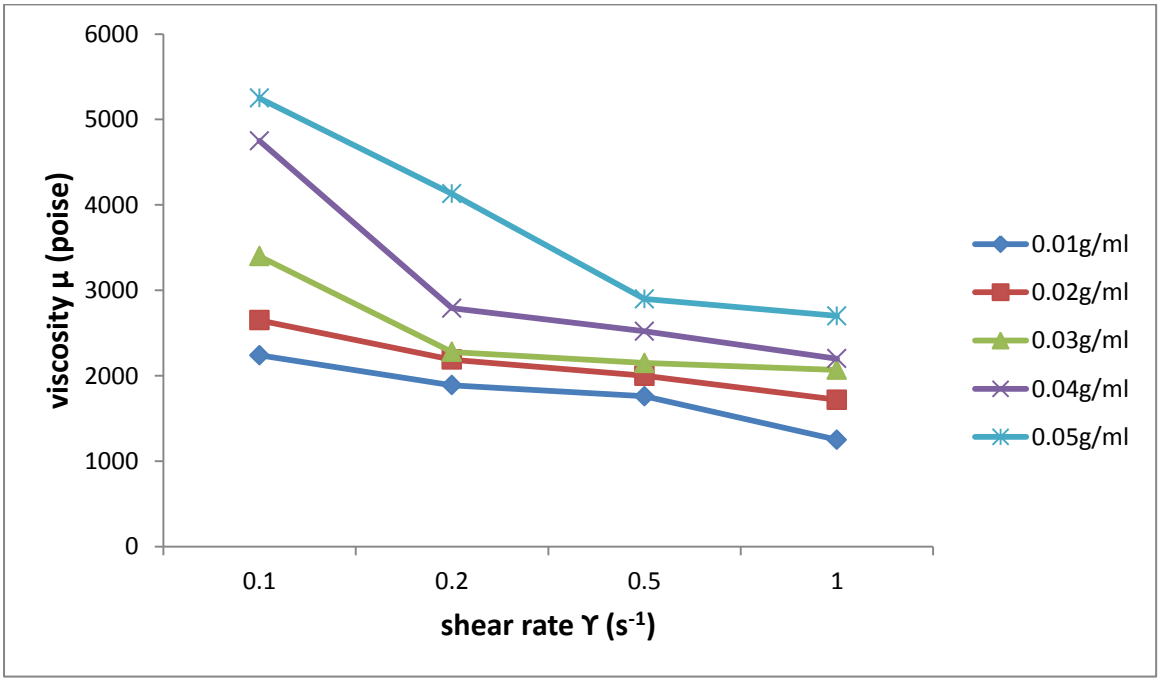

Figure 4.164: Plot of shear rate dependence of viscosity for M:P-Mud. (Data; Table 4.61)

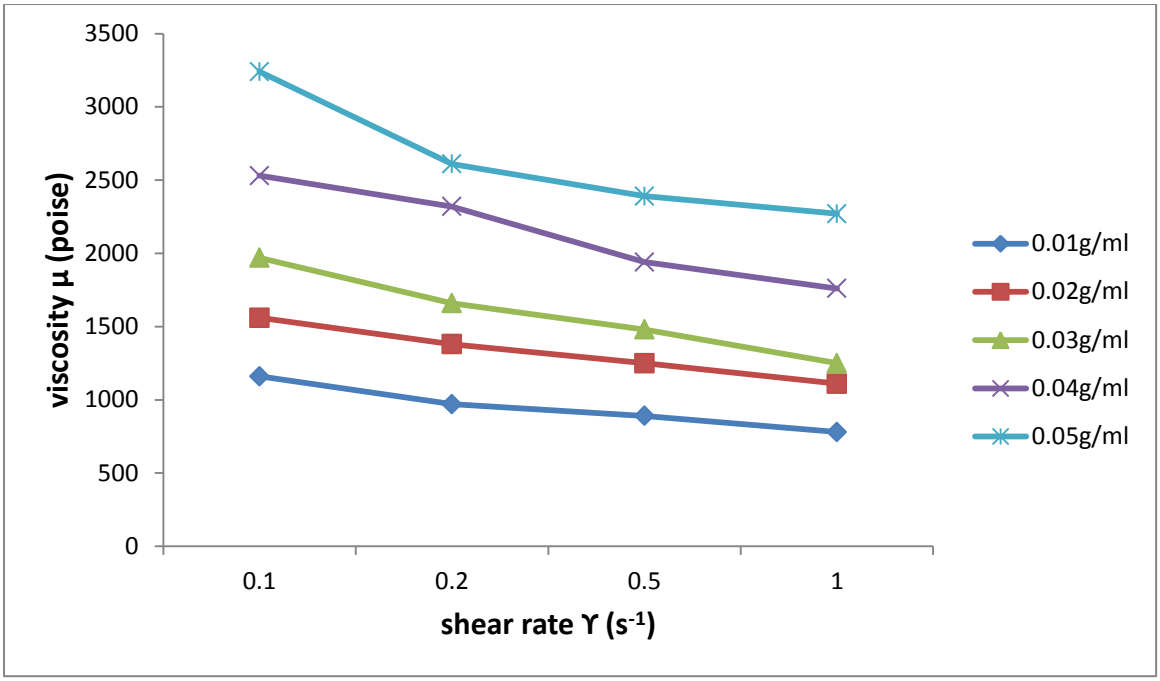

Figure 4.165: Plot of shear rate dependence of viscosity for CMS:HPS-Mud. (Data; Table 4.62)

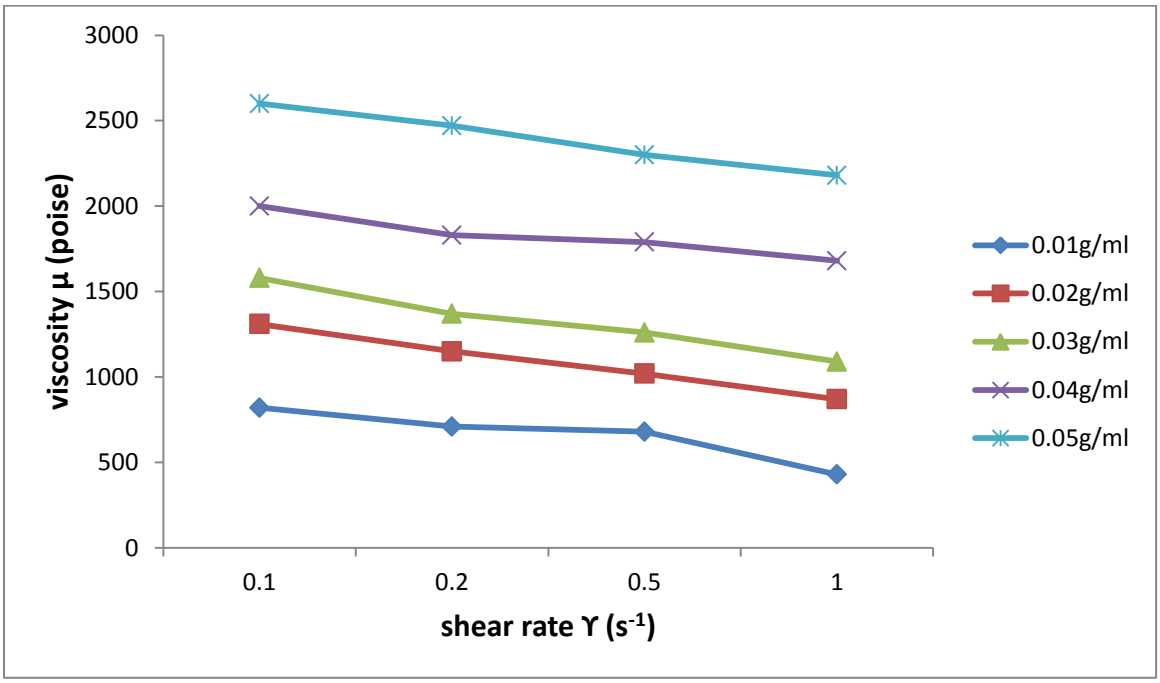

Figure 4.166: Plot of shear rate dependence of viscosity for W-Mud. (Data; Table 4.63)

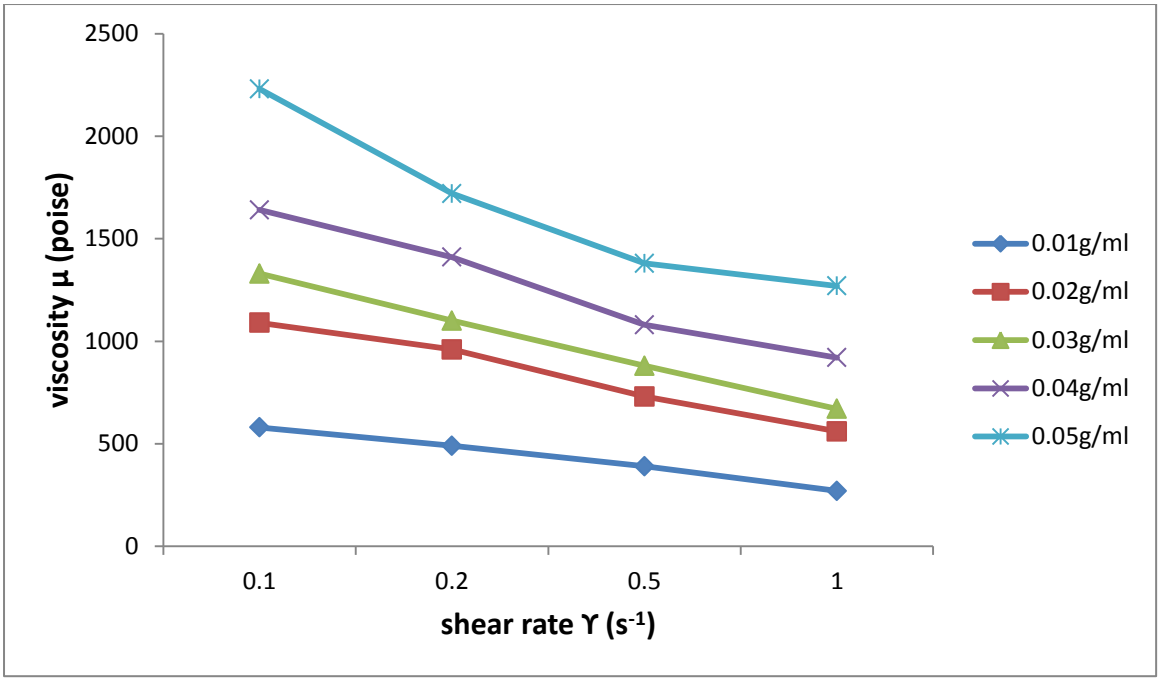

Figure 4.167: Plot of shear rate dependence of viscosity for CMS-Mud. (Data; Table 4.64)

4.2.2.4 Shear Rate Dependence of Viscosity

Figures 4.159 – 4.167 above show plots of shear rate dependence of viscosity for G:W-Mud, M:W-Mud, P:W-Mud, G:M-Mud, G:P-Mud, M:P-Mud, CMS:HPS-Mud, W-Mud and CMS-Mud respectively. Inspection of the figures shows that the viscosity of the various muds is dependent on shear rate. In this dependence, viscosity decreases with increasing shear rate (This is shear thinning). This indicates that the polymer muds possess shear thinning behaviours. Shear thinning is a rheological behaviour of a fluid in which viscosity decreases with increasing shear rate (Jax, 2010; Michael, 2009; Jay & Bruce, 2005). The molecular basis for shear thinning behaviour of the polymer mud is the effect of shear on entanglements. At low shear rates, the entanglements impede shear flow and therefore, viscosity is high, as the shear rate increases, chains begin to orient themselves in the flow direction and disentangle from one another, the viscosity then begins to decrease. Finally, the molecules become fully oriented in the direction of flow at very high shear rates. At

this point, stable entanglements are no longer possible and the viscosity reaches a low level that is again independent of shear rate (Jax, 2010; Obong, 2004; Jill & Poka, 2003).

4.2.3 Biodegradation Properties

Biodegradation properties of the various muds were determined by carrying out soil burial tests on the respective starch blends (G:W, M:W, P:W, G:M, G:P, M:P, CMS:HPS) and single or unblended starches (W, CMS). The effects of the degradation products of the starches on plants growth were also determined. The results and data for the biodegradation properties are given in Table 4.75 – 4.95

4.2.3.1 Weight Loss Characteristics after Soil Burial Tests

The weight loss data from the soil burial tests are presented in Tables 4.75 – 4.83. The weight loss characteristics or behaviours of the starches used in preparing the various muds are shown in the figure 4.168.

Table 4.75: Soil Burial Test Weight Loss Data for G:W Starch Blend

Time (Days)	Initial Weight (g)	Final Weight (g)	Weight Loss (g)	Percent Weight Loss (%)
10	50	45.26	4.74	9.48
20	50	42.30	7.70	15.40
30	50	40.60	9.40	18.80
40	50	36.08	13.92	27.84
50	50	33.80	16.20	32.40
60	50	30.06	19.94	39.88
70	50	26.23	23.77	47.54
80	50	23.87	26.13	52.26
90	50	20.41	29.59	59.18
100	50	17.75	32.85	65.70

Table 4.76: Soil Burial Test Weight Loss Data for M:W Starch Blend

Time (Days)	Initial Weight (g)	Final Weight (g)	Weight Loss (g)	Percent Weight Loss (%)
10	50	46.84	3.16	6.32
20	50	44.43	5.57	11.14
30	50	42.67	7.33	14.66
40	50	39.34	10.66	21.32
50	50	35.96	14.04	28.08
60	50	32.73	17.27	34,53
70	50	29.22	20.78	41.56
80	50	27.25	22.75	45.50
90	50	24.81	25.19	50.38
100	50	22.28	27.72	55.44

Table 4.77: Soil Burial Test Weight Loss Data for P:W Starch Blend

Time (Days)	Initial Weight (g)	Final Weight (g)	Weight Loss (g)	Percent Weight Loss (%)
10	50	47.17	2.83	5.65
20	50	45.28	4.72	9.44
30	50	43.02	6.98	13.96
40	50	42.00	8.00	16.00
50	50	39.61	10.39	20.78
60	50	36.30	13.70	27.40
70	50	34.52	15.48	30.96
80	50	30.04	19.96	39.92
90	50	26.34	23.66	47.32
100	50	23.87	26.13	52.26

Table 4.78: Soil Burial Test Weight Loss Data for G:M Starch Blend

Time (Days)	Initial Weight (g)	Final Weight (g)	Weight Loss (g)	Percent Weight Loss (%)
10	50	47.51	2.49	4.98
20	50	46.08	3.92	7.84
30	50	44.56	5.44	10.88
40	50	42.97	7.03	14.05
50	50	41.04	8.96	17.91
60	50	37.89	12.11	24.22
70	50	35.52	14.48	28.95
80	50	32.14	17.86	35.71
90	50	28.93	21.07	42.14
100	50	24.44	25.56	51.11

Table 4.79: Soil Burial Test Weight Loss Data for G:P Starch Blend

Time (Days)	Initial Weight (g)	Final Weight (g)	Weight Loss (g)	Percent Weight Loss (%)
10	50	48.00	2.00	3.99
20	50	46.50	3.50	7.00
30	50	45.60	4.40	8.79
40	50	43.93	6.47	12.94
50	50	42.07	7.93	15.86
60	50	38.66	11.34	22.67
70	50	36.58	13.42	26.83
80	50	33.88	16.12	32.24
90	50	29.61	20.39	40.07
100	50	24.50	25.50	51.00

Table 4.80: Soil Burial Test Weight Loss Data for M:P Starch Blend

Time (Days)	Initial Weight (g)	Final Weight (g)	Weight Loss (g)	Percent Weight Loss (%)
10	50	48.46	1.54	3.08
20	50	46.71	3.29	6.58
30	50	46.27	3.75	7.46
40	50	44.13	5.87	11.74
50	50	42.60	7.40	14.80
60	50	39.70	10.30	20.60
70	50	38.12	11.88	23.76
80	50	35.75	14.25	28.50
90	50	32.59	17.41	34.82
100	50	24.67	25.33	50.66

Table 4.81: Soil Burial Test Weight Loss Data for W Starch (Non-chemically modified single starch)

Time (Days)	Initial Weight (g)	Final Weight (g)	Weight Loss (g)	Percent Weight Loss (%)
10	50	48.73	1.27	2.54
20	50	47.64	2.36	4.72
30	50	46.85	3.15	6.30
40	50	45.59	4.41	8.82
50	50	43.44	6.56	13.12
60	50	41.82	8.18	16.36
70	50	40.63	9.37	18.74
80	50	38.94	11.06	22.12
90	50	35.25	14.75	29.50
100	50	31.21	18.79	37.58

Table 4.82: Soil Burial Test Weight Loss Data for CMS Starch (Chemically-modified single starch)

Time (Days)	Initial Weight (g)	Final Weight (g)	Weight Loss (g)	Percent Weight Loss (%)
10	50	49.50	0.50	1.00
20	50	49.34	0.66	1.32
30	50	49.05	0.95	1.90
40	50	48.78	1.22	2.44
50	50	48.37	1.63	3.26
60	50	47.72	2.28	4.56
70	50	47.54	2.46	4.92
80	50	46.96	3.04	6.08
90	50	46.13	3.87	7.74
100	50	44.35	5.65	11.30

Table 4.83: Soil Burial Test Weight Loss Data for CMS:HPS Starch Blend (Chemically-modified blend of starches)

Time (Days)	Initial Weight (g)	Final Weight (g)	Weight Loss (g)	Percent Weight Loss (%)
10	50	49.71	0.29	0.58
20	50	49.44	0.56	1.12
30	50	49.16	0.84	1.68
40	50	48.92	1.08	2.15
50	50	48.64	1.36	2.71
60	50	47.89	2.11	4.22
70	50	47.63	2.37	4.74
80	50	47.15	2.85	5.69
90	50	46.27	3.73	7.45
100	50	44.83	5.17	10.34

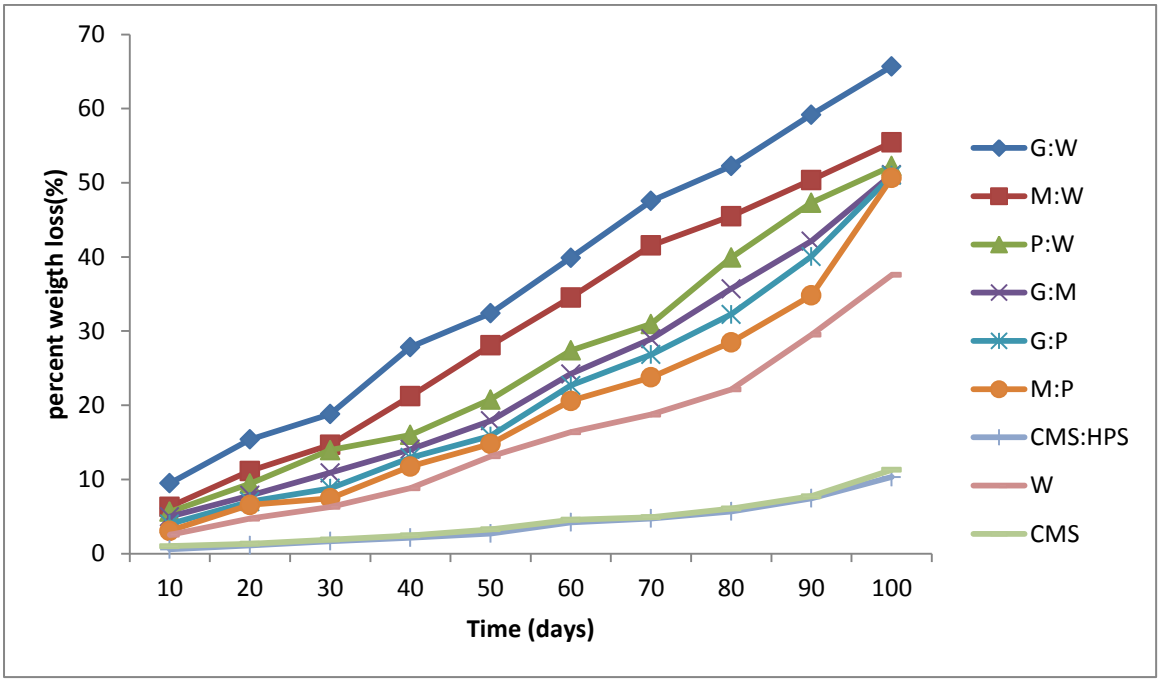

Figure 4.168: Plot of Percentage Weight Loss versus Time for the various Starches. (Data; Table 4.75-Table 4.83)

Figure 4.168 shows the plot of Percent Weight Loss (%) versus Time (days) for the various starches. It is observed from the figure that percent weight loss increased with increase in time for all the starches. This indicates continuous degradation the starches buried in the soil for the specific time interval.

More analysis of figure 4.168 shows that within 100 days time interval, G:W, containing a blend of Guinea corn starch and Waxy corn starch, gave the highest percent weight loss of 65.70% while CMS:HPS, containing a blend of chemically modified Carboxymethyl starch and Hydroxypropyl starch, gave the least percent weight loss of 10.34%. At all the time intervals, the percent weight loss of the new blends of starches (G:W, M:W, P:W, G:M, G:P, M:P) were higher than those of the aready existing starches (W, CMS, CMS:HPS). The percent weight loss of the starches increases among the starches as thus: G:W > M:W > P:W > G:M > G:P

>M:P > W > CMS > CMS:HPS. This shows that the new blends of starches were more biodegraded by microorganisms in the soil than the already existing starches. Therefore under the biodegradation consideration, the new blends of starches are more environmentally friendly and better for preparing biodegradable drilling mud than the already existing starches. This may be due to the purity of the processing technique (pregelatinization and blending in the absence of chemicals) for the new blends of starches. The presence of chemicals might have reduced the rate of biodegradation of the chemically modified starches (CMS:HPS and CMS). The chemicals used in modifying and blending these starches deaccelerated the actions of microorganisms on them. The rate of biodegradation of polymers vary depending on environmental conditions, traces of impurities and manufacturing history of the polymers (Jones, 2006; Mickey & Duke, 2005). The lower percent weight loss of W starch than the new starch blends might be due to the non-blending nature of W starch. The amount of starch in W available for microorganisms is smaller than amount in each of the new blends. CMS was neither pure nor blended, so, the small amount of starch and the presence of chemicals reduced the actions of microorganisms on the starch. The higher percent weight loss by the new starch blends than the already existing starches might also imply that the starch blends were conditioned in a way that their contents were susceptible to higher degradation, fragmentation, and eventually decrease in molecular weight. Higher degradation of starch content in the soil can be considered as an evidence for decrease in molecular weight of starch due to fragmentation during retrogradation (Obasi, 2012). Most naturally occurring polymers are completely biodegradable but nature of production and structural irregularities are often taken to be responsible for either causing or accelerating degradation of polymers (Mickey & Duke, 2005; Mario, 2003).

Table 4.84: Growth Heights of Okra plant's Shoot for the various Starches

Heights of Shoot after different Time intervals in Days

Starch Samples	10 days (cm)	20 days (cm)	30 days (cm)	40 days (cm)	50 days (cm)
G:W	40.10	54.30	63.80	70.40	75.60
M:W	35.60	55.80	60.20	66.20	70.10
P:W	33.80	48.30	53.60	59.70	62.40
G:M	30.90	40.80	47.90	54.80	58.20
G:P	28.80	37.80	43.40	49.30	55.70
M:P	27.60	34.50	41.70	47.10	50.50
W	20.30	25.20	29.50	34.70	36.90
CMS	11.50	15.20	16.30	17.90	19.10
CMS:HPS	10.20	13.60	14.80	17.20	18.30

Table 4.85: Growth Heights of Wheat plant's Shoot for the various Starches

Heights of Shoot after different Time intervals in Days

Starch Samples	10 days (cm)	20 days (cm)	30 days (cm)	40 days (cm)	50 days (cm)
G:W	40.30	59.10	69.70	75.60	79.70
M:W	38.80	56.40	67.20	71.90	76.50
P:W	38.50	51.90	63.30	68.50	73.80
G:M	35.70	46.20	57.60	67.30	71.20
G:P	34.60	43.80	51.90	60.70	64.50
M:P	32.70	39.60	45.70	53.40	58.30
W	21.40	27.30	30.60	33.80	37.40
CMS	12.10	14.80	16.20	17.10	17.80
CMS:HPS	11.80	14.20	15.70	16.30	18.90

Table 4.86: Growth Heights of Soyabean plant's Shoot for the various Starches

Heights of Shoot after different Time intervals in Days

Starch Samples	10 days (cm)	20 days (cm)	30 days (cm)	40 days (cm)	50 days (cm)
G:W	40.60	63.50	76.80	85.90	92.40
M:W	38.10	57.70	68.90	76.20	81.70
P:W	39.70	56.10	66.50	74.70	79.80
G:M	38.30	51.50	62.60	67.10	71.20
G:P	36.90	48.40	57.20	65.40	70.10
M:P	35.90	47.20	54.60	61.30	68.40
W	23.60	28.80	31.40	35.80	38.50
CMS	14.20	17.40	19.50	21.30	22.80
CMS:HPS	12.80	15.50	17.80	18.60	20.10

Table 4.87: Growth Heights of Cucumber plant's Shoot for the various Starches

Heights of Shoot after different Time intervals in Days

Starch Samples	10 days (cm)	20 days (cm)	30 days (cm)	40 days (cm)	50 days (cm)
G:W	46.50	77.20	95.70	106.40	118.10
M:W	44.80	70.40	93.50	103.70	107.20
P:W	41.20	64.90	86.30	98.30	101.80
G:M	40.30	59.60	74.10	88.50	97.70
G:P	40.10	60.20	74.30	86.70	94.30
M:P	38.60	57.80	68.20	78.40	89.60
W	24.80	29.80	35.60	39.40	43.70
CMS	15.60	17.20	20.80	22.60	24.50
CMS:HPS	14.90	16.30	18.10	20.50	22.20

Table 4.88: Growth Lengths of Okra plant's Root for the various Starches

Lengths of Root after different Time intervals in Days

Starch Samples	10 days (cm)	20 days (cm)	30 days (cm)	40 days (cm)	50 days (cm)
G:W	11.10	14.80	16.60	17.30	19.80
M:W	11.70	13.20	14.50	15.90	18.10
P:W	11.00	12.10	14.20	15.40	17.50
G:M	10.80	12.00	13.60	14.80	17.20
G:P	10.90	11.50	12.80	13.20	15.10
M:P	10.50	11.10	12.40	14.00	14.80
W	5.20	5.80	6.40	7.30	7.70
CMS	4.60	4.90	5.10	5.40	5.90
CMS:HPS	4.10	4.50	4.70	5.00	5.30

Table 4.89: Growth Lengths of Wheat plant's Root for the various Starches

Lengths of Root after different Time intervals in Days

Starch Samples	10 days (cm)	20 days (cm)	30 days (cm)	40 days (cm)	50 days (cm)
G:W	16.40	19.60	21.40	22.10	24.70
M:W	15.80	17.20	18.90	20.50	21.60
P:W	15.60	16.90	17.70	18.20	20.40
G:M	13.90	14.30	16.50	17.10	19.60
G:P	12.50	14.10	15.90	16.30	19.10
M:P	12.20	13.80	14.30	16.10	18.50
W	7.80	8.20	8.90	9.60	11.40
CMS	6.90	7.80	8.00	8.70	10.10
CMS:HPS	6.30	7.10	7.90	8.50	9.20

Table 4.90: Growth Lengths of Soyabean plant's Root for the various Starches

Lengths of Root after different Time intervals in Days

Starch Samples	10 days (cm)	20 days (cm)	30 days (cm)	40 days (cm)	50 days (cm)
G:W	18.70	21.20	24.20	25.80	27.50
M:W	18,10	20.80	22.40	24.50	26.20
P:W	17.60	18.80	21.30	22.90	24.30
G:M	15.90	16.70	19.50	20.10	21.80
G:P	14.90	16.20	18.70	19.30	19.90
M:P	13.50	15.40	17.10	18.50	19.30
W	9.70	10.20	11.50	12.80	13.60
CMS	8.10	9.80	9.90	10.70	11.20
CMS:HPS	7.80	9.10	9.80	10.40	10.90

Table 4.91: Growth Lengths of Cucumber plant's Root for the various Starches

Lengths of Root after different Time intervals in Days

Starch Samples	10 days (cm)	20 days (cm)	30 days (cm)	40 days (cm)	50 days (cm)
G:W	24.30	27.10	29.50	32.20	33.70
M:W	23.60	26.20	27.40	30.70	32.40
P:W	23.10	25.80	27.20	28.40	30.70
G:M	21.80	24.50	26.60	27.70	29.60
G:P	21.30	23.70	24.90	25.20	28.80
M:P	20.60	21.90	23.40	24.40	26.20
W	11.60	11.80	12.20	12.90	13.50
CMS	9.80	10.60	11.10	11.80	12.70
CMS:HPS	9.20	10.20	10.80	11.30	12.10

4.2.3.2 Effects of Biodegradation Products on the Growth of Plants – Okra, Wheat, Soyabean and Cucumber

The effects of biodegradation products on the growth of plants namely; Okra, Wheat, Soyabean and Cucumber are displayed on figures 4.169 – 4.184. The figures are presented in four groups. Figures 4.169 – 4.172 contain the plots of Shoot Height of each plant versus Time curves for the various starches, while figures 4.173 – 4.176 contain their replications in histograms. Figures 4.177 – 4.180 contain the plots of Root Length of each plant versus Time curves for the various starches, while figures 4.181 – 4.184 contain their replications in histograms. The experimental results used in plotting these figures are given in Tables 4.84 – 4.91.

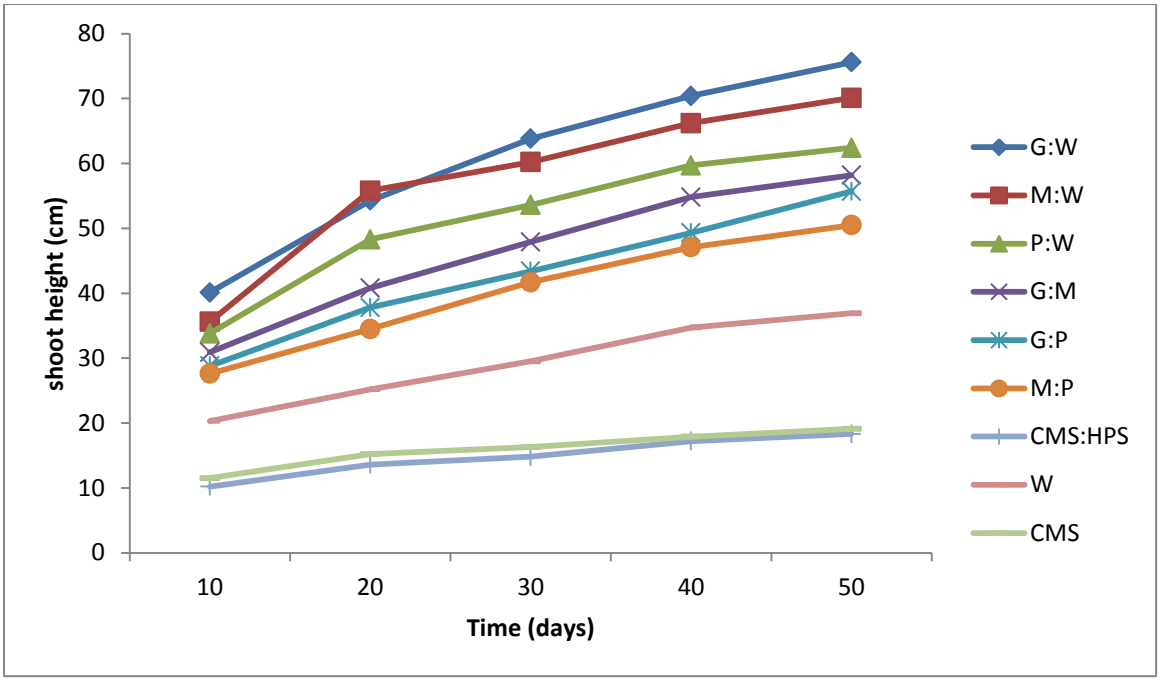

Figure 4.169: Plot of shoot height of okra plant versus time for the various starches. (Data; Table 4.84)

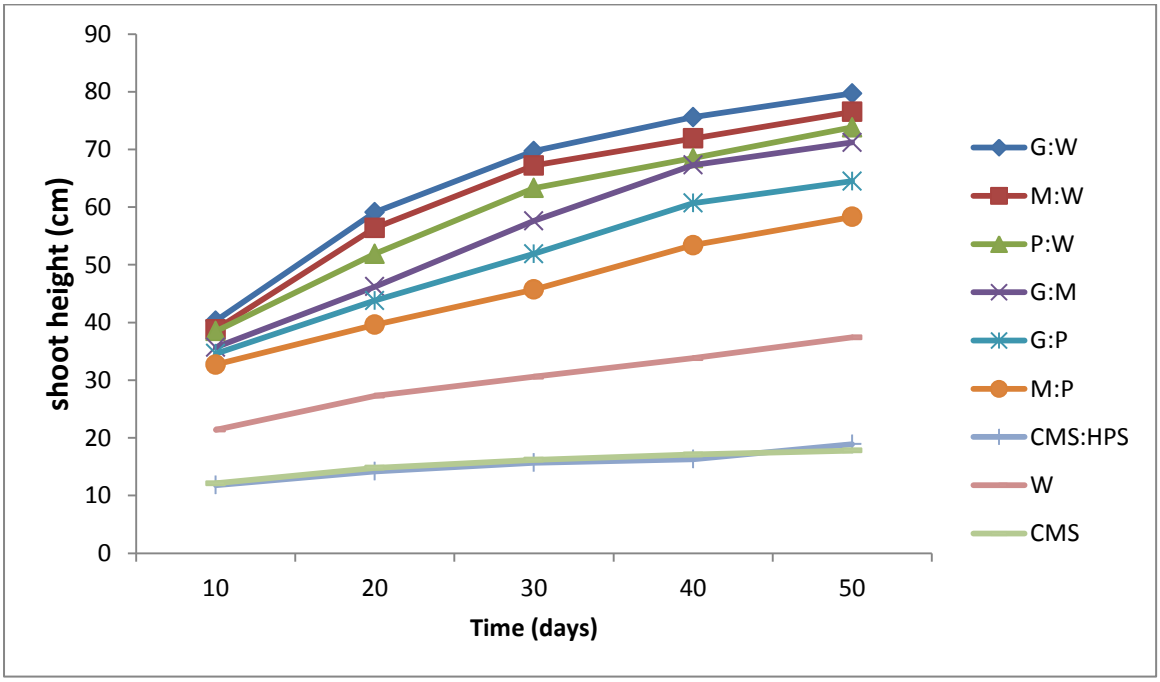

Figure 4.170: Plot of shoot height of wheat plant versus time for the various starches. (Data; Table 4.85)

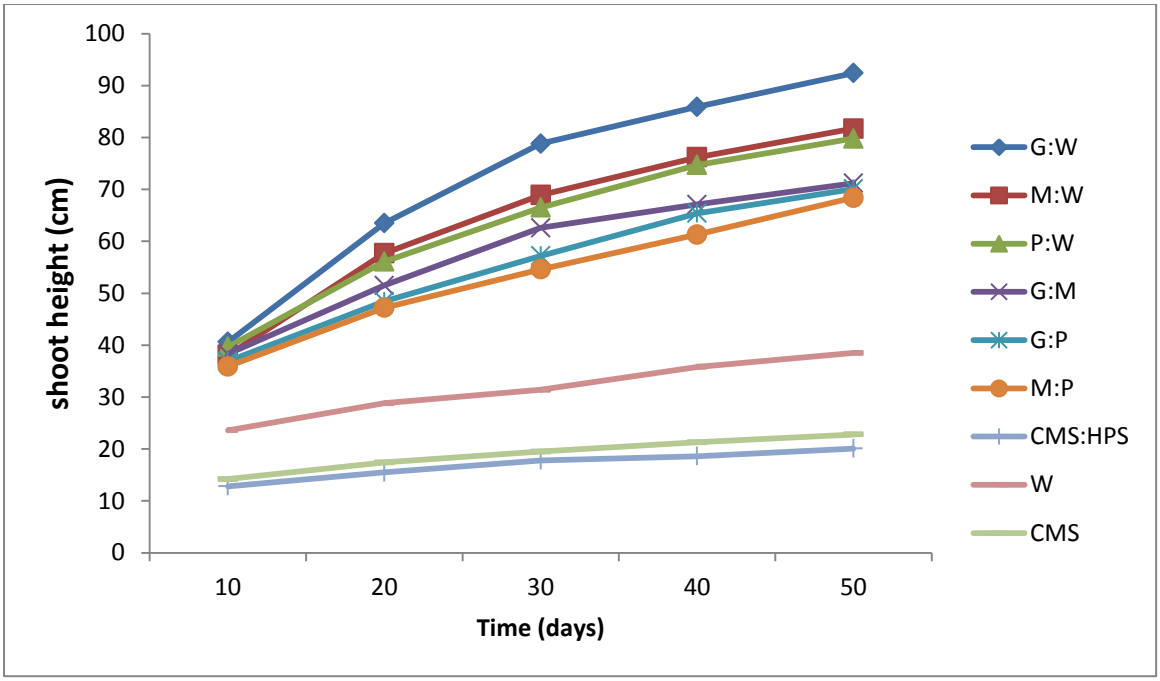

Figure 4.171: Plot of shoot height of soya bean plant versus time for the various starches. (Data; Table 4.86)

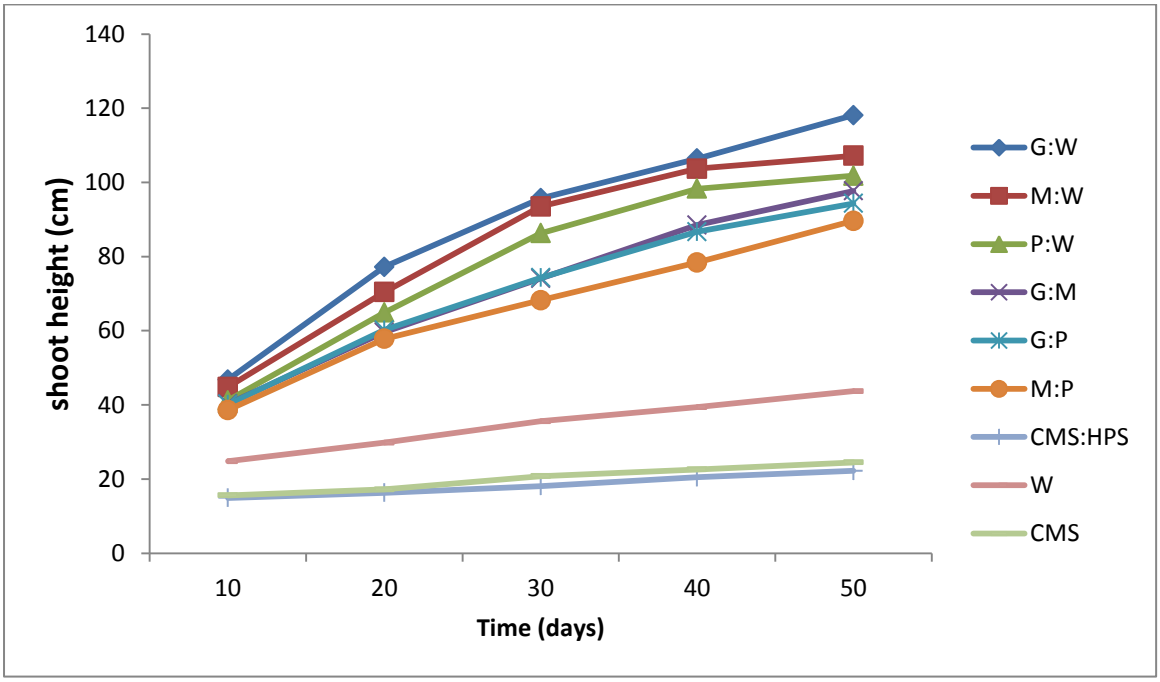

Figure 4.172: Plot of shoot height of cucumber plant versus time for the various starches. (Data; Table 4.87)

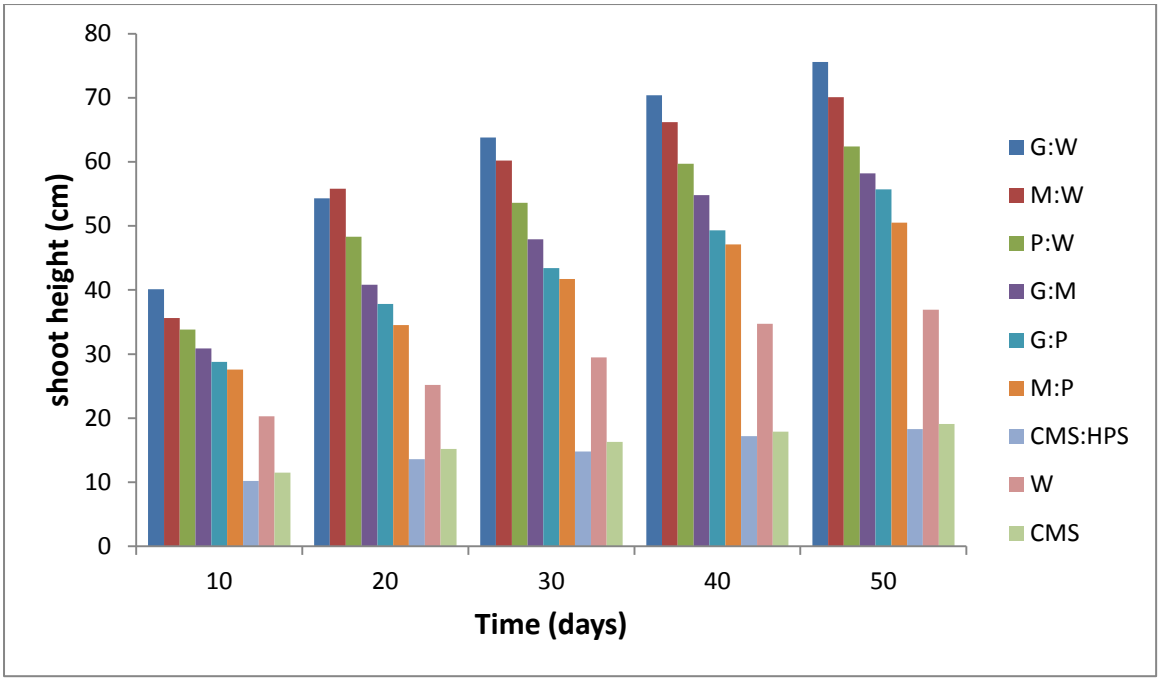

Figure 4.173: Plot of histogram for shoot height of okra plant versus time for the various starches. (Data; Table 4.84)

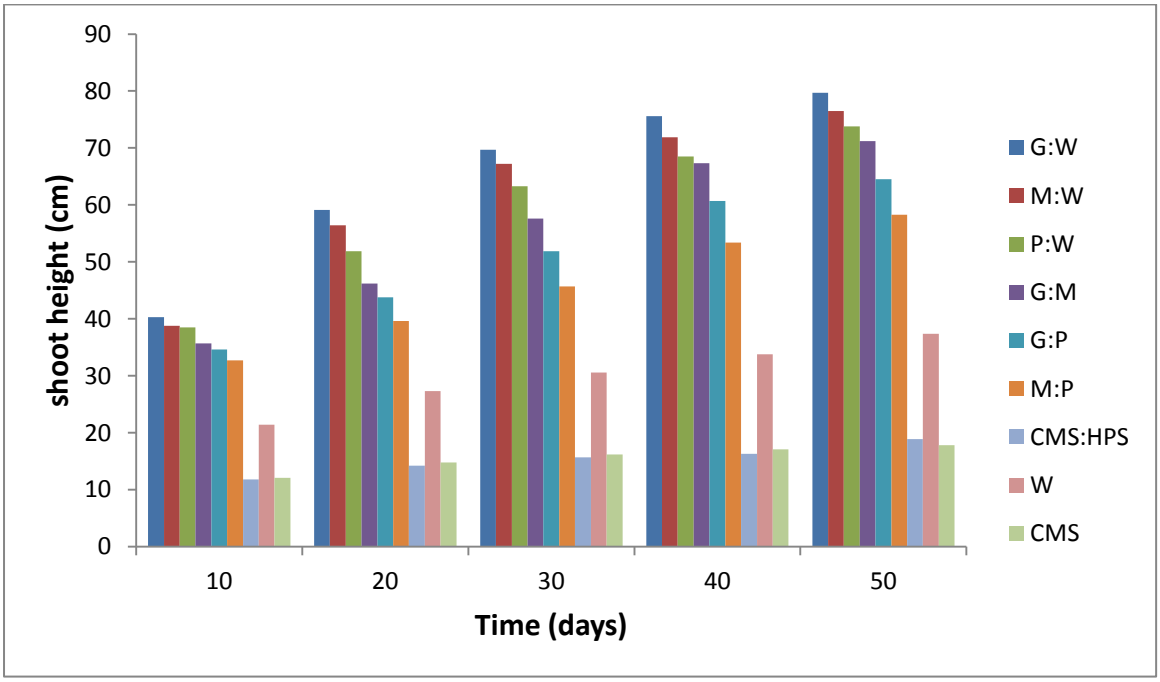

Figure 4.174: Plot of histogram for shoot height of wheat plant versus time for the various starches. (Data; Table 4.85)

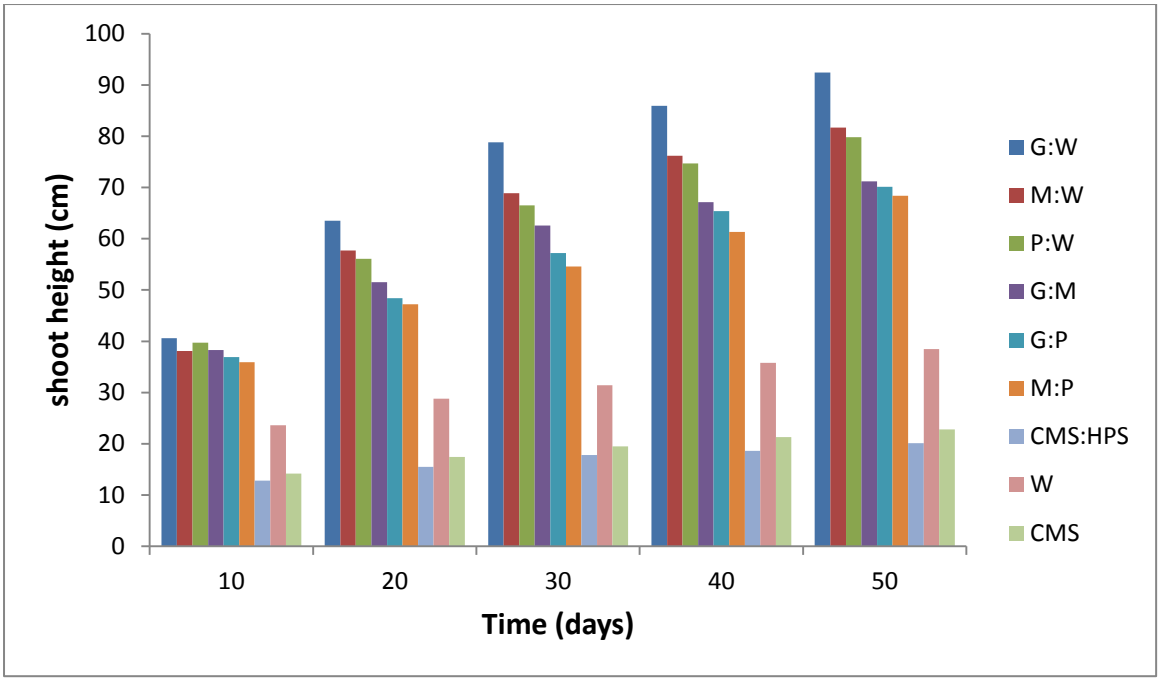

Figure 4.175: Plot of histogram for shoot height of soya bean plant versus time for the various starches. (Data; Table 4.86)

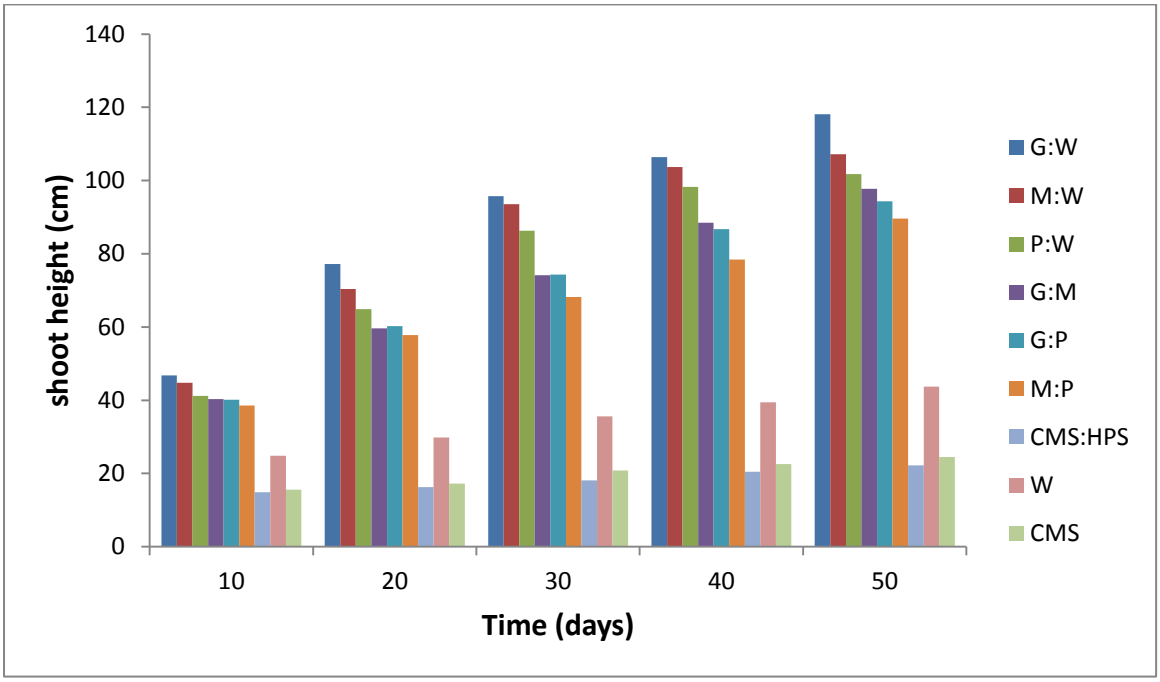

Figure 4.176: Plot of histogram for shoot height of cucumber plant versus time for the various starches. (Data; Table 4.87)

Figures 4.169 – 4.172 show the plots of Shoot Height of each plant versus Time curves for the various starches. Figures 4.173 – 4.176 show the replications of figures 4.169 – 4.172 in histograms. The figures show that the height of each plant's shoot increased with increase in time for all the starch samples. This is an indication that growth has taken place in all the plants under study. Growth is the development or increase in size such as height, length, width, of a living thing (Clever et al., 2012; Cyracus, 2012). It was also observed that after germination of each plant the rate of growth was rapid within the first 10 days and gradual within the other time intervals. The gradual increase might be attributed to the fact that the plants were approaching maturity. Further observation was that the increase in shoot heights of the plants was higher with the new blends of starches than with the already existing starches. The reason behind this might be that the new blends of starches were purer and yieded greater and more fertile degraded products during the the course of biodegradation in the soil.

The figures also show that the direction of increase in shoot heights with the various degraded products from the different starches went as follows;

CMS:HPS < CMS < W < M:P < G:P < G:M < P:W < M:W < G:W. It then means that the new blends of starches gave higher effects on the growth of plants'shoot than the already existing starches. G:W gave the highest shoot height while CMS:HPS gave the lowest shoot in all the plants under study. All these are dependent on the type, nature, amount and effectiveness of the contentents of the degraded products from each of the starches in the soil (Cisco & Whistler, 2008; Mario, 2003). The highest shoot height of 118.10cm was obtained with G:W for cucumber plant while the lowest shoot height of 18.30cm was obtained with CMS:HPS for okra plant at 50 days time interval.

Figures 4.177 – 4.180 show the plots of root length of each plant versus time curves for the various starches. Figures 4.181 – 4.184 show the replications of figures 4.177 – 4.180 in histograms. The figures show that the root lengths of all the plants increase with increase in time for the various starch samples. This also signifies that growth had taken place. The new starch blends gave higher increase root length than the already existing starches. At 50 days time interval, the longest root of 33.70cm length was obtained with G:W for cucumber plant while the shortest root of 5.30cm was obtained with CMS:HPS for okra plant. The reason for this occurrence may be related to the fact that the new starch blends including G:W were produced in a purer and more environmentally friendly way than the already or widely used starches. The growthof plant is also dependent on the soil fertility, which is affected by the type, nature, and amount of biodegraded products in the soil (Mario, 2003)

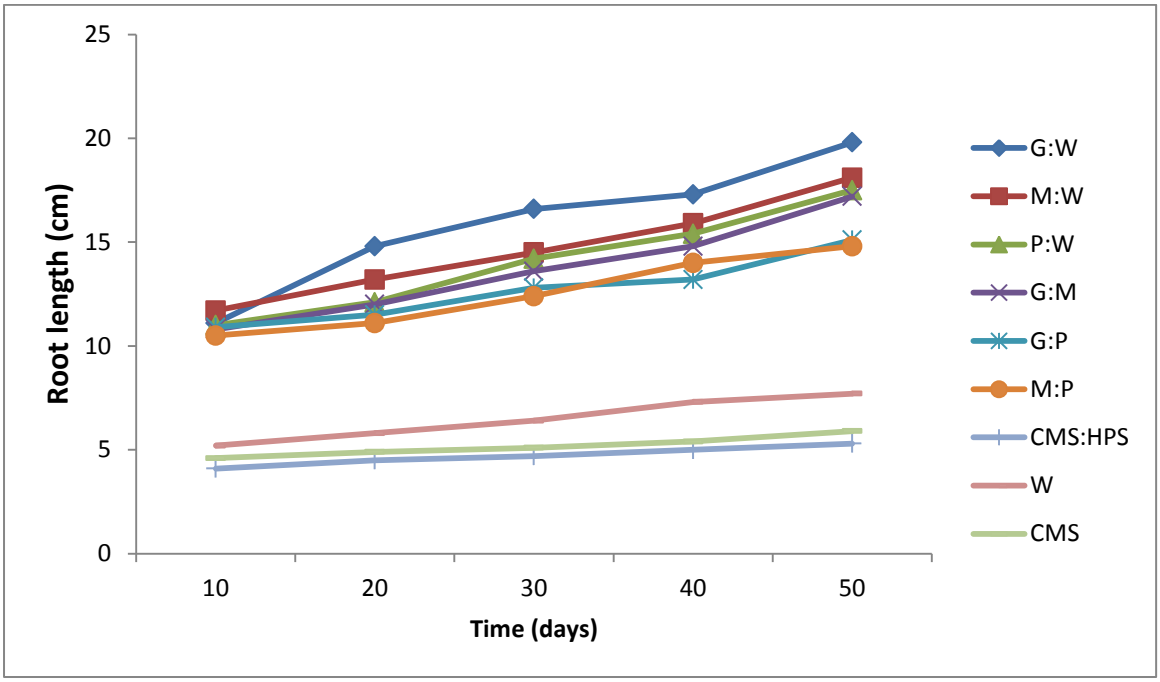

Figure 4.177: Plot of root length of Okra plant versus time for the various starches. (Data; Table 4.88)

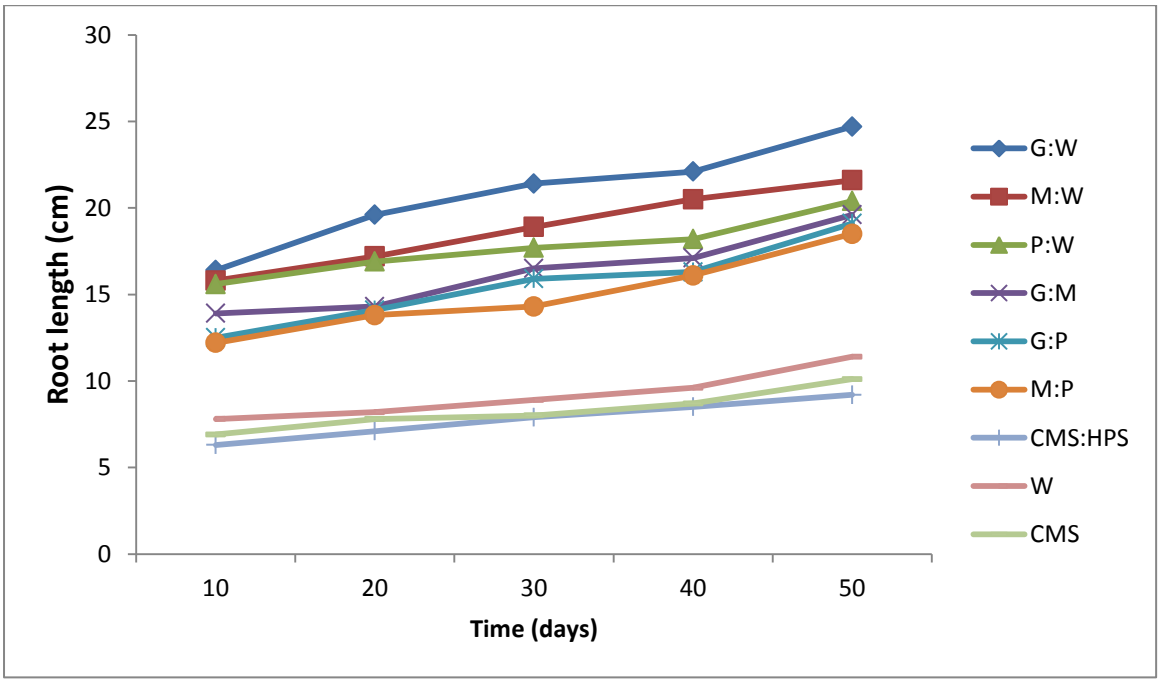

Figure 4.178: Plot of root length of Wheat plant versus time for the various starches. (Data; Table 4.89)

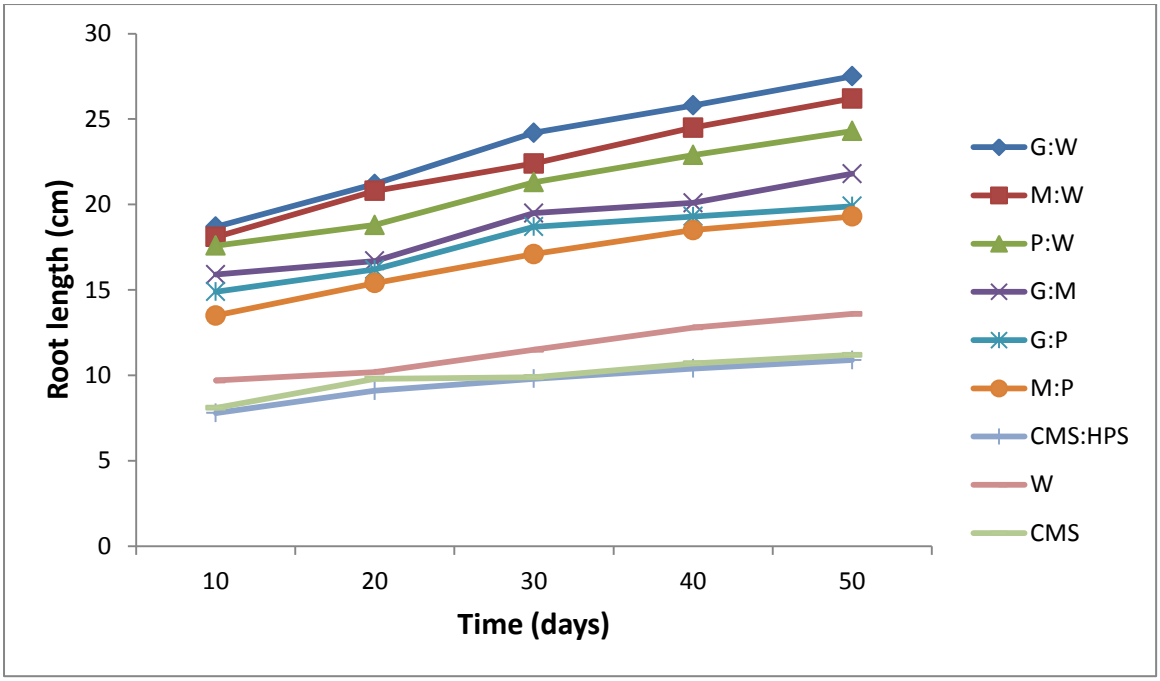

Figure 4.179: Plot of root length of Soya bean plant versus time for the various starches. (Data; Table 4.90)

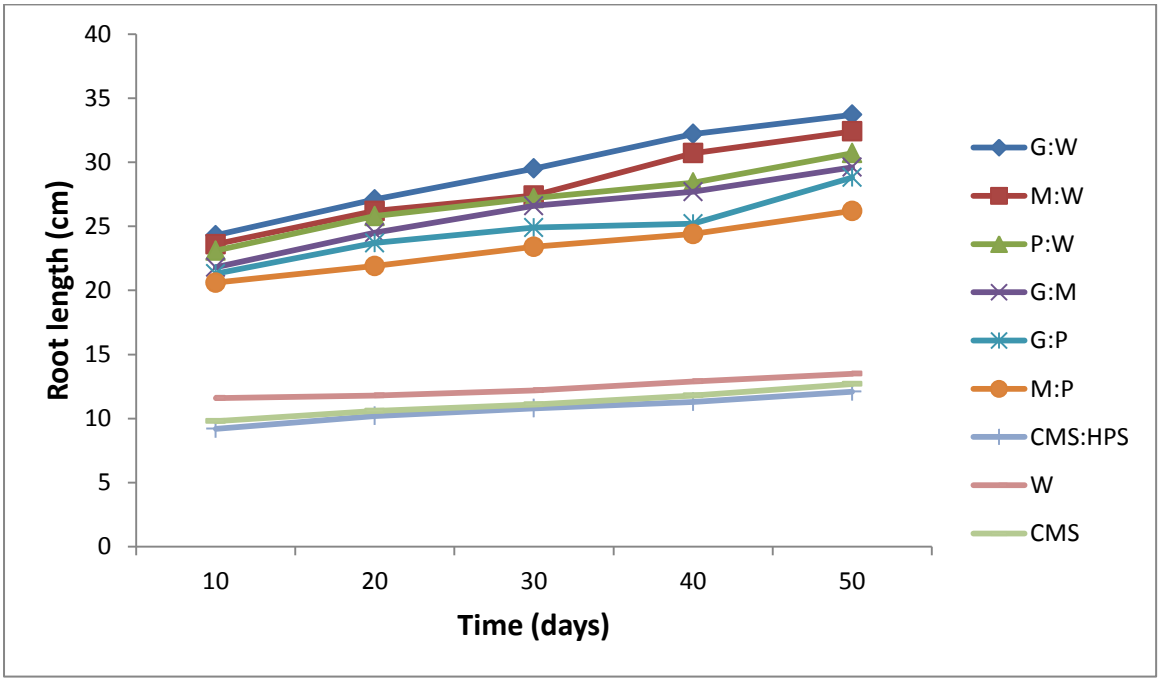

Figure 4.180: Plot of root length of Cucumber plant versus time for the various starches. (Data; Table 4.91)

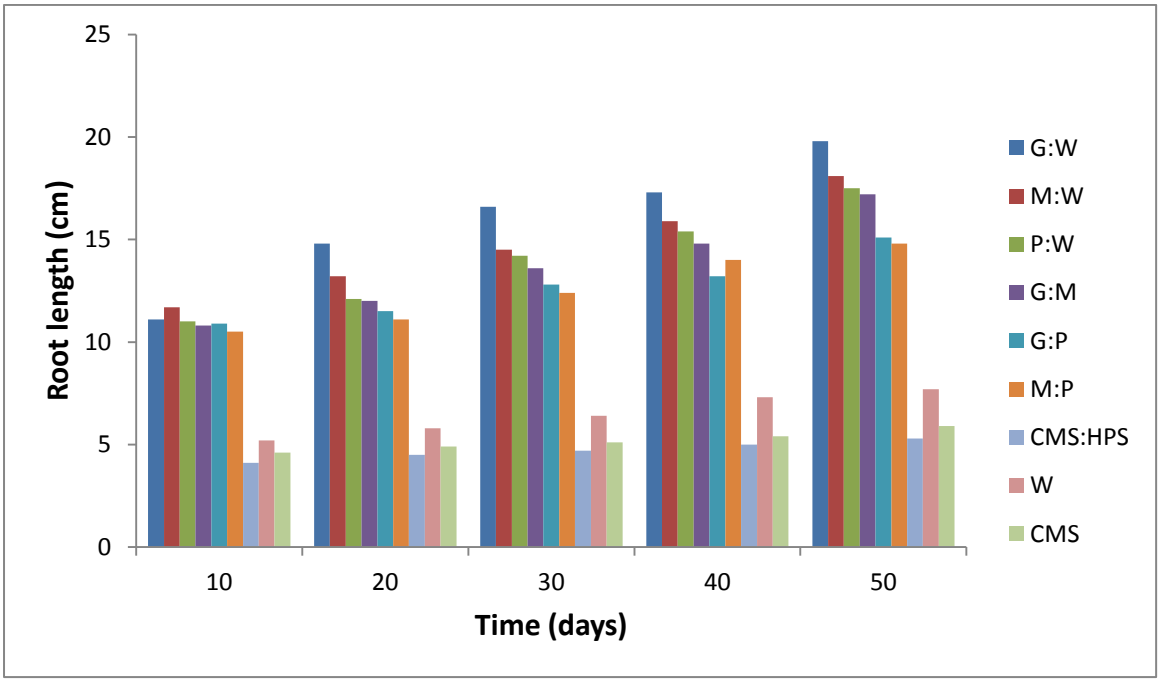

Figure 4.181: Plot of histogram for root lenght of Okra plant versus time for the various starches. (Data; Table 4.88)

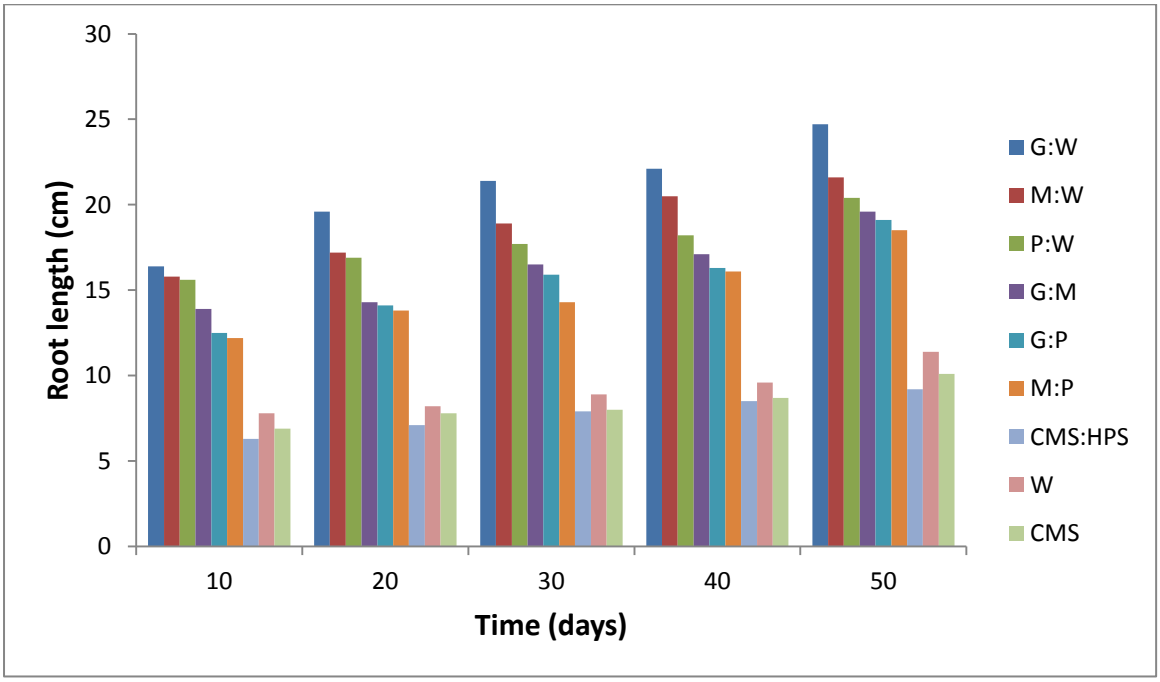

Figure 4.182: Plot of histogram for root length of Wheat plant versus time for the various starches. (Data; Table 4.89)

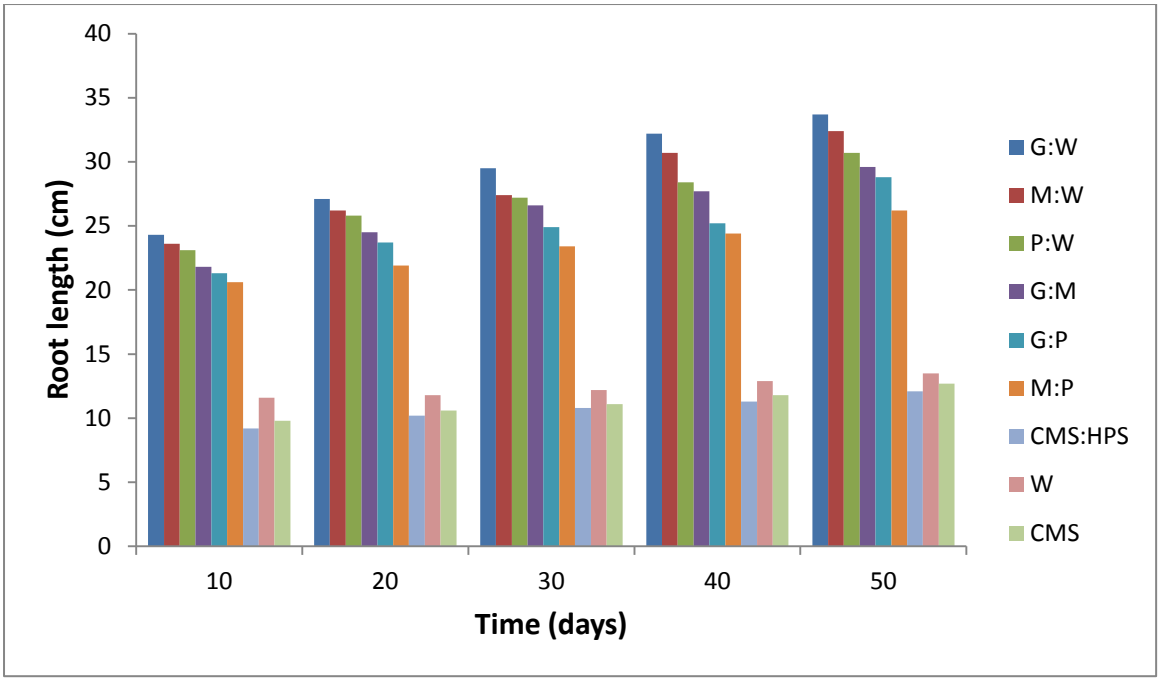

Figure 4.183: Plot of histogram for root length of Soyabean plant versus time for the various starches. (Data; Table 4.90)

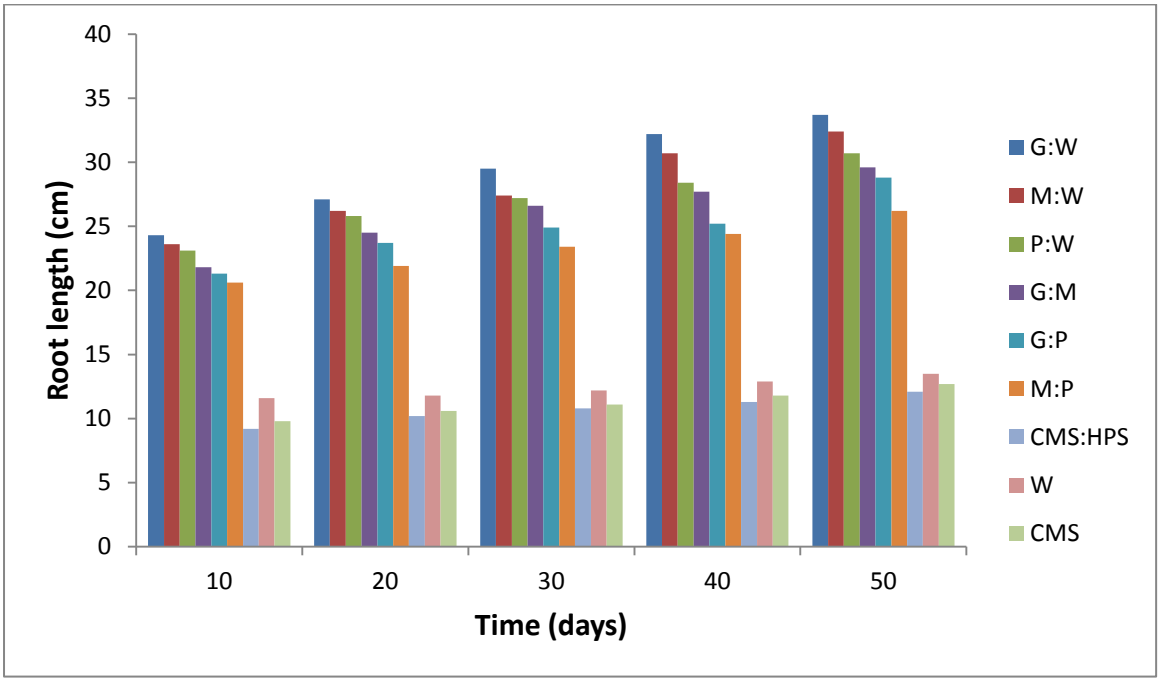

Figure 4.184: Plot of histogram for root length of Cucumber plant versus time for the various starches. (Data; Table 4.91)

Table 4.92: Total Viable Aerobic Bacteria Isolated from Soil Culturing

Sample	Total Aerobic Count	Coliform Count/ml	Staphylococal Count/ml	Bacteria Ceat
Soil	5000	2500	5000	3500

Table 4.93: Total Viable Fungal Counts Isolated from Soil Cuturing

Sample	Dilution Factor	No. of Fungal per ml of Sample		Total Count per ml of Sample		Average Counts
Soil	10^{-2}	10	10	10×10^{3}	10×10^{2}	10×10^{2}
	10^{-3}	6	8	6×10^{3}	8×10^{3}	7×10^{3}
	10^{-4}	3	2	3×10^{4}	2×10^{4}	2.5×10^{4}
	10^{-5}	1	0	1×10^{5}	-	0.5×10^{5}

Table 4.94: Identification of Moulds Isolated from Soil Culturing

Morphology		Microscopy		Suspected Oganisms
	Somatic Nature	Type of Hyphae	Kind of Spores	
White surface, black spores, white base and long Arial mycelium	Flamentors	Aseptate	Sporanigio	Mucur Pusilus
Short aerial mycelium, White surface, white spores, yellow base	Flamentors	Septate	Sporanigio	Rhizopus
Green Surface, green base, white/green spores, short aerial mycelium	Flamentors	Septate	Conidis	Aspergillus Orizae
Black surface, grey base, mycelium	Flamentors	Septate	Conidis	Aspergillus Nigar

Table 4.95: Identification of Yeast Isolated from Soil Culturing

Morphology	Gram reaction	Budding	Acid prediction	Gas prediction	Suspected organisms
White surface and Creamy base	+ve	+ve	+ve	+ve	Candida Asicae
Orange surface And creamy base	+ve	-ve	+ve	+ve	Schizo Sacchrage

4.2.3.3 Specific Microorganisms in the Soil Responsible for Biodrgradation of the Starches

Tabes 4.92 – 4.95 contain the results obtained from culturing of the soil to know the specific microorganisms responsible for the biodegradation of the starches. The experimental resuls showed that these microorganisms were responsible for the biodegradation of the starches.

(A) Bacteria

(i) Esherichia coli

(ii) Enterobacteria

(iii) Micrococus

(iv) Staphylococus

(v) Pseudomonas aerusinosa

(B) Fungi (Molds)

(i) Mucur Pusilus

(ii) Rhizopus Nigancar

(iii) Aspergillus Orizae

(i) Aspergillus Niger

(C) Yeast

(i) Candida Albicus

(ii) Schizosacchronycus

4.2.4 MATLAB Modelling Results

The results obtained from modeling the muds at different temperatures using MATLAB software are presented below.

4.2.4.1 Modelling of the Fluid Loss versus Square Root of Time for all the Muds with 0.01g/ml Starch Concentration at Room Temperature, 25^{o}C

Model equation $v = 0.003563t^4-0.1999t^3+3.889t^2-25.97t+125.9$

Coefficients (with 95% confidence bounds):

Goodness of fit: SSE: 0.2137; R-square: 0.9999

Adjusted R-square: 0.9994; RMSE: 0.4623

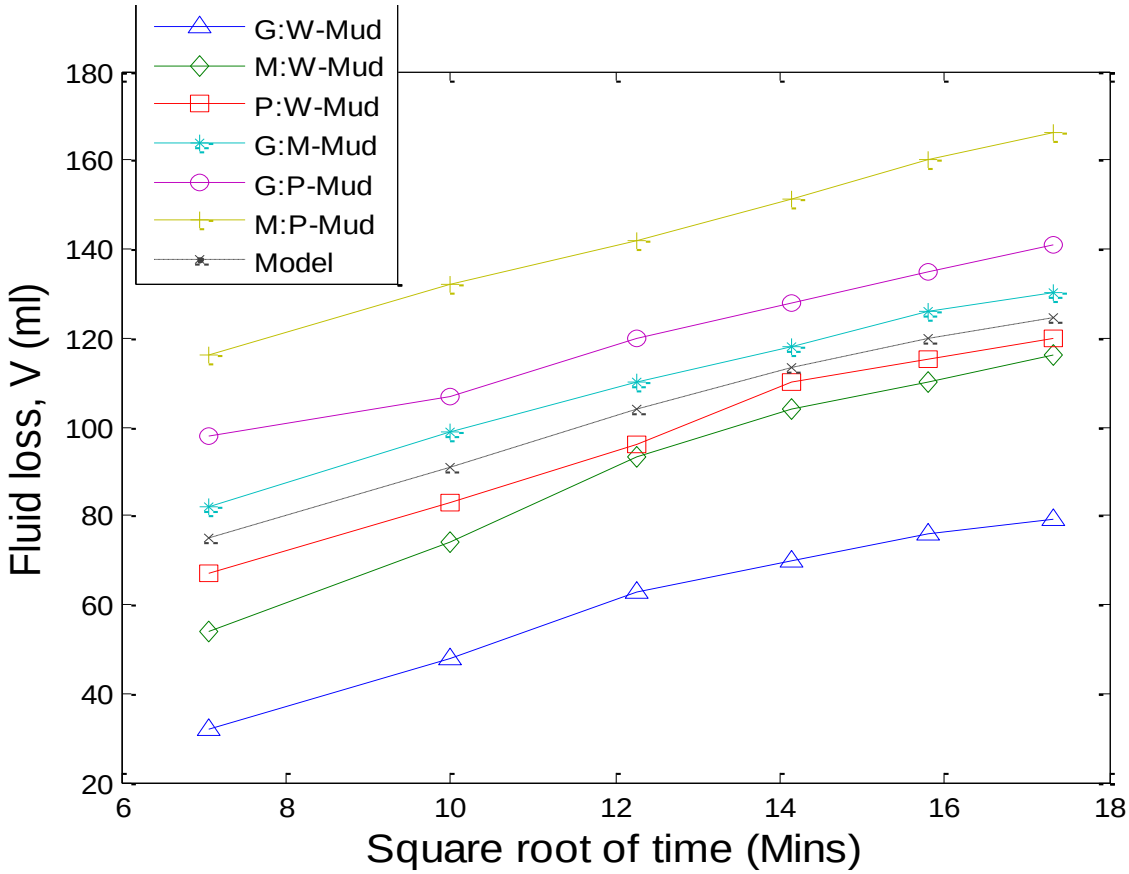

Figure 4.185: Plot of Modelled fluid loss versus square root of time for all the muds with 0.01g/ml starch concentration at room temperature, 25^{o}C. (Data; Table 4.1-Table 4.9)

In figure 4.185 and from the goodness of fit, the coefficient of regression, R^2 is 0.9999 signifying a good fit since it is close to "1" and the Sum of Squared Errors of 0.1107×10^{-5} which is close to "0" (see Table 4.96). The model curve in Figure 4.185 followed the same path with the experimental data. However, the following curves, P:W-Mud, M:W-Mud and G:W-Mud had lower deviations while G:M-Mud, G:P-Mud and M:P-mud exhibited upper deviations to the model curve.

4.2.4.2 Modelling of the Fluid Loss versus Square Root of Time for all the Muds with 0.02g/ml Starch Concentration at Room Temperature, 25°c

Model Equation is $v = -0.003297t^4+0.1521t^3-2.613t^2+24.47t-23.74$

Coefficients (with 95% confidence bounds):

Goodness of fit: SSE: 0.03502; R-square: 1,

Adjusted R-square: 0.9999, RMSE: 0.1871

In figure 4.186 and from the goodness of fit analysis showed that the coefficient of regression, R^2 is 0.9999 signifying a good fit since it is close to "1" and the Sum of Squared Errors of 0.1795×10^{-5} which is close to "0" (see Table 4.96). The model curve in Figure 4.186 followed the same path with the experimental data. Similarly, the following curves, P:W-Mud, M:W-Mud and G:W-Mud had lower deviations while G:M-Mud, G:P-Mud and M:P-mud exhibited upper deviations to the model curve.

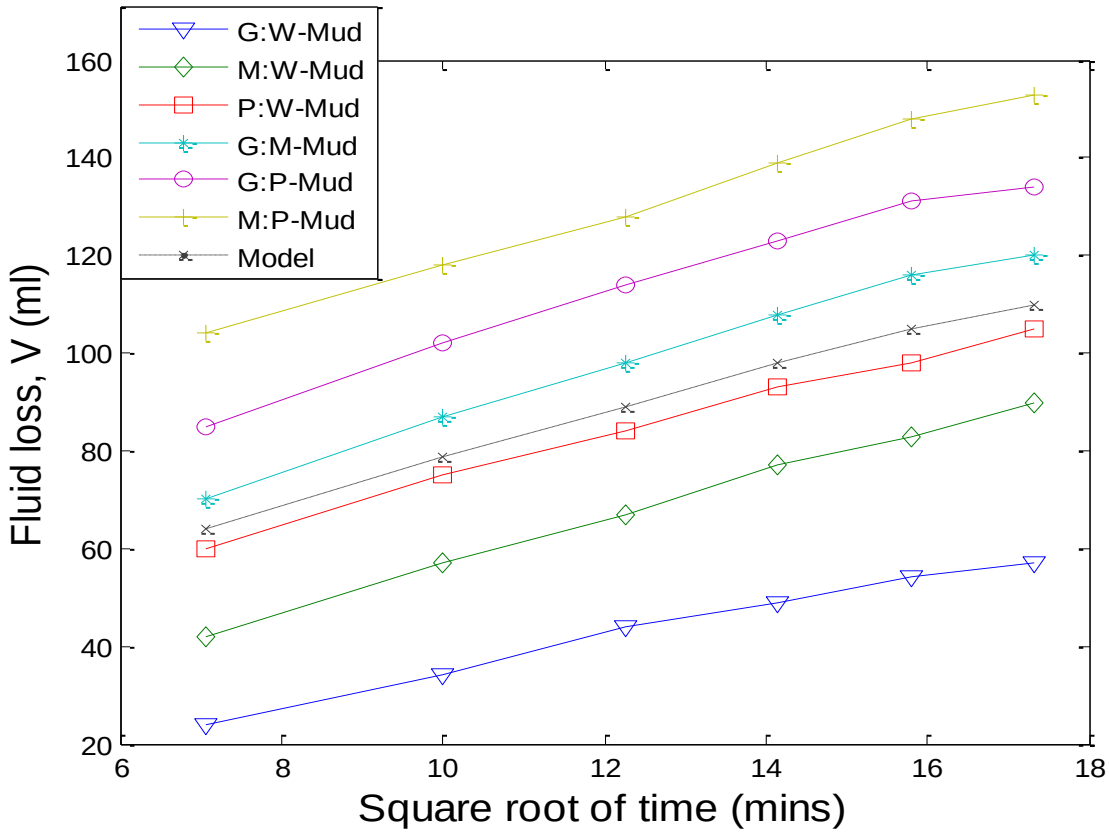

Figure 4.186: Plot of Modelled fluid loss versus square root of time for all the muds with 0.02g/ml starch concentration at room temperature, 25^{o}C. (Data; Table 4.1-Table 4.9)

4.2.4.3 Modelling of the Fluid Loss versus Square Root of Time for all the Muds with 0.03g/ml Starch Concentration at Room Temperature, 25^{o}c

Linear model Poly3: $v = -0.01065t^3+0.306t^2+2.028t+38.35$

Goodness of fit: SSE: 0.2493; R-square: 0.9998

Adjusted R-square: 0.9996, RMSE: 0.353

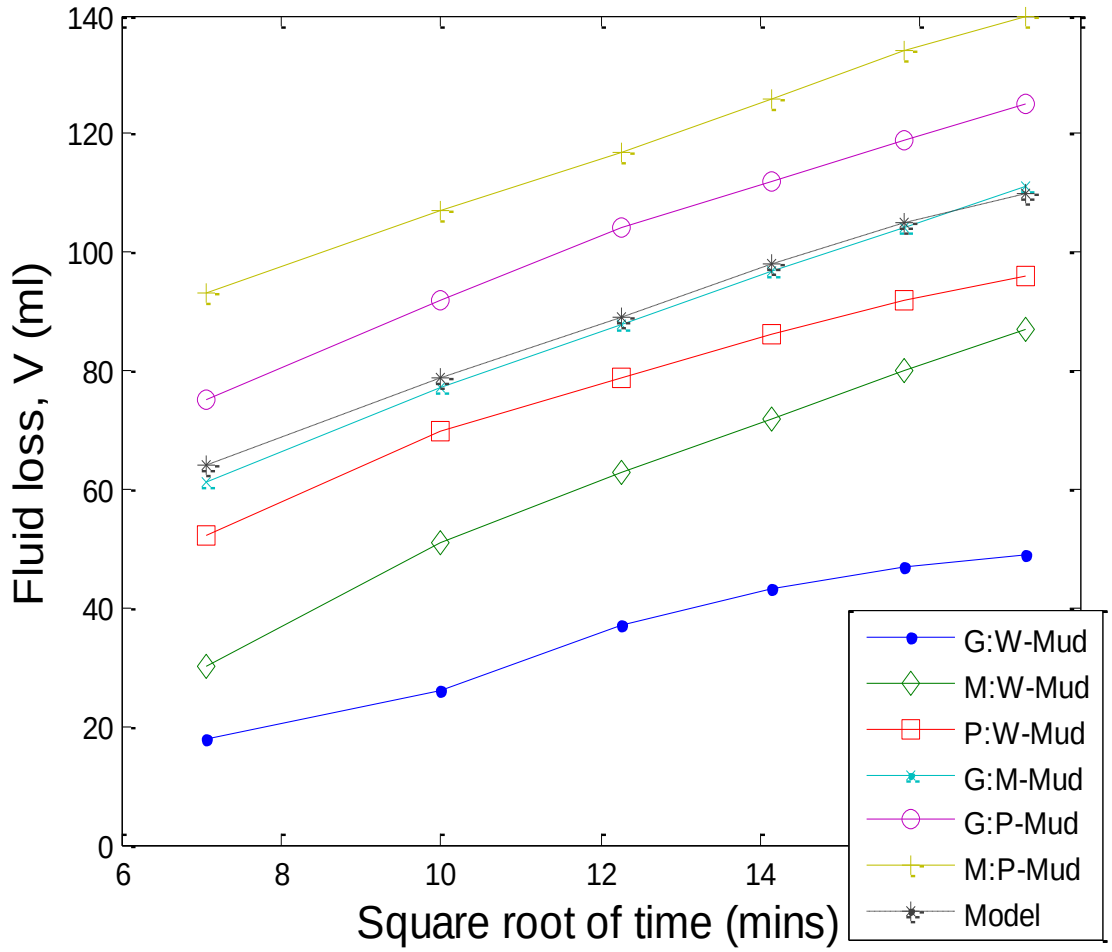

Figure 4.187: Plot of Modelled fluid loss versus square root of time for all the muds with 0.03g/ml starch concentration at room temperature, 25°C. (Data; appendix 1, Table 4.1-Table 4.9)

In figure 4.187 and from the goodness of fit, the coefficient of regression, R^2 is 0.9999 signifying a good fit since it is close to "1" and the Sum of Squared Errors of 0.09444 x 10^{-5} which is close to "0" (see Table 4.96). Hence, the G:P composite exhibited the best fit. The model curve in Figure 4.187 followed the same path with the experimental data. Similarly, the following curves, G:M-Mud, M:W-Mud and G:W-Mud had lower deviations while M:P-Mud, and G:P-Mud exhibited upper deviations to the model curve. Also, there is a close deviation between G:M –Mud and the model with an interception at 17 minutes.

4.2.4.4 Modelling of Fluid Loss versus Square Root of Time for all the Muds with 0.04g/ml Starch Concentration at Room Temperature, 25°C.

$t^{1/2}$ = [7.07, 10.00, 12.25, 14.14, 15.81, 17.32]

Linear model Poly3: $v = -0.009087t^3+0.2071t^2+3.805t+11.5$

Coefficients (with 95% confidence bounds):

Goodness of fit: SSE: 0.2076; R-square: 0.9999

Adjusted R-square: 0.9997, RMSE: 0.3222

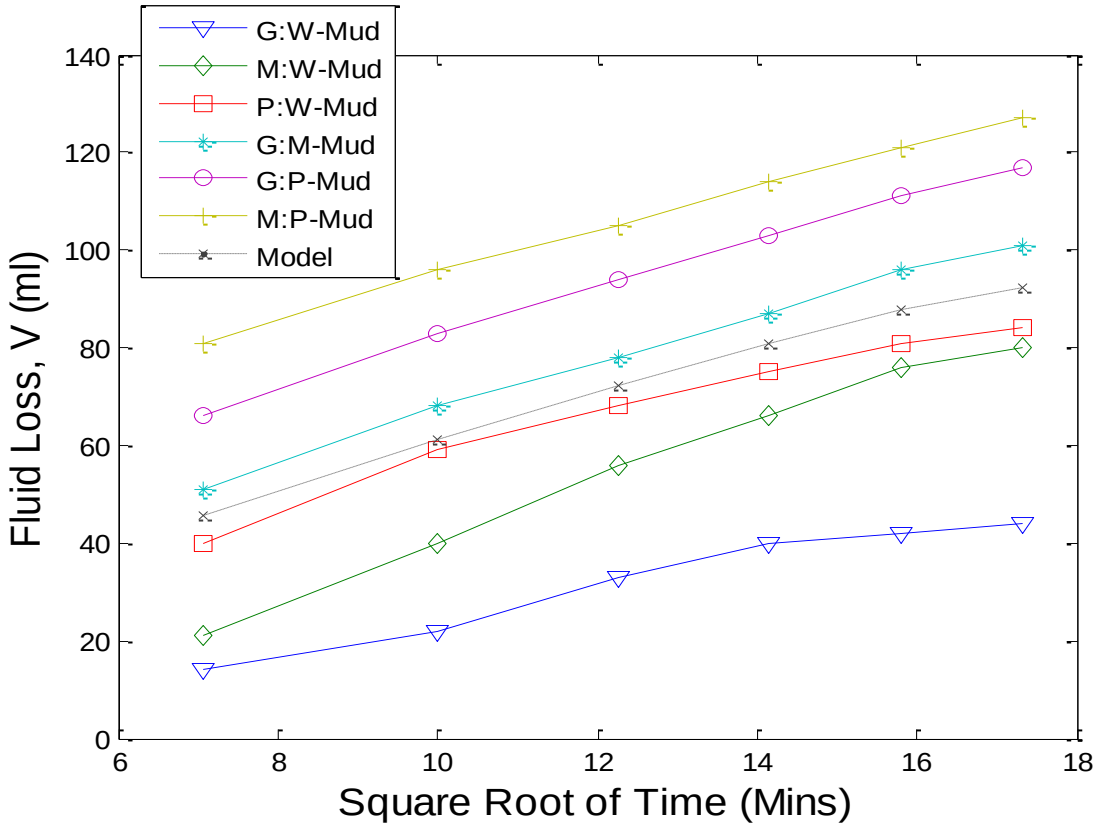

Figure 4.188: Plot of Modelled fluid loss versus square root of time for all the muds with 0.04g/ml starch concentration at room temperature, 25°C. (Data; Table 4.1-Table 4.9)

In figure 4.188 and from the goodness of fit, the coefficient of regression, R^2 is 0.9999 signifying a good fit since it is close to "1" and the Sum of Squared Errors of

0.1795 x 10^{-5} which is close to "0" (see Table 4.96). Hence, the G:M-mud composite had the best fit. The model curve in Figure 4.188 followed the same path with the experimental data. Similarly, the following curves, -P:W-Mud, M:W-Mud and G:W-Mud had lower deviations while M:P-Mud, G:P-Mud and G:M -Mud exhibited upper deviations to the model curve.

4.2.4.5 Modelling of Fluid Loss versus Square Root of Time for all the Muds with 0.05g/ml Starch Concentration at Room Temperature, 25°C

Linear model Poly2: v = -0.04358t^2+5.818t-1.087
Coefficients (with 95% confidence bounds):

Goodness of fit: SSE: 2.46; R-square: 0.9985

Adjusted R-square: 0.9975, RMSE: 0.9056

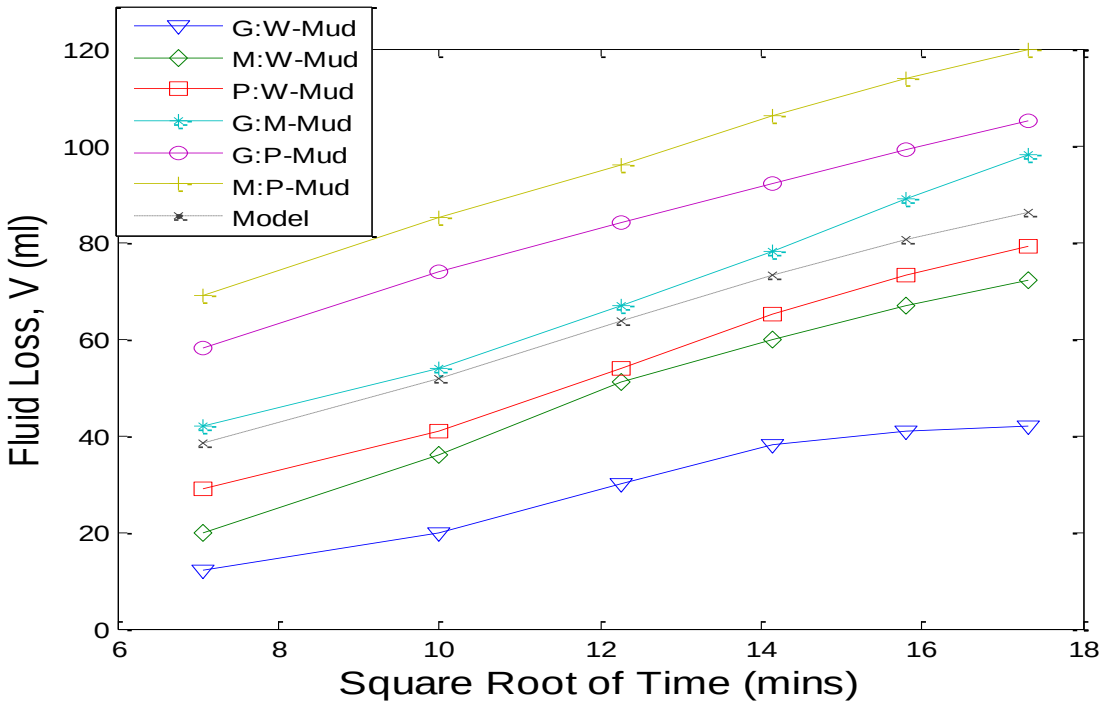

Figure 4.189: Plot of Modelled fluid loss versus square root of time for all the muds with 0.05g/ml starch concentration at room temperature, 25°C. (Data; Table 4.1-Table 4.9)

In figure 4.189, the goodness of fit analysis showed that the coefficient of regression, R^2 is 0.9999 signifying a good fit since it is close to "1" and the Sum of Squared Errors of 0.1188 x 10^{-5} which is close to "0" (see Table 4.96). Therefore, the P:W-mud exhibited the best fit. The model curve in Figure 4.189 followed the same path with the experimental data. Similarly, the following curves, P:W-Mud, M:W-Mud and G:W-Mud had lower deviations while G:M-Mud, G:P-Mud and M:P-mud exhibited upper deviations to the model curve.

4.2.4.6 Modelling of Fluid Loss versus Square Root of Time for all the Muds with 0.01g/ml Starch Concentration at High Temperature, 150^{o}C

Linear model Poly2: v = -0.04358t^2+5.818t-1.087

Coefficients (with 95% confidence bounds):

Goodness of fit: SSE: 2.46; R-square: 0.9985

Adjusted R-square: 0.9975, RMSE: 0.9056

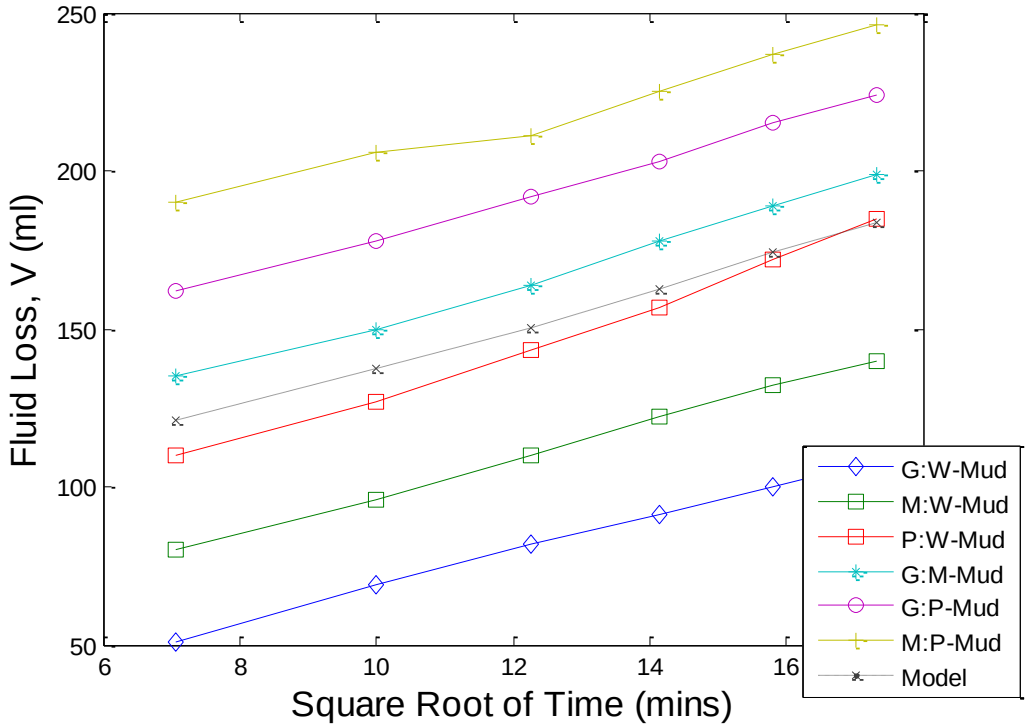

Figure 4.190: Plot of Modelled fluid loss versus square root of time for all the muds with 0.01g/ml starch concentration at high temperature, 150^{o}C. (Data; Table 4.10- Table 4.18)

In figure 4.190, the goodness of fit analysis showed that the coefficient of regression, R^2 is 0.9999 signifying a good fit since it is close to "1" and the Sum of Squared Errors of 0.2825 x 10^{-5} which is close to "0" (see Table 4.97). Therefore, the G:W-mud exhibited the best fit. The model curve in Figure 4.190 followed the same path with the experimental data. Similarly, the following curves, P:W-Mud, M:W-Mud and G:W-Mud had lower deviations while G:M-Mud, G:P-Mud and M:P-mud exhibited upper deviations to the model curve.

4.2.4.7 Modelling of fluid loss versus square root of time for all the muds with 0.02g/ml starch concentration at high temperature, 150^{o}C

Model equation, $v = -0.03431t^3+1.294t^2-9.868t+131.4$

Coefficients (with 95% confidence bounds):

Goodness of fit: SSE: 2.614; R-square: 0.9989

Adjusted R-square: 0.9972, RMSE: 1.143

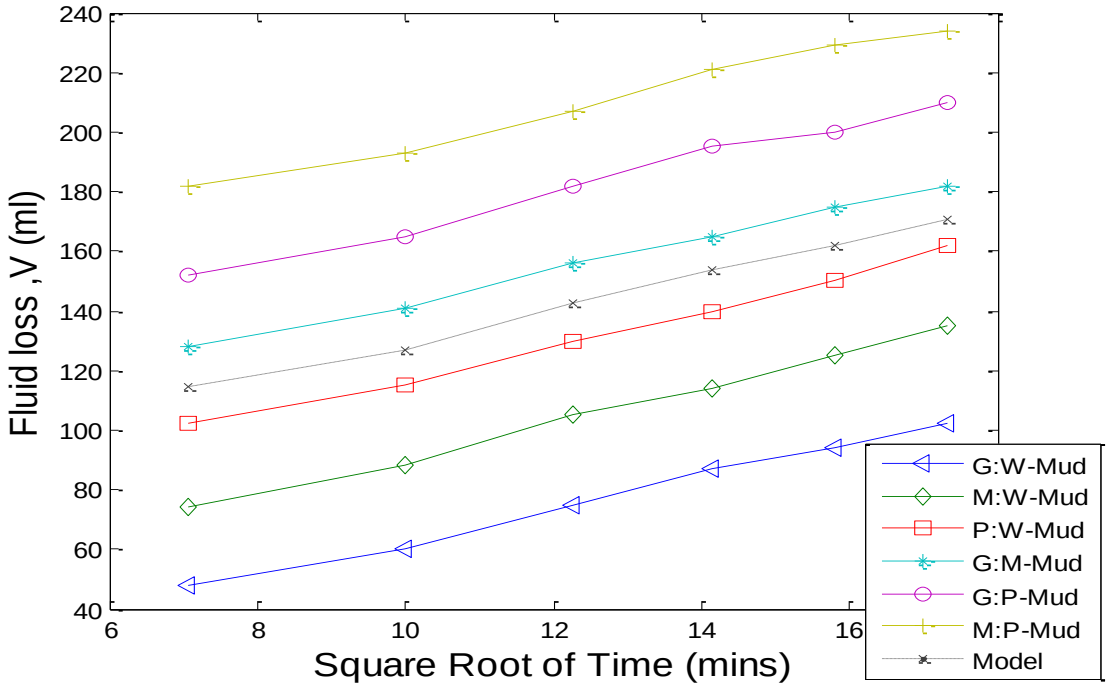

Figure 4.191: Plot of Modelled fluid loss versus square root of time for all the muds with 0.02g/ml starch concentration at high temperature, 150^{o}C. (Data; Table 4.10- Table 4.18)

In figure 4.191, the goodness of fit analysis showed that the coefficient of regression, R^2 is 0.9999 signifying a good fit since it is close to "1" and the Sum of Squared Errors of 0.2274 x 10^{-5} which is close to "0" (see Table 4.97). Therefore, the P:W-mud exhibited the best fit. The model curve in Figure 4.191 followed the same path with the experimental data. Similarly, the following curves, P:W-Mud, M:W-Mud and G:W-Mud had lower deviations while G:M-Mud, G:P-Mud and M:P-mud exhibited upper deviations to the model curve.

4.2.4.8 Modelling of fluid loss versus square root of time for all the muds with 0.03g/ml starch concentration at high temperature, 150^{o}C

Model equation is given as $v = -0.004405t^4+0.1937t^3-2.977t^2+23.75t+31.93$

Coefficients (with 95% confidence bounds):

Goodness of fit: SSE: 0.09937; R-square: 0.9999

Adjusted R-square: 0.9997, RMSE: 0.3152

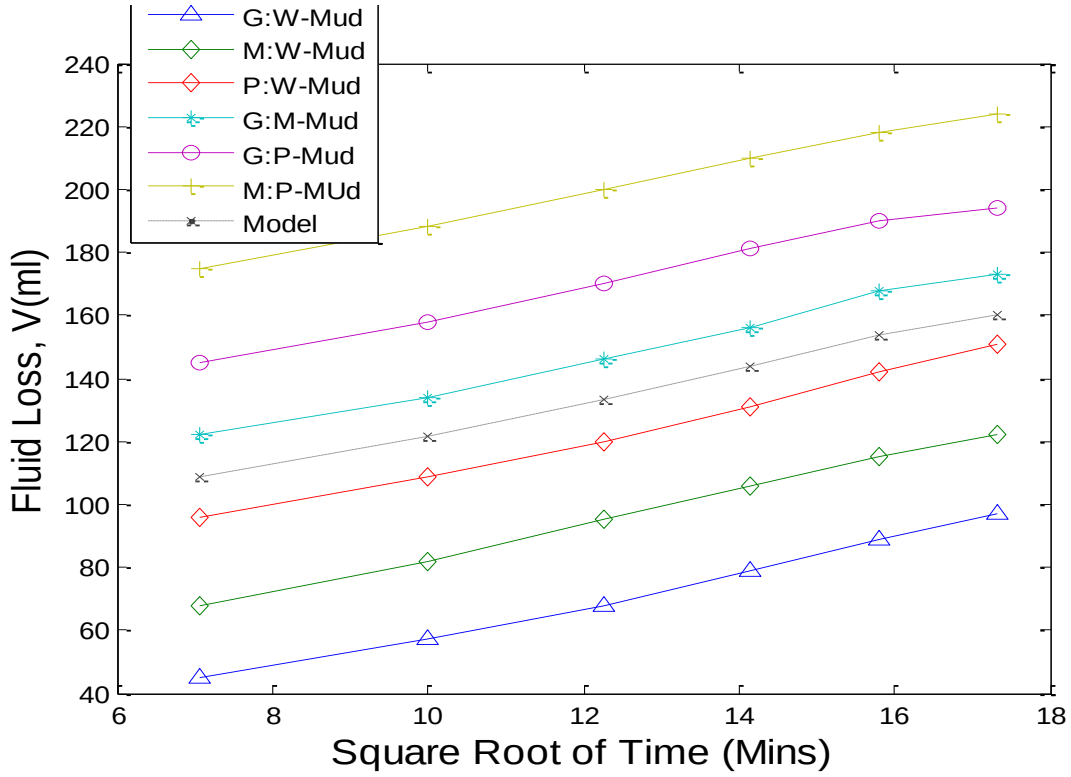

Figure 4.192: Plot of Modelled fluid loss versus square root of time for all the muds with 0.03g/ml starch concentration at high temperature, 150^{o}C. (Data; Table 4.10- Table 4.18)

In figure 4.192, the goodness of fit analysis showed that the coefficient of regression, R^2 is 0.9998 signifying a good fit since it is close to "1" and the Sum of Squared Errors of 0.3299 x 10^{-5} which is close to "0" (see Table 4.97). Therefore, the G:W-mud exhibited the best fit. The model curve in Figure 4.192 followed the same path with the experimental data. Similarly, the following curves, P:W-Mud, M:W-Mud and G:W-Mud had lower deviations while G:M-Mud, G:P-Mud and M:P-mud exhibited upper deviations to the model curve.

4.2.4.9 Modelling of fluid loss versus square root of time for all the muds with 0.04g/ml starch concentration at high temperature, 150^{o}C

Model Equation is given as, $v = 0.02629t^2+4.499t+66.94$

Coefficients (with 95% confidence bounds):

Goodness of fit: SSE: 0.9855; R-square: 0.9995

Adjusted R-square: 0.9991, RMSE: 0.5731

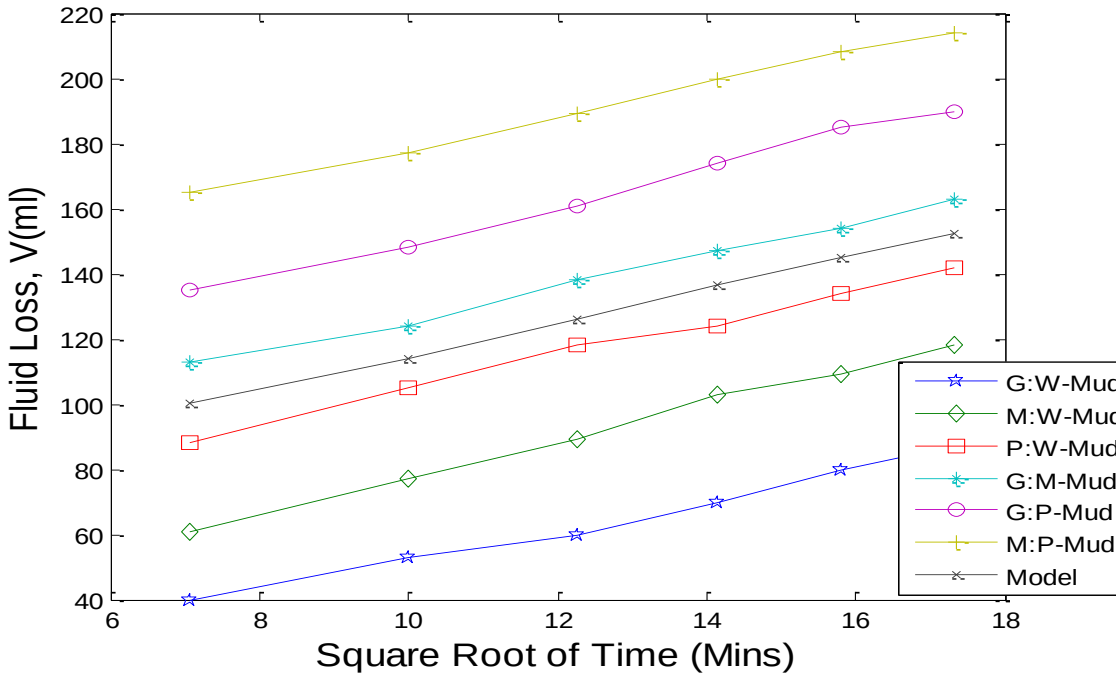

Figure 4.193: Plot of Modelled fluid loss versus square root of time for all the muds with 0.04g/ml starch concentration at high temperature, 150^{o}C. (Data; Table 4.10- Table 4.18)

In figure 4.193, the goodness of fit analysis showed that the coefficient of regression, R^2 is 0.9999 signifying a good fit since it is close to "1" and the Sum of Squared Errors of 0.1088 x 10^{-5} which is close to "0" (see Table 4.97). Therefore, the M:P-mud exhibited the best fit. The model curve in Figure 4.193 followed the same path with the experimental data. Similarly, the following curves, P:W-Mud, M:W-Mud and G:W-Mud had lower deviations while G:M-Mud, G:P-Mud and M:P-mud exhibited upper deviations to the model curve.

4.2.4.10 Modelling of fluid loss versus square root of time for all the muds with 0.05g/ml starch concentration at high temperature, 150°C.

Model Equation is given as, $v = -0.003329t^3+0.1909t^2+1.983t+69.19$

Coefficients (with 95% confidence bounds):

Goodness of fit: SSE: 0.6051; R-square: 0.9997

Adjusted R-square: 0.9992, RMSE: 0.5501

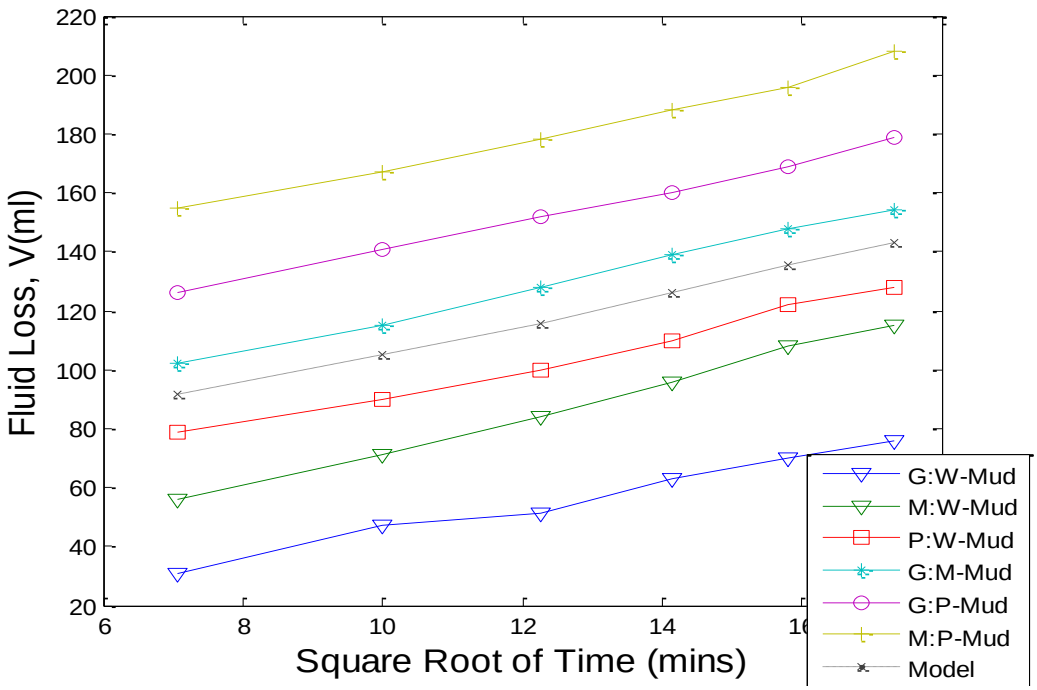

Figure 4.194: Plot of Modelled fluid loss versus square root of time for all the muds with 0.05g/ml starch concentration at high temperature, 150°C. (Data; Table 4.10- Table 4.18)

In figure 4.194, the goodness of fit analysis showed that the coefficient of regression, R^2 is 0.9999 signifying a good fit since it is close to "1" and the Sum of Squared Errors of 0.1771 x 10^{-5} which is close to "0" (see Table 4.97). Therefore, the G:P-mud exhibited the best fit. The model curve in Figure 4.194 followed the same path with the experimental data. Similarly, the following curves, P:W-Mud, M:W-Mud and G:W-Mud had lower deviations while G:M-Mud, G:P-Mud and M:P-mud exhibited upper deviations to the model curve.

4.2.4.11 Modelling of fluid loss versus square root of time for all the muds with 0.01g/ml starch concentration at high temperature, 250^{o}C

Model Equation is given as $v = -0.0441t^3+1.533t^2-9.782t+155.2$

Coefficients (with 95% confidence bounds):

Goodness of fit: SSE: 0.3625; R-square: 0.9999

Adjusted R-square: 0.9997, RMSE: 0.4257

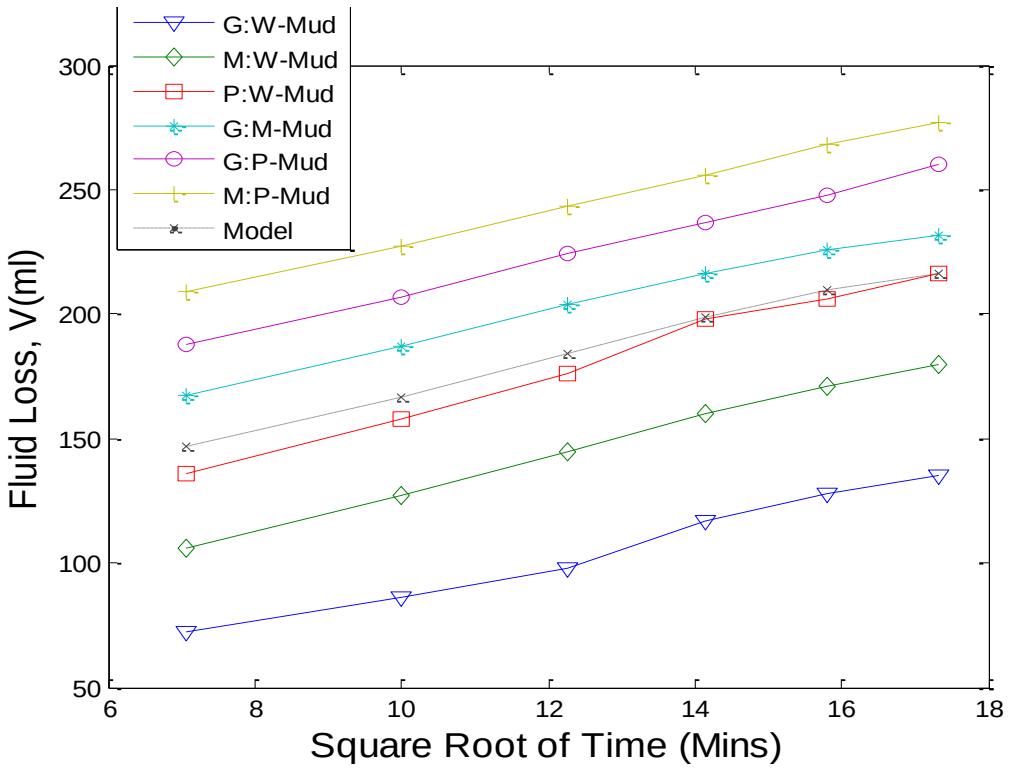

Figure 4.195: Plot of Modelled fluid loss versus square root of time for all the muds with 0.01g/ml starch concentration at high temperature, 250^{o}C. (Data; Table 4.19-Table 4.27)

In figure 4.195, the goodness of fit analysis showed that the coefficient of regression, R^2 is 0.9999 signifying a good fit since it is close to "1" and the Sum of Squared Errors of 0.3492 x 10^{-5} which is close to "0" (see Table 4.98). Therefore, the G:M-mud composite exhibited the best fit. The model curve in Figure 4.195 followed the same path with the experimental data. Similarly, the following curves, P:W-Mud, M:W-Mud and G:W-Mud had lower deviations while G:M-Mud, G:P-Mud and M:P-mud exhibited upper deviations to the model curve.

4.2.4.12 Modelling of fluid loss versus square root of time for all the muds with 0.02g/ml starch concentration at high temperature, 250°C.

Model Equation is given as $v = -0.001768t^3+0.1968t^2+2.821t+105.6$

Coefficients (with 95% confidence bounds):

Goodness of fit: SSE: 1.198; R-square: 0.9996

Adjusted R-square: 0.9991, RMSE: 0.773

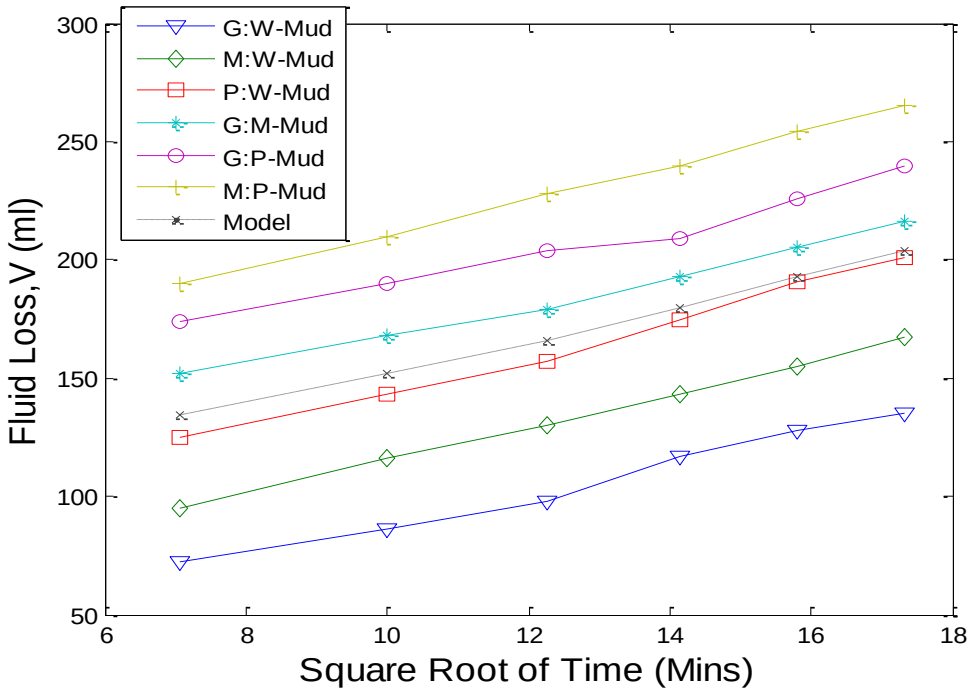

Figure 4.196: Plot of Modelled fluid loss versus square root of time for all the muds with 0.02g/ml starch concentration at high temperature, 250°C. (Data; Table 4.19-Table 4.27)

In figure 4.196, the goodness of fit analysis showed that the coefficient of regression, R^2 is 0.9999 signifying a good fit since it is close to "1" and the Sum of Squared Errors of 0.2045 x 10^{-5} which is close to "0" (see Table 4.98). Therefore, the M:W-mud exhibited the best fit. The model curve in Figure 4.196 followed the same path with the experimental data. Similarly, the following curves, P:W-Mud, M:W-Mud and G:W-Mud had lower deviations while G:M-Mud, G:P-Mud and M:P-mud exhibited upper deviations to the model curve.

4.2.4.13 Modelling of fluid loss versus square root of time for all the muds with 0.03g/ml starch concentration at high temperature, 250^{o}C

Model Equation is given as $v = -0.009323t^4+0.4689t^3-8.602t^2+73.33t-105.2$

Coefficients (with 95% confidence bounds):

Goodness of fit: SSE: 0.3084; R-square: 0.9999

Adjusted R-square: 0.9993, RMSE: 0.5553

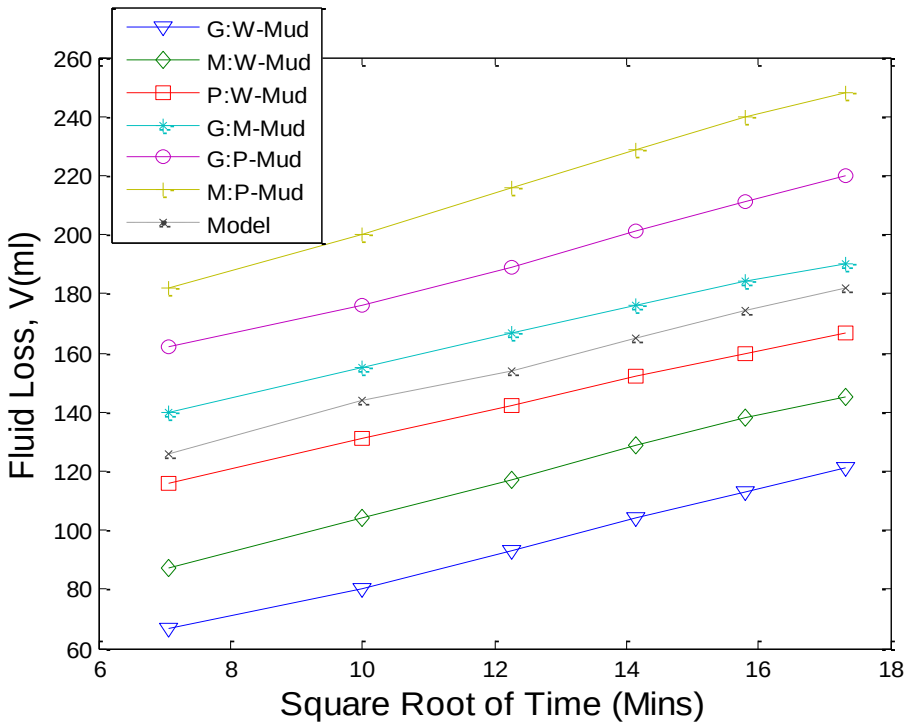

Figure 4.197: Plot of Modelled fluid loss versus square root of time for all the muds with 0.03g/ml starch concentration at high temperature, 250^{o}C. (Data; Table 4.19-Table 4.27)

In figure 4.197, the goodness of fit analysis showed that the coefficient of regression, R^2 is 0.9999 signifying a good fit since it is close to "1" and the Sum of Squared Errors of 0.0905 x 10^{-5} which is close to "0" (see Table 4.98). Therefore, the P:W-mud exhibited the best fit. The model curve in Figure 4.197 followed the same path with the experimental data. Similarly, the following curves, P:W-Mud, M:W-Mud and G:W-Mud had lower deviations while G:M-Mud, G:P-Mud and M:P-mud exhibited upper deviations to the model curve.

4.2.4.14 Modelling of fluid loss versus square root of time for all the muds with 0.04g/ml starch concentration at high temperature, 250^{o}C

The model equation is given as $v = -0.002865t^4+0.106t^3-1.162t^2+8.454t+83$

Coefficients (with 95% confidence bounds):

Goodness of fit: SSE: 0.2798; R-square: 0.9999

Adjusted R-square: 0.9995, RMSE: 0.5289

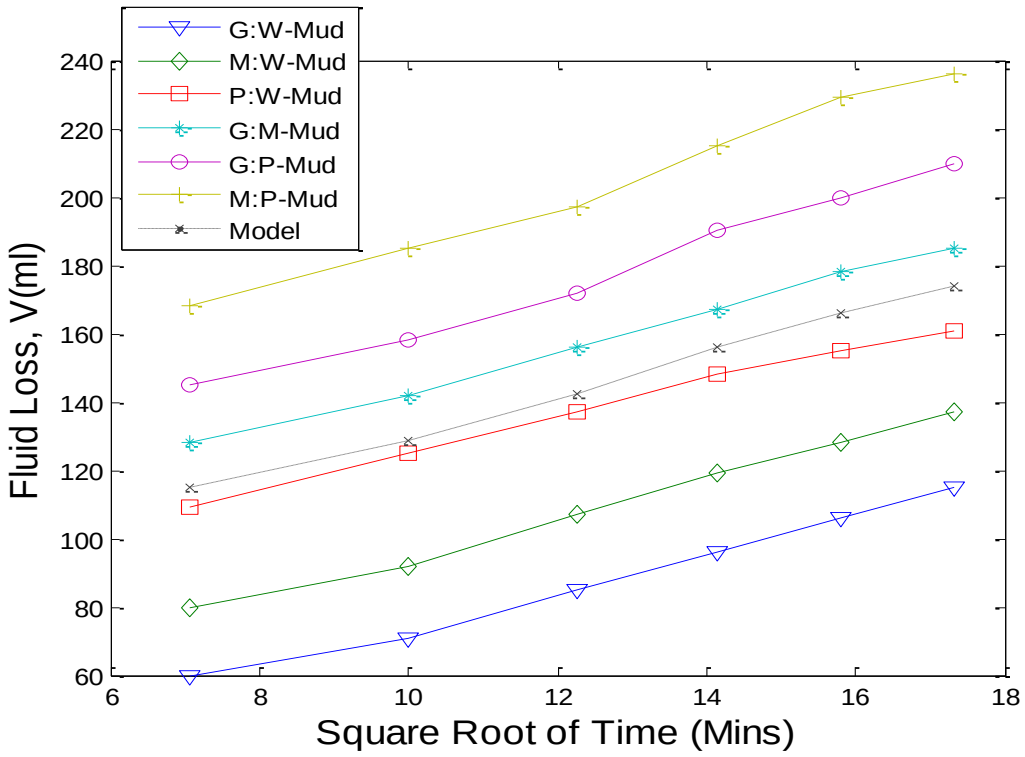

Figure 4.198: Plot of Modelled fluid loss versus square root of time for all the muds with 0.04g/ml starch concentration at high temperature, 250^{o}C. (Data; Table 4.19-Table 4.27)

In figure 4.198, the goodness of fit analysis showed that the coefficient of regression, R^2 is 0.9999 signifying a good fit since it is close to "1" and the Sum of Squared Errors of 0.1161 x 10^{-5} which is close to "0" (see Table 4.98). Therefore, the G:W-mud exhibited the best fit. The model curve in Figure 4.198 followed the same path with the experimental data. Similarly, the following curves, P:W-Mud, M:W-Mud and G:W-Mud had lower deviations while G:M-Mud, G:P-Mud and M:P-mud exhibited upper deviations to the model curve.

4.2.4.15 Modelling of fluid loss versus square root of time for all the muds with 0.05g/ml starch concentration at high temperature, 250^{o}C

The model equation is given as $v = 0.04248t^2+4.26t+70.29$

Coefficients (with 95% confidence bounds):

Goodness of fit: SSE: 0.1251; R-square: 0.9999

Adjusted R-square: 0.9999, RMSE: 0.2042

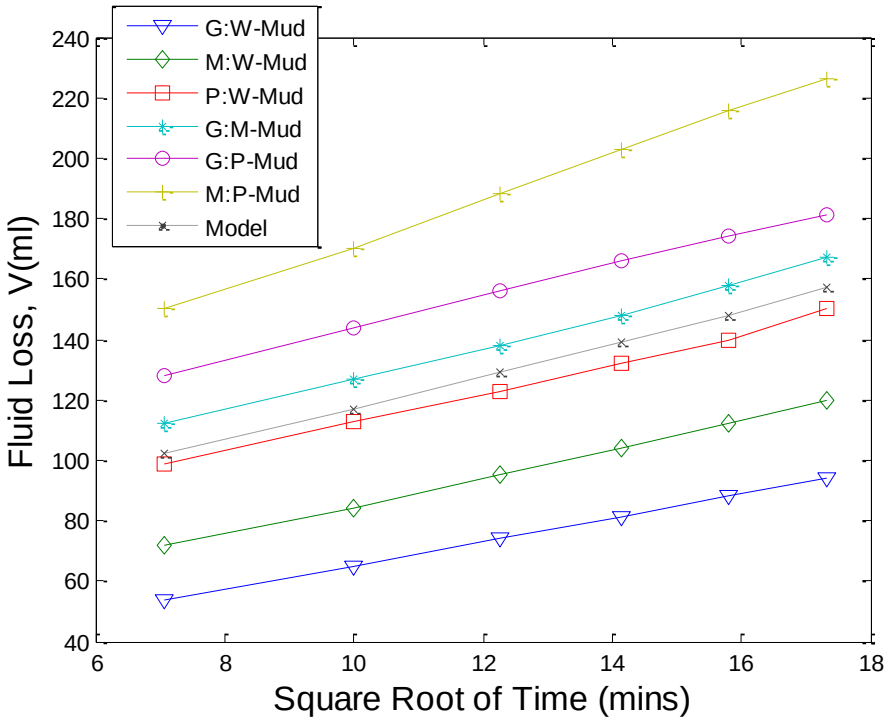

Figure 4.199: Plot of Modelled fluid loss versus square root of time for all the muds with 0.05g/ml starch concentration at high temperature, 250^{o}C. (Data; Table 4.19-Table 4.27)

In figure 4.199, the goodness of fit analysis showed that the coefficient of regression, R^2 is 0.9999 signifying a good fit since it is close to "1" and the Sum of Squared Errors of 0.1087 x 10^{-5} which is close to "0" (see Table 4.98). Therefore, the G:W-mud exhibited the best fit. The model curve in Figure 4.199 followed the same path with the experimental data. Similarly, the following curves, P:W-Mud, M:W-Mud and G:W-Mud had lower deviations while G:M-Mud, G:P-Mud and M:P-mud exhibited upper deviations to the model curve.

4.2.4.16 Modelling of the fluid loss versus square root of time for all the muds with 0.01g/ml starch concentration at high temperature, 350^{o}C.

Model equation v = 0.1309t^4-6.32$t^3$110.7t^2-824t+254.9

Coefficients (with 95% confidence bounds):

Goodness of fit: SSE: 178.4; R-square: 0.9569

Adjusted R-square: 0.7846, RMSE: 13.36

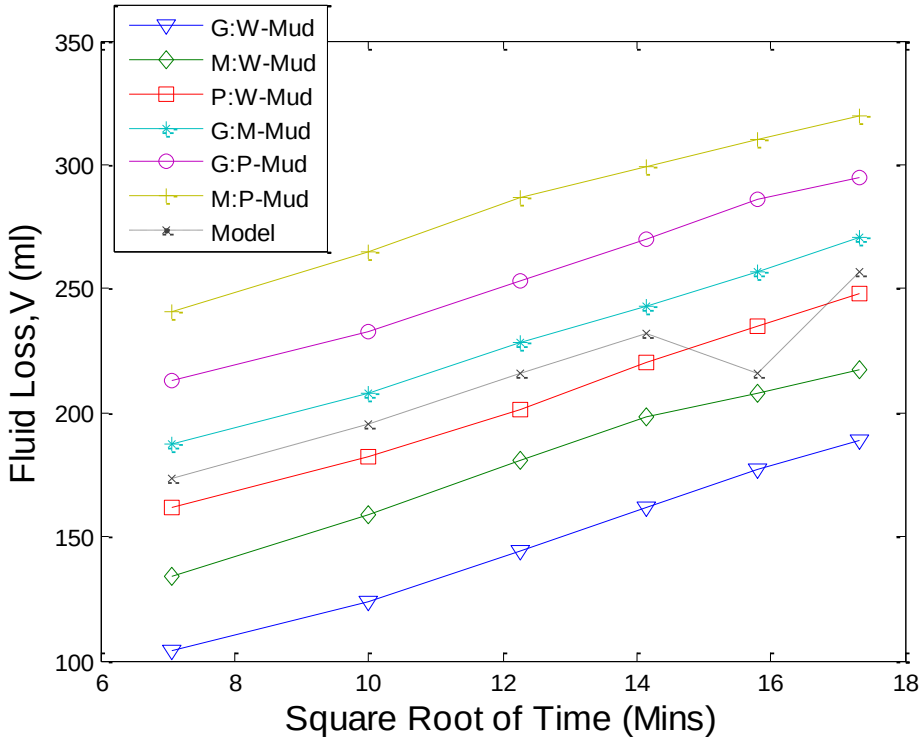

Figure 4.200: Plot of Modelled fluid loss versus square root of time for all the muds with 0.01g/ml starch concentration at high temperature, 350^{o}C. (Data; Table 4.28-Table 4.36)

In figure 4.200, the goodness of fit analysis showed that the coefficient of regression, R^2 is 0.9999 signifying a good fit since it is close to "1" and the Sum of Squared Errors of 0.5177 x 10^{-5} which is close to "0" (see Table 4.99). Therefore, the P:W-mud exhibited the best fit. The model curve in Figure 4.200 followed the same path with the experimental data. Similarly, the following curves, P:W-Mud, M:W-Mud and G:W-Mud had lower deviations while G:M-Mud, G:P-Mud and M:P-mud exhibited upper deviations to the model curve.

4.2.4.17 Modelling of the fluid loss versus square root of time for all the muds with 0.02g/ml starch concentration at high temperature, 350^{o}C

Model equation is given as $v = 0.1257t^2+4.786t+125.4$

Coefficients (with 95% confidence bounds):

Goodness of fit: SSE: 6.475; R-square: 0.9986

Adjusted R-square: 0.9976, RMSE: 1.469

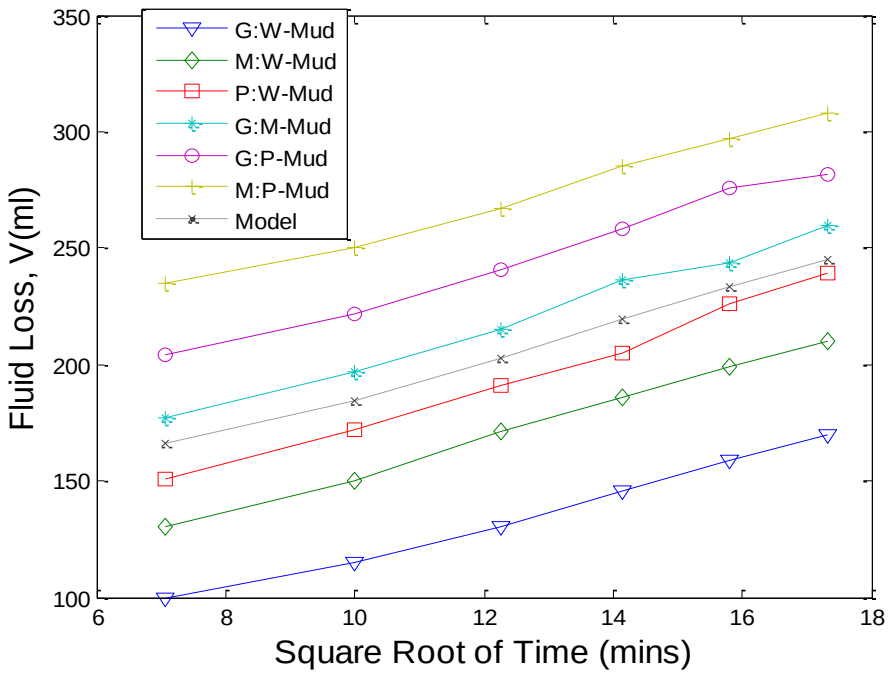

Figure 4.201: Plot of Modelled fluid loss versus square root of time for all the muds with 0.02g/ml starch concentration at high temperature, 350^{o}C. (Data; Table 4.28-Table 4.36)

In figure 4.201, the goodness of fit analysis showed that the coefficient of regression, R^2 is 0.9999 signifying a good fit since it is close to "1" and the Sum of Squared Errors of 0.3392 x 10^{-5} which is close to "0" (see Table 4.99). Therefore, the M:W-mud exhibited the best fit. The model curve in Figure 4.201 followed the same path with the experimental data. Similarly, the following curves, P:W-Mud, M:W-Mud and G:W-Mud had lower deviations while G:M-Mud, G:P-Mud and M:P-mud exhibited upper deviations to the model curve.

4.2.4.18 Modelling of the fluid loss versus square root of time for all the muds with 0.03g/ml starch concentration at high temperature, 350^{o}C

Model equation is given as $v = 0.08057t^2+4.793t+118.6$

Coefficients (with 95% confidence bounds):

Goodness of fit: SSE: 1.02; R-square: 0.9997

Adjusted R-square: 0.9995, RMSE: 0.5832

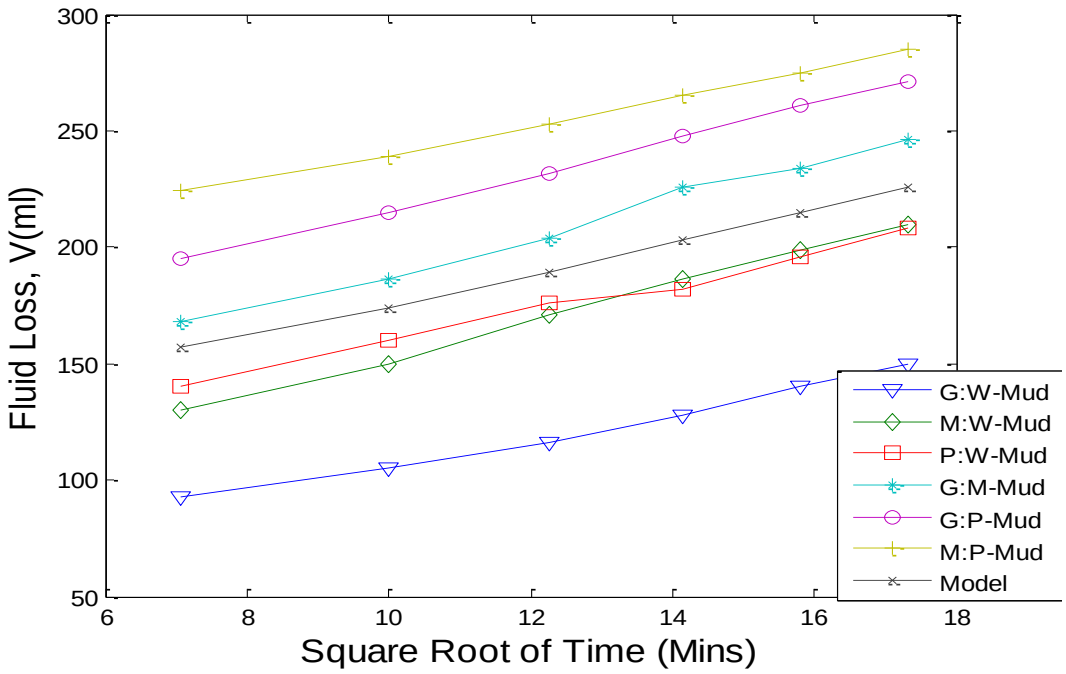

Figure 4.202: Plot of Modelled fluid loss versus square root of time for all the muds with 0.03g/ml starch concentration at high temperature, 350^{o}C. (Data; Table 4.28-Table 4.36)

In figure 4.202, the goodness of fit analysis showed that the coefficient of regression, R^2 is 0.9999 signifying a good fit since it is close to "1" and the Sum of Squared Errors of 0.3392 x 10^{-5} which is close to "0" (see Table 4.99). Therefore, the M:W-mud exhibited the best fit. The model curve in Figure 4.202 followed the same path with the experimental data. Similarly, the following curves, P:W-Mud, M:W-Mud and G:W-Mud had lower deviations while G:M-Mud, G:P-Mud and M:P-mud exhibited upper deviations to the model curve.

4.2.4.19 Modelling of the fluid loss versus square root of time for all the muds with 0.04g/ml starch concentration at high temperature, 350^{o}C

Model equation is as v = 0.1599t^2+2.817t+120

Coefficients (with 95% confidence bounds):

Goodness of fit: SSE: 0.3708; R-square: 0.9999

Adjusted R-square: 0.9998, RMSE: 0.3516

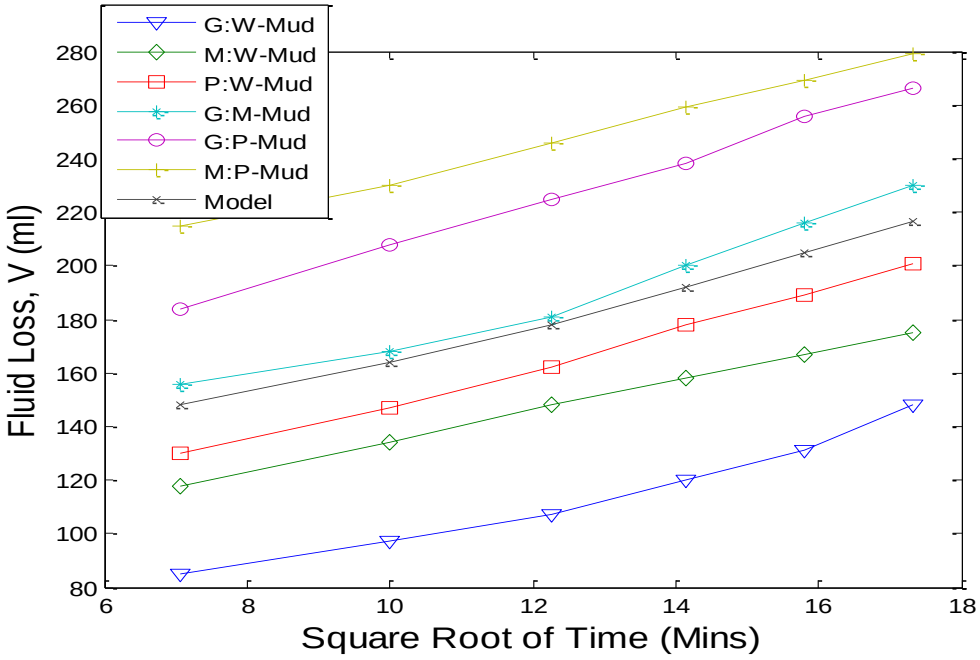

Figure 4.203: Plot of Modelled fluid loss versus square root of time for all the muds with 0.04g/ml starch concentration at high temperature, 350^{o}C. (Data; Table 4.28-Table 4.36)

In figure 4.203, the goodness of fit analysis showed that the coefficient of regression, R^2 is 0.9999 signifying a good fit since it is close to "1" and the Sum of Squared Errors of 0.1362 x 10^{-5} which is close to "0" (see Table 4.99). Therefore, the M:W-mud exhibited the best fit. The model curve in Figure 4.203 followed the same path with the experimental data. Similarly, the following curves, P:W-Mud, M:W-Mud and G:W-Mud had lower deviations while G:M-Mud, G:P-Mud and M:P-mud exhibited upper deviations to the model curve. The G:M and G:W-muds had a concave curve with a curvature at 12 mins.

4.2.4.20 Modelling of the fluid loss versus square root of time for all the muds with 0.05g/ml starch concentration at high temperature, 350^{o}C

Model equation is given as $v = -0.01366t^3+0.6191t^2-2.553t+129.3$

Coefficients (with 95% confidence bounds):

Goodness of fit: SSE: 0.1949; R-square: 0.9999

Adjusted R-square: 0.9998, RMSE: 0.3122

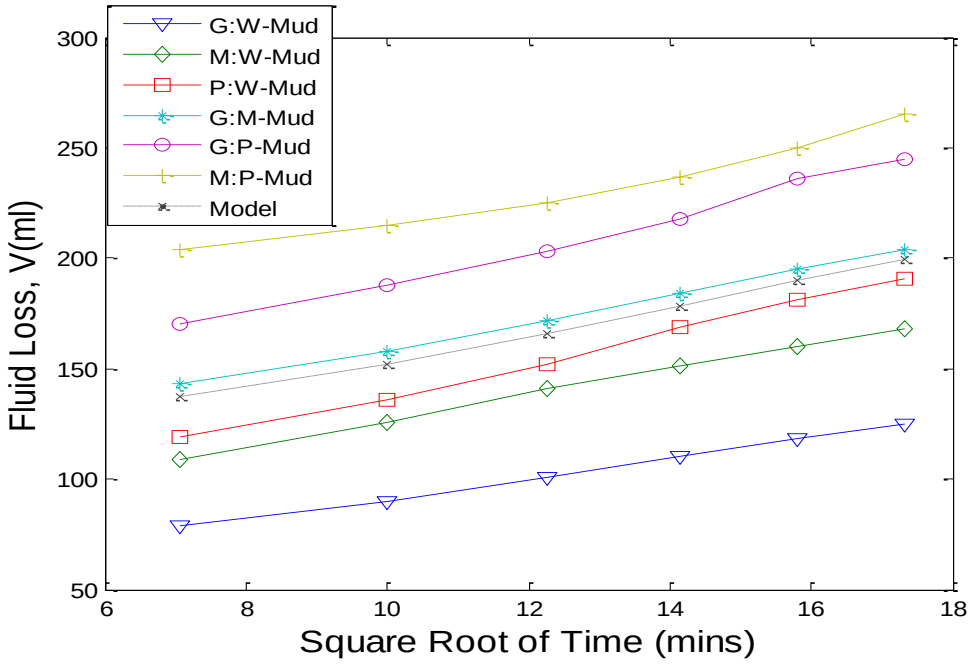

Figure 4.204: Plot of Modelled fluid loss versus square root of time for all the muds with 0.05g/ml starch concentration at high temperature, 350^{o}C. (Data; Table 4.28-Table 4.36)

In figure 4.204, the goodness of fit analysis showed that the coefficient of regression, R^2 is 0.9999 signifying a good fit since it is close to "1" and the Sum of Squared Errors of 0.1322 x 10^{-5} which is close to "0" (see Table 4.99). Therefore, the G:W-mud exhibited the best fit. The model curve in Figure 4.204 followed the same path with the experimental data. Similarly, the following curves, P:W-Mud, M:W-Mud and G:W-Mud had lower deviations while G:M-Mud, G:P-Mud and M:P-mud exhibited upper deviations to the model curve. The G:M and P:W-muds are closer to the model curve.

4.2.4.21 Modelling of the fluid loss versus square root of time for all the muds with 0.01g/ml starch concentration at high temperature, 450^{o}C

Model equation is given as $v = 0.09188t^4-4.712t^3+87.89t^2-689.1t+310$

Coefficients (with 95% confidence bounds):

Goodness of fit: SSE: 32.21; R-square: 0.9976

Adjusted R-square: 0.9879, RMSE: 5.675

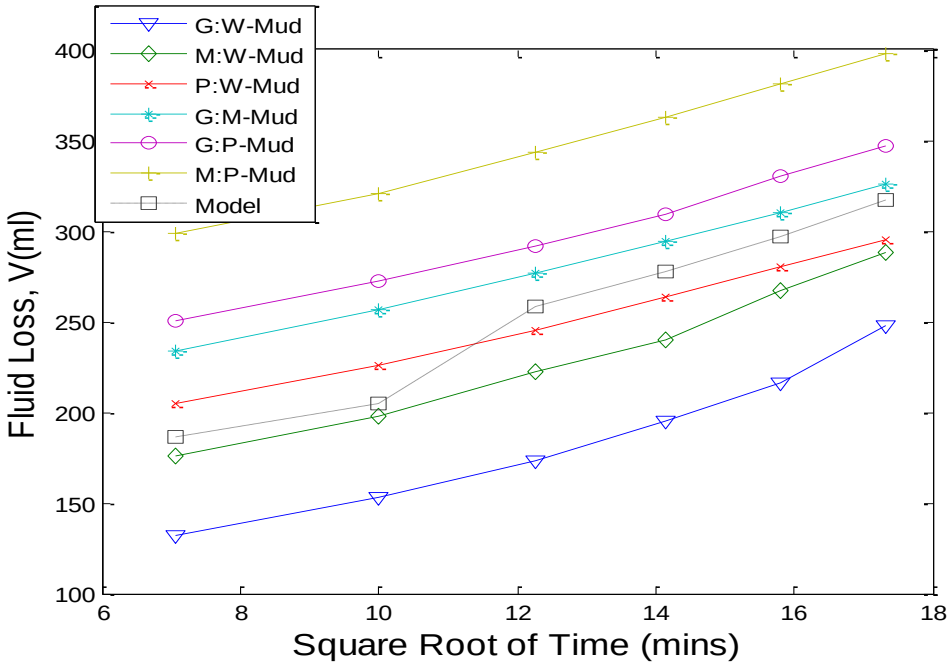

Figure 4.205: Plot of Modelled fluid loss versus square root of time for all the muds with 0.01g/ml starch concentration at high temperature, 450^{o}C. (Data; Table 4.37-Table 4.45)

In figure 4.205, the goodness of fit analysis showed that the coefficient of regression, R^2 is 0.9999 signifying a good fit since it is close to "1" and the Sum of Squared Errors of 0.1346 x 10^{-5} which is close to "0" (see Table 4.100). Therefore, the G:M-mud exhibited the best fit. The model curve in Figure 4.205 followed the same path with the experimental data. Similarly, the following curves, P:W-Mud, M:W-Mud and G:W-Mud had lower deviations while G:M-Mud, G:P-Mud and M:P-mud exhibited upper deviations to the model curve. The model curve had an interception with PW-mud at 11s^{-1}.

4.2.4.22 Modelling of the fluid loss versus square root of time for all the muds with 0.02g/ml starch concentration at high temperature, 450^{o}C

Model equation is given as $v = 0.008115t^4-0.3896t^3+7.182t^2-50.7t+316.4$

Coefficients (with 95% confidence bounds):

Goodness of fit: SSE: 1.313; R-square: 0.9998

Adjusted R-square: 0.999, RMSE: 1.146

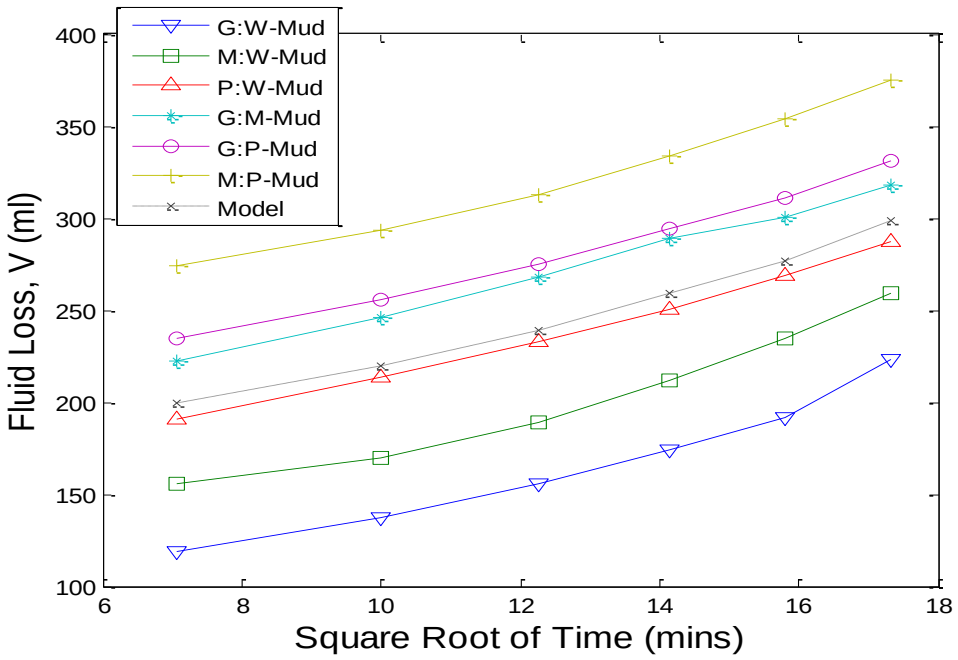

Figure 4.206: Plot of Modelled fluid loss versus square root of time for all the muds with 0.02g/ml starch concentration at high temperature, 450^{o}C. (Data; Table 4.37-Table 4.45)

In figure 4.206, the goodness of fit analysis showed that the coefficient of regression, R^2 is 0.9999 signifying a good fit since it is close to "1" and the Sum of Squared Errors of 0.4398 x 10^{-5} which is close to "0" (see Table 4.100). Therefore, the M:W-mud exhibited the best fit. The model curve in Figure 4.206 followed the same path with the experimental data. Similarly, the following curves, P:W-Mud, M:W-Mud and G:W-Mud had lower deviations while G:M-Mud, G:P-Mud and M:P-mud exhibited upper deviations to the model curve.

4.2.4.23 Modelling of the fluid loss versus square root of time for all the muds with 0.03g/ml starch concentration at high temperature, 450^{o}C

Model equation is given as $v = 0.366t^2+0.5725t+159.8$

Coefficients (with 95% confidence bounds):

Goodness of fit: SSE: 3.503; R-square: 0.9995

Adjusted R-square: 0.9991, RMSE: 1.081

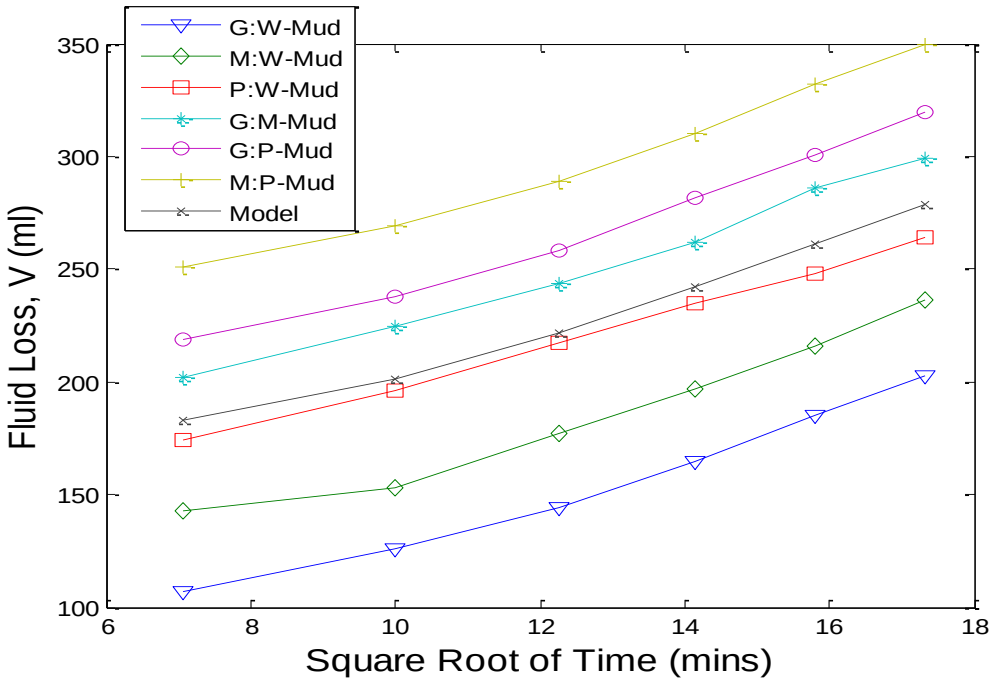

Figure 4.207: Plot of Modelled fluid loss versus square root of time for all the muds with 0.03g/ml starch concentration at high temperature, 450^{o}C. (Data; Table 4.37-Table 4.45)

In figure 4.207, the goodness of fit analysis showed that the coefficient of regression, R^2 is 0.9999 signifying a good fit since it is close to "1" and the Sum of Squared Errors of 0.1217 x 10^{-5} which is close to "0" (see Table 4.100). Therefore, the P:M-mud exhibited the best fit. The model curve in Figure 4.207 followed the same path with the experimental data. Similarly, the following curves, P:W-Mud, M:W-Mud and G:W-Mud had lower deviations while G:M-Mud, G:P-Mud and M:P-mud exhibited upper deviations to the model curve.

4.2.4.24 Modelling of the fluid loss versus square root of time for all the muds with 0.04g/ml starch concentration at high temperature, 450^{o}C

Model Equation is given as $v = -0.002598t^4+0.1042t^3-1.196t^2+12.66t+168$

Coefficients (with 95% confidence bounds):

Goodness of fit: SSE: 0.6499, R-square: 0.9999

Adjusted R-square: 0.9996, RMSE: 0.8061

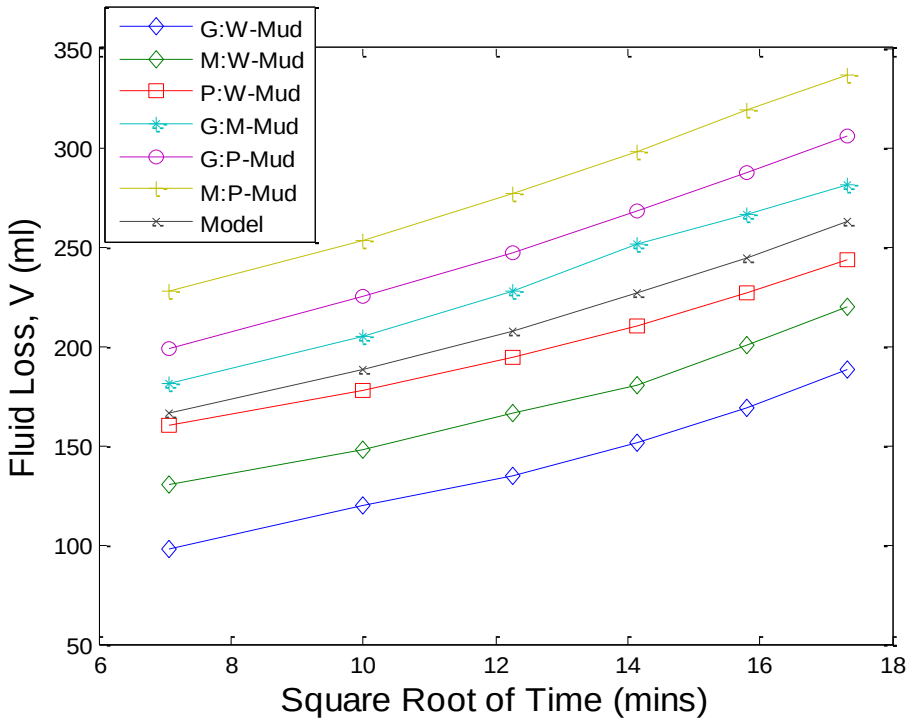

Figure 4.208: Plot of Modelled fluid loss versus square root of time for all the muds with 0.04g/ml starch concentration at high temperature, 450^{o}C. (Data; Table 4.37-Table 4.45)

In figure 4.208, the goodness of fit analysis showed that the coefficient of regression, R^2 is 0.9999 signifying a good fit since it is close to "1" and the Sum of Squared Errors of 0.3725 x 10^{-5} which is close to "0" (see Table 4.100). Therefore, the P:W-mud exhibited the best fit. The model curve in Figure 4.208 followed the same path with the experimental data. Similarly, the following curves, P:W-Mud, M:W-Mud and G:W-Mud had lower deviations while G:M-Mud, G:P-Mud and M:P-mud exhibited upper deviations to the model curve.

4.2.4.25 Modelling of the fluid loss versus square root of time for all the muds with 0.05g/ml starch concentration at high temperature, 450^{o}C

Model equation is given as $v = 0.01574t^3-0.1942t^2+6.872t+103.9$

Coefficients (with 95% confidence bounds):

Goodness of fit: SSE: 0.4148; R-square: 0.999

Adjusted R-square: 0.9998, RMSE: 0.4554

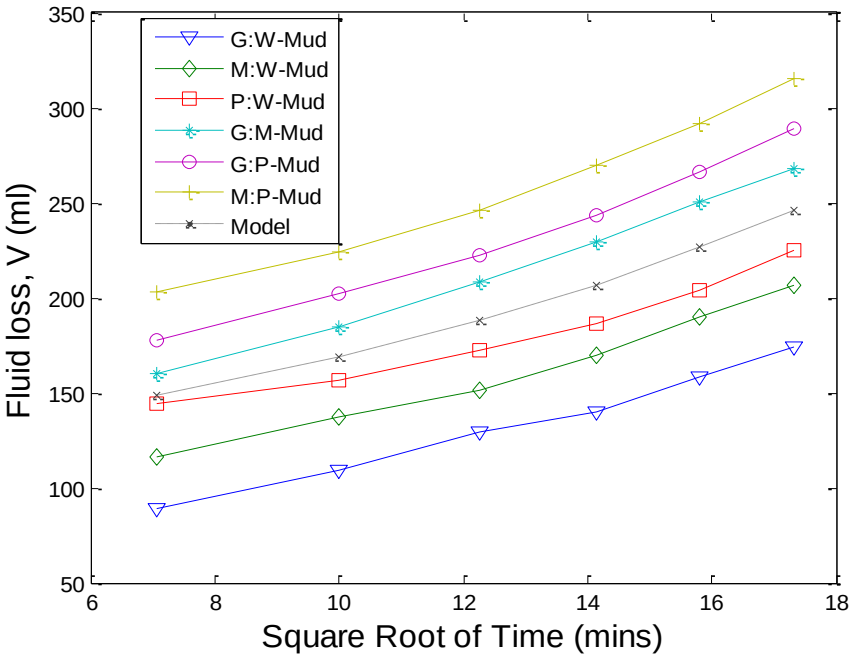

Figure 4.209: Plot of Modelled fluid loss versus square root of time for all the muds with 0.05g/ml starch concentration at high temperature, 450^{o}C. (Data; Table 4.37-Table 4.45)

In figure 4.209, the goodness of fit analysis showed that the coefficient of regression, R^2 is 0.9999 signifying a good fit since it is close to "1" and the Sum of Squared Errors of 0.5115 x 10^{-5} which is close to "0" (see Table 4.100). Therefore, the G:M-mud exhibited the best fit. The model curve in Figure 4.209 followed the same path with the experimental data. Similarly, the following curves, P:W-Mud, M:W-Mud and G:W-Mud had lower deviations while G:M-Mud, G:P-Mud and M:P-mud exhibited upper deviations to the model curve. The P:W-mud curve had close value at 6 mins.

Table 4.96: Modelled Result Parameters for Fluid loss behaviours of all the Muds containing varying starch concentrations Room Temperature, 25^0C

Starch Conc.	Parameters/Fillers	G:W	M:W	P:W	G:M	G:P	M:P
0.01g/ml	**R^2**	0.9992	0.9994	0.9985	0.9997	0.9997	**0.9999**
	SSE (x 10^{-5})	0.1333	0.1626	0.3188	0.5099	0.4011	**0.1107**
0.02g/ml	**R^2**	0.999	0.9995	0.9991	0.9995	**0.9999**	0.9994
	SSE (x 10^{-5})	0.7903	0.8249	0.8405	0.8608	**0.1795**	0.1991
0.03g/ml	**R^2**	0.9997	0.9999	0.9995	0.999	**0.9999**	0.9998
	SSE (x 10^{-5})	0.2512	0.2091	0.6839	0.8966	**0.0944**	0.3606
0.04g/ml	**R^2**	0.9996	0.999	1.436	**0.9999**	0.9998	0.9998
	SSE (x 10^{-5})	0.2857	0.2273	0.9989	**0.1795**	0.2951	0.2271
0.05g/ml	**R^2**	0.9995	0.9998	**0.9999**	0.9999	0.9996	0.9998
	SSE (x 10^{-5})	0.3605	0.2986	**0.1188**	0.2515	0.5416	0.4468

Table 4.97: Modelled Result Parameters for Fluid loss behaviours of all the Muds containing varying starch concentrations at High Temperature, 150^0C

Temperature	Parameters/Fillers	G:W	M:W	P:W	G:M	G:P	M:P
0.01g/ml	**R^2**	**0.9999**	0.9993	0.9999	0.9999	0.9997	0.9989
	SSE (x 10^{-5})	**0.2825**	0.3989	0.4635	0.3611	0.8265	0.2966
0.02g/ml	**R^2**	0.9997	0.9989	**0.9999**	0.9991	0.9987	0.9996
	SSE (x 10^{-5})	0.6184	0.2852	**0.2274**	0.2956	0.3088	0.9349
0.03g/ml	**R^2**	**0.9998**	0.9987	0.9997	0.9989	0.9994	0.9985
	SSE (x 10^{-5})	**0.3299**	0.4621	0.5734	0.5223	0.4106	0.3617
0.04g/ml	**R^2**	0.9968	0.9972	0.998	0.997	0.999	**0.9999**
	SSE (x 10^{-5})	0.4931	0.6293	0.3888	0.5299	0.2197	**0.1088**
0.05g/ml	**R^2**	0.996	0.9998	0.9993	0.9973	**0.9999**	0.9997
	SSE (x 10^{-5})	0.5551	0.4086	0.4192	0.5447	**0.1771**	0.6373

Table 4.98: Modelled Result Parameters for Fluid loss behaviours of all the Muds containing varying starch concentrations High Temperature, 250^0C

Starch Conc.	Parameters/Fillers	G:W	M:W	P:W	G:M	G:P	M:P
0.01g/ml	**R^2**	0.9988	0.9999	0.9960	**0.9999**	0.99995	0.9997
	SSE (x 10^{-5})	0.4254	0.4335	0.4162	**0.3492**	0.4608	0.4081
0.02g/ml	**R^2**	0.9982	**0.9999**	0.9979	0.9987	0.9938	0.9994
	SSE (x 10^{-5})	0.5549	**0.2045**	0.8893	0.7445	0.6763	0.3357
0.03g/ml	**R^2**	0.9999	0.9996	**0.9999**	0.9999	0.9994	0.9982
	SSE (x 10^{-5})	0.1642	0.1733	**0.0905**	0.2107	0.3346	0.3372
0.04g/ml	**R^2**	**0.9999**	0.9993	0.9997	0.9997	0.9983	0.9997
	SSE (x 10^{-5})	**0.1161**	0.1725	0.5666	0.7035	0.5464	0.4095
0.05g/ml	**R^2**	**0.9999**	0.9998	0.9999	0.9999	0.9999	0.9992
	SSE (x 10^{-5})	**0.1087**	0.2483	0.1692	0.1834	0.1455	0.3378

Table 4.99: Modelled Result Parameters for Fluid loss behaviours of all the Muds containing varying starch concentrations at High Temperature, 350^{0}C

Temperature	Parameters/Fillers	G:W	M:W	P:W	G:M	G:P	M:P
0.01g/ml	**R^2**	0.9985	0.9998	**0.9999**	0.9996	0.9998	0.9997
	SSE (x 10^{-5})	0.7821	0.7711	**0.5177**	0.8661	0.8901	0.7371
0.02g/ml	**R^2**	0.9999	**0.9999**	0.9982	0.9962	0.9993	0.9995
	SSE (x 10^{-5})	0.3642	**0.3392**	0.4953	0.5845	0.3396	0.4826
0.03g/ml	**R^2**	0.9996	**0.9999**	0.9964	0.9961	0.9999	0.9999
	SSE (x 10^{-5})	0.8314	**0.3392**	0.6473	0.5734	0.4926	0.3614
0.04g/ml	**R^2**	0.9991	**0.9999**	0.9994	0.9996	0.9988	0.9996
	SSE (x 10^{-5})	0.2508	**0.1362**	0.2055	0.2576	0.5745	0.2269
0.05g/ml	**R^2**	**0.9999**	0.9999	0.9997	0.9995	0.9994	0.9988
	SSE (x 10^{-5})	**0.1322**	0.2531	1.1591	0.3942	0.2578	0.3026

Table 4.100: Modelled Result Parameters for Fluid loss behaviours of all the Muds containing varying starch concentrations High Temperature, 450^{0}C

Starch Conc.	Parameters/Fillers	G:W	M:W	P:W	G:M	G:P	M:P
0.01g/ml	**R^2**	0.9997	0.9986	0.9999	**0.9999**	0.9996	0.9997
	SSE (x 10^{-5})	0.3449	0.5435	0.3941	**0.3246**	0.4858	0.3864
0.02g/ml	**R^2**	0.9988	**0.9999**	0.9999	0.9986	0.9999	0.9811
	SSE (x 10^{-5})	0.6754	**0.4398**	0.5278	0.7883	0.7251	0.7364
0.03g/ml	**R^2**	0.9997	0.9988	**0.9998**	0.999	0.9996	0.9997
	SSE (x 10^{-5})	0.2146	0.7983	**0.1217**	0.6684	0.2783	0.5786
0.04g/ml	**R^2**	0.9999	0.9994	**0.9999**	0.9995	0.9999	0.9999
	SSE (x 10^{-5})	0.7218	0.5505	**0.3725**	0.4422	0.6319	0.7111
0.05g/ml	**R^2**	0.9982	0.9985	0.9999	**0.9999**	0.9999	0.9999
	SSE (x 10^{-5})	0.8973	0.8637	0.5262	**0.5115**	0.7144	0.7211

4.2.4.26 Modelling of the Rate of Filtration versus time for all the muds with 0.03g/ml starch concentration at room temperature, 25°C.

The model equation becomes $f = -1.052e^{-7}t^3+7.33te^{-5}t^2-0.01801t+2.039$

f(x) = p1*x^3 + p2*x^2 + p3*x + p4

Goodness of fit: SSE: 0.001134; R-square: 0.998

Adjusted R-square: 0.995, RMSE: 0.02382

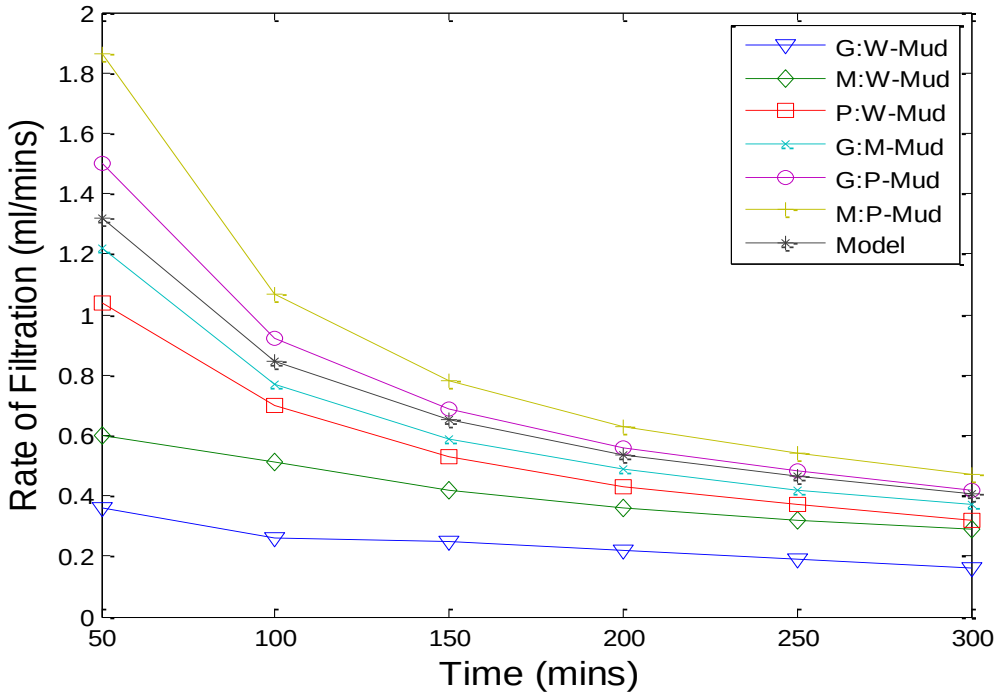

Figure 4.210: Plot of Modelled Rate of filtration versus time for all the muds with 0.03g/ml starch concentration at room temperature, 25°C. (Data; Table 4.1-Table 4.9)

In figure 4.210 and from the goodness of fit, the P:W-mud samples exhibited the best fit with coefficient of regression, R^2 is 0.9999 signifying a good fit since it is close to "1" and the Sum of Squared Errors of 0.1944 x 10^{-5} which is close to "0" (see Table 4.101). The model curve in Figure 4.210 followed the same path with the experimental data. However, the following curves, P:W-Mud, M:W-Mud, G:W-Mud, and G:M-Mud had lower deviations while G:P-Mud and M:P-mud exhibited upper deviations to the model curve.

4.2.4.27 Modelling of the Rate of Filtration versus time for all the muds with 0.03g/ml starch concentration at high temperature, 150^{o}C

The Model equation is given as

$f = -2.961e^{-7}t^{3}+0.0002008t^{2}=0.04629t+4.435$

Coefficients (with 95% confidence bounds):

Goodness of fit: SSE: 0.009298; R-square: 0.9966

Adjusted R-square: 0.9914, RMSE: 0.06818

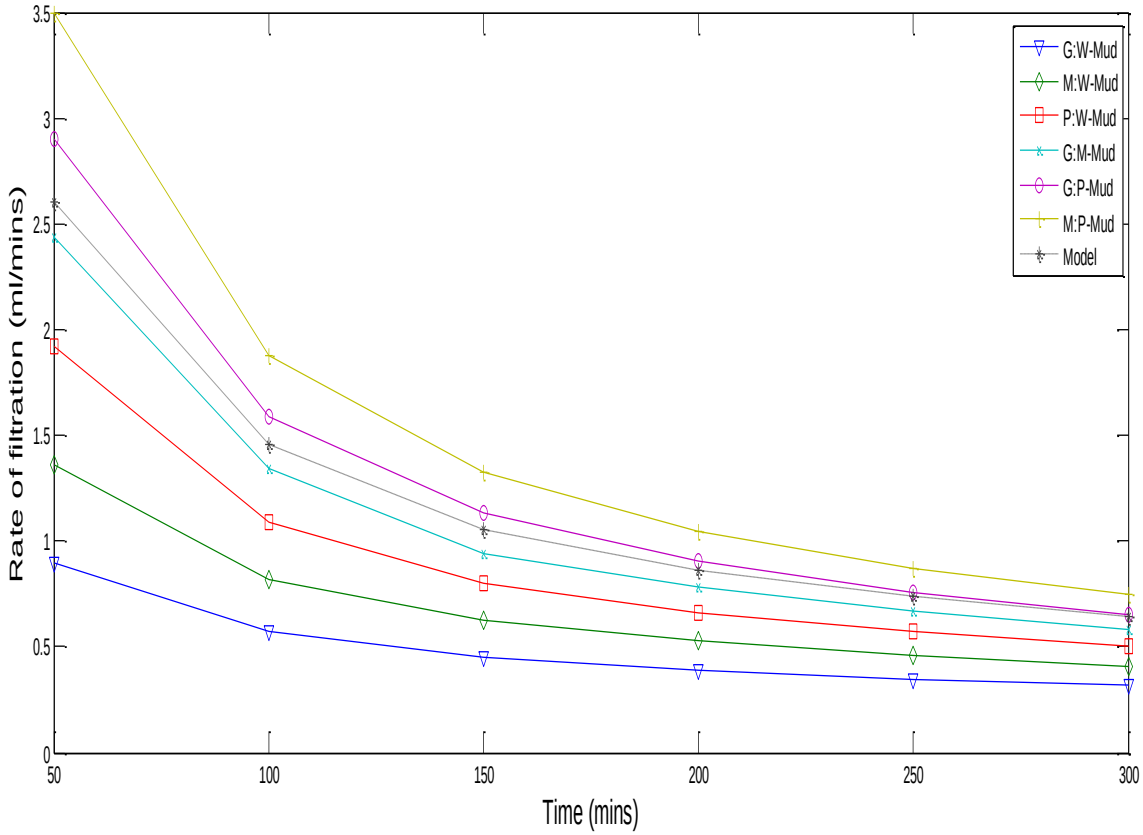

Figure 4.211: Plot of Modelled Rate of Filtration versus time for all the muds with 0.03g/ml starch concentration at high temperature, 150^{o}C. (Data; Table 4.10-Table 4.18)

The curves in Figure 4.211 showed that the goodness of fit, the P:W-mud samples exhibited the best fit with coefficient of regression, R^2 is 0.9999 signifying a good fit

since it is close to "1" and the Sum of Squared Errors of 0.1921 x 10^{-5} which is close to "0" (see Table 4.101). The model curve followed the same path with the experimental data. Also, the following curves, P:W-Mud, M:W-Mud, G:W-Mud, and G:M-Mud had lower deviations while G:P-Mud and M:P-mud exhibited upper deviations to the model curve.

4.2.4.28 Modelling of the Rate of Filtration versus time for all the muds with 0.03g/ml starch concentration at room temperature, 250^{o}C

Linear model Poly4:

$f = 2.033e^{-9}t^4-1.757e^{-6}t^3+0.0005664t^2-0.08431t+6.021$

Coefficients (with 95% confidence bounds):

Goodness of fit: SSE: 0.0006036; R-square: 0.9998

Adjusted R-square: 0.9992, RMSE: 0.0245

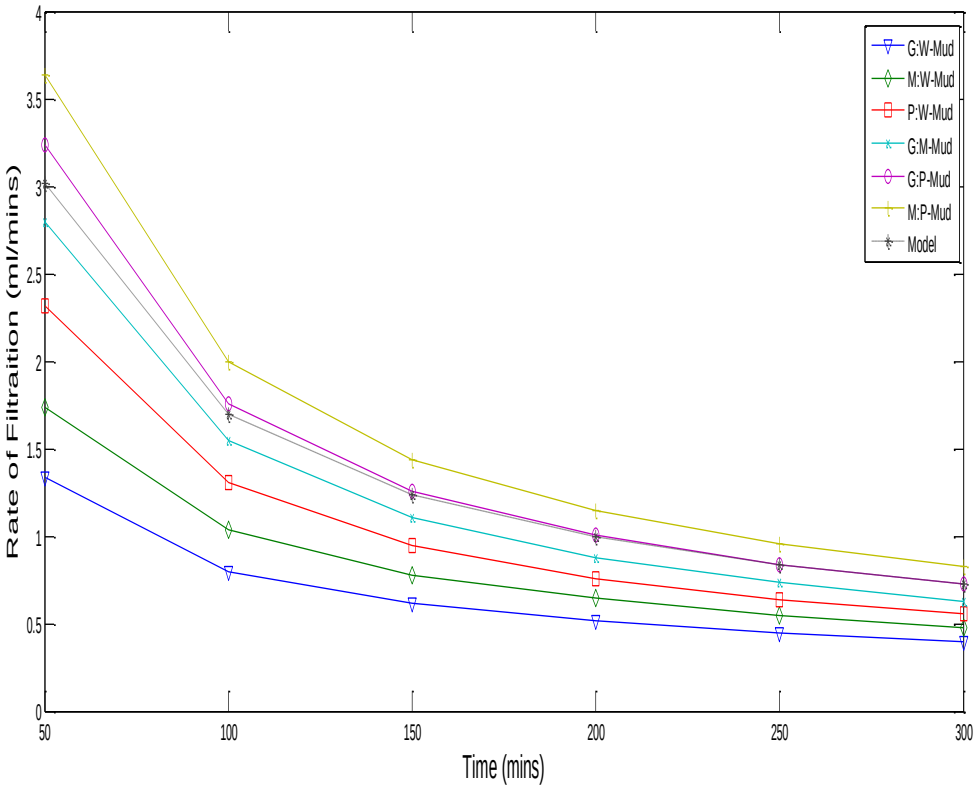

Figure 4.212: Plot of Modelled Rate of Filtration versus time for all the muds with 0.03g/ml starch concentration at high temperature, 250^{o}C. (Data; Table 4.19-Table 4.27)

The curves in Figure 4.212 showed that the goodness of fit, the G:W-mud samples exhibited the best fit with coefficient of regression, R^2 is 0.9999 signifying a good fit since it is close to "1" and the Sum of Squared Errors of 0.1433 x 10^{-5} which is close to "0" (see Table 4.101). The model curve followed the same path with the experimental data. Also, the following curves, P:W-Mud, M:W-Mud, G:W-Mud, and G:M-Mud had lower deviations while G:P-Mud and M:P-mud exhibited upper deviations to the model curve. Between 200 – 300mins, the G:P had the same path with the model curve.

4.2.4.29 Modelling of the Rate of Filtration versus time for all the muds with 0.03g/ml starch concentration at room temperature, 350^{o}C

Linear model Poly4: $f = 2.593e^{-9}t^4-2.24e^{-6}t^3+0.0007219t^2-0.1072t+7.582$

Coefficients (with 95% confidence bounds):

Goodness of fit: SSE: 0.001048; R-square: 0.9998

Adjusted R-square: 0.9991, RMSE: 0.03238

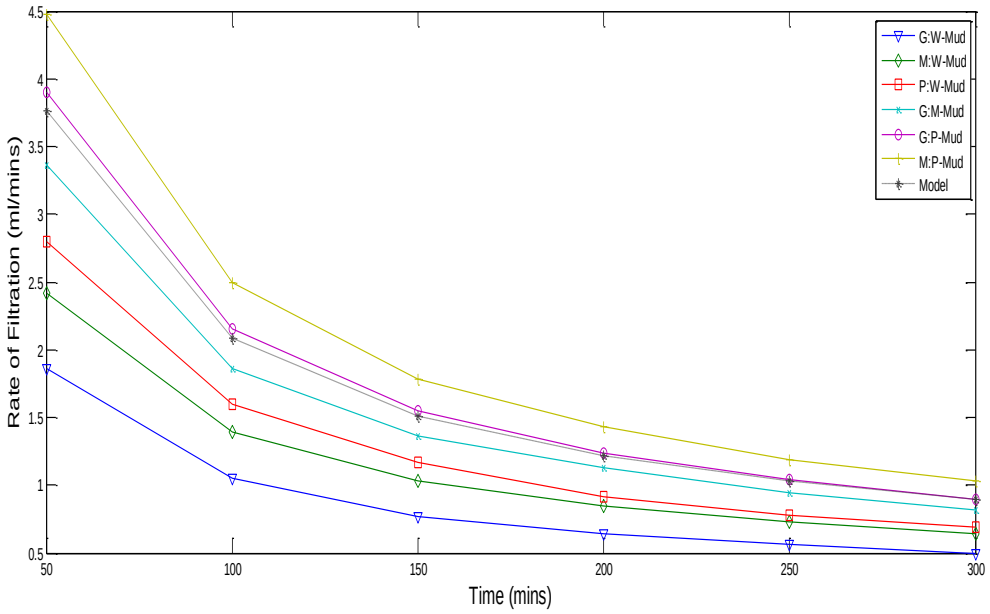

Figure 4.213: Plot of Modelled Rate of Filtration versus time for all the muds with 0.03g/ml starch concentration at high temperature, 350^{o}C. (Data; Table 4.28-Table 4.36)

The curves in Figure 4.213 showed that the goodness of fit, the G:W-mud samples exhibited the best fit with coefficient of regression, R^2 is 0.9999 signifying a good fit since it is close to "1" and the Sum of Squared Errors of 0.1751 x 10^{-5} which is close to "0" (see Table 4.101). The model curve followed the same path with the experimental data. Also, the following curves, P:W-Mud, M:W-Mud, G:W-Mud, and G:M-Mud had lower deviations while G:P-Mud and M:P-mud exhibited upper deviations to the model curve. Between 250 – 300mins, the G:P had the same path with the model curve.

4.2.4.30 Modelling of the Rate of Filtration versus time for all the muds with 0.03g/ml starch concentration at room temperature, 450^{o}C

Model equation: $r = -6.514e^{-5}t^2+0.4118t+161.6$

Coefficients (with 95% confidence bounds):

Goodness of fit: SSE: 2.815; R-square: 0.9996

Adjusted R-square: 0.9993, RMSE: 0.9687

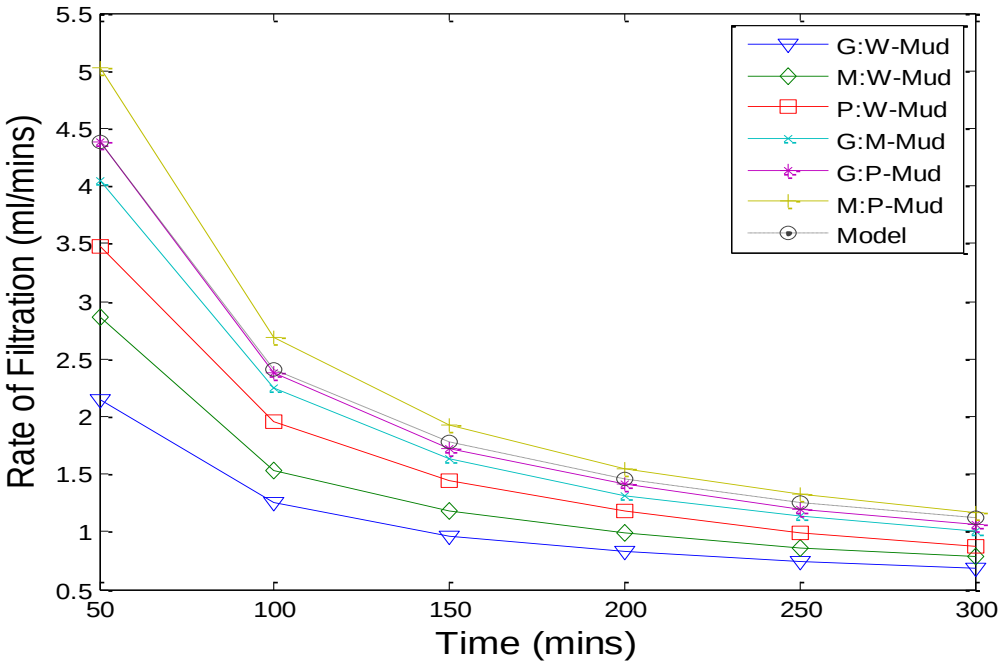

Figure 4.214: Plot of Modelled Rate of Filtration versus time for all the muds with 0.03g/ml starch concentration at high temperature, 450^{o}C. (Data; Table 4.37-Table 4.45)

The curves in Figure 4.214 showed that the goodness of fit, the G:W-mud samples exhibited the best fit with coefficient of regression, R^2 is 0.9999 signifying a good fit since it is close to "1" and the Sum of Squared Errors of 0.1016 x 10^{-5} which is close to "0" (see Table 4.101). The model curve followed the same path with the experimental data. Also, the following curves, P:W-Mud, M:W-Mud, G:W-Mud, and G:M-Mud and G:P-Mud had lower deviations while M:P-mud exhibited upper deviations to the model curve. Between 50 – 100mins, the G:P had the same path with the model curve.

Table 4.101: Modelled Result Parameters for Rate of Filtration of all the Muds containing 0.03g/ml starch concentration at different Temperatures

Temperature	Parameters/Fillers	G:W	M:W	P:W	G:M	G:P	M:P
25^{0}C	**R^2**	0.9963	0.9999	**0.9999**	0.9999	0.9998	0.9998
	SSE (x 10^{-5})	0.8929	0.6349	**0.1944**	0.3968	0.1286	0.2286
150^{0}C	**R^2**	0.9999	0.9999	**0.9999**	0.9973	0.9999	0.9998
	SSE (x 10^{-5})	0.2543	0.8929	**0.1921**	0.6652	0.3571	0.9211
250^{0}C	**R^2**	**0.9998**	0.9968	0.9998	0.9998	0.9998	0.9998
	SSE (x 10^{-5})	**0.1433**	0.3481	0.3813	0.7112	0.6671	0.1832
350^{0}C	**R^2**	**0.9999**	0.9999	0.9995	0.9999	0.9998	0.9999
	SSE (x 10^{-5})	**0.1751**	0.3111	0.1777	0.2286	0.2112	0.6349
450^{0}C	**R^2**	**0.9999**	0.9995	0.9998	0.9997	0.9999	0.9997
	SSE (x 10^{-5})	**0.1016**	0.1525	0.8036	0.1889	0.1032	0.2867

4.2.4.31 Modelling of Shear Stress as a Function of Shear Rate for G:W-Mud

Model equation is given as $s = -356r^2+3152r+302.8$

Coefficients (with 95% confidence bounds):

Goodness of fit: SSE: 2925; R-square: 0.9992

Adjusted R-square: 0.9976, RMSE: 54.08

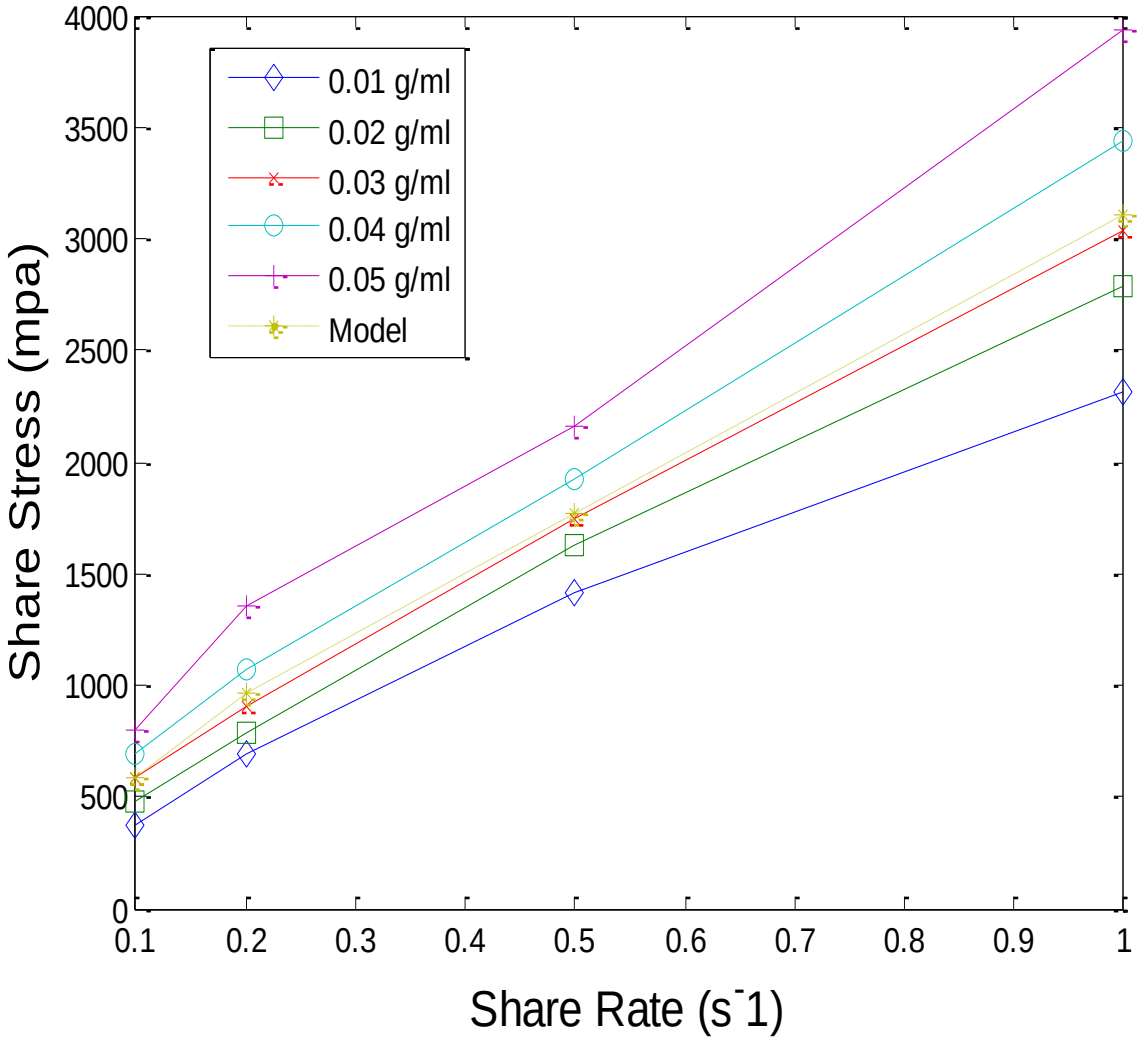

Figure 4.215: Plot of Modelled Shear Stress as a Function of Shear Rate for G:W-Mud. (Data; Table 4.56)

In figure 4.215, the goodness of fit analysis showed that the coefficient of regression, R^2 is 0.9999 signifying a good fit since it is close to "1" and the Sum of Squared Errors of 0.5115×10^{-5} which is close to "0" (see Table 4.102). Therefore, the 0.04

g/ml concentration exhibited the best fit. The model curve in Figure 4.215 followed the same path with the experimental data. Similarly, the following curves, 0.01 g/ml, 0.02 g/ml and 0.03 g/ml concentrations exhibited lower deviations with 0.03 g/ml curve having close proximity with the model. The 0.04 g/ml and 0.05 g/ml had upper deviations to the model curve.

4.2.4.32 Modelling of Shear Stress as a Function of Shear Rate for M:W-Mud

Model equation is given as $s = -424.8r^2+3001r+263.4$

Coefficients (with 95% confidence bounds):

Goodness of fit: SSE: 1250; R-square: 0.9996

Adjusted R-square: 0.9988, RMSE: 35.36

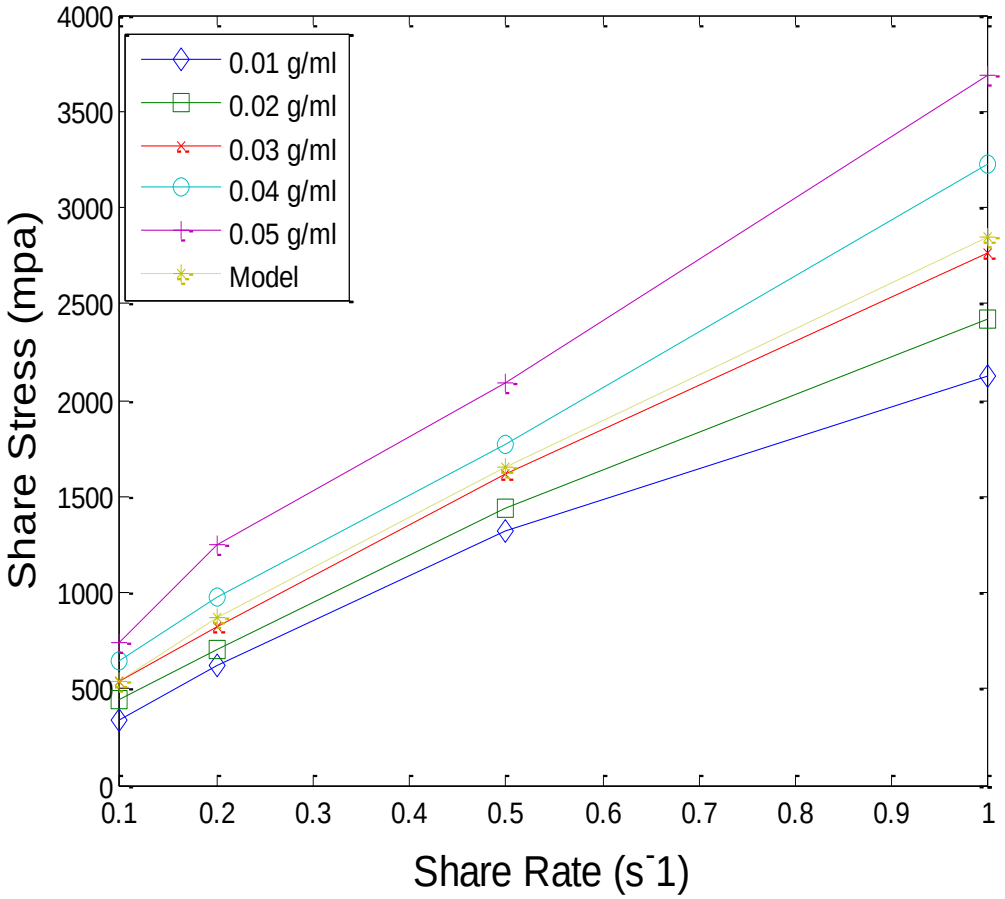

Figure 4.216: Plot of Modelled Shear Stress as a Function of Shear Rate for M:W-Mud. (Data; Table 4.57)

In figure 4.216, the goodness of fit analysis showed that the coefficient of regression, R^2 is 0.9996 signifying a good fit since it is close to "1" and the Sum of Squared Errors of 0.1604 x 10^{-5} which is close to "0" (see Table 4.102). Therefore, the 0.05 g/ml concentration exhibited the best fit. The model curve in Figure 4.216 followed the same path with the experimental data. Similarly, the following curves, 0.01 g/ml, 0.02 g/ml and 0.03 g/ml concentrations exhibited lower deviations with 0.03 g/ml curve having close proximity with the model. The 0.04 g/ml and 0.05 g/ml had upper deviations to the model curve.

4.2.4.33 Modelling of Shear Stress as a Function of Shear Rate for P:W-Mud

Model equation is given as $s = -985.9r^2+3379r+162.1$

Coefficients (with 95% confidence bounds):

Goodness of fit: SSE: 177.9; R-square: 0.9999

Adjusted R-square: 0.9998, RMSE: 13.34

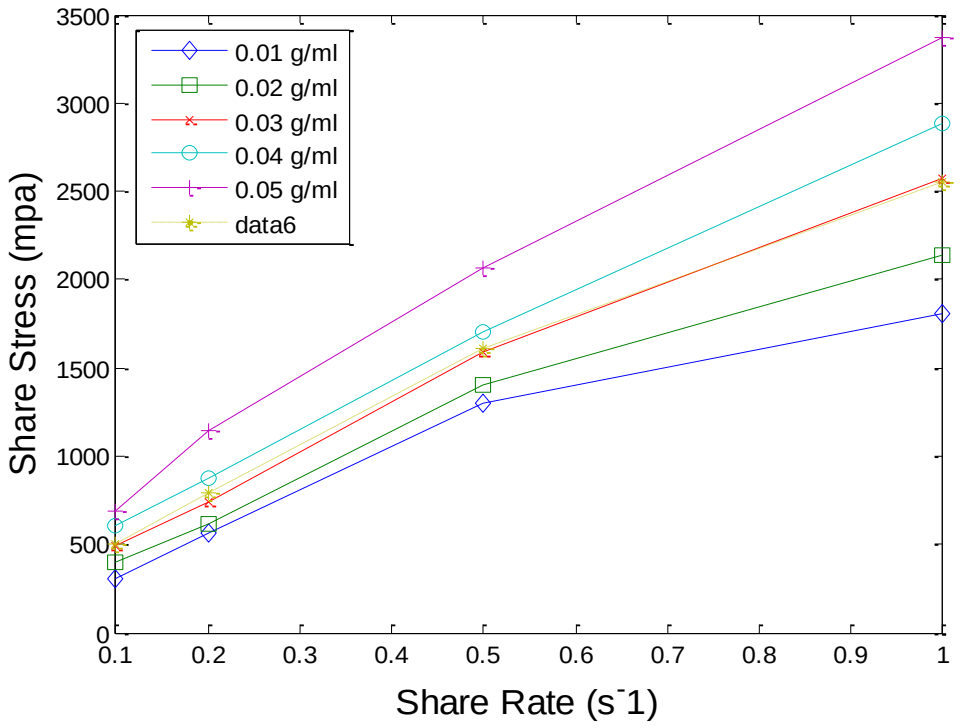

Figure 4.217: Plot of Modelled Shear Stress as a Function of Shear Rate for P:W-Mud. (Data; Table 4.58)

In figure 4.217, the goodness of fit analysis showed that the coefficient of regression, R^2 is 0.9993 signifying a good fit since it is close to "1" and the Sum of Squared Errors of 0.1048 x 10^{-5} which is close to "0" (see Table 4.102).

Therefore, the 0.03 g/ml concentration exhibited the best fit. The model curve in Figure 4.217 followed the same path with the experimental data. Similarly, the following curves, 0.01 g/ml, 0.02 g/ml and 0.03 g/ml concentrations exhibited lower deviations with 0.03 g/ml curve having close proximity with the model. The 0.04 g/ml and 0.05 g/ml had upper deviations to the model curve.

4.2.4.34 Modelling of Shear Stress as a Function of Shear Rate for G:M-Mud

Model equation is given as s = -783.7r^2+3023r+145.3

Coefficients (with 95% confidence bounds):

Goodness of fit: SSE: 577.4; R-square: 0.9997

Adjusted R-square: 0.9992

RMSE: 24.03

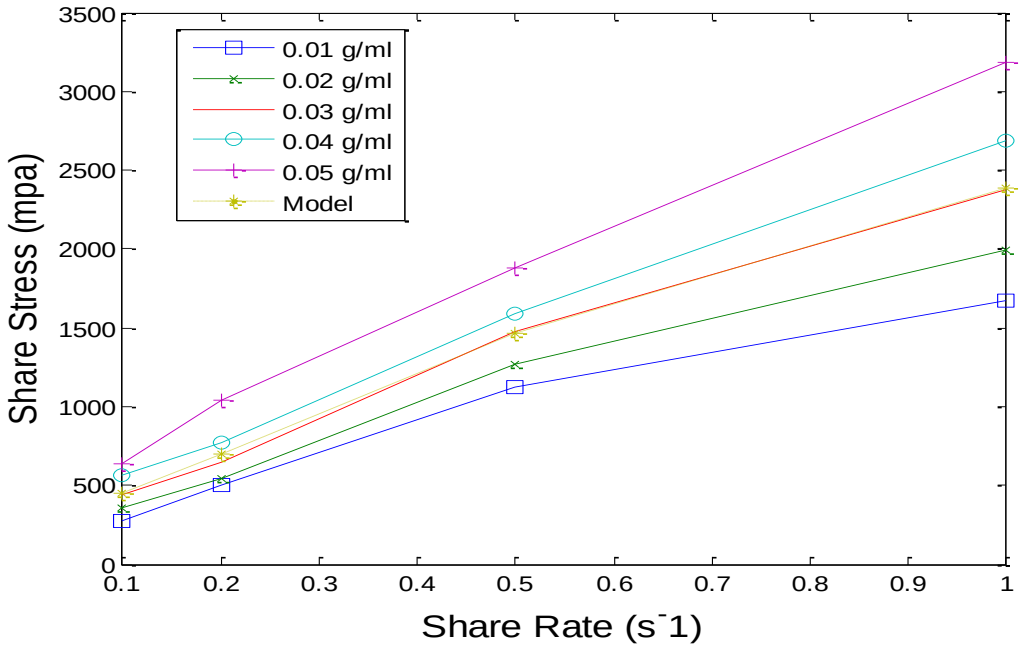

Figure 4.218: Plot of Modelled Shear Stress as a Function of Shear Rate for G:M-Mud. (Data; Table 4.59)

In figure 4.218, the goodness of fit analysis showed that the coefficient of regression, R^2 is 0.9998 signifying a good fit since it is close to "1" and the Sum of Squared Errors of 0.2291 x 10^{-5} which is close to "0" (see Table 4.102). Therefore, the 0.01 g/ml concentration exhibited the best fit. The model curve in Figure 4.218 followed the same path with the experimental data. Similarly, the following curves, 0.01 g/ml, 0.02 g/ml and 0.03 g/ml concentrations exhibited lower deviations with 0.03 g/ml curve having close proximity with the model. The 0.04 g/ml and 0.05 g/ml had upper deviations to the model curve.

4.2.4.35 Modelling of Shear Stress as a Function of Shear Rate for G:P-Mud

Model equation is given as $s = 1233r^2+610.9r+381.3$

Coefficients (with 95% confidence bounds):

Goodness of fit: SSE: 7358; R-square: 0.9963

Adjusted R-square: 0.9889, RMSE: 85.78

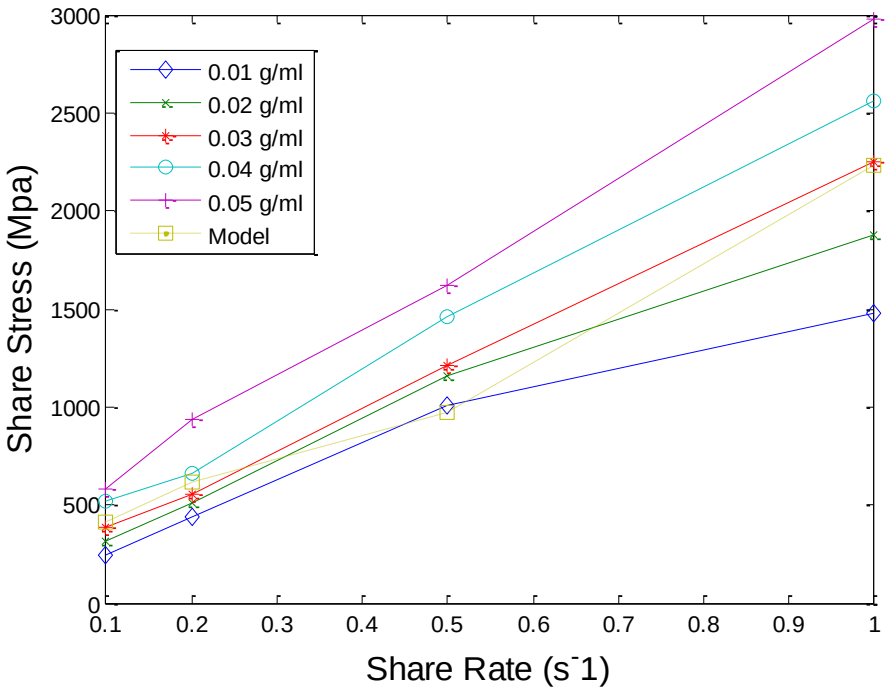

Figure 4.219: Plot of Modelled Shear Stress as a Function of Shear Rate for G:P-Mud. (Data; Table 4.60)

In figure 4.219, the goodness of fit analysis showed that the coefficient of regression, R^2 is 0.9996 signifying a good fit since it is close to "1" and the Sum of Squared Errors of 0.5616 x 10^{-5} which is close to "0" (see Table 4.102). Therefore, the 0.03 g/ml concentration exhibited the best fit. The model curve in Figure 4.219 followed the same path with the experimental data. Similarly, the following curves, 0.01 g/ml, 0.01 g/ml concentrations exhibited lower deviations while the 0.02 g.ml had opposite curve to the model. The 0.03 g/ml, 0.04 g/ml and 0.05 g/ml had upper deviations to the model curve.

4.2.4.36 Modelling of Shear Stress as a Function of Shear Rate for M:P-Mud

The model equation is given as $s = 4798r^2-3665r+839.6$

Coefficients (with 95% confidence bounds):

Goodness of fit: SSE: 8.719e+004; R-square: 0.9591

Adjusted R-square: 0.8774, RMSE: 295.3

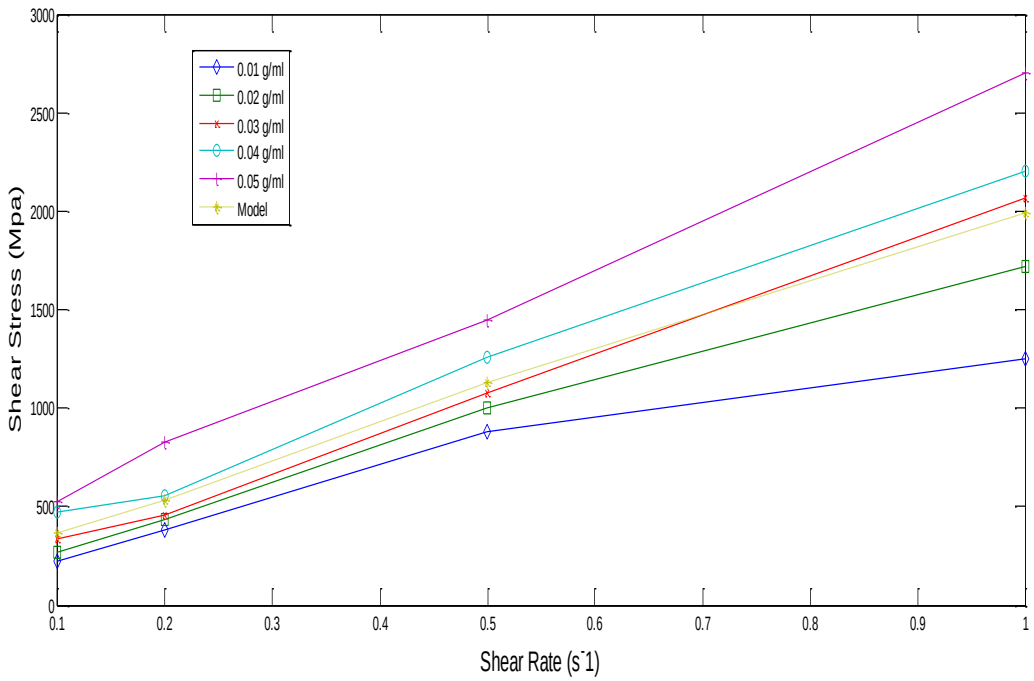

Figure 4.220: Plot of Modelled Shear Stress as a Function of Shear Rate for M:P-Mud. (Data; Table 4.61)

In figure 4.220, the goodness of fit analysis showed that the coefficient of regression, R^2 is 0.9999 signifying a good fit since it is close to "1" and the Sum of Squared Errors of 0.3581 x 10^{-5} which is close to "0" (see Table 4.102). Therefore, the 0.02 g/ml concentration exhibited the best fit. The model curve in Figure 4.220 followed the same path with the experimental data. Similarly, the following curves, 0.01 g/ml, 0.02 g/ml and 0.03 g/ml concentrations exhibited lower deviations with 0.03 g/ml curve having close proximity with the model. The 0.04 g/ml and 0.05 g/ml had upper deviations to the model curve.

Table 4.102: Modelled Result Parameters of Shear Stress as a Function of Shear Rate for all the Muds at Varying Starch Concentrations

Muds	Parameters/Fillers	0.01g/ml	0.02g/ml	0.03g/ml	0.04g/ml	0.05g/ml
G:W	**R^2**	0.9982	0.9985	0.9999	**0.9999**	0.9999
	SSE (x 10^{-5})	0.8973	0.8637	0.5262	**0.5115**	0.7144
M:W	**R^2**	0.9872	0.9961	0.9981	**0.9996**	0.9965
	SSE (x 10^{-5})	0.2451	0.9212	0.5938	**0.1604**	1.7711
P:W	**R^2**	**0.9993**	0.9987	0.9993	0.9983	0.9989
	SSE (x 10^{-5})	**0.1048**	0.2431	0.1790	0.4682	0.4669
G:M	**R^2**	**0.9998**	0.9981	0.9984	0.9991	0.9993
	SSE (x 10^{-5})	**0.2291**	0.3104	0.3873	0.2389	0.3820
G:P	**R^2**	0.9994	0.9995	**0.9996**	0.9977	0.9982
	SSE (x 10^{-5})	0.5845	0.7185	**0.5616**	0.5969	0.5996
M:P	**R^2**	0.9985	**0.9999**	0.9987	0.9956	0.9987
	SSE (x 10^{-5})	0.9945	**0.3581**	0.4441	0.8364	0.3590

CHAPTER FIVE

CONCLUSION AND RECOMMENDATIONS

5.1 CONCLUSION

The following conclusion is drawn from the research work:

Blends of starches from Millet and corns pregelatinized and blended by extrusion technique in the absence of a solvent or chemical are suitable for preparing Biodegradable Polymer Drilling Muds. The biodegradable Polymer Drilling Muds prepared with the new starch blends have better fluid loss control behaviours and filtration rates than already existing drilling muds prepared with chemically modified blend of starches, chemically-modified single starch and non-chemically-modified single starch. The muds containing the new starch blends can control fluid flow and fluid loss even at stopped circulation so as to prevent wall caving and formation damage during drilling operation. The thermal stability of the new muds at 450^{o}C implies that the muds are suitable for drilling wells having deep bottom hole temperature as high as 450^{o}C and above, whereas the functional behaviours of the already existing muds containing single starches and chemically-modified blend of starches would cease at 250^{o}C and 450^{0}C respectively due to their thermal degradation at these temperatures. The higher Sorptivity and lower Diffusivity values of the new muds show that these muds are more viscous and have greater ability of building up filter cakes at any starch concetration than the already existing muds. The values of flow index are less than 1.0 and show that all the muds are non- Newtonian and have Pseudoplastic flow model. Consistency index, shear stress, yield stress and viscosity, which are dependent on concentration, are also of higher values for the new muds denoting their higher gel strength and flocculation than the already existing muds. All the muds have shear thinning characteristics since the viscosity of each

mud decreases with increasing shear rate. The increasing percent weight loss with increase in time shows continuous biodegradation of the starches. The new muds containing the new blends of starches with higher percent weight loss are more biodegradable than the already existing muds containing starches with lower percent weight loss. The biodegraded products from the new blends of starches are purer, more eco-friendly and therefore support higher plant growth than the already existing starches. The results obtained from MATLAB modeling showed that the value of coefficient of regression R^2 is close to 1 while the value of Sum of Squared Errors SSE is close to 0 for each of the new muds at all the temperatures, and this signifies good fit of all the muds at these temparatures in the actual drilling application. Therefore, the new biodegradable polymer muds are purer, more efficient and more suitable for drilling operations in environmentally sensitive areas than the aready existing muds,

5.2 RECOMMENDATIONS

The following recommendations are made for further work;

(i) Further researchers can increase the hot rolling temperature to be above 450^0C and check the mud's behaviour for thermal stability or thermal degradation.

(ii) They can also increase and vary the concentration to be above 0.05g/ml.

(iii) The researchers can also use another physical or mechanical technique that can be as pure and efficient as extrusion for pregelatinization and modification of starch.

(iv) Subsequent researchers can carry out research or study with starch from other sources like tuber than corn or millet grains,

(v) Further researchers can increase the filtration time above 300 minutes to see if there will be different or better results,

(vi) The ratio of amylose polymer to amylopectin polymer in each starch can be determined by future researchers to know the exact amount of these polymers present in each of the new muds.

(vii) The rheological properties of the polymer muds can also be determined by researchers at higher speeds than 600 revolutions per minute.

(viii) The initial weight of starches can be increased by future researchers to be above 50g for weight loss test to know the effects on biodegradation rate.

(ix) The time of soil burial test can be increased by researchers to be above 100 days to know the effects on final weight.

(x) Further researchers can carry out the biodrgradation test in other biodegradation environments (like aquatic, landfill or compost) than soil environment.

5.3 Contributions to Knowledge

The contributons made by this work to knowledge are that:

(i) the modification, pregelatinization and blending of starches can also be done by extrusion technique other than the use of solvents or chemicals.

(ii) starch blends produced by extrusion technique in the absence of any solvent or chemical are thermally-stable and can be used to prepare thermally-stable drilling muds.

(iii) biodegradable polymer drilling mud had been produced in this study with pure and non-chemically modified blends of starches.

(iv) solvents or chemicals used in the modification of starch polymer have negative effects on their natural or pure performance characteristics.

(v) in addition to a new development, effort had been made to transfer an old existing technology (extrusion technology) to solve problems encountered in well drilling operation.

(vi) the behaviour of drilling mud at any temperature of the well can be predicted using MATLAB model.

REFERENCES

Abrams, A. (2000). Mud design to minimize rock impairment due to particle invasion. *Journal of Petroleum Tech.*, *51*(2), 68-92.

Adibhatla, B., Mohanty, K. K., Berger, P., & Lee, C. (2006). Effect of surfactants on wettabilitv of near-wellbore regions of gas reservoirs. *Journal of Petroleum Science and Engineering*, *23*(3), 26-37.

Adrian, S., & Gareth, C. K. (2009). Starch polymer.*Plastic Engineering Journal*, *8*(2), 54-65.

Akran, A. (1992). Rheological investigation of a dilute suspension. *Indian Journal of Technology*, *20*(6), 107-121.

Albert, F. N., & Mark, S. K. (2001). Starch chemistry: Its application. Chichester: Horwood Publishing, 126-145.

Alderman, N. J., Babu, D. R., Hughes, T. L. , & Maintland, G. C. (2008). The filtration and rheology of water-based drilling mud. *International Journal on Rheology, 4*(1), 1-12.

Aldol, M. M. (2004). Starch and gelling strength. New York: Plenum Press, 7-29.

Al-Riyainy, K., & Sharma, M. M. (2004). Filtration properties of oil-in- water emulsions containing solids. *SPE Journal*, *17*(2), 164 -182.

Amaefule, J. O., Kersey, D. G., Norman, D. L., & Shannon, P. M. (1998). Advances in Formation Damage Assessment and Control strategies. *Gas Processing Journal*, *13*(2), 16-31.

Amani, M. (2010). An experimental investigation of the effects of high pressures and temperatures on the flow properties of drilling fluids. *Society of Petroleum Engineers*, *57*(11), 12-25.

Amani, M. (2012). The effects of high pressures and temperatures on the fluid loss properties of water-based mud. *Energy Science and Technology* , *43*(7), 27-50.

Amanullah, M. D., & Long, Y. (2004). Corn-based starches for oil field application. *New direction for a diverse Plane*t, *13*(2), 14-23.

Amanullah, M. D., Marsden, J. R., & Shaw, H. F. (1997). An experimental study of the swelling behaviour of mudrocks in the presence of drilling mud systems. *Canadian Journal of Petroleum Tech., 36* (3), 45-66.

American Petroleum Intitute, API, (2003). Recommended practice for field testing of water-based drilling fluids (Third Edition). Texas: Author, 1-43

American Petroleum Institute. (1991). Joint association survey on 1990 drilling costs by Independent Petroleum Association of America & Mid-Continent Oil and Gas Association, USA: Author, 106-129.

American Petroleum Institute (1993). Specification for drilling fluid materials (5th ed.). Washington DC: Author, 12-44.

Anderson, F. F.; Cooper, G. A.; Maurer, W. C. & Westcott, P. A. (1991). An analysis of relative costs in drilling deep wells: Proceedings of the Society of Petroleum Engineers, 66th Annual Technical Conference and Exhibition, Dallas: Richardson Press, 55-64.

Andrew, R. N., & Robert, F. N. (2007). Starch polymer and well drilling fluid. *New Polymer Sources*, *41*(3), 41-59.

Andy, J. J., Williams, A. K., Albert, M. J., & Jack, L. B. (2000). Principles of drilling fluids control. 2nd Ed, Dallas, Texas: API Division, 11-63.

Anthony, N., & Robert, A. (2010). Evaluation of filtration behaviors of polymers as drilling fluids additives. *Petroleum Science and Technology*, *55*(9), 117-134.

API. (1997). Laboratory Testing of Drilling Fluids, (Seventh Edition), Washington DC: API Supplement, 2 - 23.

Argil1ier, J. F., Audibert, A., Janssen, M., & Demoulin, A. (2001). Performance of a new biodegradable ester-based lubricant for improving drilling operations with water based muds. *International Journal on Oilfield Chemistry*, *7*(1), 139-149.

ASTM. (2000). Standard test method for slake durability of shales and similar weak rocks: ASTM annual book of ASTM standards, America: Author, 18-63.

Audibert, A., & Dalmazzone, C. (2006). Surfactant system for water-based well fluids: Colloids and surfaces. *Physico-chem. Engineering Aspects*, *12*(3), 113-130.

Austin, P. C., & Christopher, G. V. (2008). Water-based drilling mud containing starch. *Journal of Petroleum Technology, Canada, 57*(5), 50-63.

Baghdikian, S. Y., Sharma, M. M., & Handly, L. L. (2000). Flow of clay suspensions through porous media, *Reservoir Engineering, 13*(5), 213-227.

Bada, K. (2005, August 12). Growing greener: Maximizing renewable resources. *Plastic Engineering Magazine, 5*, 25-36.

Bailey, L ., Keall, M., Audibert, A., & Lecourtier, J. (1994). Effect of clay/ polymer interactions on shale stabilization during drilling. *Langmuir, 10*(2), 1544-1569.

Balser, K., Hoppe, L., Eicher, T. ,& Wendel, M. (1996). Clay and solution interaction. 5th (ed.). Handbook of Industrial Chemistry. (119-147). Weinhein, New York: VCH Press.

Barnes, H. A, Hulton, J. F., & Wallers, W. (1999). Introduction to Rheology. Amsterdam: Elsevier, 6-64.

Bataille, I., Huguet, G., Muller, G., & Mocanu ,A. (2000). Xanthan gum and epichlorohydrin cross-linked hydroxypropylated starch for drilling fluids. *Journal of Petroleum Science and Engineering*, *17*(1), 3-28.

Behker, W. G., Godson, T. H., & Ward, T. A. (2000). Soil particles. Amsterdam: BVinod Kumar, 1-54.

Beihoffer, T. W., Dorrough, D. S., & Schmidt, D. D. (2008). The separation of electrolyte from rheological effects in studies of inhibition of shales with native moisture contents. *SPE Journal, 59*(3), 17-35.

Ben, G. & Joe, M. (2006). Well drilling fluids containing corn starch cross-linked with phosphorous oxychloride. *American Chemical Society, 7*(2) 21-43.

Beneth, E. F. & Godfrey, T. L. (2006). Inhibitive drilling fluids solve shale problems. *Petroleum Engineering Internationa*l, *21*(6), 117-118.

Bernu, C. J. (2011). High temperature stable modified starch polymers and well drilling fluids employing same. *Chemstar*, *15*(1) 1-13

Bertts, D. D., & Jerry, A. T. (2012). The use of sodium carboxymethyl
sarch and sodium carboxymethyl cellulose as fluid loss additives. *SPE Journal*, *59*(1), 1-18.

Bhattacharya, D., Singhal, R. S., & Kulkami, P. R. (2002). Carbohydrate polymer. 2nd. (ed.), Polysaccharide (247-269). Weinheim: Wiley-VCH Press.

Benna, M., Khir-Ariguib, N., Magnin, A., & Bergaya, F., (1999). Effect of pH on the rheological properties of purified sodium bentonite suspensions. *Journal of Colloid Interface Sci*., *218*(7), 442-458.

Benna, M., Kbir-Ariguib, N., Clinard, C., & Bergaya, F. (2001). Static filtration of purified sodium bentonite clay suspensions: effect of clay content. *Applied Clay Sci*, *19*(8), 103-120.

Bennion, D. B., & Thomas, F. B. (1994). Underbalanced drilling of horizontal wells: Does it really eliminate formation damage? : Formation damage control symposium. Lafayette, Louisiana, *SPE Journal*, *13*(1), 1-16.

Bergaya, F., Theng, B. K. G., & Lagaly, C. (2006). Developments in clay science. Handbook of Clay Science (1246-1268). Amsterdam: Elsevier Science.

Bill, N. L., & Mark, S. A. (2007). Chemically Modified Starches for
Drilling Application. *Chemstar*, *11*(2), 15-31.

Bingham, E. C. (2000). Fluidity. New York: McGraw Hill Book Company, 1-75.

Bishop, S. R. (2001). The experimental investigation of formation damage due to the induced flocculation of clays within a sandstone pore structure by a high salinity brine. European Formation Damage Conference, Netherlands, *SPE Journal*, *14*(3) 123-143.

Bland, K. G. (1998). Development of new water-based mud formulations and chemicals for oil industry: Developments and applications. *Spec. Publ. Soc. Chem.*, *97*(7), 83-99.

Bland, R. G. (2002). Water based glycol systems: Acceptable substitute for oil-based muds. *Oil and Gas Journal*, *54*(6), 54-68.

Bland, R. C. (2005). Quality criteria in selecting glycols as alternatives to oil-based drilling fluid systems, SPE /HSE Conference, Jakarta, Indonesia, *SPE Journal*, *18*(1), 1-21.

Bland, R. G,, Smith, G. L., Eagark, P., & Van-Oort, E. (2003). Low salinity polyglycol water-based drilling fluids as alternatives to oil-based muds. *SPE Journal*, *16*(4), 2-19.

Bo1, G. M., Wong, S.W., Davidson, C. J., & Woodland, D. C. (2002). Borehole stability in shales. SPE/European Petroleum Conference, Cannes, *SPE Journal, 15*(7), 102-118.

Bourgoyne (Jr), A. M. (1996). Applied Drilling Engineering, 2nd (edition). New York: SPE Textbook Series, 105-149.

Bradley, W. B. (1999). Failure of inclined boreholes. *Energy Resource Technol*., *102(*33), 232-249.

Brandy, A. D. (1997).The phenomena of fluid motion. *Reading Mass*, 60-83.

Brown, J. E. (2009). Well drilling fluid containing potato sarch and other additives. *Journal of Petroleum Science and Engineering*, *26*(1), 2-23.

Bryan, C. H., Gill, B. I., & Kelly, N. R. (2010). Rheological flow of modified polymer-fluid and drilling application. *Drilling Technology Journal*, *23*(13), 185-203.

Caleb, K. K. & Dan, S. B. (2004, April 16). Alternative water-based mud system which has the same performance and inhibitive characteristics as the oil-based mud systems. *Chevron Oil Company Magazine*, *84*, 13-25.

Calistus, J. R., & Mathew, A. S. (2004). Qauntitative determination of the filtration properties of drilling fluids. *SPE Journal 17*(5), 183-197.

Cambel, R.A., Austin, I. J., & Mark, N. M. (2007). Drilling problem shale. *Oil and Gas Journal*, *61*(7)77-91.

Candy, N. N., & Justus, A. F. (2006). Evaluation of the rheological models of drilling mud containing guar gum. *Society of Petroleum Engineers Journal*, *19*(2), 31-48.

Carl, G. (1990). Drilling and well completion. Cliffs N. J. (Ed.), Petroleum Engineering Book (74-126). Eeglewood: Prentice-Hall Inc.

Carraha-Charles, E. J., & Sperling, L. H. (1996). Renewable resources materials. *New Polymer Sources*, *13*(11), 34-67.

Carriere, C. J. (2009). The effect of amylose content from differing botanical sources on the nonlinear viscoelastic properties of semi-dilute solutions of maize starches. *Journal of Applied Science*, *73* (42), 229 - 256.

Caskey, J. A., King, P. H., & Martin, J. I. (2004). Effects of Polyacrylamide on Flocculation efficiency. Symposium series, America: American Institute of Chemical Engineers, 127-195.

Casmir, E. A., Lookman, T. M., & Brien, P. N. (2007). Epichlorohydrin crosslinked carboxymethylated corn starch. *American Chemical Society*, *8*(3), 34-50.

Catia, V. G. (2005). Biodegradable polymers. Bastioli (Ed.), Handbook of biodegradable materials. Bastioli, (Ed.), United Kingdom: Rapra Shrewsbury-Shropshire, 11-65.

Chang, F., & Civan, F. (1997). Practical model for chemically induced formation damage. *Journal of Petroleum Science and Engineering*. *13*(9), 123-135.

Chenevert, M. E., & Pernot, V. (1998). Control of shale swelling pressures using inhibitive water-based muds, SPE Annual Technical Conference and Exhibition in New Orleans, Louisiana, *SPE Journal*, *20*(11), 27-40.

Chimere, C. C. (2011). Biodegradable polymer drilling mud prepared from superior starch. *Journal of Brewing and Distilling*, 1(2), 16-31.

Chilingarian, G.V., & Varabutre, P. (2000). Drilling and drilling muds. Development in petroleum science (44-79), Amstredam: Elsevier.

Ching, C., Kaplan, D., & Thomas, E. (1993). Biodegradable polymers and packaging. Lanchaster, PA: Technomic Publishing Company Inc., 7-203.

Chris, M. B., & James, K. K. (2005). Drillng fluid compositions and their functions. *American Chemical Society*, *6*(1), 1-27.

Christopher, W. M., & Perlin, R. H. (2010). Industrial gums: Properties and Applications. San Diego (Ed.). Boston, New York: Academic Press Inc., 13-118.

Cisco, R. O., & Whistler, J. S. (2008). Polysaccharides and their derivatives. *Polym. Bull*., *17*(5), 63-88.

Civan, F. (2000). Reservoir formation damage: Fundamentals, modelling, and assessment. Houston Texas: Gulf Publishing company, 23-205.

Civan, F. (2001). Water sensitivity and swelling characteristics of petroleum bearing formations: Kinetics and correlation. *SPE Journal*, *22*(3), 15-36.

Clark, R. K., Scheuerman, R. F., Rath, H., & Van-Laar, H. G. (2006). Polyacrylamide /potassium chioride mud for Drilling in shale Sensitive areas, *Journal of Petroleum Technology*, *25*(12), 719-737.

Clark, D. E., & Saddok, B. (1991). Aluminium chemistry provides increased shale stability with environmental acceptability. SPE-Asia Pacific Oil and Gas Conference and Exhibition, Singapore, *SPE Journal*, *19*(11), 128-140.

Clement, T. T., & Bona, M. U. (2009). Effects of chemical modification of carbohydrate polymers. Mount Prospect II (Ed.), Berlin: ALT Press. 4-121.

Clerk, O. P.. & Clem, K. D. (2003) Mud additives and chemical modification. *American Chemical Society*, *4*(1), 1-18.

Clever D. N., Leonard N. N., & Brand, P. S. (2012). Biopolymers from Renewable Resources. *Polym. Bull*., *21*(3), 41-62.

Cliff, J. K., & Gerald, R. M. (2010). Starch: properties and materials applications. Berlin New York:Springer- Heidelberg, 1-113.

Cliffe, S., Dolan, B., & Reid, P.1. (2005). Mechanism of shale inhibition by polyols in water- based drilling fluids. Paper presented at the SPE International Symposium on Oilfield Chemistry, San Antonio, *SPE Journal*, *24*(17), 111-135.

Clifford, W., & Cain, J. (1999). Filtration theory. Philip A.Schweitzer (Edition). Hand book of separation technique for Chemical Engineers (141-215). USA: McGraw Hill.

Cole, C. (2004). Assessment and remediation of petroleum contaminated sites. Raton, F. L. (Ed.), Boca: CRC Press, 3-74.

Cook, J. M., Goldsmith, G., Geehan, T.M., Audibert, A.M., Bieber, M.T. & Lecourtier, J., et al. (1993). Mud/Shale interaction: Model wellbore studies using x-ray thermography. *SPE Journal, 12*(3), 43-55.

Coulson, J. M.; Richardson, J. F., & Bark-Hurst, J. R. (1999). Chemical Engineering. 4th (Edition), New York: Pergamon Press, 2-323.

Coussot, P., Bertrand, F., & Herzhaft, B. (2004). Rheological behavior of drilling muds, *Oil & Gas Sci. Technol*., *3*(I), 6-29.

Cyracus, H. D. (2012). Application of starch-based polymers. *Polym. Bull*., 27(2), 14-33.

Dahlgreen, H. C., & Helbig, M. (2008). Rheology of starch polymer. New York: Pergamon Press, 3-139.

Dakky, L. N., & Gronski, W. D. (2000). Guar-gum and its properties. San Diego, (Ed.) Boston, New York: Academic Press Inc., 7-123.

Dalmazzone, C., Audibert-Hayett, A., Quintero, L., Jones, T., Dewatinnes, C., & Jansen, M. (2006). Optimizing filtrate design to minimize in-situ and wellbore damage to water-wet reservoirs during drill-in. *SPE Journal*, *19*(7), 66-83.

Daniel, N. L. (1990). Encyclopedia of geological sciences. 5th (Ed.), USA: McGraw Hill, 3-216.

Darley, G. (1999). A laboratory investigation of borehole stability. *Journal of Petroleum Technology, 21*(14), 191-212.

Debussy J. H. (1992). Materials and Technology. UK: Longman, 5-327.

De Nooy, A. E., Rori, V., Masci, G., Dentini, M., & Crescenzi, V. (2002). Carbohydrates. *Res. Journal, 94*(116), 311-345.

Derek, S. H., & Perlin, A. R. (2003). Characterization of cellulose derivatives. Chichester: Horwood Publ., 3-103.

Dickson, L. L., & Philipp, T. S. (2006). Starch: Modification and characterization. New York: Springer, 2-95.

Ding, R., Qiut, Z., & Li, J. (1996). Soluble-silicate mud additives inhibit unstable clays. *Oil and Gas Journa*l, *17*(8), 66-83.

Dollimore, D., & Horridge, T. A. (1993).Clay and water interactions. *Journal of Colloid and Interface Science, 212*(5), 81-103.

Don, A. P., & Benze, T. M. (2002). Oil well drilling operations. 2nd (Ed.), Canada: Gulf Publishing Company. 10-235.

Dons, W. W., & Billy F. G. (2001). Advanced drilling and excavation technologies. 3*rd* (Ed.), Berlin: National Academy of Sciences, 6-169.

Downs, J. D., Van-Oort, E., Redman, D., Ripley, D., & Rothmann, B. (1993). TAME-a new concept in water-based drilling fluids. Offshore Europe Conference, Aberdeen, *SPE Journal, 14*(13), 119 -130.

Durant, C., Forsans, T., Ruffet, C., Onaisi, A., & Audibert, A. (2005). Influence of clays on borehole stability: Part one (Occurrence of drilling problems physico-chemical description of clays and of their interaction with fluids). *Mars-Avril, 20* (2), 12-39.

Ebewele, R. O. (2000). Polymer science and technology. N.W. Corporate Blvd. (Ed.), Boca Raton, Florida: CRC Press, 7-126.

Edmund, M. G., & Hellmann, W. (2000). Flow properties of xantham gum-based drilling fluid. *SPE Journal*, *21*(3), 18-39.

Enie, R. K., & Giles, N. T. (2001). The use of polymers as filtration controlling agents. Proceedings of 13th International Petroleum Congress and Exhibition, Turkey, *SPE Journal*, *23*(3), 24-46.

Eyler, D. H., & Pastecck, L. O. (2005). The Rheological Behaviours of Water-based Mud Containing Hydroxypropyl Starch. *SPE Journal*, *28*(7), 55-70.

Faniran, A., & Areola, O. (2000). Essentials of soil study. 4th (Ed.), London: Heinemann, 2-357.

Fannon, J. E., Gray, A., Gunawan, N., Huber, K. C., & BeMiller, J. N. (2004). Carboxymethyl cellulose: Its application as drilling mud additive. *Cellulose*, *11*(4), 44-67.

Feiffer, K., & Vierty, W. (2002). Biopolymers and applications. *Progr*, *Polym. Sc*i., *11*(4), 27-58.

Fischer, S., Voigt, W., & Pedro, K. (2000). Cellulosic polymers. *Cellulose*, *7*(2), 21-43.

Fischer, S. (2002). Starch-polymer and uses. *Cellulose*, *9*, 293.

Fordham, E. G., Maitland, .G., Meeten, G., & Sherwood, J. (2001). Drilling and pumping. *Schlumberger Cambridge Research Journal*, *22*(2), 13-31.

Fried, J. R. (2000) Polymer science and technology. 2nd (Edition), New Delhi: Prentice-Hall of India Private Limited, 1-115.

Friedheim, J., Toups, B., & Van-Oort, F. (1999). Drilling faster with water-based muds. Houston, Texas: AADE Publ., 3-131.

Fritz, S. J., & Marine, I.W. (1993). Experimental support for a predictive osmotic model of clay membranes. *Geochem & Osmochem*., *47*(31), 151-162.

Gautier, S. & Lecourtier, J. (2001). The effects of biopolymers on water-based drilling fluids. *Polym. Bull.*, *21*(14), 61-76.

Getliff, J. M., Bradhury, A. J., Sawdon, C. A., Candler, J. E., & Loklingholm, G. (2000). Can advances in drilling fluid design further reduce the environmental effects of water and organic-phase drilling fluids?, A paper presented at the Fifth SPE International Conference on Health, Safety and Environment, Stavanger, Norway, *SPE Journal*, *20*(18), 126-138.

Ghazi, M., Quaranta, C., Duplay, J., & Khodja, M. (2008). Life-cycle assessment (LCA) of drilling mud in arid area: Evaluation of specific fate factors of toxic emissions to groundwater, "first results". *SPE Journal*, *27*(4), 25-48.

Giavasis, I,; Harvey, L. M., & MCNell, B. (2002). Schleroglucan in biopolymers. Polysaccharide II (Ed.), Biotechnology, (275-319). Weinheim: Wiley-VCH.

Glinel, K.; Savage, J. P.; Oulyadi, H. & Huguet, J. (2000). Carbohydrates. *Res. Journal* , *18*(7), 143-171.

Gray, G. R., & Darley H.C.H. (1990) Composition and properties of oil well drilling fluids. 4th edition, Houston: Gulf publishing Co., 2, 28, 31 & 46.

Greaves, C., Rojas, J. C., & Chambers, B. (2001). Field application of "total fluid fragments" of drilling fluids and associated wastes, *SPE Journal*, *21*(3), 26-38.

Grieve, A. (1998). Toxicity of drilling mud. *Journal of Occupational Health*, *40*(12), 116-139.

Grim, R. E. (1998). Clay mineralogy. 2nd Edition, New York: McGraw-Hill, 5-352.

Grolimund, D., Barmettler, K., & Borkovec, M. (2001). Water Resource. *Res.Journal*, *37*, 57-71.

Gronski, W., & Hellmann, G. (2003).The functions of polymers in drilling fluids. *Papier*, *17*(5), 41-63.

Growcock, F. B., Curtis, G.W., Hoxha, B., Brooks, W.S., & Candler, J. E. (2002). Designing invert drilling fluids to yield environmentally friendly drilled cuttings. *SPE Drilling Journal*, *23*(2), 32-33.

Hale, A. H., Blytas, G. C., & Dewan, A. K. R. (2009). Physico-Chemical properties of starch. *Journal of Materilas and Application, 12,* (36), 174-201.

Hale, A. R., & Mody, F. K. (1992). Experimental investigation of the influence of chemical potential on welibore stability. *SPE Journal*, *15*(18), 117-125.

Hale, A. R., & Mody, F. K. (1996). Exprimental investigation on the rheology of chemically-modified drilling fluid additives. IADC/SPE Conference, New Orleans, Louisiana, *SPE Journal, 17*(11), 118-131.

Hall, C., & Hoff, W.D. (2012). Dynamic and static filtration: An overview. *SPE Journal*, *55*(2), 11-34.

Hans, R. (1990) Particle technology. Carl Hanser (Ed.). Verlag: Chapman and Hall, 6-153.

Haus, F., Boissel, O., & Junter, G. A. (2003). Multiple regression modelling of mineral base oil biodegradability based on their physical properties and overall chemical composition. *Chernosphere*, *23*(6), 48-56.

Heinze, T., & Liebert, T. (2001). Polysaccharides and chemical modification. *Progr. Polym. Sci*., *26*, 168-190.

Heinze, T. (2005). Carboxymethyl ethers of cellulose and starch. Friedrich Schiller University of Jane, Humboldtstrasse 10, Germany: Center of Excellence for Polysaccharide Research, 4-216.

Herman, K., Song, Y., & Jay-lin, J. (2002), Effect and mechanism of ultrahigh hydrostatic pressure on the structure and properties of starches. *Carbohydrate Polymers*, *33*(29), 233-244.

Himel, C. M., & Lee, E. G. (1991). Drilling fluids and methods of using same. *U.S. Drilling Journal*, *14*(4), 47-58.

Hofmann, R., Foster, J.W, Yon, R., & Wadle, A. (1995). Rheological properties of finely dispersed oil/water emulsion., Henkel, K. G.A. (Ed.). Germany: Henkel Referates, 1-108.

Hongwei, Y., Zhanpeng, J., & Shaoqi, S. (2004). Science of the total environment. *Environs. Journal*, *33*(52), 209- 224.

Horner, V., White, M. M., Cochran, C. D., & Diety, F. H. (2001). Microbit dynamic filtration studies. *Society of Petroleum Engineers*, 2*1*(30), 183-207.

Horsud, P., Bostrom, B., Sonstebo, E. F., & Holt, R. M. (1998). Interaction between shale and water-based drilling fluids: Laboratory exposure tests give new insight into mechanisms and field consequences of KC1 contents, *SPE Journal*, *18*(2), 15-36.

Houwink, R., & Dedecker, H. K. (1991). Elasticity, plasticity and structure of matter. 3rd (Edition), USA: Cambridge, 4-315.

Hudson, C. (1999, April 15). Evaluation of drilling rig fluids handling systems: An integrated fluids management approach, *Offshore Magazine*, *4*, 12-23.

Iheaturu, N. C. (2006).Waste management of spent drilling mud: Studies on the effect of spent oil-based drilling mud solids on the mechanical properties of filled UPR composites. Nigeria: Federal University of Technology Owerri, 53-55.

Indigo, C. C. (2009). Drilling mud wastes and management problems. *Petroleum Eng. International*, 33(18), 66-118.

Iudson, C., & Nicholson, S. (1999). Integrated fluids approach cuts waste, costs in Texas Wildlife refuge, *Petroleum Eng. International*,*17*(28), 237-251.

Jack, T. K. (2008). Drilling mud and drilling operation. *Journal of Drilling Technology*, *25*(23), 110-122.

James, C. O. (2012). Drilling mud containing chemically-modified starch. *SPE journal*, *56*(5), 35-46.

Jann, A. H., Andy, O. H., & Kobra, K. K. (2007). Technolgical advancement in well drilling. *International Petroleum journal*, *24*(2), 15-30.

Jason, M. C. & Henry, O. M. (2004). The use of starch as mud additive. *Canadian Journal of Petroleum Tech*., *24*(7), 60-72.

Jax, R. H. (2010). Determination of flow behaviours as applied to solution containing starch. *Chemstar*, *27*(3), 17-39.

Jay, B. B., & Bruce, P. N. (2005). Quantitative studies on the rheological behaviours of drilling mud containing chemically modified starch. *Petroleum Science and Technology*, *23*(20), 121-147.

Jeffrey, K. O. (2007). Biopolymers : Special drilling mud additves. *Society of Petroleum Engineers*, *21*(I), 1-19.

Jilani. S. Z., Menouar, H., Al-Majed, A. A., & Khan, M. A. (2002). Effect of overbalance pressure on formation damage, *J. Petr. Sci. Eng. 36*(26), 97-118.

Jill, R. D., & Poka, M. B. (2003). The use of specialty drilling fluids for high temperature wells. *Petroleum Science and Tech*., *21*(6), 67-88.

Jimo, T. S. (2001) Clay-polymer interaction. Nigeria: Federal University of Technology, Akure, 14-20.

Joel, I. K., Thommler, R., & Libert, L. (2006). The chemistry of schleroglucan in biopolymers. *Polysaccharide III, 5* (2), 27-50.

Jones, M. G., Hartog, I. J., & Sykes, R. M. (1996). Environmental performance indicators - the line and management tool. *SPE Journal, 19*(3), 23-41.

Jones, F. B. & Mark, N. L. (2006). A blend of carboxy methyl starch and carboxymethyl cellulose for drilling operation. *Canadian Journal of Petroleum Tech., 22*(3), 30-45.

Katchy, E. M. (2000). Principles of polymer science. 1st (Edition), Nigeria: El'Demark LTD., 33-41.

Kelvin, T. N. (2011). Carboxymethyl starch and epichlorohydrin crosslinked hydroxypropyl starch for drilling application. *Polysaccharide Research, 31*(7), 50-67.

Kennedy, J. F., Stevenson, D. L.,& Charles, A. W. (2002). Chemically- modifeid Polymers for Drilling Application. *British Polymer Journals, 15*(2), 17-36.

Kenie, M. M., & Stan, F. K. (2011). Comparative studies on properties of some polysaccharides. *Journal of Brewing and Distilling, 1* (3), 43-60.

Khodja, M., Hafid, S., & Canselier, J. P. (2005). A diagnostic of the treatment and disposal of oil well drilling waste. *Waste Eng. Albi, 05*(08), 62-83.

Khodja, M. (2008). Drilling Fluid : Performance study and environmental consideration, Toulouse, France: National Polytechnic Institute. 34-45.

Khodja, M., Canselier, J. P., Bergaya, F., Fourar, K., Cohaut, N., Benmounah, A., et al. (2010). Shale problems and water-based drilling fluid optimization in Hassi Messaoud Algerian oil field. *Appl. Clay Sci., 49*, 190-203.

Klirk, G. H. (2002). Biodegradation. 4th (Ed.) New York: Blank Inc., 211-225.

Kobert, S. A. (2009). Cellulose derivative and their uses. Chichester: Horwood Publishing, 87-110.

Labby, G. (2001). Clay-Organic Interaction. Proceedings of the International Clay Conference, New York, *Journal of Colloid and Interface Science 219*(11), 146-163.

Lamberti, C. M. C. (1999). Polymers and performance chemicals-Laboratory Test, *Albizzate, Italy, 12*(2), 18-29.

Lann, R. D. (2005). Polyanionic cellulose and uses. *Chernosphere*, *25*(12), 127-138.

Lancen, N., Pefferkorn, E., & Varoqur, R. (1994) Polyacrylamide-kaolinite interaction. *Journal of colloid and interface Science*, 202 (2), 16-40.

Lee, J. S. (2012). Rheological properties of invert emulsion drilling fluid under extreme HPHT conditions. *Society of Petroleum Engineers, 27*(2), 14-35.

Lenz, R. W. (1993) Biodegradable polymers. *Adv. Polymer Science*. *107*, 103-124.

Leung, P.1. K., & Steig, R. P. (1992). Dielectric constant measurement: A new, rapid method to characterize shale at the wellsite. *SPE Journa*l, *17*(28), 114-128.

Likos, W. J., Loehr, J. E., & Akunuri, K. (2004). Engineering evaluation of water-based drilling fluids for applications in missouri shale. Columbia: University of Missouri Columbia, 33-45.

Linus, P. K. (2002). Drilling mud containing chemically-modified corn starch. *Chemstar*, *21*(2), 14-27.

Locher, I. (1992). Study of clay mud cake structure formed during drilling. *Journal of Drill. Tech.*, *15*(3), 41-64.

Lomba, R. F., Chenevert, M. E., & Sharma, M. M. (2000). The ion-selective membrane behavior of native shales", *J. Petr. Sci. Eng.*, *18*(5), 83-105.

Long, T. T., & Jolly, A. A. (2004) Recent developments in drilling. *Petroleum Science and Technology*, *23*(21), 103 - 122.

Longeron, D., Argillier, F., & Audibert, A. (1995). An integrated experimental approach for evaluating formation damage due to drilling and completion fluids. *Petroleum Science and Technology, Netherlands*, *12*(2), 16-26.

Longey, J. A. (2006). The use of starch as fluid loss reducing agent in drilling mud. *American Chemical Soceity*, *113*(4), 36-51.

Mandy, N. D. (2001). Rheology of fluids containing polymeric particles. *Journal of Chemical Engineers*, *27*(4), 41-62.

Mangelsdorf, P. C. (2004). Corn: Its origin, evolution and improvement. Cambridge, Massachusetts: The Belknap Press of Harvard University, 101-113.

Marck, S. A., & Hercules, N. O. (2004). Glucan biopolymers: applications. *Polysaccharide II*, *3*(26), 143-159.

Mario , J., & Mark, R. (2003) Biodegradable polymers from renewable sources. *New Polymer Sources*, *21*(6), 73-90.

Marries, A. A. (2001). The chemistry of xanthan gum. *Chemstar*, *23*(2), 14-31.

Mayes, T. S. (2003). Drilling technology and its development. *Petroleum Science and Technology*, *25*(33), 217-233.

McDonald, J. A., & Portier, R. J.(2003) Feasibility studies on in-situ biological treatment of drilling muds at an abandoned site in Sicily, *Journal of Chem. Technol. and Biotechnol.78*(57), 409-426.

Mecktor, W. B., Bruno, H. T., & Lardy, T. S. (2008). Modification of colloidal portion of drilling fluids. *SPE Journal*, *28*(31), 224-248.

Michael, J. (2009). The effects of guar gum on the rheological properties of water-based mud. *SPE Journal*, *30*(8), 102-118.

Micky, D. B., & Duke, C. C. (2005). The mechanism of biodegradation. *Progr. Polym. Sci*., *27*(22), 177-192.

Middleton, J. (2000). Synthetic biodegradable polymers as orthopedic devices. *Biomaterials*, *23*(9), 135-147.

Minton, R. C. (1991). Minimizing the environmental impact of drilling operation. Aberdeen, U.K: B.P. Petroleum Development Co. Ltd., 1-20.

Modv, F. K., & Tale, A. F. (1993). Borehole-stability model to couple the mechanics and chemistry of drilling fluid/shale interactions, *J. Petr. Technol., 19*(9), 109- 120.

Mungan, N. (1999). Formation Damage, *J. Petr. Technol*., *21*(11), 122-140.

Muniz, E.S., Fantoura, S.A.B., & Lomba, R.F.T. (2004). Development of equipment and testing methodology to evaluate rock-drilling fluid interaction.The 6th North America rock mechanics symposium (NARMS), Houston, Texas: Gulf-Rocks, 8-12.

Nair, N. C. (2004). Asphaltic shale coating agent, Houston: Gulf Press, 53-54.

Neff, J. S. (2000). Environmental impacts of Synthetic based drilling fluids. Robert Ayers and Associates (Ed.). Mexico: Gulf, 35-46.

Obasi, H. C. (2012). Studies on the properties and biodegradablility of selected starch/polyproplene blends. Imo State, Nigeria: Federal University of Technology, Owerri, 127-130.

Obong, I. O. (2004). Effects of partially hydrolysed polyacrylamide on the flow and fluid loss properties of drilling muds. Nigeria: University of Port-Harcourt, 105-120.

Ogden, P. H. (1991). Chemicals in the oil industry: Development and applications. *Journal of Society of Well Drillers, 17*(21), 112-128.

Parkson, R. S., Bolen, W. N., & Gudi, B. F. (2000). Water-based drlling fluids: Composition. *Journal of Drilling Technology, 39*(3), 40-53.

Partheniades, E. (2000). Microstrucrture and Fine-grained Sediment. (3rd Edition), New York: Springer-Verlag, 181-182.

Patel, A., Stamatakis, E. S., Friedheim, J. E. & Davis, E. N. (2001). Highly inhibitive water-based fluid system provides superior chemical stabilization of reactive shale formations. *Drilling Technology Journal (DTJ), 21*(5), 107-128.

Paulsen, J. E., Saasen, A., Jensen, B., & Gringd, M. (2001). Key environmental indicators in drilling operations. *SPE Journal, 21*(31), 244- 267.

Paulsen, J. F., Saasen, A. A., Jensen, B. G., Thore, E. J., & Lelimichsen, P. K. (2002). Environmental advances in drilling fluid operations: Applying a Total Fluid Management. *SPE Journal, 15*(7), 92-114.

Peddy, L. L. (2002). Drilling and Completion Fluids and Waste Management. *DTJ, 19*(3), 23-38.

Pernot, V. F. (1999). Troublesome shale control using inhibitive water-based muds. Houston Texas: University of Texas. 54-78.

Perricou, A. C., Clapper, D. K., & Enright, D. P. (2010). A review on drilling and drilling fluids. *Journal of Petroleum Technology, 59* (13), 225-237.

Piltinitakis, F., Young, S., & Stiff, C. (2002). Designing for the future: A review of the design, development and inhibitive water-based drilling fluid. *Drilling and Waste Management Journal, 27*(23), 125-138.

Pokar, A. F., & Holt, E. T. (2002). Drilling and well completion fluids. Mexico: Gulf Publ., 112-116.

Prutt, J., & Iudson, C. (1998). Integrated approach optimizes results. *American Oil and Gas Reporter, 17*(6), 86-101.

Qartar, O. O. & Giacelo, T. B. (2010). The effects of polyacrylate on the rheological properties of water-based drilling mud. *Petroleum Tech. Journal, 51*(37), 203-225.

Quintero, L. (2002). An overview of surfactants applications in drilling fluids for the petroleum industry, *International Journal on Sci. and Technol., 23* (35), 293-309

Rahman, S. S., Rahman, M. M. & Khan, F.A. (1995). Response of low-permeability, illitic sandstone to drilling and completion fluids, *J. Petr. Sci. and Eng., 23*(41), 309-332.

Rashid M. A. (1999). Geochemistry of marine humic compound. New York: Springer-Verlag. 300-302.

Raymond, S. A., & Benco, W.O. (1992). Mechanism of clay aggregation by Polyelectrolytes, *Journal of Soil Science, 75*(61), 387-410.

Regan, R. A. & Hardy, W. O. (2002). Mechanism of clay interactions with water. *Journal of Soil Science, 115*(6), 87-107.

Reid, P.1., Elliott, C. F., Minton, R. C., Chambers, B. D., & Burt, D.A. (1993). Reduced environmental impact and improved drilling performance with water-based muds containing glycols. *SPE Journal, 18*(2), 17-31.

Renard, C., & Dupuy, J. G. (1991). Formation damage effects on horizontal-well flow efficiency. *Journal of. Pet. Technol., 43* (7), 85-106.

Retz, R. H., Friedheim, J. E., Lee, L. J., & Welch, O. O. (1991). An environmentally acceptable and held-practical, cationic polymer mud system. *SPE Journal, 16*(3), 36-44.

Rob, D. A., Michael, B. B., & Eric, I. O. (2006). The Effects of Proplene oxide on the gelling behaviour starch. *American Chemical Society, 26*(21), 115-128.

Robert, H. P. (2002). Chemicals used in drilling fluids. 5th (Edition), Chemical Engineering Hand Book (47-55). New York: Plenum Press.

Roberts, K., Kowalewaka, J. & Friberg, S. (2005). The influence of interactions between hydrolysed aluminium ions and polyacrylamides on the sedimentation of kaolin suspension. *Journal of Colloid and Interface Science, 123*(48), 226-243.

Robert, H. S. & Bell, P. N. (2011). Evaluation of the composition of starch. *Polysaccharide II, 43*(3), 33-55.

Rogers, W. F. (1991). Composition and properties of oil well drilling fluids. 5th (Edition), Houston Texas: Gulf Publishing Company, 84-91.

Rolly, J. M. (2012). Chemically modified starch for oil well drilling. *Chemstar, 14*(2), 15-34.

Rosana, F. T., Lomba, M. E., Chenevert, M., & Sharma, M. (2000). The role of osmotic effects in fluid flow through shales. *Journal of.Petr. Sci. and Eng., 21*(23), 125-149.

Roy, S. B. & Dzombak, D. A. (1996). Colloids surf: A Physicochemical analysis. *Engineering Aspects, 107*(45), 355-377.

Saddok, J. J., Clapper, D. K., Parigot, P. N. & Degouy, D. D. (1997). Oil field applications of aluminium chemistry and experience with aluminium-based drilling fluid additive. *SPE Journal, 16*(2), 18-31.

Saiers, J. E., & Hornberger, G. M. (1999). Water pollution by drilling. *Water Resources Journal*. *35*(13), 133-154.

Salisbury. D. P., & Deem, C. K. (1990). Tests show how oil muds increase shale stability. *Oil and Gas Journal, 35*(4), 57-70.

Sbittle, H. K. (2000). Development in industrial filtration. *Chemical Engineers*. 1*33*(44), 374-395.

Scarlet, E. C. & Brene, T. H. (2010). Static and dynamic filtration: The behavior of drilling fluids. *Soceity of Petroleum Engineers Journal, 57*(21), 121-134.

Schamp, N. & Huylebroeck , J. (1993). Adsorption of polymers on clays. *Journal of Polymer Science, 12*(42), 213-231.

Schlemmer, R., Friedheim, J. E., Growcock, F. B., Headley, J. A., Polnaszek, S. C., Bloys, J. B., et al. (2002). Membrane Efficiency in Shale: An Empirical Evaluation of Drilling Fluid Chemistries and Implications of Fluid Design, *SPE Journal, 27*(31), 226-248.

Schopmeyer, H. H. (2003). Waxy cornstarch as a replacement for tapioca. *Ind. Eng. Chem., 35*(33), 168-181.

Scott, B. N., Edde K. C., & Duke, M. M. (2007). The synhesis of biopolymers from biomass. *Polym. Bull., 31*(2), 11-25.

Serada, N. G. & Solovyor, E.M. (2003). Drilling of oil and gas wells. Moscow: Mir Publishers, 126-131.

Sevens, E. S. (2002). Green Polymers: An Introduction to the new Science of Biodegradable Polymers. Princeton, N. J (Ed.), New York: Princeton University Press, 1-6.

Shadravan, J. K. (2012). What Petroleum Engineers and Geoscientists should know about high pressure high temperature Wells Environment. *Energy Science and Technology, 44*(2), 16-30.

Shadravan, N. (2009). Dealing with the challenges of UBD Implementation in Southern Iranian Oilfields. *Society of Petroleum Engineers*. *33*(4), 60-80.

Shahri, S. A. (2012). A new model for determining the radius of mud loss during drilling operation in a radial fractured network. *Society of Petroleum Engineers. 57*(23), 112-134.

Shenglai, Y., Zhichao, S., Wenhui, L., Zhixue, S., Ming W., Jianwei Z., et al. (2008). Evaluation and prevention of formation damage in offshore sandstone reservoirs in China. *Pet. Sci.51*(41), 340-361

Sibel, P. & Tuncan, M. (1991) Microstructure of Fine-grained sediments. New York: Springer-Verlag, 52.

Simpson, J. P., Walker, T. O., & Jiang, G. Z. (1994). Environmentally acceptable water-based mud can prevent shale hydration and maintain borehole stability. *SPE Journal, 18*(5), 75-91.

Skalli, I., Buckley, J.S., Zhang, Y. & Morrow, N. R. (2006). Surface and core wetting effects of surfactants in oil-based drilling fluids. *Journal of. Petr. Sci*., *36*(44), 253-270.

Sobie, K.S. (1994) Polymer-Improved Oil Recovery. Blackie (Ed.). Amsterdam: CRC Press Inc., 7-66.

Song, H. C., Wang, G. X. & Bartha, R. (1990). Bioremediation potential of terrestrial fuel spills, *Appl. Environ. Microbiol*, *56*(37), 351-372.

Sorheim, R., Amundsen, C. E., Kristiansen, R. & Paulsen, J. E. (2000). Oily drill-out Cuttings: From waste to resource. *SPE Journal*, *23*(4), 66-78.

Stamatakis, E., Thaemlitz, C. J., Cotfin, G. & Reid, W. (1995). A new generation of shale inhibitors for water-based muds, *SPE Journal*, *18*(7), 175-197.

Staben, P. A., Denzel, G. D., Greg, I. B., & Chris, M. N. (2004). Drilling fluids and flow models. *SPE Journal*, *35*(36), 235-258.

Stewart, A. A. (2009). The flow properties of drilling fluid containing partially hydrolysed polyacrylamide. *Journal of Petroleum Tec*h., *28*(4), 41-62.

Steiger, R. P. (1993). Advanced triaxial swelling tests on preserved shale cores. *Journal of Petroleum Technology*, *16*(7), 117-133.

Swanson, C. L., Shogren, R. L, Fanta, G. F. & Iman S. H. (1993). Starch- plastic: Materials, preparation, pyhsical properties and biodegradability. *J. Environ. & Polym. Degrad*. *19*(8), 155-176.

Swartz, C. H., & Gschwend, P. M. (1999). Drilling fluids and the environment. *Environ Sci Technol. 32*(18), 179-200.

Tare, U. A., & Mody, F. K. (2000). Stabilizing boreholes while drilling reactive shales with silica-based drilling fluids. *Drilling Contractor*s *Journal, 41*(4), 52-74.

Thaemlitz, C. J. P. (2009). New environmentally safe high temperature water-based drilling fluid systems. *SPE Journal, 27*(11), 185-206.

Theng, B. K. G. (1999). Formation and Properties of Clay-Polymer Complexes. *Journal of Soil Science*, *21*(3), 39–53.

Timmerman, S. R. & Dakota, L. E. (2000). Starch and industrial applications. Chichester: Horwood Publ., 109-111.

Troy, D. B., Flip, N. C. & Billy, K. H. (2008). The relationship between pressure and flow rate of drilling fluids. *Chemstar*, *24*(1), 13-16.

Twynam, A. J., Caidwell, P. A. & Meads, K. I. (1994). Glycol-enhanced water-based muds: case history to demonstrate improved drilling efficiency in tectonically stresses shales. *SPE Journal*, 16(3), 18-38.

Ukachukwu, C. O., Ogbobe O., & Umoren, S. A. (2010). Preparation and characterization of biodegradable polymer mud based on millet starch. *Chemical Engineering Communication (CEC), 197*(8), 1126-1139.

Utrack, L. A. (2001). Rheology and processing of multiphase systems. Amsterdam: Hanser Publishers, 111-124.

Valentine, D. D. (1997). Introduction to clay colloid chemistry. 3rd (Edition), New York: Wiley and Sons Inc., 3-21.

Vander-Zwaag, C. H. (2006). Benchmarking the formation damage of drilling fluids. *Petr. Prod.Journal*, *32*(6), 40-52.

Van-Oort, F. (1994). A novel technique for the investigation of drilling fluid induced borehole instability in shales. *Journal of Petroleum Tech*, *20*(3), 31-52.

Van-Oort, F., Ripley, D., Ward, I., Chapman, J.W., Williamson, R., Aston, M., et al. (1999). Silicate-based drilling fluids: competent, cost-effective and benign solutions to wellbore stability problems. *27*(17), *SPE Journal*, *21*(16), 147-161.

Van-Oort, F. (2003). The physical and chemical stability of shales. *J. Petr. Sci. Eng.*, *38*(5), 213-235

Van-Oort, F., Hale, A. H., & Mody, F. K. (1996). Transport in shales and the design of improved water-based shale drilling fluids, *SPE Journal*, *23*(13), 13-24.

Van-Oort, F., Tale, A. H., Ripley, D., Ward, I., Chapman, J.W., Wiliamson, R., et al. (1996). Silicate-based drilling fluids: Competent, cost-effective and solution to wellbore shale instability, Oil and Gas Journal, *23*(11), 101-119.

Van Ort, E., Bland, R. G., Howard, S. K., Wiersma, R. J. (2001). Improving HPHT stability of water-based drilling fluids, *SPE Journal*, *30*(7), 174-187.

Velde, B. (1999). Introduction to Clay Minerals. 4th (Edition), Texas: Chapman and Hall, 20-37.

Vincent, B. & Iyklema, J. (2005). Adsorption from solution at the Solid / liquid Interface. C.D. Parfitt (Ed.), New York: Academic press, 14-31.

Vicent, J. T., Alphonse, S. M., Guton, P. A., & Delan, C. K. (2001). Studies on the gelling capacity of starch in the presence of drilling mud. *SPE Journal, 30*(11), 110-127.

Ward, I., & Williamson, R. (1998). Silicate water-based muds: A significant advance in water-based drilling fluid technology. *Oil and Gas Journal, 23*(19), 188-209.

Ward, I., Chapman, J.W. & Williamson, R. (1997). Silicate-based muds: chemical optimization based on field experience. *SPE Journal, 21*(15), 58-66.

Weir, R. K. & Bailey, A. A. (2004). Xanthan gum and epichlorohydrin cross-linked hydroxypropylated starch for drilling fluids. *Journal of Petroleum Science and Engineering, 31*(12), 123-137.

Whistler, R. L., Bemiller, J. N. & Paschal, E. G., (2007). Starch chemistry and technology. New York: Academic Press, 57-68.

Wikky, E. F. (2008). Chemically modified corn starch serves as mud additive. *Petroleum Sci. and Tech., 35*(19), 119-134.

Wilcox, T. T. & Hool, A. D. (2010). Superior drilling mud for wells with shale problems. *Petroleum Engineers International, 21*(11), 108-122.

Wylly, F. K., & Chenevert, L. B. (2012). Improved cellulosic polymer used in well drilling fluids. *Energy Sources, 35*(15), 101-115.

Young, S.Y., & Maas, T. (2001). Novel polymer chemistry increases shale stability. *Journal of Petroleum Tech., 41*(17), 127-141.

Zac, J. N., Cuffison, R. A., Blake, M. O., & Russel, B. N. (2012). Carboxymethyl starch and epichlorohydrin crosslinked carboxymethylated cellulose for drilling application. *Journal of Petroleum Science and Engineering, 33*(21), 211-225.

Zamori, M., Lal, D.T., & Dzialowski, A. K. (1990). Innovative devices for testing drilling muds, *SPE Journal, 25*(17), 147-163.

Zereek, T. M. & Bruce, N. D. (2010). Drilling fluids and high temperature wells: An overview. *Chemstar, 29* (2), 321-335.

Zhang, J., Chenevert, M. M., Talal, A., & Sharma, M. M., (2004). A new gravimetric swelling test for evaluating water and ion uptake of shales. *SPE Journal, 37*(15), 226-239.

Zhang, J., Clark, D. E., Bazali, T. M., Chenevert, T., Sharma, M. M., Rojas, J. C. & Seehong, O. (2006). Ion movement and laboratory technique to control wellbore stability. *Polymer Bulletin*, 91-106.

Zhanpeng, J., Hongwei, Y., Lixin, S. & Shaoqi, S. (2002). Integrated assessment for aerobic biodegradability of organic substances. *Chernosphere, 28*(13), 173-188.